Evaluation of Stay-in-Place Metal Forms

Douglas Nims

and

Nabil Grace

THE UNIVERSITY OF TOLEDO

LAWRENCE TECHNOLOGICAL UNIVERSITY

STATE OF OHIO DEPARTMENT OF TRANSPORTATION

FHWA

OHIO DEPARTMENT OF TRANSPORTATION
RESEARCH & DEVELOPMENT

Evaluation of Stay-in-Place Metal Forms

State Job Number 134155

Final Report

By

Douglas K. Nims
Department of Civil Engineering
The University of Toledo

And

Nabil Grace
Department of Civil Engineering
Lawrence Technological University

1. Report No. FHWA/OH-2006/13	2. Government Accession No.	3. Recipient's Catalog No.
4. Title and subtitle **Evaluation of Stay-in-Place Metal Forms**		5. Report Date **May 2006**
		6. Performing Organization Code
7. Author(s) **Douglas Nims** **Nabil Grace**		8. Performing Organization Report No.
		10. Work Unit No. (TRAIS)
9. Performing Organization Name and Address **University of Toledo** **Department of Civil Engineering** **Toledo, Ohio 43606**		11. Contract or Grant No. **134155**
		13. Type of Report and Period Covered Final Report
12. Sponsoring Agency Name and Address **Ohio Department of Transportation** **1980 West Broad Street** **Columbus, Ohio 43223**		14. Sponsoring Agency Code
15. Supplementary Notes		

16. Abstract

An experimental study was conducted to determine if the use of stay-in-place metal forms (SIPMF) resulted in reduced bridge deck concrete quality over the life of the bridge compared to bridge decks formed conventionally without SIPMF. A corollary problem addressed was to determine the potential for using ground penetrating radar (GPR) to inspect the bridge deck concrete quality immediately above the SIPMF.

Experimental studies were carried out on three Northern Ohio bridges that were partially constructed approximately 40 years ago using SIPMF. All these bridges had regions where there was no SIPMF. Cores were extracted from these bridges. The deck concrete quality in regions with SIPMF was compared to the concrete quality in regions without SIPMF. Visual inspections and compression, chloride, permeability and ultrasound tests were performed. Ultrasound is is a very discriminating technique to use for comparison. Analysis of the inspection and test data showed no significant difference between the concrete quality in regions with and without SIPMF. This is consistent with the literature.

An experimental study was carried out that compared the predicted concrete quality from a GPR survey to the concrete quality measured by testing verification cores. A GPR signal attenuation map was developed to predict the quality of the concrete in the bridge. This attenuation map was used to select the locations of the verification (ground truth) cores to be harvested. Visual inspections and compression and ultrasound tests were carried out on the ground truth cores. Ultrasound, when coupled with compression testing, is a well established technique to assess concrete condition. Analyses of the inspections and test data showed that GPR was not effective in predicting concrete quality between the bottom layer of rebar and the top of the SIPMF.

The implementation potential for SIPMF in Ohio was considered. Nothing in the present research indicates that implementation of SIMPF in Ohio will be less successful than in the neighboring northern states. Reaping the full benefits will require some time as Ohio contractors and bridge inspectors become familiar with SIMPF. Important aspects of implementation are inspection, materials, repair and specifications.

17. Key Words Bridges, Concrete, Bridge deck, Stay-in-place metal forms, SIPMF, Permanent metal deck forms, Ground penetrating radar, GPR	18. Distribution Statement No restrictions. This document is available to the public through the National Technical Information Service, Springfield, Virginia 22161
19. Security Classif. (of this report) Unclassified	20. Security Classif. (of this page) Unclassified	21. No. of Pages 544	22. Price

Form DOT F 1700.7 (8-72)   Reproduction of completed pages authorized

Disclaimer

The contents of this report reflect the views of the author who is responsible for the facts and the accuracy of the data presented herein. The contents do not necessarily reflect the official or policies of the Ohio Department of Transportation or the Federal Highway Administration. This report does not constitute a standard, specification or regulation.

Key Words

Bridges, Concrete, Bridge deck, Stay in place metal forms, SIPMF, Permanent metal deck forms, Ground penetrating radar**,** GPR

iv

Acknowledgements

Table of Contents

Table of Contents (continued)

Table of Contents (continued)

x

List of Figures

List of Figures (continued)

List of Figures (continued)

List of Figures (continued)

List of Figures (continued)

List of Figures (continued)

List of Tables

List of Tables (continued)

Chapter 1: Introduction and Bridge Information

1.1 PROBLEM STATEMENT AND OBJECTIVES

The fundamental research problem addressed was to determine if the use of Stay-in-Place Metal Forms (SIPMF, sometimes referred to in the literature as permanent metal deck forms) resulted in reduced bridge deck concrete quality over the bridge life.

A corollary problem addressed was to determine the potential for using ground penetrating radar (GPR) to inspect the bridge deck concrete immediately above the SIPMF.

The use of stay-in-place metal formwork (SIPMF), instead of the conventional plywood forming methods, offers several advantages:

1. Significant time saving in bridge deck construction.
2. Lower labor costs.
3. The ease of installation.
4. Safety of the laborers.
5. Minimal interruption to the environment or traffic below.

Due to these advantages, the Ohio Department of Transportation (ODOT) is interested in learning more about the use of SIPMF. Currently, ODOT only allows the use of SIPMF in rare circumstances. These exceptional circumstances usually exist when the access for form removal from below is very limited and dangerous. This is a sharp contrast to the neighboring states of Pennsylvania, Michigan, Indiana, and West Virginia who use SIPMF much more widely. Indeed, West Virginia requires all bridge decks to be detailed with SIPMF (West Virginia, 2004).

A significant concern in the use of SIPMF in Ohio is the inability to visually inspect the bottom of the deck throughout the life of the bridge. Inspectors use visual information and soundings to assess the quality of new concrete and identify potential problems during service. Until an adequate substitute for visual inspection is found Ohio bridge inspectors will not be comfortable with SIPMF. The present study includes the first known attempt to use ground penetrating radar (GPR) to evaluate the condition of the concrete at the bottom of the bridge deck.

Using GPR to assess concrete condition, as well as locate discontinuities in material properties, has potential to alleviate the concern with loss of visual inspection information. Several features of GPR inspection make it very intriguing as an inspection technique:

1. It is non-destructive.
2. It is a very effective method for determining if delamination exists in the concrete above the top layer of rebar.
3. GPR surveys can be conducted rapidly without impeding traffic flow. Air-launched ground penetrating radar surveys can be conducted at speeds up to 35 mph (56 kph).
4. It is safer for the inspectors.

1.2 RESEARCH OBJECTIVES

To experimentally explore the effect of SIPMF on Ohio bridges, ODOT has identified three bridges in northern Ohio that were constructed in the 1960's using SIPMF. The primary objective of this study is to combine the results from tests on cores from these bridges, review of the literature, and discussions with owners and manufacturers to assess the long-term impact of SIPMF on Ohio bridges.

A secondary objective is to experimentally determine if a state-of-the-art GPR survey of the deck of a bridge made with SIPMF can be used to assess the condition of the deck concrete just above the SIPMF. This is the first known attempt to use GPR to determine the condition of concrete.

1.3 RESEARCH APPROACH

The research for assessing the difference in concrete bridge deck performance between bridges with and without SIPMF was performed as follows:

a) An extensive literature search was performed. This was greatly facilitated by the fact that Dr. Nabil Grace, one of the authors, had conducted a parallel national study on SIPMF for the Michigan Department of Transportation.

b) Cores were extracted from the three northern Ohio Bridges that had been constructed forty years ago using SIPMF. All these bridges had regions where there was no SIPMF. Cores were extracted both from the regions with and without SIPMF.

c) The visual inspections and compression, chloride, permeability and ultrasound tests were carried out on the cores. Ultrasound is a somewhat unusual test. It was done because it is a very discriminating technique to use for comparison of concrete quality. The researchers at the University of Toledo performed the compression, permeability, and chloride ion tests. Researchers from Lawrence Technological University performed the ultrasound tests.

d) The data was analyzed to determine if there was a significant difference between the concrete quality in regions with SIPMF and regions without SIPMF.

e) Specifications for SIPMF from other states were reviewed with particular emphasis on neighboring and northern states and discussions were held with manufacturers.

The research to assess the potential for using ground penetrating radar as an inspection tool was performed as follows:

a) A literature search was performed. Resource International, Incorporated assisted in this search and provided background discussions and information on GPR.

b) A GPR survey of the OTT-2-28.41 bridge was carried out.

c) Based on the GPR survey, a signal attenuation maps were developed for the reflections from the top mat of rebar and the SIPMF. Concrete condition was predicted based on signal attenuation.

d) The GPR signal attenuation maps were used to select the locations of ground truth cores to be harvested.

e) The visual inspections and compression and ultrasound tests were carried out on the ground truth cores. Ultrasound, when coupled with compression testing, is a well established technique to assess concrete condition.

f) The concrete condition results from the ground truth cores and from the GPR survey were compared.

1.4 SUMMARY OF RESULTS

Analysis of the data showed no significant difference between the concrete in regions with and without SIPMF. This is consistent with the literature review and the experience of neighboring states.

SIPMF near expansion joints and SIPMF with holes in it experienced localized rusting near these water sources. It is recommended the number of holes be minimized and steps be taken to prevent water from flowing around the edges of the SIPMF. It has also been reported that SIPMF on underpasses in urban areas experienced deterioration from water being continually thrown on the bottom of the bridge.

Analysis of the data showed that the GPR system used was not effective as an inspection tool for the concrete immediately above the SIPMF. The GPR was effective in locating delaminations above the top layer of rebar. This is a common use for GPR and, in the present tests, the success rate in identifying top delaminations was consistent with that reported in the literature. However, the GPR gave false indications of delaminations for the concrete below the bottom rebar. Several delaminations were predicted that were not found in the ground truth cores. Many factors determine the signal attenuation and dielectric constant of the concrete. The researchers were unable to determine why the false indications occurred.

The data did reveal a correlation between concrete condition and GPR signal attenuation. This relationship supports the hypothesis that using GPR for bridge deck inspection may be possible in the future. However, it will require additional research to develop a relationship between bridge deck condition and GPR signal attenuation.

1.5 GENERAL BRIDGE INFORMATION

The three bridges sampled were selected by the research team and approved by ODOT engineers. All three of these bridges are either in the process of being totally replaced or given a new wider deck. The primary reason for widening or replacement was functional obsolescence. The first bridge, LOR-57-18.18, is located on Route 57 over the Black River in Lorain County in

ODOT District 3. This bridge was constructed in 1961 and is a typical steel truss bridge (See Figure 1.1).

Figure 1.1. LOR-57-18.18

Since the bridge lies over a deep ravine it was built such that the deck from the approach slab to the first expansion joint was formed utilizing the conventional plywood forming method. The rest of the spans where constructed using SIPMF. Figure 1.2 illustrates this.

Figure 1.2. LOR-57-18.18 SIPMF and No SIPMF Areas

Overall, the bridge was in fairly good condition except for a few areas. One noticeable problem area was along the first expansion joint. This expansion joint, where the SIPMF area meets the non-SIPMF area, showed an excessive amount of rust. Because of this, a few core samples where extracted from this area to determine the properties of the concrete in this area. Figure 1.3 provides a picture of this problem area.

Figure 1.3. LOR-57-18.18 Excessive Rust at First Expansion Joints

Another area of concern was the bridge deck. The deck showed a few areas in which the surface concrete was totally rubblized. This is illustrated in Figure 1.4.
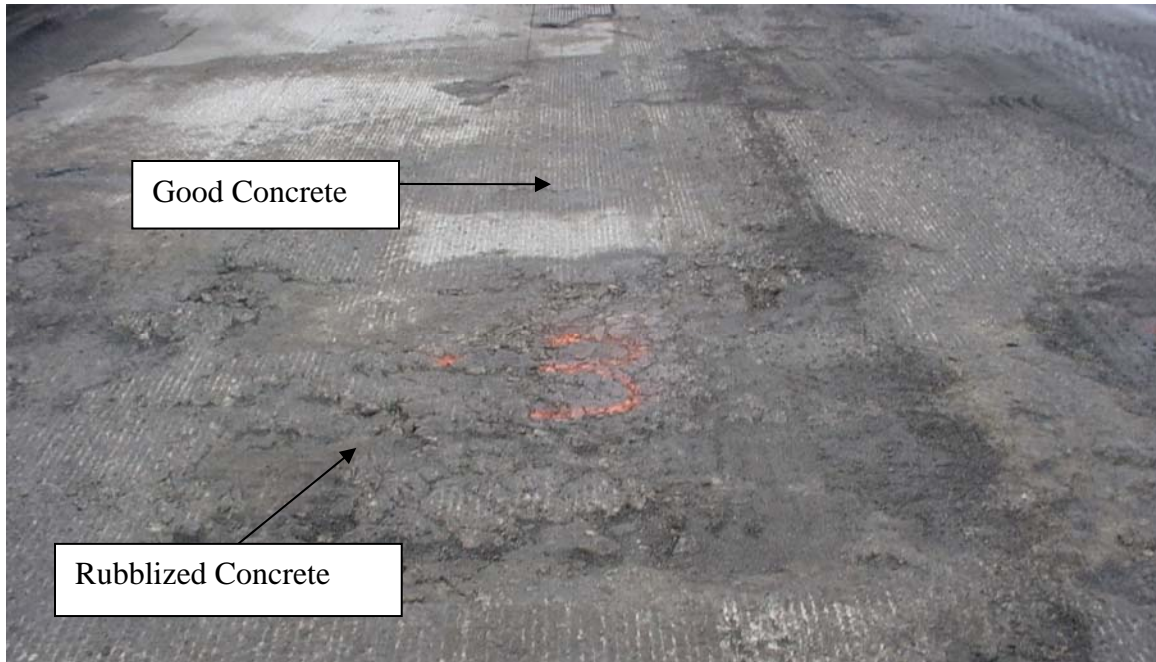
Figure 1.4. LOR-57-18.18 Rubblized Deck

Lastly, the area along the joint between the approach slab and the first span also showed an excessive amount of rust. The expansion joint at this area was totally deteriorated and water was found settled in the joint. This problem was magnified due to the fact that the drainage on bridge was not working properly. All the drains were clogged with debris, which caused the water to collect along this joint. This problem is shown in Figure 1.5.

Figure 1.5. Excessive Rust at Joint Between Approach Slab and First Span

These three problems areas caused the most concern on our visit to the bridge. Other smaller problems were also encountered. These problems ranged from small transverse cracks in the deck to slight rusting of the truss members. To get a full representation of the quality of the bridge deck, core samples were extracted from both good and bad areas of the deck. Each core was tested in either compression, permeability, chloride ion, or ultrasound. A list of each core's location, along with the test performed on each individual core, is located in Table 1.1. Figure 1.6 shows a map of each core's location. Test results and comments and for each core are in "Appendix A: LOR-57-18.18 Individual Core Data".

Table 1.1: LOR-57-18.18 Core Locations

Core Number	Ref. Exp. Jt.	Station Location	Distance from Curb (ft.) on Southside of Bridge (1 ft = .305 m)	Comments	Recommended Testing	SIPMF
S1	975 + 52.4	975 + 56.9	35.2	Most deteriorated area where no SIPMF; where plywood form meets gird	Perm. & Chloride	N
S2	975 + 52.4	975 + 51.6	29.9	Taken because SIPMF badley deteriorated underneath	Chloride Ion	Y
1E	975 + 52.4	975 + 53.1	1.6		Compression	N
1F	975 + 52.4	975 + 54	0.8		Ultrasound	N
2E	975 + 52.4	975 + 51.5	1.6		Permeability	Y
2F	975 + 52.4	975 + 51.3	0.7		Chloride Ion	Y
1C	975 + 52.4	975 + 53.4	26.5		Ultrasound	N
2C	975 + 52.4	975 + 50.7	25.9		Permeability	Y
1B	975 + 52.4	975 + 53.3	35.1		Ultrasound	N
2B	975 + 52.4	975 + 50.7	35		Chloride Ion	Y
1D	975 + 52.4	975 + 53.4	14.1		Permeability	N
2D1	975 + 52.4	975 + 51.5	14.4		Permeability	Y
2D2	975 + 52.4	975 + 50.5	14.5		Permeability	Y
2D3	975 + 52.4	975 + 50.5	13.1		Compression	Y
3F	975 + 52.4	975 + 9.6	0.8		Chloride Ion	Y
3D	975 + 52.4	975 + 8.4	19.6		Ultrasound	Y
3C	975 + 52.4	975 + 8.6	24.7		Chloride Ion	Y
4C1	975 + 52.4	974 + 80.6	21.4		Compression	Y
4C2	975 + 52.4	974 + 80.4	20.9		Ultrasound	Y
4F	975 + 52.4	974 + 79.6	0.9		Chloride Ion	Y
4E	975 + 52.4	974 + 80	1.7	Picture @ 9:12 shows bottom closeup	Permeability	Y
5E	972 + 86.1	973 + 50.1	1.7		Compression	Y
5D	972 + 86.1	973 + 49.9	12.4		Compression	Y
5C	972 + 86.1	973 + 50.4	23.2		Chloride Ion	Y
5B	972 + 86.1	973 + 50.5	32.8	Picture @ 9:58 shows bottom closeup	Permeability	Y
6E	972 + 86.1	973 + 48.9	1.7		Chloride Ion	Y
6D	972 + 86.1	973 + 48.9	12.4		Permeability	Y
6C	972 + 86.1	973 + 49.9	23.2		Ultrasound	Y
6B	972 + 86.1	973 + 49.6	32.8		Ultrasound	Y
7B	971 + 78.7	971 + 80.3	34.8		Chloride Ion	Y
8E	971 + 78.7	971 + 65.3	1.7		Ultrasound	N
8D	971 + 78.7	971 + 65.7	11.3		Compression	N
8C2	971 + 78.7	971 + 64.2	20.4		Ultrasound	N
8C1	971 + 78.7	971 + 65.3	20.6		Perm. & Chloride	N
8B	971 + 78.7	971 + 65.6	34.6		Perm. & Chloride	N
7E	971 + 78.7	971 + 80.7	1.9		Permeability	Y
7D	971 + 78.7	971 + 80.4	11.8		Ultrasound	Y
7C1	971 + 78.7	971 + 80.4	28		Permeability	Y
7C	971 + 78.7	971 + 81	17.4	Picture @ 10:55 shows cracks in deck	Chloride Ion	Y
7C1(2)	971 + 78.7	971 + 80.3	27.3		Permeability	Y

      ■ = Tests performed at Lawrence Technological University

2" cores

Core Number	Ref. Exp. Jt.	Station Location	Distance from Curb (ft.)	Comments	Recommended Testing	SIPMF
2 - 2"	975 + 52.4	975 + 51.6	31.2		Compression	Y
3 - 2"	975 + 52.4	975 + 9.3	22.8		Compression	Y
4 - 2"	975 + 52.4	974 + 80.5	21		Compression	Y
5 - 2"	972 + 86.1	973 + 49.9	22.8		Compression	Y
7 - 2"	971 + 78.7	971 + 81	20.1		Compression	Y
8 - 2"	971 + 78.7	971 + 65.4	6.9		Compression	N

Reasons for Core Location

Row 1: West side of bridge on west side of expansion joint where **no** SIPMF
Row 2: West side of bridge on east side of expansion joint where SIPMF
Row 3: Rubbelized area of deck on west side of bridge
Row 4: Rubbelized area
Row 5: Area of good concrete near middle of bridge
Row 6: Area of good concrete near middle of bridge
Row 7: East side of bridge on west side of expansion joint where SIPMF
Row 8: East side of bridge on east side of expansion joint where **no** SIPMF

Notes:

Compression Tests - 2 tests per sample; 4 samples SIPMF and 4 samples no-SIPMF per bridge
Chloride Ion Tests - 4 tests per sample; 4 samples SIPMF and 4 samples no-SIPMF per bridge
Permeability Tests - 2 tests per sample; 4 samples SIPMF and 4 samples no-SIPMF per bridge
Ultra-sound - 5 samples SIPMF and 5 samples no-SIPMF per bridge
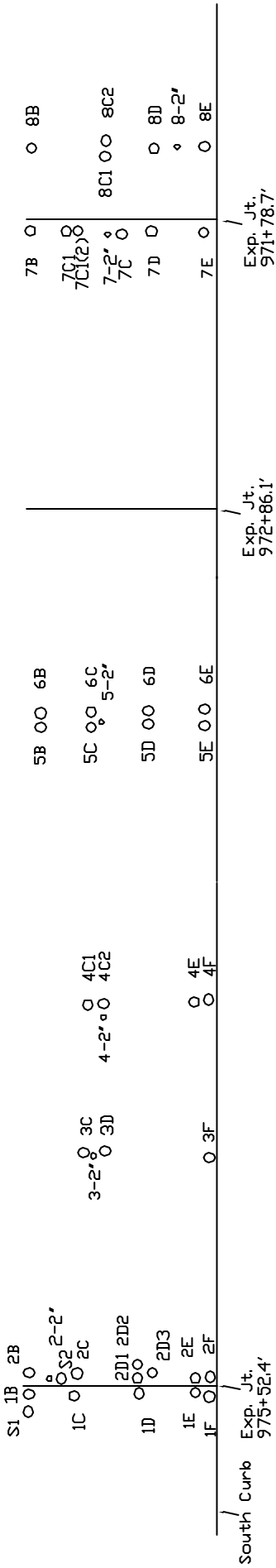
Figure 1.6

Map of Core Locations: LOR-57-18.18

The second bridge, OTT-2-28.41 is located on Route 2 over Sandusky Bay in Ottawa County in ODOT District 2. Note on the bridge number: OTT-2-28.41 is the number on the December 1962 drawings for the bridge. This number is used throughout this report. The bridge number in June 2006 is OTT-2-28.39.

This bridge was constructed in 1965 and is a precast, prestressed concrete I-Beam superstructure bridge (See Figure 1.7). This bridge utilized SIPMF on the whole deck except for the area from the exterior girder to the edge of the deck. The bridge was constructed using SIPMF because the bridge is located over a bay and access to the deck bottom was very limited.

Figure 1.7. OTT-2-28.41

Because this bridge is located over Sandusky Bay access to the deck from below was very limited. Due to this limitation, the bridge was constructed such that the whole deck utilized SIPMF except for the area from the exterior girder to the edge of the deck. This area is shown in Figure 1.8.

Figure 1.8. OTT-2-28.41 – No SIPMF Area

The one noticeable problem area was along the area where the approach slab meets the deck. This area showed an excessive amount of rust on the SIPMF. This problem originated because that the drains on the bridge were extremely clogged with debris causing the water to collect in this area. Figure 1.9 shows the heavy amount of rust on the SIPMF.

Figure 1.9. OTT-2-28.41 Excessive Rust of SIPMF

This area was the only region of noticeable concern on the bridge. The deck seemed to be in relatively good condition from our field inspection. To get a full representation of the quality of the bridge deck, core samples were extracted from both good and bad areas of the

deck. Each core was tested in either compression, permeability, chloride ion, or ultrasound. A list of each core's location, along with the test performed on each individual core, is located in Table 1.2. Figure 1.10 shows a map of the core locations. Test results and comments for each core are in "Appendix B: OTT-2-28.41 Individual Core Data.

Table 1.2: OTT-2-28.41 Core Locations

Core Number	Ref. Exp. Jt.	Station Location	Distance from Curb (ft.) on Eastside of Bridge (1 ft =.305 m)	Comments	Recommended Testing	SIPMF
A1	106 + 98	107 + 11.5	0.4		Ultrasound	N
A2	106 + 98	107 + 12.8	0.3		Chloride Ion	N
A3	106 + 98	107 + 13.9	0.3		Permeability	N
A4	106 + 98	107 + 14.8	0.4		Chloride Ion	N
A5	106 + 98	107 + 15.9	0.4		Ultrasound	N
A6	106 + 98	107 + 17.2	0.2		Permeability	N
A7	106 + 98	107 + 18.3	0.2		Compression	N
A8	106 + 98	107 + 19.6	0.3		Chloride Ion	N
A9	106 + 98	107 + 20.7	0.2		Ultrasound	N
A10	106 + 98	107 + 21.9	0.3		Permeability	N
A11	106 + 98	107 + 23	0.2		Ultrasound	N
A12	106 + 98	107 + 24.2	0.2		Compression	N
A13	106 + 98	107 + 25.6	0.3		Compression	N
A14	106 + 98	107 + 26.7	0.3		Chloride Ion	N
A15	106 + 98	107 + 27.7	0.4		Permeability	N
A16	106 + 98	107 + 28.7	0.3		Ultrasound	N
B1	106 + 98	107 + 8.6	6.7		Ultrasound	Y
B2	106 + 98	107 + 13.1	6.4		Compression	Y
B3	106 + 98	107 + 16.5	6.2		Permeability	Y
B4	106 + 98	107 + 19.5	5.9		Ultrasound	Y
B5	106 + 98	107 + 26.4	5.7		Ultrasound	Y
B6	106 + 98	107 + 29.3	5.6		Permeability	Y
B7	106 + 98	107 + 32.5	5.6		Chloride Ion	Y
			Distance from Curb (ft.) on Westside of Bridge			
C1	106 + 98	107 + 0.9	2.7	Taken because SIPMF badley deteriorated underneath	Chloride Ion	Y
C2	106 + 98	107 + 2.5	4.4	Picture shows of delamination due to rusty rebar	Permeability	Y
C3	106 + 98	107 + 5.7	4.4		Ultrasound	Y
C4	106 + 98	107 + 9.1	4.3		Chloride Ion	Y
C5	106 + 98	107 + 12.2	4.2		Chloride Ion	Y
C6	106 + 98	107 + 15.9	4.3		Chloride Ion	Y
C7	106 + 98	107 + 29	4.3		Ultrasound	Y
C8	106 + 98	107 + 32.5	4.3		Permeability	Y

▮ = Tests performed at Lawrence Technological University

2" cores (Test for Compression)						
			Distance from Curb (ft.) on Eastside of Bridge			
A17	106 + 98	107 + 29.6	0.1		Compression	N
A17-1	106 + 98	107 + 30.6	0.2		Compression	N
A18	106 + 98	107 + 31.5	0.4		Compression	N
A18-1	106 + 98	107 + 32.7	0.5		Compression	N
B8	106 + 98	107 + 34.2	5.5		Compression	Y
B9	106 + 98	107 + 36	5.5		Compression	Y
			Distance from Curb (ft.) on Westside of Bridge			
C9	106 + 98	107 + 34.8	4.3		Compression	Y
C9-1	106 + 98	107 + 35.1	4		Compression	Y
C10	106 + 98	107 + 35.3	4.1		Compression	Y
C10-1	106 + 98	107 + 37.4	3.9		Compression	Y

Reasons for Core Location
Row A: East side of bridge where **no** SIPMF
Row B: Middle of passing lane on east side of bridge where SIPMF
Row C: West side of bridge where SIPMF

Notes:
Compression Tests - 2 tests per sample; 4 samples SIPMF and 4 samples no-SIPMF per bridge
Chloride Ion Tests - 4 tests per sample; 4 samples SIPMF and 4 samples no-SIPMF per bridge
Permeability Tests - 2 tests per sample; 4 samples SIPMF and 4 samples no-SIPMF per bridge
Ultra-sound - 5 samples SIPMF and 5 samples no-SIPMF per bridge

N

↑   ↑

A1 - A18

B1 - B9

C1 - C10

21.2'

13.5'

27.4'

10.6'

35.3'

2.9'

North Abutment
STA 106+98
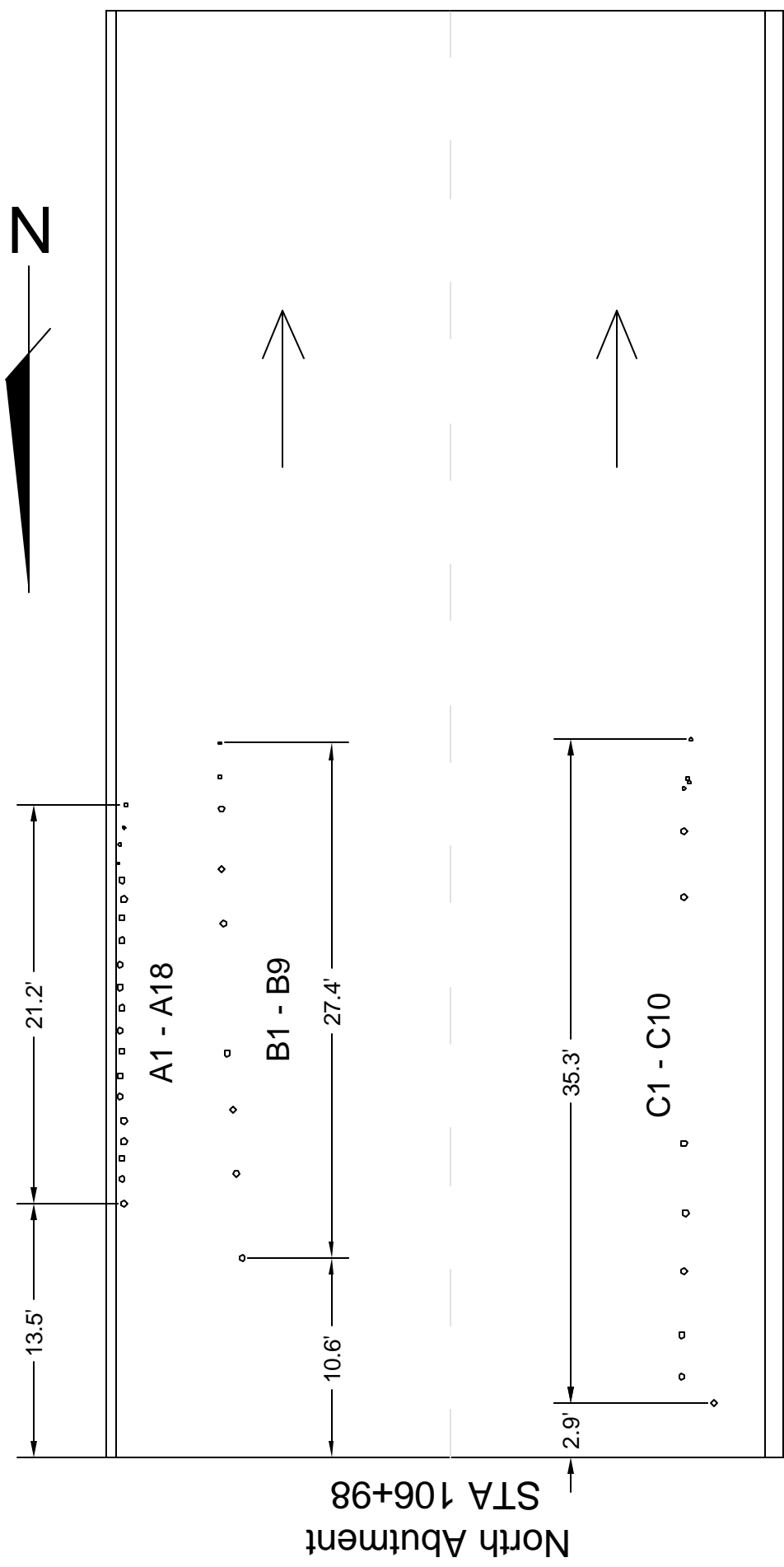
Figure 1.10
Map of Core Locations: OTT-2-28.41

The third bridge, LAK-90-23.42, is located on Interstate 90 over the Grand River in Lake County in ODOT District 12. It was constructed in 1960 and is a typical steel truss bridge (See Figure 1.11). It utilized the same construction techniques as the Lorain County Bridge: the deck from the approach slab to the first expansion joint was formed using the conventional plywood forming method. The rest of the spans were constructed using SIPMF. Once again, this construction technique was implemented because the bridge is located over a deep ravine.

Figure 1.11. LAK-90-23.42

The overall condition of the bridge was good. The SIPMF were in good condition. They showed no signs of rust. The deck also appeared to be intact. It showed very little transverse or longitudinal cracks from our initial inspection. However, the bridge did show some areas of concern. The bottom of the deck had a few areas where the concrete had begun to spall. This is illustrated in Figure 1.12.

Figure 1.12. LAK-90-23.42 Spalling of Deck Bottom

Another area of concern was along the expansion joints. The expansion joint located between the approach slab and first span showed some signs of rust. The other expansion joints also exhibited signs of rust. Once again, this problem can be attributed to the poor drainage on the bridge. All the drains on the bridge deck were clogged with debris causing the water to collect in the expansion joints. Figure 1.13 shows the rust present at the expansion joint located between the approach slab and the first span.

Figure 1.13. LAK-90-23.42 Rust at Expansion Joint

To get a full representation of the quality of the bridge deck, core samples were extracted from both good and bad areas of the deck. Each core was tested in either compression, permeability, chloride ion, or ultrasound. A list of each core's location, along with the test performed on each individual core, is located in Table 1.3. Figure 1.14 provides a map of the core locations. Test results and comments for each core are in "Appendix C: LAK-90-23.42 Individual Core Data".

Table 1.3: LAK-90-23.42 Core Locations

Core Number	Ref. Exp. Jt.	Distance from Ref. Exp. Jt.	Station Location	Distance from face of Parapet (ft.) (1 ft = .305 m) on Southside of Bridge	Comments	Recommended Testing	SIPMF
L1	838 + 23.81	-72.8	837 + 51.01	2.4		Compression	Y
L2	838 + 23.81	-71.5	837 + 52.31	2.5		Permeability	Y
L3	838 + 23.81	-70.2	837 + 53.61	2.7		Ultrasound	Y
L4	838 + 23.81	-68.9	837 + 54.91	2.6		Chloride Ion	Y
L5	838 + 23.81	-56.0	837 + 67.81	3.1		Compression	Y
L6	838 + 23.81	-54.6	837 + 69.21	2.8		Ultrasound	Y
L7	838 + 23.81	-53.4	837 + 70.41	2.5		Chloride Ion	Y
L8	838 + 23.81	-45.1	837 + 78.71	3.3		Ultrasound	Y
L9	838 + 23.81	-40.8	837 + 83.01	3.6		Permeability	Y
L10	838 + 23.81	-39.3	837 + 84.51	2.9		Ultrasound	Y
L11	838 + 23.81	-38.1	837 + 85.71	2.2		Permeability	Y
L12	838 + 23.81	-32.0	837 + 91.81	2.3		Ultrasound	Y
L13	838 + 23.81	-24.6	837 + 99.21	5.1		Chloride Ion	Y
L14	838 + 23.81	-23.9	837 + 99.91	3.3		Permeability	Y
L15	838 + 23.81	-22.2	838 + 01.61	2.8		Chloride Ion	Y
L16	838 + 23.81	-17.7	838 + 06.11	3.5		Permeability	Y
L17	838 + 23.81	-18.0	838 + 05.81	4.7		Compression	Y
L18	838 + 23.81	-18.1	838 + 05.71	5.2		Compression	Y
L19	838 + 23.81	14.7	838 + 38.51	4.6		Compression	N
L20	838 + 23.81	15.0	838 + 38.81	4.8		Compression	N
L21	838 + 23.81	14.6	838 + 38.41	6.1		Chloride Ion	N
L22	838 + 23.81	15.2	838 + 39.01	4.5		Chloride Ion	N
L23	838 + 23.81	16.2	838 + 40.01	4.7		Ultrasound	N
L24	838 + 23.81	17.5	838 + 41.31	4.9		Ultrasound	N
L25	838 + 23.81	18.6	838 + 42.41	3.3		Compression	N
L26	838 + 23.81	21.6	838 + 45.41	2.9		Ultrasound	N
L27	838 + 23.81	22.4	838 + 46.21	3.5		Permeability	N
L28	838 + 23.81	25.0	838 + 48.81	2.7		Ultrasound	N
L29	838 + 23.81	25.8	838 + 49.61	3.7		Compression	N
L30	838 + 23.81	29.4	838 + 53.21	4.1		Permeability	N
L31	838 + 23.81	30.1	838 + 53.91	4.2		Ultrasound	N
L32	838 + 23.81	35.2	838 + 59.01	5.2		Compression	N
L33	838 + 23.81	36.1	838 + 59.91	3.9		Permeability	N
L34	838 + 23.81	42.1	838 + 65.91	5.8		Chloride Ion	N
L35	838 + 23.81	42.7	838 + 66.51	4.1		Permeability	N
L36	838 + 23.81	46.8	838 + 70.61	6.1		Chloride Ion	N

** Reference expansion joint located at end of first span from the east end of bridge **

               = Tests performed at Lawrence Technological University

Notes:
Compression Tests - 2 tests per sample; 4 samples SIPMF and 4 samples no-SIPMF per bridge
Chloride Ion Tests - 4 tests per sample; 4 samples SIPMF and 4 samples no-SIPMF per bridge
Permeability Tests - 2 tests per sample; 4 samples SIPMF and 4 samples no-SIPMF per bridge
Ultra-sound - 5 samples SIPMF and 5 samples no-SIPMF per bridge

Abutment

L36

L35 L34

L33
L32

32.1'

L31
L30
L29
L28
L27
L26
L25
L24
L22 L23
L21
L20 L19

No SIPMF's

14.7'

Expansion Joint
STA 838+23.81

17.7'

L18 L17
L16
L15
L14
L13

L12

L11
L10
L9

L8

L7
L6
L5

55.1'

SIPMF's

L4
L3
L2
L1

N
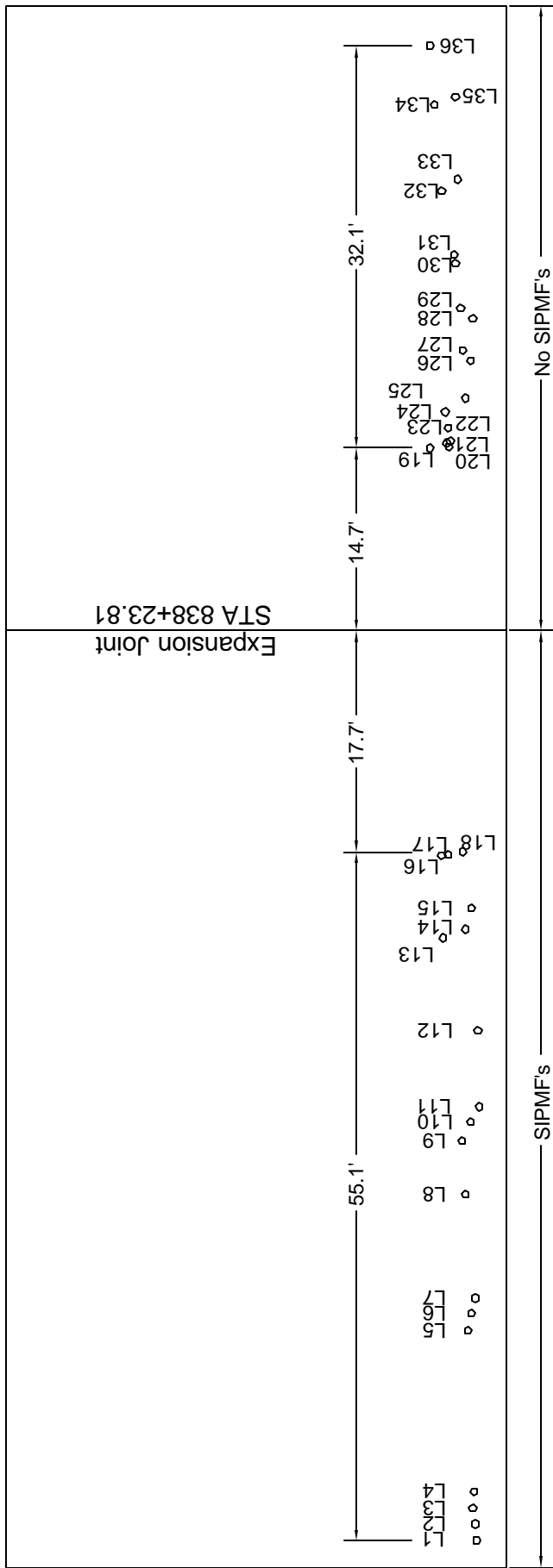
Figure 1.14

Map of Core Locations:LAK-0--23.42

Chapter 2: Stay-in-Place Metal Forms Literature Review

Stay-in-place metal forms (SIPMF) provide a viable option in the construction of a concrete bridge deck. The forms are made of thin galvanized steel sheets that span between the main girders. They remain in position for the lifetime of the bridge and require no supporting falsework (Beales and Ives, 1990). The SIPMF can be manufactured in a variety of different gage thicknesses and the depth and pitch of the form have been known to vary from project to project. A profile of a typical SIPMF is shown in Figure 2.1.
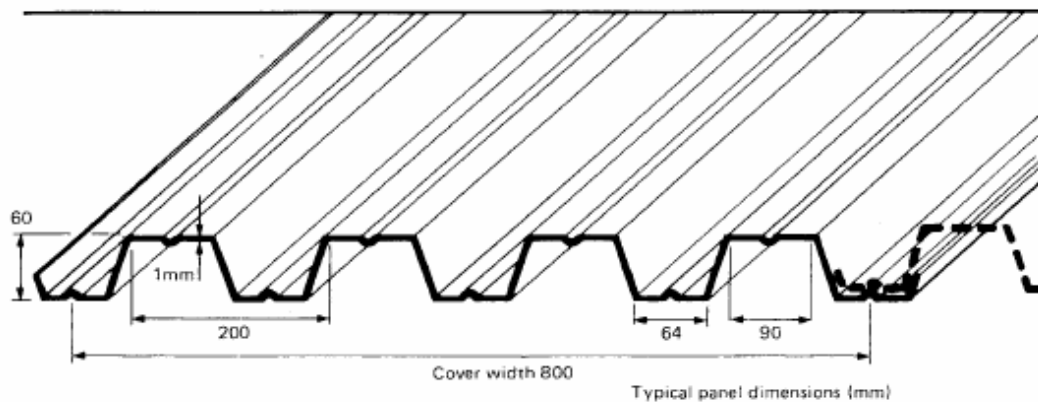
Figure 2.1. SIPMF Profile (from Beales and Ives 1990)

2.1 ADVANTAGES OF STAY-IN-PLACE METAL FORMS

The use of SIPMF is steadily increasing across the country, particularly in the south, due to the many advantages that this forming system presents over the conventional plywood forming method. The most noticeable advantage for SIPMF lies in the economic value of this system (Bakht, Mufti, and Tadros, 2002, 2002A). This system speeds up bridge deck construction, which in turn saves the owner a considerable amount of money. The construction schedule is accelerated because the SIPMF does not need to be stripped after the deck is poured. The majority of the costs in a construction project are labor costs. Since SIPMF are not stripped after the deck is poured, labor costs are reduced. This lower cost can also be attributed to lower equipment costs as well. To strip a conventional plywood deck form, equipment must be used to assist the laborers. This equipment cost is eliminated because SIPMF do not need to be

removed. Cost is also minimized when SIPMF are used to construct a bridge over another roadway. By using SIPMF, the amount of time required for a lane closure is reduced because the forms do not need to be stripped underneath. This minimizes traffic disruptions to the public and greatly increases safety of the laborers when the project is located near heavy traffic areas or when access to the underneath portion of the bridge is limited (Merrill 2002). Many contractors have stated that the use of SIPMF has resulted in lower insurance premiums due to the inherent safety of the system (Merrill 2002).

SIPMF also offer a distinct advantage in minimizing environmental disruptions. This is evident when a bridge is constructed over water or near surrounding wetlands. When the conventional plywood forming method is used, equipment may need to placed in the water or surrounding wetlands to assist the labors in stripping the forms. This in turn poses a problem to the environment. Many foreign substances may enter the water system due to the stripping process of conventional plywood forms. This environmental disruption is eliminated with the use of SIPMF.

Frosch, Blackman, and Radabaugh (2003) cited a Pennsylvania State University survey on the durability of bridge deck concrete conducted in 1971 (Cady et al. 1971). This study references Larson and Malloy (1966) and Love, Barnoff, and Larson (1967). These studies indicated that the use of SIPMF increases the structural stiffness of the bridge deck. They stated that bridge decks constructed with SIPMF have performed better than decks constructed with the conventional plywood forming method. This was evident because decks constructed with the conventional plywood forming method exhibited three times the amount of transverse cracks as decks constructed with SIPMF. The Pennsylvania State University study also concluded that SIPMF slow moisture loss from freshly placed concrete.

Economics and speed plus the other advantages are the reasons why this country has seen an increase in the use of SIPMF. The use of SIPMF is more widespread in the south because lower salt usage limits corrosion potential.

2.2 DISADVANTAGES OF STAY-IN-PLACE METAL FORMS

SIPMF offer several advantages. However, some problems have been attributed to their use. The most critical stage in deck construction using SIPMF is the placement of the concrete

(Helwig and Frank, 1993). During this phase, the SIPMF must be able to carry their own weight, the weight of the concrete, the laborers, and the equipment. The most serious problem encountered when using SIPMF deals with the failure and collapse of the metal decking during concrete placement (Merrill 2002). This type of failure can be traced back to the contractor providing the thinnest sheet metal possible in an effort to reduce his cost. For example, in one failure, the SIPMF was found to be adequate to carry the required load.   However during the installation process the SIPMF were slightly damaged. This damage was traced back to the laborers placement of reinforcing steel and a welder's cart denting the form as he crossed the SIPMF. These dents reduced the stiffness of the form causing it to buckle under the load of the concrete (Merrill 2002). Because small deformations can greatly reduce the strength of the SIPMF , many states now require a minimum gage thickness when using SIPMF. Another safety concern during construction has been that the SIPMF are used as a work platform before they are adequately tied down. This has been controlled by requiring safety stops or specifying that the SIPMF be tied down immediately (for typical details see PennDOT 2005)

Another concern of SIPMF is that corrosion problems have been experienced in some instances. These corrosion areas tend to lie along the panel edges where the SIPMF has been cut and the protective treatment has been damaged (Beales and Ives, 1990). This corrosion problem can also be attributed to a breakdown of the bridge deck waterproofing membrane. This allows water to come in contact with the SIPMF (Beales and Ives, 1990). During the visual inspections performed on the three northern Ohio bridges, corroded areas were noted along the expansion joints and near the scuppers. This can also be attributed to the expansion joint and the deck penetration at the scupper allowing water to continuously flow over the SIPMF.

One of the most common reservations inspectors have when considering the use of SIPMF is the fact that the bottom of deck cannot be visually inspected. Concerns have risen about the possibility of the SIPMF leading to improper drainage of water from the bridge deck (Goldman, Cohen, and Ramirez, 1995). The main concern is that water will become trapped between the SIPMF and the concrete, resulting in cracks in the slab originating at the bottom and traveling upwards. This confinement of water also leads to damage of the deck and SIPMF due to the freeze-thaw action in the winter months. These concerns are magnified because it is generally accepted that no bond exists between the SIPMF and the concrete because the smooth galvanized surface of the SIPMF keeps it from acting compositely with the concrete (Bakht, B.,

A.A. Mufti, and G. Tadros, 2002). From our visual inspection of the core samples, very few instances were noted where a bond existed between the concrete and the SIPMF. However, even though there was a lack of bond between the SIPMF and the concrete, few problems of corrosion along the bottom of the deck were observed.

Frosch, Blackman, and Radabaugh (2003) have also noted that a major concern about the use of SIPMF lies in area of bridge deck cracking. They have noted that this is one of the major factors leading to bridge deterioration. The cracks provide a direct route for water and chlorides to enter the deck and damage the concrete and reinforcing steel. They have stated that cracks wider than 0.007 in (0.1778 mm) lead to bridge deck deterioration. Frosch et al (2003) have also concluded that more transverse cracks were noted on bridges where SIPMF were used rather than conventional plywood forms. The results of their study stated that six of the seven bridges that used SIPMF had transverse cracks in the bridge deck. A typical transverse crack from their study is shown in Figure 2.2.
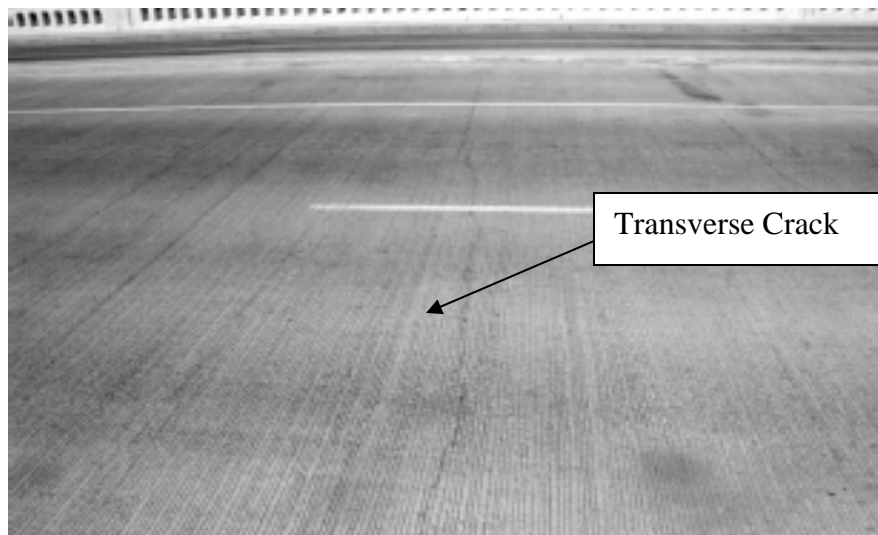
Figure 2.2. Transverse Bridge Deck Crack (Frosch et al 2003)

These transverse cracks were attributed to the fact that the concrete on the bottom was more restrained than that on the top of the bridge deck. This in turn leads to an unsymmetrical shrinkage profile that is believed to initiate more transverse cracks. Another reason why SIPMF induce more transverse cracks can be attributed to the behavior known as curling. Curling will occur because the top surface is free to shrink, where as the bottom surface is restrained. This

restriction of the bottom surface leads to the development of tensile stresses on the top surface. These stresses lead to transverse cracks. Figure 2.3 illustrates this behavior.

Before Shrinkage Tensile Stresses

Sealed Surface

After Shrinkage
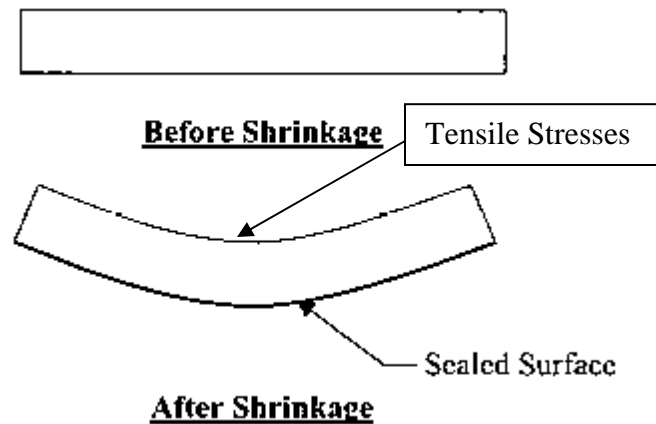
Figure 2.3. Curling (Frosch et al 2003)

However, after speaking to various individuals and from our own observations, the present researchers believe that curling is not significant. The judgment the curling is not significant is further support by the fact that no specification, even that of Indiana who sponsored the research of Frosch et al (Indiana DOT 2006), has limitations to prevent cracking associated with curling.

SIPMF also present a problem when it comes to attaching the form to the girder (Frosch et al, 2003). The typical approach of fastening the form to the girder implements the use of a 3-inch by 2-inch (76 x 50 mm) galvanized cold-rolled steel angle. This angle is attached to the flange of the girder by welding it directly to the top flange in the positive moment area or by welding it to a steel bar resting on the top flange in the negative moment area. The SIPMF are then attached to the angle by using self-tapping screws. Frosch et al noted from their inspection that the leg of the angle was usually turned upward into the deck. Since the leg of the angle was incorporated into the deck, it caused a discontinuity in the bridge deck. They stated that this may lead to a spot where cracks initiate, leading to longitudinal cracks. Figure 2.4 shows a typical detail in which the angle is turned upward into the deck.
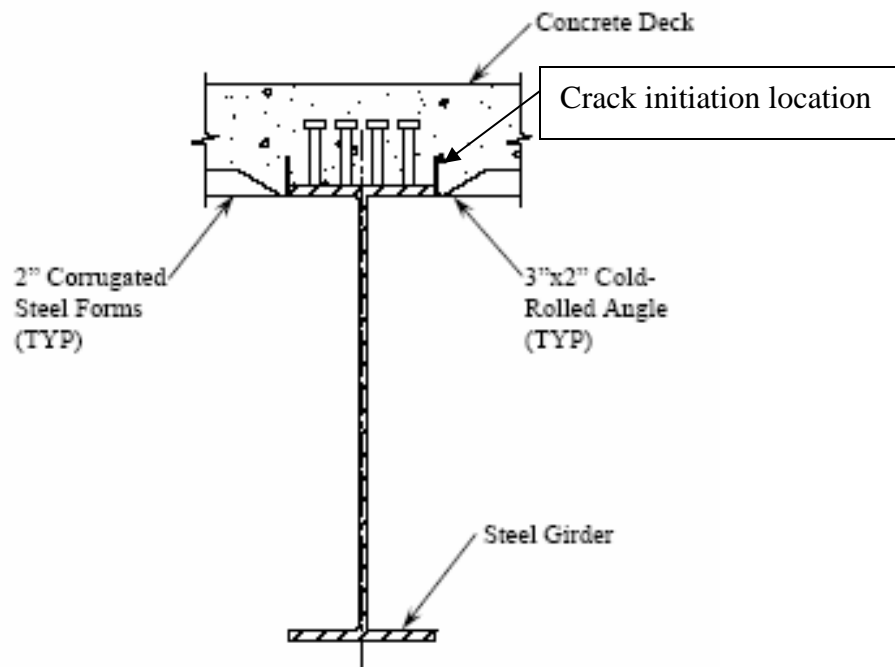
Figure 2.4. Angle Turned Upward into Deck (Frosch et al, 2003)

2.3 CODE REQUIREMENTS AND DESIGN SPECIFICATIONS

Due to the problems listed above, some engineers feel that the disadvantages of SIPMF outweigh the advantages. However, many of these problems can be corrected by implementing certain design specifications and code requirements. For example, to deal with the failure and collapse of the form during concrete placement, many states have implemented certain code requirements when using SIPMF. The state departments of transportation in Florida, Indiana, Kentucky, Massachusetts, Nebraska, North Carolina, and Virginia all state that the SIPMF must meet the requirements of ASTM A 653 and have G165 galvanizing. All the states listed above, except Florida and Kentucky, state the form material shall not be less than 20 gage (0.037 inch) (0.9398 mm) in thickness. Florida and Kentucky state the material shall not be less than 22 gage (0.0312 inch) (0.792 mm) in thickness. Certain design requirements also exist when using SIPMF. These requirements are all very similar from state to state. Listed below are the design requirements for the State of North Carolina's Department of Transportation:

1. Accommodate the dead load of the form, reinforcement and the plastic concrete, including the additional weight of the concrete due to the deflection of the metal forms, plus 50 pounds per square foot (0.002 MPa) for construction loads. Do not allow the unit working stress in the metal sheet to exceed 72.5% of the specified minimum yield strength of the material furnished nor 36 ksi (250 MPa).

2. Limit the horizontal leg of the support angle to 3 inches (76 mm). Design the support angle as a cantilever.

3. Limit the deflection under the weight of the forms, the plastic concrete and reinforcement to 1/180 of the form span or ½ inch (13mm) whichever is less; however, do not design for a total loading less than 120 pounds per square foot (0.006 MPa).

4. Base the permissible form camber on the actual dead load condition. Do not use camber to compensate for deflection in excess of the foregoing limits.

5. The design span of the form sheets is the clear distance between edges of beam or girder flanges minus 2 inches (50 mm) measured parallel to the form flutes. Design and provide form sheets with a length at least the design span of the forms.

6. Compute physical design properties in accordance with requirements of the American Iron and Steel Institute "Specification for the Design of Cold-Formed Steel Structural Members" latest published edition.

7. Provide a minimum concrete cover of 1.25 inches (32 mm) clear above metal stay-in-place form to the bottom mat of reinforcement.

8. Maintain the plan dimensions of both layers of primary deck reinforcement from the top of the concrete deck.

9. Do not weld to flanges in tension or to structural steel bridge elements fabricated from non-weldable grades of steel.

These design requirements are clearly stated to prevent a failure or collapse of the SIPMF. The code also requires extra caution when handling the SIPMF to prevent any denting of the forms. As stated previously, this is known to weaken the form, which in turn may lead to a failure.

The problem of corrosion can also be greatly reduced by implementing certain specification requirements. The SIPMF must have at least a G165 coating (as Ohio has a heavier

salt loading a G235 coating is more appropriate). This designation requires a galvanized coating to reduce the corrosion of the SIPMF. In areas where the galvanized coating has been damaged, or areas where the form has been cut, the contractor is required to clean, wire brush, and then paint the form with two coats of a galvanizing compound to reduce corrosion (North Carolina DOT, 2003). Corrosion of the SIPMF has also been attributed to certain admixtures present in the concrete. Because of this, many states do not allow concrete containing calcium chloride or any other admixture containing chloride salts. These chemicals have been shown to corrode the SIPMF (Frosch et al, 2003).

To deal with the fact that the bottom of the deck cannot be visually inspected, state departments of transportation have implemented a rigorous inspection procedure. It is required that the engineer observe all methods of construction to insure that the contractor is conforming to the code requirements. The engineer must inspect all phases of construction including the installation of the SIPMF, location and fastening of the reinforcement, composition of the concrete, mixing procedures, concrete placement and vibration, and finishing of the bridge deck (North Carolina DOT, 2003). It is noted in the specifications that if the engineer determines that the underside of the deck warrants inspection, a removal of at least one section of the SIPMF will take place. The engineer will also perform a test for soundness and bonding of the forms after the deck has been in place for a minimum of two days (North Carolina Department of Transportation). Once again, the engineer has the right to visually inspect the bottom of the deck if he has any reservations. These inspection procedures are necessary to insure that the SIPMF will perform as designed.

2.4 PREVIOUS WORK DONE IN THE FIELD OF STAY-IN-PLACE METAL FORMS

Engineers have mixed opinions about the use of SIPMF. To validate their use, research has been done on many of the "problem areas" associated with SIPMF. Helwig and Frank performed a study to measure the strength and shear stiffness of various bridge deck systems. Their study incorporated the use of a finite element program called ANSYS along with an experimental study. Their goal was to determine what strength and shear stiffness is required to adequately brace the girder. Their experimental study consisted of various deck systems composed of several different gage thicknesses. They concluded that when a SIPMF is

constructed with a gage thickness less than 22, the strength of the system is controlled by the tearing of the deck material at the corner screws. This was caused by a large deformation of the form, which in turn redistributed the force to the interior corner screws. Therefore, they concluded that when a thinner gage material is used, the strength of the system is controlled by the bearing capacity of the deck around the screw locations. From their tests on heavier gage material, 15 and 17 gage thickness, they concluded that the connection detail dominates the system. In these tests, the strength of the form was controlled by the fracture of the TEK screws, which are used to fasten the SIPMF to the support angles. In these tests, the fasteners between the deck and the support angle sheared off at the corners of the panels. Very little deformation was observed around the screws, which shows that the force was not being redistributed to the interior fasteners. This is one of the reasons why many states have a restriction when is comes to the minimum gage thickness that can be used when installing SIPMF.

The Indiana Department of Transportation, along with Purdue University, conducted a study to determine the contribution of SIPMF to formation of bridge deck cracking (Frosch, Robert J., David T. Blackman, and Roger D. Radabaugh).

Their research was broken down into five phases:

1. The first phase was a field evaluation of various bridge decks located throughout the state to investigate the scope of the problem.
2. The second phase was to instrument a typical bridge to investigate the behavior of transverse cracking.
3. The third phase was to conduct a laboratory investigation on the effects of shrinkage and restraint on a concrete bridge deck.
4. The fourth phase evaluated the effect of the formwork type on restrained shrinkage.
5. The final phase focused on the effect of reinforcement spacing and epoxy thickness on the formation of bridge deck cracks.

When the research was concluded, they listed their findings from each phase. Some important findings from each phase are listed below (Frosch et al, 2003):

1. Phase 1:
   1.1 The restraint of the deck due to SIPMF induced more transverse cracking.
2. Phase 2:

2.1 The valley in the SIPMF creates a shear key in the bottom of the deck
which may restrict the concrete during drying. This is believed to
initiate cracking in the deck.

2.2 Placing the leg of the angle in the deck to support the SIPMF leads to
discontinuity of the deck, which in turn leads to an area where cracks may
initiate.

3. Phase 3:

3.1 The primary cause of deck cracking is due to the restraint of concrete
by the SIPMF.

4. Phase 4:

4.1 SIPMF were found to significantly influence deck shrinkage due to the
sealing of the bottom surface.

5. Phase 5:

5.1 The width and spacing of the cracks was significantly affected by the
spacing of reinforcement, where as the epoxy coating thickness did not affect
the behavior.

From the results of their study, Frosch et al have concluded that alternatives to SIPMF should be considered. They have concluded that SIPMF induce more transverse cracking in the bridge deck, provide a location for cracks to initiate due to the shape of the pan, and prevent visual inspection of the bottom surface of the deck. They also suggest that the leg of angle be turned down to eliminate discontinuity of the bridge deck. This discontinuity is believed to lead to the formation of longitudinal cracks.

Previous research, including the research conducted by Purdue, states that the valleys of the SIPMF create a shear key in the bottom of the deck that restricts the concrete during drying. This is believed to lead to the formation of cracks. To eliminate this problem, Bakht, Mufti, and Tadros (2002) suggest placing a layer of foam between the SIPMF and the concrete. This would reduce the weight of the deck, while limiting the formation of cracks. The cracks would be limited because the concrete is not restrained by the valleys of the SIPMF. The foam is also expected to protect the SIPMF from chlorides and other material located in the concrete. This will lead to a more durable SIPMF. This approach was proven to be successful based on the tests conducted by Bakht, Mufti, and Tadros. They have concluded that the foam does not

weaken the deck. As a matter of fact, the New York Department of Transportation has adopted this approach (Bakht, Mufti, and Tadros, 2002). They no longer permit concrete to placed in the valleys of the SIPMF. These valleys are now filled with a foam material similar to the one proposed by Bakht, Mufti, and Tadros.

2.5 SIPMF NATIONWIDE SURVEY

The most extensive research performed on the performance of SIPMF was undertaken by Dr. Nabil Grace from Lawrence Technological University in conjunction with the Michigan Department of Transportation. Initially, Dr. Grace generated a survey composed of various questions regarding SIPMF and submitted it to all fifty states plus Washington D.C and Puerto Rico. The purpose of this survey was to address the following issues regarding the use of SIPMF (Grace and Hanson, 2002):

1. The policy of various states on the use of SIPMF.

2. Reasons for not allowing the use of SIPMF.

3. Number and status of bridge decks constructed with SIPMF.

4. The age of available SIPMF bridge decks.

5. Satisfaction of the performance of SIPMF.

6. Use of filling material in SIPMF corrugations.

7. Use of epoxy-coated reinforcement with SIPMF.

8. Methods and interval periods of inspection.

9. Types and causes of deterioration of deck slabs and corrosion of SIPMF.

10. Effect of joint leakage on SIPMF.

Thirty nine states responded to the survey, and twenty six of them allowed the use of SIPMF. Figure 2.5 shows which states allow the use of SIPMF (Grace and Hanson, 2002).
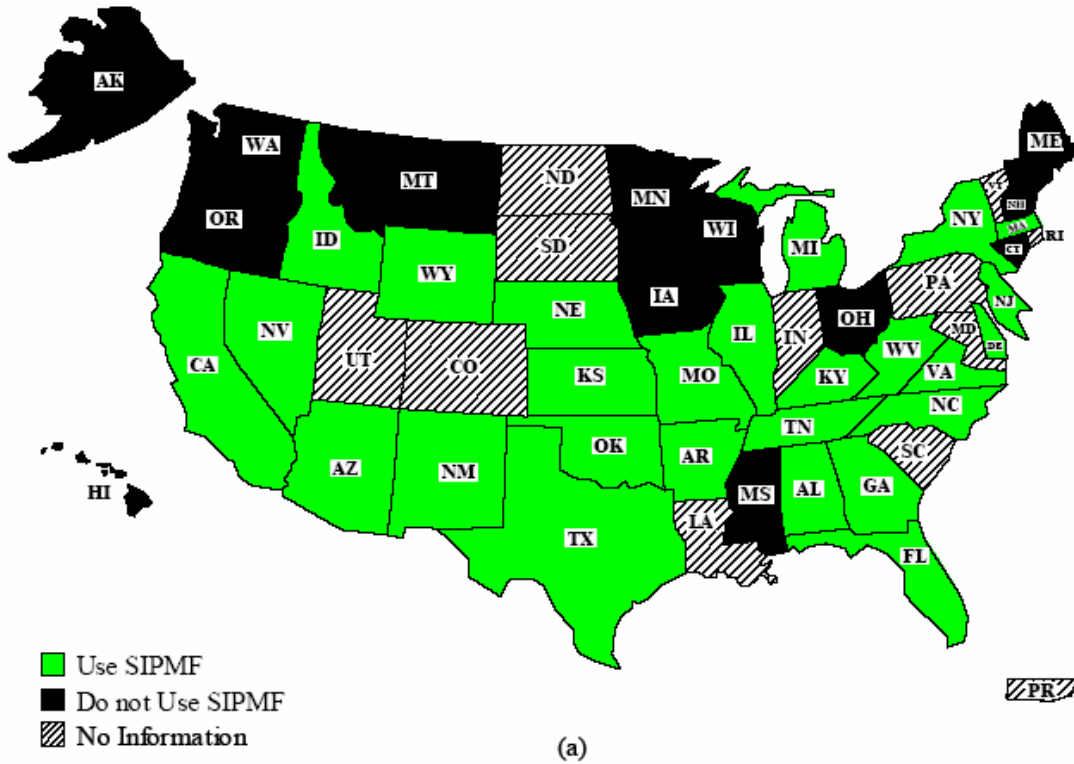
Figure 2.5. States Allowing SIPMF

From Figure 2.5, it is evident that the southern states feel more comfortable with the use of SIPMF. This can be attributed to the climatic conditions in the south. These states do not have to worry about the SIPMF corroding due to deicing chemicals used in the winter months or the problems caused by the freeze-thaw action on the bridge deck. Some of the states cited the problem of internal corrosion of the SIPMF due to the trapping of water and salt between the SIPMF and the concrete (Grace and Hanson, 2002).   Florida's attempts to prevent external corrosion by not allowing SIPMF on bridges that cross water.

When analyzing the survey results, a variety of reasons were listed for not allowing the use of SIPMF. The most cited concern was that the SIPMF interferes with the inspection of the

bottom of the bridge deck. This was stated by twelve of the thirteen states that do not allow the use of SIPMF. The engineers from these states were worried about the deck corroding from the bottom upwards. Another concern, mentioned by four states, is that the SIPMF may trap salt and water, accelerating the deterioration of the bridge deck. Figure 2.6 shows the concerns mentioned by each of the states that responded to the survey.

(a)
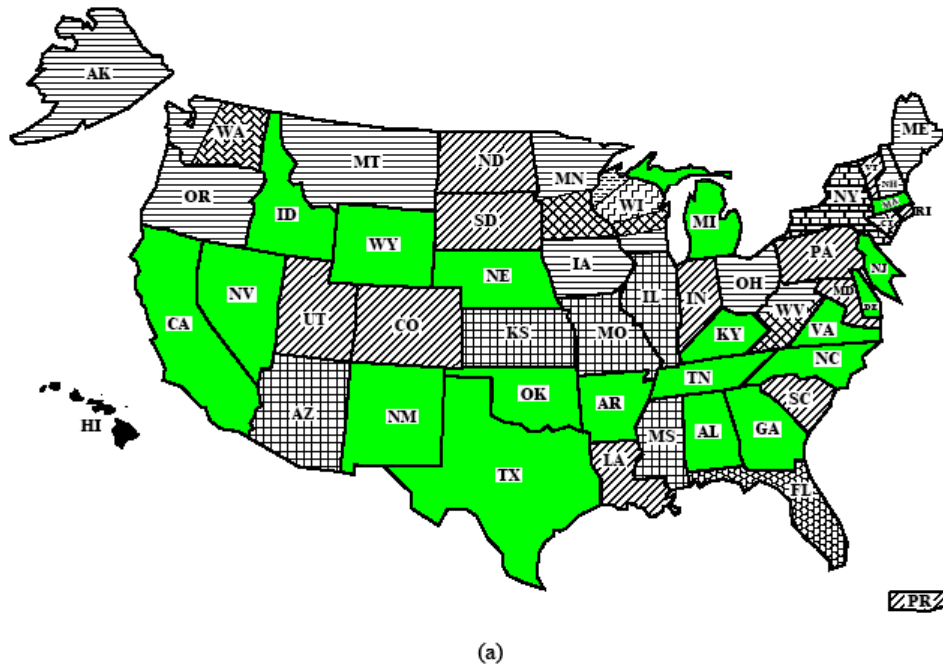
▤	SIPMF interferes with the inspection of bridge decks form underneath (12 states)
▓	Suspect that SIPMF may trap water and salt and so contribute to deck deterioration (4 states)
▦	SIPMF is allowed only on road crossings not on water crossings (Florida)
■	SIPMF unsightly when they start to corrode (Hawaii)
▦	SIPMF is not allowed at the bays where there is a closure pour (New York)
▓	Corrosion of SIPMF causes staining and objectionable aesthetics (Washington State)
▨	Tack welding to tension flange affects the growth of fatigue crack (Wisconsin)
▦	Water runs down the girder flange which causes deterioration to the girder itself (Wisconsin)
🟩	Permit the use of SIPMF
▦	Permit the use of SIPMF in special situation
▧	No Information

Figure 2.6. Reasons for Not Allowing SIPMF

The states that allow the use of SIPMF were asked if they were satisfied with the performance of SIPMF. Most of the states were either satisfied with the performance or took a neutral stance. The two states that were very dissatisfied with the performance of SIPMF were Ohio and Wisconsin. They felt SIPMF trapped water and salt accelerating the deterioration of the bridge deck. They also stated that they believe SIPMF led to the deterioration of the girder and led to the formation of fatigue cracks. Figure 2.7 provides a representation of how states feel about the performance of SIPMF. From this figure, it is also evident that the southern states are more satisfied with the performance of SIPMF. This can once again be attributed to climate in this region.

Figure 2.7. Performance of SIPMF

Drs. Grace and Hanson, also, conducted an extensive study examining bridges with and without SIPMF in Michigan. The finding was that in bridges with SIPMF and without SIPMF the deck concrete condition was not statistically different. This study also showed that the

freeze-thaw cycling did not cause damage to propagate in a beam with SIPMF (Grace and Hanson, 2004).

2.6 ALTERNATIVES TO STAY-IN-PLACE METAL FORMS

After concluding their research, many of the teams have proposed alternatives to SIPMF. To alleviate some of the concerns of SIPMF, the United Kingdom has proposed the use of "Omnia" planks and glass reinforced plastic panels (GRP) (Beales and Ives, 1990). "Omnia" planks, or precast concrete panels, are used in bridge deck construction in order to develop a composite action between the forms and the bridge deck. A few bridges in the United Kingdom were constructed using this method to determine the effect of "Omnia" planks. It was noted that bridges constructed using this method exhibited transverse and longitudinal cracks. From their initial inspection, Beales and Ives concluded that twenty percent of the planks showed signs of cracking. To determine the effects of "Omnia" planks, a study was conducted at Imperial College. This study showed that "Omnia" planks were able to withstand construction loads and the planks behaved compositely with the deck slab. However, the study also concluded that a possibility of fatigue failure is present when using this method. To eliminate this problem, careful inspection is needed. When studying the effect of GRP panels, it was noted that no deterioration of the panels occurred after ten million load cycles. The study also concluded that this method provides protection against corrosion since the use of steel is limited in this approach. However, careful consideration must be taken into account during the manufacturing process. It was noted that the manufacturing process was "unacceptable". It was deemed this way because the cover of the reinforcing steel was believed to be too small. To ensure that corrosion is not a problem, the research team suggested that the cover be increased.

Texas and Illinois have also proposed the use of precast concrete deck panels (Merrill 2002 and Volle 2002). They believe this method is superior to SIPMF. Texas suggests fabricating precast concrete panels four inches thick, leaving four inches of cast-in-place concrete (Merrill 2002). By using this method, only a single layer of reinforcing steel is needed. This allows the contractor to speed up construction, which in turn saves money, because SIPMF usually take several days or weeks to set and grade. The time required to tie the reinforcing steel is also cut in half because only one mat of steel is required, while two mats are needed when

constructing a deck using SIPMF. Precast concrete deck panels also provide an increase in safety compared to SIPMF. Instances have occurred in Texas were SIPMF have been blown off bridge decks due to high winds. Since the precast concrete panels typically weigh 3000 pounds (13.34 kN), this problem does not need to be considered. This increase in weight also eliminates the problem of collapse, which is sometimes noted when using SIPMF. These advantages, speed of construction, cost savings and safety, are the main reasons why these two states believe that precast concrete deck panels should be used rather that SIPMF. Figure 2.8 shows how a bridge deck is constructed using precast concrete deck panels (Merrill).
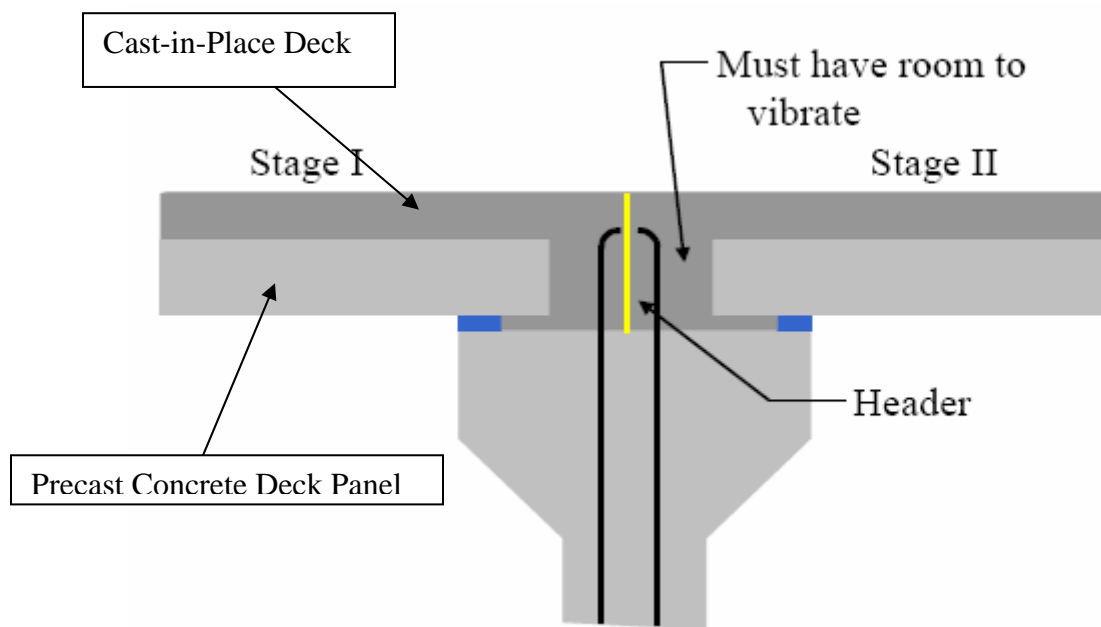
Figure 2.8. Precast Concrete Deck Panels

Although this method provides several advantages, some limitations do exist. The most significant problem associated with this method deals with the formation of longitudinal cracks (Merrill 2002). The formation of longitudinal cracks is associated with the fact that the use precast concrete deck panels result in a reduction of deck stiffness over the girders. Transverse cracking has also been noted when precast concrete deck panels are used. This problem is attributed to the fact that the bottom of the deck is restrained to shrink due to the panels. However, since these problems are also present when using SIPMF, these two states feel that precast concrete deck panels provide a more practical option when constructing a bridge deck.

Chapter 3: Visual Inspection

The goal of the research team was to successfully evaluate the use of SIPMF as a viable option in the construction of a concrete bridge deck. In order to feel confident about our findings, the research team conducted a literature review in order to address the problems that arose in the past with SIPMF. To formulate our own judgment, core samples were extracted from the three bridges identified by ODOT. As mentioned previously, these core samples where either tested for compression, permeability, chloride ion or ultrasound wave velocity.   The research team chose to evaluate SIPMF by comparing the results from cores taken in deck areas with SIPMF with the cores taken from areas where no SIPMF were present.

The first step of the comparison process involved visually inspecting all the core samples after they were extracted from the three bridges. To evaluate the core samples, a visual inspection index was created. This index consisted of:

1. The condition of the reinforcing steel.
2. The porosity of the concrete and aggregate.
3. Honeycombing present in the core.
4. Cracks present in the core.
5. Voids present in the core.

The goal of this index was to determine the overall condition of each individual core and general characteristics of each core after it had been extracted from the bridge. The reinforcing steel was inspected for the presence rust. The concrete, on the other hand, was inspected for the quantity and size of cracks; quantity and size of voids; quantity and size of honeycombing; and porosity of aggregate and cement paste.

Each core was inspected for the five quantities listed above. A rating system was created to evaluate these five observed quantities by assigning each quantity a number ranging from zero to five. A rating of zero meant the core was in bad condition for the quantity observed, while a rating of five meant the core sample was in good condition. After each observed quantity was rated, the condition of the core was represented by taking an average of all five areas. Next, a rating for the area with SIPMF and the areas without SIPMF were calculated by taking an average of the core samples from each quantity. Then, the averages for the quantities of SIPMF and non-SIPMF were compared to each other to see the effect of SIPMF. Table 3.1 summarizes

the results of the visual inspection procedure. The results of the visual inspection for individual cores from each bridge are given in tables 3.2 –3.7.

Table 3.1. Summary of Visual Inspection Index

Bridge	No SIPMF	SIPMF	No SIPMF > SIPMF by
LOR-57-18.18	69	66	4.4%
OTT-2-28.41	70	68	2.7%
LAK-90-23.42	66	65	1.5%
All Three Bridges	68	66	2.9%

The visual inspection index shows that little difference exists between areas of SIPMF and areas where the deck was formed by the conventional plywood forming method.   During the visual inspection, it was found that many of the core samples that performed poorly on the visual inspection index came from areas near expansion joints, scuppers, or areas where an edge of the SIPMF was exposed. This allowed water to remain in prolonged contact with the SIPMF causing corrosion of the SIPMF and subsequent damage to the concrete.

Table 3.2. LOR-57-18.18 Visual Inspection of Cores from Areas of No SIPMF

Bridge	Core	Steel	Concrete											
			Porosity		Honeycombing		Cracks		Voids				
		Rust Condition	*Concrete*	*Aggregate*	*Quantity*	*Size*	*Quantity*	*Size*	*Quantity*	*Size*	Σ	*Normalized to 100*	*Normalized No SIPMF Average*
	Max	5	5	5	5	5	5	5	5	5	45		
LOR-57-18.18	S1	0	1	2	2	1	2	0	2	3	13	29	
	1D	3	3	3	4	4	4	4	4	4	33	73	
	1E	5	3	4	4	4	4	4	3	4	35	78	69
	8B	5	5	4	3	3	4	4	4	4	36	80	
	8C1	4	4	4	4	4	4	4	3	3	34	76	
	8D	5	4	4	4	4	4	4	3	4	36	80	

Table 3.3. LOR-57-18.18 Visual Inspection of Cores from Areas of SIPMF

Bridge	Core	Steel	Concrete											Normalized SIPMF Average
				Porosity		Honeycombing		Cracks		Voids				
		Rust Condition	Concrete	Aggregate	Quantity	Size	Quantity	Size	Quantity	Size	Σ	Normalized to 100		
	Max	5	5	5	5	5	5	5	5	5	45		
LOR-57-18.18	S2	1	2	2	2	1	2	2	3	3	18	40	
	2B	4	3	3	3	3	3	2	3	3	27	60	
	2C	3	3	3	3	3	3	2	3	3	26	58	
	2D1	5	4	4	4	4	4	4	4	4	37	82	
	2D2	5	4	4	5	5	5	5	4	4	41	91	
	2D3	5	4	4	4	4	4	4	4	3	36	80	
	2E	4	3	4	4	4	4	4	4	3	34	76	
	2F	2	3	3	4	4	3	2	3	3	27	60	
	3C	1	3	3	3	3	3	2	3	2	23	51	
	3F	2	4	3	3	3	3	2	3	2	25	56	
	4C1	5	4	4	4	4	4	4	4	4	37	82	
	4E	3	2	4	4	4	4	2	3	3	29	64	
	4F	3	4	2	2	2	1	1	1	1	17	38	66
	5B	5	4	4	4	4	4	4	3	3	35	78	
	5C	3	4	4	4	4	4	4	2	2	31	69	
	5D	4	4	4	4	4	4	4	3	3	34	76	
	5E	5	4	4	4	4	4	4	3	3	35	78	
	6D	4	4	4	4	4	4	4	3	3	34	76	
	6E	3	3	3	3	3	4	4	3	2	28	62	
	7B	3	2	2	3	3	3	3	3	3	25	56	
	7C	2	3	3	3	3	3	2	3	3	25	56	
	7C1	3	3	3	3	3	3	2	3	2	25	56	
	7C1(2)	5	4	4	4	4	4	4	4	3	36	80	
	7E	3	4	4	3	2	4	4	3	3	30	67	

Table 3.4. OTT-2-28.41 Visual Inspection of Cores from Areas of No SIPMF

Bridge	Core	Steel	Concrete											
					Porosity		Honeycombing		Cracks		Voids				
		Rust Condition	Concrete	Aggregate	Quantity	Size	Quantity	Size	Quantity	Size	Σ	Normalized to 100	Normalized No SIPMF Average
	Max	5	5	5	5	5	5	5	5	5	45		
OTT-2-28.41	A2	4	4	4	3	3	4	4	3	3	32	71	
	A3	5	4	4	4	4	4	4	3	3	35	78	
	A4	4	4	4	4	3	4	4	3	3	33	73	
	A6	4	4	4	4	4	4	4	3	3	34	76	
	A7	5	4	4	4	4	4	4	3	3	35	78	
	A8	4	4	4	4	4	4	4	3	3	34	76	70
	A10	2	3	3	3	3	3	2	3	2	24	53	
	A12	5	3	3	3	3	4	4	3	3	31	69	
	A13	4	3	3	4	4	3	2	3	3	29	64	
	A14	4	3	3	3	3	4	4	3	3	30	67	
	A15	3	3	3	3	3	4	4	3	3	29	64	

Table 3.5. OTT-2-28.41 Visual Inspection of Cores from Areas of SIPMF

Bridge	Core	Steel	Concrete											
				Porosity		Honeycombing		Cracks		Voids				
		Rust Condition	Concrete	Aggregate	Quantity	Size	Quantity	Size	Quantity	Size	Σ	Normalized to 100	Normalized SIPMF Average
	Max	5	5	5	5	5	5	5	5	5	45		
OTT-2-28.41	B2	4	4	4	4	4	4	4	3	4	35	78	68
	B3	3	3	3	4	4	3	2	4	4	30	67	
	B6	4	4	4	4	4	4	4	4	3	35	78	
	B7	4	3	3	3	3	3	2	4	3	28	62	
	C1	2	3	3	4	4	3	3	3	3	28	62	
	C2	2	3	3	3	3	3	2	3	3	25	56	
	C4	4	4	4	4	4	3	3	3	3	32	71	
	C5	2	3	3	3	3	3	2	4	4	27	60	
	C6	4	3	3	4	4	4	4	3	3	32	71	
	C8	4	4	4	4	4	4	4	3	3	34	76	

Table 3.6. LAK-90-23.42 Visual Inspection of Cores from Areas of No SIPMF

Bridge	Core	Steel	Concrete											
			Porosity		Honeycombing		Cracks		Voids				
		Rust Condition	Concrete	Aggregate	Quantity	Size	Quantity	Size	Quantity	Size	Σ	Normalized to 100	Normalized No SIPMF Average
	Max	5	5	5	5	5	5	5	5	5	45		
LAK-90-23.42	L21	2	3	3	4	4	4	4	3	3	30	67	
	L22	4	3	3	4	4	4	4	3	3	32	71	
	L25	4	4	4	4	4	4	4	4	3	35	78	
	L27	3	3	3	3	3	3	2	3	3	26	58	
	L29	4	4	4	4	4	4	4	4	3	35	78	
	L30	2	4	4	4	4	3	2	4	3	30	67	66
	L32	4	4	4	4	4	4	4	4	3	35	78	
	L33	3	4	4	4	4	4	4	3	2	32	71	
	L34	1	3	3	3	3	3	2	4	3	25	56	
	L35	2	3	3	3	3	3	2	3	3	25	56	
	L36	2	3	3	3	3	3	2	2	2	23	51	

Table 3.7. LAK-90-23.42 Visual Inspection of Cores from Areas of SIPMF

Bridge	Core	Steel	Concrete										
			Porosity		Honeycombing		Cracks		Voids				
		Rust Condition	*Concrete*	*Aggregate*	*Quantity*	*Size*	*Quantity*	*Size*	*Quantity*	*Size*	*Σ*	*Normalized to 100*	*Normalized SIPMF Average*
	Max	5	5	5	5	5	5	5	5	5	45		
LAK-90-23.42	L1	2	3	3	3	3	4	4	3	4	29	64	
	L2	3	3	3	3	3	4	4	4	3	30	67	
	L4	4	3	3	3	3	2	2	3	3	26	58	
	L5	4	4	4	4	4	4	4	3	2	33	73	
	L7	4	4	4	4	4	4	4	3	3	34	76	
	L9	3	3	3	3	3	4	4	3	3	29	64	65
	L11	1	3	3	2	1	3	2	2	3	20	44	
	L13	2	3	3	3	3	4	4	3	3	28	62	
	L14	4	4	4	4	4	4	4	3	3	34	76	
	L15	3	3	3	3	3	3	2	3	3	26	58	
	L16	4	4	4	4	4	4	4	3	3	34	76	

Chapter 4: Compressive Tests

The condition of a bridge deck is usually indicated by the compressive strength of the concrete. In order to evaluate the condition of the bridge decks, the research team performed compression tests in accordance to AASHTO T22-97. Core samples were extracted from areas where there were SIPMF and areas where there were no SIPMF. The compression tests were performed at the University of Toledo using a 400,000 pound (1.8 mN) capacity compression machine manufactured by Tinius Olsen. A picture of the compression machine is shown in Figure 4.1.

Figure 4.1. Tinius Olsen Compression Machine

After the cores were extracted, the wearing surface and overlay were removed to provide a sample consisting of the original concrete used to cast the deck. The samples were then measured to determine their dimensions. The diameter of the cylinders was measured using a caliper. To determine the mean diameter, two measurements were performed at right angles to each other at the mid-height of the specimen. An average of these two measurements was taken to get the mean diameter of the specimen. The lengths of the specimens were also measured to

see if a correction factor needed to be applied. Once the dimensions were known, the cylinders were capped and cured according to AASHTO specifications. These cores were then tested in the Tinius Olsen Compression Machine. To calculate the compressive strength of the samples, the maximum load supplied by the compression machine was divided by the cross-sectional area. According to the AASHTO specification, a correction factor then needs to be incorporated into the results if the length-to-diameter ratio is less than 1.8.

The compression tests on LOR-57-18.18 indicated that the average compressive strength was 7,520 psi (51.8 mPa). This value was found by taking an average of the compressive strengths from both the two-inch (51 mm) diameter cores and the four-inch (102 mm) diameter cores. The two-inch (51 mm) cores were taken to provide a sampling without the presence of reinforcing steel. A correction factor was then applied to these test results as indicated in the AASHTO specification. The four-inch (102 mm) cores were sliced in order to eliminate the reinforcing steel from the sample. Using the test results, an average modulus of elasticity was found by using the formula $57,000\sqrt{f'c}$. The modulus of elasticity was determined to find the stress required to produce a given strain. The modulus of elasticity is important from a serviceability standpoint. The average modulus of elasticity for LOR-57-18.18 was 4.94×10^6 psi $(3.41\times10^4$ mPa). The test results also indicated that the average compressive strength for the samples taken in areas where SIPMF were present was 7,680 psi (53.0 mPa). This corresponds to an average modulus of elasticity of 4.99×10^6 psi $(3.44\times10^4$ mPa). In areas where no SIPMF were present, the average compressive strength was 7,160 psi (49.4 mPa). This corresponds to an average modulus of elasticity of 4.82×10^6 psi $(3.32\times10^4$ mPa). Most specimens failed due to columnar fracture (fracture type e, per AASHTO specification).

The test results on OTT-2-28.41 yielded an average compressive strength lower than that of LOR-57-18.18. The average compressive strength of the bridge deck was 6,330 psi (43.6 mPa), which corresponds to an average modulus of elasticity of 4.53×10^6 psi $(3.12\times10^4$ mPa). In areas where SIPMF were present, the average compressive strength was 6,370 psi (43.9 mPa). This in turn yields an average modulus of elasticity of 4.54×10^6 psi $(3.13\times10^4$ mPa). In areas where no SIPMF were present, the average compressive strength was 6,300 psi (43.4 mPa). This corresponds to an average modulus of elasticity of 4.51×10^6 psi $(3.11\times10^4$ mPa). These specimens also failed mostly due to columnar fracture (fracture type e, per the AASHTO

specification). However, a few failed due to a cone and shear fracture (fracture type c, per the AASHTO specification).

The test results on LAK-90-23.42 indicated that average compressive strength was higher than OTT-2-28.41, but lower than LOR-57-18.18. The average compressive strength was 7,000 psi (48.3 mPa). This in turn leads to an average modulus of elasticity of 4.77×10^6 psi (3.29×10^4 mPa). The samples extracted from areas where SIPMF were present yielded an average compressive strength of 6,920 psi (47.7 mPa). This corresponds to an average modulus of elasticity of 4.74×10^6 psi (3.27×10^4 mPa). In areas where no SIPMF were present, the average compressive strength was 7,200 psi (49.6 mPa). This corresponds to an average modulus of elasticity of 4.81×10^6 psi (3.32×10^4 mPa). All the specimens from this sampling failed due to a columnar fracture (fracture type e, per AASHTO specification). Table 4.1 summarizes the compression test results. The complete test results are presented in Tables 4.2 and 4.3.

Table 4.1: Summary of Compression Test Results
(psi = 6.90 kPa 10^6 psi = 6.90 mPa)

	Average Whole Bridge			SIPMF			No SIPMF		
	Strength (Psi)	Standard Deviation (Psi)	E (10^6 Psi)	Strength (Psi)	Standard Deviation (Psi)	E (10^6 Psi)	Strength (Psi)	Standard Deviation (Psi)	E (10^6 Psi)
LOR-57-18.18	7520	808	4.94	7680	733	4.99	7160	995	4.82
OTT-2-28.41	6330	842	4.53	6370	687	4.54	6300	971	4.51
LAK-90-23.42	7000	623	4.77	6920	482	4.74	7200	757	4.81

Table 4.2: Compression Test Results - 2" Cores

(Psi = 6.90 kPa 10^6 psi = 6.90 mPa)

2" Cores Core # OTT	Test Length (Inches)	Test Diameter (Inches)	Area (in²)	Core Weight (Lbs)	Core Density (Lbs/yd³)	Correction Factor (< 1.8D = 3.15)	Load (Lbs)	Adjusted Load (Lbs)	Strength (Psi)	Strength (Psi)	Fracture Type	Modulus of Elasticity (Psi)
A 17-1	3.12	1.75	2.41	0.57	3563.65	0.9930	15610	15501	6444	6440	c	4.574E+06
A 17	3.25	1.75	2.41	0.62	3684.26	1.0000	18920	18920	7866	7870	c	5.057E+06
A 18-1	3.18	1.75	2.41	0.60	3630.88	1.0000	15510	15510	6448	6450	e	4.578E+06
A 18	3.50	1.75	2.41	0.65	3604.37	1.0000	18700	18700	7775	7770	e	5.024E+06
B 9	3.25	1.75	2.41	0.60	3605.31	1.0000	17130	17130	7122	7120	e	4.810E+06
B 8	3.50	1.75	2.41	0.64	3555.50	1.0000	15720	15720	6536	6540	e	4.610E+06
C 10-1	3.25	1.75	2.41	0.62	3697.42	1.0000	17170	17170	7138	7140	e	4.816E+06
C 10	3.37	1.75	2.41	0.63	3616.52	1.0000	14660	14660	6095	6090	d	4.448E+06
C 9-1	3.43	1.75	2.41	0.62	3490.92	1.0000	14210	14210	5908	5910	e	4.382E+06
C 9	NA	NA	NA	NA	NA	NA		NA	NA		
LOR				Average	3605.43			Average	6815	6810		4.704E+06
2-2"	3.37	1.75	2.41	0.56	3248.52	1.0000	19220	19220	7991	7990	e	5.095E+06
2-2" (1)	3.00	1.75	2.41	0.53	3406.85	0.9770	19240	18797	7815	7820	e	5.041E+06
3-2"	3.06	1.75	2.41	0.54	3395.94	0.9800	21320	20894	8687	8690	e	5.314E+06
3-2" (1)	2.87	1.75	2.41	0.41	2756.55	0.9710	18410	17876	7432	7430	e	4.913E+06
4-2"	3.43	1.75	2.41	0.60	3366.24	1.0000	17270	17270	7180	7180	e	4.830E+06
5-2"	3.37	1.75	2.41	0.60	3426.18	1.0000	18550	18550	7712	7710	e	5.005E+06
7-2"	3.37	1.75	2.41	0.60	3451.55	1.0000	17720	17720	7367	7370	e	4.893E+06
8-2"	3.50	1.75	2.41	0.62	3408.88	1.0000	14790	14790	6149	6150	b	4.470E+06
8-2" (1)	3.37	1.75	2.41	0.61	3502.31	1.0000	20520	20520	8531	8530	e	5.264E+06
LAK				Average	3329.23			Average	7652	7650		4.985E+06
L17	3.69	1.75	2.41	0.67	3534.67	1.0000	17140	17140	7126	7130	e	4.813E+06
L18	3.63	1.75	2.41	0.64	3416.39	0.9604	15960	15328	6373	6370	e	4.549E+06
L19	2.38	1.75	2.41	0.42	3413.91	0.9425	15950	15033	6250	6250	e	4.506E+06
L20	2.50	1.75	2.41	0.45	3506.63	0.9512	17240	16399	6818	6820	e	4.707E+06
				Average	3467.90			Average	6642	6640		4.645E+06

Note: 2-2" & 2-2" (1), 3-2" & 3-2" (1), 8-2" & 8-2" (1) from same cores. (1) denotes bottom half

Table 4.3: Compression Test Results - 4" Cores

$(Psi = 6.90 \text{ kPa} \qquad 10^6 \text{ psi} = 6.90 \text{ mPa})$

4" Cores Core #	Test Length	Test Diameter	Area	Core Weight	Core Density	Correction Factor	Load	Adjusted Load	Strength	Strength	Fracture Type	Modulus of Elasticity
OTT	(Inches)	(Inches)	(in²)	(Lbs)	(Lbs/yd³)	(< 1.8D = 7.07)	(Lbs)	(Lbs)	(Psi)	(Psi)		(Psi)
A 7	4.56	3.93	12.13	4.10	3458.21	0.9082	80300	72928	6012	6010	e	4.419E+06
A 7 (1)	4.44	3.93	12.13	4.30	3724.93	0.9010	73100	65863	5430	5430	e	4.200E+06
A 12	4.44	3.93	12.13	3.90	3378.42	0.9010	68200	61448	5066	5070	e	4.059E+06
A 12 (1)	4.25	3.93	12.13	3.90	3529.46	0.8858	77100	68295	5630	5630	e	4.277E+06
A 13	6.00	3.93	12.13	5.55	3557.74	0.9622	76000	73127	6028	6030	e	4.426E+06
B 2	5.63	3.93	12.13	5.40	3689.08	0.9518	69200	65865	5430	5430	e	4.200E+06
LOR				Average	3556.31			Average	5599	5600		4.265E+06
1E	7.32	3.93	12.13	7.00	3678.07	1.0000	83800	83800	6908	6910	e	4.738E+06
2D3	6.75	3.93	12.13	6.20	3532.81	0.9766	110400	107817	8888	8890	e	5.374E+06
4C1	5.88	3.93	12.13	5.70	3728.46	0.9588	99200	95113	7841	7840	e	5.047E+06
5E	7.13	3.93	12.13	6.50	3506.36	1.0000	90200	90200	7436	7440	e	4.917E+06
5D	4.56	3.93	12.13	4.05	3416.04	0.9082	82400	74836	6169	6170	e	4.477E+06
8D	7.63	3.93	12.13	7.10	3579.04	1.0000	85700	85700	7065	7060	e	4.789E+06
LAK				Average	3573.46			Average	7385	7380		4.897E+06
L1	4.00	3.93	12.13	3.90	3750.05	0.8742	92900	81213	6695	6700	e	4.666E+06
L5	4.00	3.93	12.13	4.00	3846.21	0.8742	103600	90567	7466	7470	e	4.926E+06
L25	4.81	3.93	12.13	4.80	3838.21	0.9228	102500	94587	7798	7800	e	5.034E+06
L29	5.31	3.93	12.13	5.25	3802.75	0.9422	103800	97800	8062	8060	e	5.117E+06
L32	4.50	3.93	12.13	4.30	3675.26	0.9044	91200	82481	6800	6800	e	4.700E+06
				Average	3782.50			Average	7364	7360		4.890E+06

Average Strength of Bridges:

Bridge	Average Strength
	(psi)
OTT-2-28.41	6205
LOR-57-18.18	7515
LAK-90-23.42	7000

Average Unit Weight:

Bridge	Average Weight
	(Lbs/yd³)
OTT-2-28.41	3580.87
LOR-57-18.18	3451.34
LAK-90-23.42	3625.20

Chapter 5: Chloride Ion Test

One of the major problems leading to deterioration of bridge decks is the penetration of chlorides. When chlorides penetrate the concrete and migrate to the reinforcement, they cause corrosion and subsequent damage to the concrete bridge deck. The permeability test was undertaken to determine the rate of entry of moisture. However, a chloride analysis needs to be performed to evaluate the chloride ion concentration at different levels throughout the bridge deck. These two tests, along with the compression and ultrasound tests, allowed the research team to evaluate the durability of concrete, in areas of SIPMF, with great confidence.

The amount of chloride ion concentration is dependent on a variety of different factors. One of the obvious factors leading to high chloride ion concentration deals with the amount of cracking of the bridge deck. The cracks provide a direct route for water and chlorides to enter the deck and damage the concrete and reinforcing steel. Frosch, Blackman, and Radabaugh (2003) have stated that cracks wider than 0.007 inches (0.2 mm) lead to the ingress of chlorides. Another factor that affects the chloride ion concentration is scaling. Scaling occurs when the surface of the concrete begins to flake. This problem is magnified when the concrete is subjected to freeze-thaw action (Babaei 1982). The scaling of the bridge deck provides the chlorides, deposited during deicing, a direct route to enter the bridge deck. This has been shown to accelerate the deterioration of the reinforcing steel (Babaei 1982). Though cracking and scaling are seen to be major problems in bridge deck deterioration, spalling has been shown to lead to the most significant damage. Spalling is the result of the separation and removal of the surface level concrete. It is caused by the corrosion of the reinforcing steel located in the bridge deck. Once spalling occurs, it is difficult to stop the corrosion process since the reinforcement has begun to corrode and the concrete above the reinforcing steel has shown to have a high level of chloride ion concentration (Babaei 1982). This in turn leads to delamination and the formation of cracks, which only accelerates the deterioration of the bridge deck due to the high levels of chlorides. Lastly, the quantity of coarse aggregate in a bridge deck will affect the chloride ion concentration. This is because the chlorides are usually contained in the mortar phase (Babaei 1982).

To determine the ingress of chlorides throughout the bridge decks in our study, the research team chose to perform a chloride ion test in accordance to AASHTO T260-97. Four samples were extracted from each core at two-inch increments in order to determine the chloride

ion content in various locations of the bridge deck. This test involves using rotary type impact drill to obtain at least ten grams of pulverized concrete located at least a half an inch inside the core. These ten grams must pass through a number 50 sieve (0.300 mm) to be used in the test. After the ten grams were retrieved, the researchers proceeded to analyze the chloride ion concentration following the water soluble chloride ion content procedure in the AASHTO specification

In order to verify the test results, the research team tested a NIST reference standard. The standard reference material 1887a contains 0.0104 +/- 0.0007 % chloride. This standard was tested in the same way as the samples from our study to determine if our testing method was accurate. After performing the titration on the reference standard, it was determined that our test was accurate due to the fact that we were able to obtain a chloride ion concentration that fell between the limits listed on the NIST standard. The test results for the NIST standard sample are shown in Table 5.1.

Table 5.1: NIST Standard Test Result

Total Weight (grams)	Paper Weight (grams)	Concrete Weight (grams)	Endpoint (ml)	% Cl	NaCl Sol. 0.010132	AgNO₃ 0.0105
						0.0101
3.4639	0.4338	3.0301	4.9	0.010487		

NIST: 0.0104 +/- 0.0007

AgNO₃	mv	d mL	d mV	d mV/dmL	2nd Derivative
0.00	239.40				
1.20	246.50	1.20	7.10	5.92	
2.20	254.60	1.00	8.10	8.10	2.18
3.30	267.60	1.10	13.00	11.82	3.72
3.50	271.80	0.20	4.20	21.00	9.18
3.70	276.50	0.20	4.70	23.50	2.50
3.90	281.40	0.20	4.90	24.50	1.00
4.10	288.90	0.20	7.50	37.50	13.00
4.30	297.60	0.20	8.70	43.50	6.00
4.50	308.10	0.20	10.50	52.50	9.00
4.70	319.50	0.20	11.40	57.00	4.50
4.90	333.10	0.20	13.60	68.00	11.00
5.10	340.70	0.20	7.60	38.00	-30.00
5.30	348.60	0.20	7.90	39.50	1.50
5.50	355.10	0.20	6.50	32.50	-7.00
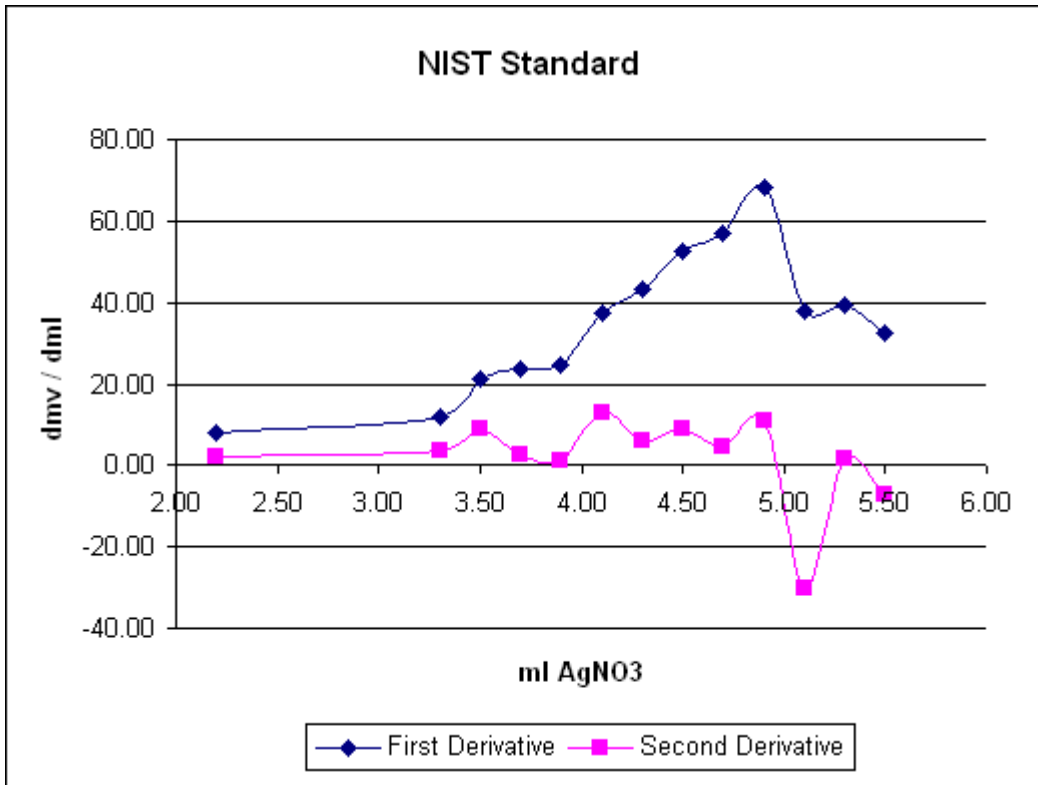
The test results showed that LOR-57-18.18 had the lowest level of chloride ion content. The average chloride ion content for the bridge was 1.52 pounds of chlorine per cubic yard (8.84 N/m^3). In areas of SIPMF, the average chloride ion content was 1.38 pounds of chlorine per cubic yard (8.03 N/m^3), compared to an average of 1.99 pounds of chlorine per cubic yard (11.58 N/m^3) in areas where no SIPMF were present. The complete test results for LOR-57-18.18 are in Table 5.2.

OTT-2-28.41 had an average chloride ion content of 2.34 pounds of chlorine per cubic yard (13.62 N/m^3). The average chloride ion content was 2.54 pounds of chlorine per cubic yard (14.78 N/m^3) in areas of SIPMF and 2.10 pounds of chlorine per cubic yard (12.22 N/m^3) in areas where no SIPMF were present. The complete test results for OTT-2-28.41 are in Table 5.3.

LAK-90-23.42 had the highest level of chloride ion content. The research team expected this outcome because LAK-90-23.42 is exposed to more deicing salt than the other two bridges. The average chloride ion content for this bridge was 3.86 pounds of chlorine per cubic yard (22.47 N/m^3). In areas of SIPMF, the average chloride ion content was 3.12 pounds of chlorine per cubic yard (18.16 N/m^3), compared to an average of 4.61 pounds of chlorine per cubic yard (26.83 N/m^3) in areas where no SIPMF were present. The complete test results for LAK-90-23.42 are in Table 5.4.

Table 5.2: LOR-57-18.18 Chloride Ion Test Results

NaCl Sol.	AgNO$_3$	Vol NaCL		Unit Weight		
0.01013176	0.0105	4.00		LAK	OTT	LOR
	0.0101			3625.2	3580.87	3451.34

Sample	Total Weight (grams)	Paper Weight (grams)	Concrete Weight (grams)	Endpoint (ml)	% Cl	Lbs Cl / yd^3
S1 1	*3.4781*	*0.4401*	*3.0380*	*8.0*	*0.0470*	*1.62*
S1 2	*3.4845*	*0.4360*	*3.0485*	*6.5*	*0.0292*	*1.01*
S1 3	*3.5063*	*0.4342*	*3.0721*	*8.6*	*0.0535*	*1.85*
S1 4	*3.4606*	*0.4426*	*3.0180*	*6.3*	*0.0271*	*0.94*
S2 1	3.4526	0.4353	3.0173	9.8	0.0733	2.53
S2 2	3.4582	0.4371	3.0211	7.4	0.0436	1.51
S2 3	3.4381	0.4354	3.0027	7.5	0.0451	1.56
S2 4	3.4426	0.4371	3.0055	9.4	0.0686	2.37
2B 1	3.4385	0.4352	3.0033	6.4	0.0315	1.09
2B 2	3.4405	0.4335	3.0070	4.6	0.0092	0.32
2B 3	3.4859	0.4398	3.0461	5.8	0.0237	0.82
2B 4	3.5312	0.4451	3.0861	4.3	0.0053	0.18
2F 1	*3.4926*	*0.4533*	*3.0393*	*6.8*	*0.0328*	*1.13*
2F 2	*3.5223*	*0.4474*	*3.0749*	*6.6*	*0.0301*	*1.04*
2F 3	*3.4990*	*0.4455*	*3.0535*	*5.1*	*0.0128*	*0.44*
2F 4	*3.5387*	*0.4424*	*3.0963*	*4.8*	*0.0091*	*0.31*
3C 1	*3.4713*	*0.4265*	*3.0448*	*7.9*	*0.0457*	*1.58*
3C 2	*3.5160*	*0.4301*	*3.0859*	*6.9*	*0.0335*	*1.16*
3C 3	*3.5057*	*0.4389*	*3.0668*	*5.8*	*0.0209*	*0.72*
3C 4	*3.4652*	*0.4442*	*3.0210*	*5.3*	*0.0153*	*0.53*
3F 1	*3.4965*	*0.4540*	*3.0425*	*7.8*	*0.0446*	*1.54*
3F 2	*3.4718*	*0.4542*	*3.0176*	*7.3*	*0.0390*	*1.35*
3F 3	*3.4746*	*0.4471*	*3.0275*	*5.4*	*0.0164*	*0.57*
3F 4	*3.5031*	*0.4390*	*3.0641*	*5.1*	*0.0127*	*0.44*
4F 1	*3.4658*	*0.4468*	*3.0190*	*8.7*	*0.0556*	*1.92*
4F 2	*3.4781*	*0.4452*	*3.0329*	*5.4*	*0.0164*	*0.57*
4F 3	*3.4852*	*0.4503*	*3.0349*	*4.9*	*0.0105*	*0.36*
4F 4	*3.4526*	*0.4479*	*3.0047*	*4.8*	*0.0094*	*0.32*
5C 1	3.4850	0.4396	3.0454	6.0	0.0262	0.90
5C 2	3.4952	0.4356	3.0596	5.2	0.0163	0.56
5C 3	3.4765	0.4389	3.0376	5.1	0.0152	0.52
5C 4	3.4502	0.4403	3.0099	5.0	0.0141	0.49
6E 1	3.4852	0.4356	3.0496	14.0	0.1238	4.27
6E 2	3.4952	0.4389	3.0563	10.8	0.0845	2.92
6E 3	3.4952	0.4425	3.0527	7.0	0.0383	1.32
6E 4	3.4725	0.4369	3.0356	6.2	0.0287	0.99
7B 1	3.5120	0.4389	3.0731	13.5	0.1168	4.03
7B 2	3.5012	0.4458	3.0554	7.3	0.0419	1.45
7B 3	3.4625	0.4495	3.0130	5.5	0.0203	0.70
7B 4	3.4952	0.4412	3.0540	5.8	0.0237	0.82
7C 1	3.4596	0.4356	3.0240	16.4	0.1544	5.33
7C 2	3.4526	0.4312	3.0214	14.6	0.1323	4.57
7C 3	3.4852	0.4389	3.0463	7.3	0.0420	1.45
7C 4	3.4829	0.4598	3.0231	5.3	0.0177	0.61
8B 1	*3.4773*	*0.4503*	*3.0270*	*12.8*	*0.1039*	*3.59*
8B 2	*3.5285*	*0.4565*	*3.0720*	*8.2*	*0.0488*	*1.68*
8B 3	*3.4793*	*0.4572*	*3.0221*	*5.9*	*0.0224*	*0.77*
8B 4	*3.5354*	*0.4468*	*3.0886*	*5.6*	*0.0184*	*0.64*
8C1 1	3.4852	0.4510	3.0342	15.2	0.1391	4.80
8C1 2	3.4962	0.4415	3.0547	14.7	0.1321	4.56
8C1 3	3.4587	0.4495	3.0092	8.3	0.0549	1.90
8C1 4	3.4621	0.4425	3.0196	5.2	0.0165	0.57
					Average	1.52
					SIPMF	1.38
					No SIPMF	1.99

Table 5.3: OTT-2-28.41 Chloride Ion Test Results

NaCl Sol.	AgNO$_3$	Vol NaCL		Unit Weight		
0.010132	0.0105	4.00		LAK	OTT	LOR
	0.0101			3625.2	3580.87	3451.34
Sample	*Total Weight*	*Paper Weight*	*Concrete Weight*	*Endpoint*	*% Cl*	*Lbs Cl / yd^3*
	(grams)	*(grams)*	*(grams)*	*(ml)*		
A2 1	3.4775	0.4298	3.0477	6.9	0.0339	1.21
A2 2	3.4719	0.4385	3.0334	7.0	0.0353	1.26
A2 3	3.5029	0.4372	3.0657	6.5	0.0291	1.04
A2 4	3.4784	0.4564	3.0220	5.8	0.0212	0.76
A4 1	3.5128	0.4541	3.0587	11.0	0.0818	2.93
A4 2	3.4456	0.4486	2.9970	6.4	0.0285	1.02
A4 3	3.5311	0.4434	3.0877	6.0	0.0230	0.83
A4 4	3.4655	0.4495	3.0160	5.3	0.0153	0.55
A8 1	3.4576	0.4319	3.0257	16.8	0.1513	5.42
A8 2	3.5002	0.4411	3.0591	8.4	0.0514	1.84
A8 3	3.5060	0.4338	3.0722	6.7	0.0313	1.12
A8 4	3.4578	0.4360	3.0218	5.9	0.0224	0.80
A14 1	3.4963	0.4489	3.0474	19.4	0.1808	6.47
A14 2	3.5156	0.4456	3.0700	16.5	0.1456	5.22
A14 3	3.4634	0.4424	3.0210	8.8	0.0567	2.03
A14 4	3.4988	0.4539	3.0449	6.8	0.0328	1.17
B7 1	3.4689	0.4489	3.0200	17.2	0.1564	5.60
B7 2	3.4859	0.4452	3.0407	12.7	0.1023	3.66
B7 3	3.5012	0.4398	3.0614	10.7	0.0782	2.80
B7 4	3.4598	0.4385	3.0213	5.4	0.0164	0.59
C1 1	3.5321	0.4320	3.1001	9.3	0.0611	2.19
C1 2	3.5039	0.4356	3.0683	7.7	0.0430	1.54
C1 3	3.5123	0.4352	3.0771	5.5	0.0173	0.62
C1 4	3.4689	0.4498	3.0191	4.7	0.0082	0.29
C4 1	3.4653	0.4345	3.0308	11.0	0.0877	3.14
C4 2	3.5085	0.4425	3.0660	7.8	0.0478	1.71
C4 3	3.4689	0.4315	3.0374	5.5	0.0201	0.72
C4 4	3.4598	0.4448	3.0150	5.3	0.0178	0.64
C5 1	3.4502	0.4498	3.0004	22.8	0.2242	8.03
C5 2	3.5153	0.4402	3.0751	11.5	0.0872	3.12
C5 3	3.5263	0.4460	3.0803	5.8	0.0208	0.74
C5 4	3.4762	0.4282	3.0480	5.3	0.0151	0.54
C6 1	3.4674	0.4422	3.0252	24.2	0.2389	8.56
C6 2	3.5461	0.4365	3.1096	14.6	0.1219	4.37
C6 3	3.5115	0.4514	3.0601	7.0	0.0350	1.25
C6 4	3.4584	0.4436	3.0148	5.4	0.0165	0.59
					Average	2.34
					SIPMF	2.54
					No SIPMF	2.10

Table 5.4: LAK-90-23.42 Chloride Ion Test Results

NaCl Sol.	AgNO₃	Vol NaCL		Unit Weight		
0.010131759	0.0105	4.00		LAK	OTT	LOR
	0.0101			3625.20	3580.87	3451.34

Sample	*Total Weight (grams)*	*Paper Weight (grams)*	*Concrete Weight (grams)*	*Endpoint (ml)*	*% Cl*	*Lbs Cl / yd³*
L4 1	3.5011	0.4356	3.0655	22.0	0.2203	7.99
L4 2	3.4418	0.4342	3.0076	21.4	0.2171	7.87
L4 3	3.4498	0.4298	3.0200	5.7	0.0227	0.82
L4 4	3.4613	0.4526	3.0087	4.4	0.0067	0.24
L7 1	3.5112	0.4468	3.0644	19.8	0.1936	7.02
L7 2	3.5403	0.4456	3.0947	9.7	0.0703	2.55
L7 3	3.5126	0.4523	3.0603	5.9	0.0248	0.90
L7 4	3.5329	0.4594	3.0735	5.7	0.0223	0.81
L13 1	3.4869	0.4521	3.0348	17.3	0.1649	5.98
L13 2	3.4398	0.4462	2.9936	6.1	0.0279	1.01
L13 3	3.4803	0.4461	3.0342	5.8	0.0238	0.86
L13 4	3.4711	0.4423	3.0288	5.5	0.0202	0.73
L15 1	3.4568	0.4521	3.0047	20.4	0.2049	7.43
L15 2	3.4562	0.4462	3.0100	14.0	0.1254	4.55
L15 3	3.4419	0.4489	2.9930	5.7	0.0229	0.83
L15 4	3.4589	0.4309	3.0280	4.5	0.0079	0.29
L21 1	3.4706	0.4559	3.0147	23.7	0.2450	8.88
L21 2	3.4839	0.4462	3.0377	11.4	0.0924	3.35
L21 3	3.4685	0.4443	3.0242	7.4	0.0436	1.58
L21 4	3.4852	0.4389	3.0463	5.7	0.0225	0.82
L22 1	3.5009	0.4538	3.0471	23.5	0.2399	8.70
L22 2	3.5089	0.4503	3.0586	8.0	0.0504	1.83
L22 3	3.4952	0.4420	3.0532	5.9	0.0249	0.90
L22 4	3.4769	0.4396	3.0373	5.3	0.0177	0.64
L34 1	3.5081	0.4356	3.0725	24.5	0.2501	9.07
L34 2	3.5065	0.4586	3.0479	7.9	0.0493	1.79
L34 3	3.4768	0.4328	3.0440	6.1	0.0274	0.99
L34 4	3.5189	0.4356	3.0833	5.6	0.0210	0.76
L36 1	3.4814	0.4512	3.0302	32.5	0.3518	12.75
L36 2	3.4985	0.4562	3.0423	28.7	0.3039	11.02
L36 3	3.4705	0.4406	3.0299	21.1	0.2118	7.68
L36 4	3.4802	0.4470	3.0332	10.6	0.0827	3.00
					Average	3.86
					SIPMF	3.12
					No SIPMF	4.61

The water soluble chloride ion test also indicated that the area located two inches below the surface exhibited the highest chloride ion content. This was expected due to the cracks present in the bridge decks. Chlorides propagated through these cracks, increasing the chloride levels throughout the top two inches of the bridge deck. A major concern of SIPMF is that they prevent visual inspection of the underside of the bridge deck. Engineers are worried that foreign substances, mainly chlorides, will erode the bottom of the deck. From our test results, it was also evident that in most cases, the bottom portion of the deck exhibited the lowest level of chloride ion content. This should help alleviate this concern. Table 5.5 shows the amount of chlorides present at each two-inch (51 mm) interval.

Table 5.5: Chloride Concentration at Each Two-Inch Interval

Bridge	Average Chloride Concentration for Each Bridge (Lbs Cl⁻ per cubic yard) (Lbs Cl⁻ per cubic yard = 5.82 N/m³)			
	2" *(51 mm)*	*4"* *(102 mm)*	*6"* *(152 mm)*	*8"* *(203 mm)*
LOR-57-18.18	2.64	1.74	1.00	0.71
OTT-2-28.41	4.84	2.64	1.24	0.66
LAK-90-23.42	8.48	4.24	1.82	0.91

As stated earlier, the main problem associated with a high level of chloride ion concentration is the corrosion of the reinforcing steel. Sprinkel and Ozyildirim (2000) have stated that a content of 1.3 pounds of chloride per cubic yard (7.66 N/m^3) is significant to cause corrosion of the reinforcing steel. They also state that the limit placed by most state departments of transportation is 2.0 pounds of chlorine per cubic yards (11.64 N/m^3). Once this threshold is passed, Sprinkel and Ozyildirim state that the reinforcing steel will begin to corrode, and the deck will not function as intended. From our tests results, it was evident that only LOR-57-18.18 possessed a chloride ion concentration lower than the limit placed by most state departments of transportation. However, the chloride ion concentration of this bridge was still higher than the 1.3 limit stated by Sprinkel and Ozyildirim. Therefore, the reinforcing steel has already started to corrode. The main reason for this corrosion of the reinforcing steel is due to the fact that the

reinforcing steel in all three of the bridges tested lacked epoxy coating. The epoxy coating has been shown to drastically decrease the corrosion of the reinforcing steel by limiting the amount of chlorides that come in contact with the steel. Since all bridges today require epoxy coating of the reinforcement steel, the problem of rebar corrosion has been greatly reduced.

The test results show that SIPMF do not significantly affect the penetration of chlorides throughout a bridge deck. Similar to the other tests performed, there was no major difference in the areas of SIPMF and areas where no permanent forms are present. The complete chloride test results are in Appendix E: Chloride Ion Test Result.

Chapter 6: Permeability Test

The permeability of concrete is a characteristic that shows the rate of entry of moisture. It is the result of a number of variables including the water to cement ratio, the curing condition, the temperature of the concrete during curing, and the level of air entrainment (Myers 2001). The type and size of aggregate has been also known to affect the permeability (Myers 2001).

The durability of a concrete structure is usually correlated to its compressive strength. However, concretes with the same strengths have shown to exhibit different levels of resistance to corrosion (Armaghani 1993). Therefore, several research teams have chosen to evaluate the durability of concrete based on the compressive strength and the permeability.

To determine the permeability of the concrete bridge decks in the present study, the research team chose to perform a permeability test in accordance with AASHTO T277-97. This test determines the concrete's resistance to the penetration of chloride ions. When chlorides penetrate into a bridge deck, they lead to the deterioration of the reinforcing steel. Corroded reinforcing steel drastically affects the durability of a bridge deck, leading to a subsequent reduction in the strength and serviceability of the structure. This in turn leads to costly repairs or premature replacement of the structure.

A two-inch specimen was cut from the core samples and prepared for testing. The concrete specimen was then placed in between two cells, one containing a 3% NaCl solution and the other containing a 0.3N NaOH solution. The test started by subjecting the specimen to 60 volts of direct current. The was conducted for six hours, monitoring the current every thirty minutes. The current was then plotted versus time. The area underneath the was then integrated to obtain a value of charge passed during the six hour test (AASHTO T 277-97). This total charge passed is a measure of the permeability of the concrete. AASHTO correlates the total charge passed into a classification rating. 1000 coulombs in recognized by AASHTO as the upper limit for concrete to provide adequate corrosion protection. However, some feel that a total charge of 1500 coulombs provides adequate protection (Myers 2001).

AASHTO's classification of concrete permeability, based on the total charge passed through the six hour test, is shown in Table 6.1 (AASHTO T 277-97).

Table 6.1. AASHTO Classification of Concrete Permeability

Charge Passed (coulombs)	Chloride Ion Penetrability
> 4,000	High
2,000 – 4,000	Moderate
1,000 – 2,000	Low
100 – 1,000	Very Low
< 100	Negligible

A permeability machine manufactured by German Instruments was used. This machine takes the current passed through the concrete during the six hour time period and converts it to a permeability classification listed in AASHTO T277-97. A picture of this machine is shown in Figure 6.1.
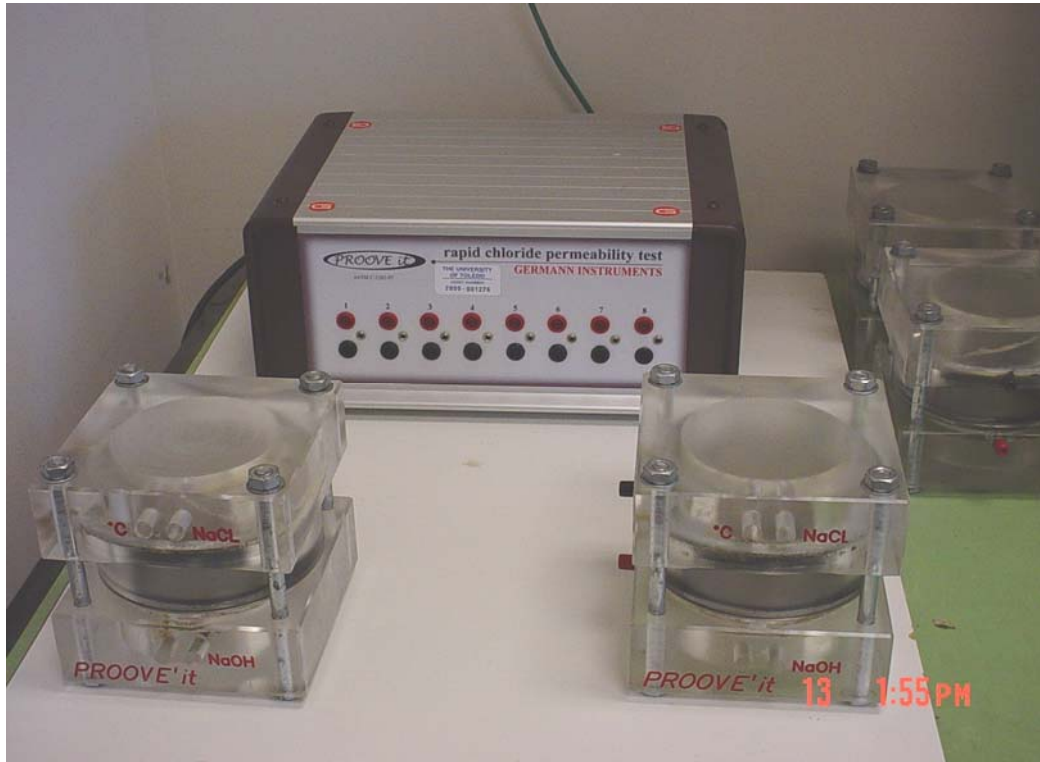
Figure 6.1. German Instrument Permeability Testing Machine

To evaluate the condition of the bridge decks in our study, two inch thick slices were cut from areas of the core samples where the original concrete was located. None of the samples contained concrete from overlays or wearing surface material. Since the permeability test requires passing a charge through the concrete, none of the samples contained reinforcing steel. This was done so that the test results provided a true representation of the permeability of the concrete.

The permeability tests on LOR-57-18.18 indicated that the average charge passed in the six-hour test was 1,650 coulombs. This leads to an AASHTO classification of low chloride ion penetrability. The test results also indicated that the average charge passed for the samples taken in areas where SIPMF were present was 1,595 coulombs. This once again leads to an AASHTO classification of low chloride ion penetrability. In areas were no SIPMF were present, the average charge passed was 1,811 coulombs. This also corresponds to an AASHTO classification of low chloride ion penetrability.

The test results on OTT-2-28.41 yielded an average charge passed greater than that of LOR-57-18.18. The average charge passed for all the samples was 2,140 coulombs, which corresponds to an AASHTO classification of moderate chloride ion penetrability. In areas where SIPMF were present, the average charge passed was 2,416 coulombs. This in turn leads to an AASHTO classification of moderate chloride ion penetrability. In areas where no SIPMF were present, the average charge passed was 2,002 coulombs. This also corresponds to an AASHTO classification of moderate chloride ion penetrability.

The test results on LAK-90-23.42 indicated that average charge passed was higher than LOR-57-18.18 and OTT-2-28.41. The average charge passed was 3,077 coulombs. This is turn leads to an AASHTO classification of moderate chloride ion penetrability. The samples extracted from areas where SIPMF were present yielded an average charge passed of 2,128 coulombs. This once again corresponds to an AASHTO classification of moderate chloride ion penetrability. In areas where no SIPMF were present, the average charge passed was 4,264 coulombs. This corresponds to an AASHTO classification of high chloride ion penetrability. The drastic difference between the SIPMF region and non SIPMF region can be attributed to the fact the bridge deck in the non SIPMF region exhibited many cracks. These cracks lead to the increase in permeability. Russel (2000) stated that the formation of microcracks due to exposure

conditions drastically affects the permeability of the concrete. Table 6.2 summarizes the permeability results.

Table 6.2: Summary of Permeability Test Results

	Average Whole Bridge		
	Charge Passed Coulombs	Standard Deviation Coulombs	AASHTO Class
LOR-57-18.18	1650	477	Low
OTT-2-28.41	2140	759	Moderate
LAK-90-23.42	3077	1471	Moderate

	SIPMF		
	Charge Passed Coulombs	Standard Deviation Coulombs	AASHTO Class
LOR-57-18.18	1595	499	Low
OTT-2-28.41	2416	1134	Moderate
LAK-90-23.42	2128	421	Moderate

	No SIPMF		
	Charge Passed Coulombs	Standard Deviation Coulombs	AASHTO Class
LOR-57-18.18	1811	422	Low
OTT-2-28.41	2002	538	Moderate
LAK-90-23.42	4264	1468	High

The Rapid Chloride Permeability Test (RCPT) has been accepted as the standard test to determine the permeability of concrete. It has gained approval due the many advantages that it presents. The most noticeable advantage is that it is a relatively quick test that provides results that are easy to interpret. However, some limitations do exist. The most criticized element of the test deals with the rise of temperature that is sometimes exhibited throughout the test (Liu and Beaudoin 2000). This problem is known to effect higher permeable concrete because as the temperature increases, the conductivity of the pore solution increases leading to a higher RCPT value (Russel 2000). This problem may lead to an RCPT value that misrepresents the true permeability of the concrete. This problem has been shown to arise when the RCPT value is

greater than 2,000 coulombs (Russel 2000). To correct for this temperature increase, several research teams have proposed multiplying the thirty minute reading by twelve (Russel 2000). To eliminate this problem, our research team chose to adopt this procedure.

As stated previously, LOR-57-18.18 test results indicated that the average charge passed in the six hour test was 1,650 coulombs. Since this value was less than 2,000 coulombs, only a few corrections for the temperature increase were needed. However, OTT-2-28.41 and LAK-90-23.42 exhibited test results greater than 2,000 coulombs. To eliminate the problem due to the rise in temperature, our research team chose to adopt the correction procedure stated by Russel (2000) to many of the values obtained from these test results.

When multiplying the thirty-minute reading by twelve, the average charge passed in the six hour test on LOR-57-18.18 was 1,612 coulombs compared to a value of 1,650 coulombs before correction. This shows that the problem due to a temperature increase does not affect lower permeability concretes. This agrees with the observation by Russel (2000). When applying the temperature correction for the test results for the samples taken in areas where SIPMF were present, the average charge passed was 1,557 coulombs. In areas were no SIPMF were present, the average charge passed, when implementing the temperature correction, was 1,777 coulombs.

The test results on OTT-2-28.41 yielded an average charge passed greater than that of LOR-57-18.18. Therefore, when implementing the temperature correction factor, the average charge passed should show a more dramatic decrease compared to that of LOR-57-18.18. The average charge passed, when applying the temperature correction, for the entire bridge deck was 2,056 coulombs, which corresponds to an AASHTO classification of moderate chloride ion penetrability. In areas where SIPMF were present, the average charge passed, when implementing the temperature correction factor, was 2,188 coulombs. When comparing this result to the average charge passed without the temperature correction, it is evident that a temperature increase did slightly affect the results. In areas where no SIPMF were present, the average charge passed was 1,990 coulombs when applying the correction for temperature increase. This corresponds to an AASHTO classification of low chloride ion penetrability compared to a classification of moderate chloride ion penetrability when the temperature correction was not applied.

The test results on LAK-90-23.42 indicated that average charge passed was higher than LOR-57-18.18 and OTT-2-28.41. Since this bridge exhibited the most permeable concrete, the temperature correction procedure should drastically decrease the results. The average charge passed, when applying the temperature correction, was 2,474 coulombs compared to 3,077 coulombs when no temperature correction was applied. The samples extracted from areas where SIPMF were present yielded an average charge passed of 1,945 coulombs when applying the temperature correction. By applying the temperature correction, the AASHTO classification moved from moderate to low chloride ion penetrability. In areas where no SIPMF were present, the average charge passed was 3,136 coulombs when applying the temperature correction. By applying the temperature correction, the value decreased by 26.5 %. This was because these test results showed a dramatic increase in temperature throughout the test. This can be seen more clearly by referring to the complete test results in "Appendix D: Permeability Test Results". Table 6.3 shows a comparison of the test results when a temperature correction is applied. From this table, and the test results, it is evident that the temperature increase plays an important role when dealing with higher permeable concretes. Table 6.4 is a summary of the test results.

Table 6.3: Permeability Test Results With Temperature Correction

Bridge	Average Whole Bridge			
	Charge Passed	Charge Passed w/ Temp. Corr.	Standard Deviation w/ Temp. Corr.	% Reduction due to Temp. Corr.
LOR-57-18.18	1650	1612	434	2.30%
OTT-2-28.41	2140	2056	592	3.93%
LAK-90-23.42	3077	2474	764	19.60%

Bridge	SIPMF			
	Charge Passed	Charge Passed w/ Temp. Corr.	Standard Deviation w/ Temp. Corr.	% Reduction due to Temp. Corr.
LOR-57-18.18	1595	1557	455	2.38%
OTT-2-28.41	2416	2188	778	9.44%
LAK-90-23.42	2128	1945	339	8.60%

Bridge	No SIPMF			
	Charge Passed	Charge Passed w/ Temp. Corr.	Standard Deviation w/ Temp. Corr.	% Reduction due to Temp. Corr.
LOR-57-18.18	1811	1777	366	1.88%
OTT-2-28.41	2002	1990	525	0.60%
LAK-90-23.42	4264	3136	596	26.45%

Table 6.4: Permeability Test Results

Core #	Location of Specimen within core		Temperature Corrected Charge Passed		Permeability Class	
	(inches from top)		(coulombs)		*(Temp. Adjusted)*	
OTT-2-28.41						
A3	1.50	9.00	1977	1214	Low	Low
A6	1.75	9.00	1667	1580	Low	Low
A10	2.50	8.75	2685	2739	Moderate	Moderate
A15	1.75	8.75	2082	1972	Moderate	Low
B3	3.50		1886		Low	
B6	4.75		2095		Moderate	
C2	5.75		1479		Low	
C8	2.75		3290		Moderate	
LOR-57-18.18						
1D	3.75		1384		Low	
2C	4.00		1083		Low	
2D1	4.88		977		Very Low	
2D2	0.50		1749		Low	
2E	2.75		1206		Low	
4E	3.25		1124		Low	
5B	0.50	4.00	1892	1513	Low	Low
6D	0.50		2240		Moderate	
7C1	2.00		1778		Low	
7C1(2)	3.00		1828		Low	
7E	0.50	4.00	2216	1073	Moderate	Low
8C1	0.50		2210		Moderate	
8B	3.50		1929		Low	
S1	3.00		1586		Low	
LAK-90-23.42						
L2	6.00		2218		Moderate	
L9	7.50		1931		Low	
L11	6.25		1743		Low	
L14	6.50		1504		Low	
L16	7.00		2331		Moderate	
L27	6.50		3013		Moderate	
L30	6.00		2352		Moderate	
L33	5.00		3475		Moderate	
L35	5.75		3702		Moderate	

Note: No rebar present in any specimens. All specimens pure concrete.

CHAPTER 7: Ultrasonic Evaluation of Cores Taken from Bridge Decks

7.1 INTRODUCTION

Cores were taken from six bridge decks, three with stay-in-place metal forms (SIPMF) and three without SIPMF. These bridge decks are LOR-57-18.18, OTT-2-28.41, and LAK-90-23.42. Five full-depth cores were taken from each bridge deck. A total of 30 cores were obtained for the ultrasonic test evaluation. The concrete cores were transported to the Structural Testing Center at Lawrence Technological University for evaluation of structural condition and assessment of condition of concrete. The cores were assessed visually, and nondestructively. The procedures for laboratory investigation are first presented. Then, data are presented for all inspection and evaluation procedures on a bridge-by-bridge basis. Finally, a summary of the comparison between the deck slabs with and without SIPMF is presented based on the inspection and investigation of the cores. The details of the bridges selected for coring and inspection are presented section 1.5. The nomenclature used in this section is bridge deck # 1 is LOR-57-18.18 without SIPMF and bridge deck # 4 is LOR-57-18.18 with SIPMF. Bridge deck # 2 OTT-2-28.41 without SIPMF and bridge deck # 5 is OTT-2-28.41 with SIPMF. Bridge deck # 3 is LAK-90-23.42 without SIPMF and bridge deck # 6 is LAK-90-23.42 with SIPMF.

7.2 PROCEDURES FOR INSPECTION OF CORES

7.2.1 Visual Inspection

Visual inspection of the cores was used to determine general physical characteristics and overall condition of the cores that were obtained for the test program. All cores were inspected visually. The characteristics of the reinforcing steel were assessed for presence and condition of epoxy coating and extent of rust. The concrete was assessed for quantity, size, and alignment of cracking; quantity and size of voids; quantity and size of honeycombing; and porosity of aggregate and cement paste. SIPMF were assessed for extent of rust.

7.2.2 Ultrasonic Testing

Ultrasonic testing was used in the test program to assess the quality and condition of concrete. In particular, variation of concrete condition with depth was determined. Tests were conducted using commercially available hardware (Figure 7.1). The measurement system

consisted of two P-wave transducers, a pulser-receiver, and a data acquisition system. The narrowband transducers operated at 100-kHz-center frequency. The 10-MHz-bandwidth pulser-receiver contained a high-voltage pulser and a high-gain receiver. The low-frequency transducers and high-voltage, high-gain pulser-receiver were particularly selected for testing concrete, which is a highly attenuating material. The data acquisition system consisted of a computer equipped with an analog-to-digital converter board with 50 MHz sampling rate and a digital oscilloscope software that was used for viewing waveforms and adjusting data acquisition parameters.

The cores were cut into slices with thicknesses ranging from approximately 1 to 3 in (25.4 mm to 76.2 mm) using a concrete saw for ultrasonic testing. Generally, six to eight pulse velocity test specimens (slices) were obtained from each core designated for ultrasonic testing. Ultrasonic pulse velocity was determined on specimens obtained from the cores using the through transmission test method in accordance with ASTM C 597 (Figure 7.1). Three repeated ultrasonic measurements were made on each specimen by placing one transducer at the center of the top surface and one transducer at the center of the bottom surface of the specimen (slice). Transit time for wave propagation was identified as the first major deviation in the amplitude of a waveform (on an amplitude vs. time record) using statistical analysis. A waveform obtained in air was subtracted from the waveforms obtained on test specimens to provide a baseline for deviation in amplitude. Then, the initial portion of the modified waveform was analyzed to determine the level of noise in the signal prior to arrival of the waveform from the test specimen. First arrival was identified as the first occurrence of deviation of amplitude by more than 3 standard deviations from the mean amplitude of the initial portion of the waveform. The resolution for transit time measurements was 0.04 μs. The wave travel path was measured as the thickness of the slice using a custom-made micrometer with a resolution of 0.001 in. Therefore, based on an adaptation of Taylor's Theorem to the propagation of uncertainty, the maximum error in pulse velocity calculations was 1.2%.
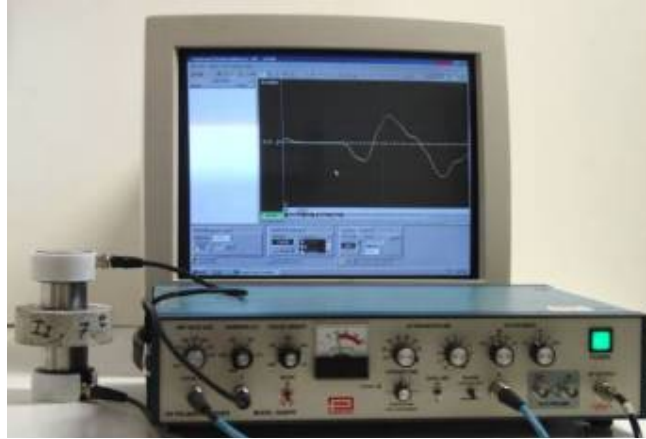
Figure 7.1. Test setup for through-transmission
ultrasonic measurements of slices of cores

7.3 INSPECTION RESULTS

Results from the laboratory investigation of the cores are presented in the following section on a bridge-by-bridge basis. This section of the report describe in detail the results of the evaluation of the cores. The inspection of cores included visual inspection and ultrasonic test.

7.3.1 Bridge Deck Number 1 (LOR-57-18.18 - No SIPMF):

Visual Inspection of Cores from LOR-57-18.18 without SIPMF

The visual inspection of cores indicated that all the cores had no wearing surface at the top surface. The steel reinforcement generally showed some signs of rust. The heights of the cores were not significantly different thus indicating uniformity of the bridge deck. The five cores removed from Bridge Deck Number 1 were carefully inspected and illustrated as follows:

Core 1C (Figure 7.2-7.3)
- 9.25 in.(228.6 mm) height.
- 2 reinforcement bars, non-epoxy coated located at 2.75 in. (69.85 mm) and 7.75 in. (196.9 mm) from top surface.
- Some rust traces on bars.
- Voids located at 1.25 in. (31.75 mm), 7 in. (177.8 mm)   , and 8.5 in. (215.6 mm)   from the top surface.

Figure 7.2. Core 1C shows rust traces

Figure 7.3. Core 1C shows small voids

Core 1F (Figure 7.4-7.5)
- 8.75 in. (222.3mm) height.
- Regions of small to moderate voids.
- 1 reinforcing bar, non-epoxy coated, located at 3.5 in. (88.9 mm) from top surface.
- Some rust existed at edges of reinforcement bar.
- 1 horizontal crack located at 2.5 in. (63.5 mm) from top surface.

Figure 7.4. Core 1F shows rust traces

Figure 7.5. Core 1F shows small voids

Core 1B (Figure 7.6-7.7)
- 6.13 in. (155.7 mm) height, approximately 9 in. (228.6 mm)till the top of the broken region.
- Core is broken at the top, with re-bar protruding vertically.
- 2 reinforcement bars are located at 3.25 in. (82.55 mm)and 5.75 in. (146.1 mm) from the bottom surface.
- Exposed steel reinforcement showed slight signs of rust.

Figure 7.6. Core 1B shows
rust in steel reinforcement

Figure 7.7. Core 1B shows small voids

Core 8E (Figure 7.8-7.9)

- 9 in. (228.6 mm) height.
- 2 reinforcement bars located at 2.5 in. (63.5 mm) and 7 in. (177.8 mm) from the top surface.
- Bars are not coated.
- Region of voids located approximately at 6 in. (152.4 mm) from the top surface.

Figure 7.8. Core 8E shows no epoxy coat for bars
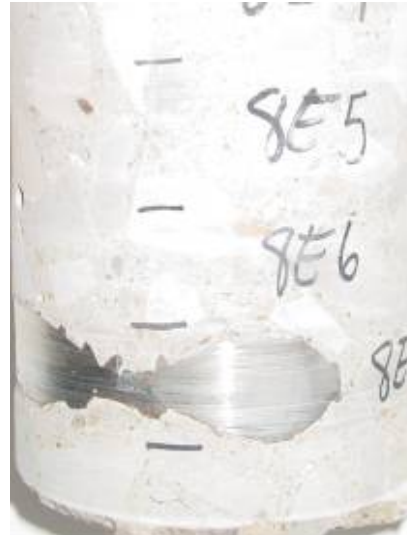
Figure 7.9. Core 8E shows small voids

Core 8C2 (Figures 7.10-7.11)

- 9 in. (228.6 mm) height.
- 3 reinforcement bars located at 2.5 in. (63.5 mm), 6.75 in. (171.5 mm), and 7.75 in. (196.9 mm) from the top surface.
- Bars are not coated and show slight signs of rust.

Figure 7.10. Core 8C2 shows rust in steel reinforcement

Figure 7.11. Core 8C2 shows small voids
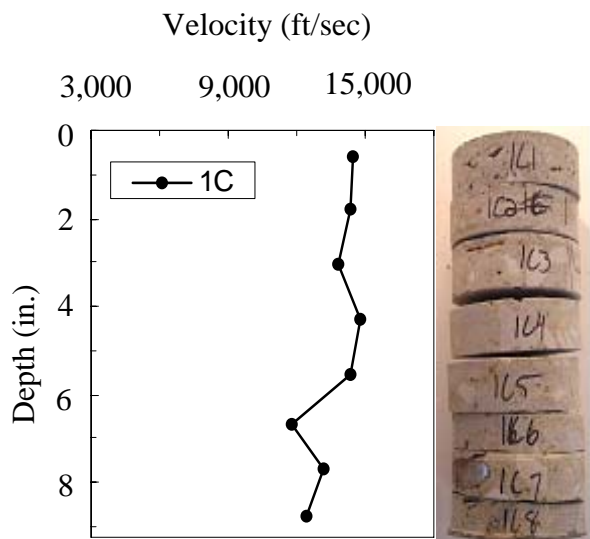
Figure 7.12. Ultrasonic velocity
with core depth for Core 1C
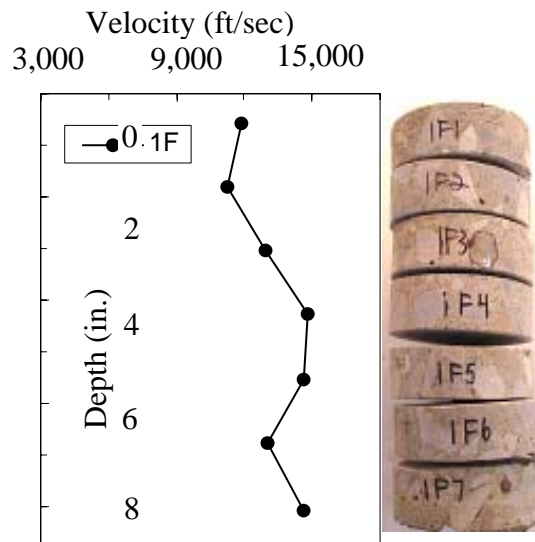
Figure 7.13. Ultrasonic velocity
with core depth for Core 1F
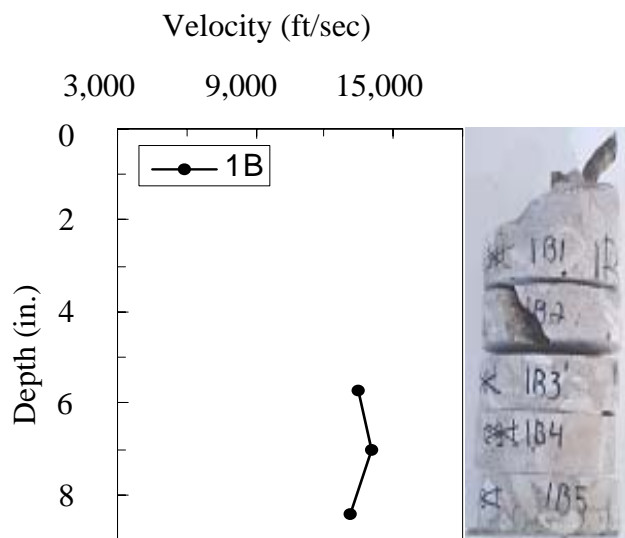
Figure 7.14. Ultrasonic velocity
with core depth for Core 1B
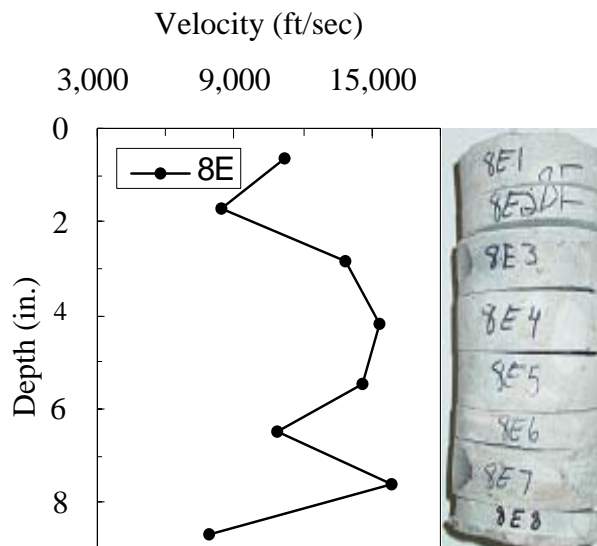
Figure 7.15. Ultrasonic velocity
with core depth for Core 8E

1 ft/sec = 0.30 m/s, 1 in. = 25.4 mm
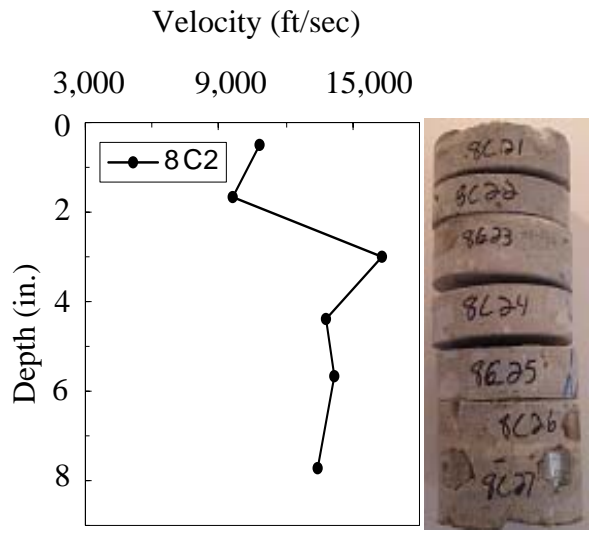
Figure 7.16. Ultrasonic velocity
with core depth for Core 8C2

1 ft/sec = 0.30 m/s, 1 in. = 25.4 mm

7.3.2 Bridge Deck Number 2 (OTT-2-28.41-No SIPMF)

Visual Inspection of Cores from OTT-2-28.41 without SIPMF

The visual inspection of cores indicated that all the cores have a wearing surface at the top. The steel reinforcement generally showed moderate to severe signs of rust. The heights of the cores were not significantly different thus indicating uniformity of the bridge deck. The five cores removed from Bridge Deck Number 2 were carefully inspected and illustrated as follows:

Core A1 (Figure 7.17-7.18)

- 11 in. (279.4 mm) height.
- 3 reinforcement bars, non-epoxy coated located at 4 in. (101.6 mm), 6 in. (152.4 mm), and 7 in. (177.8 mm) from top surface.
- Some rust traces on bars.
- Small region of honeycombing located at 2.5 in. (63.5 mm) from top surface.

Figure 7.17. Core A1 shows rust traces

Figure 7.18. Honeycombing region

Core A11 (Figure 7.19-7.20)
- 10.75 in. (273.1 mm) height.
- Regions of moderate to large voids located at 7 in. (177.8 mm) from top surface.
- 2 reinforcing bar, non-epoxy coated located at 3 in. (76.2 mm) and 4 in. (101.6 mm) from top surface.
- The bars show severe rusting.

Figure 7.19. Core A11 shows uncoated bars
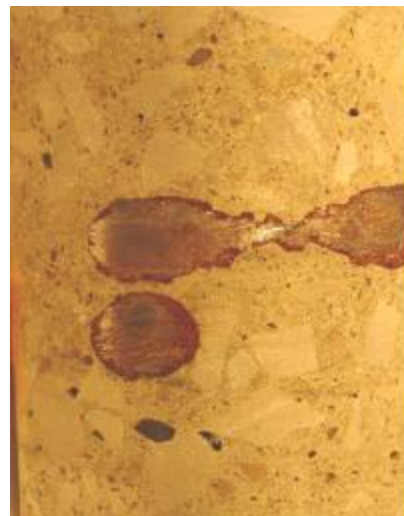
Figure 7.20. Core A11 shows severe rusting

Core A16 (Figure 7.21-7.22)

- 10.5 in. (266.7 mm) height.
- 2 reinforcement bars are located at 3.5 in. (88.9 mm) and 7 in. (177.8 mm) from the bottom surface.
- The upper bar shows severe rusting while the lower shows some rust traces.
- Region of honeycombing located at 6 in. (152.4 mm) from top.
- Region of large voids at the top-wearing surface.

Figure 7.21. Core A16 shows
rust in steel reinforcement
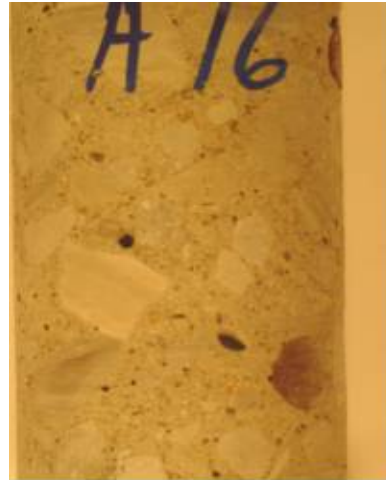
Figure 7.22. Core A16 shows
region of honeycombing

Core A5 (Figure 7.23-7.24)

- 11 in. (279.4 mm) height.
- 3 reinforcement bars located at 4.5 in. (114.3 mm), 6.5 in. (165.1 mm) and 7.5 in. (190.5 mm)from the top surface.
- Bars are not coated and show some rust traces.
- Region of honeycombing at 2.5 in. (63.5 mm) and 6.5 in. (165.1 mm) from top.

Figure 7.23. Core A5 shows
no epoxy coat on bars

Figure 7.24. Rust traces
and honeycombing

Core A9 (Figure 7.25-7.26)
- 11 in. (279.4 mm) height.
- 2 reinforcement bars located at 3 in. (76.2 mm) and 7.5 in. (190.5 mm) from top surface.
- Bars are not coated and show severe rusting.
- Region of honeycombing at 4 in. (101.6 mm) from top.

Figure 7.25. Core A9 shows
regions of honeycombing
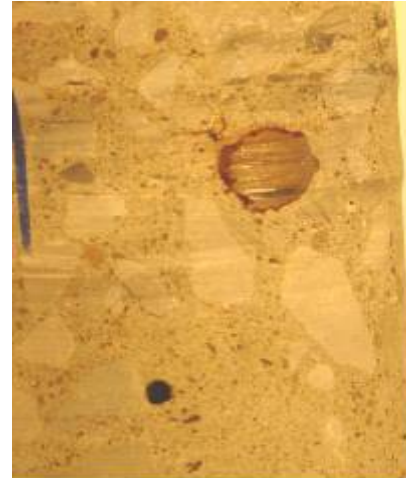
Figure 7.26. Core A9
shows severe rusting

Ultrasonic Testing of Cores fromOTT-2-28.41 without SIPMF
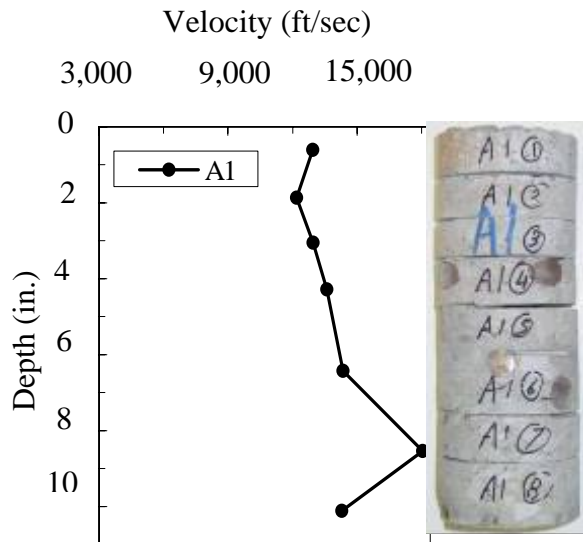
Figure 7.27. Ultrasonic velocity
with core depth for Core A1
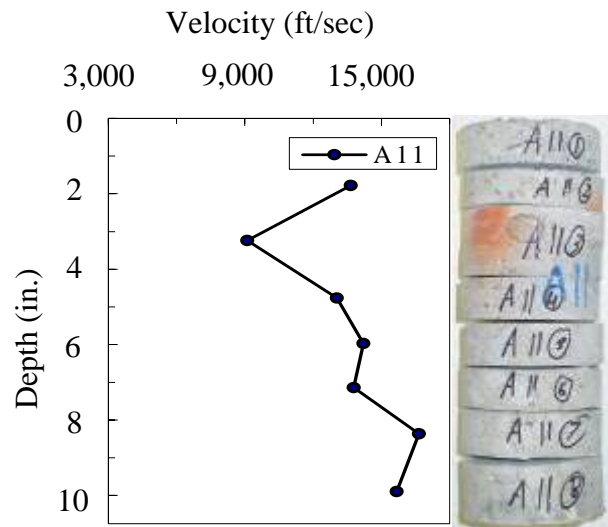
Figure 7.28. Ultrasonic velocity
with core depth for Core A11

Velocity

3,000   9,000   15,000
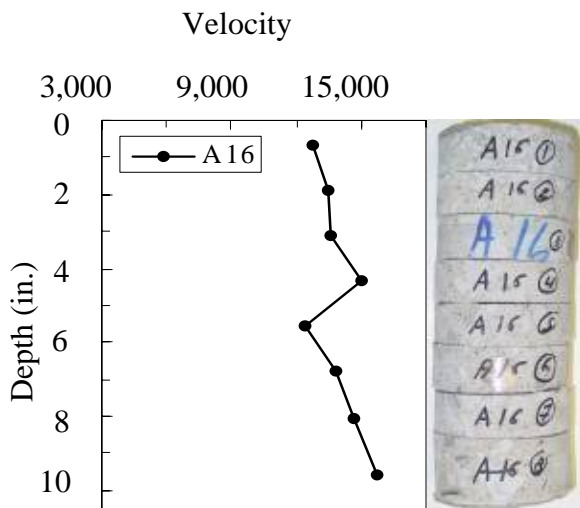
Figure 7.29. Ultrasonic velocity
with core depth for Core A16

Velocity (ft/sec)

3,000   9,000   15,000
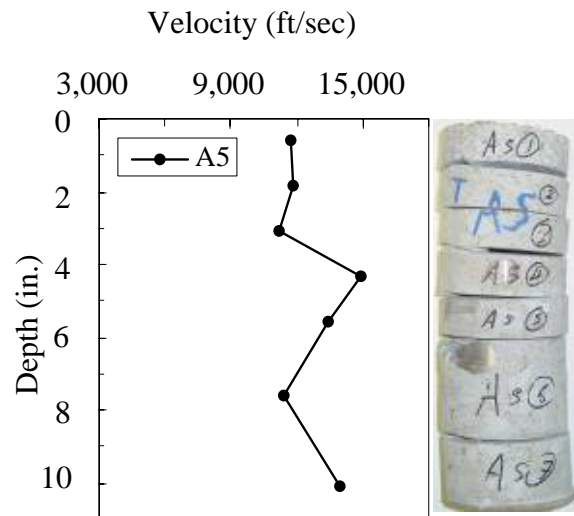
Figure 7.30. Ultrasonic velocity
with core depth for Core A5

Velocity (ft/sec)

3,000   9,000   15,000
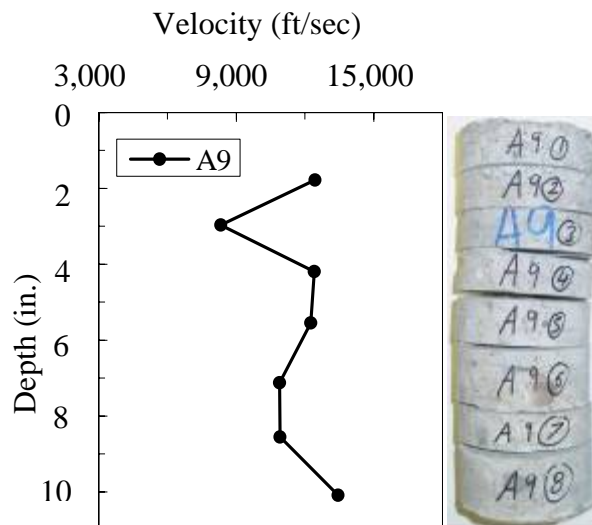
Figure 7.31. Ultrasonic velocity
with core depth for Core A9

1 ft/sec = 0.30 m/s, 1 inch = 25.4 mm

7.3.3 Bridge Deck Number 3 (LAK-90-23.42-No SIPMF):

Visual Inspection of Cores from LAK-90-23.42 without SIPMF

The visual inspection of cores indicated that the five cores had an asphalt-wearing surface. The slicing for these cores was done to have only this asphalt layer in the first slice, which was eliminated from the calculations. Some of the cores had their depth till the bottom

reinforcement due to restrictions during coring. The calculation for these cores was based on assuming a depth of 2 in. (50.8 mm) (as a concrete cover same as the one for the cores with SIPMF) for an imaginary slice with the same velocity as the preceding slice. The steel reinforcement generally showed some signs of rust. The five cores removed from Bridge Deck Number 3 were carefully inspected and illustrated as follows:

Core L23 (Figure 7.32-7.33)
- 9.5 in. (241.3 mm) height. (10.03 without the wearing surface depth and with the 2 in. (50.8 mm) imaginary slice)
- 1 reinforcement bar located at 5 in. (127 mm) from the top surface.
- Bar is not coated and shows rust traces.
- 1.5 in. (38.1 mm) asphalt wearing surface existed at the top of the core.
- Two different concrete layers.
- The aggregate in the top concrete layer is fine, while it is coarse in the bottom layer.
- Region of moderate voids located at the upper concrete layer.

Figure 7.32. Core L23 with asphalt layer at top

Figure 7.33. Bars show some rusting

Core L24 (Figure 7.34-7.35)

- 9.5 in. (241.3 mm) height. (9.97 without the wearing surface depth and with the 2 in. (50.8 mm) imaginary slice)
- 1.5 in. (38.1 mm) asphalt wearing surface existed at the top of the core.
- 2 reinforcement bars located at 5 in. (127 mm) and 6 in. (152.4 mm) from the top surface.
- Region of moderate voids at upper concrete layer.
- Brown rust traces on bars.
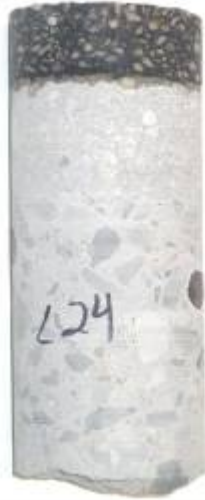
Figure 7.34. Core L24 with asphalt layer at top

Figure 7.35. Bars show some rusting

Core L26 (Figure 7.36-7.37)
- 8.75 in. (222.3 mm) height. (8.97 without the wearing surface depth and with the 2 in. (50.8 mm)imaginary slice)
- 1.5 in. (38.1 mm) asphalt wearing surface existed at the top of the core.
- 2 reinforcement bars located at 5 in. (127 mm) and 6 in. (152.4 mm) from top surface.
- Some rust traces existed on bars.
- Region of large size honeycombing at top layer of concrete.

Figure 7.36. Core L26 with asphalt layer at top

Figure 7.37. Rust and honeycombing regions

Core L28 (Figure 7.38-7.39)
- 10 in. (254 mm) height. (10.22 without the wearing surface depth and with the 2 in. (50.8 mm) imaginary slice)
- 1.5 in. (38.1 mm) asphalt wearing surface existed at the top of the core.
- 1 reinforcement bar located at 5 in. (127 mm) from top surface.
- Bar is not coated and shows some rust traces.
- Region of small to moderate voids at top concrete surface.

Figure 7.38. Core L28

Figure 7.39 Honeycombing region

Core L31 (Figure 7.40-7.41)

- 8.75 in. (222.3 mm) height. (9.15 in (232.4 mm) without the wearing surface depth and with the 2 in. (50.8 mm) imaginary slice)
- Region of small to moderate voids at top concrete surface.
- 1 reinforcement bar located at 5 in. (127 mm) from the top surface.
- Some rust at edges of reinforcement bars.
- Region of honeycombing.
- Region of small to moderate voids at upper concrete layer.

Figure 7.40. Core L31 with
asphalt layer at top

Figure 7.41. Honeycombing region

Ultrasonic Testing of Cores from LAK-90-23.42 without SIPMF
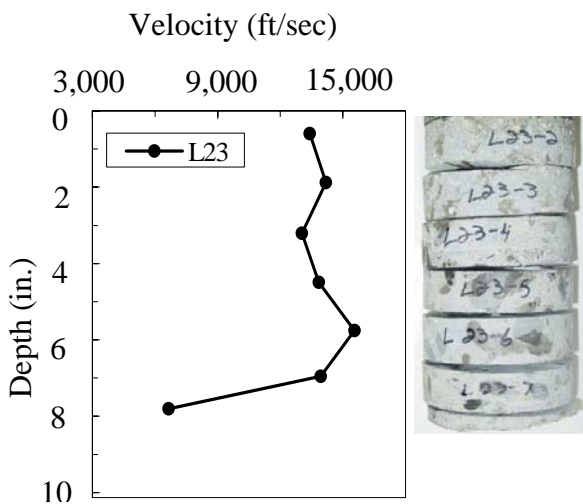
Figure 7.42. Ultrasonic velocity
with core depth for Core L23
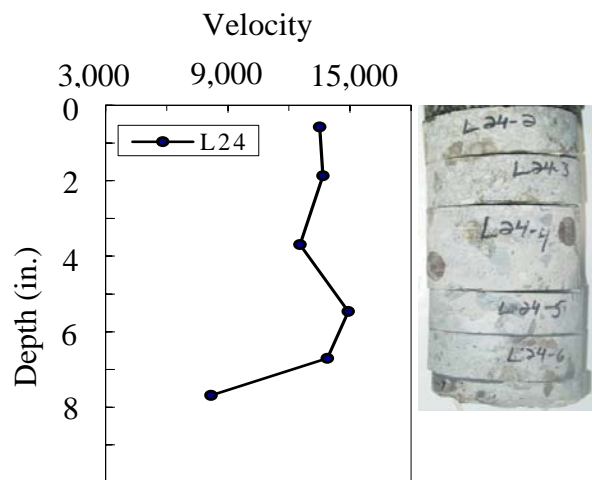
Figure 7.43. Ultrasonic velocity
with core depth for Core L24

7 - 16
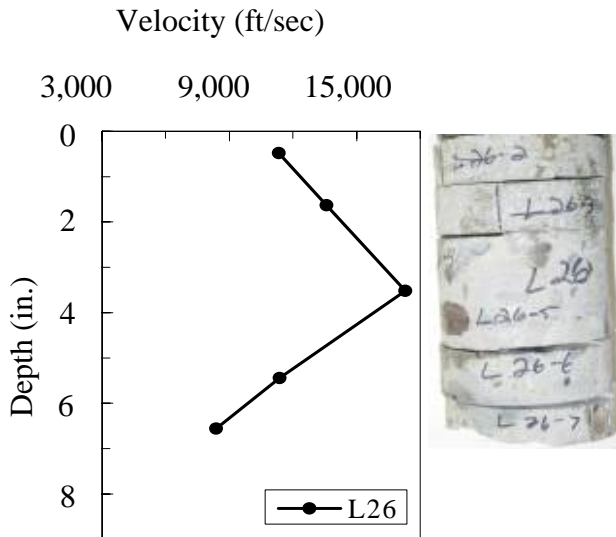
Velocity (ft/sec)

Figure 7.44. Ultrasonic velocity
with core depth for Core L26
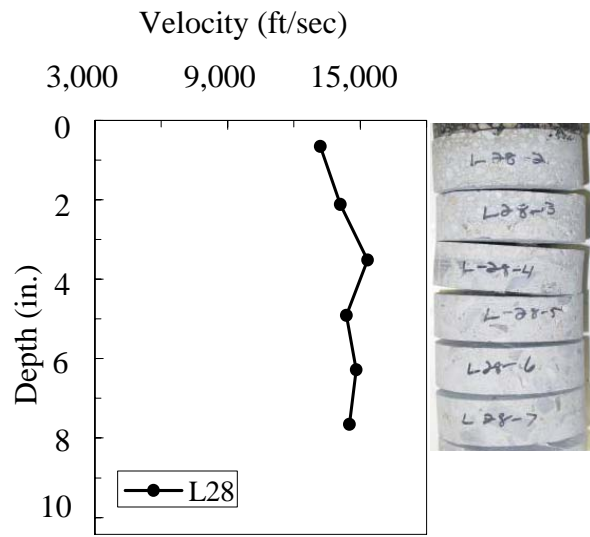
Velocity (ft/sec)

Figure 7.45. Ultrasonic velocity
with core depth for Core L28
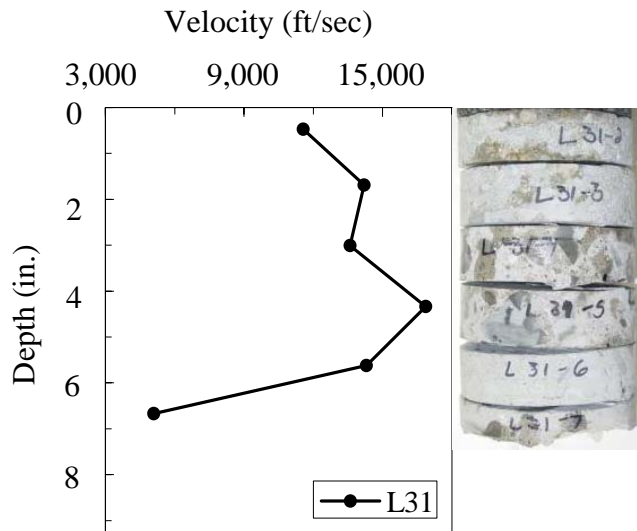
Velocity (ft/sec)

Figure 7.46. Ultrasonic velocity
with core depth for Core L31

1 ft/sec = 0.30 m/s, 1 in. = 25.4 mm

7.3.4 Bridge Deck Number 4 (LOR-57-18.18 - SIPMF):

Visual Inspection of Cores from LOR-57-18.18 with SIPMF

The visual inspection of cores indicated that all the cores had no wearing surface at the top surface. The steel reinforcement generally showed some signs of rust. The five cores removed from Bridge Deck Number 4 were carefully inspected and illustrated as follows:

Core 6B (Figure 7.41-7.48)

- 7.875 in. (200 mm) height (9.75 in. (247.7 mm) with the concrete in the region of the valley of the SIPMF).
- 2 reinforcement bars located at 3 in. (76.2 mm) and 7.5 in. (190.5 mm) from top.
- Bars are not coated and show some rust traces.
- Small region of honeycombing at 3 in. (76.2 mm) from the top surface.
- Concrete broken in region of SIPMF.

Figure 7.47. Core 6B shows small region of honeycombing

Figure 7.48. Core 6B shows small voids

Core 4C (Figure 7.49-7.50)
- 6.625 in. (168.3 mm) height (8.25 in. (209.6 mm) with the concrete in the region of the valley of the SIPMF).
- Concrete broken at the top.
- 3 reinforcing bars located at 2 in. (50.8 mm), 6 in. (152.4 mm), and 7 in. (177.8 mm), from bottom surface.
- Bars are not coated and show severe rusting
- Region of voids at 6 in. (152.4 mm) from bottom.

Figure 7.49. Broken concrete
at top of core 4C
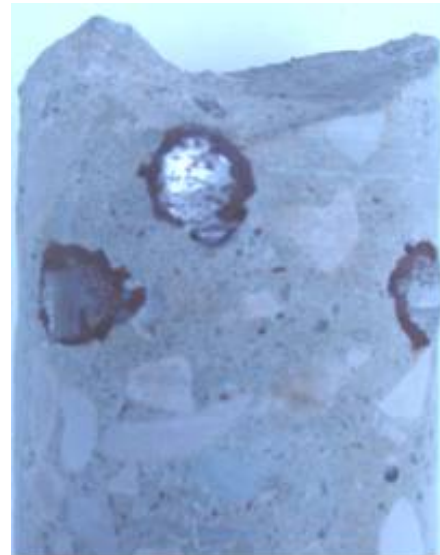
Figure 7.50. Core 4C shows
rust in steel reinforcement

Core 7D (Figure 7.51-7.52)

- 7.5 in (190.5 mm) height (9 in. (228.6 mm) with the concrete in the region of the valley of the SIPMF).
- Area of voids at 3.75 in. (95.25 mm) from top.
- Reinforcement bar located at 6 in. (152.4 mm) from bottom surface.
- Bars are not coated and show some rust.

Figure 7.51. Core 7D
shows small void

Figure 7.52. Core 7D shows
rust in steel reinforcement

Core 3D (Figure 7.53-7.54)

- 6.25 in. (158.8 mm) height (7. 5 in. (190.5 mm) with the concrete in the region of the valley of the SIPMF).
- Top of core is broken.
- 3 reinforcement bars located at 2.25 in. (57.15 mm), 6.25 in. (158.8 mm), and 7.0 in. (177.8 mm), from bottom surface.
- Bars are not coated and show severe rusting.
- Area of honeycombing at 5.5 in. (139.7 mm) from bottom surface.

Figure 7.53. Core 3D
shows small voids

Figure 7.54. Core 3D shows
rust in steel reinforcement

Core 6C (Figure 7.55-7.56)

- 7.88 in. (200.2 mm) in height (9.875 in. (250.8 mm) with the concrete in the region of the valley of the SIPMF).
- 3 reinforcement bars located at 3 in. (76.2 mm), 4 in. (101.6 mm), and 7.5 in. (190.5 mm)from top surface.
- Bars are not coated and show traces of rusting.
- Areas of medium to large voids at 1 in. (25.4 mm), and 2.25 in. (57.15 mm) from top.

Figure 7.55. Core 6C shows
rust in steel reinforcement

Figure 7.56. Core 6C
shows large voids

Ultrasonic Testing of Cores from LOR-57-18.18 with SIPMF
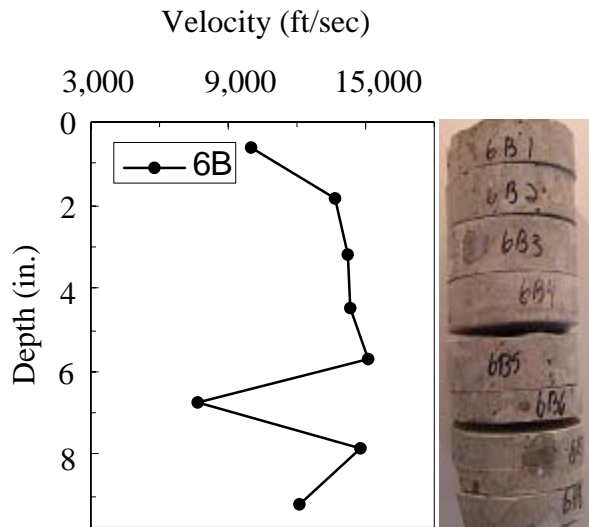
Figure 7.57. Ultrasonic velocity
with core depth for Core 6B
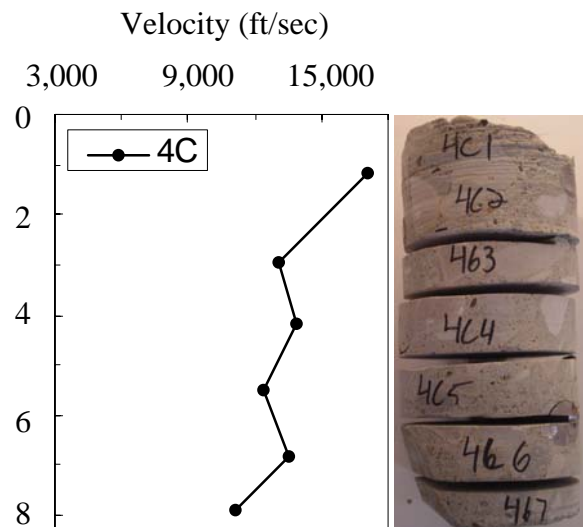
Figure 7.58. Ultrasonic velocity
with core depth for Core 4C

1 ft/sec = 0.30 m/s, 1 in. = 25.4 mm
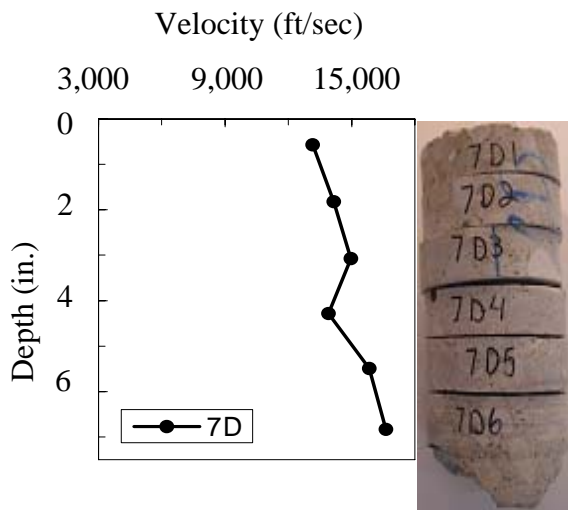
Figure 7.59. Ultrasonic velocity
with core depth for Core 7D
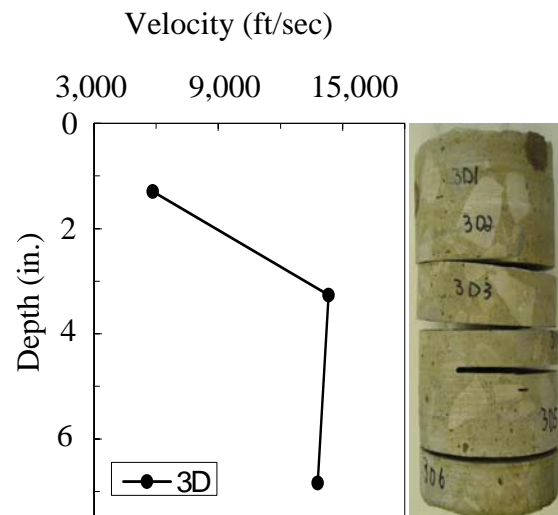
Figure 7.60. Ultrasonic velocity
with core depth for Core 3D
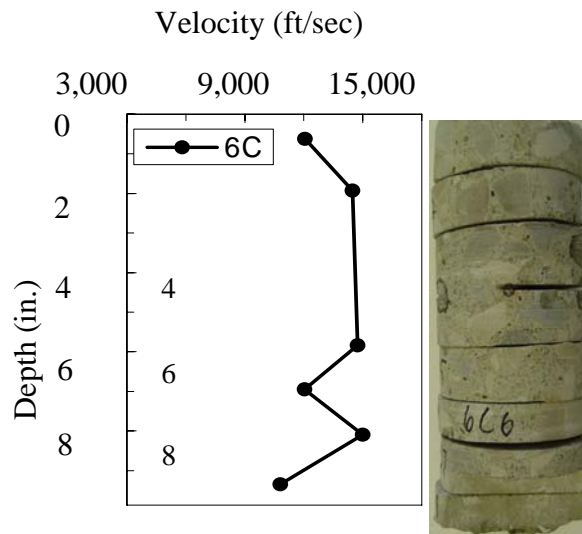
Figure 7.61. Ultrasonic velocity
with core depth for Core

1 ft/sec = 0.30 m/s, 1 in. = 25.4 mm

7.3.5 Bridge Deck Number 5 (OTT-2-28.41-SIPMF):

Visual Inspection of Cores from OTT-2-28.41 with SIPMF

The visual inspection of cores indicated that all the cores had a wearing surface at the top. The steel reinforcement generally showed moderate to severe signs of rust. The heights of the cores were not significantly different thus indicating uniformity of the bridge deck. The five cores removed from Bridge Deck Number 5 were carefully inspected and illustrated as follows:

Core B1 (Figure 7.62-7.63)
- 7.25 in. (184.2 mm) height (9.25 in. (235 mm) with the concrete in the region of the valley of the SIPMF).
- 2 reinforcement bars located at 3.5 in. (88.9 mm) and 6.5 in. (165.1 mm) from top.
- Small region of honeycombing at 2.5 in. (63.5 mm) from top surface.
- Bars are not coated and show some rust.

Figure 7.62. Core B1
shows some rust traces

Figure 7.63. Core B1 shows
region of honeycombing

Core B4 (Figure 7.64-7.65)
- 7 in. (177.8 mm) height (9 in. (228.6 mm) with the concrete in the region of the valley of the SIPMF).
- Regions of small voids.
- 2 reinforcing bars located at 1 in. (25.4 mm) and 3 in. (76.2 mm) from bottom surface, and show some rust traces.
- Brown and white traces on the SIPMF.
- Region of honeycombing at 6 in. (152.4 mm) from bottom.

Figure 7.64. Core B4 shows
regions of small voids

Figure 7.65. White
traces on SIPMF

Core B5 (Figure 7.66-7.67)
- 6.75 in. (171.5 mm) height (8.75 in. (222.3 mm) with the concrete in the region of the valley of the SIPMF).
- Area of voids at 3.75 in. (95.25 mm) from top.
- 2 reinforcing bars located at 3.75 in. (95.25 mm) and 5.5 in. (139.7 mm) from bottom surface, and show some rust traces.
- Brown and white traces on the SIPMF.

Figure 7.66. Core B5
shows small voids

Figure 7.67. Core B5 shows
no epoxy coat for bars

Core C3 (Figure 7.68-7.69)
- 7.5 in (190.5 mm) height (9.5 in. (241.3 mm) with the concrete in the region of the valley of the SIPMF).
- Core is broken into two parts.
- 1 reinforcement bars located at 3.75 in. (95.25 mm) from bottom surface.
- Bar is not coated and shows severe rusting.
- Brown and white traces on the SIPMF.

Figure 7.68. Core C3 is
broken into two pieces

Figure 7.69. Core C3 shows
rust on steel reinforcement

Core C7 (Figure 7.70-7.71)
- 7 in. height (8.7 in. with the concrete in the region of the valley of the SIPMF).
- Core is broken into two parts.
- 1 reinforcement bar located at 5.5 in. (139.7 mm) from bottom surface.
- Bar is not coated and shows some rust traces.
- White traces on the SIPMF.
- Region of small to moderate voids.

Figure 7.70. Core C7 shows rust in steel reinforcement

Figure 7.71. White traces on SIPMF

Ultrasonic Testing of Cores from OTT-2-28.41 with SIPMF
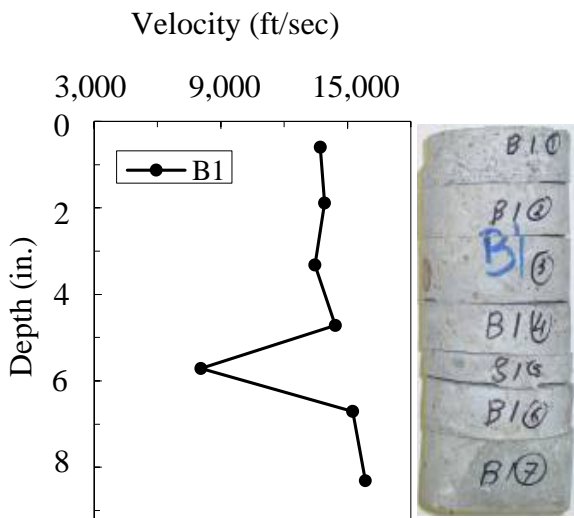
Figure 7.72. Ultrasonic velocity with core depth for Core B1
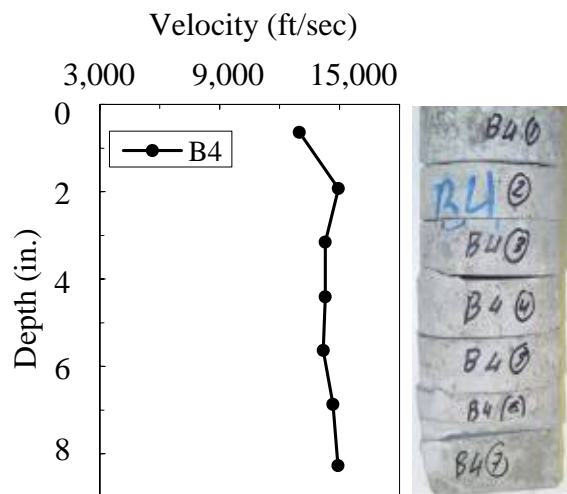
Figure 7.73. Ultrasonic velocity with core depth for Core B4

1 ft/sec = 0.30 m/s, 1 in. = 25.4 mm
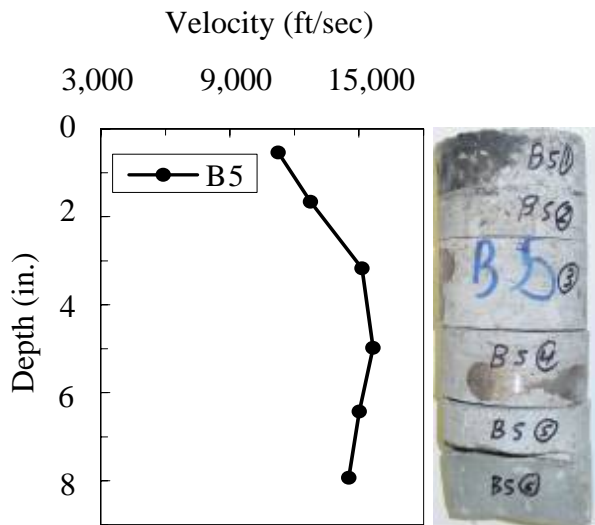
Figure 7.74. Ultrasonic velocity
with core depth for Core B5
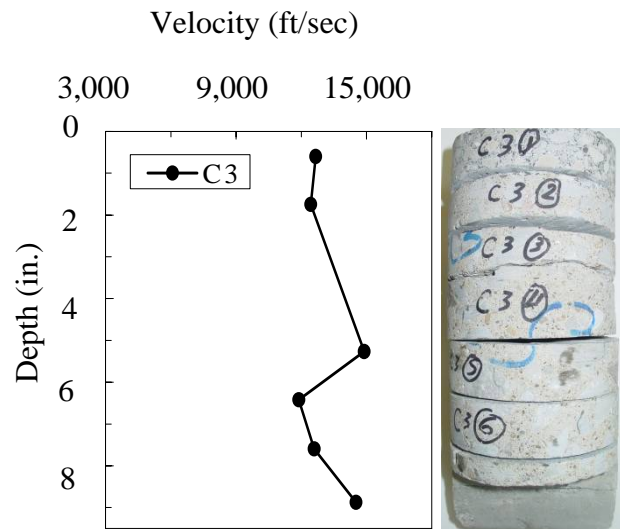
Figure 7.75. Ultrasonic velocity
with core depth for Core C3

1 ft/sec = 0.30 m/s, 1 in. = 25.4 mm
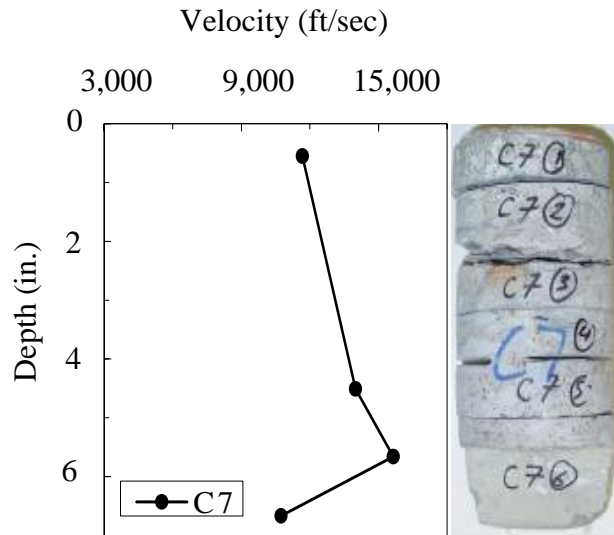
Figure 7.76. Ultrasonic velocity
with core depth for Core C7

1 ft/sec = 0.30 m/s, 1 in. = 25.4 mm

7.3.6 Bridge Deck Number 6 (LAK-90-23.42-SIPMF):

Visual Inspection of Cores from LAK-90-23.42 with SIPMF

The visual inspection of cores indicated that four of the five cores had an asphalt-wearing surface. The slicing for these cores was done to have only this asphalt layer in the first slice, which was eliminated from the calculations. Two different concrete layers were observed below the asphalt-wearing surface. The steel reinforcement generally showed some signs of rust. The five cores removed from Bridge Deck Number 6 were carefully inspected and illustrated as follows:

Core L3 (Figure 7.77-7.78)
- 10.25 in. (260.4 mm) height (12.25 in. (311.2 mm) with the concrete in the region of the valley of the SIPMF).
- Regions of large size honeycombing.
- 1 reinforcement bar located at 6 in. (152.4 mm) from the top surface.
- Some rust traces on the bar.
- Some cracks existed in the surface between the two concrete layers.

| Figure 7.77. Core L3 with asphalt wearing surface | Figure 7.78. Regions of cracks and honeycombing |

Core L6 (Figure 7.79-7.80)

- 10.25 in. (260.4 mm) height (11.75 in. (298.5 mm) with the concrete in the region of the valley of the SIPMF).
- 1 reinforcement bar located at 9.5 in. (241.3 mm) from the top surface.
- Rust traces on the bar.
- Region of small to moderate voids at the top layer of concrete.
- Region of honeycombing at the bottom layer of concrete.

Figure 7.79. Core L6 with
asphalt wearing surface

Figure 7.80. Voids region

Core L8 (Figure 7.81-7.82)
- 10.25 in. (260.4 mm) height (12 in. (304.8 mm) with the concrete in the region of the valley of the SIPMF).
- 1 reinforcement bar located at 9.5 in. (241.3 mm) from the top surface.
- Some rust traces on bars.
- Region of small voids at upper layer of concrete.
- Region of cracks and honeycombing at the surface between the two concrete layers.
- White traces on SIPMF.

Figure 7.81. Core L8 with
asphalt wearing surface

Figure 7.82. White traces
on SIPMF of core L8

Core L10 (Figure 7.83-7.84)
- 10.25 in. (260.4 mm) height (11.75 in. (298.5 mm) with the concrete in the region of the valley of the SIPMF).
- 1 reinforcement bar located at 9.5 in. (241.3mm) from the top surface.
- The bar is not coated and shows some rust traces.
- Region of small to moderate voids at upper layer of concrete.
- Core is broken approximately in the middle.

Figure 7.83. Core L10 with
asphalt wearing surface

Figure 7.84. Core is broken into two pieces

Core L12 (Figure 7.85-7.86)

- 9.5 in. (241.3 mm) height (11. 5 in. (292.1 mm) with the concrete in the region of the valley of the SIPMF).
- 1 reinforcement bar located at 9.0 in. (228.6 mm) from the top surface.
- Some rust traces on the bar.
- Region of small voids.
- Core is broken at top.
- White traces on SIPMF.

Figure 7.85. Core L12 shows rust traces on steel reinforcement

Figure 7.86. White traces on SIPMF

Ultrasonic Testing of Cores from LAK-90-23.42 with SIPMF
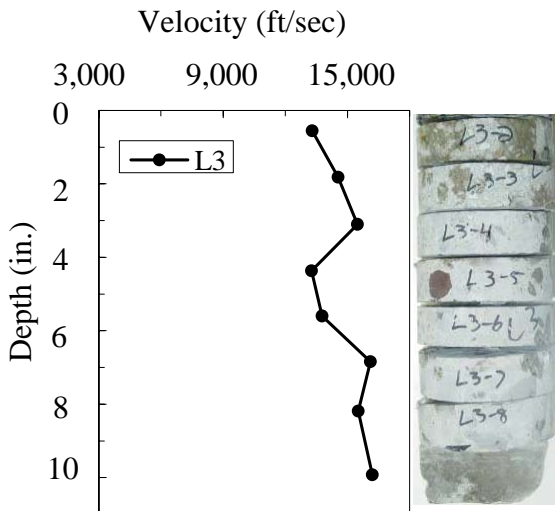
Figure 7.87. Ultrasonic velocity with core depth for Core L3
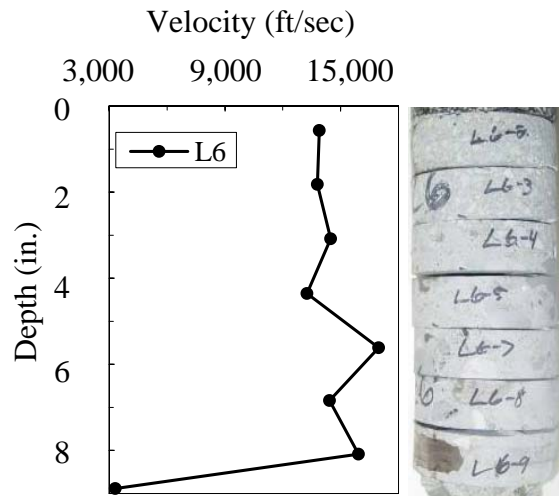
Figure 7.88. Ultrasonic velocity with core depth for Core L6

1 ft/sec = 0.30 m/s, 1 in. = 25.4 mm
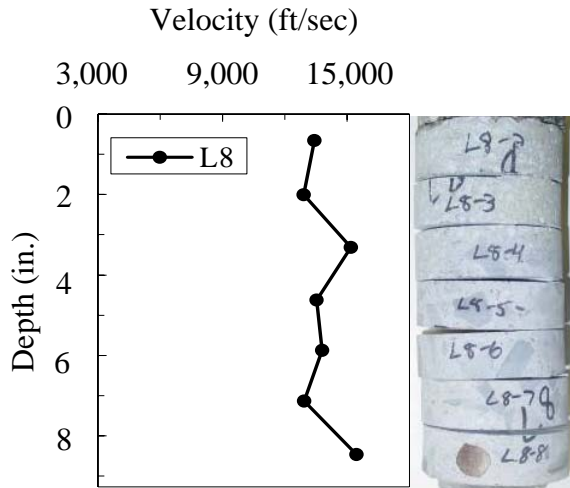
Figure 7.89. Ultrasonic velocity
with core depth for Core L8
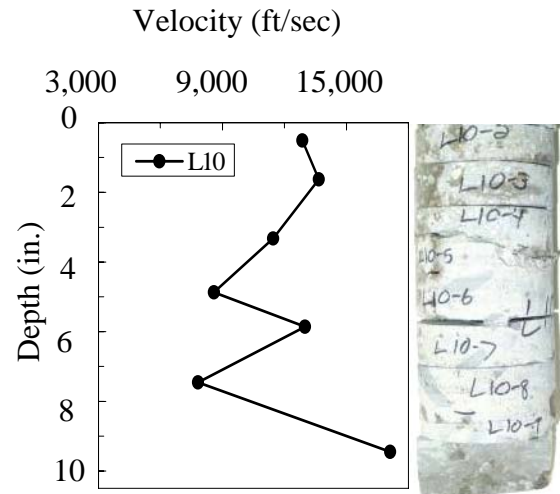
Figure 7.90. Ultrasonic velocity
with core depth for Core L10

1 ft/sec = 0.30 m/s, 1 in. = 25.4 mm
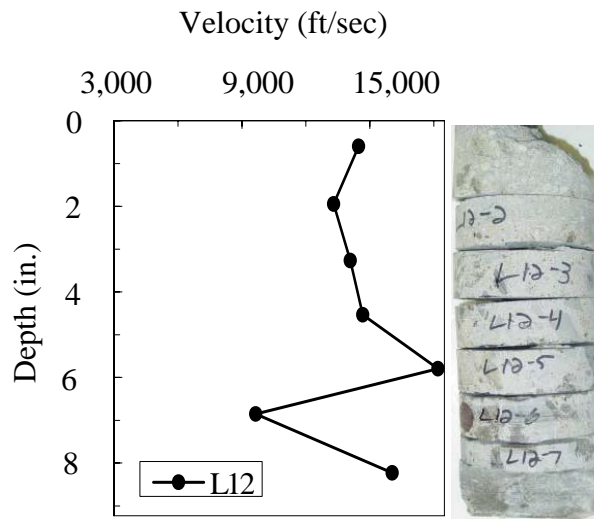
Figure 7.91. Ultrasonic velocity
with core depth for Core L12

1 ft/sec = 0.30 m/s, 1 in. = 25.4 mm

7 - 31

7.4 SUMMARY OF BRIDGE DECK INSPECTION AND CORING

This investigation included six concrete bridge decks located in Ohio. These bridge decks included: I. LOR-57-18.18 (bridge decks 1 and 4), II. OTT-2-28.41 (bridge decks 2 and 5), and III. LAK-90-23.42 (bridge decks 3 and 6). The investigation was done on a total of six concrete bridge decks, three decks constructed without SIPMF (bridge decks number 1 through 3) and three decks constructed with SIPMF (bridge decks number 4 through 6), which were analyzed and compared.

Comparisons were made using visual inspection and ultrasonic pulse velocity tests. Inspection indices were developed to quantify visual inspection test. Statistical analysis was used to compare all the test results obtained for decks constructed with and without SIPMF

7.4.1 Inspection of Cores

7.4.1.1 Visual Inspection

Visual inspection was used to determine general physical characteristics and overall condition of the cores that were obtained from the inspected bridges. A visual inspection index (*VII*) was developed to quantify the condition of cores based on visual inspection. The parameter was determined using visual inspection and rating of various characteristics of the reinforcing steel (when present in a core), concrete, and SIPMF. The characteristics analyzed for reinforcing steel were presence and condition of epoxy coating, and extent of rust. The characteristics analyzed for concrete were quantity, size, and alignment of cracking; quantity and size of voids; quantity and size of honeycombing; and porosity of aggregate and cement paste. The characteristics analyzed for SIPMF were the extent of rust. A numerical value is specified to indicate the condition of the various characteristics. The value of *VII* is calculated by dividing the summation of the numerical values for all the characteristics by the summation of the maximum potential numerical values, and converting to a percentage (by multiplying by 100). This parameter has a potential range of 0 to 100 (poor to excellent) that represents the overall quality of a core. *VII* ranged from 59 to 89 for bridge decks without SIPMF. The average *VII* for decks without SIPMF was 77. *VII* ranged from 57 to 81 for bridge decks with SIPMF. The average *VII* for bridge decks with SIPMF was 70.

Table 7.1: Visual Inspection Index (VII) for cores from No SIPMF deck slabs

No SIPMF												
		Steel	Concrete									
			Porosity		Honeycombing		Cracks		Voids				
Bridge Deck Number	Core	Condition of Rust	Concrete	Aggregate	Quantity	Size	Quantity	Size	Quantity	Size	Σ	VII $VII = (\Sigma / 27) * 100$	Average VII
		3	3	3	3	3	3	3	3	3	27		
1 LOR-57-18.18 without SIPMF	1C	2	3	3	2	1.5	3	3	2	2	22	81	84
	1F	2	3	3	3	3	2.5	2.5	2	2	23	85	
	1B	2	3	3	3	3	1	1	2	2	20	74	
	8E	3	3	3	2.5	2	3	3	2	2	24	89	
	8C2	2.5	3	3	2.5	2.5	3	3	2	2	24	89	
2 OTT-2-28.41 without SIPMF	A1	2.5	3	3	2	1.5	3	3	2	2	22	81	77
	A11	0	3	3	2	2	3	3	2.5	2.5	21	78	
	A16	1	3	3	1.5	1.5	3	3	2	1.5	20	74	
	A5	2	3	3	1	1	3	3	2	2	20	74	
	A9	0	3	3	2	2	3	3	2.5	2.5	21	78	
3 LAK-90-23.42 without SIPMF	L23	2	1	3	2	1.5	3	3	1	2	19	70	69
	L24	2	1.5	3	2.5	1	3	3	1	2	19	70	
	L26	2	1	3	1	0	3	3	1	2	16	59	
	L28	3	1.5	3	2	2	3	3	0	2	20	74	
	L31	2	2	3	2	1.5	3	3	1	2	20	74	

Table 7.2: Visual Inspection Index (VII) for cores from SIPMF deck slabs

Bridge Deck Number	Core	Steel	Concrete									SIPMF	Σ	VII = (Σ / 27) * 100	Average VII
			Porosity		Honeycombing		Cracks		Voids					
		Condition of Rust	Concrete	Aggregate	Quantity	Size	Quantity	Size	Quantity	Size	Condition of Rust			
		3	3	3	3	3	3	3	3	3	NA/3	27-30		
4 LOR-57-18.18 with SIPMF	6B	2	3	3	2	2	3	3	2	2	NA	22/27	81	
	4C	0	3	3	2	2	3	3	2	2	NA	20/27	74	
	7D	2	3	3	2	2	1.5	1.5	2	2	NA	19/27	70	70
	3D	0	1.5	3	2	2	3	3	1	1	NA	17/27	63	
	6C	2	3	3	0	0	3	3	1.5	1.5	NA	17/27	63	
5 OTT-2-28.41 with SIPMF	B1	2	3	3	2	2	3	3	2	2	2	24	80	
	B4	2	3	3	2	2	3	3	2	2	1.5	24	80	
	B5	2	3	3	2	0	3	3	2	2	1	21	70	71
	C3	0	3	3	2	2	1.5	1.5	2	2	0	17	57	
	C7	2	3	3	3	3	1	1	2	2	0	20	67	
6 LAK-90-23.42 with SIPMF	L3	2	1	3	1	0	3	3	1	2	3	19	63	
	L6	2	1	3	2	2	3	3	1	2	1.5	21	70	
	L8	2	1.5	3	2	2	2.5	2.5	1	2	2	21	70	69
	L10	1.5	2	3	1.5	2	1	1	1.5	2	2.5	18	60	
	L12	2	1	3	3	3	3	3	1	1.5	3	24	80	

7.4.1.2 Ultrasonic Testing

Ultrasonic velocity was measured on individual slices of each core. The ultrasonic measurements for each core are presented at the end of each coring location section. All of the ultrasonic data (velocity vs. depth) obtained in the test program are summarized in Figures 7.92 through 7.97. Average trends are shown in Figures 7.98 through 7.101. Average velocities for cores were calculated as weighted averages obtained by taking into consideration the thickness and corresponding pulse velocity of each slice from a core. This approach was used, as the thicknesses of specimens obtained for a core were variable. Some of the cores had an asphalt-wearing surface. The slicing for these cores was done so that only this asphalt layer was attached in the first slice, which was eliminated from the calculations. Some of the cores for the deck slabs without SIPMF extended only to the top level of the bottom reinforcement due to restrictions during coring. The calculation of the velocity for these cores was based on assuming a depth of 2 in. for an imaginary slice with the same velocity as the preceding slice.

To better quantify the results of this analysis, a parameter termed Quality Index (*QI*) was introduced. The profile of wave velocity with depth can be quantified by taking the product of incremental wave velocity (for a given slice) and length of that particular slice. This is effectively represented as area contained by the velocity vs. length (along a core depth) plot. This area, considered alone, would bias results of longer cores. Therefore, a normalization of the quantity was achieved by dividing this summed area by total length of the core. The normalized value, *QI*, had units consistent with velocity (ft/s) and represented a weighted average of the wave velocity with depth over the entire profile (Figure 7.102). This parameter provided an effective means for comparison of the integrity of concrete between different cores. The results of this analysis for each core are presented in Tables 7.3-7.11. The *QI* representing all bridge deck cores without SIPMF (calculated for the total length of all analyzed cores from bridge decks without SIPMF) was 12,984 ft/s (Table 7.12). The *QI* representing all bridge deck cores with SIPMF (calculated for the total length of all analyzed cores from bridge decks with SIPMF) was 13,663 ft/s (Table 7.14). Even though the *QI* for bridge decks with SIPMF was greater than *QI* for bride decks without SIPMF, the difference in *QI* between the two bridge deck systems was considered negligible (5.0%). Results from the through-transmission ultrasonic measurements demonstrated the similarity of the integrity of the concrete in the two bridge deck systems.

The average *QI* for cores obtained from bridge decks without SIPMF was 12,969 ft/s (Table 7.12) and the average *QI* for cores obtained from bridge decks with SIPMF was 13,652 ft/s (Table 7.14). The average *QI* for all the cores tested in the study was 13,311 ft/s. The average *QI* for the bridge decks were compared statistically to determine equivalency between the decks. A student's t-test was conducted to compare the average *QI* for decks constructed with and without SIPMF based on the values provided in Tables 7.12 and 7.14. The data were compared using a two-tailed analysis with a 95% confidence interval. The $t_{critical}$ value for this dataset was equal to 2.23 and the t-statistic was calculated to be 7.81. The average *QI* for cores obtained from the two types of bridge decks were deemed statistically similar, as the t-statistic was less than $t_{critical}$.

The variation of pulse velocity with depth was investigated by dividing the cores into three equal regions with depth: top, middle, and bottom. The results of this analysis are presented in Tables 7.3 through 7.11 for individual cores. The region specific results are summarized in tables 7.13 and 7.15 for each bridge deck. Average *QI* is presented for each region of the cores. In addition, ratios of region-specific *QI* to average *QI* for a given bridge deck are provided. It was observed that average *QI* and region-specific *QI* were similar for cores from both bridge deck systems. A student's t-test was conducted to compare the region-specific *QI* for decks constructed with and without SIPMF based on the values provided in Tables 7.13 and 7.15. The data were compared using a two-tailed analysis with a 95% confidence interval. The $t_{critical}$ value for this dataset was equal to 2.23 and the t-statistic values were calculated to be 0.86, 0.10, and 2.03 for *QI* of top, middle, and bottom regions, respectively. The region-specific *QI* for cores obtained from the two types of bridge decks were considered statistically similar for as the t-statistic was less than $t_{critical}$. The region specific analysis did not indicate specially beneficial or adverse effect of the presence of SIPMF on the bridge deck as a function of the depth.

Table 7.3: Ultrasonic velocity for Cores 1C, 1F, 1B, and 8E.

Slice No.	Thickness (in.)	Mid Point depth (h) (in.)	Velocity (V) (ft/s)	Σ V(Δh) (in.ft/s)	Slice No.	Thickness (in.)	Mid Point depth (h) (in.)	Velocity (V) (ft/s)	Σ V(Δh) (in.ft/s)
		Core 1C					Core 1F		
	1 in. = 25.4 mm	1 in. = 25.4 mm	1 ft/s = 0.30 m/s	1 in. ft/s = 0.0076 m²/s		1 in. = 25.4 mm	1 in. = 25.4 mm	1 ft/s = 0.30 m/s	1 in. ft/s = 0.0076 m²/s
1	1.17	0.59	14,412	8,474.12	1	1.14	0.57	11,875	6,768.75
2	1.06	1.82	14,369	17,697.59	2	1.08	1.80	11,219	14,244.99
3	1.19	3.06	13,819	17,460.22	3	1.12	3.03	12,951	14,782.05
4	1.11	4.32	14,736	18,041.19	4	1.14	4.28	14,779	17,361.31
5	1.17	5.57	14,350	18,209.45	5	1.15	5.55	14,663	18,653.80
6	0.81	6.67	11,744	14,385.62	6	1.00	6.75	13,034	16,620.48
7	1.01	7.70	13,190	12,761.01	7	1.38	8.06	14,610	28,237.30
8	0.93	8.78	12,394	19,661.90					
Σ =	9.25			126,691.1	Σ =	8.75			116,668.6
V_{max} =			14,736		V_{max} =			14,779	
QI_{avrg} =				13,696.34	QI_{avrg} =				13,333.56
QI_{top} =				14,270.61	QI_{top} =				11,786.60
QI_{mid} =				14,268.20	QI_{mid} =				14,258.78
QI_{bot} =				12,550.20	QI_{bot} =				13,955.31
QI_{top} / V_{max} =				0.97	QI_{top} / V_{max} =				0.80
QI_{top} / QI_{avrg} =				1.04	QI_{top} / QI_{avrg} =				0.88
QI_{mid} / V_{max} =				0.97	QI_{mid} / V_{max} =				0.96
QI_{mid} / QI_{avrg} =				1.04	QI_{mid} / QI_{avrg} =				1.07
QI_{bot} / V_{max} =				0.85	QI_{bot} / V_{max} =				0.94
QI_{bot} / QI_{avrg} =				0.92	QI_{bot} / QI_{avrg} =				1.05

{(--) Indicates no available data}

Table 7.3: Ultrasonic velocity for Cores 1C, 1F, 1B, and 8E, continued

	Core 1B					Core 8E			
Slice No.	Thickness (in.)	Mid Point depth (h) (in.)	Velocity (V) (ft/s)	$\Sigma V(\Delta h)$ (in.ft/s)	Slice No.	Thickness (in.)	Mid Point depth (h) (in.)	Velocity (V) (ft/s)	$\Sigma V(\Delta h)$ (in.ft/s)
	1 in. = 25.4 mm	1 in. = 25.4 mm	1 ft/s = 0.30 m/s	1 in. ft/s = 0.0076 m^2/s		1 in. = 25.4 mm	1 in. = 25.4 mm	1 ft/s = 0.30 m/s	1 in. ft/s = 0.0076 m^2/s
1	5.00		(--)	(--)	1	1.27	0.64	11,205	7,126.43
2		2.5			2	0.69	1.73	8,395	10,739.93
3	1.10	5.73	13,468	77,188.14	3	1.26	2.82	13,838	12,126.94
4	1.17	7.05	14,081	18,136.71	4	1.20	4.17	15,301	19,638.57
5	1.18	8.41	13,114	26,258.58	5	1.12	5.45	14,609	19,111.77
					6	0.73	6.49	10,893	13,317.63
					7	1.30	7.62	15,882	15,147.12
					8	0.60	8.70	7,943	15,174.04
Σ =	9.00			121,583.42	Σ =	9.00			112,382.43
V_{max} =			14,081		V_{max} =			15,882	
QI_{avrg} =				13,509.27	QI_{avrg} =				12,486.94
QI_{top} =				13,468.14	QI_{top} =				10,820.53
QI_{mid} =				13,473.75	QI_{mid} =				14,598.42
QI_{bot} =				13,585.92	QI_{bot} =				12,041.86
QI_{top} / V_{max} =				0.96	QI_{top} / V_{max} =				0.68
QI_{top} / QI_{avrg} =				1.00	QI_{top} / QI_{avrg} =				0.87
QI_{mid} / V_{max} =				0.96	QI_{mid} / V_{max} =				0.92
QI_{mid} / QI_{avrg} =				1.00	QI_{mid} / QI_{avrg} =				1.17
QI_{bot} / V_{max} =				0.96	QI_{bot} / V_{max} =				0.76
QI_{bot} / QI_{avrg} =				1.01	QI_{bot} / QI_{avrg} =				0.96

{(--) Indicates no available data}

Table 7.4: Ultrasonic velocity for Cores 8C2, 6B, 4C and 7D

Core 8C2				Core 6B				
Slice No.	Thickness (in.)	Mid Point depth (h) (in.)	Velocity (V) (ft/s)	Σ V(Δh) (in.ft/s)	Slice No.	Thickness (in.)	Mid Point depth (h) (in.)	Velocity (V) (ft/s)	Σ V(Δh) (in.ft/s)
	1 in. = 25.4 mm	1 in. = 25.4 mm	1 ft/s = 0.30 m/s	1 in. ft/s = 0.0076 m^2/s		1 in. = 25.4 mm	1 in. = 25.4 mm	1 ft/s = 0.30 m/s	1 in. ft/s = 0.0076 m^2/s
1	1.05	0.53	10,783	5,671.91	1	1.17	0.59	10,029	5,872.05
2	0.88	1.66	9,594	11,567.23	2	1.14	1.87	13,660	15,179.91
3	1.41	2.97	16,285	16,986.99	3	1.23	3.18	14,259	18,316.30
4	1.10	4.40	13,764	21,414.05	4	1.10	4.47	14,310	18,478.12
5	1.13	5.69	14,164	17,982.79	5	1.16	5.73	15,130	18,526.24
6	2.58				6	0.63	6.76	7,714	11,694.43
7		7.71	13,411	45,191.71	7	1.34	7.87	14,726	12,502.87
					8	1.08	9.21	12,065	24,471.65
Σ =	9.00			118,814.69	Σ =	9.75			125,041.58
V_{max} =			16,285		V_{max} =			15,130	
QI_{avrg} =				13,201.63	QI_{avrg} =				12,824.78
QI_{top} =				11,549.87	QI_{top} =				12,424.23
QI_{mid} =				14,461.91	QI_{mid} =				13,995.27
QI_{bot} =				13,593.11	QI_{bot} =				12,054.84
QI_{top} / V_{max} =				0.71	QI_{top} / V_{max} =				0.82
QI_{top} / QI_{avrg} =				0.87	QI_{top} / QI_{avrg} =				0.97
QI_{mid} / V_{max} =				0.89	QI_{mid} / V_{max} =				0.92
QI_{mid} / QI_{avrg} =				1.10	QI_{mid} / QI_{avrg} =				1.09
QI_{bot} / V_{max} =				0.83	QI_{bot} / V_{max} =				0.80
QI_{bot} / QI_{avrg} =				1.03	QI_{bot} / QI_{avrg} =				0.94

{(--) Indicates no available data}

Table 7.4: Ultrasonic velocity for Cores 8C2, 6B, 4C and 7D, continued

		Core 4C					Core 7D		
Slice No.	Thickness (in.)	Mid Point depth (h) (in.)	Velocity (V) (ft/s)	Σ V(Δh) (in.ft/s)	Slice No.	Thickness (in.)	Mid Point depth (h) (in.)	Velocity (V) (ft/s)	Σ V(Δh) (in.ft/s)
	1 in. = 25.4 mm	1 in. = 25.4 mm	1 ft/s = 0.30 m/s	1 in. ft/s = 0.0076 m²/s		1 in. = 25.4 mm	1 in. = 25.4 mm	1 ft/s = 0.30 m/s	1 in. ft/s = 0.0076 m²/s
1	2.35	1.17	17,042	19,981.92	1	1.14	0.57	13,160	7,481.30
2					2	1.16	1.82	14,154	17,071.33
3	0.90	2.96	13,104	27,007.53	3	1.15	3.08	14,974	18,299.90
4	1.20	4.19	13,924	16,497.38	4	1.07	4.29	13,906	17,515.85
5	1.13	5.52	12,336	17,499.09	5	1.14	5.50	15,847	17,978.54
6	1.12	6.81	13,480	16,674.27	6	1.33	6.84	16,629	32,792.97
7	0.71	7.89	11,109	17,286.68					
Σ =	8.25			114,946.88	Σ =	7.50			111,139.89
V_{max} =			17,042		V_{max} =			16,629	
QI_{avrg} =				13,932.95	QI_{avrg} =				14,818.65
QI_{top} =				16,047.60	QI_{top} =				13,740.13
QI_{mid} =				13,321.47	QI_{mid} =				14,530.56
QI_{bot} =				12,434.81	QI_{bot} =				16,185.26
QI_{top} / V_{max} =				0.94	QI_{top} / V_{max} =				0.83
QI_{top} / QI_{avrg} =				1.15	QI_{top} / QI_{avrg} =				0.93
QI_{mid} / V_{max} =				0.78	QI_{mid} / V_{max} =				0.87
QI_{mid} / QI_{avrg} =				0.96	QI_{mid} / QI_{avrg} =				0.98
QI_{bot} / V_{max} =				0.73	QI_{bot} / V_{max} =				0.97
QI_{bot} / QI_{avrg} =				0.89	QI_{bot} / QI_{avrg} =				1.09

{(--) Indicates no available data}

Table 7.5: Ultrasonic velocity for Cores 3D and 6C

	Core 3D					Core 6C			
Slice No.	Thickness (in.)	Mid Point depth (h) (in.)	Velocity (V) (ft/s)	Σ V(Δh) (in.ft/s)	Slice No.	Thickness (in.)	Mid Point depth (h) (in.)	Velocity (V) (ft/s)	Σ V(Δh) (in.ft/s)
	1 in. = 25.4 mm	1 in. = 25.4 mm	1 ft/s = 0.30 m/s	1 in. ft/s = 0.0076 m^2/s		1 in. = 25.4 mm	1 in. = 25.4 mm	1 ft/s = 0.30 m/s	1 in. ft/s = 0.0076 m^2/s
1	2.59	1.29	5,835	7,544.44	1	1.245	0.62	12,064	7,509.81
2					2	1.087	1.93	14,470	17,333.42
3	1.10	3.27	14,323	19,899.06	3	2.508	2.51	(--)	(--)
4	2.36	(--)	(--)	(--)	4				
5					5	1.132	5.83	14,740	56,937.13
6	1.06	6.97	13,802	59,383.85	6	0.829	6.95	12,049	15,015.24
					7	1.176	8.09	15,000	15,458.74
					8	1.055	9.35	10,814	21,915.41
Σ =	7.50			86,827.36	Σ =	9.88			134,169.76
V_{max} =			14,323		V_{max} =			15,000	
QI_{avrg} =				11,576.98	QI_{avrg} =				13,586.81
QI_{top} =				7,087.50	QI_{top} =				13,557.09
QI_{mid} =				13,732.18	QI_{mid} =				14,311.69
QI_{bot} =				13,911.26	QI_{bot} =				12,891.65
QI_{top} / V_{max} =				0.49	QI_{top} / V_{max} =				0.90
QI_{top} / QI_{avrg} =				0.61	QI_{top} / QI_{avrg} =				1.00
QI_{mid} / V_{max} =				0.96	QI_{mid} / V_{max} =				0.95
QI_{mid} / QI_{avrg} =				1.19	QI_{mid} / QI_{avrg} =				1.05
QI_{bot} / V_{max} =				0.97	QI_{bot} / V_{max} =				0.86
QI_{bot} / QI_{avrg} =				1.20	QI_{bot} / QI_{avrg} =				0.95

{(--) Indicates no available data}

Table 7.6: Ultrasonic velocity for Cores A1, A11, A16, and A5

Slice No.	Thickness (in.)	Mid Point depth (h) (in.)	Velocity (V) (ft/s)	Σ V(Δh) (in.ft/s)	Slice No.	Thickness (in.)	Mid Point depth (h) (in.)	Velocity (V) (ft/s)	Σ V(Δh) (in.ft/s)
	1 in. = 25.4 mm	1 in. = 25.4 mm	1 ft/s = 0.30 m/s	1 in. ft/s = 0.0076 m^2/s		1 in. = 25.4 mm	1 in. = 25.4 mm	1 ft/s = 0.30 m/s	1 in. ft/s = 0.0076 m^2/s
1	1.20	0.60	12,942	7,771.56	1	1.23	0.61	--	--
2	1.15	1.87	12,193	15,981.42	2	1.02	1.78	13,656	24,317.28
3	1.02	3.05	12,959	14,829.19	3	1.81	3.24	9,101	16,581.15
4	1.26	4.28	13,599	16,395.34	4	1.15	4.76	13,045	16,867.21
5&6	2.82	6.42	14,339	29,861.67	5	1.18	5.97	14,207	16,456.43
7	1.21	8.53	18,051	34,222.76	6	1.08	7.14	13,776	16,421.58
8	1.76	10.12	14,294	38,180.94	7	1.28	8.36	16,641	18,579.91
					8	1.70	9.90	15,662	**38,115.14**
Σ =	11			157,242.88	Σ =	10.75			147,338.69
V$_{max}$ =			18,050		V$_{max}$ =			16,641	
QI_{avrg} =				14,294.81	QI_{avrg} =				13,705.92
QI_{top} =				12,723.96	QI_{top} =				12,333.92
QI_{mid} =				14,169.65	QI_{mid} =				13,054.80
QI_{bot} =				15,990.81	QI_{bot} =				15,729.06
QI_{top} / V$_{max}$ =				0.70	QI_{top} / Vs$_{max}$ =				0.74
QI_{top} / QI_{avrg} =				0.89	QI_{top} / QI_{avrg} =				0.90
QI_{mid} / V$_{max}$ =				0.78	QI_{mid} / V$_{max}$ =				0.78
QI_{mid} / QI_{avrg} =				0.99	QI_{mid} / QI_{avrg} =				0.95
QI_{bot} / V$_{max}$ =				0.89	QI_{bot} / V$_{max}$ =				0.95
QI_{bot} / QI_{avrg} =				1.12	QI_{bot} / QI_{avrg} =				1.15

{(--) Indicates no available data}

Table 7.6: Ultrasonic velocity for Cores A1, A11, A16, and A5, continued

Core A16					Core A5				
Slice No.	Thickness (in.)	Mid Point depth (h) (in.)	Velocity (V) (ft/s)	Σ V(Δh) (in.ft/s)	Slice No.	Thickness (in.)	Mid Point depth (h) (in.)	Velocity (V) (ft/s)	Σ V(Δh) (in.ft/s)
	1 in. = 25.4 mm	1 in. = 25.4 mm	1 ft/s = 0.30 m/s	1 in. ft/s = 0.0076 m²/s		1 in. = 25.4 mm	1 in. = 25.4 mm	1 ft/s = 0.30 m/s	1 in. ft/s = 0.0076 m²/s
1	1.29	0.64	12,778	8,228.89	1	1.122	0.56	11,688	6,556.69
2	1.10	1.91	13,456	16,611.53	2	1.177	1.82	11,865	14,830.17
3	1.18	3.12	13,611	16,381.33	3	1.073	3.06	11,177	14,226.52
4	1.11	4.34	15,082	17,451.27	4	1.197	4.30	14,963	16,269.71
5	1.13	5.53	12,379	16,379.45	5	1.098	5.56	13,456	17,865.69
6	1.24	6.79	13,873	16,531.36	6	2.804	7.62	11,454	25,667.81
7	1.10	8.04	14,654	17,771.32	7	1.87	10.07	13,914	44,044.86
8	1.84	9.58	15,753	37,974.40					
Σ	10.5			147,329.54	Σ =	11.00			139,461.45
V_{max} =			15,753		V_{max} =			14,963	
QI_{avrg} =				14,031.38	QI_{avrg} =				12,678.31
QI_{top} =				13,276.91	QI_{top} =				11,731.83
QI_{mid} =				13,751.38	QI_{mid} =				13,390.35
QI_{bot} =				15,065.86	QI_{bot} =				12,912.77
QI_{top} / V_{max} =				0.84	QI_{top} / V_{max} =				0.78
QI_{top} / QI_{avrg} =				0.95	QI_{top} / QI_{avrg} =				0.93
QI_{mid} / V_{max} =				0.87	QI_{mid} / V_{max} =				0.89
QI_{mid} / QI_{avrg} =				0.98	QI_{mid} / QI_{avrg} =				1.06
QI_{bot} / V_{max} =				0.96	QI_{bot} / V_{max} =				0.86
QI_{bot} / QI_{avrg} =				1.07	QI_{bot} / QI_{avrg} =				1.02

{(--) Indicates no available data}

Table 7.7: Ultrasonic velocity for Cores A9, B1, B4, and B5

		Core A9					Core B1		
Slice No.	Thickness (in.)	Mid Point depth (h) (in.)	Velocity (V) (ft/s)	Σ V(Δh) (in.ft/s)	Slice No.	Thickness (in.)	Mid Point depth (h) (in.)	Velocity (V) (ft/s)	Σ V(Δh) (in.ft/s)
	1 in. = 25.4 mm	1 in. = 25.4 mm	1 ft/s = 0.30 m/s	1 in. ft/s = 0.0076 m²/s		1 in. = 25.4 mm	1 in. = 25.4 mm	1 ft/s = 0.30 m/s	1 in. ft/s = 0.0076 m²/s
1	1.146	0.57	--	--	1	1.21	0.60	13,705	8,263.84
2	1.074	1.78	12,431	22,167.23	2	1.18	1.89	13,915	17,782.44
3	1.078	2.96	8,318	12,203.06	3	1.49	3.32	13,451	19,528.05
4	1.191	4.19	12,406	12,794.94	4	1.13	4.72	14,426	19,551.14
5	1.313	5.54	12,248	16,669.89	5	0.66	5.71	8,051	11,111.37
6	1.637	7.12	10,884	18,220.10	6	1.15	6.71	15,253	11,613.22
7	1.03	8.5	10,911	15,624.91	7	1.88	8.31	15,845	39,835.92
8	1.829	10.08	13,449	30,931.12					
Σ	11.00			128,611.26	Σ =	9.25			127,686.00
V_{max} =			13,449		V_{max} =			15,845	
QI_{avrg} =				11,691.93	QI_{avrg} =				13,803.89
QI_{top} =				11,203.51	QI_{top} =				13,754.96
QI_{mid} =				11,802.84	QI_{mid} =				12,410.41
QI_{bot} =				12,069.44	QI_{bot} =				15,246.31
QI_{top} / V_{max} =				0.83	QI_{top} / V_{max} =				0.87
QI_{top} / QI_{avrg} =				0.96	QI_{top} / QI_{avrg} =				1.00
QI_{mid} / V_{max} =				0.88	QI_{mid} / V_{max} =				0.78
QI_{mid} / QI_{avrg} =				1.01	QI_{mid} / QI_{avrg} =				0.90
QI_{bot} / V_{max} =				0.90	QI_{bot} / V_{max} =				0.96
QI_{bot} / QI_{avrg} =				1.03	QI_{bot} / QI_{avrg} =				1.10

{(--) Indicates no available data}

Table 7.7: Ultrasonic velocity for Cores A9, B1, B4, and B5, continued

	Core B4					Core B5			
Slice No.	Thickness (in.)	Mid Point depth (h) (in.)	Velocity (V) (ft/s)	Σ V(Δh) (in.ft/s)	Slice No.	Thickness (in.)	Mid Point depth (h) (in.)	Velocity (V) (ft/s)	Σ V(Δh) (in.ft/s)
	1 in. = 25.4 mm	1 in. = 25.4 mm	1 ft/s = 0.30 m/s	1 in. ft/s = 0.0076 m^2/s		1 in. = 25.4 mm	1 in. = 25.4 mm	1 ft/s = 0.30 m/s	1 in. ft/s = 0.0076 m^2/s
1	1.29	0.64	12,984	8,361.61	1	1.08	0.54	11,240	6,063.76
2	1.10	1.92	14,946	17,923.77	2	0.94	1.66	12,745	13,434.72
3	1.17	3.15	14,289	17,869.81	3	1.87	3.17	15,146	21,110.45
4	1.17	4.41	14,289	17,940.11	4	1.53	4.98	15,645	27,840.22
5	1.11	5.63	14,196	17,504.43	5	1.15	6.43	15,013	22,255.01
6	1.17	6.87	14,663	17,784.31	6	1.63	7.94	14,536	34,027.60
7	1.46	8.27	14,928	31,655.38					
Σ =	9.00			129,039.43	Σ =	8.75			124,731.76
V_{max} =			14,946		V_{max} =			15,645	
QI_{avrg} =				14,337.71	QI_{avrg} =				14,255.0
QI_{top} =				14,001.92	QI_{top} =				12,606.77
QI_{mid} =				14,269.34	QI_{mid} =				15,374.60
QI_{bot} =				14,741.88	QI_{bot} =				14,783.81
QI_{top} / V_{max} =				0.94	QI_{top} / V_{max} =				0.81
QI_{top} / QI_{avrg} =				0.98	QI_{top} / QI_{avrg} =				0.88
QI_{mid} / V_{max} =				0.95	QI_{mid} / V_{max} =				0.98
QI_{mid} / QI_{avrg} =				1.00	QI_{mid} / QI_{avrg} =				1.08
QI_{bot} / V_{max} =				0.99	QI_{bot} / V_{max} =				0.94
QI_{bot} / QI_{avrg} =				1.03	QI_{bot} / QI_{avrg} =				1.04

{(--) Indicates no available data}

Table 7.8: Ultrasonic velocity for Cores C3 and C7

Core C3					Core C7				
Slice No.	Thickness (in.)	Mid Point depth (h) (in.)	Velocity (V) (ft/s)	Σ V(Δh) (in.ft/s)	Slice No.	Thickness (in.)	Mid Point depth (h) (in.)	Velocity (V) (ft/s)	Σ V(Δh) (in.ft/s)
	1 in. = 25.4 mm	1 in. = 25.4 mm	1 ft/s = 0.30 m/s	1 in. ft/s = 0.0076 m²/s		1 in. = 25.4 mm	1 in. = 25.4 mm	1 ft/s = 0.30 m/s	1 in. ft/s = 0.0076 m²/s
1	1.20	0.60	12669.49	7,576.36	1	1.10	0.55	11,875	6,543.13
2	0.98	1.75	12436.22	14,468.96	2	1.43	1.93	--	--
3	0.91	2.76	--	--	3	1.15	3.34	--	--
4	1.36	3.96	--	--	4	0.96	4.51	13,997	51,230.63
5	1.12	5.27	14893.62	48,072.22	5	1.10	5.66	15,653	17,050.52
6	1.05	6.42	11886.36	15,400.40	6	0.67	6.67	10,737	16,839.75
7	1.17	7.59	12596.98	14,379.59					
8	1.26	8.87	14525.46	26,461.47					
Σ =	9.50			126,359.00	Σ =	7.00			91,664.02
V_{max} =			14,894		V_{max} =			15,653	
QI_{avrg} =				13,300.9	QI_{avrg} =				13,094.8
QI_{top} =				12,743.88	QI_{top} =				12,239.76
QI_{mid} =				13,896.88	QI_{mid} =				13,459.87
QI_{bot} =				13,262.08	QI_{bot} =				13,584.95
QI_{top} / V_{max} =				0.86	QI_{top} / V_{max} =				0.78
QI_{top} / QI_{avrg} =				0.96	QI_{top} / QI_{avrg} =				0.93
QI_{mid} / V_{max} =				0.93	QI_{mid} / V_{max} =				0.86
QI_{mid} / QI_{avrg} =				1.04	QI_{mid} / QI_{avrg} =				1.03
QI_{bot} / V_{max} =				0.89	QI_{bot} / V_{max} =				0.87
QI_{bot} / QI_{avrg} =				1.00	QI_{bot} / QI_{avrg} =				1.04

{(--) Indicates no available data}

Table 7.9: Ultrasonic velocity for Cores L23, L24, L26, and L28

		Core L23					Core L24		
Slice No.	Thickness (in.)	Mid Point depth (h) (in.)	Velocity (V) (ft/s)	Σ V(Δh) (in.ft/s)	Slice No.	Thickness (in.)	Mid Point depth (h) (in.)	Velocity (V) (ft/s)	Σ V(Δh) (in.ft/s)
	1 in. = 25.4 mm	1 in. = 25.4 mm	1 ft/s = 0.30 m/s	1 in. ft/s = 0.0076 m²/s		1 in. = 25.4 mm	1 in. = 25.4 mm	1 ft/s = 0.30 m/s	1 in. ft/s = 0.0076 m²/s
2	1.18	0.59	13,409	7,911.36	2	1.15	0.57	13,514	7,743.61
3	1.203	1.88	14,186	17,843.39	3	1.20	1.87	13,670	17,579.38
4	1.231	3.20	13,040	17,952.04	4	2.21	3.69	12,551	23,925.02
5	1.152	4.50	13,846	17,384.94	5	1.10	5.46	14,918	24,342.66
6	1.17	5.76	15,559	18,564.84	6	1.16	6.71	13,882	17,933.23
7	1.025	6.96	13,927	17,679.50	7	0.56	7.69	8,169	10,775.50
8	0.457	7.80	6,642	8,666.93	8	2.00	8.97	--	18,632.59
9	2.0	9.03	--	14,814.07					
Σ =	10.03			120,817.0	Σ =	9.97			120,931.98
V_{max} =			15,559		V_{max} =			14,918	
QI_{avrg} =				12,045.57	QI_{avrg} =				12,133.03
QI_{top} =				13,626.21	QI_{top} =				13,417.37
QI_{mid} =				14,346.02	QI_{mid} =				13,862.08
QI_{bot} =				8,164.48	QI_{bot} =				9,119.65
QI_{top} / V_{max} =				0.88	QI_{top} / V_{max} =				0.90
QI_{top} / QI_{avrg} =				1.13	QI_{top} / QI_{avrg} =				1.11
QI_{mid} / V_{max} =				0.92	QI_{mid} / V_{max} =				0.93
QI_{mid} / QI_{avrg} =				1.19	QI_{mid} / QI_{avrg} =				1.14
QI_{bot} / V_{max} =				0.52	QI_{bot} / V_{max} =				0.61
QI_{bot} / QI_{avrg} =				0.68	QI_{bot} / QI_{avrg} =				0.75

{(--) Indicates no available data}

Table 7.9: Ultrasonic velocity for Cores L23, L24, L26, and L28, continued

	Core L26					Core L28			
Slice No.	Thickness (in.)	Mid Point depth (h) (in.)	Velocity (V) (ft/s)	Σ V(Δh) (in.ft/s)	Slice No.	Thickness (in.)	Mid Point depth (h) (in.)	Velocity (V) (ft/s)	Σ V(Δh) (in.ft/s)
	1 in. = 25.4 mm	1 in. = 25.4 mm	1 ft/s = 0.30 m/s	1 in. ft/s = 0.0076 m²/s		1 in. = 25.4 mm	1 in. = 25.4 mm	1 ft/s = 0.30 m/s	1 in. ft/s = 0.0076 m²/s
	0.96	0.48	11,333	5,445.29	2	1.31	0.65	13,185	8,623.31
3	1.09	1.63	13,575	14,345.50	3	1.20	2.11	14,104	19,916.61
4	2.44		17,301	29,168.69	4	1.20	3.52	15,332	20,702.90
5					5	1.15	4.90	14,375	20,552.04
6	1.15	5.44	11,369	27,514.78	6	1.19	6.28	14,813	20,068.84
7	0.83	6.56	8,377	11,027.19	7	1.14	7.65	14,515	20,077.33
8	2.00	7.97	--	21,293.54	8	2.00	9.22	--	37,328.53
Σ =	8.97			107,705.97	Σ =	10.22			147,269.55
V_{max} =			17,301		V_{max} =			15,332	
QI_{avrg} =				12,007.35	QI_{avrg} =				14,409.94
QI_{top} =				13,390.50	QI_{top} =				13,944.94
QI_{mid} =				13,499.50	QI_{mid} =				14,747.35
QI_{bot} =				9,132.06	QI_{bot} =				14,537.52
QI_{top} / V_{max} =				0.77	QI_{top} / V_{max} =				0.91
QI_{top} / QI_{avrg} =				1.12	QI_{top} / QI_{avrg} =				0.97
QI_{mid} / V_{max} =				0.78	QI_{mid} / V_{max} =				0.96
QI_{mid} / QI_{avrg} =				1.12	QI_{mid} / QI_{avrg} =				1.02
QI_{bot} / V_{max} =				0.53	QI_{bot} / V_{max} =				0.95
QI_{bot} / QI_{avrg} =				0.76	QI_{bot} / QI_{avrg} =				1.01

{(--) Indicates no available data}

Table 7.10: Ultrasonic velocity for Cores L31, L3, L6, and L8

	Core L31					Core L3			
Slice No.	Thickness (in.)	Mid Point depth (h) (in.)	Velocity (V) (ft/s)	Σ V(Δh) (in.ft/s)	Slice No.	Thickness (in.)	Mid Point depth (h) (in.)	Velocity (V) (ft/s)	Σ V(Δh) (in.ft/s)
	1 in. = 25.4 mm	1 in. = 25.4 mm	1 ft/s = 0.30 m/s	1 in. ft/s = 0.0076 m²/s		1 in. = 25.4 mm	1 in. = 25.4 mm	1 ft/s = 0.30 m/s	1 in. ft/s = 0.0076 m²/s
2	0.94	0.47	11,556	5,448.83	2	1.11	0.55	13,293	7,351.18
3	1.23	1.71	14,201	15,931.18	3	1.23	1.82	14,540	17,595.90
4	1.15	3.05	13,597	18,652.52	4	1.15	3.10	15,484	19,326.05
5	1.24	4.40	16,861	20,544.00	5	1.19	4.37	13,270	18,192.27
6	1.08	5.71	14,295	20,407.59	6	1.08	5.60	13,776	16,624.59
7	0.75	6.77	5,095	10,320.50	7	1.21	6.84	16,104	18,530.73
8	2.00	8.15	--	12,105.98	8	1.29	8.19	15,529	21,294.65
					9	2.00	9.92	16,193	43,690.68
Σ =	9.15			103,410.58	Σ =	10.92			162,606.05
V_{max} =			16,861		V_{max} =			16,193	
QI_{avrg} =				11,301.70	QI_{avrg} =				14,890.66
QI_{top} =				13,123.19	QI_{top} =				14,370.95
QI_{mid} =				15,043.18	QI_{mid} =				14,383.72
QI_{bot} =				5,738.74	QI_{bot} =				15,917.32
QI_{top} / V_{max} =				0.78	QI_{top} / V_{max} =				0.89
QI_{top} / QI_{avrg} =				1.16	QI_{top} / QI_{avrg} =				0.97
QI_{mid} / V_{max} =				0.89	QI_{mid} / V_{max} =				0.89
QI_{mid} / QI_{avrg} =				1.33	QI_{mid} / QI_{avrg} =				0.97
QI_{bot} / V_{max} =				0.34	QI_{bot} / V_{max} =				0.98
QI_{bot} / QI_{avrg} =				0.51	QI_{bot} / QI_{avrg} =				1.07

{(--) Indicates no available data}

Table 7.10: Ultrasonic velocity for Cores L31, L3, L6, and L8, continued

	Core L6					Core L8			
Slice No.	Thickness (in.)	Mid Point depth (h) (in.)	Velocity (V) (ft/s)	Σ V(Δh) (in.ft/s)	Slice No.	Thickness (in.)	Mid Point depth (h) (in.)	Velocity (V) (ft/s)	Σ V(Δh) (in.ft/s)
	1 in. = 25.4 mm	1 in. = 25.4 mm	1 ft/s = 0.30 m/s	1 in. ft/s = 0.0076 m^2/s		1 in. = 25.4 mm	1 in. = 25.4 mm	1 ft/s = 0.30 m/s	1 in. ft/s = 0.0076 m^2/s
2	1.13	0.57	13,885	7,865.74	2	1.31	0.66	13,422	8,791.50
3	1.17	1.82	13,797	17,415.42	3	1.12	2.01	12,905	17,807.55
4	1.14	3.08	14,490	17,817.25	4	1.22	3.31	15,188	18,334.43
5	1.19	4.35	13,259	17,603.10	5	1.13	4.62	13,534	18,823.64
6	1.11	5.61	16,982	19,017.58	6	1.10	5.88	13,800	17,155.77
7	1.13	6.84	14,426	19,303.97	7	1.14	7.14	12,932	16,858.23
8	1.15	8.09	15,931	18,908.35	8	1.24	8.47	15,463	28,465.15
9	0.23	8.88	3,310	8,052.88					
Σ =	9.00			125,984.30	Σ =	9.09			126,236.26
V_{max} =			16,982		V_{max} =			15,463	
QI_{avrg} =				13,998.26	QI_{avrg} =				13,887.38
QI_{top} =				14,366.14	QI_{top} =				13,433.79
QI_{mid} =				14,356.42	QI_{mid} =				14,090.12
QI_{bot} =				13,272.21	QI_{bot} =				14,138.22
QI_{top} / V_{max} =				0.85	QI_{top} / V_{max} =				0.87
QI_{top} / QI_{avrg} =				1.03	QI_{top} / QI_{avrg} =				0.97
QI_{mid} / V_{max} =				0.85	QI_{mid} / V_{max} =				0.91
QI_{mid} / QI_{avrg} =				1.03	QI_{mid} / QI_{avrg} =				1.01
QI_{bot} / V_{max} =				0.78	QI_{bot} / V_{max} =				0.91
QI_{bot} / QI_{avrg} =				0.95	QI_{bot} / QI_{avrg} =				1.02

{(--) Indicates no available data}

Table 7.11: Ultrasonic velocity for Cores L10 and L12

Core L10					Core L12				
Slice No.	Thickness (in.)	Mid Point depth (h) (in.)	Velocity (V) (ft/s)	Σ V(Δh) (in.ft/s)	Slice No.	Thickness (in.)	Mid Point depth (h) (in.)	Velocity (V) (ft/s)	Σ V(Δh) (in.ft/s)
	1 in. = 25.4 mm	1 in. = 25.4 mm	1 ft/s = 0.30 m/s	1 in. ft/s = 0.0076 m^2/s		1 in. = 25.4 mm	1 in. = 25.4 mm	1 ft/s = 0.30 m/s	1 in. ft/s = 0.0076 m^2/s
2	1.01	0.50	12,870	6,492.86	2	1.21	0.60	14,483	8,726.11
3	1.14	1.62	13,666	14,856.24	3	1.26	1.95	13,305	18,726.31
4	1.17	2.83	11,455	15,094.10	4	1.15	3.27	14,093	18,086.74
5	1.82	4.37	8,594	15,444.76	5	1.15	4.54	14,681	18,239.80
6					6	1.14	5.80	18,205	20,731.26
7	1.08	5.86	12,993	16,132.85	7	0.74	6.85	9,648	14,703.70
8	2.02	7.46	7,826	16,605.28	8	1.77	8.23	16,051	31,797.85
9									
10	1.89	9.46	17,111	41,082.78					
Σ =	10.4			125,708.8	Σ =	9.11			131,011.76
V$_{max}$ =			17,111		V$_{max}$ =			18,205	
QI_{avrg} =				12,087.39	QI_{avrg} =				14,381.09
QI_{top} =				12,519.72	QI_{top} =				13,916.26
QI_{mid} =				10,582.54	QI_{mid} =				15,457.15
QI_{bot} =				13,159.92	QI_{bot} =				13,769.88
QI_{top} / V$_{max}$ =				0.73	QI_{top} / V$_{max}$ =				0.76
QI_{top} / QI_{avrg} =				1.04	QI_{top} / QI_{avrg} =				0.97
QI_{mid} / V$_{max}$ =				0.62	QI_{mid} / V$_{max}$ =				0.85
QI_{mid} / QI_{avrg} =				0.88	QI_{mid} / QI_{avrg} =				1.07
QI_{bot} / V$_{max}$ =				0.77	QI_{bot} / V$_{max}$ =				0.76
QI_{bot} / QI_{avrg} =				1.09	QI_{bot} / QI_{avrg} =				0.96

{(--) Indicates no available data}

Table 7.12: Summary of pulse velocity test results for No SIPMF Bridge Decks

Bridge Deck Number	Core	Height, h (in.)	Σ V(Δh) (in.ft/s)	QI_{avrg} for Core (ft/s)	QI_{avrg} for Bridge Deck (ft/s)
		1 in. = 25.4 mm	1 in. ft/s = 0.0076 m²/s	1 ft/s = 0.30 m/s	1 ft/s = 0.30 m/s
1 LOR-57-18.18 without SIPMF	1C	9.25	126,691	13,696	13,246
	1F	8.75	116,669	13,334	
	1B	9.00	121,583	13,509	
	8E	9.00	112,382	12,487	
	8C2	9.00	118,815	13,202	
2 OTT-2-28.41 without SIPMF	A1	11.00	157,243	14,295	13,280
	A11	10.75	147,339	13,706	
	A16	10.50	147,330	14,031	
	A5	11.00	139,461	12,678	
	A9	11.00	128,611	11,692	
3 LAK-90-23.42 without SIPMF	L23	10.03	120,817	12,046	12,380
	L24	9.97	120,932	12,133	
	L26	8.97	107,706	12,007	
	L28	10.22	147,270	14,410	
	L31	9.15	103,411	11,302	
Average				**12,969**	
Standard Deviation				**990**	
Σ		**148**	**1,916,260**		
QI (ft/s)	**12,984**				

Table 7.13: Summary of region-specific pulse velocity analysis for No SIPMF Bridge Decks

Bridge Deck Number	Core	QI_{avrg} (ft/s)	QI_{top} (ft/s)	QI_{top} / QI_{avrg}	QI_{mid} (ft/s)	QI_{mid} / QI_{avrg}	QI_{bot} (ft/s)	QI_{bot} / QI_{avrg}
		1 ft/s = 0.30 m/s	1 ft/s = 0.30 m/s		1 ft/s = 0.30 m/s		1 ft/s = 0.30 m/s	
1 LOR-57-18.18 without SIPMF	1C	13,696	14,271	1.04	14,268	1.04	12,550	0.92
	1F	13,334	11,787	0.88	14,259	1.07	13,955	1.05
	1B	13,509	13,468	1.00	13,474	1.00	13,586	1.01
	8E	12,487	10,821	0.87	14,598	1.17	12,042	0.96
	8C2	13,202	11,550	0.87	14,462	1.10	13,593	1.03
2 OTT-2-28.41 without SIPMF	A1	14,295	12,724	0.89	14,170	0.99	15,991	1.12
	A11	13,706	12,334	0.90	13,055	0.95	15,729	1.15
	A16	14,031	13,277	0.95	13,751	0.98	15,066	1.07
	A5	12,678	11,732	0.93	13,390	1.06	12,913	1.02
	A9	11,692	11,204	0.96	11,803	1.01	12,069	1.03
3 LAK-90-23.42 without SIPMF	L23	12,046	13,626	1.13	14,346	1.19	8,164	0.68
	L24	12,133	13,417	1.11	13,862	1.14	9,120	0.75
	L26	12,007	13,391	1.12	13,500	1.12	9,132	0.76
	L28	14,410	13,945	0.97	14,747	1.02	14,538	1.01
	L31	11,301	13,123	1.16	15,043	1.33	5,739	0.51
Average		**12,968**	**12,711**	**0.98**	**13,915**	**1.08**	**12,279**	**0.94**

Table 7.14: Summary of pulse velocity test results for SIPMF Bridge Decks

Bridge Deck Number	Core	Height, h (in.)	Σ V(Δh) (in.ft/s)	QI avrg for Core (ft/s)	QI avrg for Bridge Deck (ft/s)
		1 in. = 25.4 mm	1 in. ft/s = 0.0076 m²/s	1 ft/s = 0.30 m/s	1 ft/s = 0.30 m/s
4 LOR-57-18.18 with SIPMF	6B	9.75	125,042	12,825	13,348
	4C	8.25	114,947	13,933	
	7D	7.50	111,140	14,819	
	3D	7.50	86,827	11,577	
	6C	9.88	134,170	13,587	
5 OTT-2-28.41 with SIPMF	B1	9.25	127,686	13,804	13,758
	B4	9.00	129,039	14,338	
	B5	8.75	124,732	14,255	
	C3	9.50	126,359	13,301	
	C7	7.00	91,664	13,095	
6 LAK-90-23.42 with SIPMF	L3	10.92	162,606	14,900	13,851
	L6	9.00	125,984	13,998	
	L8	9.09	126,236	13,887	
	L10	10.40	125,709	12,087	
	L12	9.11	131,012	14,381	
Average				13,652	
Standard Deviation				943	
Σ		135	1,843,153		
QI (ft/s)	13,663				

Table 7.15: Summary of region-specific pulse velocity analysis for SIPMF Bridge Decks.

Bridge Deck Number	Core	QI_{avrg} (ft/s)	QI_{top} (ft/s)	QI_{top} / QI_{avrg}	QI_{mid} (ft/s)	QI_{mid} / QI_{avrg}	QI_{bot} (ft/s)	QI_{bot} / QI_{avrg}
		1 ft/s = 0.30 m/s	1 ft/s = 0.30 m/s		1 ft/s = 0.30 m/s		1 ft/s = 0.30 m/s	
4 LOR-57-18.18 with SIPMF	6b	12825	12424	0.97	13995	1.09	12055	0.94
	4c	13933	16048	1.15	13321	0.96	12435	0.89
	7d	14819	13740	0.93	14531	0.98	16185	1.09
	3d	11577	7087	0.61	13732	1.19	13911	1.20
	6c	13587	13557	1.00	14312	1.05	12892	0.95
5 OTT-2-28.41 with SIPMF	B1	13804	13755	1.00	12410	0.90	15246	1.10
	B4	14338	14002	0.98	14269	1.00	14742	1.03
	B5	14255	12607	0.88	15375	1.08	14784	1.04
	C3	13301	12744	0.96	13897	1.04	13262	1.00
	C7	13095	12240	0.93	13460	1.03	13585	1.04
6 LAK-90-23.42 with SIPMF	L3	14891	14371	0.97	14384	0.97	15917	1.07
	L6	13998	14366	1.03	14356	1.03	13272	0.95
	L8	13887	13434	0.97	14090	1.01	14138	1.02
	L10	12087	12520	1.04	10582	0.88	13160	1.09
	L12	14381	13916	0.97	15457	1.07	13770	0.96
Average		**13652**	**13121**	**0.96**	**13878**	**1.02**	**13957**	**1.02**
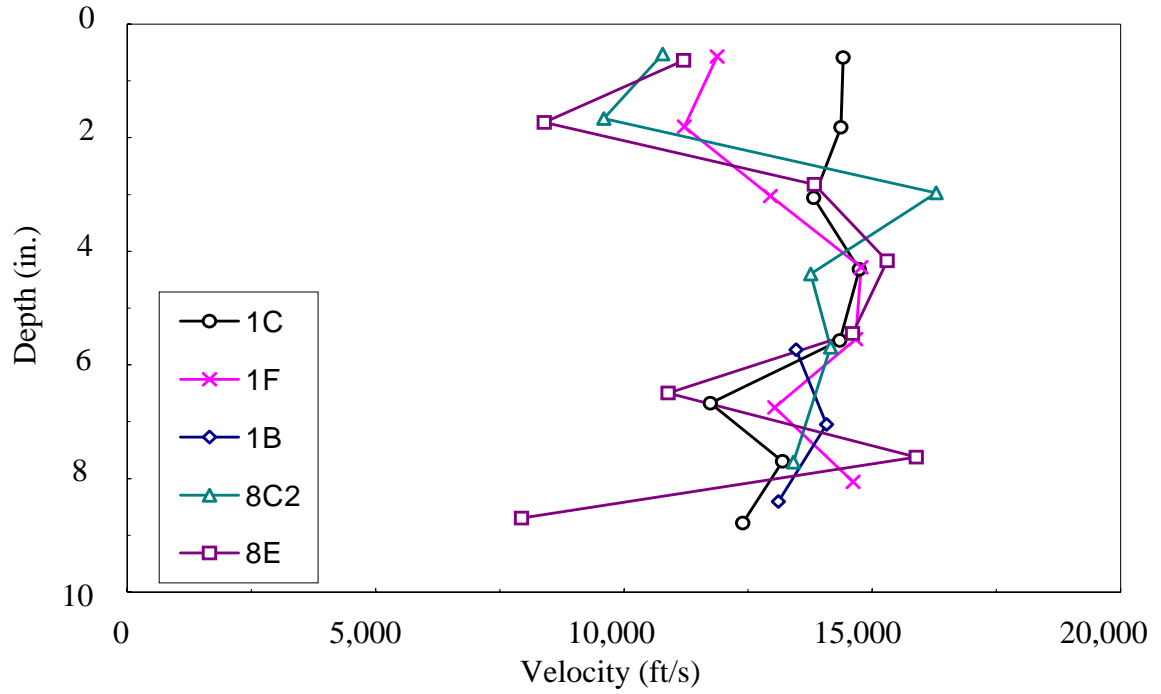
Figure 7.92. Velocity profiles for cores from LOR-57-18.18 without SIPMF
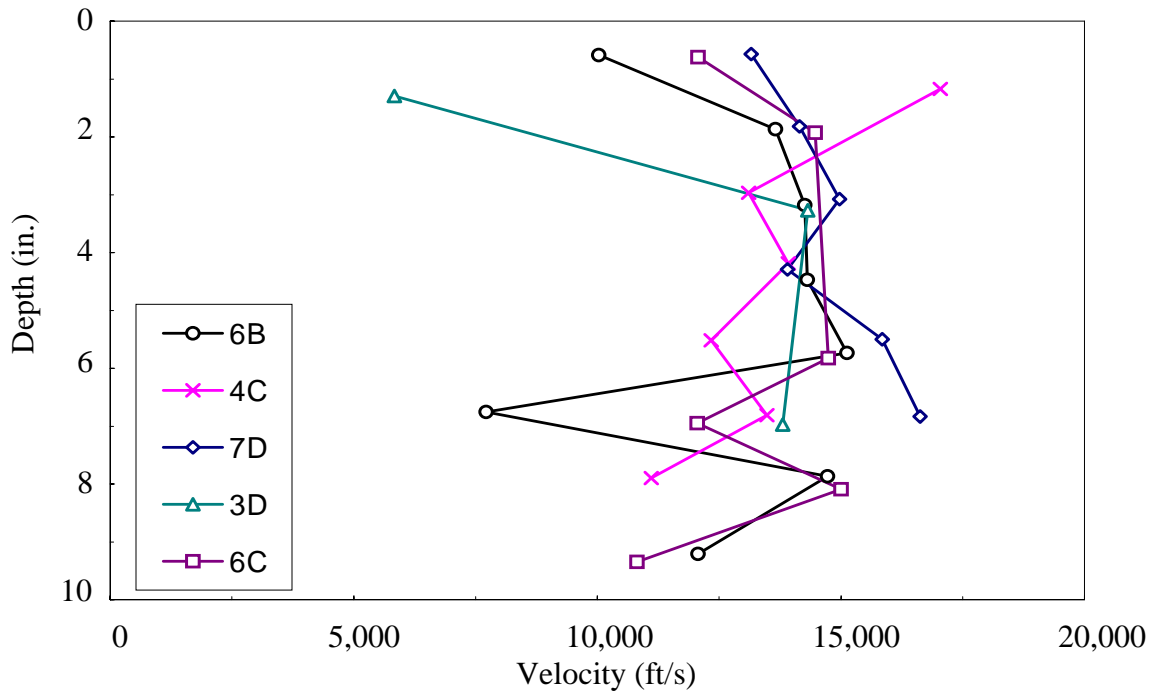
Figure 7.93. Velocity profiles for cores OTT-2-28.41without SIPMF
1 ft/sec = 0.30 m/s, 1 in. = 25.4 mm
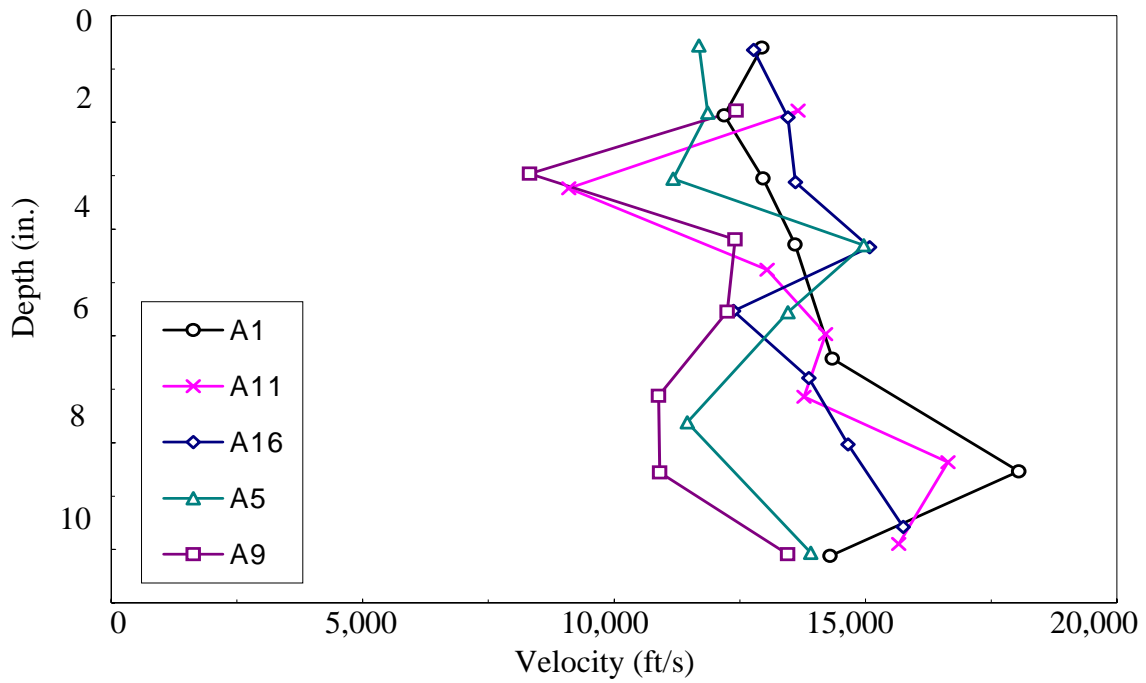
Figure 7.94. Velocity profiles for cores from LAK-90-23.42 without SIPMF
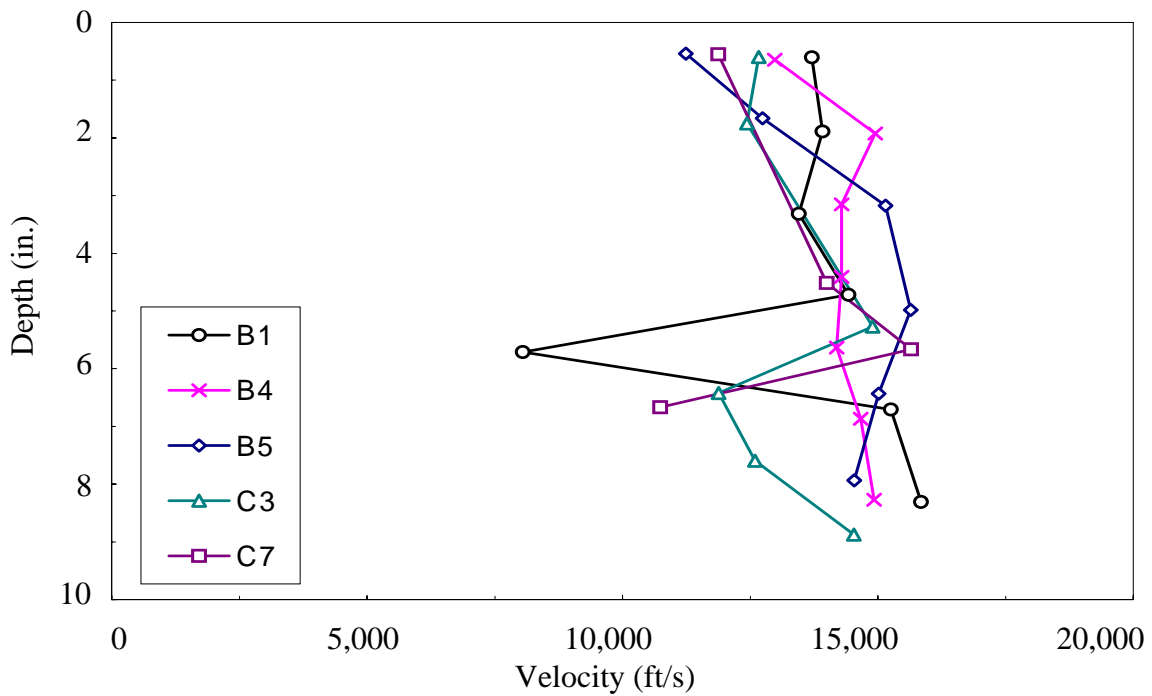
Figure 7.95. Velocity profiles for cores LOR-57-18.18 with SIPMF.
1 ft/sec = 0.30 m/s, 1 in. = 25.4 mm
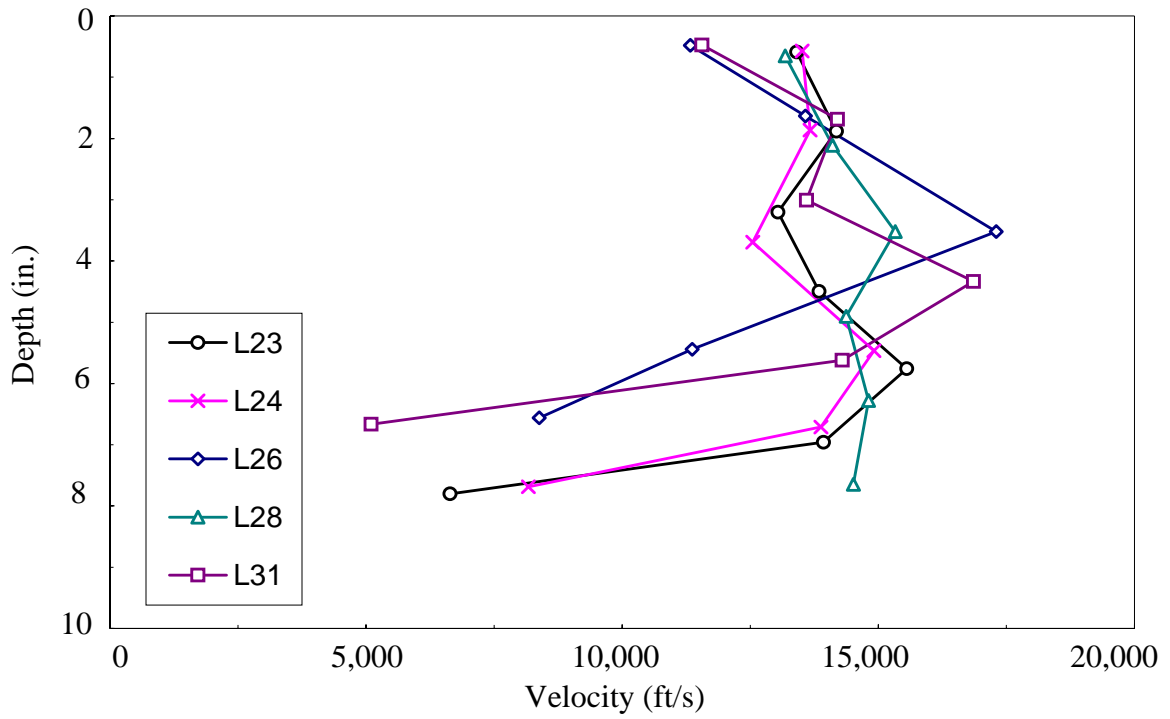
Figure 7.96. Velocity profiles for cores from OTT-2-28.41 with SIPMF
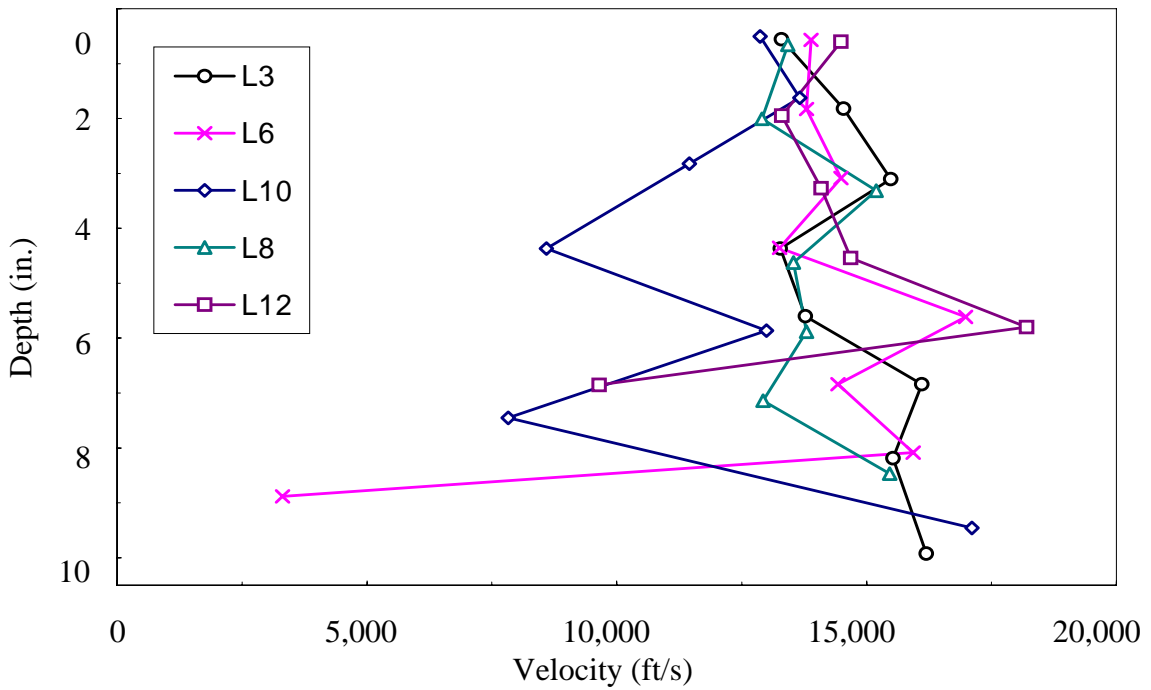
Figure 7.97. Velocity profiles for cores LAK-90-23.42 with SIPMF.
1 ft/sec = 0.30 m/s, 1 in. = 25.4 mm
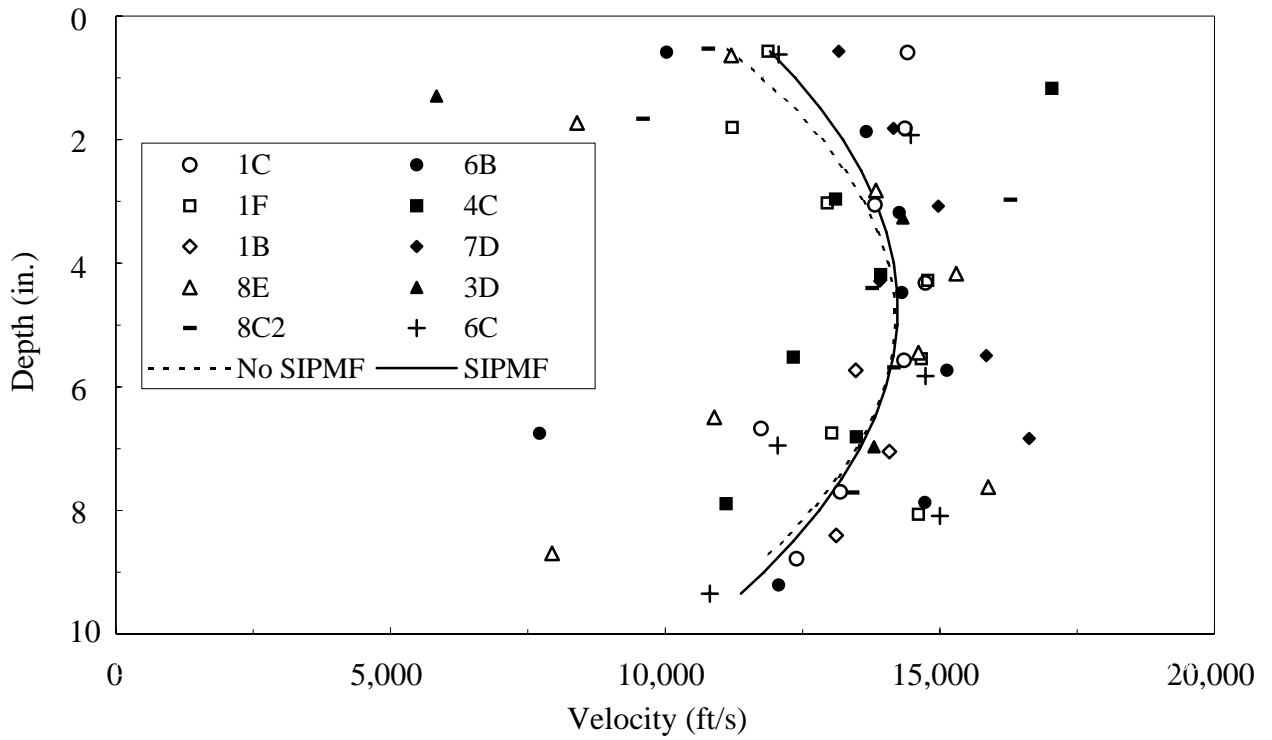
Figure 7.98. Summary of all ultrasonic pulse velocity measurements with depth from LOR-57-18.18
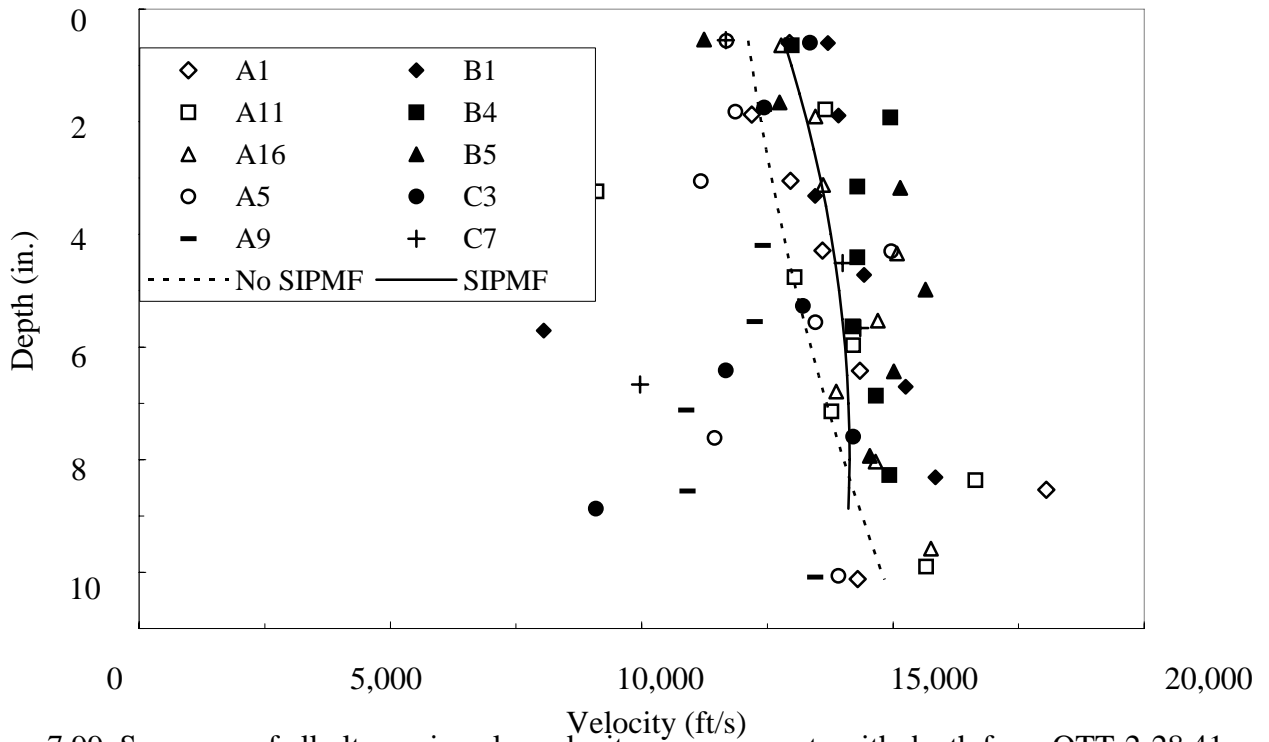
Figure 7.99. Summary of all ultrasonic pulse velocity measurements with depth from OTT-2-28.41
1 ft/sec = 0.30 m/s, 1 in. = 25.4 mm
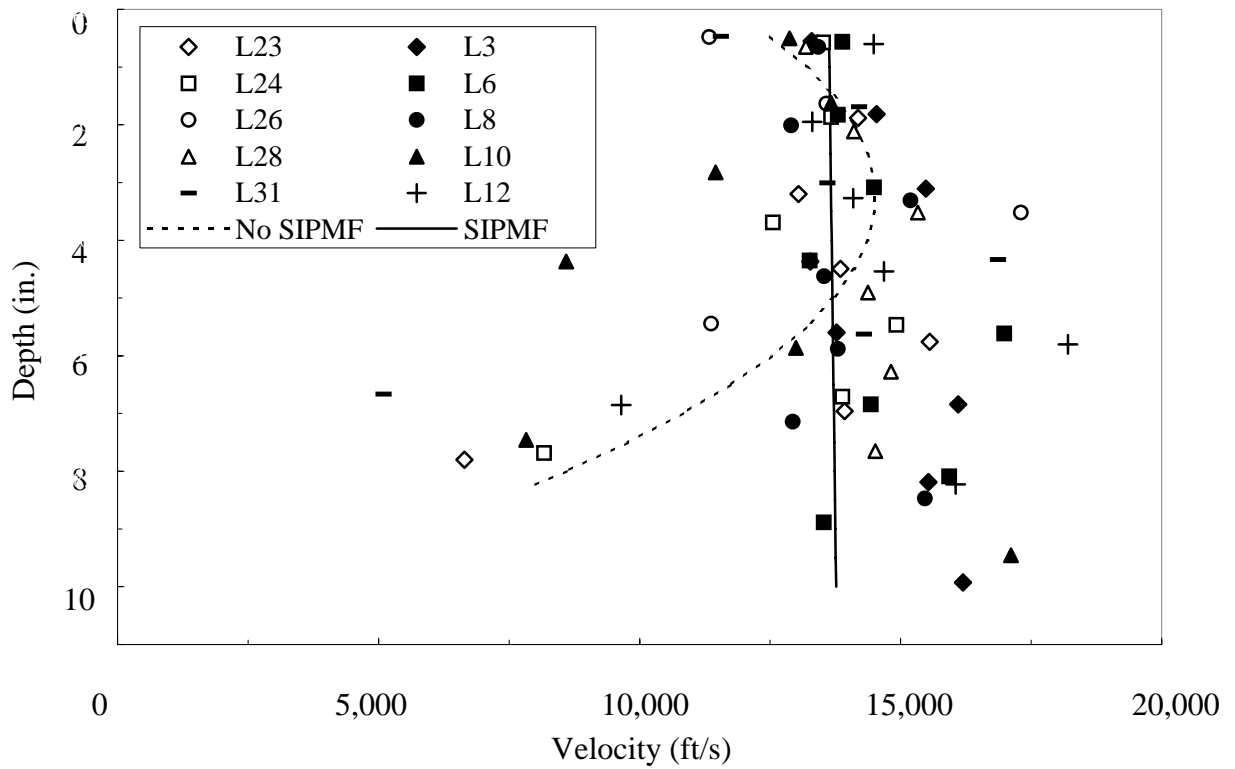
Figure 7.100. Summary of all ultrasonic pulse velocity measurements with depth for LAK-90-23.42
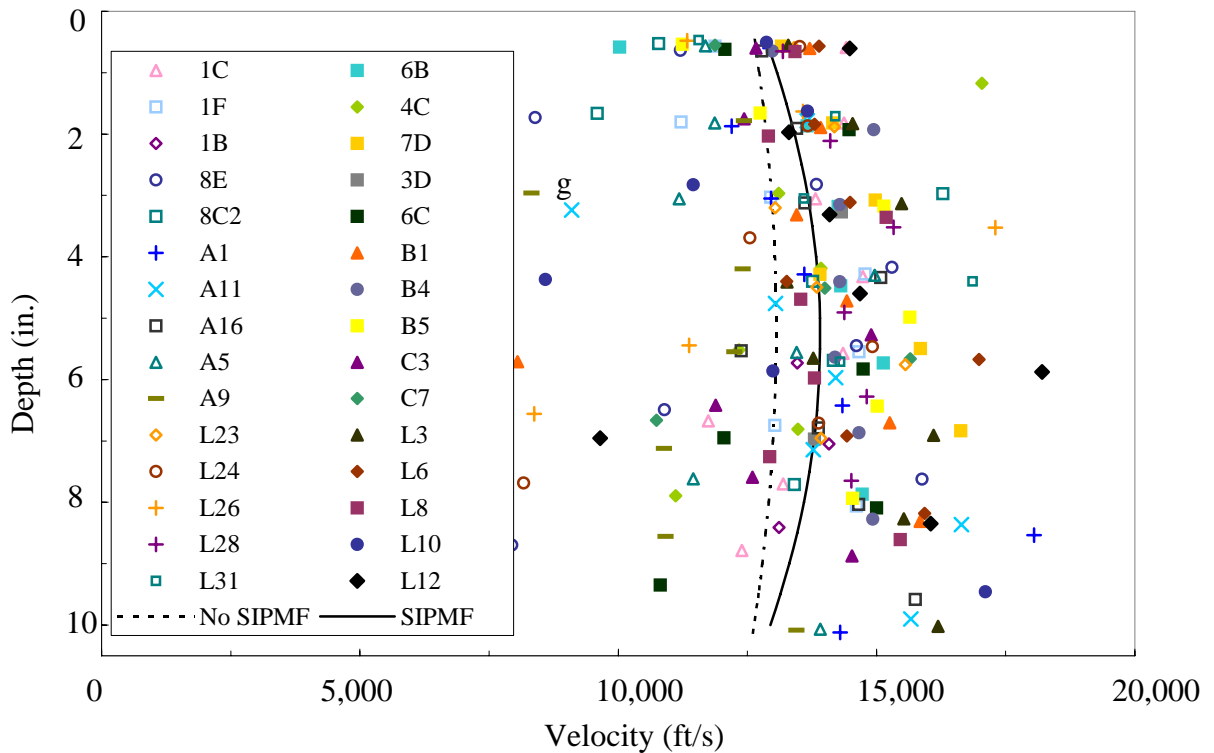
Figure 7.101. Summary of all ultrasonic pulse velocity measurements with depth for all Bridge decks
1 ft/sec = 0.30 m/s, 1 in. = 25.4 mm
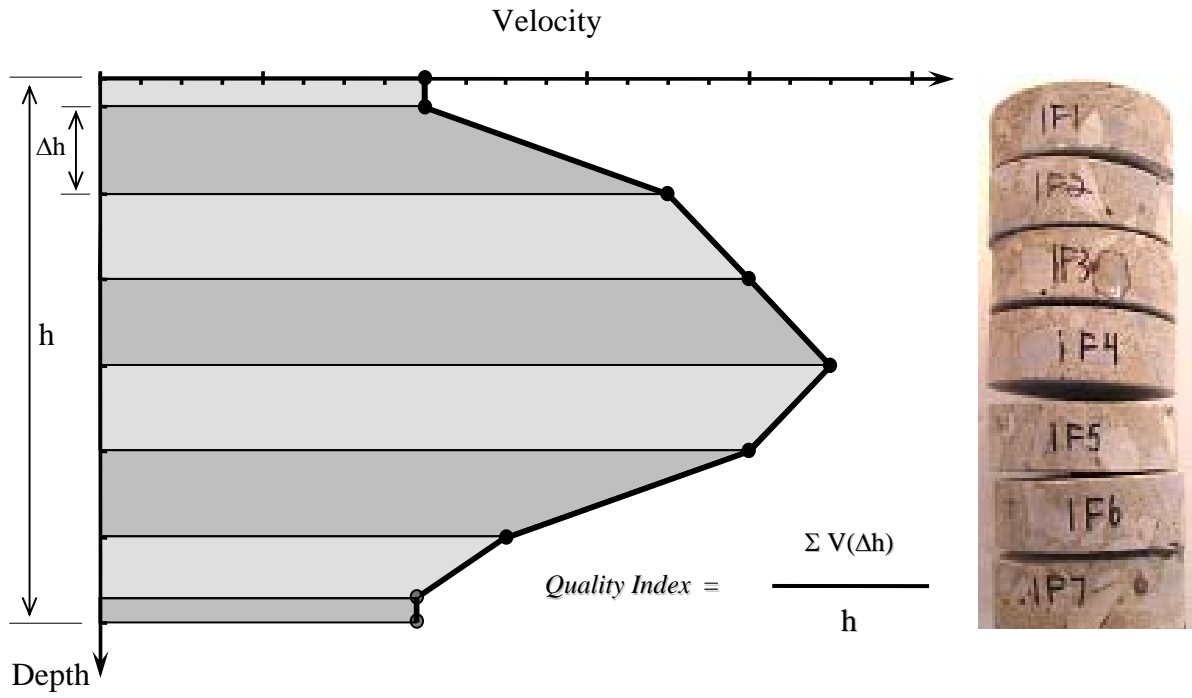
Figure 7.102. Quality Index(QI) calculation.

$$Quality\ Index\ =\ \frac{\Sigma\ V(\Delta h)}{h}$$

7.5 ULTRASOUND TESTING CONCLUSIONS

A study was conducted to evaluate the performance of concrete bridge decks constructed using SIPMF. Comparisons were made between decks without SIPMF and decks with SIPMF. The test program was conducted on bridge decks located in Northern Ohio. The decks were exposed to high seasonal temperature variations and cyclic freeze thaw due to the prevailing climatic conditions in the state. Evaluations were made using analysis of cores obtained from bridge decks. The cores were investigated using visual inspection, and ultrasonic tests. The ultrasonic tests provided a means for evaluating the response of cores with depth of bridge deck. The test results were analyzed initially to compare all bridge decks without SIPMF to bridge decks with SIPMF.

The results obtained from the region specific pulse-velocity analysis maybe found somehow different from the results obtained from the overall trend lines. This is attributed to the fact that the trend line is only affected by the pulse velocity reading, while the region specific quality index is affected by both the pulse velocity reading as well as the slice thickness, which is represented as the area contained by the velocity vs. length (along a specific slice) plot.

Based on the visual inspection of cores, it was determined that the two bridge deck systems were similar. Statistical analysis of ultrasonic pulse velocity test also indicated similarity of the bridge deck systems for all the decks. The ultrasonic test results with depth did not indicate specifically beneficial or adverse effects of the presence of SIPMF on the bridge decks. Overall, the performance of concrete bridge decks constructed with SIPMF was determined to be similar to the performance of concrete bridge decks constructed without SIPMF in this test program.

Chapter 8: Comparison of Test Results

After completing the compression, permeability, chloride ion and ultrasound tests an overall evaluation was done to compare the areas where there were SIPMF and areas where there was no SIPMF. this overall comparison study was done by taking an average for each test result in the areas where SIPMF were present comparing it to the average for areas were the deck was formed by the conventional plywood forming method. Table 8.1 and Figure 8.1 summarize the results from this comparison study. From the table, it is evident that the concrete from the areas of SIPMF was of better overall quality than the concrete from areas where no SIPMF were present. Bridge by bridge details of this comparison are presented in Tables 8.2 – 8.4 and Figures 7.98 – 7.100.

The overall finding is that there is no significant difference in deck concrete condition between regions with SIPMF and regions without SIPMF.

Table 8.1: Comparison Summary of Test Results

Bridge	Compression Test AASHTO: T 22 (Psi) 1 Psi = 0.006895 MPa		Permeability Test AASHTO: T 277 (Coulombs)		Chloride Ion Test AASHTO: T 260 (Lbs Cl / yd³) 1 inch = 25.4 mm, 1 lb/yd³ = 5.89 N/m³							
	No SIPMF	SIPMF	No SIPMF	SIPMF	No SIPMF				SIPMF			
				w/ temp. correction	2"	4"	6"	8"	2"	4"	6"	8"
LOR-57-18.18	7163	7685	1777	1577	3.34	2.42	1.51	0.72	2.43	1.55	0.85	0.71
OTT-2-28.41	6300	6372	1990	2188	4.01	2.34	1.26	0.82	5.5	2.88	1.23	0.53
LAK-90-23.42	7146	6918	3136	2128	9.85	4.5	2.79	1.31	7.11	4	0.85	0.52
Average	6870	6992	2301	1964	5.73	3.09	1.85	0.95	5.01	2.81	0.98	0.59

Compression Test: SIPMF > No SIPMF by 1.74%

Permeability Test: SIPMF > No SIPMF by 14.63%

Chloride Ion Test:

        2": SIPMF > No SIPMF by 12.56%

        4": SIPMF > No SIPMF by 9.06%

        6": SIPMF > No SIPMF by 47.3%

        8": SIPMF > No SIPMF by 37.89%
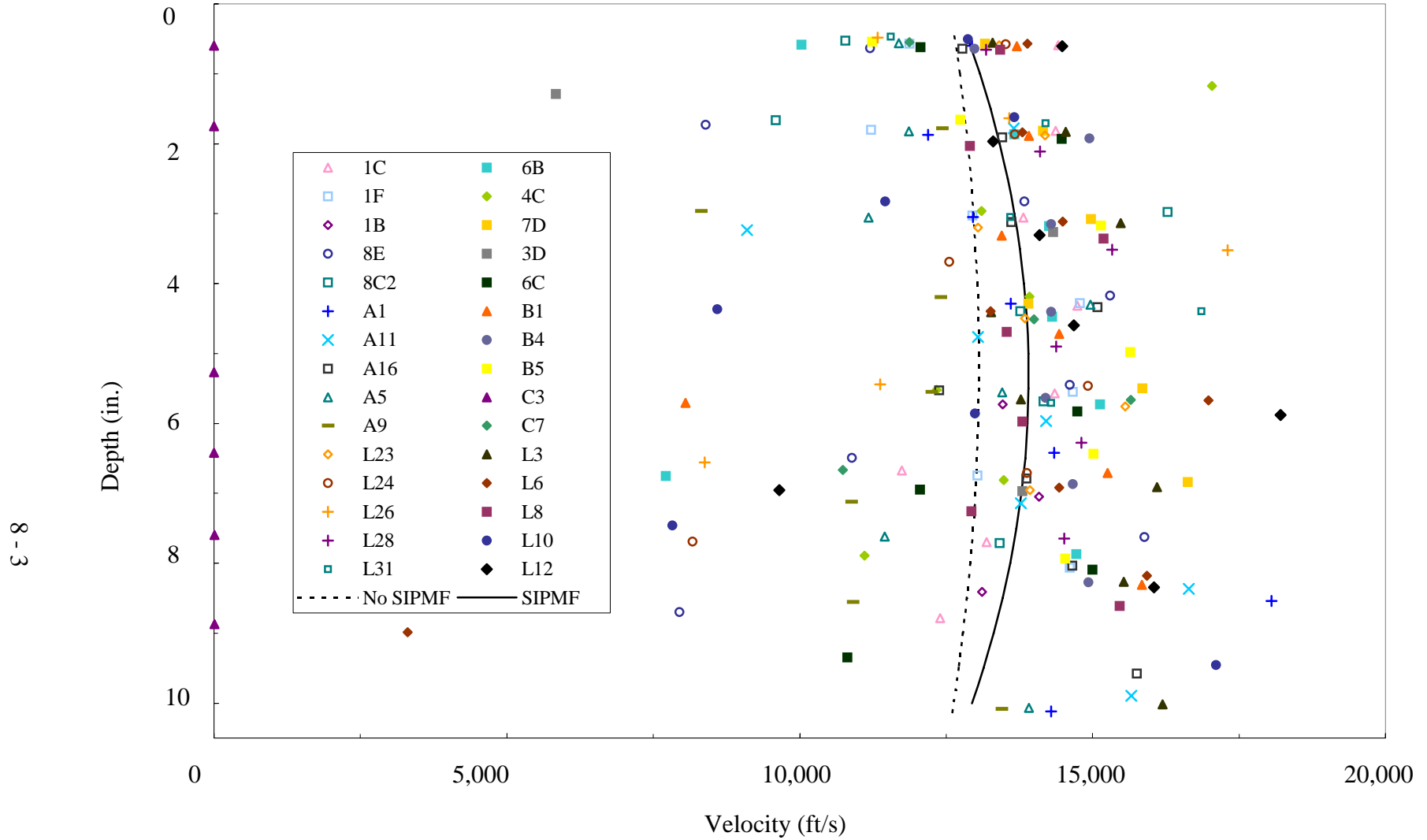
Figure 8.1. (Same as Figure 7.102) Summary of all ultrasonic pulse velocity measurements with depth for all bridge decks

1 ft/sec = 0.30 m/s, 1 in. = 25.4 mm

Table 8.2: LOR-57-18.18 SIPMF vs. No SIPMF

Core Number	Core Location		Compression Test		Permeability Test		Chloride Ion Test				SIPMF
	Station Location	Distance (ft.) from South Curb	AASHTO: T 22 (Psi)		AASHTO: T 277 (Coulombs)		AASHTO: T 260 (Lbs Cl / yd3)				
							2"	4"	6"	8"	
S1	975 + 56.9	35.2			1586		1.62	1.01	1.85	0.94	N
S2	975 + 51.6	29.9					2.53	1.51	1.56	2.37	Y
1B	975 + 53.3	35.1									N
1C	975 + 53.4	26.5									N
1D	975 + 53.4	14.1			1384						N
1E	975 + 53.1	1.6	6910								N
1F	975 + 54.0	0.8									N
2 - 2"	975 + 51.6	31.2	7990	7820							Y
2B	975 + 50.7	35					1.09	0.32	0.82	0.18	Y
2C	975 + 50.7	25.9			1083						Y
2D1	975 + 51.5	14.4			977						Y
2D2	975 + 50.5	14.5			1749						Y
2D3	975 + 50.5	13.1	8890								Y
2E	975 + 51.5	1.6			1206						Y
2F	975 + 51.3	0.7					1.13	1.04	0.44	0.31	Y
3 - 2"	975 + 9.3	22.8	8690	7430							Y
3C	975 + 8.6	24.7					1.58	1.16	0.72	0.53	Y
3D	975 + 8.4	19.6									Y
3F	975 + 9.6	0.8					1.54	1.35	0.57	0.44	Y
4 - 2"	974 + 80.5	21	7180								Y
4C1	974 + 80.6	21.4	7840								Y
4C2	974 + 80.4	20.9									Y
4E	974 + 80.0	1.7			1124						Y
4F	974 + 79.6	0.9					1.92	0.57	0.36	0.32	Y
5 - 2"	973 + 49.9	22.8	7710								Y
5B	973 + 50.5	32.8			1892	1513					Y
5C	973 + 50.4	23.2					0.9	0.56	0.52	0.49	Y
5D	973 + 49.9	12.4	6170								Y
5E	973 + 50.1	1.7	7440								Y
6B	973 + 49.6	32.8									Y
6C	973 + 49.9	23.2									Y
6D	973 + 48.9	12.4			2350						Y
6E	973 + 48.9	1.7					4.27	2.92	1.32	0.99	Y
7 - 2"	971 + 81.0	20.1	7370								Y
7B	971 + 80.3	34.8					4.03	1.45	0.7	0.82	Y
7C	971 + 81.0	17.4					5.33	4.57	1.45	0.61	Y
7C1	971 + 80.4	28			2028						Y
7C1(2)	971 + 80.3	27.3			1828						Y
7D	971 + 80.4	11.8									Y
7E	971 + 80.7	1.9			2319	1073					Y
8 - 2"	971 + 65.4	6.9	6150	8530							N
8B	971 + 65.6	34.6			1929		3.59	1.68	0.77	0.64	N
8C1	971 + 65.3	20.6			2346		4.8	4.56	1.9	0.57	N
8C2	971 + 64.2	20.4									N
8D	971 + 65.7	11.3	7060								N
8E	971 + 65.3	1.7									N
		No SIPMF	7162.50		1811		3.34	2.42	1.51	0.72	
		SIPMF	7684.55		1595		2.43	1.55	0.85	0.71	

8 - 4

Table 8.3: OTT-2-28.41 SIPMF vs. No SIPMF

Core Number	Core Location		Compression Test		Permeability Test		Chloride Ion Test				SIPMF
	Station Location	*Distance (ft.) from East Curb*	*AASHTO: T 22* (*Psi*)		*AASHTO: T 277* (*Coulombs*)		*AASHTO: T 260* (*Lbs Cl / yd3*)				
							2"	*4"*	*6"*	*8"*	
A1	107 + 11.5	0.4									N
A2	107 + 12.8	0.3					1.21	1.26	1.04	0.76	N
A3	107 + 13.9	0.3			1977	1214					N
A4	107 + 14.8	0.4					2.93	1.02	0.83	0.55	N
A5	107 + 15.9	0.4									N
A6	107 + 17.2	0.2			1667	1580					N
A7	107 + 18.3	0.2	6010	5430							N
A8	107 + 19.6	0.3					5.42	1.84	1.12	0.8	N
A9	107 + 20.7	0.2									N
A10	107 + 21.9	0.3			2997	2240					N
A11	107 + 23	0.2									N
A12	107 + 24.2	0.2	5070	5630							N
A13	107 + 25.6	0.3	6030								N
A14	107 + 26.7	0.3					6.47	5.22	2.03	1.17	N
A15	107 + 27.7	0.4			2233	2107					N
A16	107 + 28.7	0.3									N
A17	107 + 29.6	0.1	7870								N
A17-1	107 + 30.6	0.2	6440								N
A18	107 + 31.5	0.4	7770								N
A18-1	107 + 32.7	0.5	6450								N
B1	107 + 8.6	6.7									Y
B2	107 + 13.1	6.4	5430								Y
B3	107 + 16.5	6.2			1886						Y
B4	107 + 19.5	5.9									Y
B5	107 + 26.4	5.7									Y
B6	107 + 29.3	5.6			2247						Y
B7	107 + 32.5	5.6					5.6	3.66	2.8	0.59	Y
B8	107 + 34.2	5.5	6540								Y
B9	107 + 36	5.5	7120								Y
C1	107 + 0.9	2.7					2.19	1.54	0.62	0.29	Y
C2	107 + 2.5	4.4			1479						Y
C3	107 + 5.7	4.4									Y
C4	107 + 9.1	4.3					3.14	1.71	0.72	0.64	Y
C5	107 + 12.2	4.2					8.03	3.12	0.74	0.54	Y
C6	107 + 15.9	4.3					8.56	4.37	1.25	0.59	Y
C7	107 + 29	4.3									Y
C8	107 + 32.5	4.3			4050						Y
C9	107 + 34.8	4.3									Y
C9-1	107 + 35.1	4	5910								Y
C10	107 + 35.3	4.4	6090								Y
C10-1	107 + 37.4	3.9	7140								Y
		No SIPMF	*6300.00*		*2002*		*4.01*	*2.34*	*1.26*	*0.82*	
		SIPMF	*6371.67*		*2416*		*5.50*	*2.88*	*1.23*	*0.53*	

Table 8.4: LAK-90-23.42 SIPMF vs. No SIPMF

Core Number	Core Location		Compression Test	Permeability Test	Chloride Ion Test				SIPMF
	Station Location	*Distance (ft.) from South Curb*	*AASHTO: T 22* (Psi)	*AASHTO: T 277* (Coulombs)	*AASHTO: T 260* (Lbs Cl / yd3)				
					2"	*4"*	*6"*	*8"*	
L1	837 + 51.01	2.4	6700						Y
L2	837 + 52.31	2.5		2460					Y
L3	837 + 53.61	2.7							Y
L4	837 + 54.91	2.6			7.99	7.87	0.82	0.2	Y
L5	837 + 67.81	3.1	7470						Y
L6	837 + 69.21	2.8							Y
L7	837 + 70.41	2.5			7.02	2.55	0.9	0.8	Y
L8	837 + 78.71	3.3							Y
L9	837 + 83.01	3.6		2089					Y
L10	837 + 84.51	2.9							Y
L11	837 + 85.71	2.2		2018					Y
L12	837 + 91.81	2.3							Y
L13	837 + 99.21	5.1			5.98	1.01	0.86	0.7	Y
L14	837 + 99.91	3.3		1504					Y
L15	838 + 01.61	2.8			7.43	4.55	0.83	0.3	Y
L16	838 + 06.11	3.5		2571					Y
L17	838 + 05.81	4.7	7130						Y
L18	838 + 05.71	5.2	6370						Y
L19	838 + 38.51	4.6	6250						N
L20	838 + 38.81	4.8	6820						N
L21	838 + 38.41	6.1			8.88	3.35	1.58	0.8	N
L22	838 + 39.01	4.5			8.7	1.83	0.9	0.6	N
L23	838 + 40.01	4.7							N
L24	838 + 41.31	4.9							N
L25	838 + 42.41	3.3	7800						N
L26	838 + 45.41	2.9							N
L27	838 + 46.21	3.5		3977					N
L28	838 + 48.81	2.7							N
L29	838 + 49.61	3.7	8060						N
L30	838 + 53.21	4.1		2606					N
L31	838 + 53.91	4.2							N
L32	838 + 59.01	5.2	6800						N
L33	838 + 59.91	3.9		4302					N
L34	838 + 65.91	5.8			9.07	1.79	0.99	0.8	N
L35	838 + 66.51	4.1		6169					N
L36	838 + 70.61	6.1			12.75	11.02	7.68	3	N
		No SIPMF	*7146.00*	*4264*	*9.85*	*4.50*	*2.79*	*#*	
		SIPMF	*6917.50*	*2128*	*7.11*	*4.00*	*0.85*	*#*	

Chapter 9 Ground Penetrating Radar Study

9.1 INTRODUCTION

A significant concern in the use of stay-in-place metal forms (SIPMF) in Ohio is the inability to visually inspect the bottom of the deck throughout the life of the bridge. Inspectors use visual information and soundings to assess the quality of new concrete and identify potential problems during service. Until an adequate substitute for visual inspection is found bridge engineers will not be comfortable with SIPMF. This chapter reports the results of the first known attempt to use ground penetrating radar (GPR) to evaluate the quality of the concrete at the bottom of the bridge deck by examining the GPR signal reflected from the SIPMF.

Ground penetrating radar is a very effective technique for determining if delamination exists in the upper layer of concrete. Air-launched ground penetrating radar surveys can be conducted at speeds up to 35 mph (56 kph). Using GPR to assess concrete condition, as well as locate discontinuities in material properties, has great potential to increase the efficiency of bridge deck inspection. There are also safety benefits from using GPR, as it can be completed at normal traffic speeds without impeding traffic flow. Thus, GPR has tremendous potential as a tool for inspecting the concrete at the bottom of the bridge deck.

The effectiveness of GPR as a non-destructive technique to determine the quality of concrete immediately above SIMPF and below the lower layer of rebar in a bridge deck was evaluated by conducting a GPR survey on OTT-2-28.41. This is one of the three bridges that was previously studied (see section 1.5). This bridge was selected by the research team and approved by ODOT.

This survey implemented the use of both ground coupled and air launched radar signals to determine the quality of the concrete just above the SIPMF. The sole variable considered in using the GPR to assess the quality of the concrete was signal attenuation. A low reflected signal to input signal ratio was interpreted to mean poor quality concrete. Conversely, relatively low signal loss was interpreted to mean the concrete quality was good. After the GPR surveys were completed, the first area examined was the region where the cores had been previously taken from. It was found that the areas of high radar signal attenuation did not coincide with the

location of these existing cores. Therefore, the additional verification (ground truth) cores were extracted along the length of the bridge and analyzed for delaminations and concrete quality.

The ground truth cores were inspected visually and tested in compression and ultrasonically. The results of these three assessments were compared to the GPR results to determine if the GPR survey accurately captured the quality of the deck concrete. In this chapter, the procedure and results are discussed sequentially for the visual, compression and ultrasound tests. Then the combined results of these tests are compared to the GPR results.

After analyzing the ground truth cores, using visual inspection and compression and ultrasound tests, it was found that GPR was reliable in predicting delaminations in the bridge deck above the top layer of rebar. However, GPR was not as reliable in determining delaminations in the region below the top layer of rebar and above the SIPMF.

9.2   GPR Literature Review

There are two basic types of GPR systems, ground-coupled systems and air-launched . Ground-coupled radar systems must keep in contact with the ground during a survey, so they are often dragged by hand or towed slowly (3-8 mph (5-13 kph)). Air launched GPR systems are often used in the transportation field because it utilizes a non-contact horn antenna suspended over the surface of the road or bridge deck and can perform surveys at speeds between 25 and 35 mph (40 and 56 kph).

Currently, GPR is used in civil engineering for detecting voids and delaminations in concrete pavements, determining asphalt and concrete layer thickness, and evaluating moisture or density variations in pavement (Maierhofer 2003, Barnes and Trottier 2004, Maser 1996, Scott et al 2003). Some of the benefits of using GPR in quality assessments of roadways include the fact that few or no cores need to be taken to get an accurate representation of what lies beneath the surface and equipment can be driven at road speed, eliminating the need for traffic control and the risk to workers and motorists (Heiler et al 1995). Comparing the radar results to ground truth cores taken from the area of survey dramatically increases the accuracy of the GPR results (AASHTO 2000).

GPR emits electromagnetic energy in the form of radio frequency wave pulses that can travel in dielectric materials, reflect from conductive materials in their path, and allow measurements of the reflected or transmitted waves (Shin and Grivas 2003). GPR operates in the wavelength range of 0.1 meters to 10 meters, which is on the low end of the radio wavelength

spectrum (AASHTO 2000). The electromagnetic energy is emitted in a conical shape out from the antenna and is sent into the subsurface where it travels through different media. As the energy comes to an interface between two media, it may be absorbed, reflected back or transmitted through depending on the electromagnetic properties of the two materials (Heiler et al 1995, Hugenschmidt 2002). The energy that is reflected back through the surface is received by the antennae and recorded.

Before they are reflected back up through the surface, the input pulses of energy undergo energy losses due to several reasons: absorption by the medium, dividing energy at interfaces, scattering of the wave from variously oriented objects, and the expanding conical wave front (Heiler et al 1995). Because of the conical emission of energy, objects appear at locations other than directly above their actual location and seem much larger than they actually are (Heiler et al 1995).

Electromagnetic waves pass through materials that do not conduct electricity; these materials are categorized as dielectric materials (Shin and Grivas 2003). Dielectric materials are classified according to their dielectric constant, which is a measure of ability to store electrical energy (AASHTO 2000). For example, air has a dielectric constant of one and fresh water has a dielectric constant of roughly 81. The velocity of the wave through a given medium varies in inverse proportion to the square root of the material's dielectric constant. For example, if a radar wave passes through a material having a dielectric constant of 4, it will travel half as fast as it does through air and twice as fast as it would through a material having a dielectric constant of 16 (AASHTO 2000). The dielectric constant of concrete is complex: it can depend on the moisture content, aggregate type, curing time, water to cement ratio, admixtures, and the presence of chlorides and is usually in the range of 6-11 (AASHTO 2000).

Normally, GPR will provide two independent measurable quantities: travel time and attenuation. The travel time is two-way travel time of the electromagnetic wave through a given material and attenuation is the weakening of the wave as it moves through the material due to some of the energy being lost. Attenuation results in less depth of penetration of the radio wave. From these two independent variables, it is possible to calculate both the dielectric constant of a material and its thickness using the equations below. If more variables are desired, a broader range of data must be collected from the radar wave. The reflection from a large metal plate

placed under the radar unit serves as the initial amplitude measurement in the following equation.

$$\varepsilon_1 = \left[\frac{\left(1 + \dfrac{A_1}{A_m}\right)}{\left(1 - \dfrac{A_1}{A_m}\right)} \right]^2$$

where, ε_1 = the dielectric constant of the surface layer

A_1 = the amplitude of the surface reflection, volts

A_m = the amplitude of reflection from a large metal plate, volts

The amplitude difference that exists between two material layers is a function of the difference in the dielectric constant between the two layers. Two material layers may have different material characteristics, but if the dielectric constants are not different, then there will not be a noticeable GPR reflection (AASHTO 2000). The greater the difference in dielectric constants; the larger the difference in amplitude of the returned signal.

Converting the two-way travel time to information about the depth to the interface can be completed using the following equation:

$$h_1 = v \times \Delta t_1$$

where, h_1 = the thickness of the layer

v = the velocity of the radar wave

Δt_1 = the two way traveling time of the wave in the material

The velocity of the radar wave in the material is primarily dependent on the dielectric constant of the material. Since the velocity of a wave in a medium varies in inverse proportion to the dielectric constant, it can be calculated using the following equation:

$$v = \frac{c}{\sqrt{\varepsilon_1}}$$

where, c = the speed of the electromagnetic wave in a vacuum

Therefore, by substitution, the following equation is obtained:

$$h_1 = \frac{(c \times \Delta t_1)}{\sqrt{\varepsilon_1}}$$

If the thickness is assumed to remain constant and its value is known, then the only remaining variable is the two way travel time, Δt_1. Rearranging the previous equation results in an equation where the material dielectric constant can be determined, as follows:

$$\varepsilon_1 = \left[\frac{(c \times \Delta t_1)}{h_1} \right]^2$$

A change in properties of a medium will impact the dielectric constant. In concrete, the most significant properties are moisture content and the presence of air or water filled voids. An increase in moisture content will decrease the speed with which the wave travels therefore increasing the materials dielectric constant, while an increase in air voids will increase the speed with which the wave travels therefore decreasing the materials dielectric constant. A gap filled with salt water, as may occur between the SIPMF and the deck, will increase attenuation of the radar signal.

9.3 GPR EXAMINATION OF EXISTING CORES

The existing study area of the bridge (chapter 1) is located within the first one hundred feet in the southbound lanes. The GPR data collection in this area was completed using both air launched and ground coupled systems.

First, the ground-coupled system was used at low speed (3-8 mph (5-13 kph)) to obtain data points at approximately 1-inch (25.4 mm) intervals along the study area. A series of passes was carried out on a spacing of two feet longitudinally so that an adequate representation of the quality of the deck could be generated. This method of collection results in the highest resolution of the quality of the concrete.

Next, the air-launched system was used at low speed (3-8 mph (5-13 kph)) to obtain data points at 1-inch (25.4 mm) intervals along the study area. Again, a series of multiple passes was carried out over the width of the bridge to obtain adequate information.

Finally, the air-launched system was used at normal speed (25-35 mph(40-56 kph)) to obtain data points at 2 inch (51mm) intervals over the entire length of the bridge. This part of the survey was completed because traveling at normal speeds during data acquisition is the safest of the methods and would most likely occur in future surveys. The entire length of the bridge was surveyed so an expanded study could be conducted if the study of the existing cores was not conclusive.

The raw data from the survey was then compiled by Resource International, Incorporated (Rii). The Rii report is included as the appendix to this chapter. It was found that GPR gives a reflection from the transverse rebar in the upper layer of the bridge deck and from the SIPMF. The lower layer of transverse rebar, which is located directly below the upper layer, lies in the shadow of the upper transverse rebar as shown in Figure 9.1. Therefore, there is no reflection from the transverse rebar at the bottom of the bridge deck. The radar results for a section of bridge deck are shown in Figures 9.2 and 9.3 on the following pages. The ground-coupled results are shown in Figure 9.2 and the air-launched results are shown in Figure 9.3.
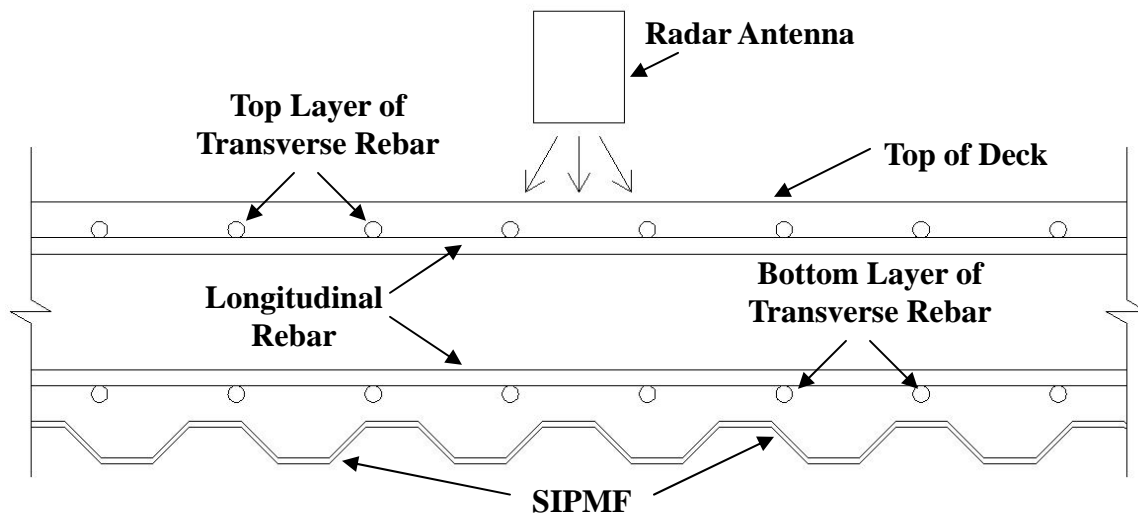
Figure 9.1. Typical Cross Section of Bridge Deck
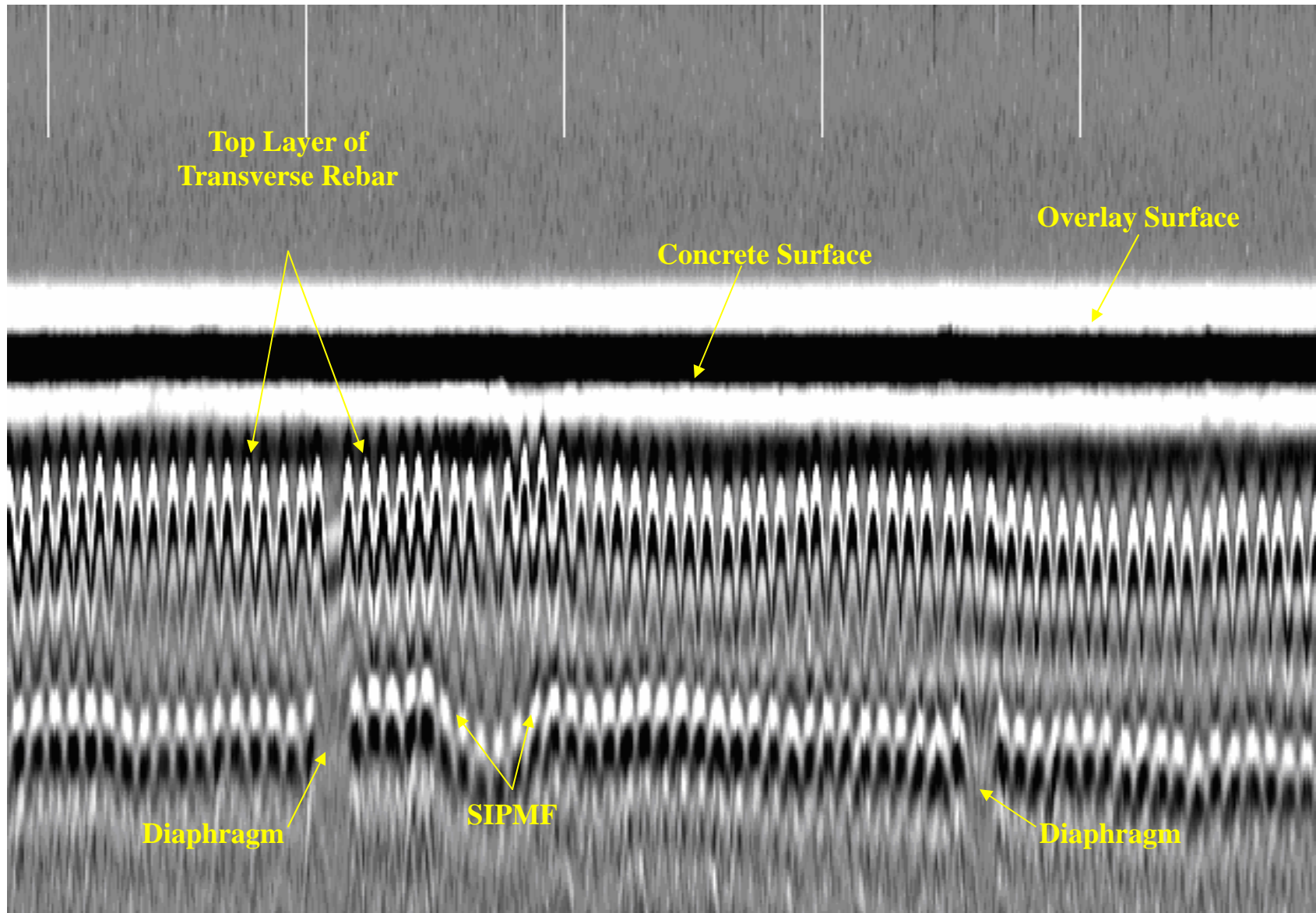
Figure 9.2. Ground Coupled Radar Results
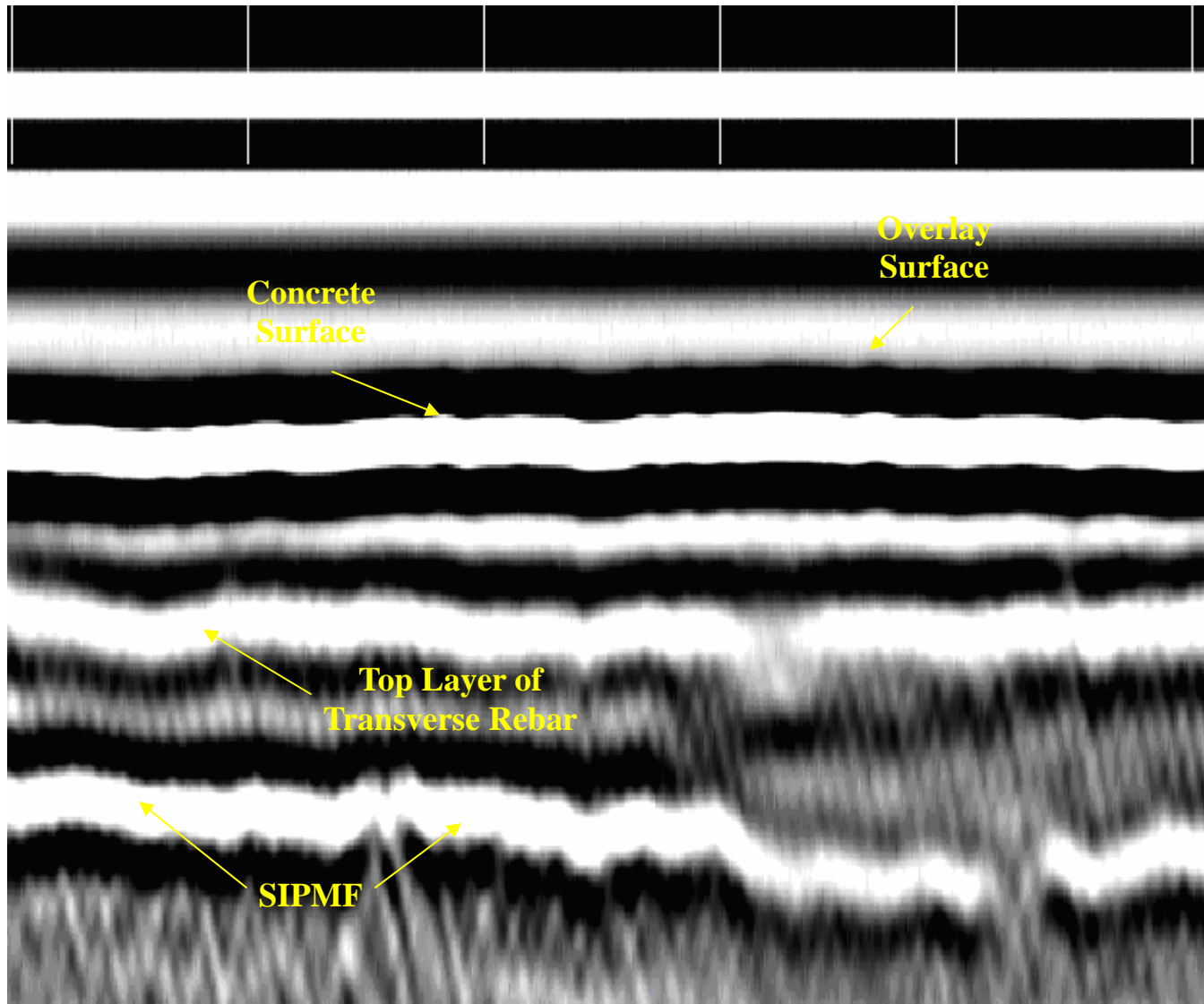
Figure 9.3. Air Launched Radar Results

Rii compiled maps of the strength of the reflected radar signal from the top layer of rebar and from the SIPMF over the region the original cores were taken from and the entire length of the bridge. Delaminations are one of the principle causes of high attenuation. Therefore, it was hypothesized that high attenuation indicated areas with delaminations. It was found that areas of high attenuation, indicating potential delaminations, existed over the entire length of the structure. Figure 9.4 is the delamination map over the region the existing cores were taken from. Figure 9.5 is the delamination map over the entire length of the bridge. If an area had low attenuation of the radar signal, it is blue on the delamination map. If the area had high attenuation, it is red on the map. Areas of intermediate attenuation are yellow.

There were three limitations to using the GPR data from the existing cores to reach broad conclusions about the efficacy of GPR. The existing cores covered a very small portion of the bridge, the existing cores were not located in areas where the GPR predicted severe delamination, and the cavities left by the core extraction reduce the accuracy of the GPR in the local region of the cores. Therefore, it was decided to harvest additional verification cores.
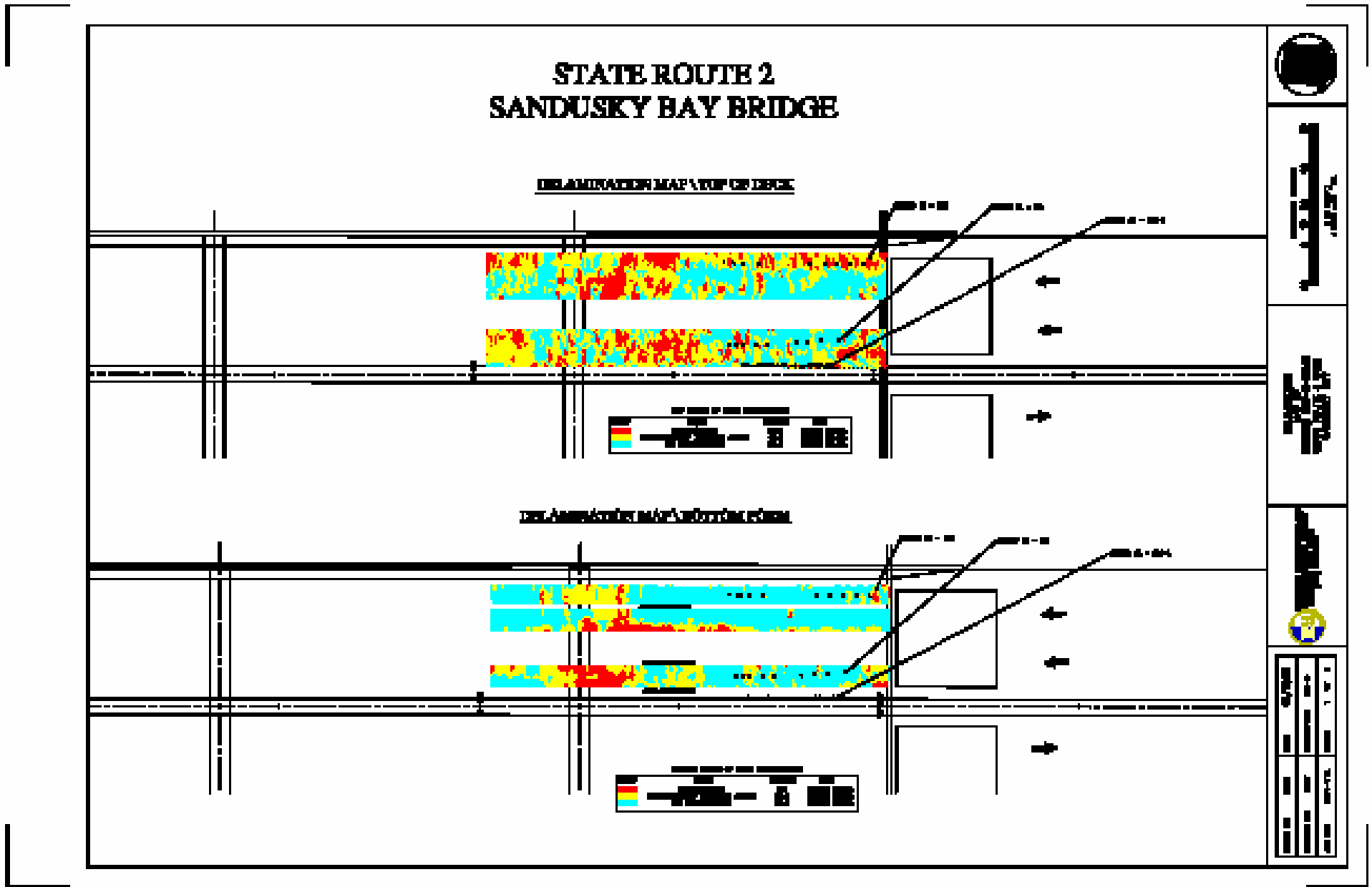
Figure 9.4. GPR Delamination Map of Existing Core Locations

Figure 9.5a. GPR Delamination Map from the South Abutment to Pier 20
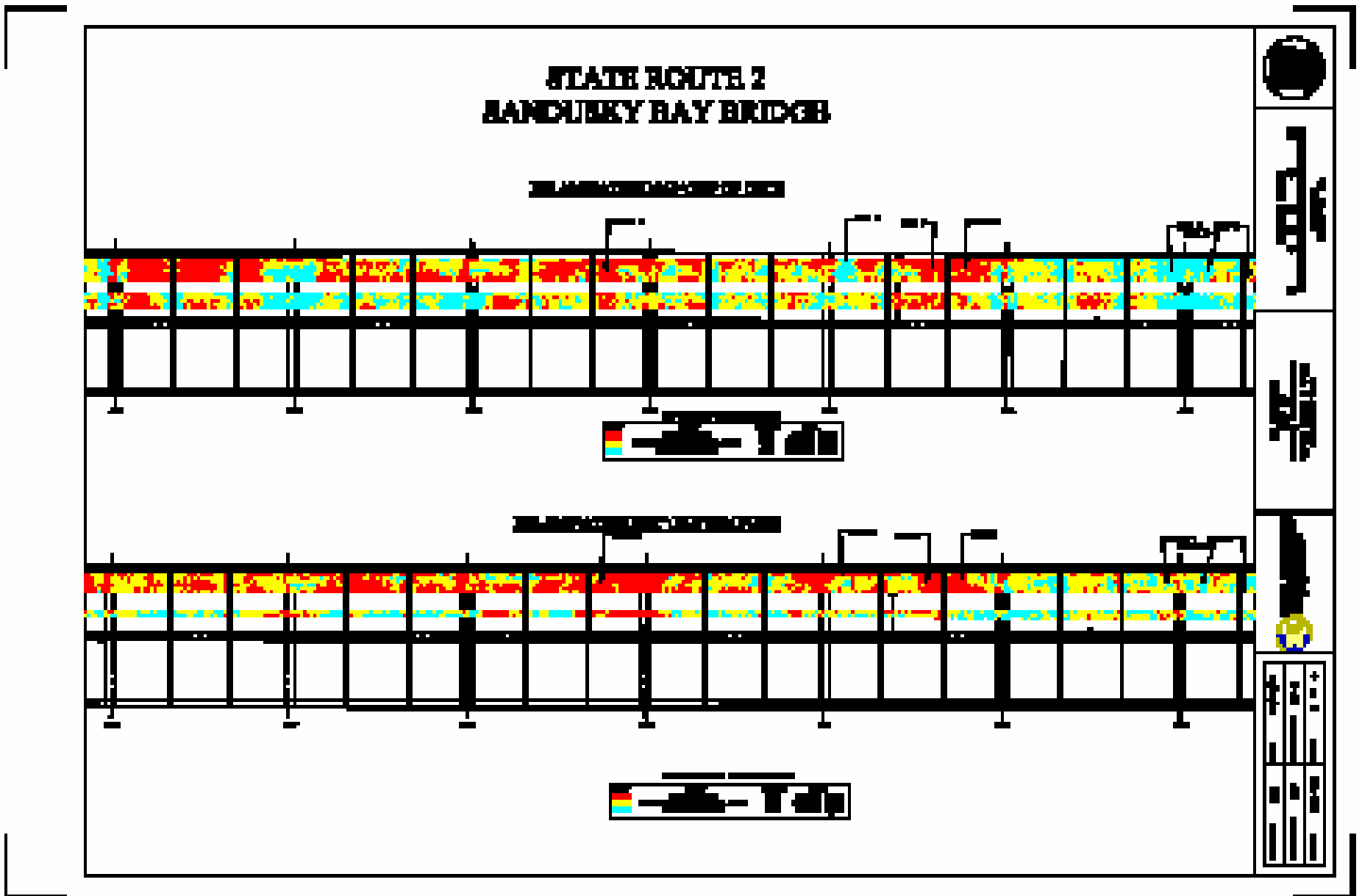
Figure 9.5b. GPR Delamination Map from Pier 19 to Pier 13
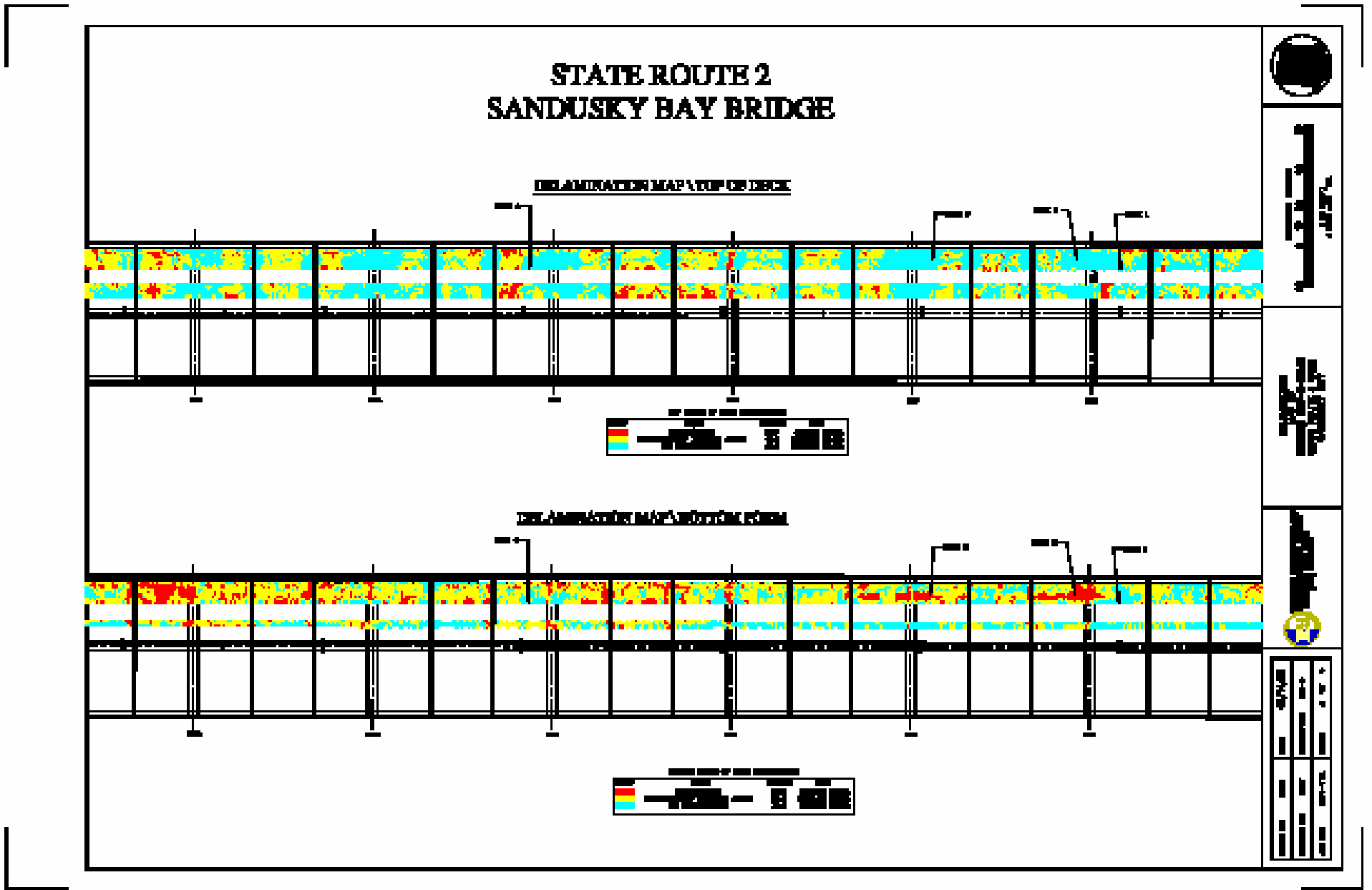
Figure 9.5c. GPR Delamination Map from Pier 12 to Pier 7
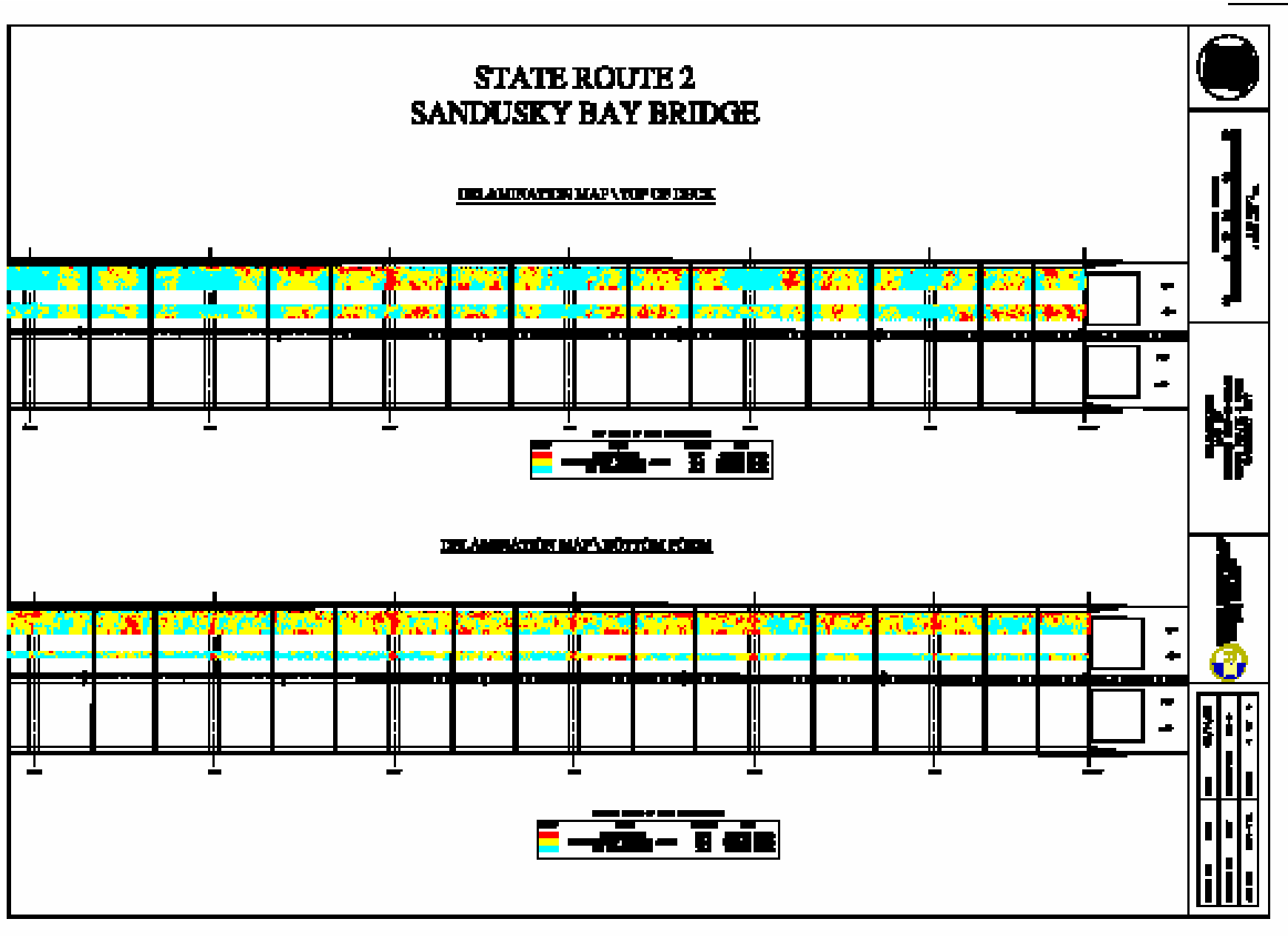
Figure 9.5d. GPR Delamination Map from Pier 6 to the North Abutment

9.4 Ground Truth Survey

Generally, the areas of high attenuation found during the survey of the entire bridge do not coincide with the location of the existing cores. Therefore, it was decided that additional verification (ground truth) cores should be extracted along the length of the bridge in various places: some where the both the top and bottom show low attenuation, some where the bottom shows high attenuation but the top shows low attenuation, and some where both the top and bottom show high attenuation.

The target was to harvest cores at eight to twelve locations. Sixteen candidate locations were selected based on Figure 9.5. Ground truth cores were extracted from ten of the candidate locations along the length of the bridge. At each location, at least two cores were harvested: one core for compression testing and one core for ultrasonic testing.

Low attenuation of the GPR signal was hypothesized to predict a core without delaminations. While high attenuation was hypothesized to predict the core to have delaminations. Each location was classified as good/good, good/bad, or bad/bad depending on the attenuation of the radar signal in the top and bottom of the deck respectively and corresponding to information obtained from the GPR survey. The attenuation at the top of the deck was determined from the strength of the reflection from the top layer of rebar, while the attenuation at the bottom was determined from the strength of the reflection from the SIPMF. If high attenuation of the radar signal occurred off the top layer of rebar, it was hypothesized that there was a delamination in the top of the deck. If there is low attenuation off the top layer of rebar, but high attenuation off the SIPMF, it was hypothesized that delamination existed between the top layer of rebar and the SIPMF. Table 9.1 shows the correlation of high and low attenuation from the top layer of rebar and the SIPMF with the expected quality of the concrete deck.

It was also a concern that the gap that exists between the SIPMF and the concrete deck would result in high attenuation of the radar signal and give a false indication of delamination in the concrete. During core extraction, it was found that none of the cores was bonded to the SIPMF. Therefore, the void just above the SIPMF could give a false indication of a delamination.

It was also a goal for this study to assess if it was possible to determine the strength or quality of concrete using GPR. Based on the literature review, it was determined that the

reflected GPR signal has not yet been correlated to concrete strength. The speed at which the GPR wave travels through the bridge deck is a function of the dielectric constant and the losses are a function of absorption, scattering, changes in dielectric constant of the medium, the shape of the wavefront. The dielectric constant changes due to a number of variables, including the mix design, free water in voids, air voids, admixtures, aggregate type, water to cement ratio, the presence of chlorides, etc. These properties are not directly linked to the elastic properties of concrete or to the strength of concrete. Because of this complexity, dielectric constant and attenuation have not been linked to concrete strength.

Table 9.1: Radar Signal Attenuation

Radar Signal Attenuation		
Top Layer of Rebar	**SIPMF**	**Expected Condition**
Low	Low	No delaminations present in entire column
Low	High	Delamination below the top layer of rebar and above the SIPMF
High	High	Delamination present at least above the top layer of rebar
High	Low	Not possible, an upper layer delamination would cause high attenuation in both the top layer of rebar and SIPMF reflections.

9.4.1   Visual Inspection of Ground Truth Cores

The ground truth cores and the hole from which they were extracted were visually inspected immediately upon removal and an index was created. The index consisted of:

1. The condition of the concrete at the surface.
2. The condition of the concrete in the top layer.
3. The condition of the concrete at the bottom layer.
4. Presence of rust on SIPMF.
5. Delaminations in the concrete.

The goal of this index was to determine the overall condition of each individual core and general characteristics of each core after it had been extracted from the bridge. The reinforcing steel was inspected for the presence of rust and the concrete was inspected for the presence of cracks and air voids.

Each core was inspected in the five areas listed above, and a rating system was created to evaluate these five areas by assigning each area a number ranging from zero to five. A rating of zero implied the worst condition possible, while a rating of five meant the core sample was in good condition for the area inspected.

Photographs and descriptions of the cores are presented below.

Location:

Station location 113+00.3 and 4.9 feet (1.494 m) from the face of the curb on the west side of the bridge.

Comments:
- Core height 7 inches (177.8 mm) with 4.25 inch (108 mm) overlay.
- Some rust present on bottom of core.
- Numerous air voids present.

Figure 9.6. Core GT-1A

Location:

Station location 113+00.3 and 5.4 (1.646 m) feet from the face of the curb on the west side of the bridge.

Comments:
- Core height 6.75 inches (171.5 mm) with 4 inch (101.6 mm) overlay.
- White residue present on bottom of core.
- Numerous voids in concrete up to 0.25 inches (6.35 mm)in diameter

Figure 9.7. Core GT-1B

Location:

Station location 112+99.8 and 4.9 feet (1.494 m) from the face of the curb on the west side of the bridge.

Comments:
- Core height 5.25 inches (133.4 mm) with 4 inch (101.6 mm) overlay.
- Core fractured due to excavation.
- Rebar at 3.5" (88.9 mm) from top.
- Numerous air voids in concrete.

Figure 9.8. Core GT-1C

Location:

Station location 112+99.8 and 5.3 feet (1.615 m) from the face of the curb on the west side of the bridge.

Comments:
- Core height 6.75 inches (171.5 mm) with 3.75 inch (95.25 mm) overlay.
- Rebar at 5.5 inches (139.7 mm) from top.
- Heavy rust present on bottom of core.
- Large voids present in concrete up to 0.5 (12.7 mm) inches in diameter.

Figure 9. 9. Core GT-1D

Location:

Station location 113+22.4 and 5.1 feet (1.554 m) from the face of the curb on the west side of the bridge.

Comments:
- Core height 7.25 (184.2 mm) inches with overlay thicknesses of 1.75 inches (44.45 mm) and 1.5 inches (38.1 mm).
- Heavy rust present on bottom of core.
- Small voids present in concrete.

Figure 9.10. Core Number: GT-2A

Location:

Station location 113+22.4 and 5.6 feet (1.707 m) from the face of the curb on the west side of the bridge.

Comments:
- Core height 7 inches (177.8 mm) with overlay thicknesses of 1.5 inches (38.1 mm) and 1 inch (25.4 mm).
- Heavy rust present on bottom of core.
- Small voids present in concrete.

Figure 9.11. Core : GT-2B

Location:

Station location 113+95.3 and 5.0 feet (1.524 m) from the face of the curb on the west side of the bridge

Comments:
- Core height 7.75 inches (196.8 mm) with 4 inch (101.6 mm) overlay.
- Core fractured at 6.25 inches (158.8 mm) from the top due to extraction.
- Rebar present at 6.5 inches (165.1 mm) from the top.
- Numerous air voids in concrete.

Figure 9.12. Core GT-3A

Location:

Station location 113+95.3 and 5.6 feet (1.707 m) from the face of the curb on the west side of the bridge

Comments:
- Core height 7.5 inches (190.5 mm) with overlay thicknesses of 2 inches (50.8 mm) and 1 inch (25.4 mm).
- Numerous voids present in concrete.

Figure 9.13. Core GT-3B

Location:

Station location 118+44.2 and 5.0 feet (1.524 m) from the face of the curb on the west side of the bridge.

Comments:
- Core height 7.75 inches (196.9 mm) with 1.5 inch (38.1 mm) overlay.
- Core delaminated 3 inches (76.2 mm) from the top, above the top layer of rebar.
- Numerous voids present in concrete.

Figure 9.14. Core GT-6A

Location:

Station location 118+44.2 and 5.6 feet (1.707 m) from the face of the curb on the west side of the bridge.

Comments:
- Core height 8 inches (203.2 mm) with 1.5 inch (38.1 mm) overlay.
- Core delaminated 3 inches (76.2 mm) from the top, above the top layer of rebar.
- Numerous voids in concrete up to 0.375 inches in diameter.

Figure 9.15. Core GT-6B

Location:

Station location 118+61.2 and 5.0 feet (1.524 m) from the face of the curb on the west side of the bridge.

Comments:
- Core height 8 inches (203.2 mm) with 1.5 inch (38.1 mm) overlay.
- Rebar present at 6.5 inches (165.1 mm) from the top.
- Small voids present in the concrete.

Figure 9.16. Core Number: GT-7A

Location:

Station location 118+61.2 and 5.5 feet (1.676 m) from the face of the curb on the west side of the bridge.

Comments:
- Core height 8 inches (203.2 mm) with 1.5 inch (38.1 mm) overlay.
- Small voids present in the concrete.

Figure 9.17. Core Number: GT-7B

Location:

Station location 119+64.8 and 3.2 feet (0.975 m) from the face of the curb on the west side of the bridge.

Comments:
- Core height 8.5 inches (215.9 mm) with 2 inch (50.8 mm) overlay.
- Heavy rust present on bottom of core.
- Core delaminated 3.75 inches (95.25 mm) from the top, above the top layer of rebar.
- Numerous voids in concrete.

Figure 9.18. Core Number: GT-8A

Location:

Station location 119+64.8 and 3.6 feet (1.097 m) from the face of the curb on the west side of the bridge.

Comments:
- Core height 8.25 inches (203.2 mm) with 2 inch (203.2 mm) overlay
- Some rust present on bottom of core
- Core delaminated 3.5 inches (203.2 mm) from top
- Rebar located at 5 inches (203.2 mm) and 7.25 inches (203.2 mm) from the top.
- Small air voids present in the concrete.

Figure 9.19. Core Number: GT-8B

Location:

Station location 119+65.3 and 3.1 feet (0.945 m) from the face of the curb on the west side of the bridge.

Comments:
- Core height 8.25 inches (209.6 mm) with 2 inch (50.8 mm) overlay.
- Core delaminated 4 inches (101.6 mm) from top, just above the top layer of rebar.
- Core fractured at bottom due to extraction.
- Rebar located at 4.5 inches (114.3 mm) from the top heavily corroded.
- Rebar located at 8.25 inches (209.6 mm) from the top.
-

Figure 9.20 Core Number: GT-8C

Location:

Station location 119+83.0 and 4.1 feet (1.250 m) from the face of the curb on the west side of the bridge.

Comments:
- Core height 8.5 inches (215.9 mm) with 1.75 inch (44.45 mm) overlay.
- Core delaminated at overlay, above the top layer of rebar.
- Rebar located at 8 inches (203.2 mm) from top.
- Numerous voids present up to 0.375 inches (9.525 mm) in diameter.

Figure 9.21. Core Number: GT-9A

Location:

Station location 119+83.0 and 4.6 feet (1.402 m) from the face of the curb on the west side of the bridge.

Comments:
- Core height 8.5 inches (215.9 mm) with 1.5 inch (38.1 mm) overlay.
- Core delaminated at overlay, above the top layer of rebar.
- Rebar located at 7.25 inches (184.2 mm), 5 inches (127 mm), and 8 inches (203.2 mm) from the top.
- Numerous voids in concrete up to 0.25 inches (6.35 mm) in diameter..

Figure 9.22. Core Number: GT-9B

Location:

Station location 0+25.7 and 1.3 feet (0.396 m) from the face of the curb on the west side of the bridge.

Comments:
- Core height 8.75 inches (222.3 mm) with 2.25 inch (57.15 mm) overlay.
- Rebar located at 4.75 inches (120.7 mm) from the top with minor rust.
- Numerous voids present in concrete.

Figure 9.23. Core Number: GT-10A

Location:

Station location 0+25.8 and 1.5 feet (0.457 m) from the face of the curb on the west side of the bridge.

Comments:
- Core height 10.5 inches (203.2 mm) with 2 inch (50.8 mm) overlay.
- Rebar located at 4 inches (101.6 mm), 5 inches (127 mm), and 7.5 inches (190.5 mm) from the top.
- Core fractured at bottom due to excavation.
- Small voids present in concrete

Figure 9.24. Core Number: GT-10B

Location:

Station location 1+47.2 and 5.0 feet (1.524 m) from the face of the curb on the west side of the bridge.

Comments:
- Core height 8.5 inches (215.9 mm) with 1.75 inch (44.45 mm) overlay.
- Core fractured due to excavation.
- Small voids present in concrete up to 0.25 inches (6.35 mm) in diameter.

Figure 9.25. Core Number: GT-11A

Location:

Station location 1+47.2 and 5.5 feet (1.676 m) from the face of the curb on the west side of the bridge.

Comments:
- Core height 8.5 inches (215.9 mm) with 1.75 inch (44.45 mm) overlay.
- Numerous voids in concrete up to 0.25 inches (6.35 mm) in diameter.

Figure 9.26. Core Number: GT-11B

Location:

Station location 7+29.8 and 3.0 feet (0.914 m) from the face of the curb on the west side of the bridge.

Comments:
- Core height 10 inches (254 mm) with 2 inch (50.8 mm) overlay.
- Rebar located at 3.75 inches (95.25 mm) and 7.5 inches (190.5 mm) from the top.
- Small amounts of voids in concrete.

Figure 9.27. Core Number: GT-16A

Location:

Station location 7+29.7 and 4.0 feet (1.219 m) from the face of the curb on the west side of the bridge.

Comments:
- Core height 10 inches (254 mm) with 2 inch (50.8 mm) overlay.
- Rebar located at 3.75 inches (95.25 mm) and 7.5 inches (190.5 mm) from the top.
- White residue present on bottom of core.
- Small amount of voids in concrete.

Figure 9.28. Core Number: GT-16B

The results of the visual inspection are shown in table 9.2. According to the records, the design compressive strength of the concrete on OTT-2-28.41 is 3000 psi (20.69 mPa). The original design was an 8 inches (203.2 mm) deck slab thickness. In 1980, a 1.25 inch (31.75 mm) layer of asphalt was applied to the top of the deck and in 1994 the asphalt layer was removed and replaced with 1.25 inch (31.75 mm) of Micro-Silica Modified Concrete (Geckle, 2005). The visual inspection found conditions that where different. At certain locations, such as coring locations GT-1, 2, and 3, the overlay was of greater thickness than the rest of the bridge. The GPR scan does not depict this change in thickness; this means the dielectric constant of the overlay is the same as the deck concrete. In addition, in areas where two overlay layers existed, such as coring location GT-2, the GPR could not differentiate between them.

Table 9.2: OTT-2-28.41 Visual Inspection of Ground Truth Cores

Core	Concrete			SIPMF Rust		Delamination			Σ	Average
	Surface	Top	Bottom	Present	Score	Present	Location	Score		
	5	5	5	Y/N	5	Y/N		5	25	
1A	5	5	4	Y	3	N	N/A	5	22	88
1B	5	5	4	Y	3	N	N/A	5	22	88
1C	5	5	N/A	N/A	N/A	N	N/A	5	15	100
1D	5	5	4	Y	3	N	N/A	5	22	88
2A	5	5	4	Y	4	N	N/A	5	23	92
2B	5	5	4	Y	4	N	N/A	5	23	92
3A	4	5	4	N	5	N	N/A	5	23	92
3B	4	5	4	N	5	N	N/A	5	23	92
6A	4	2	4	N	5	Y	Top	3	18	72
6B	4	2	4	N	5	Y	Top	4	19	76
7A	4	5	4	N	5	N	N/A	5	23	92
7B	4	5	4	N	5	N	N/A	5	23	92
8A	3	2	3	Y	4	Y	Top	1	13	52
8B	3	2	3	Y	2	Y	Top	0	10	40
8C	3	2	N/A	N/A	N/A	Y	Top	1	6	40
9A	3	2	4	N	5	Y	Overlay	1	15	60
9B	3	2	4	N	5	Y	Overlay	1	15	60
10A	5	5	5	N	5	N	N/A	5	25	100
10B	5	5	5	N	5	N	N/A	5	25	100
11A	3	5	5	N	5	N	N/A	5	23	92
11B	3	5	5	N	5	N	N/A	5	23	92
16A	3	5	5	N	5	N	N/A	5	23	92
16B	3	5	5	N	5	N	N/A	5	23	92

82

9.4.2 Compression Tests of Ground Truth Cores

The ground truth cores were tested in compression in accordance with AASHTO T22-97. The specification and procedure were identical to the earlier tests (chapter 4). The core samples obtained had a diameter of approximately 4" (101.6 mm)diameter. First, the test cores were sliced to remove the sections that contained reinforcement. This was followed by capping the cylinders to achieve a plane test surface. After capping, core dimensions, diameter and test lengths were obtained. In addition, the cylinders were weighed to calculate the density of concrete. The diameter and length of the specimen were used to calculate the required correction factor for low L/D ratios., the capped cylinders were then cured. After curing, the cores were tested in a 400,000-pound (1780 kN) capacity Tinius Olsen universal test machine in the concrete lab at The University of Toledo. The need to slice the cores to get rid of the reinforcement led to cores with L/D ratio less than one and as the AASHTO T22-97 gives correction factor only for L/D ratio with range 1 to 1.75. The correction factor values for cores with a lower L/D were extrapolated.

The design strength of the concrete for OTT-2-28.41 is 3,000 psi (20.69 MPa) . The average compressive strength found in the tests was 4,490 psi (30.96 MPa). All failures were columnar. The test results are consistent with the design strength, but display a wide range. The reason for the wide range is not completely understood. Part of the wide range is certainly due to the low L/D ratio for some cores and the fact that some cores come from regions with delaminations. Figure 9.29 shows the testing of a typical specimen and table 9.3 gives the compression test results.

9.29a: Prepared Specimen

9.29b: Specimen in the Test Machine

9.29c: Columnar Failure

Figure 9.29. Compression Test

Table 9.3: Ground Truth Cores Compression Test Results

Core	Weight lbs	Length in	Dia. in	Area in^2	Vol. in^3	Density lbs/yd^3	L/D	Correction Factor	Load lb	Adjusted Load lb	Strength psi
	1 lb = 4.448 N	1 in = 25.4 mm	1 in = 25.4 mm	1 in^2 = 645.16 mm^2	1 in^2 = 16387.06 mm^3	1 lbs/yd^3 =5.82 N/m^3			1 lb = 4.448 N	1 lb = 4.448 N	1 psi = 0.006895 MPa
GT-1B-T	3.96	4.1	3.91	12.01	49.53	3,730	1.05	0.88	83,300	73,570	6,130
GT-1B- B	2.84	2.8	3.94	12.18	33.87	3,910	0.71	0.79	62,000	49,137	4,040
GT-1C- T	2.57	2.6	3.94	12.18	31.96	3,758	0.67	0.78	84,500	65,628	5,390
GT-1D- T	3.27	3.4	3.88	11.79	39.80	3,829	0.87	0.84	79,800	66,955	5,680
GT-2A - B	5.62	5.5	3.91	11.98	65.91	3,978	1.41	0.95	46,300	43,937	3,670
GT-3A-T	3.83	4.0	3.88	11.79	47.17	3,793	1.03	0.88	61,900	54,332	4,610
GT-6A- B	4.56	4.5	3.88	11.79	53.44	3,984	1.17	0.91	54,500	49,630	4,210
GT-7A- M	4.15	4.1	3.94	12.18	49.85	3,888	1.04	0.88	54,500	47,934	3,940
GT-8C-M	2.29	2.3	3.91	11.98	28.09	3,799	0.60	0.75	60,000	45,000	3,750
GT-9B-M	2.86	2.9	3.91	11.98	34.45	3,872	0.74	0.80	40,500	32,578	2,720
GT-10B-T	3.02	3.0	3.94	12.18	36.53	3,854	0.76	0.81	77,700	63,159	5,190
GT-11A-B	3.18	3.3	3.88	11.79	38.33	3,868	0.84	0.83	64,800	53,868	4,570
GT-11A-M	3.12	3.1	3.91	11.98	37.45	3,891	0.80	0.82	45,900	37,730	3,150
GT-16A-M	2.56	2.6	3.88	11.79	30.96	3,855	0.68	0.78	76,300	59,588	5,050
GT-16A-T	3.06	3.2	3.88	11.79	37.59	3,800	0.82	0.83	75,600	62,553	5,300
Average						3,854				53,707	4,490

9.4.3 Ultrasound Tests of Ground Truth Cores

9.4.3.1 Introduction

Ultrasound investigation is well established as tool suitable for assessing the quality of concrete. The ultrasound tests were carried out at Lawrence Technological University. It is extremely accurate when it is accompanied by a complementary test such as the compression tests described in section 9.4.2 (Malhortra 1991, Krautkramer 1990, Sapovics 2005). The main objective of the ultrasound analysis and inspection of the ground truth cores was to determine that quality of the concrete. This measure of quality, complemented by the visual and compression tests, was then used as a standard for evaluating the predictions of the ground penetrating radar. The accepted relation between pulse velocity and quality of concrete is presented in table 9.4.

Table 9.4. Correlation between Ultrasonic Pulse Velocity and Quality of Concrete

(Krautkramer and Krautkramer 1990)

Ultrasound Pulse Velocity	Quality of concrete
15,000 fps	Very Good
12,000 fps	Good
10,000 fps	Moderate to questionable
7,000 fps	Bad
Below 7,000 fps	Very bad

(1 fps = 0.3048 m/s)

Ten of the full-depth ground truth cores taken from OTT-2-28.41 were transported to the Structural Testing Center at Lawrence Technological University (LTU) for evaluation of structural condition and assessment of condition of concrete. The cores were assessed visually and ultrasonically. The visual inspection and ultrasound tests were carried out by the procedures described in sections 7.2.1 and 7.2.2. The individual core data and a summary for the visual inspection and ultrasound testing procedures are presented below.

9.4.3.2 Inspection Results

Visual Inspection of Ground Truth Cores

The visual inspection of cores indicated that all the cores had wearing surface at the top surface. The heights of the cores were variable thus indicating non-uniformity of the bridge deck. The ten cores removed from the bridge deck were carefully inspected and illustrated as follows:

Core GT-1A (Figures 9.30-9.31)

- 6.88 in. (174.8 mm) height.
- 3.75 in. (95.25 mm) thickness of wearing surface.
- The concrete in the region of the valley of the SIPMF was broken.
- Fine aggregates were in the wearing surface and coarse aggregates in the remaining thickness.
- More porosity in the wearing surface.
- Honey combing in the wearing surface of 0.2 in (5.08 mm).
- Some rust and salt traces on the bottom of the core.
- The concrete in the region of the valley of the SIPMF was broken.

Figure 9.30. Large Depth of wearing surface

Figure 9.31. Rust and salt traces

Core GT-2B (Figures 9.32-9.33)
- 7.13 in. (181.1 mm) height.
- 1.66 in. (42.16 mm) thickness of wearing surface.
- Fine aggregates were in the wearing surface and coarse aggregates in the remaining thickness.
- More porosity in the wearing surface.
- Honey combing of 0.4 in. (10.16 mm) size at 5 in. (127 mm) and 0.25 in. (6.35 mm) at 6.25 in. (158.8 mm).
- Severe rust and salt traces on the bottom of the core.
- The concrete in the region of the valley of the SIPMF was broken.

Figure 9.32. Core 2B shows more porosity in the wearing surface

Figure 9.33. Severe rust and salt traces

Core 3B (Figures 9.34-9.35)

- 7.5 in. (190.5 mm) height.
- 2 wearing surface layers of 2 in. (50.8 mm) and 1.66 in. (42.16 mm) thicknesses.
- Fine aggregates were in the wearing surface and coarse aggregates in the remaining thickness.
- More porosity in the wearing surface.
- Some honey combing at several places.
- Voids of 0.2 in. (5.08 mm) at 3in. (76.2 mm), 3.75 in. (95.25 mm) and 4.75 in. (120.7 mm)
- Some salt traces on the bottom of the core.
- The concrete in the region of the valley of the SIPMF was broken.

Figure 9.35. Void at 3.75 in.

Figure 9.34. Two wearing surface layers

Core 6B (Figure 9.36)

- 7.5 in. (190.5 mm) height.
- Wearing surface layer of 1.5 in. (38.1 mm).
- Fine aggregates were in the wearing surface and coarse aggregates in the remaining thickness.
- More porosity in the wearing surface.
- Some honey combing at several locations.
- Voids of 0.4 in. (10.16 mm) at 2.75 in. (69.85 mm) and 0.13 in. (3.302) at 1.75 in. (44.45 mm).
- Horizontal crack at 2.88 in. (73.15 mm)
- The concrete in the region of the valley of the SIPMF was broken.

Figure 9.36. Core 6B shows
horizontal crack

Core 7B (Figures 9.37-9.38)

- 8.0 in. (203.2 mm) height.
- Wearing surface layer of 1.5 in. (38.1 mm)
- Fine aggregates were in the wearing surface and coarse aggregates in the remaining thickness.
- More honey combing in the wearing surface.
- Low porosity in both layers.
- Small voids at several locations.
- Small traces of salt at the bottom of the core.
- The concrete in the region of the valley of the SIPMF was broken.

Figure 9.38. Small traces of salt
at the bottom of Core 7B

Figure 9.37. Core 7B shows more honey
combing in the wearing surface

Core 8A (Figures 9.39-9.40)

- 8.3 in. (210.8 mm) height.
- Wearing surface layer of 2.0 in. (50.8 mm).
- Fine aggregates were in the wearing surface and coarse aggregates in the remaining thickness.
- More honey combing in the wearing surface.
- Voids of size 0.5 in. (12.7 mm) at 4.5 in. (114.3 mm), 0.4 in. (10.16 mm) at 5.5 in. (139.7 mm), and 0.2 in. (5.08 mm) at 2.5 in. (63.5 mm).
- Severe rust traces at the bottom of the core from SIPMF.
- The core was broken at 3.5 in. (88.9 mm).
- The concrete in the region of the valley of the SIPMF was broken.

Figure 9.40. Rust traces at the bottom

Figure 9.39. Core 8A
broken in the middle

Core 9A (Figures 9.41-9.42)

- 8.13 in. (206.5 mm) height.
- Wearing surface layer of 1.75 in. (44.45 mm).
- Fine aggregates were in the wearing surface and coarse aggregates in the remaining thickness.
- Honey combing of 0.5 in. (12.7 mm) at 7.0 in. (177.8 mm).
- Voids of size 0.25 in (6.35 mm). at 5.25 in. (133.4 mm), 6.25 in. (158.8 mm) , and 7.5 in. (190.5 mm)
- Reinforcement bar had small traces of rust.
- The core was broken at the bottom of the wearing surface.
- The concrete in the region of the valley of the SIPMF was broken.

Figure 9.41. Core 9A broken at the bottom of wearing surface

Figure 9.42. Some rust traces on reinforcement

Core 10A (Figures 9.43)

- 8.75 in. (222.3 mm) height.
- Wearing surface layer of 2.25 in. (57.15 mm)
- Fine aggregates were in the wearing surface and coarse aggregates in the remaining thickness.
- Honey combing of 0.25 in. (6.35 mm) size at 1.25 in. (31.75 mm)
- Voids of 0.25 in. (6.35 mm) size at 7.5 in. (190.5 mm)
- More voids in the wearing surface.
- Reinforcement bar had small traces of rust.
- The concrete in the region of the valley of the SIPMF was broken.

Figure 9.43. Core 9A broken in the
region of the valley of the SIPMF

Core 11B (Figures 9.44-9.45)

- 8.25 in. (209.6 mm) height.
- Wearing surface layer of 2.75 in. (69.85 mm)
- Fine aggregates were in the wearing surface and coarse aggregates in the remaining thickness.
- Honey combing in both layers.
- Voids of 0.32 in. (8.127 mm) size at 3.25 in. (82.55 mm), 4.0 in. (101.6 mm) , and 7.0 in. (177.8 mm)
- The concrete in the region of the valley of the SIPMF was broken.

Figure 9.44. Honey combing in both layers

Figure 9.45. Voids and honey combing

Core 16B (Figures 9.46-9.47)

- 9.75 in. (174.8 mm) height.
- Wearing surface layer of 2.0 in. (50.8 mm).
- Fine aggregates were in the wearing surface and coarse aggregates in the remaining thickness.
- More porosity in the wearing surface.
- Honey combing in both layers.
- Voids of 0.38 in. (9.652 mm) size at 5.75 in. (146.1 mm).
- 2 reinforcement bars with small traces of rust.
- Salt traces at the bottom of the core.
- The concrete in the region of the valley of the SIPMF was broken.

Figure 9.46. Core 16B with 2
reinforcement bars

Figure 9.47. Salt traces at the bottom
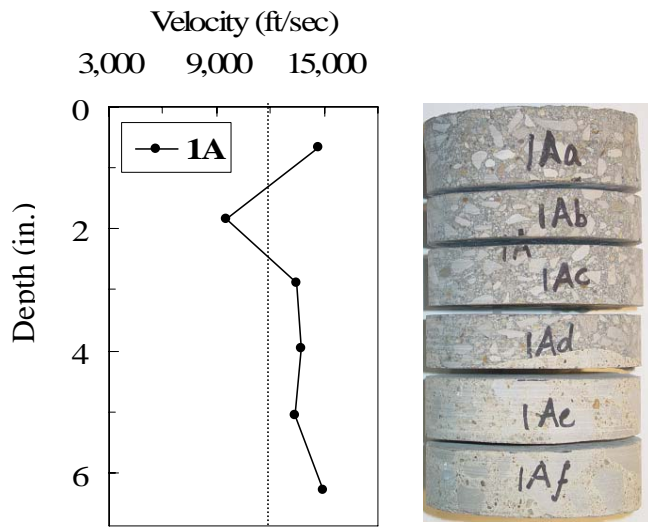
Figure 9.48. Ultrasonic velocity
with core depth for Core 1A
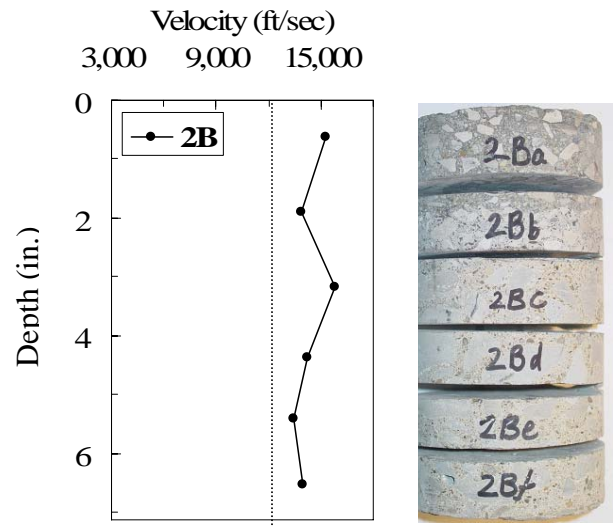
Figure 9.49. Ultrasonic velocity
with core depth for Core 2B
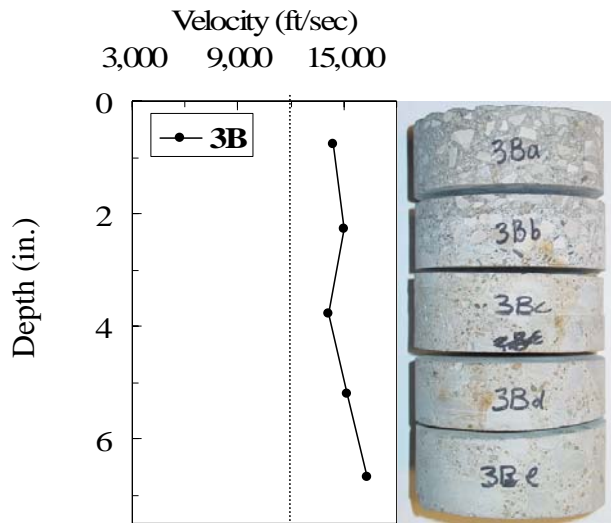
Figure 9.50. Ultrasonic velocity
with core depth for Core 3B
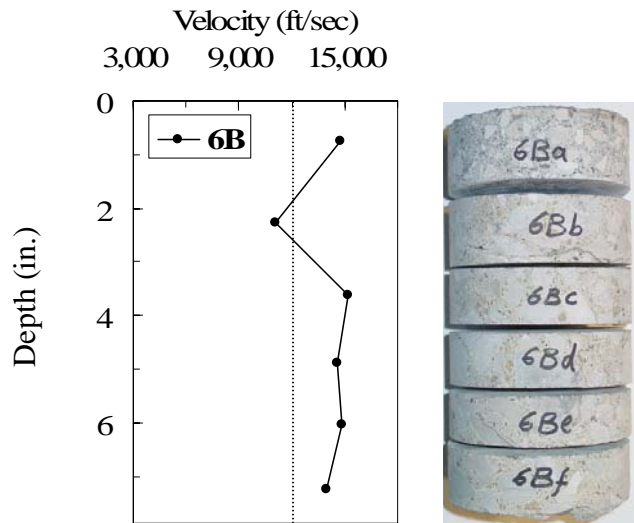
Figure 9.51. Ultrasonic velocity
with core depth for Core 6B

1 fps = 0.3048 m/s
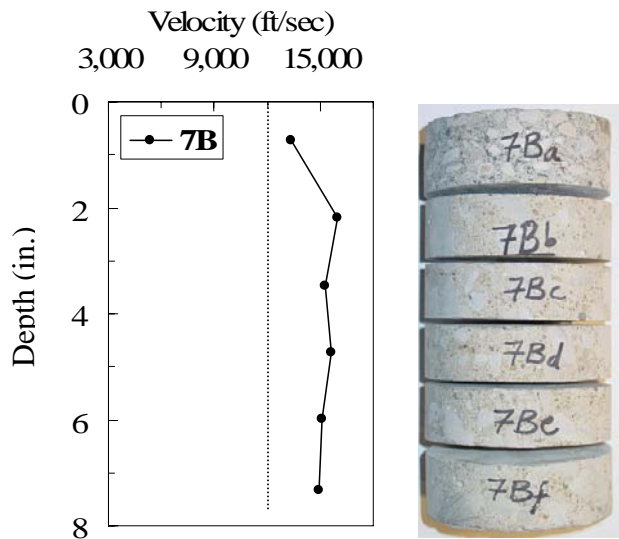
Figure 9.52. Ultrasonic velocity
with core depth for Core 7B
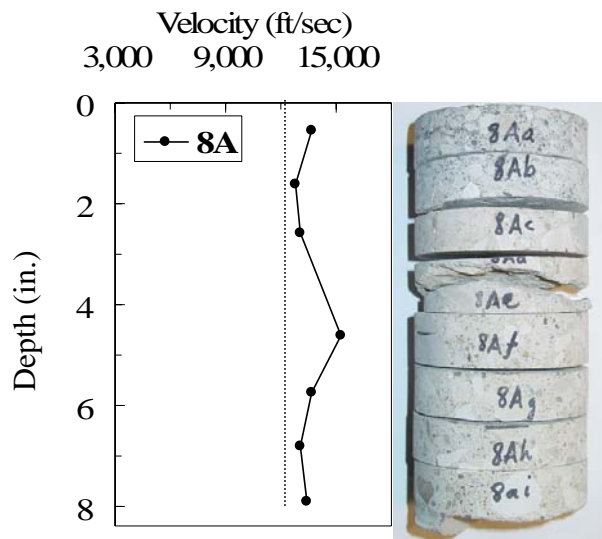
Figure 9.53. Ultrasonic velocity
with core depth for Core 8A
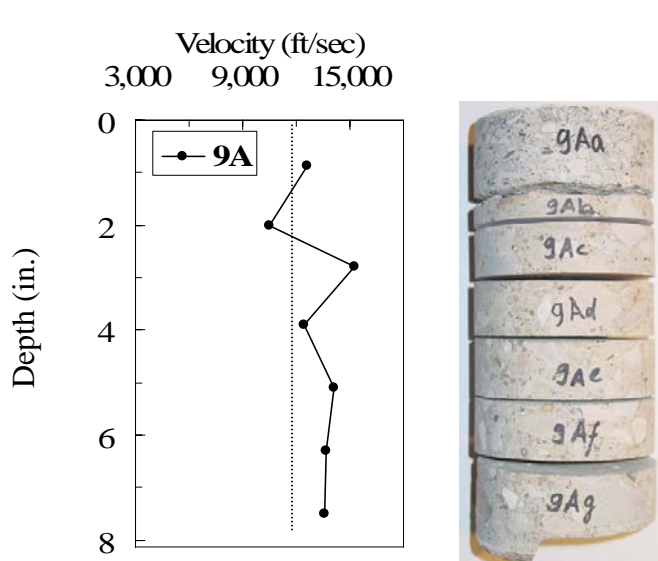
Figure 9.54. Ultrasonic velocity
with core depth for Core 9A
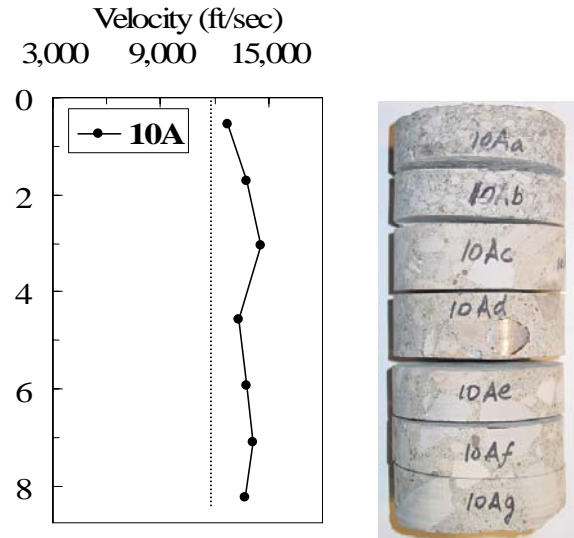
Figure 9.55. Ultrasonic velocity
with core depth for Core 10A

1 fps = 0.3048 m/s
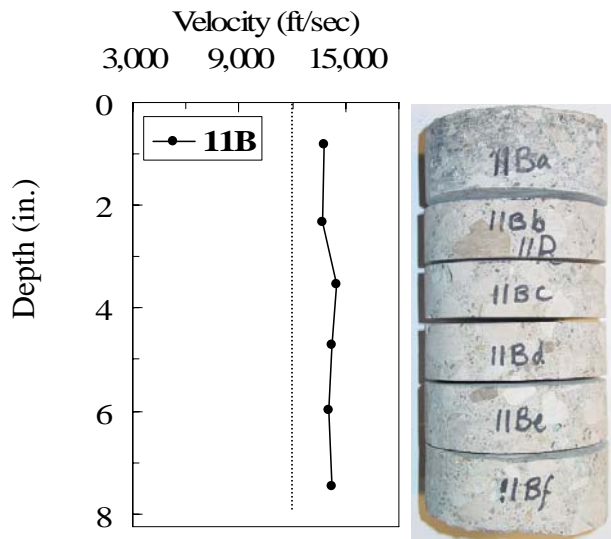
Figure 9.56. Ultrasonic velocity
with core depth for Core 11A
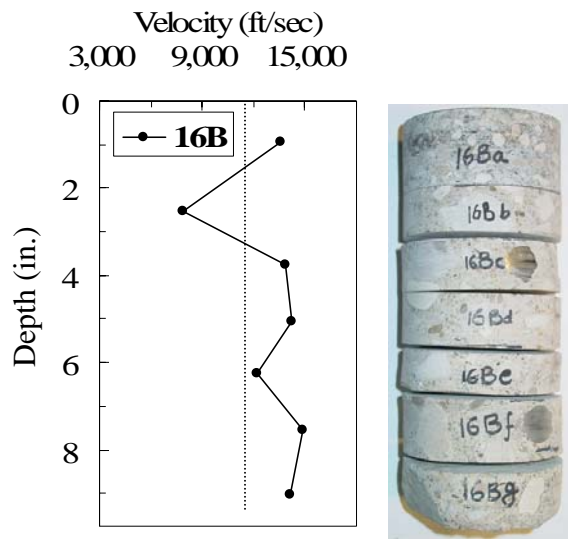
Figure 9.57. Ultrasonic velocity
with core depth for Core 16B

1 fps = 0.3048 m/s

9.4.3.3 Summary of visual inspection and ultrasonic tests of ground truth cores

Inspection indices similar to sections 7.4.1.1 and 7.4.1.2 were developed to quantify the visual inspection and ultrasonic test results of the ten cores. As before, these indices are referred to as the visual inspection index (*VII*) and Quality Index (*QI*), respectively.

Ground Truth Core Visual Inspection Summary

For the ground truth cores, the *VII* ranged from 56 to 89 with an average value of 73 (Table 9.5).

Overall, based on visual inspection of the collected cores, the condition of this bridge deck was essentially similar to the condition reported for other cores taken from other bridge decks reported in Chapter 7.

Table 9.5: Visual Inspection Index (VII) for ground truth cores from OTT-2-28.41

Core	Steel Condition of Rust	Concrete Porosity Concrete	Porosity Aggregate	Honeycombing Quantity	Honeycombing Size	Cracks Quantity	Cracks Size	Voids Quantity	Voids Size	SIPMF Condition of Rust	Σ	VII $VII = (\Sigma/27)*100$	Average VII
	N/A - 3	3	3	3	3	3	3	3	3	N/A - 3	24 - 30		
GT 1A	N/A	1.5	3	3	3	3	3	3	3	1.5	**24**	89	
GT 2B	N/A	0.5	3	3	3	3	3	3	3	0	**21.5**	80	
GT 3B	N/A	1.5	3	1.5	1.5	3	3	1.5	1.5	2.5	**19**	70	
GT 6B	N/A	3	3	2	2	1.5	0	1	1	NA	**13.5**	56	
GT 7B	N/A	2.5	2.5	2	2	3	3	3	3	2.5	**23.5**	87	73
GT 8A	N/A	3	3	1	1	1.5	1.5	1	1	0	**13**	48	
GT 9A	2	3	3	2	2	3	3	2	2	3	**25**	83	
GT 10A	2	3	3	2	2	3	3	1	1	3	**23**	77	
GT 11B	N/A	3	3	0	0	3	3	2	2	3	**19**	70	
GT 16B	2	2	2	2	2	3	3	2	2	2	**22**	73	

Ground Truth Core Ultrasonic Testing Summary

Ultrasonic velocity was measured on individual slices of each core. The ultrasonic measurements for each core are presented at the end of each coring location section. All of the ultrasonic data (velocity vs. depth) obtained in the test program are presented in Figures 9.58. Average trends are shown in Figures 9.59.

The normalized value, *QI*, has units consistent with velocity (ft/s) (1ft/s = 0.3048 m/s) and represented a weighted average of the wave velocity with depth over the entire profile (Figure 7.102). This parameter provided an effective means for comparison of the quality of concrete between different cores. The results of this analysis are presented in Tables 9.6-9.8. The *QI* representing all bridge deck cores (calculated for the total length of all analyzed cores) was 13,918 ft/s (4242.206 m/s) (Table 9.9). It should be mentioned that even though the *QI* for the OTT-2-28.41 deck was greater than *QI* (Chapter 7), the difference in QI between two bridge deck systems was considered negligible (5.0%).

The variation of pulse velocity with depth was investigated by dividing the cores into three equal regions with depth: top, middle, and bottom. The results of this analysis are presented in Tables 9.6 through 9.8, and 9.10. Average *QI* is presented for each region of the cores. In addition, ratios of region-specific *QI* to average *QI* are provided.

Table 9.6: Ultrasonic velocity for Cores GT 1A, GT 2B, GT 3B, and GT 6B

	Core GT 1A					Core GT 2B			
Slice No.	Thickness (in.)	Mid Point depth (h) (in.)	Velocity (V) (ft/s)	Σ V(Δh) (in.ft/s)	Slice No.	Thickness (in.)	Mid Point depth (h) (in.)	Velocity (V) (ft/s)	Σ V(Δh) (in.ft/s)
	1 in. = 25.4 mm	1 in. = 25.4 mm	1 ft/s = 0.30 m/s	1 in. ft/s = 0.0076 m²/s		1 in. = 25.4 mm	1 in. = 25.4 mm	1 ft/s = 0.30 m/s	1 in. ft/s = 0.0076 m²/s
a	1.336	0.67	14,644	9,778.29	a	1.272	0.64	15,291	9,727.28
b	0.827	1.85	9,575	14,288.41	b	1.087	1.91	13,865	18,582.38
c	1.034	2.88	13,457	11,849.41	c	1.242	3.17	15,839	18,704.63
d	0.942	3.96	13,685	14,738.44	d	0.981	4.38	14,262	18,159.18
e	1.050	5.06	13,386	14,808.42	e	0.881	5.40	13,422	14,201.17
f	1.195	6.28	14,938	26,213.97	f	1.187	6.53	13,998	23,783.39
Σ	6.88			91,676.94	Σ =	7.13			103,158.03
V_{max} =			14,937.50		V_{max} =			15,838.65	
QI_{avrg} =				13,334.83	QI_{avrg} =				14,478.32
QI_{top} =				12,519.14	QI_{top} =				14,700.87
QI_{mid} =				13,308.54	QI_{mid} =				14,943.58
QI_{bot} =				14,176.80	QI_{bot} =				13,790.52
QI_{top} / V_{max} =				0.84	QI_{top} / V_{max} =				0.93
QI_{top} / QI_{avrg} =				0.94	QI_{top} / QI_{avrg} =				1.02
QI_{mid} / V_{max} =				0.89	QI_{mid} / V_{max} =				0.94
QI_{mid} / QI_{avrg} =				1.00	QI_{mid} / QI_{avrg} =				1.03
QI_{bot} / V_{max} =				0.95	QI_{bot} / V_{max} =				0.87
QI_{bot} / QI_{avrg} =				1.06	QI_{bot} / QI_{avrg} =				0.95

Table 9.6: Ultrasonic velocity for Cores GT 1A, GT 2B, GT 3B, and GT 6B (continued)

	Core GT 3B					Core GT 6B			
Slice No.	Thickness (in.)	Mid Point depth (h) (in.)	Velocity (V) (ft/s)	Σ V(Δh) (in.ft/s)	Slice No.	Thickness (in.)	Mid Point depth (h) (in.)	Velocity (V) (ft/s)	Σ V(Δh) (in.ft/s)
	1 in. = 25.4 mm	1 in. = 25.4 mm	1 ft/s = 0.30 m/s	1 in. ft/s = 0.0076 m²/s		1 in. = 25.4 mm	1 in. = 25.4 mm	1 ft/s = 0.30 m/s	1 in. ft/s = 0.0076 m²/s
a	1.525	0.76	14,441	11,011.48	a	1.487	0.74	14,752	10,968.10
b	1.368	2.28	15,000	22,298.10	b	1.381	2.27	11,062	19,666.80
c	1.497	3.78	14,176	21,893.04	c	1.169	3.63	15,215	17,927.17
d	1.215	5.20	15,184	20,906.52	d	1.144	4.88	14,585	18,565.59
e	1.622	6.69	16,353	36,708.93	e	0.975	6.03	14,863	16,921.71
					f	1.271	7.24	13,931	26,309.41
Σ	7.50			112,818.07	Σ =	7.88			110,358.78
V_{max} =			16,353.33		V_{max} =			15,214.84	
QI_{avrg} =				15,042.41	QI_{avrg} =				14,013.81
QI_{top} =				14,654.88	QI_{top} =				13,252.19
QI_{mid} =				14,566.90	QI_{mid} =				14,375.28
QI_{bot} =				15,905.44	QI_{bot} =				14,413.97
QI_{top} / V_{max} =				0.90	QI_{top} / V_{max} =				0.87
QI_{top} / QI_{avrg} =				0.97	QI_{top} / QI_{avrg} =				0.95
QI_{mid} / V_{max} =				0.89	QI_{mid} / V_{max} =				0.94
QI_{mid} / QI_{avrg} =				0.97	QI_{mid} / QI_{avrg} =				1.03
QI_{bot} / V_{max} =				0.97	QI_{bot} / V_{max} =				0.95
QI_{bot} / QI_{avrg} =				1.06	QI_{bot} / QI_{avrg} =				1.03

{(--) Indicates no available data}

Table 9.7: Ultrasonic velocity for Cores GT 7B, GT 8A, GT 9A, and GT 10A

	Core GT 7B					Core GT 8A			
Slice No.	Thickness (in.)	Mid Point depth (h) (in.)	Velocity (V) (ft/s)	Σ V(Δh) (in.ft/s)	Slice No.	Thickness (in.)	Mid Point depth (h) (in.)	Velocity (V) (ft/s)	Σ V(Δh) (in.ft/s)
	1 in. = 25.4 mm	1 in. = 25.4 mm	1 ft/s = 0.30 m/s	1 in. ft/s = 0.0076 m²/s		1 in. = 25.4 mm	1 in. = 25.4 mm	1 ft/s = 0.30 m/s	1 in. ft/s = 0.0076 m²/s
a	1.476	0.74	13,370	9,866.74	a	1.094	0.55	13,669	7,473.39
b	1.224	2.19	15,941	21,339.01	b	0.903	1.62	12,820	14,184.93
c	1.147	3.49	15,246	20,136.13	c	0.859	2.57	13,087	12,351.33
d	1.126	4.73	15,635	19,178.52	d	0.403	3.28	--	
e	1.161	5.98	15,117	19,210.00	e	0.429	3.76	--	
f	1.337	7.33	14,919	30,318.49	f	1.126	4.61	15,292	28,983.39
					g	0.985	5.74	13,681	16,344.66
					h	1.005	6.81	13,086	14,293.73
					i	0.989	7.88	13,441	20,842.13
Σ =	8.00			120,048.89	Σ =	8.38			114,473.56
V_{max} =			15,940.76		V_{max} =			15,292.12	
QI_{avrg} =				15,006.11	QI_{avrg} =				13,668.48
QI_{top} =				14,504.68	QI_{top} =				13,224.93
QI_{mid} =				15,514.37	QI_{mid} =				14,409.62
QI_{bot} =				14,999.29	QI_{bot} =				13,370.90
QI_{top} / V_{max} =				0.91	QI_{top} / V_{max} =				0.86
QI_{top} / QI_{avrg} =				0.97	QI_{top} / QI_{avrg} =				0.97
QI_{mid} / V_{max} =				0.97	QI_{mid} / V_{max} =				0.94
QI_{mid} / QI_{avrg} =				1.03	QI_{mid} / QI_{avrg} =				1.05
QI_{bot} / V_{max} =				0.94	QI_{bot} / V_{max} =				0.87
QI_{bot} / QI_{avrg} =				1.00	QI_{bot} / QI_{avrg} =				0.98

{(--) Indicates no available data}

Table 9.7: Ultrasonic velocity for Cores GT 7B, GT 8A, GT 9A, and GT 10A (continued)

Core GT 9A				Core GT 10A			
Slice No.	Thickness (in.)	Mid Point depth (h) (in.)	Velocity (V) (ft/s)	Σ V(Δh) (in.ft/s)	Slice No.	Thickness (in.)	Mid Point depth (h) (in.)	Velocity (V) (ft/s)	Σ V(Δh) (in.ft/s)

Core GT 9A					Core GT 10A				
Slice No.	Thickness (in.)	Mid Point depth (h) (in.)	Velocity (V) (ft/s)	Σ V(Δh) (in.ft/s)	Slice No.	Thickness (in.)	Mid Point depth (h) (in.)	Velocity (V) (ft/s)	Σ V(Δh) (in.ft/s)
	1 in. = 25.4 mm	1 in. = 25.4 mm	1 ft/s = 0.30 m/s	1 in. ft/s = 0.0076 m^2/s		1 in. = 25.4 mm	1 in. = 25.4 mm	1 ft/s = 0.30 m/s	1 in. ft/s = 0.0076 m^2/s
a	1.758	0.88	12,629	11,101.16	a	1.101	0.55	12,746	7,018.24
b	0.492	2.01	10,490	13,075.16	b	1.036	1.72	13,770	15,558.20
c	1.046	2.79	15,271	9,982.17	c	1.419	3.06	14,539	18,859.02
d	1.156	3.89	12,452	15,342.61	d	1.412	4.58	13,371	21,220.43
e	1.220	5.09	14,120	15,863.41	e	1.100	5.94	13,750	18,457.68
f	1.178	6.29	13,634	16,725.63	f	1.019	7.10	14,153	16,248.14
g	1.239	7.51	13,580	24,935.33	g	1.033	8.23	13,730	22,854.14
Σ	8.13			107,025.47	Σ =	8.75			120,215.85
V_{max} =			15,270.88		V_{max} =			14,538.93	
QI_{avrg} =				13,172.37	QI_{avrg} =				13,738.95
QI_{top} =				12,186.09	QI_{top} =				13,511.34
QI_{mid} =				13,664.34	QI_{mid} =				13,805.07
QI_{bot} =				13,666.66	QI_{bot} =				13,900.45
QI_{top} / V_{max} =				0.80	QI_{top} / V_{max} =				0.93
QI_{top} / QI_{avrg} =				0.93	QI_{top} / QI_{avrg} =				0.98
QI_{mid} / V_{max} =				0.89	QI_{mid} / V_{max} =				0.95
QI_{mid} / QI_{avrg} =				1.04	QI_{mid} / QI_{avrg} =				1.00
QI_{bot} / V_{max} =				0.89	QI_{bot} / V_{max} =				0.96
QI_{bot} / QI_{avrg} =				1.04	QI_{bot} / QI_{avrg} =				1.01

{(--) Indicates no available data}

Table 9.8: Ultrasonic velocity for Cores GT 11B and GT 16B

Slice No.	Core GT 11B				Slice No.	Core GT 16B			
	Thickness (in.)	Mid Point depth (h) (in.)	Velocity (V) (ft/s)	$\Sigma V(\Delta h)$ (in.ft/s)		Thickness (in.)	Mid Point depth (h) (in.)	Velocity (V) (ft/s)	$\Sigma V(\Delta h)$ (in.ft/s)
	1 in. = 25.4 mm	1 in. = 25.4 mm	1 ft/s = 0.30 m/s	1 in. ft/s = 0.0076 m^2/s		1 in. = 25.4 mm	1 in. = 25.4 mm	1 ft/s = 0.30 m/s	1 in. ft/s = 0.0076 m^2/s
a	1.659	0.83	13,821	11,460.93	a	1.893	0.95	13,597	12,868.18
b	1.163	2.31	13,712	20,446.67	b	1.077	2.52	7,915	16,945.26
c	1.115	3.53	14,512	17,121.37	c	1.177	3.74	13,874	13,261.40
d	1.137	4.73	14,206	17,232.94	d	1.256	5.05	14,267	18,386.42
e	1.212	5.98	14,028	17,630.74	e	0.976	6.25	12,194	15,959.06
f	1.593	7.45	14,219	32,180.33	f	1.404	7.53	14,871	17,326.59
					g	1.425	9.04	14,137	31,902.87
Σ	8.25			116,072.97	Σ =	9.75			126,649.78
Vmax =			14,511.72		V_{max} =			14,870.76	
QI_{avrg} =				14,069.45	QI_{avrg} =				12,989.
QI_{top} =				13,796.81	QI_{top} =				11,346.46
QI_{mid} =				14,259.19	QI_{mid} =				13,425.57
QI_{bot} =				14,152.36	QI_{bot} =				14,197.13
QI_{top} / V_{max} =				0.95	QI_{top} / V_{max} =				0.76
QI_{top} / QI_{avrg} =				0.98	QI_{top} / QI_{avrg} =				0.87
QI_{mid} / V_{max} =				0.98	QI_{mid} / V_{max} =				0.90
QI_{mid} / QI_{avrg} =				1.01	QI_{mid} / QI_{avrg} =				1.03
QI_{bot} / V_{max} =				0.98	QI_{bot} / V_{max} =				0.95
QI_{bot} / QI_{avrg} =				1.01	QI_{bot} / QI_{avrg} =				1.09

{(--) Indicates no available data}

Table 9.9: Summary of pulse velocity test results

	Core	Height, h (in.)	Σ V(Δh) (in.ft/s)	*QI* avrg for Core (ft/s)	*QI* avrg for Bridge Deck (ft/s)
		1 in. = 25.4 mm	1 in. ft/s = 0.0076 m²/s	1 ft/s = 0.30 m/s	1 ft/s = 0.30 m/s
Sandusky Bridge	1A	6.88	91,677	13,335	13,951
	2B	7.13	103,158	14,478	
	3B	7.50	112,818	15,042	
	6B	7.88	110,359	14,014	
	7B	8.00	120,049	15,006	
	8A	8.38	114,474	13,668	
	9A	8.13	107,025	13,172	
	10A	8.75	120,216	13,739	
	11B	8.25	116,073	14,070	
	16B	9.75	126,650	12,990	
Average				**13,951**	
Standard Deviation				**718**	
Σ		**80.65**	**1,122,499**		
QI (ft/s)	**13,918**				

Table 9.10: Summary of ground truth pulse velocity analysis

Bridge Deck	Core	QI_{avrg} (ft/s)	QI_{top} (ft/s)	QI_{top}/QI_{avrg}	QI_{mid} (ft/s)	QI_{mid}/QI_{avrg}	QI_{bot} (ft/s)	QI_{bot}/QI_{avrg}
OTT-2-28.41	1A	13,335	12,519	0.94	13,309	1.00	14,177	1.06
	2B	14,478	14,701	1.02	14,944	1.03	13,791	0.95
	3B	15,042	14,655	0.97	14,567	0.97	15,905	1.06
	6B	14,014	13,252	0.95	14,375	1.03	14,414	1.03
	7B	15,006	14,505	0.97	15,514	1.03	14,999	1.00
	8A	13,668	13,225	0.97	14,410	1.05	13,371	0.98
	9A	13,172	12,186	0.93	13,664	1.04	13,667	1.04
	10A	13,739	13,511	0.98	13,805	1.00	13,900	1.01
	11B	14,070	13,797	0.98	14,259	1.01	14,152	1.01
	16B	12,990	11,346	0.87	13,426	1.03	14,197	1.09
Average		**13,951**	**13,370**	**0.96**	**14,227**	**1.02**	**14,257**	**1.02**

1 ft/s = 0.30 m/s
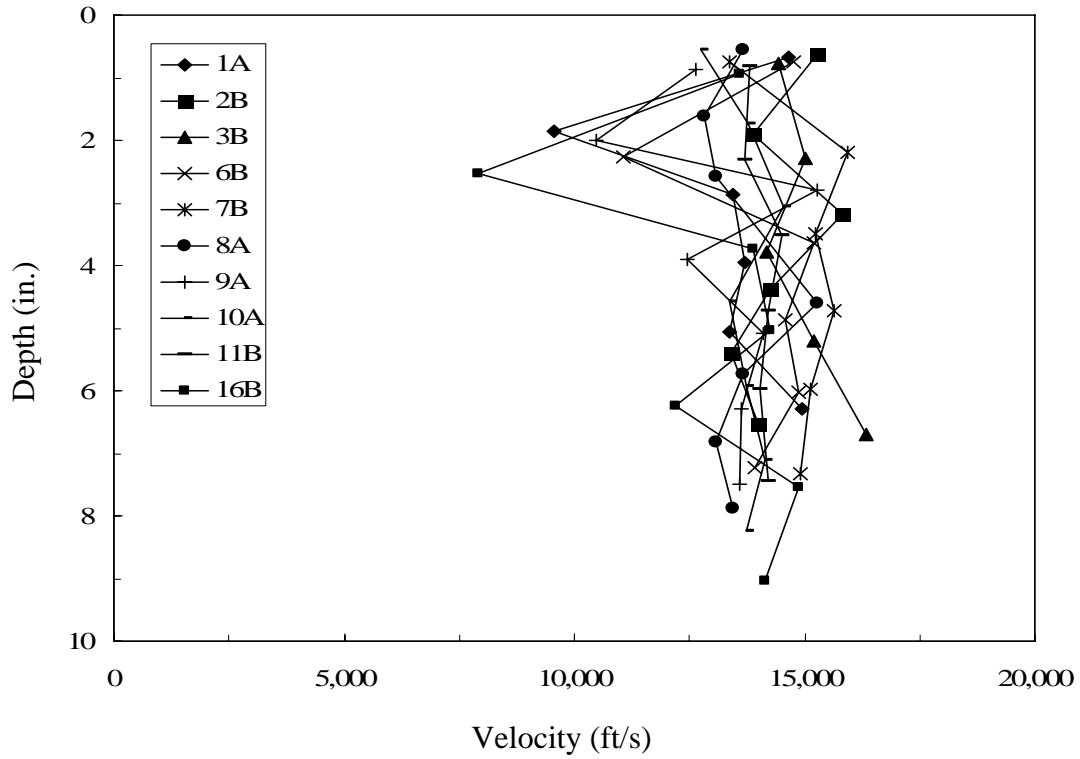
Figure 9.58. Velocity profiles for all the cores
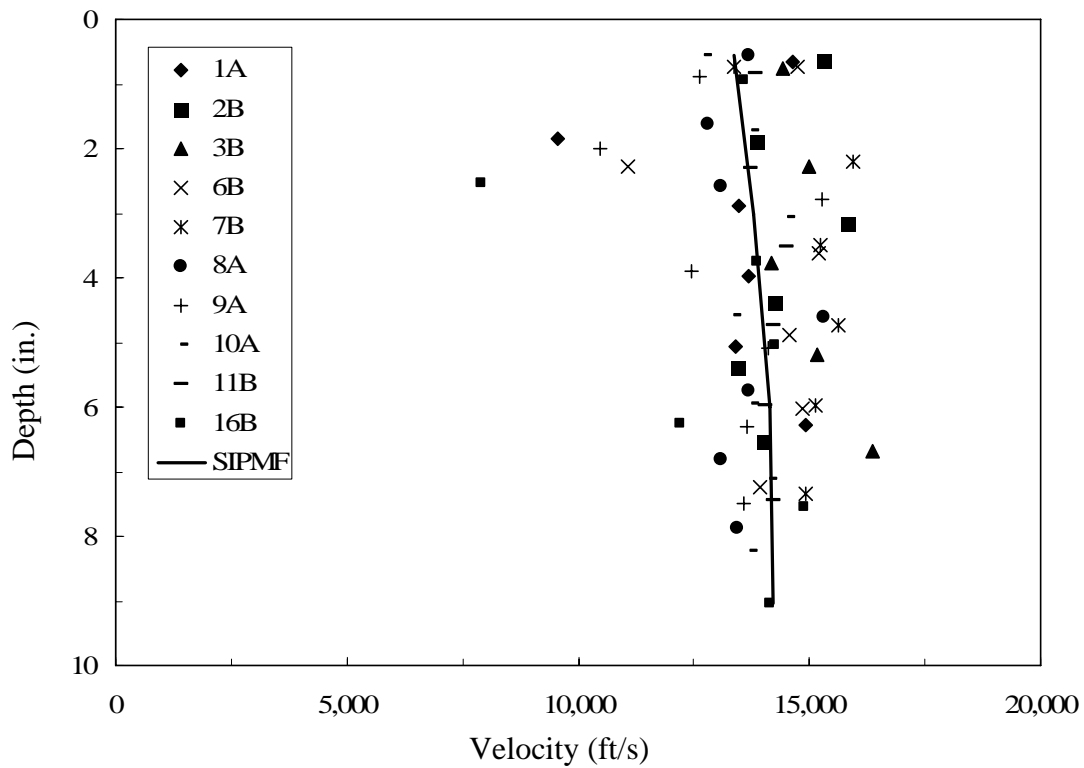
Figure 9.59. Summary of all ultrasonic pulse velocity measurements with depth
1 ft/s = 0.30 m/s

9.4.3.4 Conclusion of Ultrasonic Tests of Ground Truth Cores

An ultrasonic study was conducted to evaluate the performance of ground truth cores taken from OTT-2-28.41. Evaluations were made using analysis of cores obtained from the OTT-2-28.41 bridge deck using the GPR signal attenuation map. The cores were investigated using visual inspection and ultrasonic tests. The ultrasonic tests were used to evaluate the quality of the bridge deck concrete through its depth.

Based on the results of the visual inspection of cores and analysis of ultrasonic pulse velocity test, it was determined that the ground truth cores and the cores taken earlier were similar.

9.5 ANALYSIS OF ORIGINAL AND GROUND TRUTH CORES

9.5.1 Analysis of Original Cores

The original cores were taken form the north end of the OTT-2- 28.41 bridge. These cores were studied to see if there was a relationship between the ultrasound wave velocity and the condition of the concrete indicated by the GPR survey.

As shown in table 9.11 below, it was found that there is a slight correlation between the quality of the concrete ascertained from ultrasound tests of the existing cores (Chapter 1) and the GPR results. The delamination map for the region the original cores were extracted from (Section 9.3) shows that cores taken in an area where GPR found delaminations corresponds to lower pulse wave velocities obtained from the ultrasound tests. On the other hand, the cores that were taken from the areas where GPR found no delaminations, the ultrasound tests returned higher pulse velocity values. This correlation is suggestive of a relationship between GPR attenuation and concrete quality. However, because the GPR study was performed after the extraction of the cores the readings in areas leading up to and directly over the core locations may be inaccurate.

Table 9.11: Comparison of Ultrasound Velocities to GPR Attenuation for Original Cores

Ultrasound Velocity (ft/s) 1 ft/s = 0.30 m/s		
High Attenuation (Red)	**Intermediate Attenuation (Yellow)**	**Low Attenuation (Blue)**
12,723 (A1 top)	11,731 (A5 top)	13,754 (B1 top)
11,203 (A9 top)	12,334 (A11 top)	14,001 (B4 top)
12,606 (B5 top)	13,276 (A16 top)	15,246 (B1 bottom)
12,239 (C7 top)	12,743 (C3 top)	14,471 (B4 bottom)
		14,784 (B5 bottom)
		13,585 (C7 bottom)
Average Ultrasound Velocity		
12,193	12,521	14,407

9.5.2 Analysis of Ground Truth Cores

The ground truth cores were taken in clusters along the entire length of the bridge. The locations were selected based on the condition of the bridge deck indicated by the GPR survey. The locations agreed upon by UT and Rii. The goal was to extract at least two cores from each location: one for ultrasound testing and one for compression testing. The core locations were selected based primarily on the attenuation of the GPR signal. Locations were selected that met one of three criteria: 1) low attenuation at the top and bottom, 2) locations that had low attenuation at the top and high attenuation at the bottom, and 3) locations that had high attenuation at the top and bottom. The top of the core is defined as the height above the top rebar and the bottom is defined as the depth below the top rebar to the stay-in-place-metal form. It was hypothesized that low attenuation corresponded to good concrete quality. As stated above, this hypothesis had some support in the comparison of the ultrasound pulse velocities to GPR signal attenuation for the original group of cores (table 9.11).

The cores were also visually inspected upon extraction. The visual inspection focused on delaminations and evidence of deterioration or rust at the bottom of the core. Both the core and the cavity it was extracted from were examined. The drying water on the cores highlighted the cracks.

Table 9.12 presents the results of the visual and ultrasound inspection the ground truth cores. These results are grouped by core location in table 9.13.

Table 9.12: GPR Signal Attenuation versus Visual and Ultrasound Results by Core

Core		Material	GPR Attenuation	Visual Inspection	Ultrasound	Comments
GT-1A	Top	Overlay	Low	Good	Moderate	All agree
	Bot	Base	Low	Good	Good	All agree
GT-1B	Top	Overlay	Low	Good	---	Visual and GPR agree. No ultrasound
	Bot	Base	Low	Good	---	Visual and GPR agree. No ultrasound
GT-1C	Top	Overlay	Low	Good	---	Visual and GPR agree. No ultrasound
	Bot	Base	Low	---	---	No visual or ultrasound.
GT-1D	Top	Overlay	Low	Good	---	Visual and GPR agree. No ultrasound
	Bot	Base	Low	Good	---	Visual and GPR agree. No ultrasound
GT-2A	Top	Overlay	Low	Good	---	Visual and GPR agree. No ultrasound
	Bot	Base	High	Good	---	False negative by visual. No ultrasound
GT-2B	Top	Overlay	Low	Good	Good	All agree
	Bot	Base	High	Good	Good	False negative by visual and ultrasound
GT-3A	Top	Overlay	Low	Good	---	Visual and GPR agree. No ultrasound
	Bot	Base	High	Good	---	False negative by visual. No ultrasound
GT-3B	Top	Overlay	Low	Good	Good	All agree
	Bot	Base	High	Good	Good	False negative by visual and ultrasound
GT-6A	Top	Overlay	Low	Bad	---	False positive by visual. No ultrasound. There was a delamination above the top rebar that the GPR did not pick up.
	Bot	Base	Low	Good	---	Visual and GPR agree. No ultrasound
GT-6B	Top	Overlay	Low	Bad	Moderate	False positive by visual and ultrasound. There was a delamination above the top rebar that the GPR did not pick up. This delamination was included in the ultrasound slice reducing the pulse velocity.
	Bot	Base	Low	Good	Good	All agree
GT-7A	Top	Overlay	Low	Good	---	Visual and GPR agree. No ultrasound
	Bot	Base	Low	Good	---	Visual and GPR agree. No ultrasound
GT-7B	Top	Overlay	Low	Good	Good	All agree
	Bot	Base	Low	Good	Good	All agree
GT-8A	Top	Overlay	High	Bad	Good	GPR OK. The ultrasound slice did not include the delamination.
	Bot	Base	High	Good	Good	False negative by visual and ultrasound
GT-8B	Top	Overlay	High	Bad	---	Visual and GPR agree. No ultrasound
	Bot	Base	High	Good	---	False negative by visual. No ultrasound
GT-8C	Top	Overlay	High	Bad	---	Visual and GPR agree. No ultrasound
	Bot	Base	High	Good	---	False negative by visual. No ultrasound
GT-9A	Top	Overlay	High	Bad	Moderate	All agree
	Bot	Base	High	Good	Good	False negative by visual and ultrasound
GT-9B	Top	Overlay	High	Bad	---	Visual and GPR agree. No ultrasound
	Bot	Base	High	Good	---	False negative by visual. No ultrasound
GT-10A	Top	Overlay	Low	Good	Good	All agree
	Bot	Base	High	Good	Good	False negative by visual and ultrasound
GT-10B	Top	Overlay	Low	Good	---	Visual and GPR agree. No ultrasound
	Bot	Base	High	Good	---	False negative by visual. No ultrasound
GT-11A	Top	Overlay	High	Good	Good	False negative by visual and ultrasound
	Bot	Base	High	Good	Good	False negative by visual and ultrasound
GT-11B	Top	Overlay	High	Good	---	False negative by visual. No ultrasound
	Bot	Base	High	Good	---	False negative by visual. No ultrasound
GT-16A	Top	Overlay	High	Good	---	False negative by visual. No ultrasound
	Bot	Base	High	Good	---	False negative by visual. No ultrasound
GT-16B	Top	Overlay	High	Good	Moderate	False negative by visual and ultrasound
	Bot	Base	High	Good	Good	False negative by visual and ultrasound

Low Attenuation = Good Concrete
High Attenuation = Poor Concrete

Table 9.13: Comparison of Signal Attenuation and Actual Condition by Location

Core	Level	Material	GPR Attenuation	Visual Inspection	Ultrasound	Comments
GT-1	Top	Overlay	Good	Good	Moderate	All agree
	Bottom	Base	Good	Good	Good	All agree
GT-2	Top	Overlay	Good	Good	Good	All agree
	Bottom	Base	Bad	Good	Good	All agree
GT-3	Top	Overlay	Good	Good	Good	All agree
	Bottom	Base	Bad	Good	Good	GPR false negative
GT-6	Top	Overlay	Good	Bad	Moderate	GPR false positive
	Bottom	Base	Good	Good	Good	All agree
GT-7	Top	Overlay	Good	Good	Good	All agree
	Bottom	Base	Good	Good	Good	All agree
GT-8	Top	Overlay	Bad	Bad	Good	GPR OK See note in Table 9.12. All agree.
	Bottom	Base	Bad	Good	Good	GPR false negative
GT-9	Top	Overlay	Bad	Bad	Moderate	All agree
	Bottom	Base	Bad	Good	Good	GPR false negative
GT-10	Top	Overlay	Good	Good	Good	All agree
	Bottom	Base	Bad	Good	Good	GPR false negative
GT-11	Top	Overlay	Bad	Good	Good	GPR false negative
	Bottom	Base	Bad	Good	Good	GPR false negative
GT-16	Top	Overlay	Bad	Good	Moderate	GPR false negative
	Bottom	Base	Bad	Good	Good	GPR false negative

Table 9.14 summarizes the results of the GPR survey compared to the visual and ultrasound results. Overall, the GPR was successful in locating delaminations above the top rebar. This is as expected from the literature and is consistent with GPR being a good tool for assessing redecking and resurfacing quantities. The GPR was not successful predicting the delaminations or quality of concrete when the signal had to be reflected off the SIPMF. The exact mechanisms that lead to the lack of accurate results are not known. The gap between the concrete and the SIPMF, scatter throughout the column due to inhomogeniety, changes in moisture, additives or chlorides that affect the dielectric constant are some of the possibilities for a higher attenuation not related to concrete quality.

Table 9.14: Summary of GPR Results

20 Trials: 10 tops and 10 Bottoms	
Overall	
GPR consistent with other methods	11
GPR false negative	8
GPR false positive	1
Total Trials	20
10 Tops	
GPR consistent with other methods	7
GPR false negative	2
GPR false positive	1
10 Bottoms	
GPR consistent with other methods	4
GPR false negative	6
GPR false positive	0

A brief statistical analysis was performed on these results. Because of the small size of the sample and the binary nature of the data, a binomial distribution was used.

For the tops, the goal is to decide if the finding of 7 correct results is consistent with a correct rate of 80% that is supported by the literature. Therefore, for the tops, the null hypothesis (H0) was "probability of correct detection is greater than 80%" and H1 was "the probability of correct detection is less than 80%". Five or few correct responses would lead to rejection of H0

at the 0.056 level. Thus, from our data, there is no strong evidence that our result for the tops differs from that found in the literature.

For the bottoms, the worst that could be done is accepting the GPR survey as having a low error rate when it did not. Therefore, H0 is "The probability of correct detection is less than 75%" and H1 is "The probability of correct detection is greater than 75%". This requires than rejecting H0 requires strong evidence in support of H1. Specifically, in our case it would require 9 correct observations to reject H0 at the 0.056 level. Since we found 4 correct responses, H0 is not rejected.

For the bottoms, it is of interest to know if taking more samples is likely to change the statistical result. Therefore, the probability of a type II error is of interest. A type II error is failing to reject H0 when H1 is true. With our data, the probability we are failing to reject H0 when H1 is true is 2%.

The analysis yields four significant insights

1) Table 9.11 indicates there is a probable relationship between GPR attenuation and concrete quality

2) There were no false positives at the bottoms. The GPR need not report bad condition concrete as good condition concrete.

3) The statistical analysis of the tops indicates our results are consistent with the literature, so our overall GPR method and approach were reasonable.

4) The statistical analysis of the bottoms indicates that the GPR cannot reliably give insight into the condition of the concrete immediately above the SIPMF.

The analysis is hopeful in that it suggests a relationship between concrete condition and GPR survey results and that the GPR did not report any false positives at the bottom. However, the lack of a clear theoretical model and inconsistency of the experimental results for the signal reflected off the SIPMF indicates that more work needs to be done before GPR can be recommended as an inspection tool for the concrete just above the SIPMF. An example of ongoing work is that of Scott (2006), who is investigating ways to vary the frequency to extract more information from a GPR survey.

9.6 GROUND PENETRATING RADAR CONCLUSION

GPR is a widely accepted technique for identifying bridge deck areas with delaminations. It was attempted to extend the GPR technique to assess the condition of concrete immediately above the SIPMF. It was found that GPR was reliable in determining if the concrete above the top layer of rebar was delaminated. However, it was found that GPR was undependable in determining if the concrete between the top layer of rebar and the SIPMF was delaminated.

Maps of the strength of the reflected radar signal from the top layer of rebar and from the SIPMF were then compiled over the entire length of the bridge by Rii. The results of these maps where used to study the original cores. It was found that there was a slight correlation between GPR signal strength and concrete condition. It was also found that study of the original cores was not adequate to make a judgment on the efficacy of using GPR to examine the condition of the concrete just above the SIPMF.

Generally, the areas of high attenuation found during the survey of the entire bridge do not coincide with the location of the original cores. Therefore, it was decided that additional ground truth cores would be extracted at critical locations along the length of the bridge. The ground truth cores were inspected visually at extraction and prior to testing. The cores were subjected to compression and ultrasound testing. Comparing the established tests to the GPR survey results it was found that the GPR testing conducted was as reliable as that reported in the literature for identifying delaminations above the top layer of rebar. However, the GPR was not reliable in identifying delaminations or concrete condition below the top rebar. Our sample was small, but the statistical results indicate that further GPR studies to investigate the condition of the concrete immediately above the SIMPF undertaken with the current techniques would probably not be fruitful.

It was also a goal for this study to assess if it was possible to determine the strength or quality of concrete using GPR. Based on the literature review, it was determined that the return from a GPR signal has not yet been correlated to concrete strength. The speed at which the GPR wave travels through the bridge deck is a function of the dielectric constant and the losses are a function of scattering and changes in dielectric constant of the medium. The dielectric constant changes due to a number of variables, including the mix design, free water in voids, air voids, admixtures, aggregate type, water to cement ratio, the presence of chlorides, etc. These

properties are not directly linked to the elastic properties of concrete or to the strength of concrete.

Chapter 10: Conclusions, Recommendations and Implementation

10.1. THE RESEARCH PROBLEM

The fundamental problem addressed by this research was to determine if the use of stay-in-place metal forms (SIPMF) resulted in reduced bridge deck concrete quality over the life of the bridge compared to bridges without SIPMF.

Since SIPMF conceal the bottom of the bridge deck from inspectors, a corollary problem addressed was to determine the potential for using ground penetrating radar (GPR) to inspect the bridge deck concrete immediately above the SIPMF.

10.2. CONCLUSIONS AND RECOMMENDATIONS

Analysis of the data from the visual inspection and compression, chloride ion, permeability, and ultrasound tests showed no significant difference between the deck concrete in regions with and without SIPMF. This is consistent with the literature review.

SIPMF near expansion joints and SIPMF with holes in it experienced localized rusting near these water sources. It is recommended that the number of holes be minimized and steps be taken to prevent water from flowing around the edges of the SIPMF. It has also been reported that SIPMF on underpasses in urban areas experienced deterioration from water being continually thrown on the bottom of the bridge.

Analysis of the data from the visual inspection and compression and ultrasound tests showed that the GPR system used was not effective as an inspection tool for the concrete immediately above the SIPMF. The GPR was effective in locating delaminations above the top layer of rebar. The efficacy of the GPR system in locating delaminations above the top rebar was consistent with that reported in the literature. However, the GPR gave false indications of delaminations for the concrete below the top rebar. Many factors determine the attenuation and dielectric constant of the concrete. The researchers were unable to determine why the false indications occurred. Additional testing with the current GPR techniques appears unlikely to lead to information about the condition of the concrete immediately above the SIPMF.

10.3. IMPLEMENTATION

Nothing in the present research indicates that implementation of SIMPF in Ohio will be less successful than in the neighboring northern states of Michigan, Pennsylvania, or Indiana. Four key aspects of implementation are inspection, materials, repair and specification.

Proper implementation of SIPMF offers several advantages compared to the conventional plywood forming methods. Some of these advantages are:

1. Lower labor costs.
2. Significant time saving in bridge deck construction.
3. The ease of installation.
4. Safety of the laborers.
5. Minimal interruption to the environment or traffic below.

The biggest objection to implementation of SIPMF is the inability to inspect the bottom of the deck during construction and service. At the present time, there is no nondestructive inspection technique that any state uses to completely replace visual inspection. Typically, states have handled the construction issue by rigorous topside inspection during the pour, controlling rebar location, controlling aggregate size and possibly post-pour sounding of the deck bottom. The states are very comfortable with this.

The issue of service inspection does not appear to have been addressed in a systematic way. It appears the reason this is not a barrier to the use of SIPMF is that the circumstances where lack of visual inspection conceals a significant problem are rare.   The basic issue is this: after many years of service when the deck needs extensive rehabilitation, how can deep damage be detected. The damage and delamination above the top rebar mat can be reasonably inspected with ground penetrating radar. However, the depth the damage extends below the top rebar mat can not be easily detected. If the deep damage is contiguous with damage above the upper rebar mat, it will be exposed during hydrodemolition, or other technique used to remove upper level concrete that is in poor condition, and pose no long term safety risk. A pocket of poor condition concrete or heavily corroded rebar that gives no indication above the top mat or by telltale rust of the SIPMF would not be detected by any technique the present researchers are aware of. As intact SIPMF inhibits the flow of water through the deck and research (Grace, 2004) has shown

that freezing and thawing does not significantly damage the concrete above the SIPMF, the formation of a hidden deep pocket of damage is unlikely.

A note of caution, some states are developing inspection techniques that focus on the bond between the concrete and the SIPMF. As the SIPMF is not a structural component after the concrete hardens and it has been shown that the absence of a bond is not deleterious to the condition of the concrete or rebar, inspection techniques that focus on this bond are not, in the opinion of the present researchers, making a measurement that gives insight into the concrete or rebar condition.

Typical materials are galvanized steel of various grades (grade 80 is the most common) in accordance with ASTM A653/A653M with tolerances governed by ASTM 924. Deck thicknesses run from 22 gage to 16 gage (0.033 to 0.066 inches (0.84 to 1.68 mm)). The most common coating is G165 (Z505) with some G235 (Z720) manufactured.   The coating designation is in ounces of zinc per foot squared (1 oz/ft^2 = 305.15 g/m^2). G235 being 2.35 ounces/foot^2 (717 g/m^2). The approximate thickness is 0.0017 inch per oz/ft^2 (0.0427 mm per 305.15 g/m^2) (GavInfoCenter 2005). Corrugations range from 2 to 4½ inches (50 to 113 mm) in depth. Section properties are calculated in accordance with requirements of the American Iron and Steel Institute "Specification for the Design of Cold-Formed Steel Structural Members" latest published edition.

Repair to damaged galvanizing on SIPMF is straightforward. ASTM 780 is specification for repair to galvanized coating which has provisions for field repair and some states provide additional direction. A suggested specification clause is "All permanently exposed form metal, where the galvanized coating has been damaged shall be repaired in accordance with ASTM 780 or shall be thoroughly and satisfactorily cleaned, wire brushed, and painted with two coats of zinc oxide-zinc dust primer in accordance with Federal Specification TT-P-641(d), type II, with no color added. Minor heat discoloration in areas of welds need not be touched up." The FS TT-P-641 painting is in compliance with ASTM 780. Sandblasting could be substituted for wire brushing.

Specifications must address the needs of designers, contractors, inspectors and bridge maintenance personnel. Implementation trials are underway in Ohio (ODOT 2006) and a draft

specification has been written (ODOT 2005). A generic outline of a typical specification is provided in section 2.3. The current draft specification needs further development, but is in general accordance with section 2.3. The final specification should have four parts addressing design, construction, inspection, and long term repair, respectively. The requirements of the overall specification should be in appropriate ODOT design, construction, inspection and maintenance documents. Key state provisions in a specification are minimum thickness for the SIMPF, minimum coating thickness, and welding restrictions. The current Ohio draft specification has a minimum SIPMF thickness of 20 gage which is reasonable to insure a safe working platform and requires a G235 coating which is appropriate because the Ohio environment is more corrosive than the southern states which use the G165 coating. The present Ohio prohibition on all welding is more restrictive than most specifications which permit welding to compression and composite flanges. The researchers suggest consideration in the specification be given to provisions that

- Restrict admixtures containing calcium chloride or any other admixture containing chloride salts
- Control rebar size
- Control rebar standoff from the forms

Bibliography

AASHTO PP 40-00, "Application of Non-Contact Ground Penetrating Radar (GPR) to Highways." <u>AASHTO Standard Recommended Practice,</u> American Association of State Highway and Transportation Officials. Washington, D.C., 2000.

AASHTO T 22-97. "Compressive Strength of Cylindrical Concrete Specimens." <u>AASHTO Standard Specification</u>, Part II Tests. American Association of State Highway and Transportation Officials. Washington D.C., 1997.

AASHTO T 24 Obtaining and Testing Drilled Cores and Sawed Beams of Concrete

AASHTO T 260-97. "Sampling and Testing for Total Chloride Ion in Concrete and Concrete Raw Materials."

AASHTO T 277-97. "Electrical Indication of Concrete's Ability to Resist Chloride." <u>AASHTO Standard Specification</u>, Part II Tests. American Association of State Highway and Transportation Officials. Washington D.C., 1997.

Aldea, CM., P. Surendra, and A. Karr, 1999, "Effect of Cracking on Water and Chloride Permeability of Concrete." <u>ASCE Journal of Material in Civil Engineering</u>. Vol. 11, No. 3, Aug. 1999: 181-187.

Armaghani, J.M. 1993, "Testing of Concrete Permeability for Durability Evaluation." <u>Structural Engineering in Natural Hazards Mitigation: Proceedings of Papers Presented at the Structures Congress 1993</u>. American Society of Civil Engineers: New York, NY, 1993: 989-995.

ASTM C39-86 Standard Method of Test for Compressive Strength of Cylindrical Concrete Specimens.

Babaei, K. and R. L. Terrel, 1982, "Deterioration of Concrete Bridge Decks and Review of the WSOT Bridge Deck Program." Report No. WA-RD-55.1, Washington State Transportation Center. Seattle: Sept. 1982.

Bakht, B., A.A. Mufti, and G. Tadros, 2002A, "Transverse Confinement of Deck Slabs by Metallic Stay-in-Place Metal Forms." 4th Structural Specialty Conference, Canadian Society for Civil Engineers 30th Annual Conference, Montreal, Quebec, Canada, June 5-8, 2002: 1-7.

Bakht, B., A.A. Mufti, and G. Tadros. 2002, "Metal Forms Replace Reinforcement in BridgeDeck Slabs." 1st International Conference on Advanced Structural Steels. Hung Hum, Kowloon, Hong Kong, December 9-11, 2002.

Bakht, B., A.A. Mufti, and G. Tadros. 2003, "Failure Test on Unreinforced Concrete Slab on Stay-in-Place Metal Forms." <u>Steel and Composite Structures – An International Journal</u> 2003.

Bakht, B., and A.A. Mufti. 1997, "Stay-in-Place Concrete Formwork for Deck Slabs of GirderBridges." <u>The Institution of Engineers</u> 78 (1997): 129-135.

Barnes, C. L. and J. F. Trottier , 2004, "Effectiveness of Ground Penetrating Radar in Predicting Deck Repair Quantities." <u>Journal of Infrastructure Systems</u>, Vol. 10, June 2004: 69-76.

Beales, C. and D.A. Ives, 1990, "The Behaviour of Permanent Formwork." Research Report 254, Transport and Road Research Laboratory, Department of Transport. United Kingdom, 1990.

Berube, M.A., et al. 2003, "Laboratory and Field Investigations of the Influence of Sodium Chloride on Alkali-Silica Reactivity," Cement and Concrete Research 33 (2003): 77-84.

Cady P.D., R.E.Carrier, T.A. Bakr and J.C. Theisen, 1971, "Final Report of the Durability of Bridge Deck Concrete," The Pennsylvania State University, Dec. 1971.

Cox, W.R., and K. R. Pruski, 2002, "High Performance Concrete Structures: A Work in Progress." Austin: Texas Department of Transportation. July 31, 2002.

Feldman, R., et al. 1994, "Investigation of the Rapid Chloride Permeability Test." ACI Materials Journal. May-June 1994: 246-255.

Florida. Department of Transportation. 2002, Design Specifications. Tallahassee: Florida Department of Transportation, 2002.

Frosch, R. J., D. T. Blackman and R. D. Radabaugh. 2003, "Investigation of Bridge Deck Cracking in Various Bridge Superstructure Systems." Report No. FHWA/IN/JTRP-2002/25. Joint Transportation Research Program, Purdue University: Feb. 2003.

GavInfoCenter, 2005, "Understanding Caoting Weight Designations for Zinc Based Coating on Steel Sheet," GaIvInfoNote1, Rev. 2.5, 2005

Geckle, D., 2005, ODOT District 2 Transportation Engineer, personal communication, August, 2005.

Goldman, A., M.D. Cohen and J.A. Ramirez, 1995, "Stay-In-Place Deck Panels. Part 1. Final Report and Executive Summary. Report No. FHWA/IN/JHRP-94/11-1. Joint Transportation Research Program, Purdue University: Sept. 1995.

Charlottesville, 2000.

Grace, N. and J. Hanson, 2002, "Survey on the Performance and Inspection Techniques for Bridge Decks Constructed with Stay-in-Place-Metal-Forms." Civil Engineering Department, Lawrence Technological University: November 21, 2002.

Grace, N. and J. Hanson, 2004, "Inspection and Deterioration of Bridge Decks Constructed Using Stay-In-Place Metal Forms and Epoxy-Coated Reinforcement", Lawrence Technological University, Southfield, MI, October, 2004

Ground Penetrating Radar Institute, 2006, website, http://www.gprinstitute.org/ . Accessed spring 2005 and spring 2006.

Heiler, M., S. McNeil and J. Garrett, 1995, "Ground penetrating radar for highway and bridge deck condition assessment and inventory." Nondestructive Evaluation of Aging Bridges and Highways. Vol. 2456, June 1995: 195-206.

Helwig, T.A., and K.H. Frank, 1993, "Lateral Bracing of Plate Girders Using Deck Forms." Structural Engineering in Natural Hazards Mitigation: Proceedings of Papers Presented at the Structures Congress 1993. American Society of Civil Engineers: New York, NY, 1993: 939-944.

Hooton, R.D., et al. 1997, "Influence of Silica Fume on Chloride Resistance of Concrete."
Proceedings, PCI/FHWA International Symposium on High Performance Concrete. New
Orleans: Oct. 20-22, 1997: 245-256.

Hugenschmidt, J., 2002, "Concrete bridge inspection with a mobile GPR system." Construction
and Building Materials 16, 2002: 147-154.

Huston, D., et al., 2000 "GIMA ground penetrating radar system for monitoring concrete bridge
decks." Journal of Applied Geophysics 43, 2000: 139-146.

Indiana. Department of Transportation. 2006, Design Specifications, section 702.13 (e)
Indianapolis: Indiana Department of Transportation, 2006.

Kentucky. Department of Transportation. 2002, Design Specifications. Louisville: Kentucky
Department of Transportation, 2002.

Krautkrämer, J. and Krautkrämer, H, 1990, Ultrasonic Testing of Materials, Spring-Verlag,
1990.

Larson, T.D., and J.J. Malloy, 1966, "Durability of Bridge Deck Concrete – Report 3," Vol. 1,
Pennsylvania State University, Mar. 1966, 188 pp.

Liu, Z. and J.J. Beaudoin, 2000, "Permeability of Cement Systems to Chloride Ingress and
Related Test Methods." Cement, Concrete, and Aggregates. CCAGDP, Vol. 22, No. 1,
Jun. 2000. 16-23.

Love, Jr., J.S., R.M. Barnoff and T.D. Larson, 1967, "Composite Action form Corrugated Bridge
Deck Forms," The Pennsylvania State University, Mar. 1967, 37 pp.

Maierhofer, C., 2003, "Nondestructive Evaluation of Concrete Infrastructure with Ground
Penetrating Radar." Journal of Materials in Civil Engineering, Vol. 15, June 2003: 287-
297.

Malhotra, V.M. and N.J. Carino, 1991, Handbook on Nondestructive Testing of Concrete, CRC
Press, 1991.

Maser, K. R., 1996, "Condition Assessment of Transportation Infrastructure Using Ground-
Penetrating Radar." Journal of Infrastructure Systems, Vol. 2, June 1996: 94-101.

Massachusetts. Department of Transportation. 2002, Design Specifications. Boston:
Massachusetts Department of Transportation, 2002.

Merrill, Brian D. 2002, "Texas' Use of Precast Concrete Stay-In-Place Forms for Bridge Decks."
Austin: Texas Department of Transportation, 2002.

Misra, S., A. Yamamoto, T. Tsutsumi and K. Motohashi, 1994, "Application of Rapid Chloride
Permeability Test to Quality Control of Concrete." ACI SP-145, Durability of Concrete
1994.

Mohammed, T. U., Nobuaki Otsuki, and Hidenori Hamada, 2003, "Corrosion of Steel Bars in
Cracked Concrete Under Marine Environment." ASCE Journal of Material in Civil
Engineering, Vol. 15, No. 5, 1 Oct. 2003: 460-469.

Myers, J.J., 2001, "Permeability Performance of High Performance Concrete Subjected to Various Curing Regimes." National Research Council. <u>Journal of Transportation Research Board</u>. Washington D.C.: Feb. 2001.

Myers, J. J., W. Touma, and R.L Carrasquillo, 1997, "Permeability of High Performance Concrete: Rapid Chloride Ion Test vs. Chloride Ponding Test." PCI/FHWA International Symposium on High Performance Concrete. <u>Advanced Concrete Solutions for Bridges and Transportation Structures.</u> New Orleans, Louisiana. Oct. 1997. 268-282.

Nebraska.. Department of Transportation. 2002, <u>Design Specifications.</u> Lincoln: Nebraska Department of Transportation, 2002.

North Carolina. Department of Transportation. 2003, <u>Design Specifications.</u> Raleigh: North Carolina Department of Transportation, 2003.

Nukala, P.K.V., et al. 1995, "Stay-In-Place Deck Panels. Horizontal Shear Strength of Bridge Deck Panels- Part 2. Report No. FHWA/IN/JHRP-94/11-2. Joint Transportation Research Program, Purdue University: Aug. 1995.

Ohio. Department of Transportation. 2005, Structural Engineering. Steel SIP Form Notes 2005 CMS Version #1.

Ohio. Department of Transportation. 2006, "Build Bridges, Faster, Smarter, Pilot Projects", http://www.dot.state.oh.us/se/SI9/SI9.asp, accessed March 2006.

Olhoeft, G. R., 1996, "Application of Ground Penetrating Radar." Proceedings of the 6th International Conference on Ground Penetrating Radar, September 30 – October 3, 1996: 1-4.

Pennsylvania. Department of Transportation. 2005, Construction Specification BC – 732M, "Standard Permanent Metal Deck Forms", July 29, 2005.

Russel, H.G., 2000, "The Rapid Chloride Permeability Test." <u>HPC Bridge Views</u>, Issue No. 12, November/December 2000: 1-4.

Scott, M., et al., 2003, "A comparison of nondestructive evaluation methods for bridge deck assessment." <u>NDT&E International</u> 36, 2003: 245-255.

Shin, H., and D.A. Grivas, 2003, "How Accurate is Ground-Penetrating Radar for Bridge Deck Condition Assessment?" <u>Transportation Research Record</u>, Issue 1845, 2003: 139-147.

Soltesz, S.. 2003, "Washing Bridges to Reduce Chloride." Report No. FHWA-OR-DF-04-05, Oregon Department of Transportation. Salem: Dec. 2003.

Sprinkel, M. M., and C. Ozyildirim. 2000, "Evaluation of High Performance Concrete Overlays Placed on Route 60 Over Lynnhaven Inlet in Virginia." VTRC 01-R1, Virginia Transportation Research Council: Charlottesville, 2000.

Stanish, K.D., R.D. Hooton, and M.D.A. Thomas, 1997, "Testing the Chloride Penetration Resistance of Concrete: A Literature Review." FHWA Contract DTFH61-97-R-00022, Prediction of Chloride Penetration in Concrete. University of Toronto: 1997.

Scott, M., N. Gagarin, P. Mills, and M. Oskard, 2006, "Step Frequency Ground Penetrating Radar Applications to Highway Infrastructure Measurement and System Integration Feasibility with Complementary Sensors", presentation at 2006 TRB Meeting, accessed through http://www.gprinstitute.org/workshops/TRB06/presentations.html March 2006.

Steel Deck Institute. 2003, "Designing with Steel Form Deck." Steel Deck Institute. 2003.

Udegbunam, O., et al. 1999, "Developing a Rapid Measure of Concrete Permeability for use in QA/QC Specifications." Paper No: 990565, 78th Annual Meeting Transportation Research Board. Washington D.C., Jan. 10-14, 1999.

Virginia. Department of Transportation. 2002, Design Specifications. Richmond: Virginia Department of Transportation, 2002.

Volle, T., 2002, "Construction of Bridge Decks with Precast Prestressed Deck Planks." Report No. FHWA/IL/PRR-139. Springfield: Illinois Department of Transportation, Apr. 2002.

Washington. Department of Transportation. 2002, Design Specifications. Olympia: Washington State Department of Transportation, 2002.

West Virginia. Department of Transportation. 1994, Division of Highways. Evaluation of Bridge Decks Using Epoxy Coated Reinforcement. 1994.

West Virginia. Department of Transportation. 2004, Division of Highways. Engineering Division. Bridge Design Manual. March 1, 2004.

Whiting, D,. "Rapid Determination of the Chloride Permeability of Concrete." Final Report No. FHWA/RD-81-119. Federal Highway Administration, NTIS No. PB82140724.

Willet, D. A., and B. Rister, 2002, "Ground Penetrating Radar Pavement Layer Thickness Evaluation." Kentucky Transportation Center Research Report, December 2002, 39-146.

Wioleta, A., et al. 2000, "Field Performance of Epoxy-Coated Reinforcing Steel in Virginia Bridge Decks." VTRC 00-R16, Virginia Transportation Research Council:

Appendix A
LOR-57-18.18 Individual Core Data

Core Number: S1

Location:

Station location 975 + 56.9 and 35.2 feet from the face of the curb on south side of the bridge.

Chloride Ion Test:

At two inches:
 % CL⁻:   0.0470
 # CL⁻ / yd³: 1.62

At four inches:
 % CL⁻:   0.0292
 # CL⁻ / yd³: 1.01

At six inches:
 % CL⁻:   0.0535
 # CL⁻ / yd³: 1.85

At eight inches:
 % CL⁻:   0.0271
 # CL⁻ / yd³: 0.94

Permeability Test:

 Charge Passed: 1,757 C
 Adjusted Charge: 1,586 C
 Permeability Class: Low

Comments:
- Core taken at this location because it was the most deteriorated area where there was no SIPMF.
- Length of core was 7.5 inches including a 2.0 inch wearing surface.
- Core split in three by two transverse cracks, one where wearing surface meets deck and one where bottom rebar mat is located.
- Rebar heavily rusted.
- Various voids present throughout core, up to 0.5 inch in diameter.

Core Number: S2

Location:

Station location 975 + 51.6 and 29.9 feet from the face of the curb on the south side of the bridge.

Chloride Ion Test:

At two inches:
    % CL⁻:   0.0733
    # CL⁻ / yd³: 2.53

At four inches:
    % CL⁻:   0.0436
    # CL⁻ / yd³: 1.51

At six inches:
    % CL⁻:   0.0451
    # CL⁻ / yd³: 1.56

At eight inches:
    % CL⁻:   0.0686
    # CL⁻ / yd³: 2.37

Comments:
- Core taken at this location because SIPMF badly deteriorated underneath.
- Length of core ranged from 7.75 inches to 9.5 inches.
- No bond between SIPMF and deck. SIPMF badly corroded. Rust and white residue present on bottom of core and SIPMF.
- Rebar heavily rusted.
- Numerous voids present in concrete up to 3/8 inches in diameter.
- Large void present at bottom, 8 inches from top of core, where bottom mat of rebar is located. Void is 1 inch in diameter and extends halfway into core.

Core Number: 1B

Location:

Station location 975 + 53.3 and 35.1 feet from the face of the curb on the south side of the bridge.

Ultrasound Test:

$\sum$ V(Δh): 121,583 in ft/s
Maximum Velocity: 14,081 ft/s
Quality Index Avrg.: 13,509 ft/s

Comments:
- 6.13 inches in height, approximately 9 inches till the top of the broken region.
- Core in broken at the top, with re-bar protruding vertically.
- Two reinforcement bars located at 3.25 inches and 5.75 inches from bottom surface.
- Exposed steel reinforcement showed slight signs of rust.
- Small voids present in concrete.

Core Number: 1C

Location:

Station location 975 + 53.4 and 26.5 feet from the face of the curb on the south side of the bridge.

Ultrasound Test:

∑ V(Δh): 126,691 in ft/s
Maximum Velocity: 14,736 ft/s
Quality Index Avrg.: 13,696 ft/s

Comments:
- Core 9.25 inches in height.
- Two reinforcement bars, non-epoxy coated located at 2.75 inches and 7.75 inches from top surface.
- Some traces of rust on bars.
- Voids located at 1.25 inches, 7 inches, and 8.5 inches from top surface.

Core Number: 1D
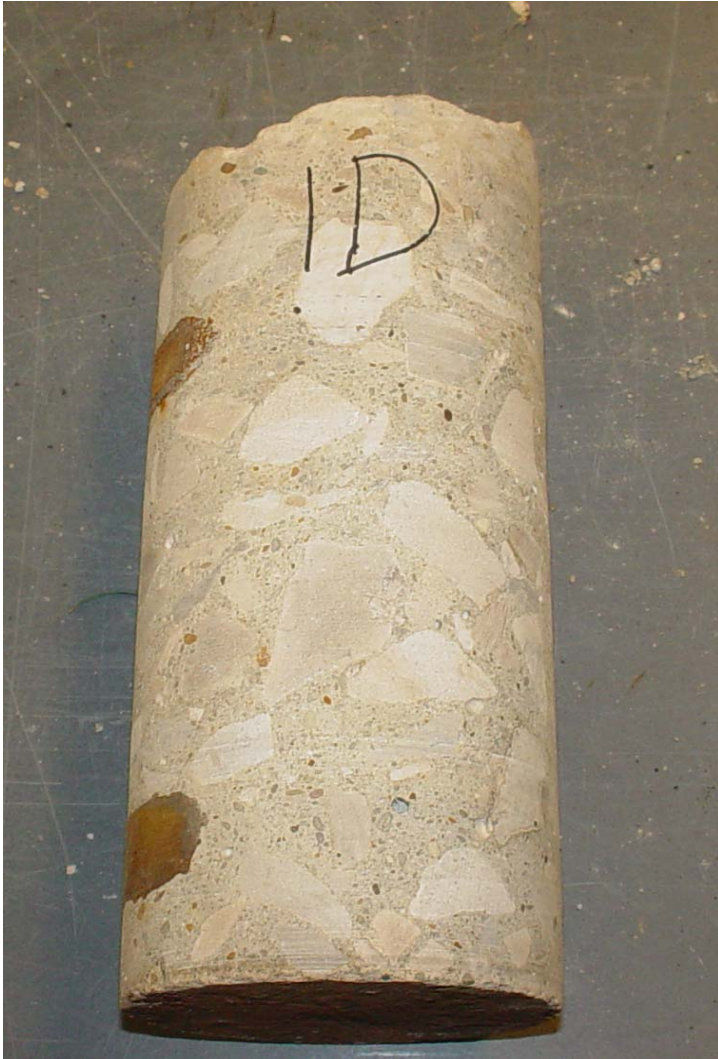
Location:

Station location 975 + 53.4 and 14.1 feet from the face of the curb on the south side of the bridge.

Permeability Test:

Charge Passed: 1,533 C
Adjusted Charge: 1,348 C
Permeability Class: Low

Comments:
- Original core length 8.5 inches.
- Numerous voids present in concrete up to 1/8 inch in diameter.
- Rebar shows signs of rust.

Core Number: 1E

Location:

Station location 975 + 53.1 and 1.6 feet from the face of the curb on the south side of the bridge.

Compression Test:

Cut and Capped Length: 7.32"
Load: 83,800 Lbs
Adjusted Load: 83,800
Corrected Psi: 6,910 Psi

Comments:
- Original core length 8.5 inches.
- Numerous voids present in concrete up to 1/8 inch in diameter.

Core Number: 1F

Location:

Station location 975 + 54.0 and 0.8 feet from the face of the curb on the south side of the bridge.

Ultrasound Test:

$\sum$ V(Δh): 116.669 in ft/s
Maximum Velocity: 14,779 ft/s
Quality Index Avrg.: 13,334 ft/s

Comments:
- Core height 8.75 inches.
- Regions of small to moderate voids.
- One reinforcing bar, non-epoxy coated, located at 3.5 inches from top surface.
- Some rust existed at edges of reinforcement bar.
- One horizontal crack located at 2.5 inches from top surface.

Core Number: 2- 2"
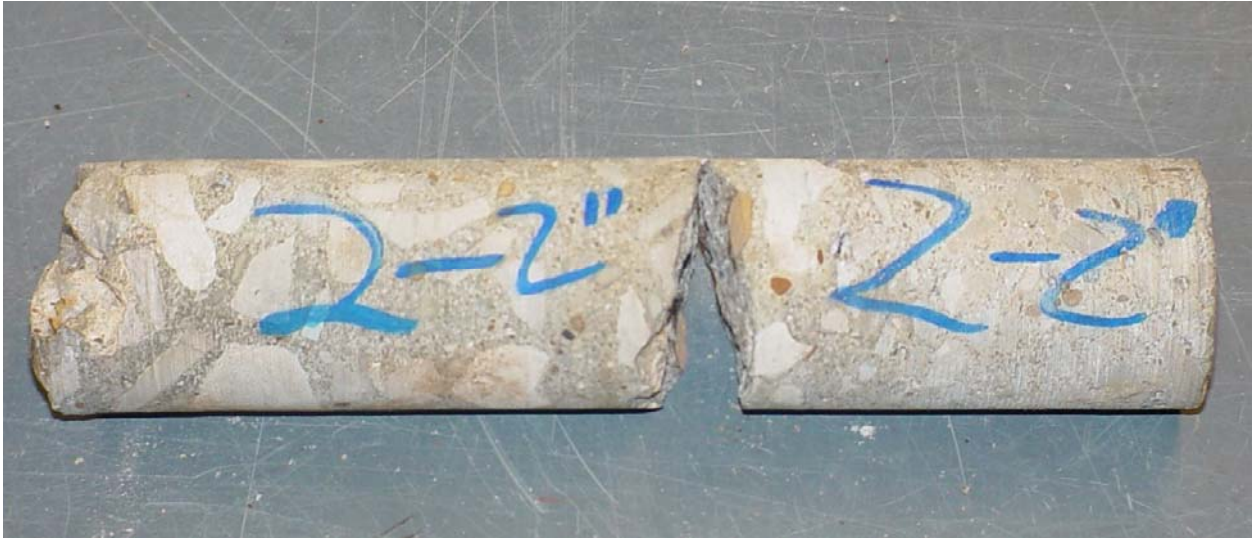
Location:

Station location 975 + 51.6 and 31.2 feet from the face of the curb on the south side of the bridge.

Compression Test:

2-2"
Cut and Capped Length: 3.37"
Load: 19,220 Lbs
Adjusted Load: 19,220 Lbs
Corrected Psi: 7,990 Psi

2-2" (1)
Cut and Capped Length: 3.00"
Load: 19,240 Lbs
Adjusted Load: 18,797 Lbs
Corrected Psi: 7,820 Psi

Comments:
- Original core length 8.75 inches.
- Many voids present in concrete up to 1/4 inch in diameter.
- Traces of rust found on core.

Core Number: 2B

Location:

Station location 975 + 50.7 and 35 feet from the face of the curb on the south side of the bridge.

Chloride Ion Test:

At two inches:
  % CL⁻:   0.0315
  # CL⁻ / yd³: 1.09

At four inches:
  % CL⁻:   0.0092
  # CL⁻ / yd³: 0.32

At six inches:
  % CL⁻:   0.0237
  # CL⁻ / yd³: 0.82

At eight inches:
  % CL⁻:   0.0053
  # CL⁻ / yd³: 0.18

Comments:
- Original core length 6.75 – 8.75 inches.
- No bond between SIPMF and deck. White residue found on SIPMF and concrete.
- Rebar severely rusted.
- Numerous voids present in concrete up to 1/8 inch in diameter.
- Transverse crack located at bottom rebar mat, 7.5 inches from the top, due to severe rust of rebar. Crack is 3/4 of the way through core.

Core Number: 2C

Location:

Station location 975 + 50.7 and 25.9 feet from the face of the curb on the south side of the bridge.

Permeability Test:

Charge Passed: 1,200 C
Adjusted Charge: 1,083 C
Permeability Class: Low

Comments:
- Original concrete length 7.75 – 9.5 inches.
- No bond between SIPMF and deck.
- Core fractured at first rebar mat, 2.25 inches from top, due to heavily corroded rebar.
- Core fractured at 8.25 inches from top due to extraction of core.

Core Number: 2D1

Location:

Station location 975 + 51.5 and 14.4 feet from the face of the curb on the south side of the bridge.

Permeability Test:

Charge Passed: 1,083 C
Adjusted Charge: 977 C
Permeability Class: Very Low

Comments:
- Original core length 8.5 inches.
- No bond between SIPMF and deck.
- Rebar shows traces of rust.

Core Number: 2D2

Location:

Station location975 + 50.5 and 14.5 feet from the face of the curb on the south side of the bridge.

Permeability Test:

Charge Passed: 1,938 C
Adjusted Charge: 1,749 C
Permeability Class: Low

Comments:
- Original core length 8.5 inches.
- No bond between SIPMF and deck.
  - Rebar shows traces of rust.

Core Number: 2D3

Location:

Station location 975 + 50.5 and 13.1 feet from the face of the curb on the south side of the bridge.

Compression Test:

Cut and Capped Length: 6.75"
Load: 110,400 Lbs
Adjusted Load: 107,817 Lbs
Corrected Psi: 8,890 Psi

Comments:
- Original core length 8 – 10 inches.
- Numerous voids present in concrete up to 1/2 inch in diameter.
- No bond between SIPMF and deck. White residue found on SIPMF and core.

Core Number: 2E
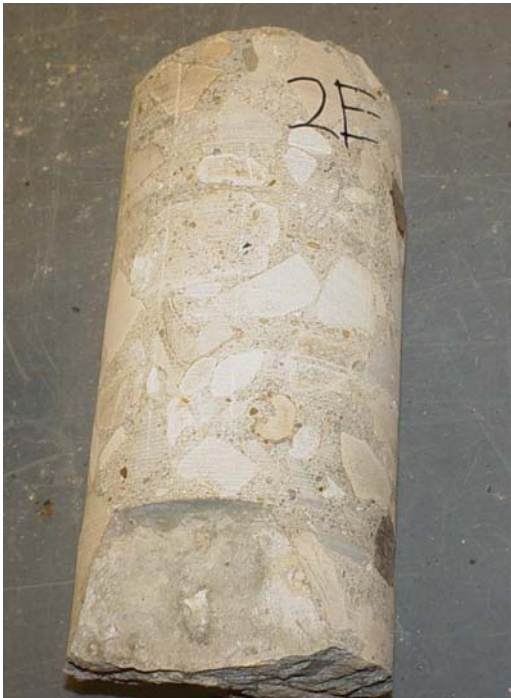
Location:
Station location 975 + 51.5 and 1.6 feet from the face of the curb on the south side of the bridge.

Permeability Test:

Charge Passed: 1,336 C
Adjusted Charge: 1,206 C
Permeability Class: Low

Comments:
- Original core length 8.5 inches.
- No bond between SIPMF and deck. Concrete on bottom of core, against SIPMF, rubbelized.
- Rebar shows signs of rust.
- Numerous voids present in concrete up to 1/8 inch in diameter.

Core Number: 2F

Location:

Station location 975 + 51.3 and 0.7 feet from the face of the curb on the south side of the bridge.

Chloride Ion Test:

At two inches:
% CL$^-$:	0.0328
# CL$^-$ / yd^3:	1.13

At four inches:
% CL$^-$:	0.0301
# CL$^-$ / yd^3:	1.04

At six inches:
% CL$^-$:	0.128
# CL$^-$ / yd^3:	0.44

At eight inches:
% CL$^-$:	0.0091
# CL$^-$ / yd^3:	0.31

Comments:
- Original core length 7.75 – 9.5 inches.
- No bond between SIPMF and deck. White residue found on SIPMF and bottom of core.
- Core fractured at first rebar mat, 2.5 inches from the top, due to severe corrosion of rebar.
- Other steel reinforcement severely rusted as well.
- Numerous voids present in concrete up to 3/8 inch in diameter.

Core Number: 3 - 2"
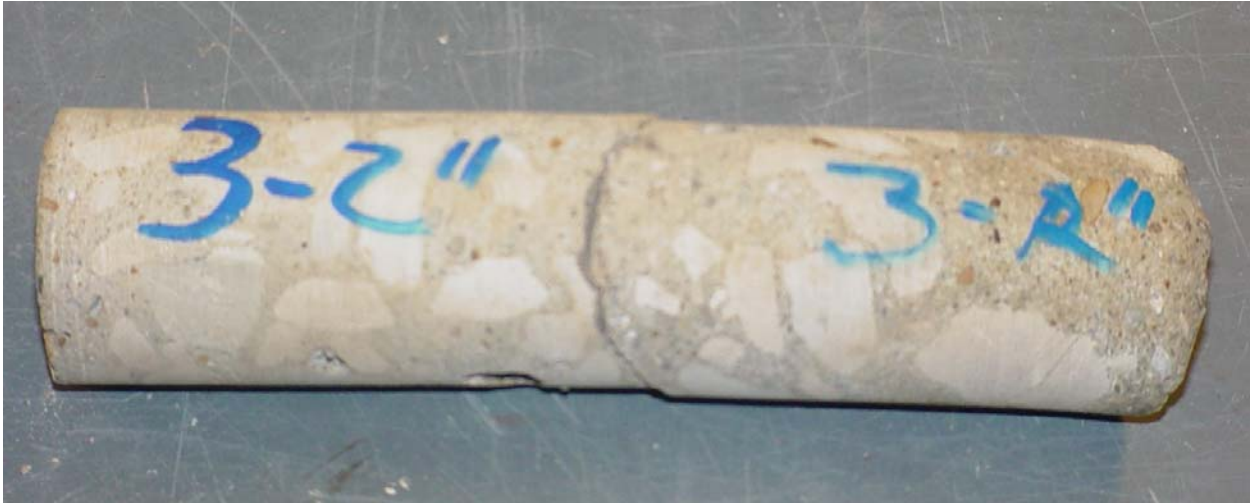
Location:

Station location 975 + 9.3 and 22.8 feet from the face of the curb on the south side of the bridge.

Compression Test:

3-2"
Cut and Capped Length: 3.06"
Load: 21,320 Lbs
Adjusted Load: 20,894 Lbs
Corrected Psi: 8,690 Psi

3-2" (1)
Cut and Capped Length: 2.87"
Load: 18,410 Lbs
Adjusted Load: 17,876 Lbs
Corrected Psi: 7,430 Psi

Comments:
- Original length 8 inches.
- Honeycombing present at bottom of core.
- Numerous voids present up to 3/8 inch in diameter.
- Core fractured during excavation process.

Core Number: 3C

Location:

Station location 975 + 8.6 and 24.7 feet from the face of the curb on the south side of the bridge.

Chloride Ion Test:

At two inches:
  % CL⁻:   0.0457
  # CL⁻ / yd³: 1.58

At four inches:
  % CL⁻:   0.0335
  # CL⁻ / yd³: 1.16

At six inches:
  % CL⁻:   0.0209
  # CL⁻ / yd³: 0.72

At eight inches:
  % CL⁻:   0.0153
  # CL⁻ / yd³: 0.53

Comments:

- Core length 6 – 8 inches.
- No bond between SIPMF and deck.
- Core fractured where SIPMF meets deck, 6 in from top.
- Rebar heavily corroded.
- Numerous voids present in concrete up to 3/8 inch diameter.
- Large void present 3 inches from top. Void is and inch in diameter.

Core Number: 3D
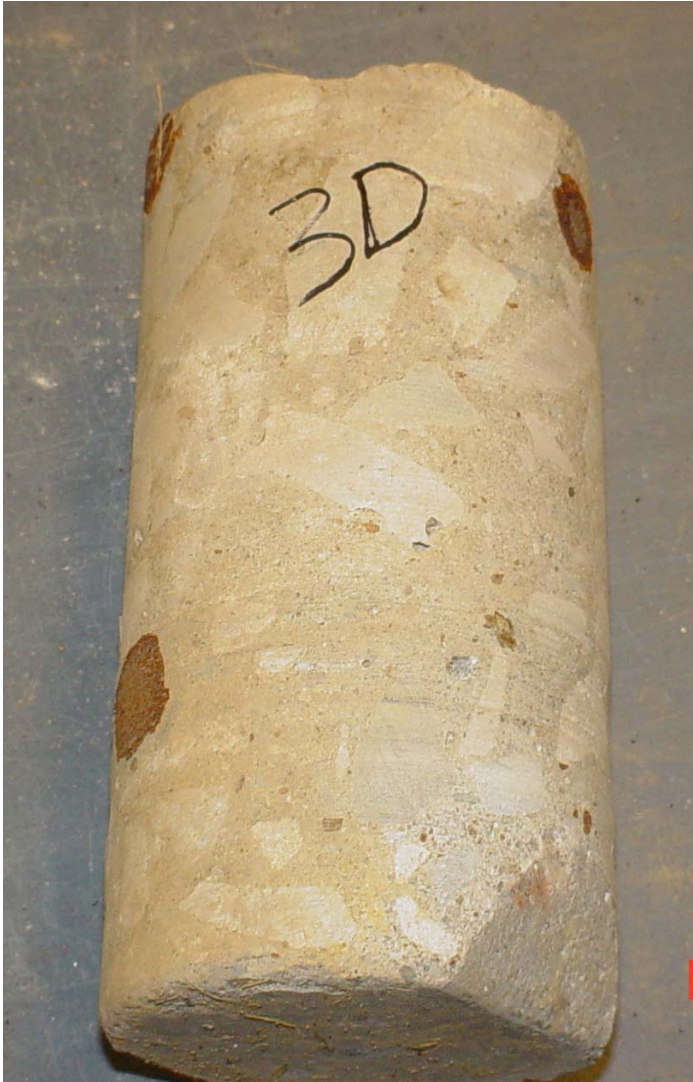
Location:

Station location 975 + 8.4 and 19.6 feet from the face of the curb on the south side of the bridge.

Ultrasound Test:

$\sum$ V(Δh): 86,827 in ft/s
Maximum Velocity: 14,323 ft/s
Quality Index Avrg.: 11,577 ft/s

Comments:
- Core height 6.25 inches, 7.5 inches with the concrete in the region of the valley of the SIPMF.
- Top of core broken.
- Three reinforcement bars located at 2.25 inches, 6.25 inches, and 7.0 inches from bottom surface.
- Bars are not coated and show severe rusting.
- Area of honeycombing at 5.5 inches from bottom surface.
- Small voids present in concrete.

Core Number: 3F

Location:

Station location 975 + 9.6 and 0.8 feet from the face of the curb on the south side of the bridge.

Chloride Ion:

At two inches:
    % CL⁻:   0.0446
    # CL⁻ / yd³: 1.54

At four inches:
    % CL⁻:   0.0390
    # CL⁻ / yd³: 1.35

At six inches:
    % CL⁻:   0.0164
    # CL⁻ / yd³: 0.57

At eight inches:
    % CL⁻:   0.0127
    # CL⁻ / yd³: 0.44

Comments:
- Core length 9.5 inches.
- Core fractured at first rebar mat, 2 inches from top, due to severe corrosion of rebar.
- Large void 4.5 inches below top. Void in 1/2 inch in diameter.
- No bond between SIPMF and deck.
- All rebar heavily rusted.
- Honeycombing present on bottom of core.

Core Number: 4 – 2"

Location:

Station location 974 + 80.5 and 21 feet from the face of the curb on the south side of the bridge.

Compression Test:

Cut and Capped Length: 3.43"
Load: 17,270 Lbs
Corrected Load: 17,270 Lbs
Corrected Psi: 7,180 Psi

Comments:
- Original length 5 inches.
- Numerous voids present up to 3/8 inch in diameter.
- Large void 3/8 inch in diameter located 1 inch from top.

Core Number: 4C1

Location:

Station location 974 + 80.6 and 21.4 feet from the face of the curb on the south side of the bridge.

Compression Test:

Cut and Capped Length: 5.88"
Load: 99,200 Lbs
Adjusted Load: 95,113 Lbs
Corrected Psi: 7,840 Psi

Comments:
- Original length 6.75 inches.
- Numerous voids present up to 1/8 inch in diameter.
- No bond between SIPMF and deck.
- Core fractured at top during coring operation.

Core Number: 4C2

Location:

Station location 974 + 80.4 and 20.9 feet from the face of the curb on the south side of the bridge.

Ultrasound Test:

$\sum$ V(Δh): 114,947 in ft/s
Maximum Velocity: 17,042 ft/s
Quality Index Avrg.: 13,933 ft/s

Comments:
- Core height 6.625 inches, 8.25 inches with the concrete in the region of the valley of the SIPMF.
- Concrete broken at the top.
- Three reinforcing bars located at 2 inches, six inches, and 7 inches from bottom surface.
- Bars are not coated and show severe rusting.
- Region of voids at 6 inches from bottom.

Core Number: 4E

Location:

Station location 974 + 80 and 1.7 feet from the face of the curb on the south side of the bridge.

Permeability Test:

Charge Passed: 1,245 C
Adjusted Charge: 1,124 C
Permeability Class: Low

Comments:
- Original length 9 inches.
- Core fractured 1 inch below surface due to numerous voids present at location.
- Rebar severely rusted.
- Good bond between SIPMF and deck. Concrete located against SIPMF beginning to rubblize.

Core Number: 4F

Location:

Station location 974+ 79.6 and 0.9 feet from the face of the curb on the south side of the bridge.

Chloride Ion Test:

At two inches:
  % CL⁻:   0.0556
  # CL⁻ / yd³: 1.92

At four inches:
  % CL⁻:   0.0164
  # CL⁻ / yd³: 0.57

At six inches:
  % CL⁻:   0.0105
  # CL⁻ / yd³: 0.36

At eight inches:
  % CL⁻:   0.0094
  # CL⁻ / yd³: 0.32

Comments:
- Total length 7 inches.
- Core fractured at both rebar locations due to severe corrosion of rebar.
- Numerous voids present up to 1/4 inch in diameter.
- No bond SIPMF and deck. Bottom of core rubblized.

Core Number: 5 – 2"

Location:

Station location 973 + 49.9 and 22.8 feet from the face of the curb on the south side of the bridge.

Compression Test:

Cut and Capped Length: 3.37"
Load: 18,550 Lbs
Adjusted Load: 18,550 Lbs
Corrected Psi: 7,710 Psi

Comments:
- Rebar shows traces of rust.
- Numerous small voids up to 1/8 inch in diameter.

Core Number: 5B

Location:

Station location 973 + 50.5 and 32.8 feet from the face of the curb on the south side of the bridge.

Permeability Test:

5B (T)
  Charge Passed: 2,096 C
  Adjusted Charge: 1,892 C
  Permeability Class: Low

5B (B)
  Charge Passed: 1,676 C
  Adjusted Charge: 1,513 C
  Permeability Class: Low

Comments:
- Original Length was 9.5 inches.
- Rebar in good condition.
- Voids present in concrete up to 1/4 inch in diameter.
- No bond SIPMF and concrete.

Core Number: 5C

Location:

Station location 973 + 50.4 and 23.2 feet from the face of the curb on the south side of the bridge.

Chloride Ion Test:

At two inches:
   % CL⁻:   0.0262
   # CL⁻ / yd³: 0.90

At four inches:
   % CL⁻:   0.0163
   # CL⁻ / yd³: 0.56

At six inches:
   % CL⁻:   0.0152
   # CL⁻ / yd³: 0.52

At eight inches:
   % CL⁻:   0.0141
   # CL⁻ / yd³: 0.49

Comments:
- Length of core 9.5 inches.
- Rebar shows traces of rust.
- Numerous voids in concrete up to 1/2 inch in diameter.
- No bond SIPMF and concrete. Bottom of core, where in contact with SIPMF, rubblized.

Core Number: 5D

Location:

Station location 973 + 49.9 and 12.4 feet from the face of the curb on the south side of the bridge.

Compression Test:

Cut and Capped Length: 4.56"
Load: 82,400 Lbs
Adjusted Load: 74,836 Lbs
Corrected Psi: 6,170 Psi

Comments:
- Length 8 – 9.5 inches.
- Rebar shows traces of rust.
- No bond SIPMF and deck. White residue found on SIPMF and concrete.
- Numerous voids up to 1/8 inch in diameter.

Core Number: 5E
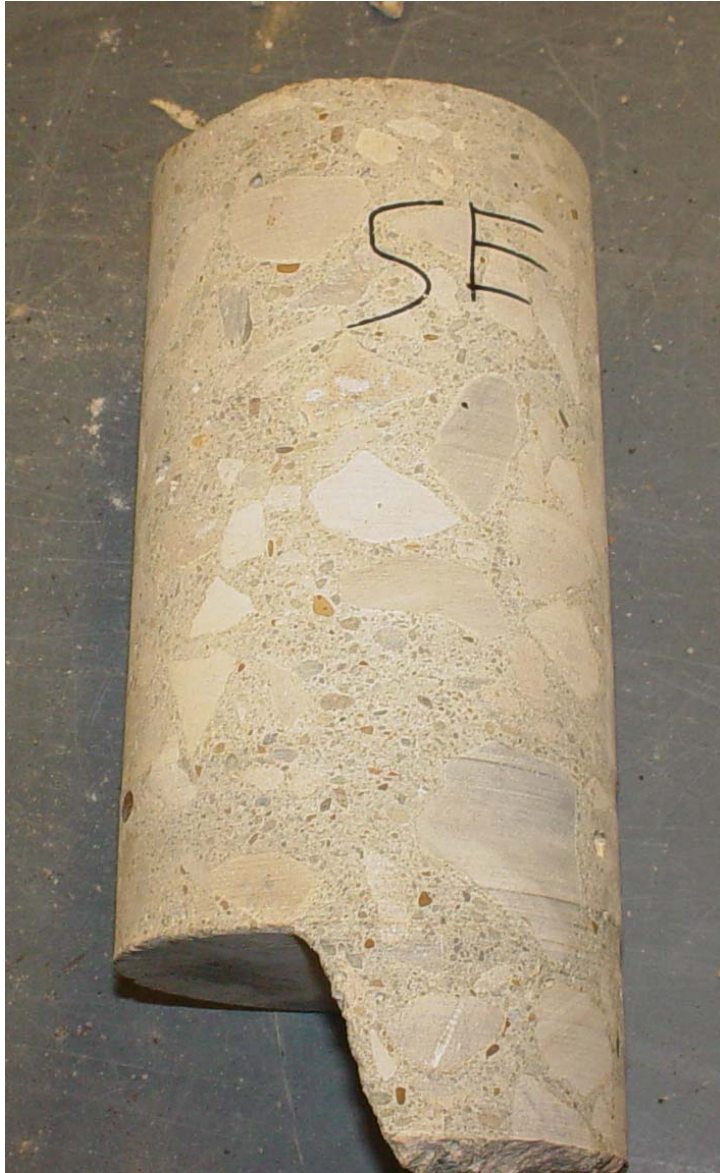
Location:

Station location 973 + 50.1 and 1.7 feet from the face of the curb on the south side of the bridge.

Compression Test:

Cut and Capped Length: 7.13"
Load: 90,200 Lbs
Adjusted Load: 90,200 Lbs
Corrected Psi: 7,440 Psi

Comments:
- Length 7.75 – 9.5 inches
- Numerous voids present in concrete up to 1/4 inch in diameter.
- No bond SIPMF and deck. White residue found on bottom of core
- No rebar in core.

Core Number: 6B
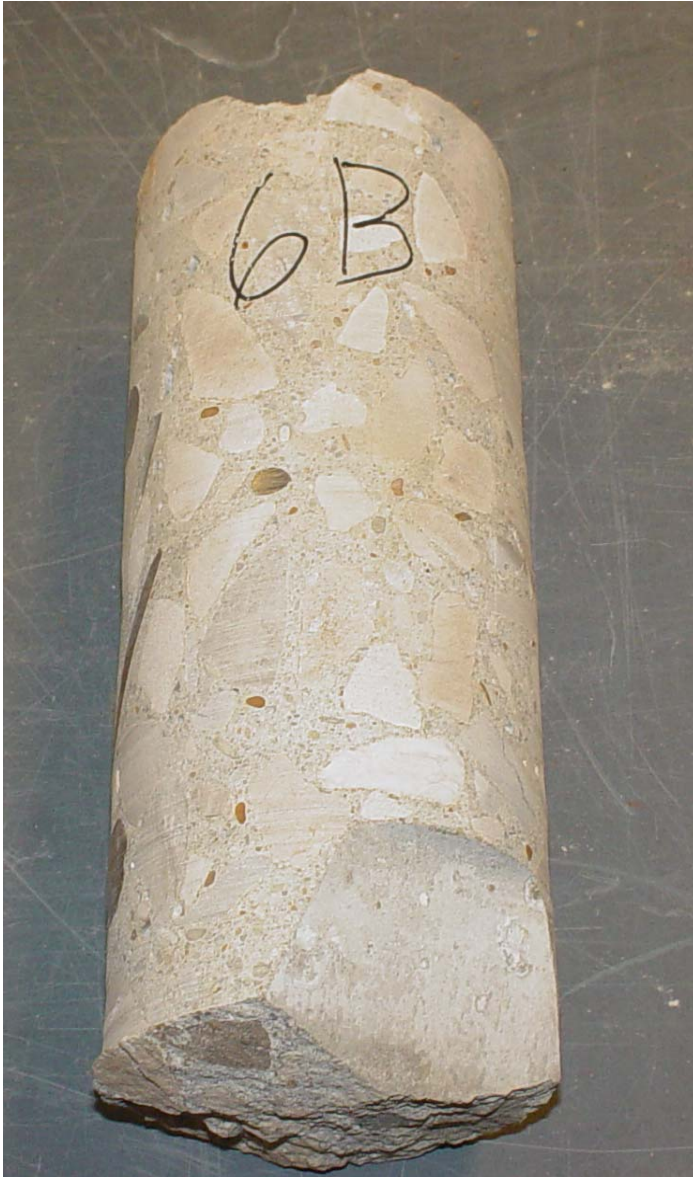
Location:

Station location 973 + 49.6 and 32.8 feet from the face of the curb on the south side of the bridge.

Ultrasound Test:

$\sum$ V(Δh): 125,042 in ft/s
Maximum Velocity: 15,130 ft/s
Quality Index Avrg.: 12,825 ft/s

Comments:
- 7.875 inches in height, 9.75 inches with the concrete in the region of the valley of the SIPMF.
- Two reinforcement bars located at 3 inches and 7.5 inches from the top.
- Bars are not coated and show some rust traces.
- Small region of honeycombing at 3 inches from the top surface.
- Concrete broken in region of SIPMF.

Core Number: 6C

Location:

Station location 973 + 49.9 and 23.2 feet from the face of the curb on the south side of the bridge.

Ultrasound Test:

$\sum$ V(Δh): 134,170 in ft/s
Maximum Velocity: 15,000 ft/s
Quality Index Avrg.: 13,587 ft/s

Comments:
- 7.88 inches in height, 9.875 in. with the concrete in the region of the valley of the SIPMF.
- Three reinforcement bars located at 3 inches, 4 inches, and 7.5 inches from top surface.
- Bars are not coated and show traces of rusting.
- Areas of medium to large voids at 1 inch and 2.25 inches from top.

Core Number: 6D

Location:

Station location 973 + 48.9 and 12.4 feet from the face of the curb on the south side of the bridge.

Permeability Test:

Charge Passed: 2,604 C
Adjusted Charge: 2,350 C
Permeability Class: Moderate

Comments:
- Length 9.5 inches.
- No bond SIPMF and deck. Bottom of core beginning to deteriorate.
- Rebar shows traces of rust.
- Numerous voids in concrete up to 3/16 inch in diameter.

Core Number: 6E

Location:

Station location 973 + 48.9 and 1.7 feet from the face of the curb on the south side of the bridge.

Chloride Ion Test:

At two inches:
  % CL⁻:   0.1238
  # CL⁻ / yd³: 4.27

At four inches:
  % CL⁻:   0.0845
  # CL⁻ / yd³: 2.92

At six inches:
  % CL⁻:   0.0383
  # CL⁻ / yd³: 1.32

At eight inches:
  % CL⁻:   0.0287
  # CL⁻ / yd³: 0.99

Comments:
- Length 8.5 – 9.5 inches.
- No bond between SIPMF and concrete.
- Rebar severely rusted.
- Numerous voids present in concrete up to 3/8 inch in diameter.
- Bottom of core fractured during extraction of core.

Core Number: 7 – 2"
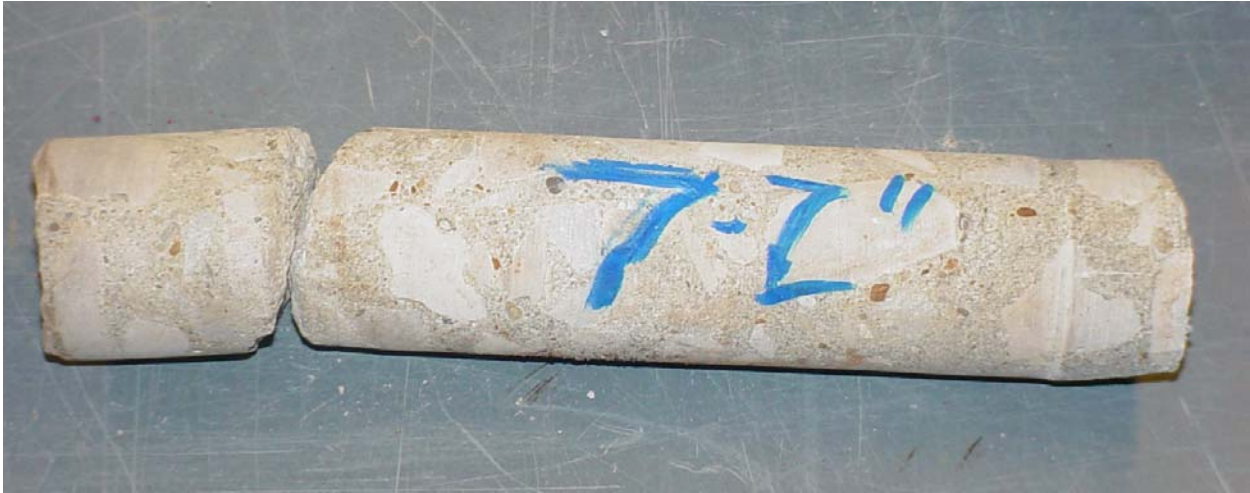
Location:

Station location 971 + 81 and 20.1 feet from the face of the curb on the south side of the bridge.

Compression Test:

Cut and Capped Length: 3.37"
Load: 17,720 Lbs
Adjusted Load: 17,720 Lbs
Corrected Psi: 7,370 Psi

Comments:
- Original length 5.5 inches.
- Core fractured 1 inch below top of core due to extraction core.
- Numerous void present in concrete up to 1/8 inch in diameter.

Core Number: 7B

Location:

Station location 971 + 80.3 and 34.8 feet from the face of the curb on the south side of the bridge.

Chloride Ion Test:

At two inches:
% CL⁻:   0.1168
# CL⁻ / yd³: 4.03

At four inches:
% CL⁻:   0.0419
# CL⁻ / yd³: 1.45

At six inches:
% CL⁻:   0.0203
# CL⁻ / yd³: 0.70

At eight inches:
% CL⁻:   0.0237
# CL⁻ / yd³: 0.82

Comments:
- Length 7.25 – 8.75 inches.
- No bond between SIPMF and deck. White residue found on SIPMF and concrete.
- Fractured 1 inch below top due to many voids in concrete.
- Rebar shows traces of rust.
- Numerous voids present in concrete up to 1/8 inch in diameter.

Core Number: 7C

Location:

Station location 971 + 81 and 17.4 feet from the face of the curb on the south side of the bridge.

Chloride Ion Test:

At two inches:
% CL⁻:	0.1544
# CL⁻ / yd³:	5.33

At four inches:
% CL⁻:	0.1323
# CL⁻ / yd³:	4.57

At six inches:
% CL⁻:	0.0420
# CL⁻ / yd³:	1.45

At eight inches:
% CL⁻:	0.0177
# CL⁻ / yd³:	0.61

Comments:
- Length 6.25 – 8 inches.
- No bond SIPMF and concrete. White residue found on SIPMF and concrete.
- Rebar shows traces of rust.
- Core fractured 1 inch below top of core due to numerous voids.
- Numerous voids up to 1/8 inch in diameter.

Core Number: 7C1

Location:

Station location 971 + 80.4 and 28 feet from the face of the curb on the south side of the bridge.

Permeability Test:

Charge Passed: 2,247 C
Adjusted Charge: 2,020 C
Permeability Class: Moderate

Comments:
- Length 7.25 – 9.5 inches.
- Core fractured 1.25 inches below top due to numerous voids.
- No bond SIPMF and concrete. White residue found on bottom of core.
- Rebar shows traces of rust.
- Numerous voids in concrete up to 3/8 inch in diameter.

Core Number: 7C1 (2)

Location:

Station location 971 + 80.3 and 27.3 feet from the face of the curb on the south side of the bridge.

Permeability Test:

Charge Passed: 2,026 C
Adjusted Charge: 1,828 C
Permeability Class: Low

Comments:
- Length 9.25 inches.
- No bond SIPMF and concrete. Rust present on bottom of core.
- Rebar shows traces of rust.
- Numerous voids in concrete up to 1/4 inch in diameter.
- Length 9.25 inches.

Core Number: 7D
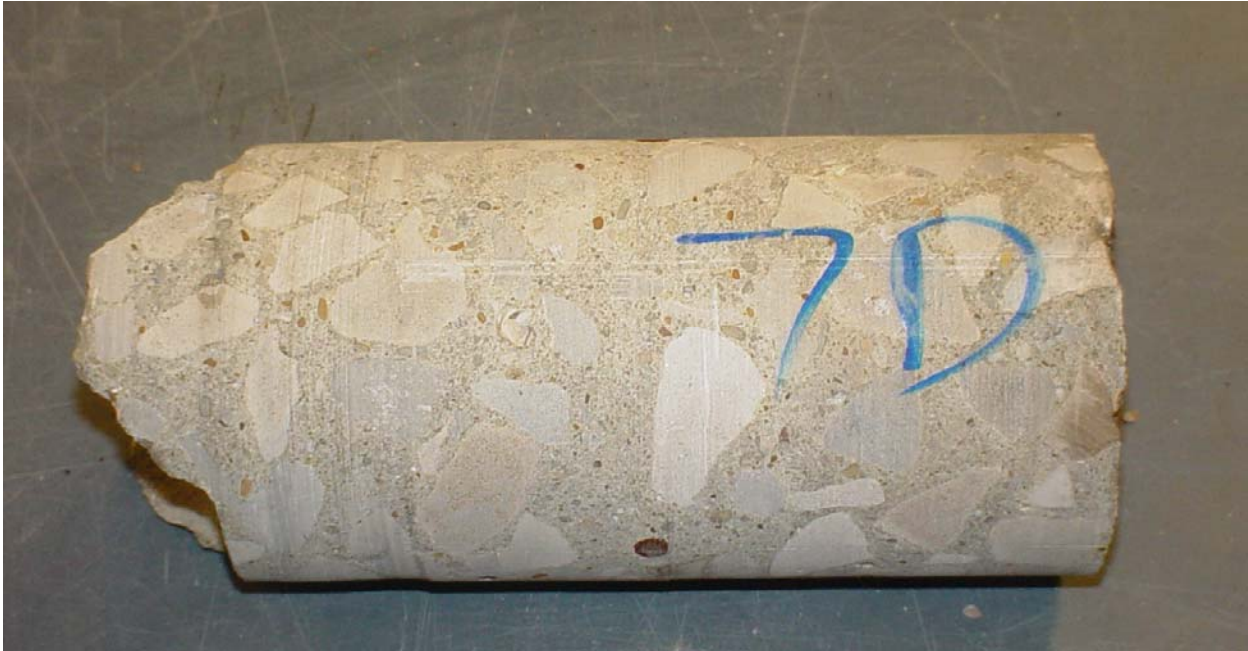
Location:

Station location 971 + 80.4 and 11.8 feet from the face of the curb on the south side of the bridge.

Ultrasound Test:

$\sum$ V(Δh): 111,139 in ft/s
Maximum Velocity: 16,629 ft/s
Quality Index Avrg.: 14,819 ft/s

Comments:
- 7.5 inches in height, 9 inches with the concrete in the region of the valley of the SIPMF.
- Area of voids at 3.75 inches from the top.
- Reinforcement bar located at 6 inches from the bottom surface.
- Bars are not coated and show some rust.
- Small voids present in concrete.

Core Number: 7E

Location:

Station location 971 + 80.7 and 1.9 feet from the face of the curb on the south side of the bridge.

Permeability Test:

7E (T)
 Charge Passed: 2,570 C
 Adjusted Charge: 2,319 C
 Permeability Class: Moderate

7E (B)
 Charge Passed: 1,189 C
 Adjusted Charge: 1,073 C
 Permeability Class: Low

Comments:
- Length 9.75 inches.
- No bond between SIPMF and concrete. White residue found on SIPMF and concrete.
- Bottom of core rubblized and honeycombing present on one side.
- Rebar traces of rust.

Core Number: 8 – 2"

Location:

Station location 971 + 65.4 and 6.9 feet from the face of the curb on the south side of the bridge.

Compression Test:

8 – 2"
  Cut and Capped Length: 3.50"
  Load: 14,790 Lbs
  Adjusted Load: 14,790 Lbs
  Corrected Psi: 6,150 Psi

8 – 2" (1)
  Cut and Capped Length: 3.37"
  Load: 20,520 Lbs
  Adjusted Load: 20,520 Lbs
  Corrected Psi: 8,530 Psi

Comments:
- Length 9 inches.
- Numerous voids present in concrete up to 1/8 inch in diameter.

Core Number: 8B

Location:

Station location 971 + 65.6 and 34.6 feet from the face of the curb on the south side of the bridge.

Chloride Ion Test:

At two inches:
   % CL⁻:   0.1039
   # CL⁻ / yd³: 3.59

At four inches:
   % CL⁻:   0.0488
   # CL⁻ / yd³: 1.68

At six inches:
   % CL⁻:   0.0224
   # CL⁻ / yd³: 0.77

At eight inches:
   % CL⁻:   0.0184
   # CL⁻ / yd³: 0.64

Permeability Test:

Charge Passed: 2,137 C
Adjusted Charge: 1,929 C
Permeability Class: Low

Comments:
- Core length 9 inches.
- Rebar shows traces of rust.
- Bottom chipped due to excavation of core.
- Concrete in good condition.

Core Number: 8C1

Location:

Station location 971 + 65.6 and 34.6 feet from the face of the curb on the south side of the bridge.

Chloride Ion Test:

At two inches:
  % CL⁻:   0.1391
  # CL⁻ / yd³: 4.80

At four inches:
  % CL⁻:   0.1321
  # CL⁻ / yd³: 4.56

At six inches:
  % CL⁻:   0.0549
  # CL⁻ / yd³: 1.90

At eight inches:
  % CL⁻:   0.0165
  # CL⁻ / yd³: 0.57

Permeability Test:

Charge Passed: 2,599 C
Adjusted Charge: 2,346 C
Permeability Class: Moderate

Comments:
- Core length 9.5 inches.
- Rebar shows traces of rust.
- Numerous voids present in concrete up to 1/4 inch in diameter.

Core Number: 8C2

Appendix A: LOR-57-18.18 Individual Core Data

Location:

Station location 971 + 64.2 and 20.4 feet from the face of the curb on the south side of the bridge.

Ultrasound:

$\sum$ V(Δh): 118,815 in ft/s
Maximum Velocity: 16,285 ft/s
Quality Index Avrg.: 13,202 ft/s

Comments:
- Core 9 inches in height.
- Three reinforcement bars located at 2.5 inches, 6.75 inches, and 7.75 inches from the top surface.
- Bars are not coated and show slight signs of rust.
- Small voids present in concrete.

Core Number: 8D

Location:

Station location 971 + 65.7 and 11.3 feet from the face of the curb on the south side of the bridge.

Compression Test:

Cut and Capped Length: 7.63"
Load: 85,700 Lbs
Adjusted Load: 85,700 Lbs
Corrected Psi: 7,060 Psi

Comments:

- Core length 9.5 inches.
- Numerous voids present in concrete up to 1/8 inch in diameter.

Core Number: 8E

Location:

Station location 971 + 65.3 and 1.7 feet from the face of the curb on the south side of the bridge.

Ultrasound Test:

$\sum V(\Delta h)$: 112,382 in ft/s
Maximum Velocity: 15,882 ft/s
Quality Index Avrg.: 12,487 ft/s

Comments:
- Core length 9 inches.
- Two reinforcement bars located at 2.5 inches and 7 inches from the top surface.
- Bars are not coated.
- Region of voids located approximately at 6 inches from the top surface.
- Small voids present in concrete.

Appendix B
OTT-2-28.41 Individual Core Data

Core Number: A1

Location:

Station location 107 + 11.5 and 0.4 feet from the face of the curb on the east side of the bridge.

Ultrasound Test:

$\sum$ V(Δh): 157,243 in ft/s
Maximum Velocity: 18,050 ft/s
Quality Index Avrg.: 14,295 ft/s

Comments:
- Core height 11 inches.
- Three reinforcement bars, non-epoxy coated located at 4 inches, 6 inches, and 7 inches from top surface.
- Some rust traces on bars.
- Small region of honeycombing located at 2.5 in. from top surface.

Core Number: A2

Location:

Station location 107 + 12.8 and 0.3 feet from the face of the curb on the east side of the bridge.

Chloride Ion Test:

At two inches:
  % CL⁻:   0.0339
  # CL⁻ / yd³: 1.21

At four inches:
  % CL⁻:   0.0353
  # CL⁻ / yd³: 1.26

At six inches:
  % CL⁻:   0.0291
  # CL⁻ / yd³: 1.04

At eight inches:
  % CL⁻:   0.0212
  # CL⁻ / yd³: 0.76

Comments:
- Core length 11 inches with 1.75 in wearing surface.
- Rebar shows traces of rust.
- Numerous amounts of voids in concrete up to 1/4 inch in diameter.
- Bottom of core damage during excavation.

Core Number: A3
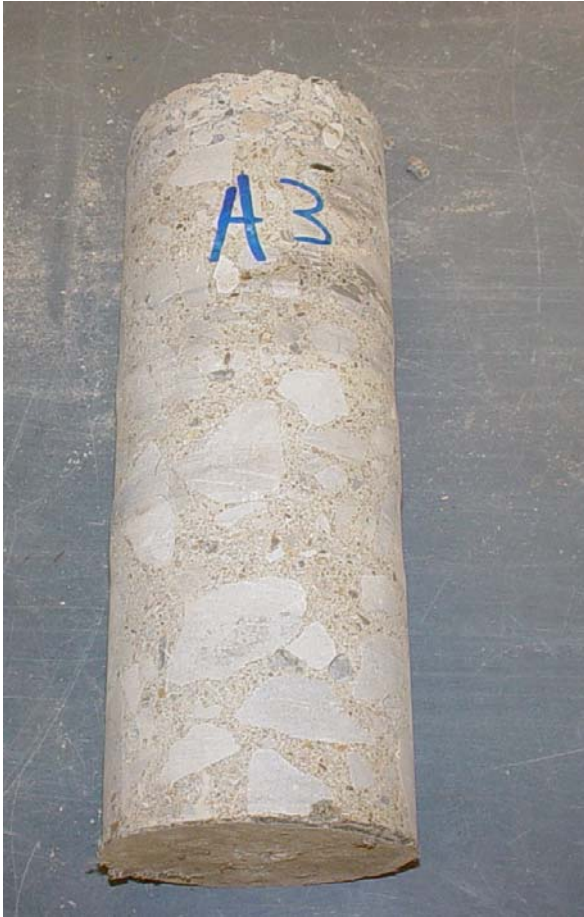
Location:

Station location 107 + 13.9 and 0.3 feet from the face of the curb on the east side of the bridge.

Permeability Test:

A3 (T)
  Charge Passed: 2,191 C
  Adjusted Charge: 1,977 C
  Permeability Class: Low

A3 (B)
  Charge Passed: 1,345 C
  Adjusted Charge: 1,214 C
  Permeability Class: Low

Comments:
- Core length 11 inches with 1.25 inch wearing surface.
- Rebar shows traces of rust.
- Numerous amounts of voids in concrete up to 1/4 inch in diameter.

Core Number: A4

Location:

Station location 107 + 14.8 and 0.4 feet from the face of the curb on the east side of the bridge.

Chloride Ion Test:

At two inches:
  % CL$^-$:   0.0818
  # CL$^-$ / yd^3:   2.93

At four inches:
  % CL$^-$:   0.0285
  # CL$^-$ / yd^3:   1.02

At six inches:
  % CL$^-$:   0.0230
  # CL$^-$ / yd^3:   0.83

At eight inches:
  % CL$^-$:   0.0153
  # CL$^-$ / yd^3:   0.55

Comments:
- Core length 10.75 inches with 1.5 inch wearing surface.
- Rebar shows traces of rust.
- Numerous amounts of voids in concrete up to 1/4 inch in diameter.
- Large void 3 inches from top, 7/8 inches long and 1/4 inch wide.
- Core fractured 9 inches below top due to large amounts of voids.

Core Number: A5

Location:

Station location 107 + 15.9 and 0.4 feet from the face of the curb on the east side of the bridge.

Ultrasound Test:

$\sum$ V(Δh): 139,461 in ft/s
Maximum Velocity: 14,963 ft/s
Quality Index Avrg.: 12,678 ft/s

Comments:
- Core height 11 inches.
- Three reinforcement bars located at 4.5 inches, 6.5 inches and 7.5 inches from the top surface.
- Bars are not coated and show some rust traces.
- Region of honeycombing at 2.5 inches and 6.5 inches from top.
- Small voids present in concrete.

Core Number: A6

Location:

Station location 107 + 17.2 and 0.2 feet from the face of the curb on the east side of the bridge.

Permeability Test:

A6 (T)
  Charge Passed: 1,847 C
  Adjusted Charge: 1,667 C
  Permeability Class: Low

A6 (B)
  Charge Passed: 1,751 C
  Adjusted Charge: 1,580 C
  Permeability Class: Low

Comments:
- Core length 11.25 inches with 1.75 inch wearing surface.
- Rebar shows traces of rust.
- Numerous amounts of voids in concrete up to 1/4 inch in diameter.

Core Number: A7
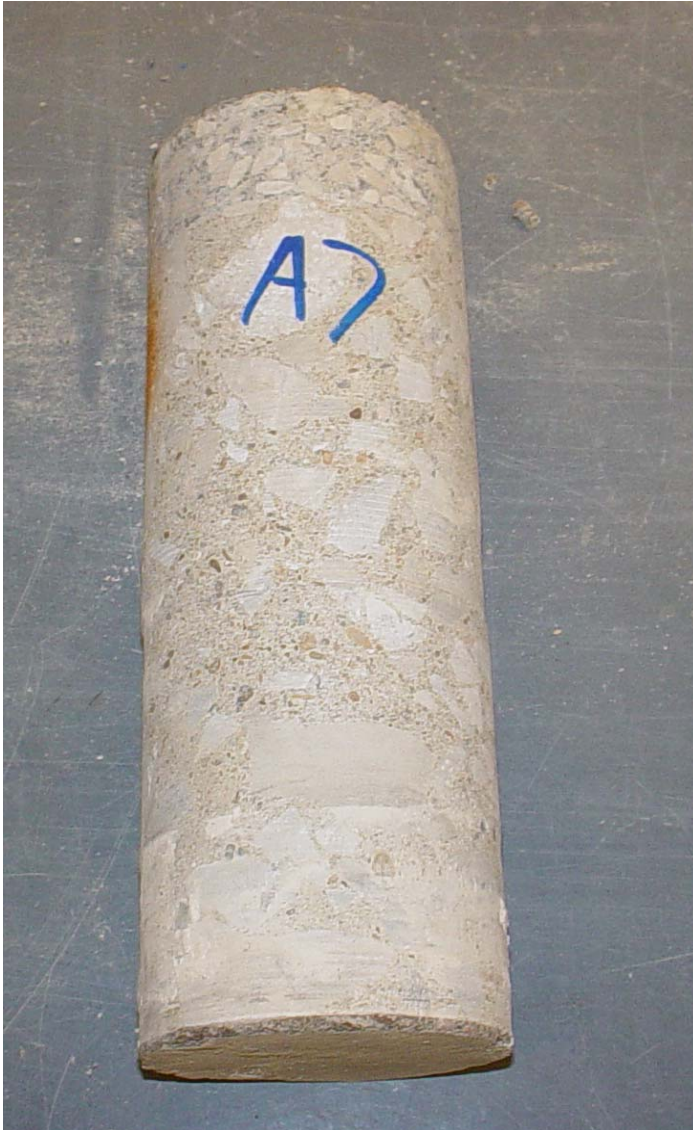
Location:

Station location 107 + 18.3 and 0.2 feet from the face of the curb on the east side of the bridge.

Compression Test:

A7
 Cut and Capped Length: 4.56"
 Load: 80,300 Lbs
 Adjusted Load: 72,928 Lbs
 Corrected Psi: 6,010

A7 (1)
 Cut and Capped Length: 4.44"
 Load: 73,100 Lbs
 Adjusted Load: 65,863 Lbs
 Corrected Psi: 5,430 Psi

Comments:
- Core length 10.75 inches with 1.75 inch wearing surface.
- Numerous amounts of voids in concrete up to 1/4 inch in diameter.

Core Number: A8
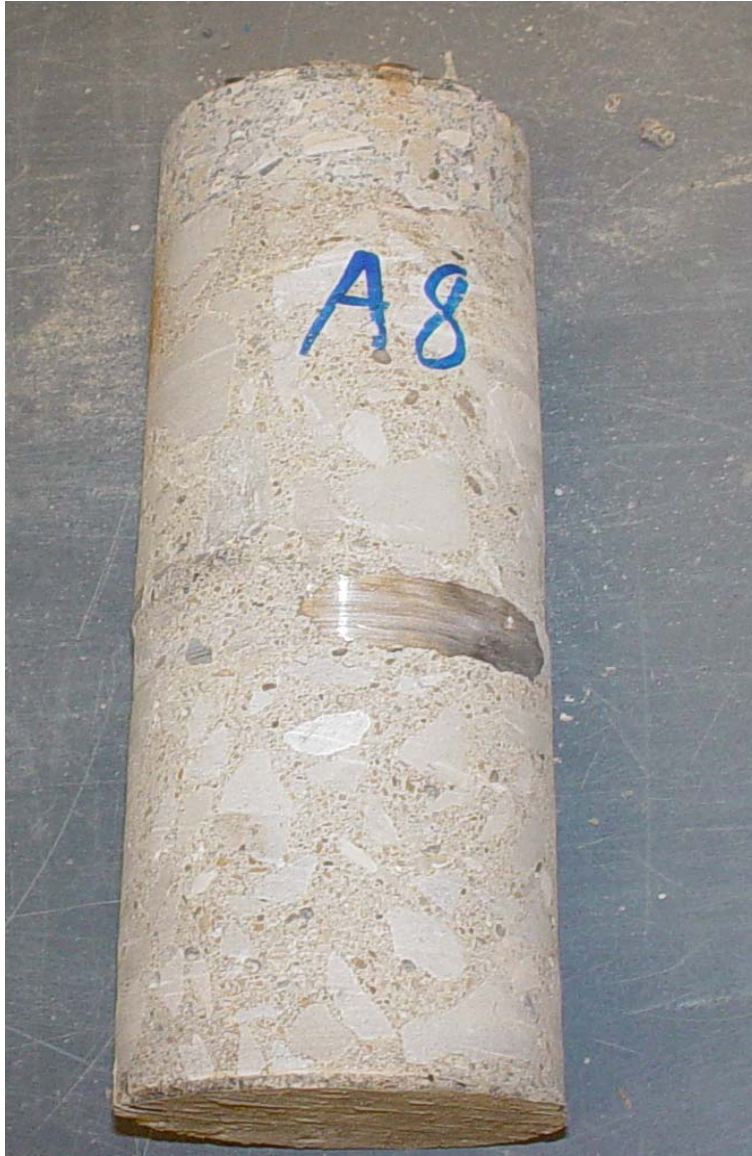
Location:

Station location $107 + 19.6$ and 0.3 feet from the face of the curb on the east side of the bridge.

Chloride Ion Test:

At two inches:
% CL⁻:	0.1513
# CL⁻ / yd³:	5.42

At four inches:
% CL⁻:	0.0514
# CL⁻ / yd³:	1.84

At six inches:
% CL⁻:	0.0313
# CL⁻ / yd³:	1.12

At eight inches:
% CL⁻:	0.0224
# CL⁻ / yd³:	0.80

Comments:
- Core length 11 inches with 1.75 inch wearing surface.
- Numerous amounts of voids in concrete up to 3/8 inch in diameter.
- Rebar shows traces of rust.

Core Number: A9

Location:

Station location $107 + 20.7$ and 0.2 feet from the face of the curb on the east side of the bridge.

Ultrasound Test:

$\sum V(\Delta h)$: 128,611 in ft/s
Maximum Velocity: 13,499 ft/s
Quality Index Avrg.: 11,692 ft/s

Comments:
- Core height 11 inches.
- Two reinforcement bars located at 3 inches and 7.5 inches from top surface.
- Bars are not coated and show severe rusting.
- Region of honeycombing at 4 inches from top.

Core Number: A10

Location:

Station location 107 + 21.9 and 0.3 feet from the face of the curb on the east side of the bridge.

Permeability Test:

A10 (T)
  Charge Passed: 3,321 C
  Adjusted Charge: 2,997 C
  Permeability Class: Moderate

A10 (B)
  Charge Passed: 2,482 C
  Adjusted Charge: 2,240 C
  Permeability Class: Moderate

Comments:
- Core length 11 inches with 1.75 inch wearing surface.
- Numerous amounts of voids in concrete up to 3/8 inch in diameter.
- Rebar heavily rusted.
- Core fractured where wearing surface meets deck due to a large amount of voids.

Core Number: A11

Location:

Station location 107 + 23 and 0.2 feet from the face of the curb on the east side of the bridge.

Ultrasound Test:

$\sum$ V(Δh): 147,339 in ft/s
Maximum Velocity: 16,641 ft/s
Quality Index Avrg.: 13,706 ft/s

Comments:
- Core height 10.75 inches.
- Regions of moderate to large voids located at 7 inches from top surface.
- Two reinforcing bars, non-epoxy coated located at 3 inches and 4 inches from top surface.
- The bars show severe rusting.

Core Number: A12
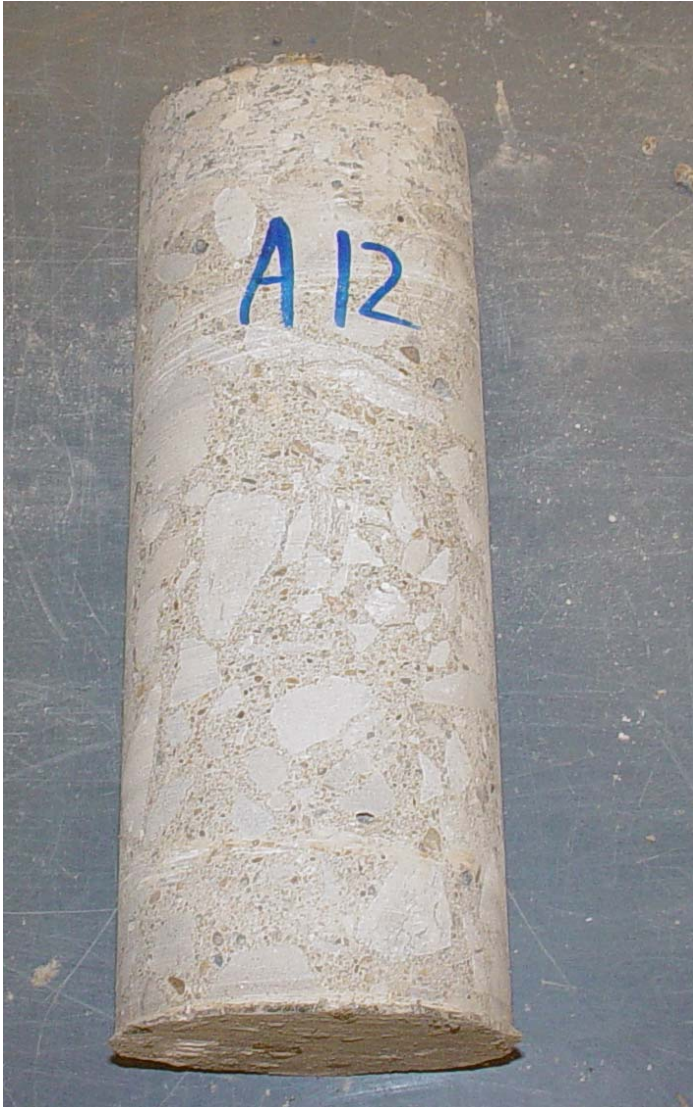
Location:

Station location 107 + 24.2 and 0.2 feet from the face of the curb on the east side of the bridge.

Compression Test:

A12
 Cut and Capped Length: 4.44"
 Load: 68,200 Lbs
 Adjusted Load: 61,448 Lbs
 Corrected Psi: 5,070 Psi

A12 (1)
 Cut and Capped Length: 4.25"
 Load: 77,100 Lbs
 Adjusted Load: 68,295 Lbs
 Corrected Psi: 5,630 Psi

Comments:
- Core length 10.75 inches with 1.5 inch wearing surface.
- Numerous amounts of voids in concrete up to 5/16 inch in diameter.

Core Number: A13

Location:

Station location 107 + 25.6 and 0.3 feet from the face of the curb on the east side of the bridge.

Compression Test:

Cut and Capped Length: 6.00"
Load: 76,000 Lbs
Adjusted Load: 73,127 Lbs
Corrected Psi: 6,030 Psi

Comments:
- Core length 10.75 inches with 1.75 inch wearing surface.
- Numerous amounts of voids in concrete up to 1/8 inch in diameter.
- Rebar shows traces of rust.
- Aggregate cracked 5.5 inches from top, crack is 1 3/8 inch long.
- Core cracked wear wearing surface meets deck. Crack is 1/4 a way around core.

Core Number: A14

Location:

Station location 107 + 26.7 and 0.3 feet from the face of the curb on the east side of the bridge.

Chloride Ion Test:

At two inches:
  % CL⁻:   0.1808
  # CL⁻ / yd³: 6.47

At four inches:
  % CL⁻:   0.1456
  # CL⁻ / yd³: 5.22

At six inches:
  % CL⁻:   0.0567
  # CL⁻ / yd³: 2.03

At eight inches:
  % CL⁻:   0.0328
  # CL⁻ / yd³: 1.17

Comments:
- Core length 10.75 inches with 2 inch wearing surface.
- Numerous amounts of voids in concrete up to 3/8 inch in diameter.
- Rebar shows traces of rust.

Core Number: A15

Location:

Station location 107 + 27.7 and 0.4 feet from the face of the curb on the east side of the bridge.

Permeability Test:

A15 (T)
  Charge Passed: 2,474 C
  Adjusted Charge: 2,233 C
  Permeability Class: Moderate

A15 (B)
  Charge Passed: 2,335 C
  Adjusted Charge: 2,107 C
  Permeability Class: Moderate

Comments:
- Core length 10.75 inches with 1.75 inch wearing surface.
- Numerous amounts of voids in concrete up to 3/8 inch in diameter.
- Rebar heavily rusted.

Core Number: A16

Location:

Station location 107 + 28.7 and 0.3 feet from the face of the curb on the east side of the bridge.

Ultrasound Test:

$\sum$ V(Δh): 147,330 in ft/s
Maximum Velocity: 15,753 ft/s
Quality Index Avrg.: 14,031 ft/s

Comments:
- Core height 10.5 inches. .
- Two reinforcement bars located at 3.5 inches and 7 inches from the bottom surface.
- The upper bar shows severe rusting while the lower shows some rust traces.
- Region of honeycombing located at 6 inches from top.
- Region of large voids at the top-wearing surface.

Core Number: A17

Location:

Station location 107 + 29.6 and 0.1 feet from the face of the curb on the east side of the bridge.

Compression Test:

Cut and Capped Length: 3.25"
Load: 18,920 Lbs
Adjusted Load: 18,920 Lbs
Corrected Psi: 7,870 Psi

Comments:
- Core length 11 inches with 3 inch wearing surface.
- Core fractured during excavation.
- Concrete in good condition.

Core Number: A17-1

Location:

Station location 107 + 30.6 and 0.2 feet from the face of the curb on the east side of the bridge.

Compression Test:

Cut and Capped Length: 3.12"
Load: 15,610 Lbs
Adjusted Load: 15,501 Lbs
Corrected Psi: 6,440 Psi

Comments:
- Core length 10 inches with 2.75 inch wearing surface.
- Numerous voids present in concrete up to 1/4 inch in diameter.

Core Number: A18

Location:

Station location 107 + 31.5 and 0.4 feet from the face of the curb on the east side of the bridge.

Compression Test:

Cut and Capped Length: 3.5"
Load: 18,700 Lbs
Adjusted Load: 18,700 Lbs
Corrected Psi: 7,770 Psi

Comments:
- Core length 8.5 inches with 2 inch wearing surface.
- Numerous voids present in concrete up to 1/8 inch in diameter.
- Core cracked longitudinally 3 inches from top. Length of crack 2.5 inches.

Core Number: A18-1

Location:

Station location 107 + 32.7 and 0.5 feet from the face of the curb on the east side of the bridge.

Compression Test:

Cut and Capped Length: 3.18"
Load: 15,510 Lbs
Adjusted Load: 15,510 Lbs
Corrected Psi: 6,450 Psi

Comments:
- Core length 10.75 inches with 2 inch wearing surface.
- Numerous voids present in concrete up to 3/8 inch in diameter.
- Core fractured during excavation.

Core Number: B1

Location:

Station location 107 + 8.6 and 6.7 feet from the face of the curb on the east side of the bridge.

Ultrasound Test:

$\sum$ V(Δh): 127,686 in ft/s
Maximum Velocity: 15,485 ft/s
Quality Index Average: 13,804 ft/s

Comments:
- Core height 7.25 inches, 9.25 inches with the concrete in the region of the valley of the SIPMF.
- Two reinforcement bars located at 3.5 inches and 6.5 inches from top.
- Small region of honeycombing at 2.5 inches from top surface.
- Bars are not coated and show some rust.

Core Number: B2

Location:

Station location 107 + 13.1 and 6.4 feet from the face of the curb on the east side of the bridge.

Compression Test:

Cut and Capped Length: 5.63"
Load: 69,200 Lbs
Adjusted Load: 65,865 Lbs
Corrected Psi: 5,430 Psi

Comments:
- Core length 7.5 inches with 1.25 inch wearing surface.
- Numerous amounts of voids up to 1/4 inch in diameter.
- No bond SIPMF and concrete. White residue and rust present on SIPMF and concrete.

Core Number: B3

Location:

Station location 107 + 16.5 and 6.2 feet from the face of the curb on the east side of the bridge.

Permeability Test:

Charge Passed: 2,090 C
Adjusted Charge: 1,886 C
Permeability Class: Low

Comments:
- Core length 9.25 inches with 1.25 inch wearing surface.
- Good bond between SIPMF and deck. Bottom of concrete beginning to rubbelize.
- Core fractured 2.75 inches from top due to heavy rusting of rebar.
- Bottom rebar shows traces of rust.
- Numerous voids in concrete up to 1/8 inch in diameter.

Core Number: B4

Location:

Station location 107 + 19.5 and 5.9 feet from the face of the curb on the east side of the bridge.

Ultrasound Test:

$\sum$ V(Δh): 129,039 in ft/s
Maximum Velocity: 14,946 ft/s
Quality Index Avrg.: 14,338 ft/s

Comments:
- Core height 7 inches, 9 inches with the concrete in the region of the valley of the SIPMF.
- Regions of small voids.
- Two reinforcing bars located at 1 inch and 3 inches from bottom surface, and show some rust traces.
- Brown and white traces on the SIPMF.
- Region of honeycombing at 6 inches from bottom.

Core Number: B5

Location:

Station location $107 + 26.4$ and 5.7 feet from the face of the curb on the east side of the bridge.

Ultrasound Test:

$\sum V(\Delta h)$: 124,732 in ft/s
Maximum Velocity:
  15,645 ft/s
Quality Index Avrg.:
  14,255 ft/s

Comments:
- Core height 6.75 inches, 8.75 inches with the concrete in the region of the valley of the SIPMF.
- Area of voids at 3.75 inches from top.
- Two reinforcing bars located at 3.75 inches and 5.5 inches from bottom surface, and show some rust traces.
- Brown and white traces on the SIPMF.

Core Number: B6

Location:

Station location 107 + 29.3 and 5.6 feet from the face of the curb on the east side of the bridge.

Permeability Test:

Charge Passed: 2,490 C
Adjusted Charge: 2,247 C
Permeability Class: Moderate

Comments:
- Core length 6.75 – 8.5 inches with 1.5 inch wearing surface.
- No bond between SIPMF and deck. White residue present on SIPMF and concrete.
- Core fractured 2 inches from top due to large amounts of voids. Length of crack 2.5 inches.
- Bottom rebar shows traces of rust.
- Numerous voids in concrete up to 1/4 inch in diameter.

Core Number: B7

Location:

Station location 107 + 32.5 and 5.6 feet from the face of the curb on the east side of the bridge.

Chloride Ion Test:

At two inches:
    % CL$^-$:   0.1564
    # CL$^-$ / yd^3:   5.60

At four inches:
    % CL$^-$:   0.1023
    # CL$^-$ / yd^3:   3.66

At six inches:
    % CL$^-$:   0.0782
    # CL$^-$ / yd^3:   2.80

At eight inches:
    % CL$^-$:   0.0164
    # CL$^-$ / yd^3:   0.59

Comments:
- Core length 9 inches with 1.75 inch wearing surface.
- No bond between SIPMF and deck. White residue present on SIPMF and concrete.
- Core fractured 6.5 inches from top due to heavy rusting of rebar.
- Bottom rebar shows traces of rust.
- Numerous voids in concrete up to 1/4 inch in diameter.

Core Number: B8

Location:

Station location 107 + 34.2 and 5.5 feet from the face of the curb on the east side of the bridge.

Compression Test:

Cut and Capped Length: 3.50"
Load: 15,720 Lbs
Adjusted Load: 15,720 Lbs
Corrected Psi: 6,540 Psi

Comments:
- Core length 7.25 inches with 1.75 inch wearing surface.
- No bond between SIPMF and deck. White residue present on concrete
- Core fractured 3.5 inches from top due to excavation of core.

Core Number: B9

Location:

Station location 107 + 36 and 5.5 feet from the face of the curb on the east side of the bridge.

Compression Test:

Cut and Capped Length: 3.25"
Load: 17,130 Lbs
Adjusted Load; 17,130 Lbs
Corrected Psi: 7,120 Psi

Comments:
- Core length 7.25 inches with 2 inch wearing surface.
- No bond between SIPMF and deck. White residue present on bottom of concrete.
- Core fractured 2.75 inches from top due to heavy rust.

Core Number: C1

Location:

Station location 107 + 0.9 and 2.7 feet from the face of the curb on the west side of the bridge.

Chloride Ion Test:

At two inches:
% CL^-:	0.0611
# CL^- / yd^3:	2.19

At four inches:
% CL^-:	0.0430
# CL^- / yd^3:	1.54

At six inches:
% CL^-:	0.0173
# CL^- / yd^3:	0.62

At eight inches:
% CL^-:	0.0082
# CL^- / yd^3:	0.29

Comments:
- Core length 7.75 – 10.5 inches with 1.5 inch wearing surface.
- No bond between SIPMF and deck. White residue and heavy rust present on bottom of concrete and SIPMF
- SIPMF badly deteriorated.
- Core fractured 8 inches from top due to heavy rusting of SIPMF.
- Rebar badly rusted.
- Numerous amounts of voids present in concrete up to 1/4 inch in diameter.

Core Number: C2

Location:

Station location 107 + 2.5 and 4.4 feet from the face of the curb on the west side of the bridge.

Permeability Test:

Charge Passed: 1,639 C
Adjusted Charge: 1,479 C
Permeability Class: Low

Comments:
- Core length 7.75 – 9.75 inches with 1.5 inch wearing surface.
- No bond between SIPMF and deck. White residue and heavy rust present on bottom of concrete and SIPMF
- Core fractured 2.75 inches from top due to heavy rusting of rebar.
- Rebar badly rusted.
- Numerous amounts of voids present in concrete up to 1/4 inch in diameter.

Core Number: C3

Location:

Station location 107 + 5.7 and 4.4 feet from the face of the curb on the west side of the bridge.

Ultrasound Test:

$\sum$ V(Δh): 126,359 in ft/s
Maximum Velocity: 14,894 ft/s
Quality Index Avrg.: 13,301 ft/s

Comments:
- Core height 7.5 inches, 9.5 inches with the concrete in the region of the valley of the SIPMF.
- Core is broken into two parts.
- One reinforcement bar located at 3.75 inches from bottom surface.
- Bar is not coated and shows severe rusting.
- Brown and white traces on the SIPMF.

Core Number: C4

Location:

Station location 107 + 9.1 and 4.3 feet from the face of the curb on the west side of the bridge.

Chloride Ion Test:

At two inches:
  % CL$^-$:   0.0877
  # CL$^-$ / yd^3:   3.14

At four inches:
  % CL$^-$:   0.0478
  # CL$^-$ / yd^3:   1.71

At six inches:
  % CL$^-$:   0.0201
  # CL$^-$ / yd^3:   0.72

At eight inches:
  % CL$^-$:   0.0178
  # CL$^-$ / yd^3:   0.64

Comments:
- Core length 7.75 – 9.75 inches with 1.5 inch wearing surface.
- No bond between SIPMF and deck. White residue present on bottom of concrete and SIPMF.
- Core fractured 3 inches from top due to large number of voids. Length of crack 2.5 inches.
- Rebar shows traces of rust
- Numerous amounts of voids present in concrete up to 1/4 inch in diameter.

Core Number: C5

Location:

Station location 107 + 12.2 and 4.2 feet from the face of the curb on the west side of the bridge.

Chloride Ion Test:

At two inches:
    % CL^-:   0.2242
    # CL^- / yd^3:   8.03

At four inches:
    % CL^-:   0.0872
    # CL^- / yd^3:   3.12

At six inches:
    % CL^-:   0.0208
    # CL^- / yd^3:   0.74

At eight inches:
    % CL^-:   0.0151
    # CL^- / yd^3:   0.54

Comments:
- Core length 9 inches with 1.75 inch wearing surface.
- No bond between SIPMF and deck. White residue present on bottom of concrete and SIPMF.
- Core fractured 3 inches from top due to heavy rusting of rebar.
- Rebar severely rusted.
- Numerous amounts of voids present in concrete up to 1/8 inch in diameter.

Core Number: C6

Location:

Station location 107 + 15.9 and 4.3 feet from the face of the curb on the west side of the bridge.

Chloride Ion Test:

At two inches:
 % CL^-:   0.2389
 # CL^- / yd^3: 8.56

At four inches:
 % CL^-:   0.1219
 # CL^- / yd^3: 4.37

At six inches:
 % CL^-:   0.0350
 # CL^- / yd^3: 1.25

At eight inches:
 % CL^-:   0.0165
 # CL^- / yd^3: 0.59

Comments:
- Core length 7- 9 inches with 1.5 inch wearing surface.
- No bond between SIPMF and deck. White residue present on bottom of concrete and SIPMF.
- Rebar traces of rust.
- Numerous amounts of voids present in concrete up to 1/4 inch in diameter.

Core Number: C7

Location:

Station location 107 + 29 and 4.3 feet from the face of the curb on the west side of the bridge.

Ultrasound Test:

$\sum V(\Delta h)$: 91,664 in ft/s
Maximum Velocity: 15,653 ft/s
Quality Index Avrg.: 13,095 ft/s

Comments:
- Core height 7 inches, 8.7 inches with the concrete in the region of the valley of the SIPMF.
- Core is broken into two parts.
- One reinforcement bar located at 5.5 inches from bottom surface.
- Bar is not coated and shows some rust traces.
- White traces on the SIPMF.
- Region of small to moderate voids.

Core Number: C8

Location:

Station location 107 + 32.5 and 4.3 feet from the face of the curb on the west side of the bridge.

Permeability Test:

Charge Passed: 4,487 C
Adjusted Charge: 4,050 C
Permeability Class: High

Comments:
- Core length 7 inches with 2.5 inch wearing surface.
- No bond between SIPMF and deck. White residue present on bottom of concrete and SIPMF.
- Rebar traces of rust.
- Numerous amounts of voids present in concrete up to 1/4 inch in diameter.

Appendix B: OTT-2-28.41 Individual Core Data

**Appendix C
LAK-90-23.42 Individual Core Data**

Core Number: L1

Location:

Station location 837 + 51.01 and 2.4 feet from the face of the parapet on the south side of the bridge.

Compression:

Cut and Capped Length: 4.00"
Load: 92,900 Lbs
Adjusted Load: 81,213 Lbs
Corrected Psi: 6,700 Psi

Comments:
- Core length 12 inches with 1 inch wearing surface and 3 inch overlay.
- No bond between SIPMF and concrete. White residue found on SIPMF and concrete.
- Rebar badly corroded.
- Large voids in overlay up to 1/2 inch in diameter.
- Numerous amounts of voids in concrete up to 1/8 inch in diameter.

Core Number: L2

Location:

Station location 837 + 52.31 and 2.5 feet from the face of the parapet on the south side of the bridge.

Permeability Test:

Charge Passed: 2,726 C
Adjusted Charge: 2,460 C
Permeability Class: Moderate

Comments:
- Core length 12.25 inches with 1 inch wearing surface and 3.25 inch overlay.
- Good bond between SIPMF and concrete.
- Rebar badly corroded.
- Large voids in overlay up to 1/4 inch in diameter. Many concentrated where overlay meets concrete.
- Numerous amounts of voids in concrete up to 1/4 inch in diameter.

Core Number: L3

Location:

Station location 837 + 53.61 and 2.7 feet from the face of the parapet on the south side of the bridge.

Ultrasound Test:

$\sum V(\Delta h)$: 162,606 in ft/s
Maximum Velocity: 16,193 ft/s
Quality Index Avrg.: 14,891 ft/s

Comments:
- Core height 10.25 inches, 12.25 inches with the concrete in the region of the valley of the SIPMF.
- Regions of large size honeycombing.
- One reinforcement bar located at 6 inches from the top surface.
- Some rust traces on the bar.
- Some cracks existed in the surface between the two concrete layers.

Core Number: L4

Location:

Station location 837 + 54.91 and 2.6 feet from the face of the parapet on the south side of the bridge.

Chloride Ion Test:

At two inches:
  % CL⁻:   0.2203
  # CL⁻ / yd³: 7.99

At four inches:
  % CL⁻:   0.2171
  # CL⁻ / yd³: 7.87

At six inches:
  % CL⁻:   0.0227
  # CL⁻ / yd³: 0.82

At eight inches:
  % CL⁻:   0.0067
  # CL⁻ / yd³: 0.24

Comments:
- Core length 10 - 12 inches with 1 inch wearing surface and 3 inch overlay.
- No bond between SIPMF and concrete. White residue present on SIPMF and concrete.
- Rebar shows traces of rust.
- Large void in overlay 3 inches from the top. Length of crack is 1.5 inches and 3/4 of an inch deep.
- Large amounts of voids where overlay meets concrete.
- Numerous amounts of voids in concrete up to 1/8 inch in diameter.
- Numerous amounts of voids in overlay up to 1/4 inch in diameter.

Core Number: L5

Location:

Station location 837 + 67.81 and 3.1 feet from the face of the parapet on the south side of the bridge.

Compression Test:

Cut and Capped Length: 4.00"
Load: 103,600 Lbs
Adjusted Load: 90,567 Lbs
Corrected Psi: 7,470 Psi

Comments:
- Core length 10.5 inches with 1.5 inch wearing surface and 3.5 inch overlay.
- No bond between SIPMF and concrete. White residue present on SIPMF and concrete.
- Rebar shows traces of rust.
- Numerous amounts of voids in concrete up to 1/4 inch in diameter.
- Numerous amounts of voids in overlay up to 3/8 inch in diameter.

Core Number: L6

Location:

Station location 837 + 69.21 and 2.8 feet from the face of the parapet on the south side of the bridge.

Ultrasound Test:

$\sum$ V(Δh): 125,984 in ft/s
Maximum Velocity: 16,982 ft/s
Quality Index Avrg.: 13,998 ft/s

Comments:
- Core height 10.25 inches, 11.75 inches with the concrete in the region of the valley of the SIPMF.
- One reinforcement bar located at 9.5 inches from the top surface.
- Rust traces on the bar.
- Region of small to moderate voids at the top layer of concrete.
- Region of honeycombing at the bottom layer of concrete.

Core Number: L7

Location:

Station location 837 + 70.41 and 2.5 feet from the face of the parapet on the south side of the bridge.

Chloride Ion Test:

At two inches:
  % CL⁻:   0.1936
  # CL⁻ / yd³: 7.02

At four inches:
  % CL⁻:   0.0703
  # CL⁻ / yd³: 2.55

At six inches:
  % CL⁻:   0.0248
  # CL⁻ / yd³: 0.90

At eight inches:
  % CL⁻:   0.0223
  # CL⁻ / yd³: 0.81

Comments:
- Core length 10 - 12 inches with 1 inch wearing surface and 3 inch overlay.
- No bond between SIPMF and concrete. White residue present on SIPMF and concrete.
- Rebar shows traces of rust.
- Numerous amounts of voids in overlay up to 1/4 inch in diameter.
- Concrete in good condition.

Core Number: L8

Location:

Station location 837 + 78.71 and 3.3 feet from the face of the parapet on the south side of the bridge.

Ultrasound Test:

$\sum$ V(Δh): 126,236 in ft/s
Maximum Velocity: 15,463 ft/s
Quality Index Avrg.: 13,887 ft/s

Comments:
- Core height 10.25 inches, 12 inches with the concrete in the region of the valley of the SIPMF.
- One reinforcement bar located at 9.5 inches from the top surface.
- Some rust traces on bars.
- Region of small voids at upper layer of concrete.
- Region of cracks and honeycombing at the surface between the two concrete layers.
- White traces on SIPMF.

Core Number: L9

Location:

Station location 837 + 83.01 and 3.6 feet from the face of the parapet on the south side of the bridge.

Permeability Test:

Charge Passed: 2,315 C
Adjusted Charge: 2,089 C
Permeability Class: Moderate

Comments:
- Core length 10.25 - 12 inches with 1 inch wearing surface and 3.25 inch overlay.
- No bond between SIPMF and concrete. White residue present on SIPMF and concrete.
- Rebar shows traces of rust.
- Numerous amounts of voids in overlay up to 5/8 inch in diameter.
- Numerous amounts of voids in concrete up to 1/8 inch in diameter.

Core Number: L10

Location:

Station location 837 + 84.51 and 2.9 feet from the face of the parapet on the south side of the bridge.

Ultrasound Test:

$\sum$ V(Δh): 125,709 in ft/s
Maximum Velocity: 17,111 ft/s
Quality Index Avrg.: 12,087 ft/s

Comments:
- Core height 10.25 inches, 11.75 inches with the concrete in the region of the valley of the SIPMF.
- One reinforcement bar located at 9.5 inches from the top surface.
- The bar is not coated and shows some rust traces.
- Region of small to moderate voids at upper layer of concrete.
- Core is broken approximately in the middle.

Core Number: L11

Location:

Station location 837 + 85.71 and 2.2 feet from the face of the parapet on the south side of the bridge.

Permeability Test:

Charge Passed: 2,236 C
Adjusted Charge: 2,018 C
Permeability Class: Moderate

Comments:
- Core length 11 inches with 3/4 inch wearing surface and 3 inch overlay.
- No bond between SIPMF and concrete. White residue present on SIPMF and concrete.
- Rebar heavily rusted.
- Core fractured 4.5 inches from the top. Numerous amounts of voids present at fracture.
- Numerous amounts of voids in overlay up to 3/8 inch in diameter.
- Numerous amounts of voids in concrete up to 1/4 inch in diameter.

Core Number: L12

Location:

Station location 837 + 91.81 and 2.3 feet from the face of the parapet on the south side of the bridge.

Ultrasound Test:

$\sum$ V(Δh): 131,012 in ft/s
Maximum Velocity: 18,205 ft/s
Quality Index Avrg.: 14,381 ft/s

Comments:
- Core height 9.5 inches, 11. 5 inches with the concrete in the region of the valley of the SIPMF.
- One reinforcement bar located at 9.0 inches from the top surface.
- Some rust traces on the bar.
- Region of small voids.
- Core is broken at top.
- White traces on SIPMF.

Core Number: L13

Location:

Station location 837 + 99.21 and 5.1 feet from the face of the parapet on the south side of the bridge.

Chloride Ion Test:

At two inches:
    % CL⁻:   0.1649
    # CL⁻ / yd³: 5.98

At four inches:
    % CL⁻:   0.0279
    # CL⁻ / yd³: 1.01

At six inches:
    % CL⁻:   0.0238
    # CL⁻ / yd³: 0.86

At eight inches:
    % CL⁻:   0.0202
    # CL⁻ / yd³: 0.73

Comments:
- Core length 9.75 inches with 1.25 inch wearing surface and 3.5 inch overlay.
- Rebar heavily rusted.
- Numerous amounts of voids in overlay up to 1/4 inch in diameter.
- Numerous amounts of voids in concrete up to 1/8 inch in diameter.

Core Number: L14

Location:

Station location 837 + 99.91 and 3.3 feet from the face of the parapet on the south side of the bridge.

Permeability Test:

Charge Passed: 1,667 C
Adjusted Charge: 1,504 C
Permeability Class: Low

Comments:
- Core length 10 inches with 1.25 inch wearing surface and 3.5 inch overlay.
- Rebar shows traces of rust.
- Numerous amounts of voids in overlay up to 1/4 inch in diameter.
- Numerous amounts of voids in concrete up to 1/8 inch in diameter.

Core Number: L15

Location:

Station location 838 + 01.61 and 2.8 feet from the face of the parapet on the south side of the bridge.

Chloride Ion Test:

At two inches:
 % CL⁻: 0.2049
 # CL⁻ / yd³: 7.43

At four inches:
 % CL⁻: 0.1254
 # CL⁻ / yd³: 4.55

At six inches:
 % CL⁻: 0.0229
 # CL⁻ / yd³: 0.83

At eight inches:
 % CL⁻: 0.0079
 # CL⁻ / yd³: 0.29

Comments:
- Core length 9 inches with 1.5 inch wearing surface and 3.5 inch overlay.
- Rebar shows traces of rust.
- Core fractured 5.5 inches below top due to severe rusting of rebar.
- Numerous amounts of voids in overlay up to 1/4 inch in diameter.
- Numerous amounts of voids in concrete up to 1/8 inch in diameter.

Chloride Ion Test:

At two inches:
 % CL^-: 0.2049
 # CL^- / yd^3: 7.43

At four inches:
 % CL^-: 0.1254
 # CL^- / yd^3: 4.55

At six inches:
 % CL^-: 0.0229
 # CL^- / yd^3: 0.83

At eight inches:
 % CL^-: 0.0079
 # CL^- / yd^3: 0.29

Core Number: L16
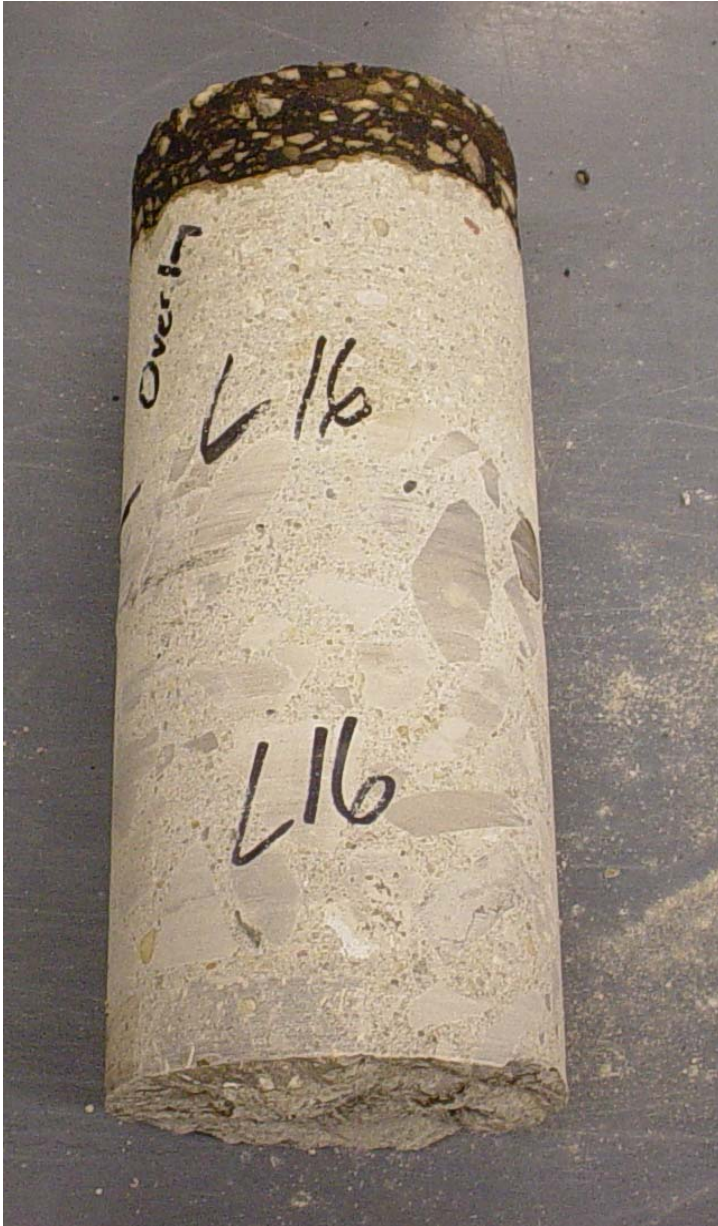
Location:

Station location 838 + 06.11 and 3.5 feet from the face of the parapet on the south side of the bridge.

Permeability Test:

Charge Passed: 2,849 C
Adjusted Charge: 2,571 C
Permeability Class: Moderate

Comments:

- Core length 10 inches with 1.25 inch wearing surface and 3.25 inch overlay.
- Rebar shows traces of rust.
- Numerous amounts of voids in overlay up to 1/4 inch in diameter.
- Numerous amounts of voids in concrete up to 1/8 inch in diameter.

Core Number: L17

Location:

Station location 838 + 05.81 and 4.7 feet from the face of the parapet on the south side of the bridge.

Compression Test:

Cut and Capped Length: 3.69"
Load: 17,140 Lbs
Adjusted Load: 17,140 Lbs
Corrected Psi: 7,130 Psi

Comments:
- Core length 7.25 inches with 3 inch overlay.
- Numerous amounts of voids in overlay up to 1/8 inch in diameter.
- Numerous amounts of voids in concrete up to 1/8 inch in diameter.

Core Number: L18

Location:

Station location 838 + 05.71 and 5.2 feet from the face of the parapet on the south side of the bridge.

Compression Test:

Cut and Capped Length: 3.63"
Load: 15,960 Lbs
Adjusted Load: 15,328 Lbs
Corrected Psi: 6,370 Psi

Comments:
- Core length 8.5 inches with 3/4 inch wearing surface and 3 inch overlay.
- Core fractured during excavation.
- Numerous amounts of voids in overlay up to 1/8 inch in diameter.
- Numerous amounts of voids in concrete up to 1/8 inch in diameter.

Core Number: L19
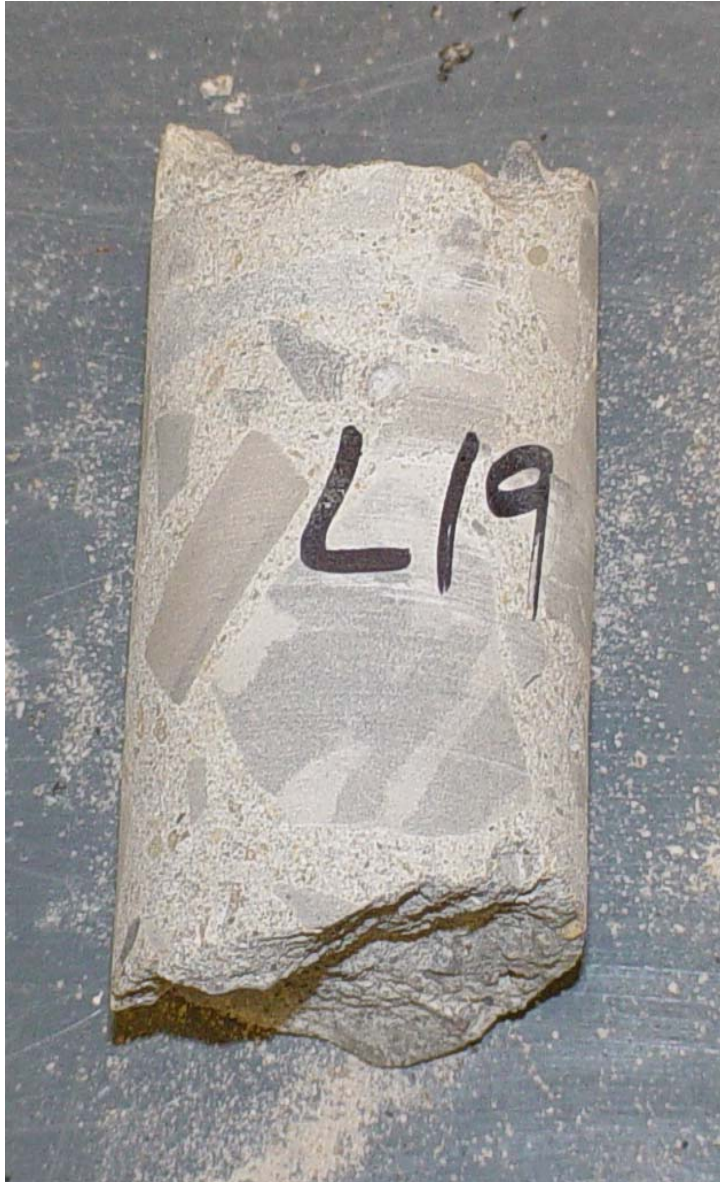
Location:

Station location 838 + 38.51 and 4.6 feet from the face of the parapet on the south side of the bridge.

Compression Test:

Cut and Capped Length: 2.38"
Load: 15,950 Lbs
Adjusted Load: 15,033 Lbs
Corrected Psi: 6,250 Psi

Comments:
- Core badly broken up during coring.

Core Number: L20

Location:

Station location 838 + 38.81 and 4.8 feet from the face of the parapet on the south side of the bridge.

Compression Test:

Cut and Capped Length: 2.50"
Load: 17,240 Lbs
Adjusted Load: 16,399 Lbs
Corrected Psi: 6,820 Psi

Comments:
- Core length 7 inches with 3.5 inch overlay.
- Large void in overlay 1.25 inches from top. Void is 3/4 inch in diameter.
- Numerous amounts of voids in overlay up to 1/8 inch in diameter.
- Numerous amounts of voids in concrete up to 1/4 inch in diameter.

Core Number: L21

Location:

Station location 838 + 38.41 and 6.1 feet from the face of the parapet on the south side of the bridge.

Chloride Ion Test:

At two inches:
% CL$^-$:	0.2450
# CL$^-$ / yd^3:	8.88

At four inches:
% CL$^-$:	0.0924
# CL$^-$ / yd^3:	3.35

At six inches:
% CL$^-$:	0.0436
# CL$^-$ / yd^3:	1.58

At eight inches:
% CL$^-$:	0.0225
# CL$^-$ / yd^3:	0.82

Comments:
- Core length 9 inches with 1.5 inch wearing surface and 3 inch overlay.
- Rebar severely rusted.
- Numerous amounts of voids in overlay up to 1/4 inch in diameter.
- Numerous amounts of voids in concrete up to 1/4 inch in diameter.

Core Number: L22

Location:

Station location 838 + 38.41 and 4.5 feet from the face of the parapet on the south side of the bridge.

Chloride Ion Test:

At two inches:
% CL$^-$:	0.2399
# CL$^-$ / yd^3:	8.70

At four inches:
% CL$^-$:	0.0504
# CL$^-$ / yd^3:	1.83

At six inches:
% CL$^-$:	0.0249
# CL$^-$ / yd^3:	0.90

At eight inches:
% CL$^-$:	0.0177
# CL$^-$ / yd^3:	0.64

Comments:
- Core length 10 inches with 1.5 inch wearing surface and 3 inch overlay.
- Numerous amounts of voids in overlay up to 3/8 inch in diameter.
- Numerous amounts of voids in concrete up to 1/8 inch in diameter.

Core Number: L23

Location:

Station location 838 + 40.01 and 4.7 feet from the face of the parapet on the south side of the bridge.

Ultrasound Test:

$\sum V(\Delta h)$: 120,817 in ft/s
Maximum Velocity: 15,559 ft/s
Quality Index Avrg.: 12,046 ft/s

Comments:
- Core height 9.5 inches, 10.03 inches without the wearing surface depth and with the 2 inch imaginary slice.
- One reinforcement bar located at 5 inches from the top surface.
- Bar is not coated and shows rust traces.
- 1.5 inch asphalt wearing surface existed at the top of the core.
- Two different concrete layers.
- The aggregate in the top concrete layer is fine, while it is coarse in the bottom layer.
- Region of moderate voids located at the upper concrete layer.

Core Number: L24
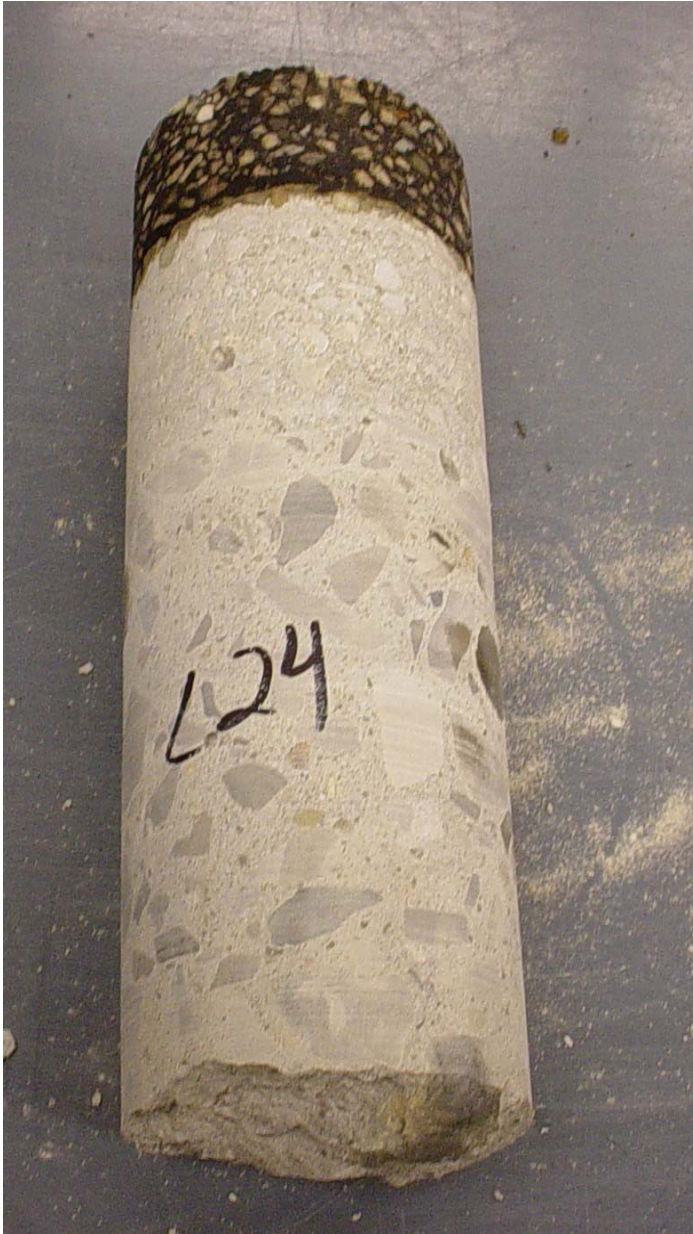
Location:

Station location 838 + 41.31 and 4.9 feet from the face of the parapet on the south side of the bridge.

Ultrasound Test:

$\sum$ V(Δh): 120,932 in ft/s
Maximum Velocity: 14,918 ft/s
Quality Index Avrg.: 12,133 ft/s

Comments:
- Core height 9.5 inches, 9.97 inches without the wearing surface depth and with the 2 inch imaginary slice.
- 1.5 inch asphalt wearing surface existed at the top of the core.
- Two reinforcement bars located at 5 inches and 6 inches from the top surface.
- Region of moderate voids at upper concrete layer.
- Brown rust traces on bars.

Core Number: L25
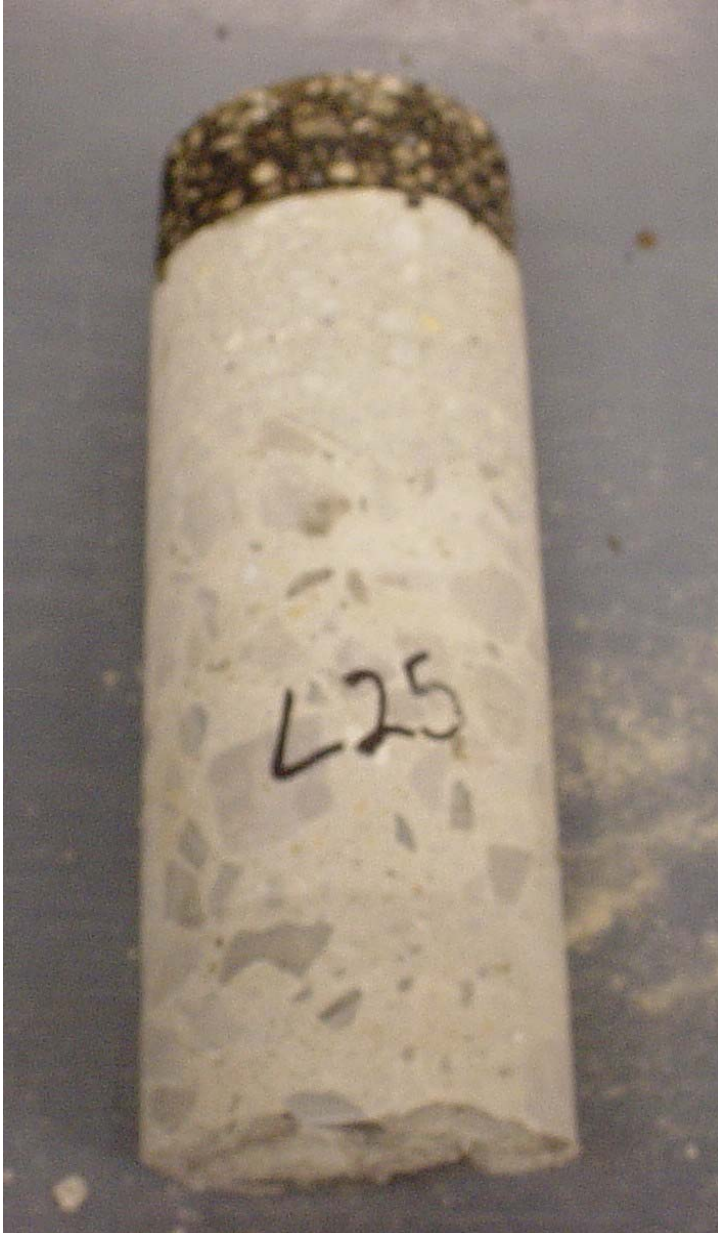
Location:

Station location 838 + 42.41 and 3.3 feet from the face of the parapet on the south side of the bridge.

Compression Test:

Cut and Capped Length: 4.81"
Load: 102,500 Lbs
Adjusted Load: 94,587 Lbs
Corrected Psi: 7800 Psi

Comments:
- Core length 10 inches with 1.5 inch wearing surface and 3.25 inch overlay.
- Numerous amounts of voids in overlay up to 1/4 inch in diameter.
- Concrete in good condition.

Core Number: L26

Location:

Station location 838 + 45.41 and 2.9 feet from the face of the parapet on the south side of the bridge.

Ultrasound Test:

$\sum$ V(Δh): 107,706 in ft/s
Maximum Velocity: 17,301 ft/s
Quality Index Avrg.: 12,007 ft/s

Comments:
- Core height 8.75 inches, 8.97 inches without the wearing surface depth and with the 2 inch imaginary slice.
- 1.5 inch asphalt wearing surface existed at the top of the core.
- Two reinforcement bars located at 5 inches and 6 inches from top surface.
- Some rust traces existed on bars.
- Region of large size honeycombing at top layer of concrete.

Core Number: L27

Location:

Station location 838 + 46.21 and 3.5 feet from the face of the parapet on the south side of the bridge.

Permeability Test:

Charge Passed: 4,407 C
Adjusted Charge: 3,977 C
Permeability Class: Moderate

Comments:
- Core length 10 inches with 1.5 inch wearing surface and 3.25 inch overlay.
- Numerous amounts of voids in overlay up to 3/8 inch in diameter.
- Numerous amounts of voids in concrete up to 3/16 inch in diameter.
- Core fractured 5.5 inches from the top due to heavy rusting of rebar and numerous voids.

Core Number: L28

Location:

Station location 838 + 48.81 and 2.7 feet from the face of the parapet on the south side of the bridge.

Ultrasound Test:

$\sum$ V(Δh): 147,270 in ft/s
Maximum Velocity: 15,332 ft/s
Quality Index Avrg.: 14,410 ft/s

Comments:
- Core height 10 inches, 10.22 inches without the wearing surface depth and with the 2 inch imaginary slice.
- 1.5 inch asphalt wearing surface existed at the top of the core.
- One reinforcement bar located at 5 inches from top surface.
- Bar is not coated and shows some rust traces.
- Region of small to moderate voids at top concrete surface.

Core Number: L29
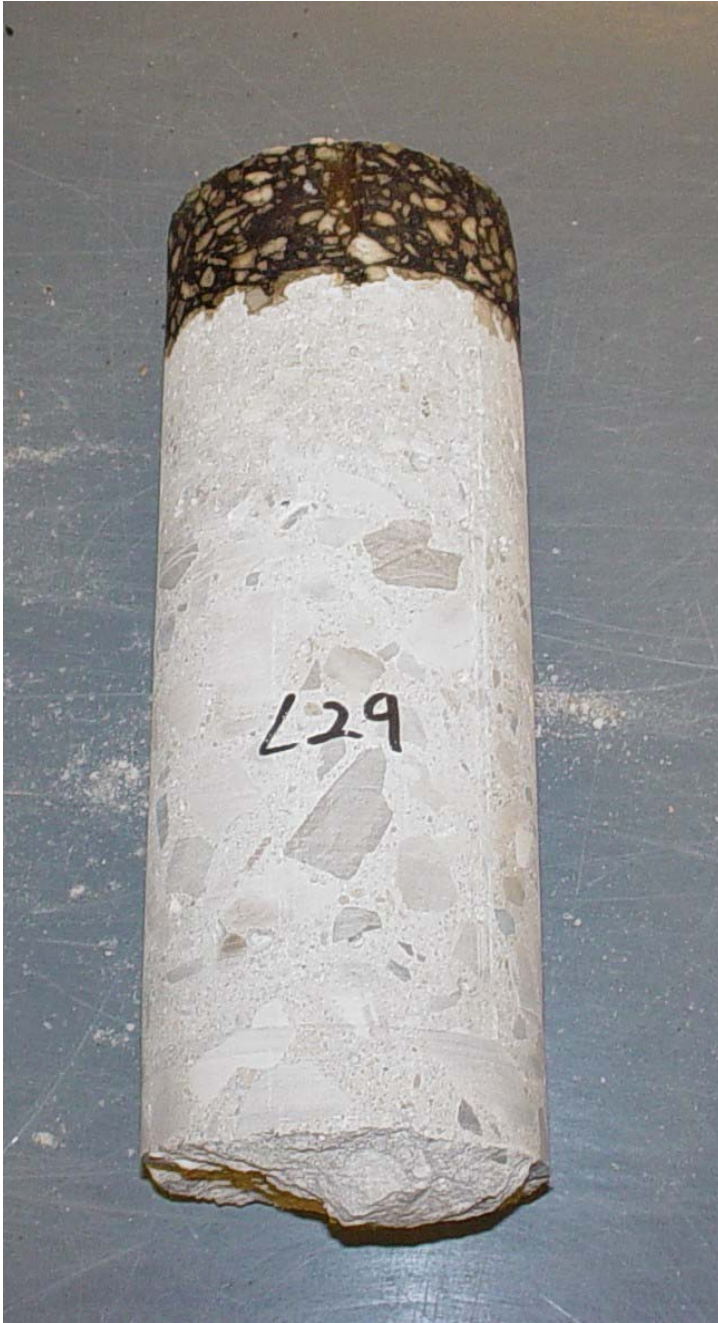
Location:

Station location 838 + 49.61 and 3.7 feet from the face of the parapet on the south side of the bridge.

Compression Test:

Cut and Capped Length: 5.31"
Load: 103,800 Lbs
Adjusted Load: 97,800 Lbs
Corrected Psi: 8,060 Psi

Comments:
- Core length 10.25 inches with 1.5 inch wearing surface and 3 inch overlay.
- Numerous amounts of voids in overlay up to 3/8 inch in diameter.
- Numerous amounts of voids in concrete up to 1/8 inch in diameter.

Core Number: L30

Location:

Station location 838 + 53.21 and 4.1 feet from the face of the parapet on the south side of the bridge.

Permeability Test:

Charge Passed: 2,887 C
Adjusted Charge: 2,606 C
Permeability Class: Moderate

Comments:
- Core length 10 inches with 1.5 inch wearing surface and 3 inch overlay.
- Rebar heavily rusted.
- Core fractured 4.5 inches from the top where the overlay meets the concrete. Fracture due to heavy rusting of rebar.
- Numerous amounts of voids in overlay up to 1/4 inch in diameter.
- Numerous amounts of voids in concrete up to 1/8 inch in diameter.

Core Number: L31

Location:

Station location 838 + 53.91 and 4.2 feet from the face of the parapet on the south side of the bridge.

Ultrasound Test:

$\sum$ V(Δh): 103,411 in ft/s
Maximum Velocity: 16,861 ft/s
Quality Index Avrg.: 11,302 ft/s

Comments:
- Core height 8.75 inches, 9.15 inches without the wearing surface depth and with the 2 inch imaginary slice.
- Region of small to moderate voids at top concrete surface.
- One reinforcement bar located at 5 inches from the top surface.
- Some rust at edges of reinforcement bars.
- Region of honeycombing.
- Region of small to moderate voids at upper concrete layer.

Core Number: L32

Location:

Station location 838 + 59.01 and 5.2 feet from the face of the parapet on the south side of the bridge.

Compression Test:

Cut and Capped Length: 4.50"
Load: 91,200 Lbs
Adjusted Load: 82481 Lbs
Corrected Psi: 6,800 Psi

Comments:
- Core length 10.5 inches with 1.5 inch wearing surface and 3.5 inch overlay.
- Numerous amounts of voids in overlay up to 1/2 inch in diameter.
- Numerous amounts of voids in concrete up to 1/4 inch in diameter.

Core Number: L33

Location:

Station location 838 + 59.91 and 3.9 feet from the face of the parapet on the south side of the bridge.

Permeability Test:

Charge Passed: 4,767 C
Adjusted Charge: 4,302 C
Permeability Class: High

Comments:
- Core length 9.75 inches with 1.75 inch wearing surface and 3.5 inch overlay.
- Rebar shows traces of rust.
- Numerous amounts of voids in overlay up to 5/8 inch in diameter.
- Numerous amounts of voids in concrete up to 1/4 inch in diameter.

Core Number: L34

Location:

Station location 838 + 65.91 and 5.8 feet from the face of the parapet on the south side of the bridge.

Chloride Ion Test:

At two inches:
% CL⁻:	0.2501
# CL⁻ / yd³:	9.07

At four inches:
% CL⁻:	0.0493
# CL⁻ / yd³:	1.79

At six inches:
% CL⁻:	0.0274
# CL⁻ / yd³:	0.99

At eight inches:
% CL⁻:	0.0210
# CL⁻ / yd³:	0.76

Comments:
- Core length 8 inches with 1.5 inch wearing surface and 3 inch overlay.
- Rebar severely rusted.
- Core fractured 5 inches from the top due to heavy rusting of rebar.
- Numerous amounts of voids in overlay up to 1/8 inch in diameter.

Core Number: L35

Location:

Station location 838 + 66.51 and 4.1 feet from the face of the parapet on the south side of the bridge.

Permeability Test:

Charge Passed: 6,865 C
Adjusted Charge: 6,169 C
Permeability Class: High

Comments:
- Core length 8.75 inches with 1.5 inch wearing surface and 3 inch overlay.
- Rebar severely rusted.
- Core fractured 5.25 inches from the top due to heavy rusting of rebar.
- Numerous amounts of voids in overlay up to 1/4 inch in diameter.
- Numerous amounts of voids in concrete up to 1/8 inch in diameter.

Core Number: L36

Location:

Station location 838 + 70.61 and 6.1 feet from the face of the parapet on the south side of the bridge.

Chloride Ion Test:

At two inches:
  % CL$^-$: 0.3518
  # CL$^-$ / yd^3: 12.75

At four inches:
  % CL$^-$: 0.3039
  # CL$^-$ / yd^3: 11.02

At six inches:
  % CL$^-$: 0.2118
  # CL$^-$ / yd^3: 7.68

At eight inches:
  % CL$^-$: 0.0827
  # CL$^-$ / yd^3: 3.00

Comments:
- Core length 9 inches with 1.5 inch wearing surface and 3 inch overlay.
- Rebar severely rusted.
- Core fractured 5 inches from the top due to heavy rusting of rebar.
- Large void where overlay meets concrete. Void is 1/2 inch in diameter and 3/4 inch deep.
- Numerous amounts of voids in overlay up to 1/4 inch in diameter.
- Numerous amounts of voids in concrete up to 1/8 inch in diameter.

Appendix D
Permeability Test Results
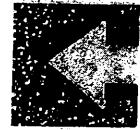
PROOVE it

ASTM C 1202-97

GERMANN INSTRUMENTS

DENMARK
Phone: +45 3967 7117
Fax: +45 3967 3167

USA
Phone: (847)329-9999
Fax: (847)329-9888

Test report

Voltage Used:	60	
Testing time:	06:00 hour	
Charge passed:	1757	
Adjusted Charge passed:	1586	
Permeability class:	Low	
Instrument number:	994704	
Channel number:	4	
Report date:	7/1/2004	
Testing by:	Chris Tuminello	
Reference:	LOR-57-18.18	
Sample diameter:	100	
Comment:	S1 - No SIPMF	
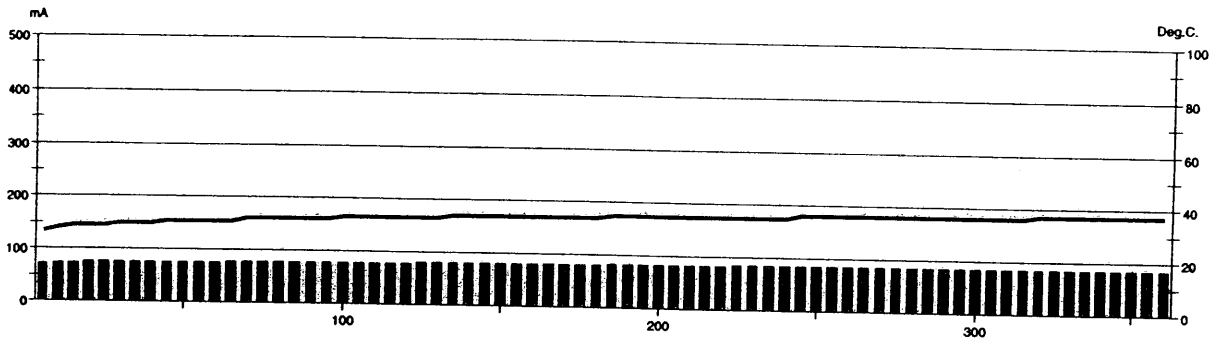
Time	°C	mA	Time	°C	mA	Time	°C	mA	Time	°C	mA
00:05	27	71.2	01:35	32	78.3	03:05	35	81.6	04:35	36	85.7
00:10	28	73.2	01:40	33	78.5	03:10	35	81.7	04:40	36	85.8
00:15	29	74.2	01:45	33	78.7	03:15	35	82.0	04:45	36	85.7
00:20	29	74.9	01:50	33	78.8	03:20	35	82.3	04:50	36	85.7
00:25	29	75.5	01:55	33	79.0	03:25	35	82.6	04:55	36	85.7
00:30	30	75.8	02:00	33	79.2	03:30	35	83.0	05:00	36	85.6
00:35	30	76.1	02:05	33	79.4	03:35	35	83.4	05:05	36	85.5
00:40	30	76.3	02:10	33	79.6	03:40	35	83.6	05:10	36	85.4
00:45	31	76.5	02:15	34	79.7	03:45	35	83.9	05:15	36	85.4
00:50	31	76.6	02:20	34	79.9	03:50	35	84.1	05:20	37	85.8
00:55	31	76.8	02:25	34	80.0	03:55	35	84.4	05:25	37	85.8
01:00	31	76.9	02:30	34	79.9	04:00	35	84.6	05:30	37	85.7
01:05	31	77.1	02:35	34	80.1	04:05	36	84.7	05:35	37	85.5
01:10	32	77.4	02:40	34	80.6	04:10	36	85.0	05:40	37	85.4
01:15	32	77.5	02:45	34	80.7	04:15	36	85.3	05:45	37	85.6
01:20	32	77.8	02:50	34	80.8	04:20	36	85.4	05:50	37	85.8
01:25	32	78.0	02:55	34	81.0	04:25	36	85.5	05:55	37	85.8
01:30	32	78.2	03:00	34	81.2	04:30	36	85.6	06:00	37	85.9
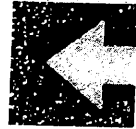
Test report

Voltage Used:	60
Testing time:	06:00 hour
Charge passed:	1533
Adjusted Charge passed:	1384
Permeability class:	Low
Instrument number:	994704
Channel number:	4
Report date:	7/2/2004
Testing by:	Chris Tuminello
Reference:	LOR-57-18.18
Sample diameter:	100
Comment:	1D - No SIPMF
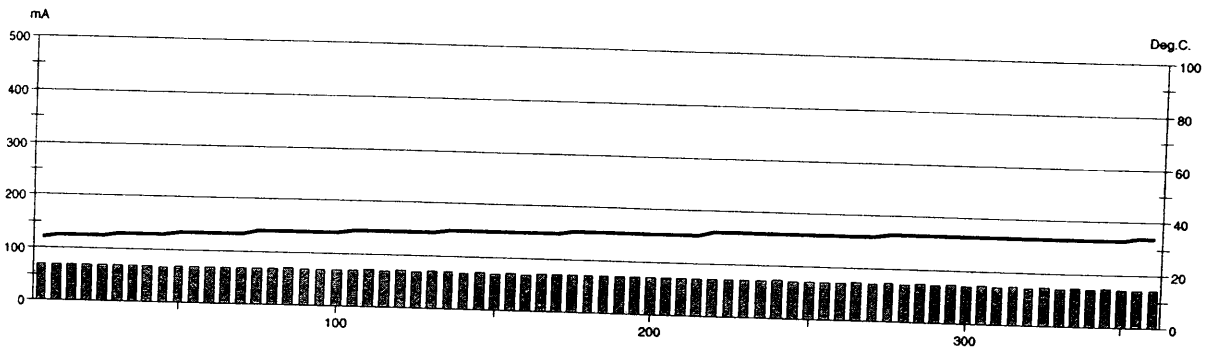
Time	°C	mA	Time	°C	mA	Time	°C	mA	Time	°C	mA
00:05	24	69.3	01:35	28	70.3	03:05	31	71.4	04:35	33	72.8
00:10	25	69.2	01:40	28	69.7	03:10	31	72.0	04:40	33	71.5
00:15	25	69.2	01:45	29	70.1	03:15	31	71.4	04:45	33	73.1
00:20	25	69.3	01:50	29	70.6	03:20	31	71.6	04:50	33	71.3
00:25	25	69.4	01:55	29	69.3	03:25	31	71.8	04:55	33	73.0
00:30	26	69.5	02:00	29	71.3	03:30	31	72.3	05:00	33	71.5
00:35	26	69.6	02:05	29	69.4	03:35	31	72.4	05:05	33	73.2
00:40	26	68.7	02:10	29	72.2	03:40	32	71.1	05:10	33	71.8
00:45	26	67.8	02:15	30	70.8	03:45	32	71.9	05:15	33	73.0
00:50	27	69.4	02:20	30	70.2	03:50	32	72.5	05:20	33	71.6
00:55	27	68.1	02:25	30	71.5	03:55	32	70.9	05:25	33	73.7
01:00	27	69.4	02:30	30	69.9	04:00	32	72.6	05:30	33	71.9
01:05	27	69.1	02:35	30	71.9	04:05	32	71.4	05:35	33	72.6
01:10	27	68.2	02:40	30	70.3	04:10	32	71.0	05:40	33	71.1
01:15	28	70.2	02:45	30	72.3	04:15	32	72.5	05:45	33	72.8
01:20	28	68.5	02:50	30	70.7	04:20	32	71.5	05:50	33	71.0
01:25	28	70.5	02:55	31	72.5	04:25	32	72.7	05:55	34	72.2
01:30	28	69.3	03:00	31	71.5	04:30	32	71.3	06:00	34	70.8

PROOVE it

ASTM C 1202-97

GERMANN INSTRUMENTS

DENMARK
Phone: +45 3967 7117
Fax: +45 3967 3167

USA
Phone: (847)329-9999
Fax: (847)329-9888

Test report

Voltage Used:	60
Testing time:	06:00 hour
Charge passed:	1200
Adjusted Charge passed:	1083
Permeability class:	Low
Instrument number:	994704
Channel number:	6
Report date:	7/16/2004
Testing by:	Chris Tuminello
Reference:	LOR-57-18.18
Sample diameter:	100
Comment:	2C - SIPMF

Time	°C	mA	Time	°C	mA	Time	°C	mA	Time	°C	mA
00:05	25	55.5	01:35	29	56.1	03:05	30	55.4	04:35	31	55.7
00:10	26	55.7	01:40	29	56.4	03:10	30	55.6	04:40	31	55.4
00:15	26	56.0	01:45	29	55.9	03:15	30	55.7	04:45	31	55.5
00:20	26	55.7	01:50	29	55.9	03:20	30	55.5	04:50	31	55.1
00:25	27	55.1	01:55	29	56.0	03:25	31	56.0	04:55	31	55.2
00:30	27	54.8	02:00	29	56.2	03:30	31	55.5	05:00	31	55.1
00:35	27	54.6	02:05	29	55.8	03:35	31	55.4	05:05	31	54.9
00:40	27	55.4	02:10	30	55.9	03:40	31	55.2	05:10	31	55.3
00:45	28	55.0	02:15	30	55.9	03:45	31	56.1	05:15	31	55.0
00:50	28	55.4	02:20	30	55.9	03:50	31	55.7	05:20	31	55.0
00:55	28	55.7	02:25	30	55.9	03:55	31	55.3	05:25	31	55.0
01:00	28	55.5	02:30	30	56.0	04:00	31	55.4	05:30	31	55.9
01:05	28	55.4	02:35	30	55.8	04:05	31	55.1	05:35	31	55.4
01:10	28	55.3	02:40	30	55.9	04:10	31	55.1	05:40	31	55.5
01:15	28	55.6	02:45	30	55.9	04:15	31	55.7	05:45	31	55.0
01:20	29	56.0	02:50	30	55.5	04:20	31	55.5	05:50	31	54.8
01:25	29	55.6	02:55	30	55.5	04:25	31	55.6	05:55	31	54.9
01:30	29	56.0	03:00	30	55.5	04:30	31	56.5	06:00	31	55.5

D3

PROOVE it

ASTM C 1202-97

Test report

Voltage Used:	60
Testing time:	06:00 hour
Charge passed:	1200
Adjusted Charge passed:	1083
Permeability class:	Low
Instrument number:	994704
Channel number:	6
Report date:	7/16/2004
Testing by:	Chris Tuminello
Reference:	LOR-57-18.18
Sample diameter:	100
Comment:	2C - SIPMF

Time	°C	mA	Time	°C	mA	Time	°C	mA	Time	°C	mA
00:05	25	55.5	01:35	29	56.1	03:05	30	55.4	04:35	31	55.7
00:10	26	55.7	01:40	29	56.4	03:10	30	55.6	04:40	31	55.4
00:15	26	56.0	01:45	29	55.9	03:15	30	55.7	04:45	31	55.5
00:20	26	55.7	01:50	29	55.9	03:20	30	55.5	04:50	31	55.1
00:25	27	55.1	01:55	29	56.0	03:25	31	56.0	04:55	31	55.2
00:30	27	54.8	02:00	29	56.2	03:30	31	55.5	05:00	31	55.1
00:35	27	54.6	02:05	29	55.8	03:35	31	55.4	05:05	31	54.9
00:40	27	55.4	02:10	30	55.9	03:40	31	55.2	05:10	31	55.3
00:45	28	55.0	02:15	30	55.9	03:45	31	56.1	05:15	31	55.0
00:50	28	55.4	02:20	30	55.9	03:50	31	55.7	05:20	31	55.0
00:55	28	55.7	02:25	30	55.9	03:55	31	55.3	05:25	31	55.0
01:00	28	55.5	02:30	30	56.0	04:00	31	55.4	05:30	31	55.9
01:05	28	55.4	02:35	30	55.8	04:05	31	55.1	05:35	31	55.4
01:10	28	55.3	02:40	30	55.9	04:10	31	55.1	05:40	31	55.5
01:15	28	55.6	02:45	30	55.9	04:15	31	55.7	05:45	31	55.0
01:20	29	56.0	02:50	30	55.5	04:20	31	55.5	05:50	31	54.8
01:25	29	55.6	02:55	30	55.5	04:25	31	55.6	05:55	31	54.9
01:30	29	56.0	03:00	30	55.5	04:30	31	56.5	06:00	31	55.5

D4

PROOVE it

Test report

Voltage Used:	60
Testing time:	06:00 hour
Charge passed:	1083
Adjusted Charge passed:	977
Permeability class:	Very Low
Instrument number:	994704
Channel number:	5
Report date:	7/15/2004
Testing by:	Chris Tuminello
Reference:	LOR-57-18.18
Sample diameter:	100
Comment:	2D1 - SIPMF
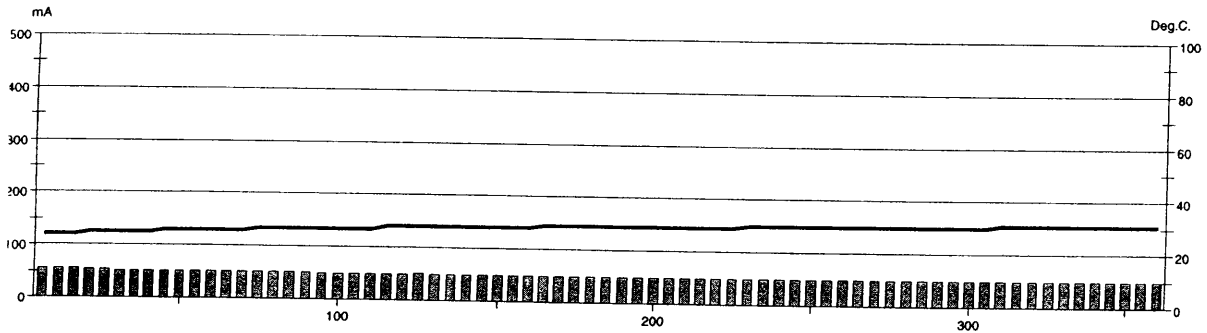
Time	°C	mA	Time	°C	mA	Time	°C	mA	Time	°C	mA
00:05	24	56.2	01:35	27	50.1	03:05	29	49.7	04:35	30	49.3
00:10	24	55.4	01:40	27	49.9	03:10	29	49.7	04:40	30	49.3
00:15	24	54.8	01:45	27	49.8	03:15	29	49.6	04:45	30	49.1
00:20	25	54.0	01:50	27	49.8	03:20	29	49.4	04:50	30	49.3
00:25	25	52.9	01:55	28	49.5	03:25	29	49.4	04:55	30	49.2
00:30	25	52.2	02:00	28	49.9	03:30	29	49.5	05:00	30	49.1
00:35	25	51.7	02:05	28	50.4	03:35	29	49.6	05:05	30	49.1
00:40	25	51.5	02:10	28	50.1	03:40	29	49.8	05:10	31	48.9
00:45	26	51.2	02:15	28	49.7	03:45	29	49.7	05:15	31	48.9
00:50	26	51.0	02:20	28	49.6	03:50	30	49.7	05:20	31	49.3
00:55	26	50.9	02:25	28	50.1	03:55	30	49.7	05:25	31	49.4
01:00	26	50.8	02:30	28	49.8	04:00	30	49.8	05:30	31	49.2
01:05	26	51.4	02:35	28	49.6	04:05	30	49.8	05:35	31	49.2
01:10	26	50.9	02:40	28	49.7	04:10	30	49.5	05:40	31	48.9
01:15	27	50.5	02:45	29	49.6	04:15	30	49.2	05:45	31	49.1
01:20	27	50.4	02:50	29	49.5	04:20	30	49.1	05:50	31	49.0
01:25	27	50.4	02:55	29	49.6	04:25	30	49.4	05:55	31	48.9
01:30	27	50.7	03:00	29	49.6	04:30	30	49.3	06:00	31	49.3
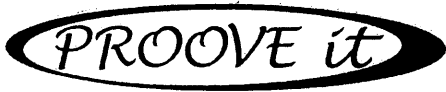
D5

PROOVE it

ASTM C 1202-97

Test report

Voltage Used:	60
Testing time:	06:00 hour
Charge passed:	1938
Adjusted Charge passed:	1749
Permeability class:	Low
Instrument number:	994704
Channel number:	7
Report date:	6/29/2004
Testing by:	Chris Tuminello
Reference:	LOR-57-18.18
Sample diameter:	100
Comment:	2D2 - SIPMF
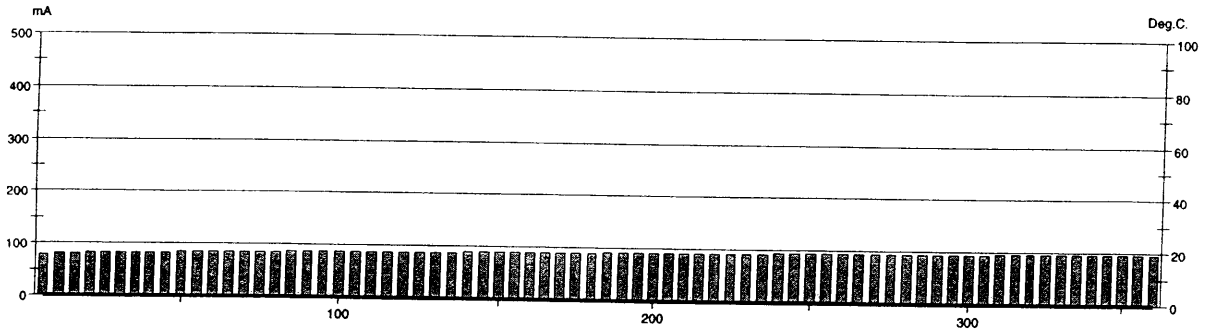
Time	°C	mA	Time	°C	mA	Time	°C	mA	Time	°C	mA
00:05	0	78.9	01:35	0	86.4	03:05	0	90.6	04:35	0	93.7
00:10	0	80.2	01:40	0	86.4	03:10	0	90.7	04:40	0	93.9
00:15	0	80.9	01:45	0	86.5	03:15	0	90.9	04:45	0	94.0
00:20	0	81.5	01:50	0	86.7	03:20	0	91.2	04:50	0	94.1
00:25	0	82.0	01:55	0	86.9	03:25	0	91.5	04:55	0	94.4
00:30	0	82.4	02:00	0	87.2	03:30	0	91.7	05:00	0	94.6
00:35	0	82.9	02:05	0	87.5	03:35	0	91.8	05:05	0	94.8
00:40	0	83.3	02:10	0	87.7	03:40	0	92.0	05:10	0	94.9
00:45	0	83.6	02:15	0	88.0	03:45	0	92.2	05:15	0	95.1
00:50	0	83.9	02:20	0	88.3	03:50	0	92.4	05:20	0	95.2
00:55	0	84.3	02:25	0	88.6	03:55	0	92.5	05:25	0	95.3
01:00	0	84.7	02:30	0	88.9	04:00	0	92.7	05:30	0	95.4
01:05	0	85.0	02:35	0	89.2	04:05	0	92.8	05:35	0	95.5
01:10	0	85.2	02:40	0	89.4	04:10	0	93.0	05:40	0	95.6
01:15	0	85.5	02:45	0	89.7	04:15	0	93.2	05:45	0	95.7
01:20	0	85.8	02:50	0	89.9	04:20	0	93.3	05:50	0	95.8
01:25	0	86.0	02:55	0	90.1	04:25	0	93.5	05:55	0	95.8
01:30	0	86.3	03:00	0	90.3	04:30	0	93.6	06:00	0	95.8

D6

PROOVE it

ASTM C 1202-97

Test report

Voltage Used:	60
Testing time:	06:00 hour
Charge passed:	1336
Adjusted Charge passed:	1206
Permeability class:	Low
Instrument number:	994704
Channel number:	5
Report date:	6/29/2004
Testing by:	Chris Tuminello
Reference:	LOR-57-18.18
Sample diameter:	100
Comment:	2E - SIPMF
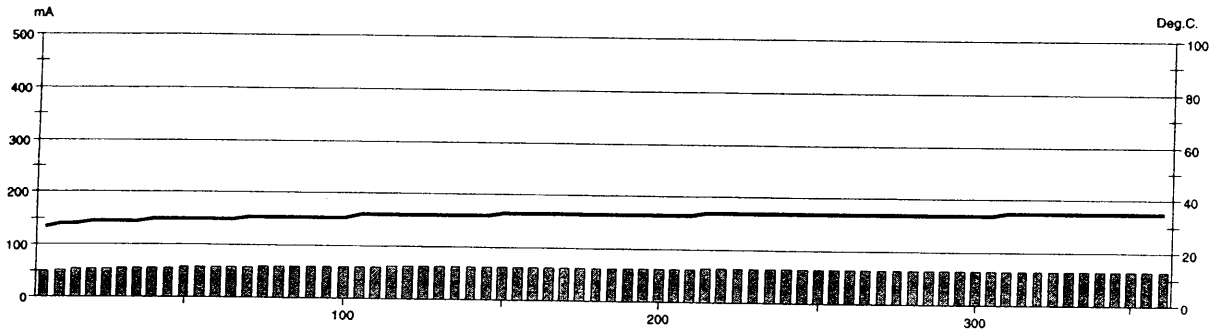
Time	°C	mA	Time	°C	mA	Time	°C	mA	Time	°C	mA
00:05	27	49.9	01:35	31	60.4	03:05	33	63.2	04:35	34	64.6
00:10	28	51.6	01:40	31	60.7	03:10	33	63.3	04:40	34	64.6
00:15	28	52.8	01:45	32	61.0	03:15	33	63.4	04:45	34	64.7
00:20	29	53.7	01:50	32	61.2	03:20	33	63.5	04:50	34	64.8
00:25	29	54.5	01:55	32	61.5	03:25	33	63.6	04:55	34	64.9
00:30	29	55.1	02:00	32	61.8	03:30	33	63.6	05:00	34	64.9
00:35	29	55.7	02:05	32	62.1	03:35	34	63.7	05:05	34	64.9
00:40	30	56.2	02:10	32	62.3	03:40	34	63.7	05:10	35	65.0
00:45	30	56.7	02:15	32	62.3	03:45	34	63.8	05:15	35	65.0
00:50	30	57.2	02:20	32	62.2	03:50	34	63.8	05:20	35	65.0
00:55	30	57.7	02:25	32	62.4	03:55	34	64.0	05:25	35	65.1
01:00	30	58.1	02:30	33	62.5	04:00	34	64.1	05:30	35	65.1
01:05	30	58.5	02:35	33	62.6	04:05	34	64.1	05:35	35	65.1
01:10	31	58.9	02:40	33	62.6	04:10	34	64.2	05:40	35	65.2
01:15	31	59.3	02:45	33	62.8	04:15	34	64.3	05:45	35	65.2
01:20	31	59.7	02:50	33	62.9	04:20	34	64.4	05:50	35	65.2
01:25	31	60.0	02:55	33	62.9	04:25	34	64.5	05:55	35	65.1
01:30	31	60.2	03:00	33	63.0	04:30	34	64.6	06:00	35	65.2
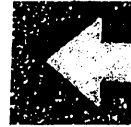
D7

PROOVE it

ASTM C 1202-97

Test report

Voltage Used:	60
Testing time:	06:00 hour
Charge passed:	1245
Adjusted Charge passed:	1124
Permeability class:	Low
Instrument number:	994704
Channel number:	3
Report date:	6/29/2004
Testing by:	Chris Tuminello
Reference:	LOR-57-18.18
Sample diameter:	100
Comment:	4E - SIPMF
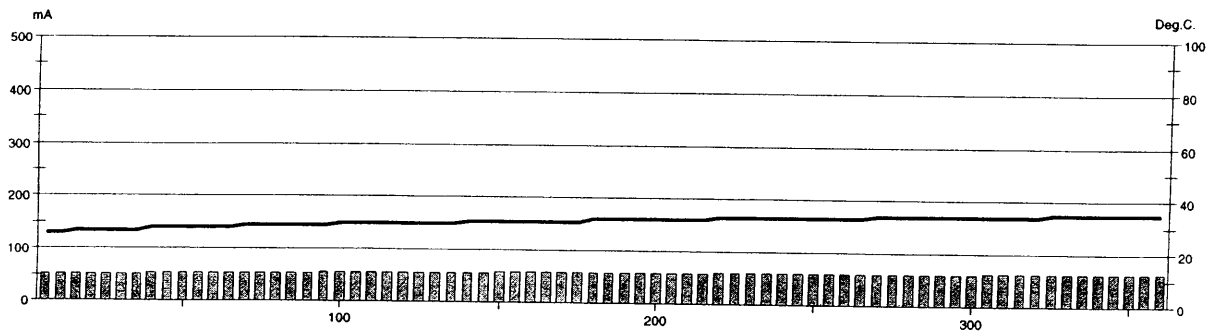
Time	°C	mA	Time	°C	mA	Time	°C	mA	Time	°C	mA
00:05	26	52.1	01:35	29	54.8	03:05	32	58.1	04:35	34	60.7
00:10	26	52.0	01:40	30	55.0	03:10	32	58.3	04:40	34	60.8
00:15	27	52.0	01:45	30	55.1	03:15	32	58.5	04:45	34	61.0
00:20	27	52.0	01:50	30	55.4	03:20	32	58.6	04:50	34	61.1
00:25	27	52.1	01:55	30	55.6	03:25	32	58.8	04:55	34	61.2
00:30	27	52.2	02:00	30	55.8	03:30	32	58.9	05:00	34	61.3
00:35	27	52.4	02:05	30	56.0	03:35	32	59.1	05:05	34	61.4
00:40	28	52.5	02:10	30	56.2	03:40	33	59.2	05:10	34	61.5
00:45	28	52.7	02:15	30	56.4	03:45	33	59.4	05:15	34	61.7
00:50	28	52.9	02:20	31	56.6	03:50	33	59.5	05:20	34	61.7
00:55	28	53.1	02:25	31	56.8	03:55	33	59.7	05:25	35	61.9
01:00	28	53.3	02:30	31	57.0	04:00	33	59.9	05:30	35	62.0
01:05	28	53.5	02:35	31	57.1	04:05	33	60.0	05:35	35	62.1
01:10	29	53.7	02:40	31	57.3	04:10	33	60.1	05:40	35	62.2
01:15	29	53.9	02:45	31	57.5	04:15	33	60.2	05:45	35	62.3
01:20	29	54.1	02:50	31	57.7	04:20	33	60.3	05:50	35	62.4
01:25	29	54.3	02:55	31	57.8	04:25	33	60.5	05:55	35	62.4
01:30	29	54.5	03:00	32	58.0	04:30	34	60.6	06:00	35	62.6
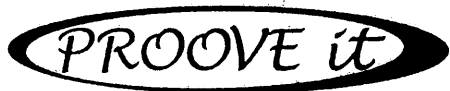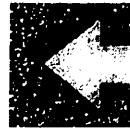
D8

ASTM C 1202-97

Test report

Voltage Used:	60
Testing time:	06:00 hour
Charge passed:	1676
Adjusted Charge passed:	1513
Permeability class:	Low
Instrument number:	994704
Channel number:	5
Report date:	7/15/2004
Testing by:	Chris Tuminello
Reference:	LOR-57-18.18
Sample diameter:	100
Comment:	5B(B) - SIPMF
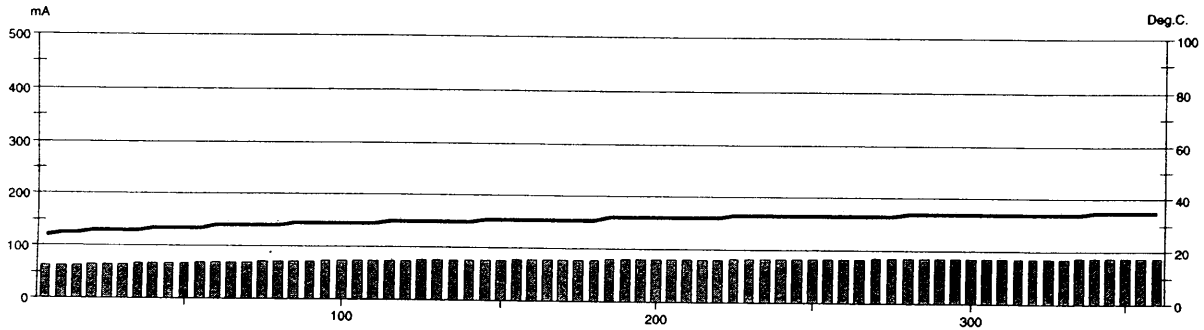
Time	°C	mA	Time	°C	mA	Time	°C	mA	Time	°C	mA
00:05	24	61.6	01:35	29	72.6	03:05	32	79.3	04:35	33	84.0
00:10	25	62.6	01:40	29	73.1	03:10	32	79.6	04:40	34	84.2
00:15	25	63.5	01:45	29	73.5	03:15	32	80.0	04:45	34	84.3
00:20	26	64.3	01:50	29	73.9	03:20	32	80.4	04:50	34	84.6
00:25	26	65.0	01:55	30	74.2	03:25	32	80.6	04:55	34	84.8
00:30	26	65.5	02:00	30	74.5	03:30	32	80.9	05:00	34	85.0
00:35	26	66.1	02:05	30	74.8	03:35	32	81.1	05:05	34	85.2
00:40	27	66.6	02:10	30	75.2	03:40	32	81.3	05:10	34	85.3
00:45	27	67.2	02:15	30	75.6	03:45	33	81.5	05:15	34	85.4
00:50	27	67.9	02:20	30	76.0	03:50	33	81.9	05:20	34	85.5
00:55	27	68.5	02:25	31	76.4	03:55	33	82.1	05:25	34	85.7
01:00	28	69.1	02:30	31	76.8	04:00	33	82.4	05:30	34	85.8
01:05	28	69.6	02:35	31	77.3	04:05	33	82.6	05:35	34	86.0
01:10	28	70.1	02:40	31	77.7	04:10	33	82.9	05:40	35	86.1
01:15	28	70.7	02:45	31	78.0	04:15	33	83.2	05:45	35	86.2
01:20	28	71.2	02:50	31	78.3	04:20	33	83.4	05:50	35	86.4
01:25	29	71.7	02:55	31	78.6	04:25	33	83.6	05:55	35	86.6
01:30	29	72.2	03:00	31	79.0	04:30	33	83.8	06:00	35	86.7
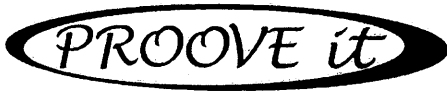
PROOVE it

ASTM C 1202-97

Test report

Voltage Used:	60
Testing time:	06:00 hour
Charge passed:	2604
Adjusted Charge passed:	2350
Permeability class:	Moderate
Instrument number:	994704
Channel number:	6
Report date:	7/1/2004
Testing by:	Chris Tuminello
Reference:	LOR-57-18.18
Sample diameter:	100
Comment:	6D - SIPMF
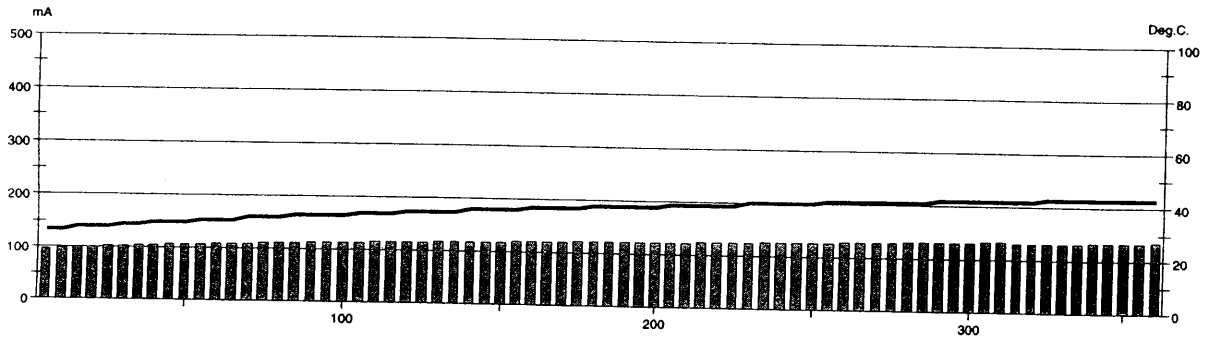
Time	°C	mA	Time	°C	mA	Time	°C	mA	Time	°C	mA
00:05	27	96.9	01:35	33	113.4	03:05	38	122.3	04:35	41	130.2
00:10	27	98.8	01:40	33	114.1	03:10	38	122.3	04:40	41	130.7
00:15	28	100.3	01:45	34	114.7	03:15	38	122.5	04:45	41	131.1
00:20	28	101.5	01:50	34	115.3	03:20	38	122.8	04:50	42	131.6
00:25	28	102.7	01:55	34	115.9	03:25	39	123.2	04:55	42	132.0
00:30	29	103.7	02:00	35	116.5	03:30	39	123.7	05:00	42	132.5
00:35	29	104.6	02:05	35	116.7	03:35	39	124.3	05:05	42	132.9
00:40	30	105.5	02:10	35	117.3	03:40	39	124.8	05:10	42	133.1
00:45	30	106.4	02:15	35	117.5	03:45	39	125.4	05:15	42	131.7
00:50	30	107.2	02:20	36	118.2	03:50	40	125.9	05:20	42	131.4
00:55	31	107.9	02:25	36	118.7	03:55	40	126.3	05:25	43	132.1
01:00	31	108.7	02:30	36	119.2	04:00	40	126.8	05:30	43	132.5
01:05	31	109.4	02:35	36	119.8	04:05	40	127.4	05:35	43	132.1
01:10	32	110.1	02:40	37	120.3	04:10	40	127.8	05:40	43	133.8
01:15	32	110.7	02:45	37	120.8	04:15	41	128.3	05:45	43	134.3
01:20	32	111.4	02:50	37	121.3	04:20	41	128.8	05:50	43	133.1
01:25	33	112.1	02:55	37	121.7	04:25	41	129.2	05:55	43	134.8
01:30	33	112.8	03:00	38	122.0	04:30	41	129.7	06:00	43	135.2
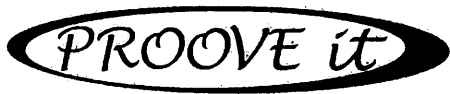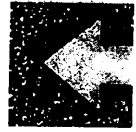
D10

PROOVE it

ASTM C 1202-97

Test report

Voltage Used:	60
Testing time:	06:00 hour
Charge passed:	2247
Adjusted Charge passed:	2028
Permeability class:	Moderate
Instrument number:	994704
Channel number:	7
Report date:	7/6/2004
Testing by:	Chris Tuminello
Reference:	LOR-57-18.18
Sample diameter:	100
Comment:	7C1 - SIPMF
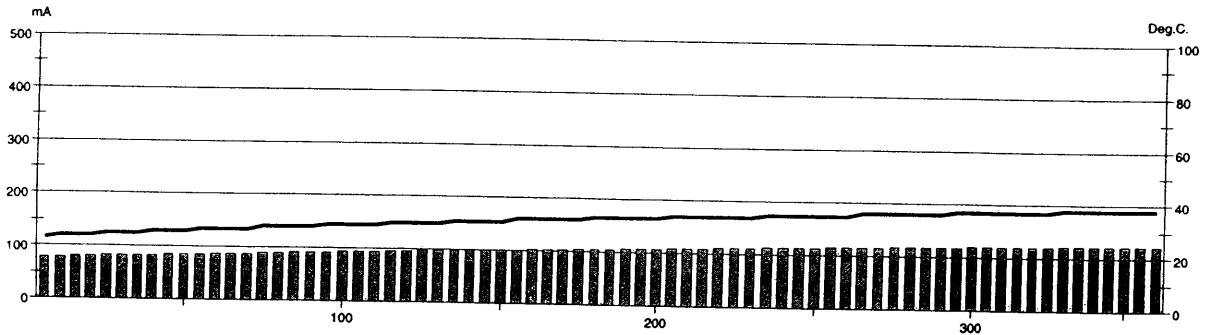
Time	°C	mA	Time	°C	mA	Time	°C	mA	Time	°C	mA
00:05	23	77.8	01:35	29	92.2	03:05	33	105.4	04:35	36	117.7
00:10	24	79.1	01:40	29	93.0	03:10	33	106.9	04:40	36	118.4
00:15	24	80.1	01:45	29	93.9	03:15	33	107.1	04:45	36	118.3
00:20	24	80.9	01:50	29	94.7	03:20	33	108.2	04:50	36	118.8
00:25	25	81.6	01:55	30	95.5	03:25	34	108.4	04:55	37	119.3
00:30	25	82.3	02:00	30	96.3	03:30	34	109.8	05:00	37	119.9
00:35	25	82.9	02:05	30	97.1	03:35	34	110.2	05:05	37	120.1
00:40	26	83.5	02:10	30	97.9	03:40	34	111.3	05:10	37	120.3
00:45	26	84.2	02:15	31	98.7	03:45	34	111.9	05:15	37	121.1
00:50	26	84.9	02:20	31	99.4	03:50	34	112.3	05:20	37	121.2
00:55	27	85.7	02:25	31	100.2	03:55	35	113.5	05:25	37	121.4
01:00	27	86.5	02:30	31	100.6	04:00	35	113.4	05:30	38	121.7
01:05	27	87.3	02:35	32	100.0	04:05	35	114.4	05:35	38	122.1
01:10	27	88.0	02:40	32	101.6	04:10	35	114.9	05:40	38	122.0
01:15	28	88.8	02:45	32	103.2	04:15	35	116.1	05:45	38	122.6
01:20	28	89.7	02:50	32	103.4	04:20	35	116.0	05:50	38	123.0
01:25	28	90.5	02:55	32	104.9	04:25	36	116.3	05:55	38	123.0
01:30	28	91.3	03:00	33	105.7	04:30	36	117.1	06:00	38	123.5

D11

ASTM C 1202-97

GERMANN INSTRUMENTS

DENMARK
Phone: +45 3967 7117
Fax: +45 3967 3167

USA
Phone: (847)329-9999
Fax: (847)329-8888

Test report

Voltage Used:	60
Testing time:	06:00 hour
Charge passed:	2026
Adjusted Charge passed:	1828
Permeability class:	Low
Instrument number:	994704
Channel number:	1
Report date:	7/15/2004
Testing by:	Chris Tuminello
Reference:	LOR-57-18.18
Sample diameter:	100
Comment:	7C1(2) - SIPMF
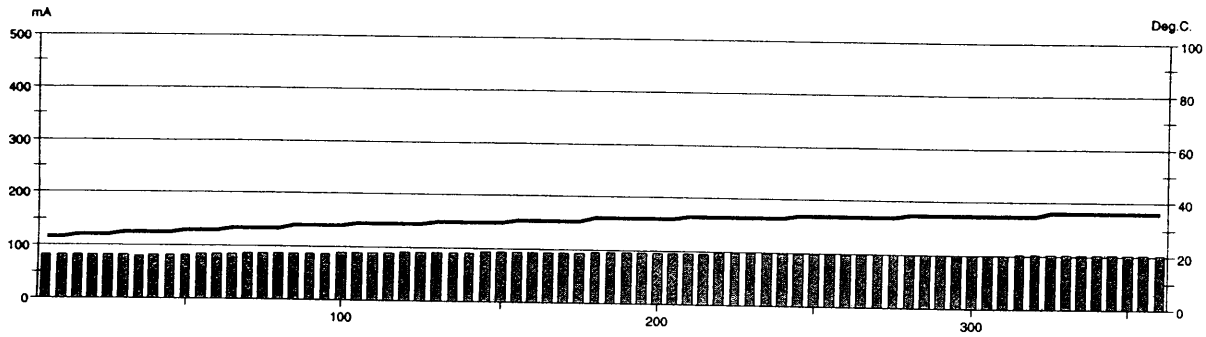
Time	°C	mA	Time	°C	mA	Time	°C	mA	Time	°C	mA
00:05	23	83.7	01:35	28	88.1	03:05	32	95.5	04:35	34	99.7
00:10	23	82.4	01:40	28	89.5	03:10	32	95.7	04:40	35	99.9
00:15	24	82.3	01:45	29	89.9	03:15	32	95.9	04:45	35	100.3
00:20	24	82.1	01:50	29	89.8	03:20	32	96.2	04:50	35	100.4
00:25	24	81.9	01:55	29	90.1	03:25	32	96.4	04:55	35	100.6
00:30	25	81.6	02:00	29	90.8	03:30	33	96.5	05:00	35	100.7
00:35	25	81.2	02:05	29	91.1	03:35	33	96.9	05:05	35	101.1
00:40	25	82.2	02:10	30	91.6	03:40	33	97.1	05:10	35	101.2
00:45	25	82.3	02:15	30	91.9	03:45	33	97.6	05:15	35	101.6
00:50	26	83.6	02:20	30	92.1	03:50	33	97.8	05:20	35	101.7
00:55	26	84.7	02:25	30	92.7	03:55	33	98.0	05:25	36	102.0
01:00	26	85.2	02:30	30	93.0	04:00	33	98.2	05:30	36	102.2
01:05	27	85.7	02:35	31	93.4	04:05	34	98.6	05:35	36	102.3
01:10	27	86.2	02:40	31	93.9	04:10	34	98.8	05:40	36	102.4
01:15	27	86.4	02:45	31	94.1	04:15	34	98.9	05:45	36	102.7
01:20	27	86.4	02:50	31	94.4	04:20	34	99.1	05:50	36	102.9
01:25	28	87.0	02:55	31	94.7	04:25	34	99.2	05:55	36	103.2
01:30	28	87.4	03:00	32	95.1	04:30	34	99.5	06:00	36	103.6
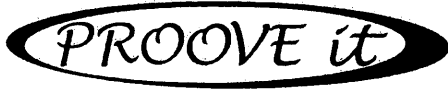
ASTM C 1202-97

GERMANN INSTRUMENTS

DENMARK
Phone: +45 3967 7117
Fax: +45 3967 3167

USA
Phone: (847)329-9999
Fax: (847)329-8888

Test report

Voltage Used:	60
Testing time:	06:00 hour
Charge passed:	2570
Adjusted Charge passed:	2319
Permeability class:	Moderate
Instrument number:	994704
Channel number:	5
Report date:	7/14/2004
Testing by:	Chris Tuminello
Reference:	LOR-57-18.18
Sample diameter:	100
Comment:	7E(T) - SIPMF
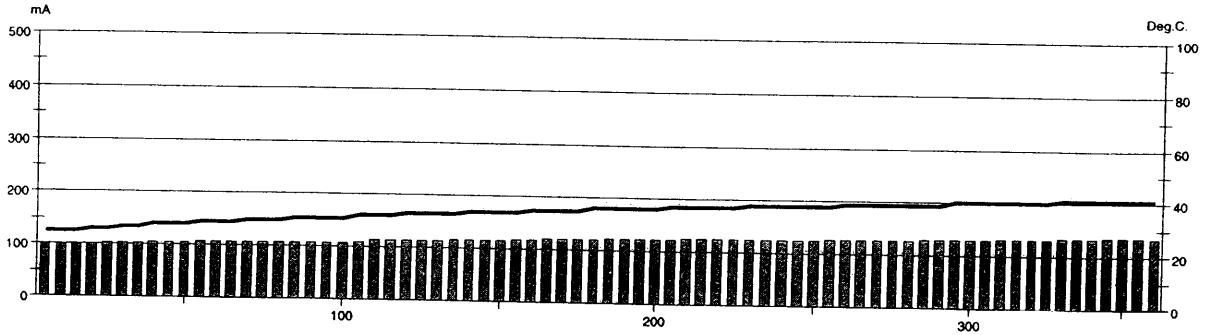
Time	°C	mA	Time	°C	mA	Time	°C	mA	Time	°C	mA
00:05	25	97.8	01:35	31	107.6	03:05	36	121.8	04:35	39	127.8
00:10	25	99.0	01:40	31	108.2	03:10	36	122.3	04:40	39	128.3
00:15	25	99.9	01:45	32	109.4	03:15	36	123.0	04:45	39	128.4
00:20	26	100.8	01:50	32	113.1	03:20	36	123.4	04:50	39	129.1
00:25	26	101.7	01:55	32	114.1	03:25	37	123.8	04:55	40	129.3
00:30	27	102.6	02:00	33	114.2	03:30	37	124.4	05:00	40	129.8
00:35	27	103.3	02:05	33	113.2	03:35	37	124.9	05:05	40	130.3
00:40	28	104.0	02:10	33	114.2	03:40	37	125.4	05:10	40	130.7
00:45	28	104.8	02:15	33	116.3	03:45	37	125.7	05:15	40	130.8
00:50	28	105.6	02:20	34	116.1	03:50	38	124.6	05:20	40	131.3
00:55	29	106.3	02:25	34	115.4	03:55	38	124.5	05:25	40	132.6
01:00	29	107.1	02:30	34	115.3	04:00	38	125.0	05:30	41	134.5
01:05	29	107.1	02:35	34	118.4	04:05	38	125.4	05:35	41	133.8
01:10	30	106.3	02:40	35	119.1	04:10	38	125.6	05:40	41	134.2
01:15	30	106.2	02:45	35	119.5	04:15	38	126.2	05:45	41	135.7
01:20	30	106.2	02:50	35	120.1	04:20	39	126.6	05:50	41	135.7
01:25	31	106.7	02:55	35	120.7	04:25	39	127.2	05:55	41	135.2
01:30	31	107.5	03:00	36	121.2	04:30	39	127.5	06:00	41	134.2
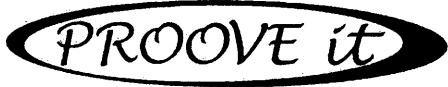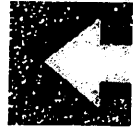
D13

PROOVE it

ASTM C 1202-97

Test report

Voltage Used:	60
Testing time:	06:00 hour
Charge passed:	1189
Adjusted Charge passed:	1073
Permeability class:	Low
Instrument number:	994704
Channel number:	5
Report date:	7/13/2004
Testing by:	Chris Tuminello
Reference:	LOR-57-18.18
Sample diameter:	100
Comment:	7E(B) - SIPMF
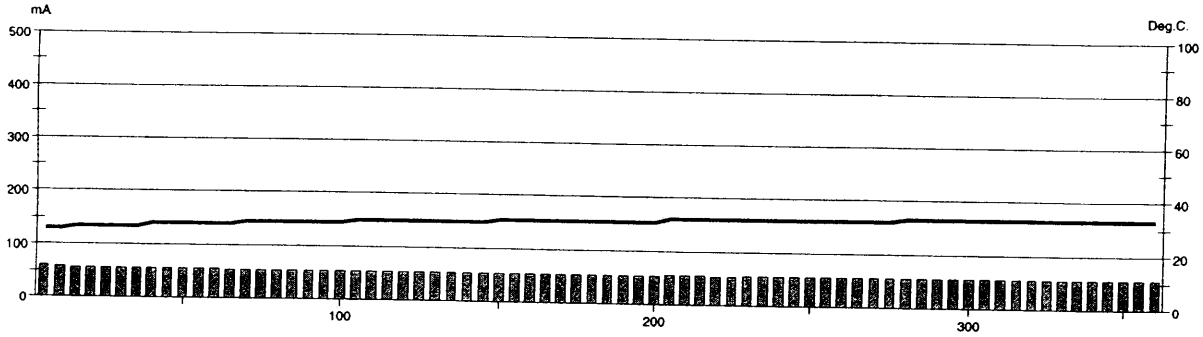
Time	°C	mA	Time	°C	mA	Time	°C	mA	Time	°C	mA
00:05	26	59.5	01:35	29	53.7	03:05	31	54.0	04:35	32	55.4
00:10	26	57.5	01:40	29	54.2	03:10	31	54.0	04:40	33	55.6
00:15	27	56.8	01:45	30	54.3	03:15	31	54.2	04:45	33	55.5
00:20	27	56.1	01:50	30	54.3	03:20	31	54.5	04:50	33	55.4
00:25	27	55.7	01:55	30	54.2	03:25	32	54.7	04:55	33	55.6
00:30	27	55.4	02:00	30	54.3	03:30	32	54.8	05:00	33	55.8
00:35	27	55.1	02:05	30	54.2	03:35	32	54.7	05:05	33	55.8
00:40	28	55.0	02:10	30	54.3	03:40	32	54.6	05:10	33	55.7
00:45	28	55.0	02:15	30	54.4	03:45	32	54.5	05:15	33	55.6
00:50	28	55.0	02:20	30	54.4	03:50	32	54.9	05:20	33	55.8
00:55	28	54.9	02:25	30	54.4	03:55	32	54.8	05:25	33	55.8
01:00	28	54.8	02:30	31	54.4	04:00	32	55.0	05:30	33	56.0
01:05	28	54.6	02:35	31	54.3	04:05	32	55.1	05:35	33	56.0
01:10	29	54.3	02:40	31	54.3	04:10	32	55.0	05:40	33	55.9
01:15	29	54.2	02:45	31	54.3	04:15	32	55.1	05:45	33	56.2
01:20	29	54.1	02:50	31	54.1	04:20	32	55.4	05:50	33	56.4
01:25	29	53.9	02:55	31	54.3	04:25	32	55.3	05:55	33	56.3
01:30	29	53.8	03:00	31	54.2	04:30	32	55.3	06:00	33	56.0
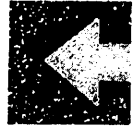
D14

PROOVE it

ASTM C 1202-97

Test report

Voltage Used:	60
Testing time:	06:00 hour
Charge passed:	2137
Adjusted Charge passed:	1929
Permeability class:	Low
Instrument number:	994704
Channel number:	7
Report date:	7/1/2004
Testing by:	Chris Tuminello
Reference:	LOR-57-18.18
Sample diameter:	100
Comment:	8B - No SIPMF
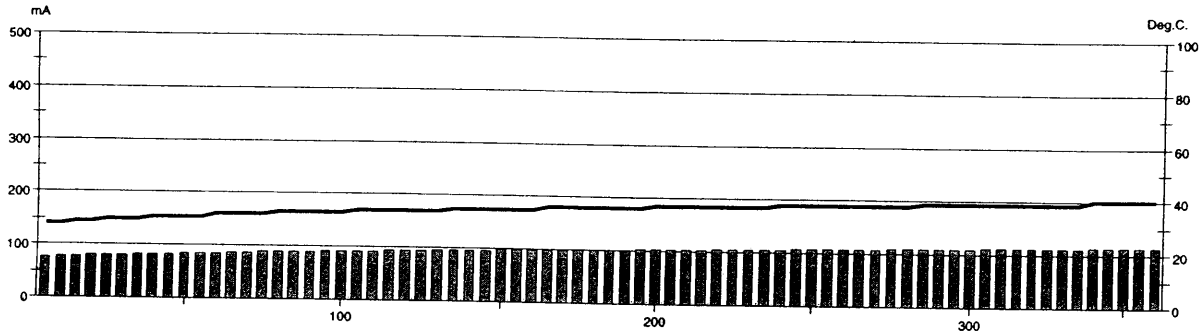
Time	°C	mA	Time	°C	mA	Time	°C	mA	Time	°C	mA
00:05	28	75.9	01:35	33	91.0	03:05	36	101.0	04:35	38	108.4
00:10	28	77.4	01:40	33	91.6	03:10	36	101.5	04:40	38	108.8
00:15	29	78.5	01:45	34	92.1	03:15	36	102.0	04:45	39	109.1
00:20	29	79.6	01:50	34	92.6	03:20	37	102.5	04:50	39	109.4
00:25	30	80.0	01:55	34	93.2	03:25	37	102.9	04:55	39	109.9
00:30	30	80.9	02:00	34	93.9	03:30	37	103.3	05:00	39	110.3
00:35	30	81.9	02:05	34	94.6	03:35	37	103.6	05:05	39	110.7
00:40	31	82.8	02:10	34	95.1	03:40	37	104.4	05:10	39	111.1
00:45	31	83.6	02:15	35	95.4	03:45	37	104.7	05:15	39	111.3
00:50	31	84.5	02:20	35	96.1	03:50	37	105.2	05:20	39	111.7
00:55	31	85.2	02:25	35	96.3	03:55	37	105.4	05:25	39	112.0
01:00	32	85.8	02:30	35	97.1	04:00	38	105.9	05:30	39	112.5
01:05	32	86.6	02:35	35	97.5	04:05	38	106.4	05:35	39	112.7
01:10	32	87.4	02:40	35	98.2	04:10	38	107.0	05:40	40	112.9
01:15	32	88.2	02:45	36	98.7	04:15	38	107.0	05:45	40	113.1
01:20	33	89.1	02:50	36	99.3	04:20	38	107.7	05:50	40	113.3
01:25	33	89.8	02:55	36	100.0	04:25	38	107.9	05:55	40	113.7
01:30	33	90.4	03:00	36	100.4	04:30	38	107.9	06:00	40	113.9

PROOVE it

ASTM C 1202-97

Test report

Voltage Used:	60
Testing time:	06:00 hour
Charge passed:	2599
Adjusted Charge passed:	2346
Permeability class:	Moderate
Instrument number:	994704
Channel number:	1
Report date:	7/15/2004
Testing by:	Chris Tuminello
Reference:	LOR-57-18.18
Sample diameter:	100
Comment:	8C1 - No SIPMF
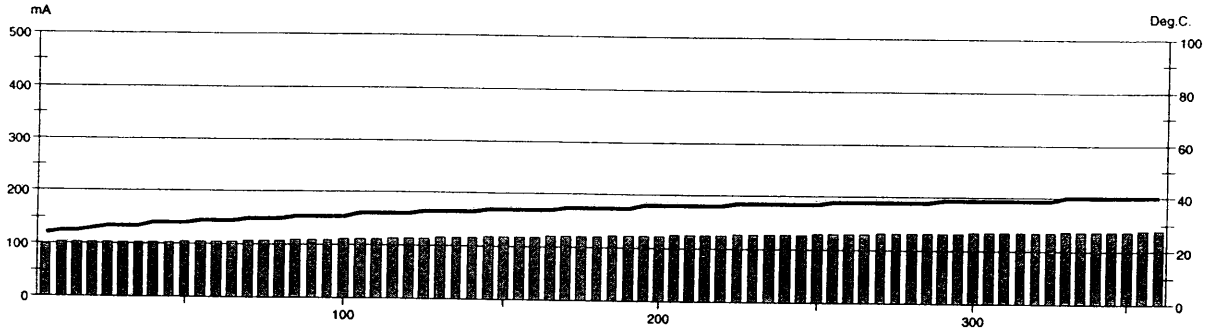
Time	°C	mA	Time	°C	mA	Time	°C	mA	Time	°C	mA
00:05	24	98.4	01:35	31	110.3	03:05	35	122.0	04:35	38	131.2
00:10	25	102.3	01:40	31	111.0	03:10	35	122.4	04:40	38	131.5
00:15	25	102.9	01:45	32	111.5	03:15	36	123.0	04:45	38	131.7
00:20	26	102.9	01:50	32	112.6	03:20	36	123.6	04:50	39	132.2
00:25	27	102.8	01:55	32	113.2	03:25	36	124.3	04:55	39	132.6
00:30	27	102.3	02:00	32	114.0	03:30	36	124.7	05:00	39	133.1
00:35	27	101.8	02:05	33	114.5	03:35	36	125.3	05:05	39	133.5
00:40	28	102.2	02:10	33	115.6	03:40	36	125.8	05:10	39	133.8
00:45	28	102.9	02:15	33	116.3	03:45	37	126.2	05:15	39	134.1
00:50	28	104.8	02:20	33	117.0	03:50	37	126.7	05:20	39	134.5
00:55	29	104.2	02:25	34	117.5	03:55	37	127.2	05:25	39	134.9
01:00	29	105.3	02:30	34	118.0	04:00	37	127.7	05:30	40	135.2
01:05	29	106.0	02:35	34	118.5	04:05	37	128.2	05:35	40	136.0
01:10	30	106.6	02:40	34	119.1	04:10	37	128.6	05:40	40	136.4
01:15	30	107.3	02:45	34	119.8	04:15	38	129.1	05:45	40	136.7
01:20	30	107.5	02:50	35	120.3	04:20	38	129.8	05:50	40	137.1
01:25	31	108.6	02:55	35	120.8	04:25	38	130.1	05:55	40	137.7
01:30	31	109.3	03:00	35	121.4	04:30	38	130.6	06:00	40	138.0
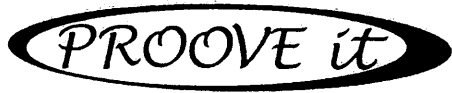
PROOVE it

ASTM C 1202-97

Test report

Voltage Used:	60
Testing time:	06:00 hour
Charge passed:	2191
Adjusted Charge passed:	1977
Permeability class:	Low
Instrument number:	994704
Channel number:	1
Report date:	6/28/2004
Testing by:	Chris Tuminello
Reference:	OTT-2-28.41
Sample diameter:	100
Comment:	A3(T) - No SIPMF
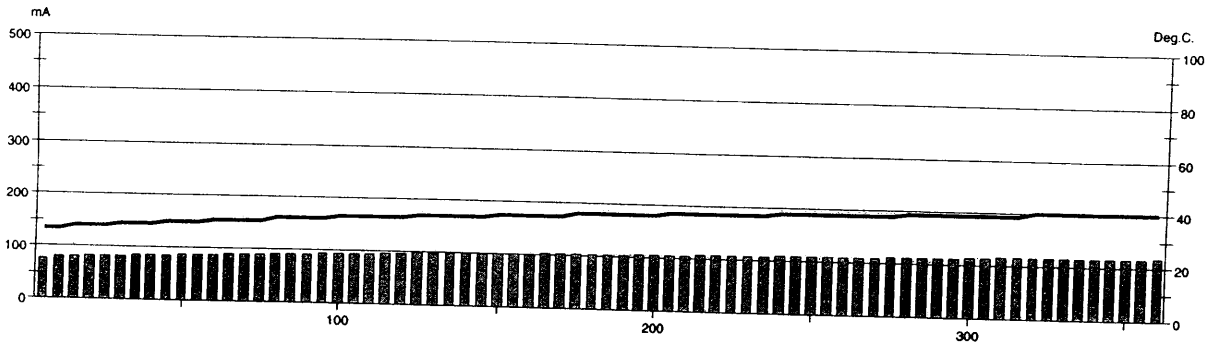
Time	°C	mA	Time	°C	mA	Time	°C	mA	Time	°C	mA
00:05	27	76.9	01:35	32	92.9	03:05	36	103.3	04:35	38	111.0
00:10	27	80.0	01:40	33	93.5	03:10	36	103.7	04:40	39	111.1
00:15	28	81.0	01:45	33	94.3	03:15	36	104.6	04:45	39	111.7
00:20	28	81.6	01:50	33	94.8	03:20	36	104.8	04:50	39	111.7
00:25	28	82.6	01:55	33	96.0	03:25	37	105.5	04:55	39	112.0
00:30	29	83.3	02:00	33	96.7	03:30	37	105.8	05:00	39	112.8
00:35	29	84.1	02:05	34	97.4	03:35	37	106.4	05:05	39	113.8
00:40	29	84.9	02:10	34	97.8	03:40	37	106.9	05:10	39	115.0
00:45	30	85.8	02:15	34	98.2	03:45	37	107.1	05:15	39	115.0
00:50	30	86.4	02:20	34	98.7	03:50	37	107.4	05:20	40	115.2
00:55	30	87.2	02:25	34	99.3	03:55	37	108.1	05:25	40	115.9
01:00	31	87.8	02:30	35	99.9	04:00	38	108.6	05:30	40	115.9
01:05	31	88.6	02:35	35	100.5	04:05	38	108.5	05:35	40	116.3
01:10	31	89.5	02:40	35	100.9	04:10	38	108.8	05:40	40	116.2
01:15	31	90.0	02:45	35	101.7	04:15	38	109.4	05:45	40	116.7
01:20	32	90.7	02:50	35	101.9	04:20	38	109.6	05:50	40	117.0
01:25	32	91.4	02:55	36	102.6	04:25	38	110.1	05:55	40	116.8
01:30	32	92.1	03:00	36	102.8	04:30	38	110.3	06:00	40	117.5
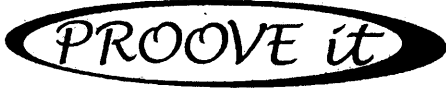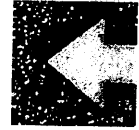
PROOVE it

ASTM C 1202-97

Test report

Voltage Used:	60
Testing time:	06:00 hour
Charge passed:	1345
Adjusted Charge passed:	1214
Permeability class:	Low
Instrument number:	994704
Channel number:	1
Report date:	6/28/2004
Testing by:	Chris Tuminello
Reference:	OTT-2-28.41
Sample diameter:	100
Comment:	A3(B) - No SIPMF
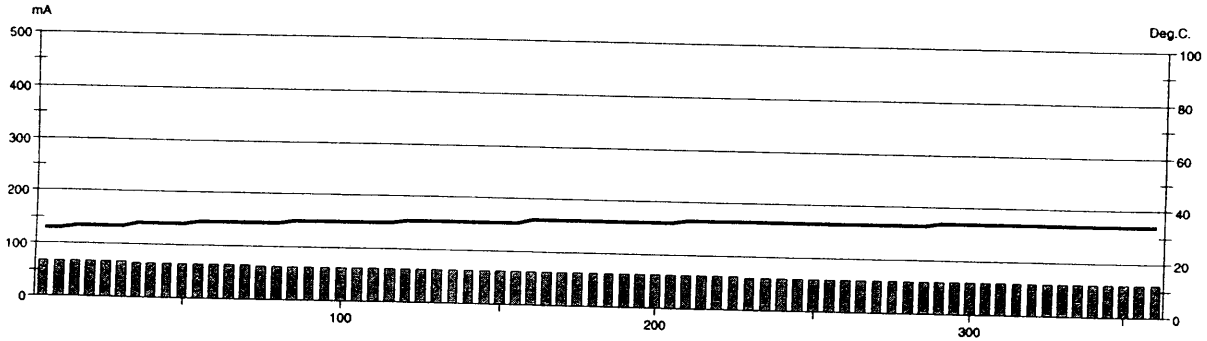
Time	°C	mA	Time	°C	mA	Time	°C	mA	Time	°C	mA
00:05	26	66.3	01:35	30	63.3	03:05	32	61.9	04:35	33	60.6
00:10	26	67.2	01:40	30	63.2	03:10	32	61.9	04:40	33	60.5
00:15	27	66.9	01:45	30	63.1	03:15	32	61.8	04:45	33	60.4
00:20	27	66.5	01:50	30	63.0	03:20	32	61.8	04:50	34	60.4
00:25	27	66.2	01:55	30	63.0	03:25	32	61.7	04:55	34	60.3
00:30	27	65.9	02:00	31	63.0	03:30	33	61.7	05:00	34	60.4
00:35	28	65.7	02:05	31	62.9	03:35	33	61.6	05:05	34	60.4
00:40	28	65.4	02:10	31	62.8	03:40	33	61.5	05:10	34	60.3
00:45	28	65.2	02:15	31	62.8	03:45	33	61.4	05:15	34	60.3
00:50	28	64.3	02:20	31	62.7	03:50	33	61.2	05:20	34	60.2
00:55	29	64.0	02:25	31	62.7	03:55	33	61.2	05:25	34	60.1
01:00	29	63.9	02:30	31	62.6	04:00	33	61.1	05:30	34	60.0
01:05	29	63.8	02:35	31	62.5	04:05	33	61.0	05:35	34	59.8
01:10	29	63.7	02:40	32	62.4	04:10	33	61.0	05:40	34	59.7
01:15	29	63.6	02:45	32	62.2	04:15	33	60.9	05:45	34	59.7
01:20	29	63.5	02:50	32	62.2	04:20	33	60.8	05:50	34	59.6
01:25	30	63.5	02:55	32	62.1	04:25	33	60.8	05:55	34	59.5
01:30	30	63.4	03:00	32	62.0	04:30	33	60.7	06:00	34	59.4
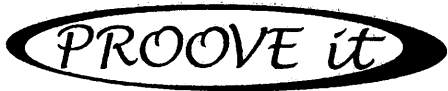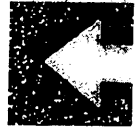
D18

PROOVE it

ASTM C 1202-97

GERMANN INSTRUMENTS

Test report

Voltage Used:	60
Testing time:	06:00 hour
Charge passed:	1847
Adjusted Charge passed:	1667
Permeability class:	Low
Instrument number:	994704
Channel number:	2
Report date:	7/16/2004
Testing by:	Chris Tuminello
Reference:	OTT-2-28.41
Sample diameter:	100
Comment:	A6(T) - No SIPMF
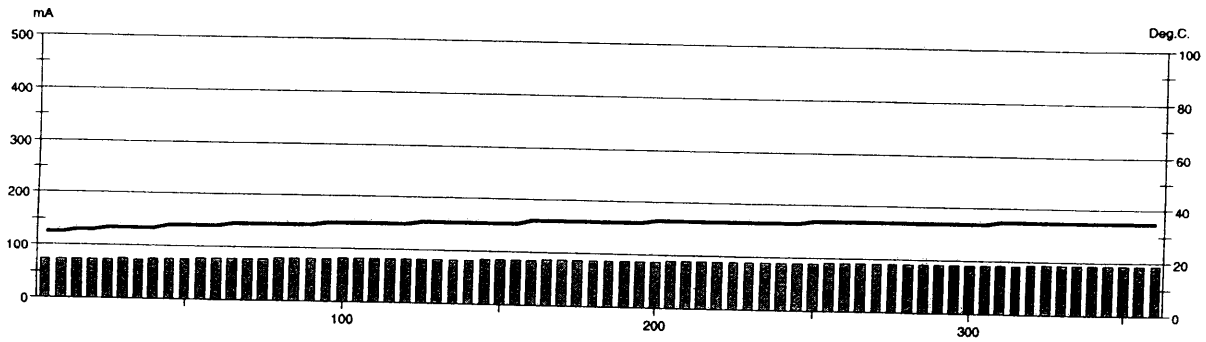
Time	°C	mA	Time	°C	mA	Time	°C	mA	Time	°C	mA
00:05	25	73.0	01:35	30	80.6	03:05	32	87.3	04:35	34	91.5
00:10	25	73.1	01:40	30	81.6	03:10	32	87.2	04:40	34	91.6
00:15	26	73.1	01:45	30	81.6	03:15	32	87.4	04:45	34	91.9
00:20	26	72.8	01:50	30	81.5	03:20	33	87.8	04:50	34	91.9
00:25	27	73.4	01:55	30	81.6	03:25	33	88.4	04:55	34	91.8
00:30	27	75.0	02:00	30	83.4	03:30	33	88.5	05:00	34	92.3
00:35	27	74.7	02:05	31	83.5	03:35	33	89.0	05:05	34	92.6
00:40	27	75.9	02:10	31	83.3	03:40	33	89.2	05:10	35	92.5
00:45	28	76.0	02:15	31	83.2	03:45	33	89.4	05:15	35	92.3
00:50	28	76.6	02:20	31	83.0	03:50	33	89.9	05:20	35	92.7
00:55	28	77.3	02:25	31	84.4	03:55	33	89.8	05:25	35	93.0
01:00	28	77.6	02:30	31	85.2	04:00	33	90.0	05:30	35	93.1
01:05	29	78.0	02:35	31	85.6	04:05	33	90.2	05:35	35	93.2
01:10	29	78.5	02:40	32	85.9	04:10	34	90.0	05:40	35	92.9
01:15	29	78.6	02:45	32	86.1	04:15	34	90.6	05:45	35	92.9
01:20	29	80.1	02:50	32	86.6	04:20	34	90.9	05:50	35	93.7
01:25	29	80.0	02:55	32	86.7	04:25	34	90.9	05:55	35	93.6
01:30	29	79.8	03:00	32	86.8	04:30	34	90.9	06:00	35	93.4
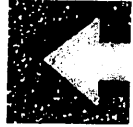
D19

ASTM C 1202-97

Test report

Voltage Used:	60
Testing time:	06:00 hour
Charge passed:	1751
Adjusted Charge passed:	1580
Permeability class:	Low
Instrument number:	994704
Channel number:	4
Report date:	7/6/2004
Testing by:	Chris Tuminello
Reference:	OTT-2-18.18
Sample diameter:	100
Comment:	A6(B) - No SIPMF
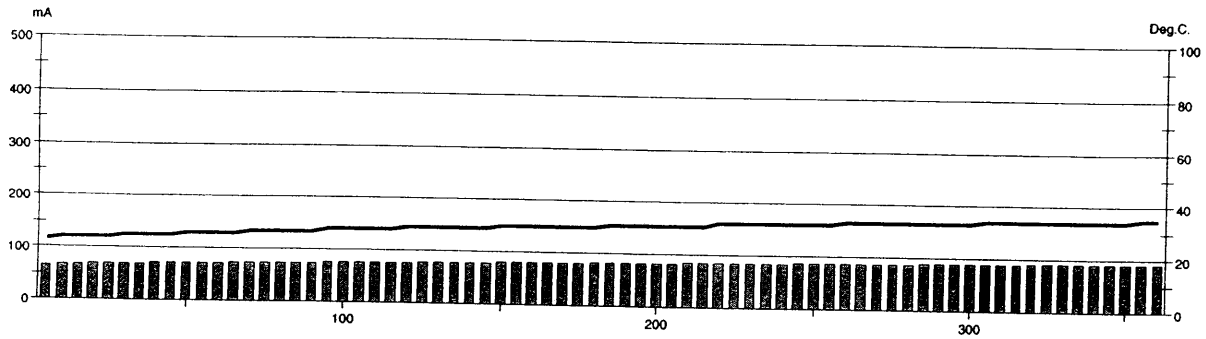
Time	°C	mA	Time	°C	mA	Time	°C	mA	Time	°C	mA
00:05	23	65.1	01:35	28	75.1	03:05	31	82.1	04:35	33	87.8
00:10	24	67.6	01:40	28	75.5	03:10	31	82.4	04:40	33	88.0
00:15	24	67.9	01:45	28	76.0	03:15	31	83.0	04:45	33	88.3
00:20	24	68.3	01:50	28	76.3	03:20	31	83.3	04:50	33	88.6
00:25	24	68.8	01:55	28	76.7	03:25	31	83.7	04:55	33	89.0
00:30	25	69.4	02:00	29	77.0	03:30	31	84.0	05:00	33	89.2
00:35	25	69.8	02:05	29	77.3	03:35	31	84.1	05:05	34	89.6
00:40	25	70.4	02:10	29	77.6	03:40	32	84.5	05:10	34	89.9
00:45	25	70.8	02:15	29	78.1	03:45	32	84.8	05:15	34	90.2
00:50	26	71.3	02:20	29	78.5	03:50	32	85.1	05:20	34	90.5
00:55	26	71.8	02:25	29	78.8	03:55	32	85.5	05:25	34	90.7
01:00	26	72.2	02:30	30	79.3	04:00	32	85.8	05:30	34	90.9
01:05	26	72.6	02:35	30	79.5	04:05	32	86.1	05:35	34	90.9
01:10	27	73.0	02:40	30	79.8	04:10	32	86.4	05:40	34	91.2
01:15	27	73.5	02:45	30	80.3	04:15	32	86.7	05:45	34	91.6
01:20	27	73.9	02:50	30	80.6	04:20	33	87.0	05:50	34	91.7
01:25	27	74.3	02:55	30	81.0	04:25	33	87.3	05:55	35	91.9
01:30	27	74.7	03:00	30	81.6	04:30	33	87.6	06:00	35	92.2
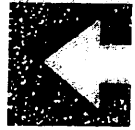
PROOVE it

ASTM C 1202-97

Test report

Voltage Used:	60
Testing time:	06:00 hour
Charge passed:	3321
Adjusted Charge passed:	2997
Permeability class:	Moderate
Instrument number:	994704
Channel number:	1
Report date:	6/29/2004
Testing by:	Chris Tuminello
Reference:	OTT-2-28.41
Sample diameter:	100
Comment:	A10(T) - No SIPMF
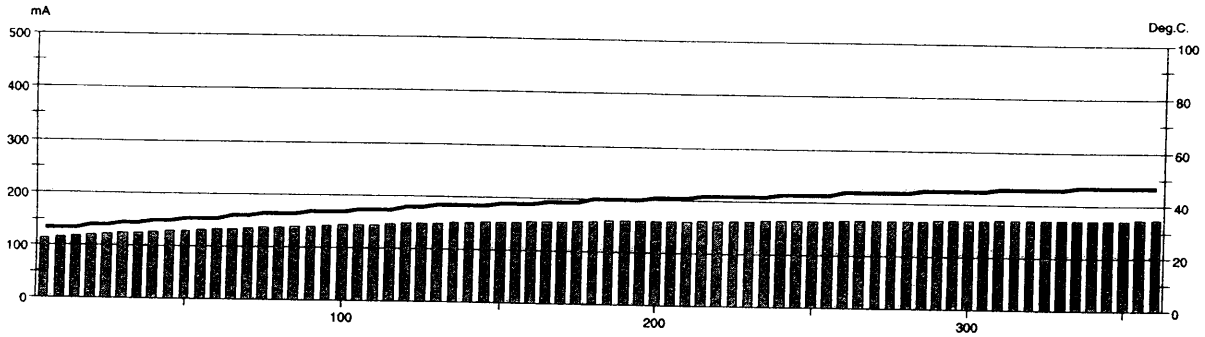
Time	°C	mA	Time	°C	mA	Time	°C	mA	Time	°C	mA
00:05	27	114.8	01:35	34	142.7	03:05	40	159.6	04:35	44	168.1
00:10	27	117.1	01:40	34	144.0	03:10	40	160.1	04:40	44	168.3
00:15	27	119.2	01:45	35	145.0	03:15	40	160.4	04:45	45	168.5
00:20	28	121.0	01:50	35	146.1	03:20	41	161.0	04:50	45	168.9
00:25	28	122.7	01:55	35	147.2	03:25	41	161.6	04:55	45	169.4
00:30	29	124.3	02:00	36	148.5	03:30	41	161.8	05:00	45	170.0
00:35	29	125.8	02:05	36	149.6	03:35	42	161.9	05:05	45	170.6
00:40	30	127.4	02:10	37	150.4	03:40	42	162.4	05:10	46	171.1
00:45	30	128.9	02:15	37	151.4	03:45	42	162.9	05:15	46	171.4
00:50	31	130.5	02:20	37	152.3	03:50	42	163.6	05:20	46	171.4
00:55	31	131.9	02:25	37	153.2	03:55	42	164.1	05:25	46	171.6
01:00	31	133.4	02:30	38	153.8	04:00	43	164.2	05:30	46	171.9
01:05	32	134.8	02:35	38	154.6	04:05	43	164.7	05:35	47	172.2
01:10	32	136.2	02:40	38	155.4	04:10	43	165.5	05:40	47	172.5
01:15	33	137.6	02:45	39	156.2	04:15	43	166.0	05:45	47	172.8
01:20	33	138.9	02:50	39	157.3	04:20	44	166.5	05:50	47	172.9
01:25	33	140.2	02:55	39	158.0	04:25	44	167.3	05:55	47	173.4
01:30	34	141.4	03:00	40	158.6	04:30	44	167.9	06:00	47	173.4
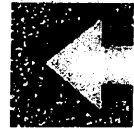
D21

ASTM C 1202-97

Test report

Voltage Used:	60
Testing time:	06:00 hour
Charge passed:	2482
Adjusted Charge passed:	2240
Permeability class:	Moderate
Instrument number:	994704
Channel number:	1
Report date:	6/29/2004
Testing by:	Chris Tuminello
Reference:	OTT-2-28.41
Sample diameter:	100
Comment:	A10(B) - No SIPMF
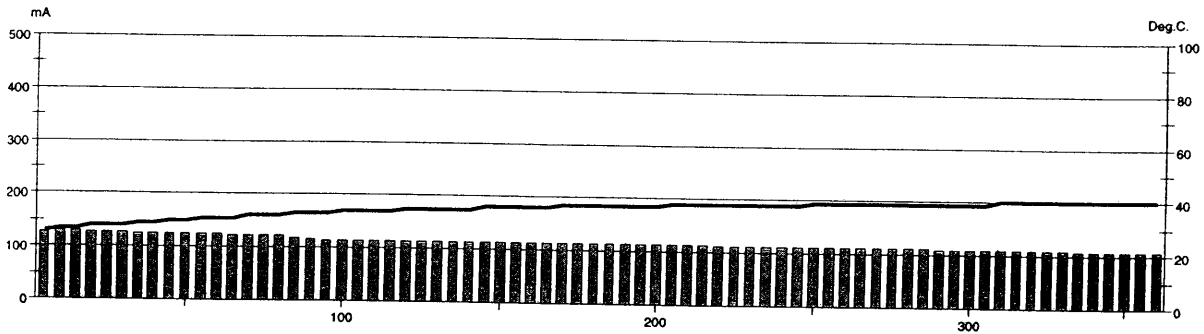
Time	°C	mA	Time	°C	mA	Time	°C	mA	Time	°C	mA
00:05	26	127.3	01:35	33	113.8	03:05	37	113.8	04:35	39	110.8
00:10	27	129.5	01:40	34	113.2	03:10	37	113.7	04:40	39	110.7
00:15	27	128.9	01:45	34	113.1	03:15	37	113.7	04:45	39	110.6
00:20	28	128.3	01:50	34	113.3	03:20	37	113.6	04:50	39	110.2
00:25	28	127.5	01:55	34	113.2	03:25	38	113.3	04:55	39	110.0
00:30	28	126.8	02:00	35	113.2	03:30	38	113.2	05:00	39	109.9
00:35	29	126.1	02:05	35	113.3	03:35	38	112.8	05:05	39	109.7
00:40	29	125.7	02:10	35	113.4	03:40	38	112.7	05:10	40	109.4
00:45	30	125.4	02:15	35	113.5	03:45	38	112.6	05:15	40	109.0
00:50	30	124.8	02:20	35	113.6	03:50	38	112.4	05:20	40	108.8
00:55	31	124.2	02:25	36	113.6	03:55	38	112.3	05:25	40	108.7
01:00	31	124.0	02:30	36	113.6	04:00	38	112.1	05:30	40	108.4
01:05	31	123.3	02:35	36	113.7	04:05	38	111.8	05:35	40	108.2
01:10	32	122.9	02:40	36	113.9	04:10	39	111.8	05:40	40	107.9
01:15	32	121.8	02:45	36	113.8	04:15	39	111.5	05:45	40	107.7
01:20	32	122.6	02:50	37	113.8	04:20	39	111.5	05:50	40	107.6
01:25	33	118.7	02:55	37	113.9	04:25	39	111.2	05:55	40	107.7
01:30	33	115.5	03:00	37	113.8	04:30	39	111.0	06:00	40	107.3

PROOVE it

ASTM C 1202-97

Test report

Voltage Used:	60
Testing time:	06:00 hour
Charge passed:	2474
Adjusted Charge passed:	2233
Permeability class:	Moderate
Instrument number:	994704
Channel number:	7
Report date:	7/2/2004
Testing by:	Chris Tuminello
Reference:	OTT-2-28.41
Sample diameter:	100
Comment:	A15(T) - No SIPMF
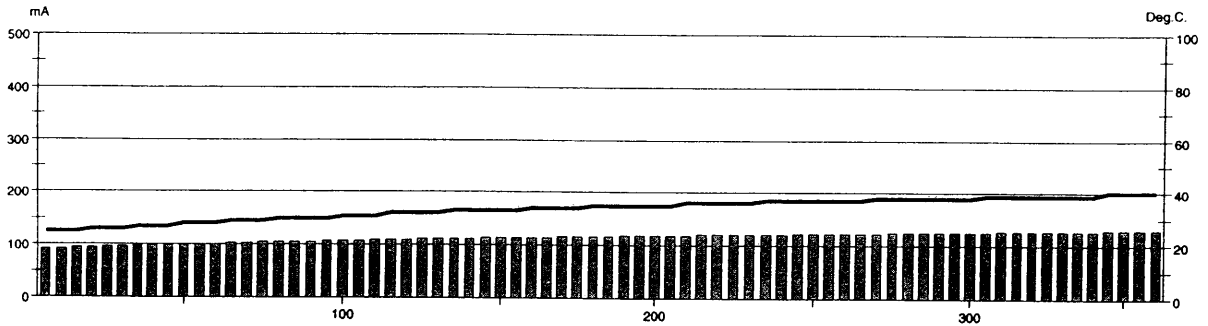
Time	°C	mA	Time	°C	mA	Time	°C	mA	Time	°C	mA
00:05	25	91.1	01:35	30	106.7	03:05	35	116.8	04:35	38	124.0
00:10	25	92.1	01:40	31	107.5	03:10	35	117.3	04:40	38	124.2
00:15	25	93.3	01:45	31	107.9	03:15	35	117.8	04:45	38	124.7
00:20	26	94.5	01:50	31	108.3	03:20	35	118.1	04:50	38	125.1
00:25	26	95.5	01:55	32	109.3	03:25	35	118.5	04:55	38	125.3
00:30	26	96.4	02:00	32	110.1	03:30	36	119.0	05:00	38	125.8
00:35	27	97.2	02:05	32	110.8	03:35	36	119.6	05:05	39	126.1
00:40	27	98.1	02:10	32	111.4	03:40	36	119.9	05:10	39	126.4
00:45	27	99.0	02:15	33	111.8	03:45	36	120.4	05:15	39	126.7
00:50	28	99.9	02:20	33	112.1	03:50	36	120.8	05:20	39	127.2
00:55	28	100.6	02:25	33	112.8	03:55	37	121.3	05:25	39	127.5
01:00	28	101.4	02:30	33	113.5	04:00	37	121.5	05:30	39	127.7
01:05	29	102.4	02:35	33	113.8	04:05	37	121.9	05:35	39	128.0
01:10	29	103.0	02:40	34	114.4	04:10	37	122.2	05:40	39	128.3
01:15	29	103.9	02:45	34	114.9	04:15	37	122.6	05:45	40	128.5
01:20	30	104.6	02:50	34	115.4	04:20	37	123.0	05:50	40	128.8
01:25	30	105.4	02:55	34	115.9	04:25	37	123.3	05:55	40	129.0
01:30	30	106.0	03:00	35	116.2	04:30	38	123.7	06:00	40	129.3
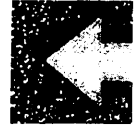
D23

PROOVE it

GERMANN INSTRUMENTS

DENMARK
Phone: +45 3967 7117
Fax: +45 3967 3167
USA
Phone: (847)329-9999
Fax: (847)329-8888

Test report

Voltage Used:	60
Testing time:	06:00 hour
Charge passed:	2335
Adjusted Charge passed:	2107
Permeability class:	Moderate
Instrument number:	994704
Channel number:	1
Report date:	7/13/2004
Testing by:	Chris Tuminello
Reference:	OTT-2-28.41
Sample diameter:	100
Comment:	A15(B) - No SIPMF
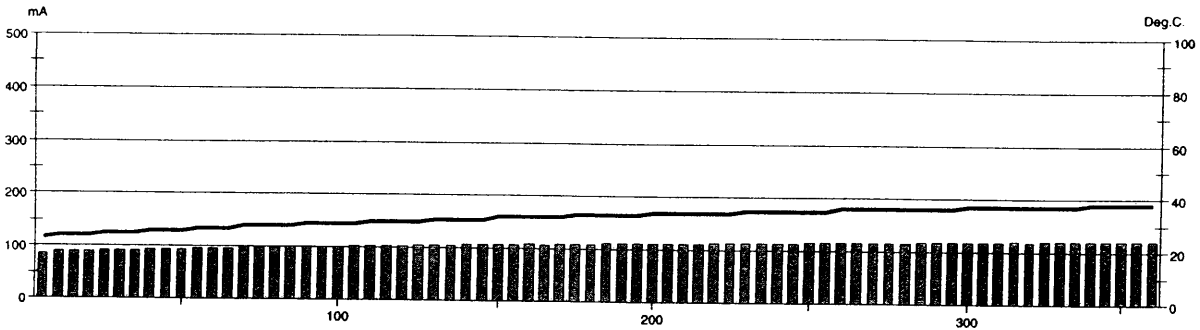
Time	°C	mA	Time	°C	mA	Time	°C	mA	Time	°C	mA
00:05	23	85.9	01:35	29	101.2	03:05	33	110.6	04:35	36	116.9
00:10	24	88.8	01:40	29	101.1	03:10	33	110.8	04:40	36	117.1
00:15	24	89.4	01:45	29	101.9	03:15	33	110.7	04:45	36	117.8
00:20	24	90.2	01:50	30	103.0	03:20	34	111.9	04:50	36	118.0
00:25	25	91.0	01:55	30	103.3	03:25	34	112.3	04:55	36	118.7
00:30	25	91.3	02:00	30	103.5	03:30	34	112.6	05:00	37	119.1
00:35	25	91.6	02:05	30	104.8	03:35	34	112.6	05:05	37	119.0
00:40	26	93.0	02:10	31	105.2	03:40	34	113.6	05:10	37	119.0
00:45	26	93.5	02:15	31	105.5	03:45	34	113.9	05:15	37	119.8
00:50	26	93.8	02:20	31	106.4	03:50	35	113.7	05:20	37	119.4
00:55	27	95.0	02:25	31	106.7	03:55	35	114.5	05:25	37	119.5
01:00	27	95.8	02:30	32	106.6	04:00	35	114.9	05:30	37	119.9
01:05	27	96.0	02:35	32	107.8	04:05	35	114.9	05:35	37	119.7
01:10	28	97.3	02:40	32	108.3	04:10	35	115.5	05:40	38	119.6
01:15	28	97.9	02:45	32	108.1	04:15	35	115.9	05:45	38	120.3
01:20	28	99.0	02:50	32	109.3	04:20	36	115.9	05:50	38	120.3
01:25	28	99.8	02:55	33	109.7	04:25	36	116.5	05:55	38	120.3
01:30	29	100.8	03:00	33	109.8	04:30	36	116.9	06:00	38	120.4

PROOVE it

ASTM C 1202-97

Test report

Voltage Used:	60
Testing time:	06:00 hour
Charge passed:	2090
Adjusted Charge passed:	1886
Permeability class:	Low
Instrument number:	994704
Channel number:	4
Report date:	6/28/2004
Testing by:	Chris Tuminello
Reference:	OTT-2-28.41
Sample diameter:	100
Comment:	B3 - SIPMF
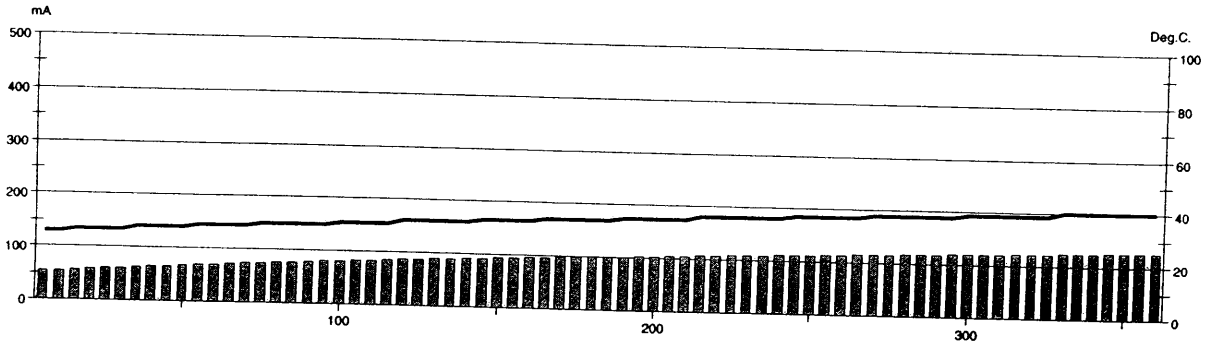
Time	°C	mA	Time	°C	mA	Time	°C	mA	Time	°C	mA
00:05	26	52.8	01:35	30	79.7	03:05	34	100.5	04:35	38	116.6
00:10	26	54.4	01:40	31	81.0	03:10	35	101.5	04:40	38	117.4
00:15	27	56.1	01:45	31	82.3	03:15	35	102.5	04:45	38	118.1
00:20	27	57.7	01:50	31	83.7	03:20	35	103.5	04:50	38	118.8
00:25	27	59.2	01:55	31	84.9	03:25	35	104.5	04:55	38	119.6
00:30	27	60.8	02:00	32	86.2	03:30	35	105.4	05:00	39	120.3
00:35	28	62.3	02:05	32	87.4	03:35	36	106.4	05:05	39	120.9
00:40	28	63.8	02:10	32	88.6	03:40	36	107.4	05:10	39	121.6
00:45	28	65.3	02:15	32	89.7	03:45	36	108.3	05:15	39	122.3
00:50	28	66.8	02:20	32	90.9	03:50	36	109.2	05:20	39	122.9
00:55	29	68.2	02:25	33	92.0	03:55	36	110.1	05:25	39	123.6
01:00	29	69.7	02:30	33	93.1	04:00	36	111.0	05:30	40	124.2
01:05	29	71.2	02:35	33	94.2	04:05	37	111.9	05:35	40	124.9
01:10	29	72.6	02:40	33	95.3	04:10	37	112.7	05:40	40	125.5
01:15	30	74.1	02:45	34	96.3	04:15	37	113.5	05:45	40	126.2
01:20	30	75.5	02:50	34	97.4	04:20	37	114.3	05:50	40	126.8
01:25	30	77.0	02:55	34	98.5	04:25	37	115.1	05:55	40	127.5
01:30	30	78.3	03:00	34	99.5	04:30	38	115.9	06:00	40	128.2

D25

Test report

Voltage Used:	60
Testing time:	06:00 hour
Charge passed:	2490
Adjusted Charge passed:	2247
Permeability class:	Moderate
Instrument number:	994704
Channel number:	7
Report date:	6/29/2004
Testing by:	Chris Tuminello
Reference:	OTT-2-28.41
Sample diameter:	100
Comment:	B6 - SIPMF
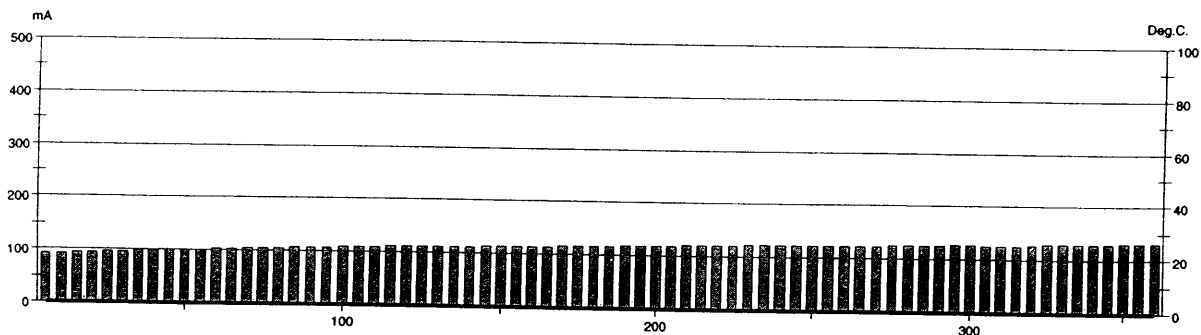
Time	°C	mA	Time	°C	mA	Time	°C	mA	Time	°C	mA
00:05	0	90.7	01:35	0	108.0	03:05	0	116.6	04:35	0	124.9
00:10	0	92.5	01:40	0	108.6	03:10	0	117.3	04:40	0	125.4
00:15	0	93.7	01:45	0	109.1	03:15	0	117.4	04:45	0	126.0
00:20	0	94.8	01:50	0	109.6	03:20	0	118.8	04:50	0	125.8
00:25	0	96.1	01:55	0	110.5	03:25	0	119.2	04:55	0	126.8
00:30	0	97.0	02:00	0	111.0	03:30	0	119.6	05:00	0	126.6
00:35	0	98.0	02:05	0	111.5	03:35	0	120.6	05:05	0	126.1
00:40	0	99.0	02:10	0	111.6	03:40	0	120.7	05:10	0	125.9
00:45	0	99.6	02:15	0	111.8	03:45	0	121.3	05:15	0	125.9
00:50	0	100.7	02:20	0	112.7	03:50	0	121.8	05:20	0	128.3
00:55	0	101.4	02:25	0	113.5	03:55	0	122.0	05:25	0	128.9
01:00	0	102.3	02:30	0	114.3	04:00	0	122.5	05:30	0	128.5
01:05	0	103.0	02:35	0	114.3	04:05	0	122.7	05:35	0	129.3
01:10	0	104.3	02:40	0	114.9	04:10	0	123.0	05:40	0	130.1
01:15	0	105.0	02:45	0	114.9	04:15	0	123.2	05:45	0	130.2
01:20	0	105.8	02:50	0	115.4	04:20	0	123.2	05:50	0	130.7
01:25	0	106.6	02:55	0	115.9	04:25	0	122.9	05:55	0	131.9
01:30	0	107.1	03:00	0	116.4	04:30	0	122.9	06:00	0	132.7
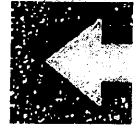
PROOVE it

GERMANN INSTRUMENTS

DENMARK
Phone: +45 3967 7117
Fax: +45 3967 3167

USA
Phone: (847)329-9999
Fax: (847)329-8888

Test report

Voltage Used:	60
Testing time:	06:00 hour
Charge passed:	1639
Adjusted Charge passed:	1479
Permeability class:	Low
Instrument number:	994704
Channel number:	3
Report date:	6/29/2004
Testing by:	Chris Tuminello
Reference:	OTT-2-28.41
Sample diameter:	100
Comment:	C2 - SIPMF
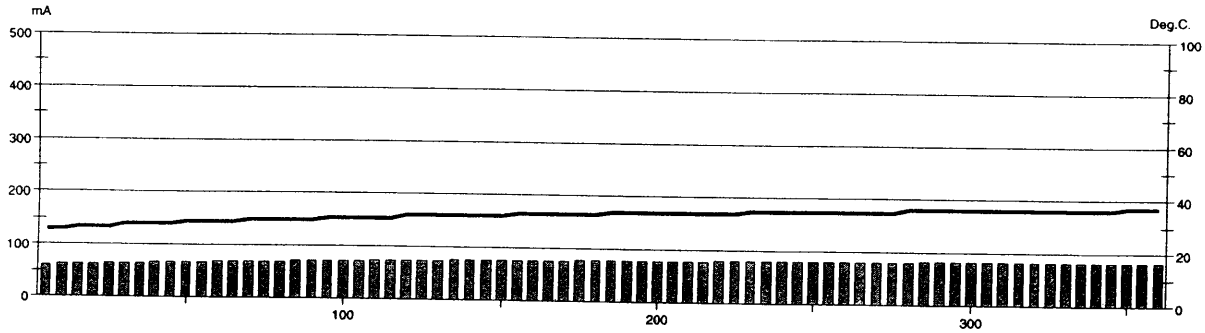
Time	°C	mA	Time	°C	mA	Time	°C	mA	Time	°C	mA
00:05	26	60.8	01:35	31	71.7	03:05	34	77.8	04:35	35	81.3
00:10	26	61.9	01:40	31	72.1	03:10	34	78.0	04:40	36	81.4
00:15	27	62.8	01:45	31	72.5	03:15	34	78.2	04:45	36	81.6
00:20	27	63.6	01:50	31	72.9	03:20	34	78.5	04:50	36	81.7
00:25	27	64.4	01:55	31	73.3	03:25	34	78.7	04:55	36	81.9
00:30	28	65.0	02:00	32	73.7	03:30	34	79.0	05:00	36	82.0
00:35	28	65.6	02:05	32	74.1	03:35	34	79.1	05:05	36	82.1
00:40	28	66.2	02:10	32	74.4	03:40	34	79.3	05:10	36	82.2
00:45	28	66.7	02:15	32	74.8	03:45	34	79.5	05:15	36	82.3
00:50	29	67.3	02:20	32	75.2	03:50	35	79.7	05:20	36	82.4
00:55	29	67.8	02:25	32	75.5	03:55	35	79.9	05:25	36	82.6
01:00	29	68.3	02:30	32	75.8	04:00	35	80.1	05:30	36	82.7
01:05	29	68.9	02:35	33	76.1	04:05	35	80.3	05:35	36	82.8
01:10	30	69.4	02:40	33	76.4	04:10	35	80.5	05:40	36	82.9
01:15	30	69.8	02:45	33	76.6	04:15	35	80.6	05:45	36	82.9
01:20	30	70.3	02:50	33	77.0	04:20	35	80.8	05:50	37	83.1
01:25	30	70.7	02:55	33	77.2	04:25	35	81.0	05:55	37	83.2
01:30	30	71.2	03:00	33	77.5	04:30	35	81.1	06:00	37	83.3
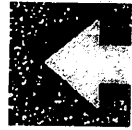
PROOVE it

ASTM C 1202-97

Test report

Voltage Used:	60
Testing time:	06:00 hour
Charge passed:	2315
Adjusted Charge passed:	2089
Permeability class:	Moderate
Instrument number:	994704
Channel number:	5
Report date:	6/30/2004
Testing by:	Chris Tuminello
Reference:	LAK-90-23.42
Sample diameter:	100
Comment:	L9 - SIPMF
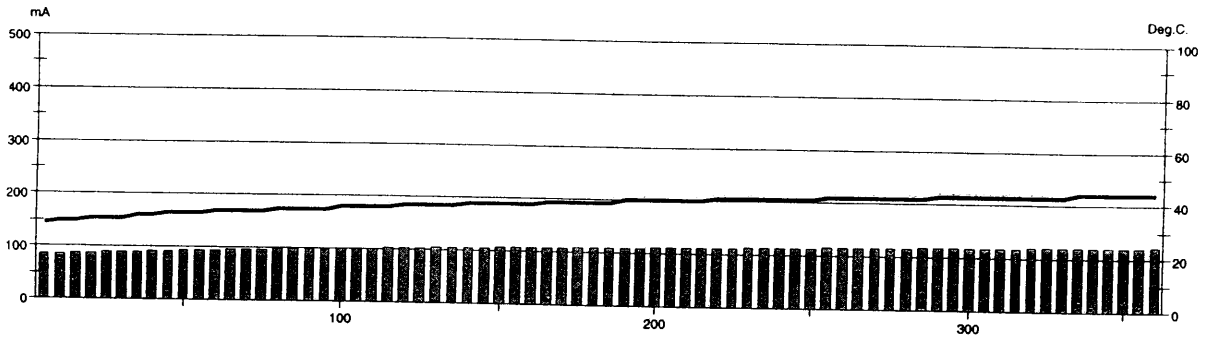
Time	°C	mA	Time	°C	mA	Time	°C	mA	Time	°C	mA
00:05	29	84.9	01:35	35	99.3	03:05	39	109.3	04:35	42	116.7
00:10	30	85.8	01:40	36	100.0	03:10	40	109.7	04:40	42	117.1
00:15	30	86.6	01:45	36	100.6	03:15	40	110.1	04:45	42	117.4
00:20	31	87.3	01:50	36	101.4	03:20	40	110.7	04:50	43	117.6
00:25	31	88.6	01:55	36	101.9	03:25	40	111.1	04:55	43	118.0
00:30	31	89.4	02:00	37	102.8	03:30	40	111.4	05:00	43	118.3
00:35	32	90.4	02:05	37	103.1	03:35	40	111.5	05:05	43	118.7
00:40	32	91.3	02:10	37	103.8	03:40	41	112.0	05:10	43	119.0
00:45	33	92.0	02:15	37	104.5	03:45	41	112.5	05:15	43	119.2
00:50	33	92.8	02:20	38	105.1	03:50	41	112.9	05:20	43	119.6
00:55	33	93.4	02:25	38	105.6	03:55	41	113.5	05:25	43	119.9
01:00	34	94.5	02:30	38	106.2	04:00	41	113.9	05:30	43	120.2
01:05	34	95.0	02:35	38	106.4	04:05	41	114.5	05:35	44	120.4
01:10	34	96.0	02:40	38	106.9	04:10	41	114.9	05:40	44	120.7
01:15	34	96.6	02:45	39	107.4	04:15	42	115.3	05:45	44	120.9
01:20	35	97.2	02:50	39	107.9	04:20	42	115.6	05:50	44	121.3
01:25	35	97.9	02:55	39	108.3	04:25	42	116.1	05:55	44	121.5
01:30	35	98.5	03:00	39	108.8	04:30	42	116.4	06:00	44	121.7
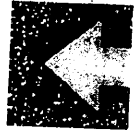
D28

PROOVE it

ASTM C 1202-97

GERMANN INSTRUMENTS

DENMARK
Phone: +45 3967 7117
Fax: +45 3967 3167

USA
Phone: (847)329-9999
Fax: (847)329-8888

Test report

Voltage Used:	60
Testing time:	06:00 hour
Charge passed:	4487
Adjusted Charge passed:	4050
Permeability class:	High
Instrument number:	994704
Channel number:	8
Report date:	7/1/2004
Testing by:	Chris Tuminello
Reference:	OTT-2-28.41
Sample diameter:	100
Comment:	C8 - SIPMF
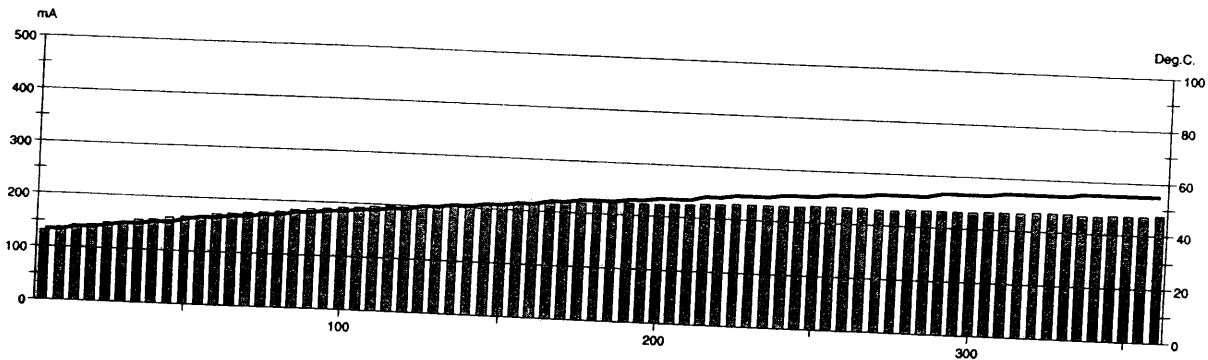
Time	°C	mA	Time	°C	mA	Time	°C	mA	Time	°C	mA
00:05	27	131.1	01:35	37	189.2	03:05	45	221.8	04:35	52	230.8
00:10	27	137.6	01:40	37	191.8	03:10	46	222.8	04:40	52	232.6
00:15	28	142.5	01:45	38	194.1	03:15	46	223.1	04:45	52	232.7
00:20	28	145.9	01:50	38	196.2	03:20	47	223.4	04:50	53	232.7
00:25	29	149.1	01:55	39	198.3	03:25	47	225.4	04:55	53	232.3
00:30	30	152.3	02:00	39	199.9	03:30	47	226.2	05:00	53	232.0
00:35	30	155.5	02:05	40	202.1	03:35	48	226.7	05:05	53	233.5
00:40	31	158.8	02:10	40	204.1	03:40	48	227.8	05:10	54	233.7
00:45	31	161.9	02:15	41	205.9	03:45	49	229.0	05:15	54	233.8
00:50	32	165.1	02:20	41	207.7	03:50	49	229.0	05:20	54	235.7
00:55	33	168.1	02:25	42	209.7	03:55	49	229.4	05:25	54	236.0
01:00	33	171.0	02:30	42	211.2	04:00	50	230.0	05:30	54	236.5
01:05	34	173.8	02:35	43	213.6	04:05	50	230.5	05:35	55	235.1
01:10	34	176.2	02:40	43	215.3	04:10	50	231.9	05:40	55	235.3
01:15	35	179.0	02:45	44	216.5	04:15	51	231.7	05:45	55	235.7
01:20	35	181.7	02:50	44	217.8	04:20	51	232.0	05:50	55	236.0
01:25	36	184.4	02:55	45	219.2	04:25	51	232.2	05:55	55	236.6
01:30	36	186.9	03:00	45	220.5	04:30	52	230.9	06:00	55	237.9
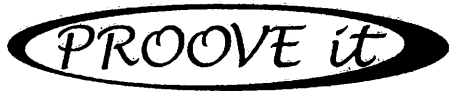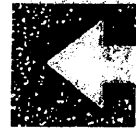
D29

PROOVE it

GERMANN INSTRUMENTS

DENMARK
Phone: +45 3967 7117
Fax: +45 3967 3167

USA
Phone: (847)329-9999
Fax: (847)329-8868

Test report

Voltage Used:	60
Testing time:	06:00 hour
Charge passed:	2726
Adjusted Charge passed:	2460
Permeability class:	Moderate
Instrument number:	994704
Channel number:	8
Report date:	6/30/2004
Testing by:	Chris Tuminello
Reference:	LAK-90-23.42
Sample diameter:	100
Comment:	L2 - SIPMF
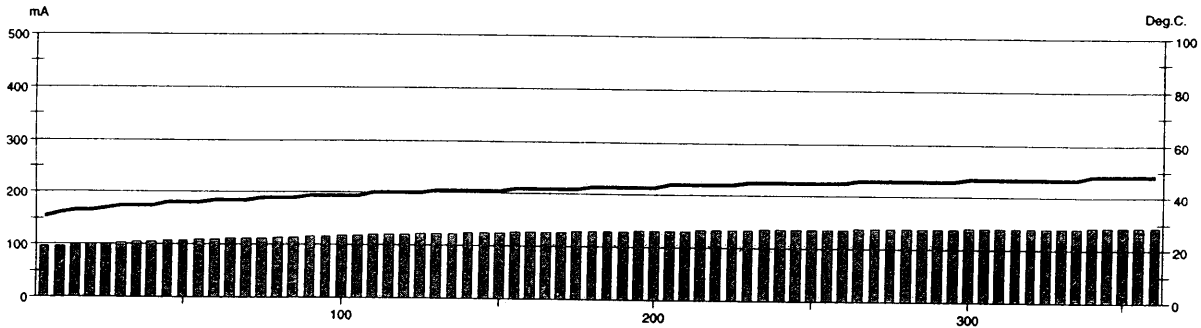
Time	°C	mA	Time	°C	mA	Time	°C	mA	Time	°C	mA
00:05	31	95.4	01:35	39	116.9	03:05	43	129.8	04:35	46	138.2
00:10	32	96.6	01:40	39	117.8	03:10	43	130.4	04:40	46	138.5
00:15	33	98.2	01:45	39	118.7	03:15	43	130.9	04:45	46	138.8
00:20	33	99.8	01:50	40	119.5	03:20	43	131.4	04:50	46	139.1
00:25	34	101.3	01:55	40	120.3	03:25	44	131.9	04:55	46	139.4
00:30	35	102.7	02:00	40	121.1	03:30	44	132.7	05:00	47	139.6
00:35	35	103.8	02:05	40	122.0	03:35	44	133.3	05:05	47	139.9
00:40	35	105.0	02:10	41	122.8	03:40	44	133.8	05:10	47	140.1
00:45	36	106.2	02:15	41	123.5	03:45	44	134.3	05:15	47	140.4
00:50	36	107.4	02:20	41	124.2	03:50	45	134.9	05:20	47	140.7
00:55	36	108.5	02:25	41	124.9	03:55	45	135.3	05:25	47	141.0
01:00	37	109.6	02:30	41	125.6	04:00	45	135.6	05:30	47	141.2
01:05	37	110.6	02:35	42	126.2	04:05	45	136.0	05:35	47	141.7
01:10	37	111.7	02:40	42	126.9	04:10	45	136.4	05:40	48	142.4
01:15	38	112.6	02:45	42	127.5	04:15	45	136.8	05:45	48	142.6
01:20	38	113.8	02:50	42	128.1	04:20	45	137.1	05:50	48	142.9
01:25	38	114.9	02:55	42	128.7	04:25	46	137.5	05:55	48	143.4
01:30	39	116.0	03:00	43	129.3	04:30	46	137.8	06:00	48	143.7
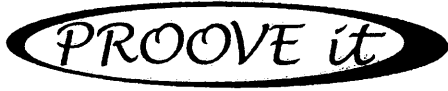
D30

ASTM C 1202-97

Test report

Voltage Used:	60
Testing time:	06:00 hour
Charge passed:	2236
Adjusted Charge passed:	2018
Permeability class:	Moderate
Instrument number:	994704
Channel number:	3
Report date:	6/30/2004
Testing by:	Chris Tuminello
Reference:	LAK-90-23.42
Sample diameter:	100
Comment:	L11 - SIPMF
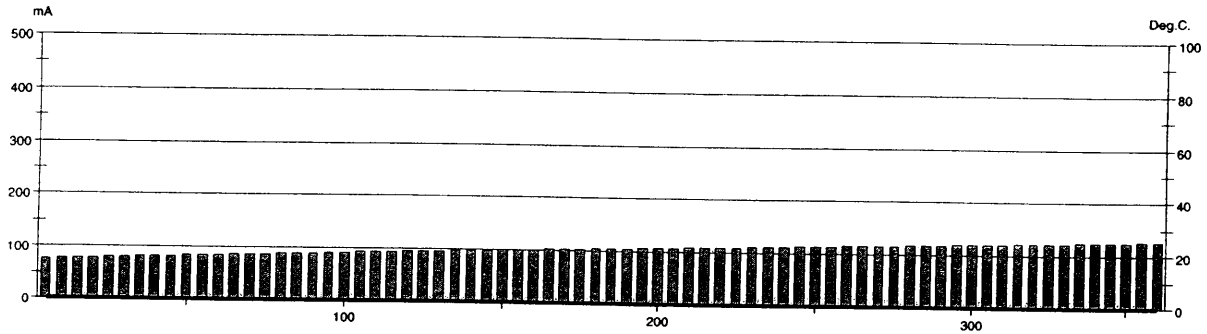
Time	°C	mA	Time	°C	mA	Time	°C	mA	Time	°C	mA
00:05	0	76.8	01:35	0	91.1	03:05	0	104.8	04:35	0	117.1
00:10	0	77.4	01:40	0	91.9	03:10	0	105.5	04:40	0	117.9
00:15	0	78.4	01:45	0	92.7	03:15	0	106.2	04:45	0	118.6
00:20	0	79.2	01:50	0	93.5	03:20	0	106.9	04:50	0	119.2
00:25	0	80.0	01:55	0	94.4	03:25	0	107.7	04:55	0	119.6
00:30	0	80.7	02:00	0	95.2	03:30	0	108.3	05:00	0	120.2
00:35	0	81.6	02:05	0	96.0	03:35	0	109.1	05:05	0	120.8
00:40	0	82.4	02:10	0	96.6	03:40	0	109.7	05:10	0	121.4
00:45	0	83.1	02:15	0	97.4	03:45	0	110.3	05:15	0	122.1
00:50	0	84.0	02:20	0	98.2	03:50	0	111.0	05:20	0	122.7
00:55	0	84.8	02:25	0	98.9	03:55	0	111.8	05:25	0	123.2
01:00	0	85.6	02:30	0	99.6	04:00	0	112.4	05:30	0	123.6
01:05	0	86.4	02:35	0	100.3	04:05	0	113.0	05:35	0	124.2
01:10	0	87.1	02:40	0	101.1	04:10	0	113.7	05:40	0	124.8
01:15	0	87.9	02:45	0	101.9	04:15	0	114.2	05:45	0	125.3
01:20	0	88.6	02:50	0	102.7	04:20	0	115.0	05:50	0	125.9
01:25	0	89.4	02:55	0	103.4	04:25	0	115.7	05:55	0	126.5
01:30	0	90.2	03:00	0	104.1	04:30	0	116.2	06:00	0	126.9

ASTM C 1202-97
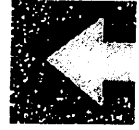
Test report

Voltage Used:	60
Testing time:	06:00 hour
Charge passed:	1667
Adjusted Charge passed:	1504
Permeability class:	Low
Instrument number:	994704
Channel number:	2
Report date:	6/30/2004
Testing by:	Chris Tuminello
Reference:	LAK-90-23.42
Sample diameter:	100
Comment:	L14 - SIPMF
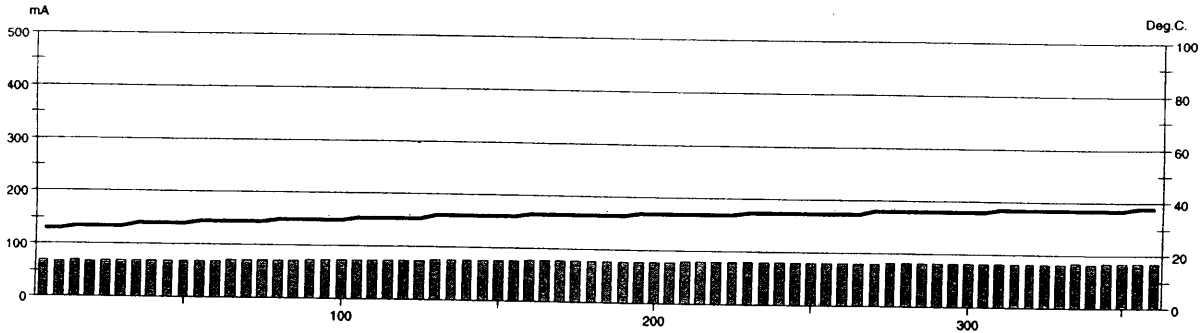
Time	°C	mA	Time	°C	mA	Time	°C	mA	Time	°C	mA
00:05	26	69.0	01:35	30	73.1	03:05	33	78.4	04:35	36	81.5
00:10	26	68.0	01:40	30	73.3	03:10	33	78.9	04:40	36	81.6
00:15	27	68.1	01:45	31	73.3	03:15	34	79.0	04:45	36	81.7
00:20	27	68.0	01:50	31	74.2	03:20	34	78.8	04:50	36	82.1
00:25	27	68.2	01:55	31	73.8	03:25	34	78.8	04:55	36	82.4
00:30	27	68.5	02:00	31	74.6	03:30	34	79.7	05:00	36	82.4
00:35	28	68.8	02:05	31	74.6	03:35	34	79.9	05:05	36	82.5
00:40	28	69.3	02:10	32	75.5	03:40	34	79.9	05:10	37	83.0
00:45	28	69.6	02:15	32	75.2	03:45	34	80.3	05:15	37	83.1
00:50	28	69.6	02:20	32	75.4	03:50	35	80.0	05:20	37	83.4
00:55	29	70.0	02:25	32	76.5	03:55	35	80.8	05:25	37	83.3
01:00	29	70.3	02:30	32	76.8	04:00	35	80.5	05:30	37	83.4
01:05	29	70.7	02:35	32	76.8	04:05	35	80.8	05:35	37	83.8
01:10	29	71.2	02:40	33	77.3	04:10	35	80.6	05:40	37	83.7
01:15	29	71.6	02:45	33	77.3	04:15	35	81.2	05:45	37	83.8
01:20	30	71.6	02:50	33	77.4	04:20	35	81.3	05:50	37	84.0
01:25	30	72.1	02:55	33	78.2	04:25	35	81.4	05:55	38	84.6
01:30	30	73.0	03:00	33	78.5	04:30	36	81.3	06:00	38	84.3
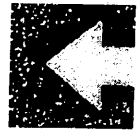
D32

ASTM C 1202-97

Test report

Voltage Used:	60
Testing time:	06:00 hour
Charge passed:	2849
Adjusted Charge passed:	2571
Permeability class:	Moderate
Instrument number:	994704
Channel number:	6
Report date:	6/30/2004
Testing by:	Chris Tuminello
Reference:	LAK-90-23.42
Sample diameter:	100
Comment:	L16 - SIPMF
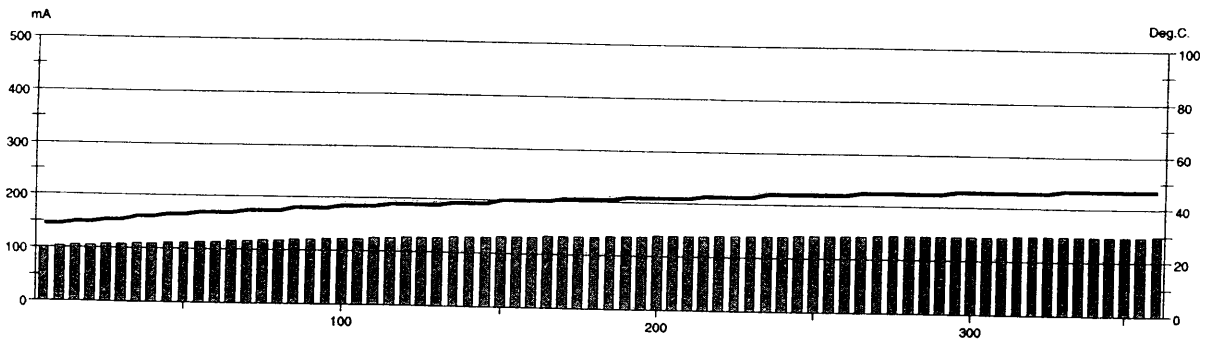
Time	°C	mA	Time	°C	mA	Time	°C	mA	Time	°C	mA
00:05	29	101.1	01:35	36	122.0	03:05	41	135.6	04:35	45	144.6
00:10	29	102.4	01:40	37	122.9	03:10	42	136.2	04:40	45	144.9
00:15	30	103.9	01:45	37	123.8	03:15	42	136.7	04:45	45	145.2
00:20	30	105.3	01:50	37	124.8	03:20	42	137.3	04:50	45	145.6
00:25	31	106.6	01:55	38	125.7	03:25	42	137.9	04:55	46	146.0
00:30	31	107.9	02:00	38	126.6	03:30	42	138.4	05:00	46	145.8
00:35	32	109.1	02:05	38	127.4	03:35	43	139.1	05:05	46	146.0
00:40	32	110.3	02:10	38	128.3	03:40	43	139.7	05:10	46	146.2
00:45	33	111.5	02:15	39	129.0	03:45	43	140.1	05:15	46	146.5
00:50	33	112.7	02:20	39	129.8	03:50	43	140.6	05:20	46	146.9
00:55	34	113.8	02:25	39	130.5	03:55	44	141.1	05:25	46	147.2
01:00	34	114.9	02:30	40	131.1	04:00	44	141.5	05:30	47	147.5
01:05	34	116.0	02:35	40	131.9	04:05	44	142.0	05:35	47	147.6
01:10	35	117.0	02:40	40	132.6	04:10	44	142.8	05:40	47	147.8
01:15	35	118.1	02:45	40	133.3	04:15	44	143.2	05:45	47	147.9
01:20	35	119.1	02:50	41	133.9	04:20	44	143.6	05:50	47	148.1
01:25	36	120.0	02:55	41	134.5	04:25	45	143.8	05:55	47	148.4
01:30	36	121.0	03:00	41	135.0	04:30	45	144.2	06:00	47	148.7
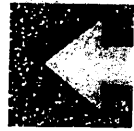
PROOVE it

ASTM C 1202-97

Test report

Voltage Used:	60
Testing time:	06:00 hour
Charge passed:	4407
Adjusted Charge passed:	3977
Permeability class:	Moderate
Instrument number:	994704
Channel number:	1
Report date:	6/30/2004
Testing by:	Chris Tuminello
Reference:	LAK-90-23.42
Sample diameter:	100
Comment:	L27 - No SIPMF
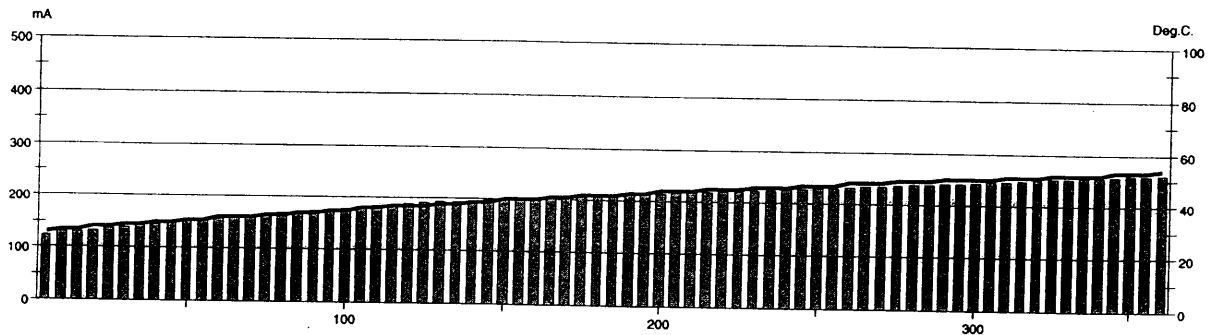
Time	°C	mA	Time	°C	mA	Time	°C	mA	Time	°C	mA
00:05	26	122.9	01:35	35	177.3	03:05	42	211.1	04:35	49	236.4
00:10	27	128.8	01:40	35	179.5	03:10	43	212.1	04:40	49	237.8
00:15	27	129.4	01:45	36	182.1	03:15	43	213.2	04:45	49	239.2
00:20	28	132.2	01:50	36	184.9	03:20	44	214.5	04:50	50	240.5
00:25	28	135.8	01:55	37	187.2	03:25	44	216.1	04:55	50	242.0
00:30	29	139.5	02:00	37	189.2	03:30	44	217.9	05:00	50	243.7
00:35	29	142.7	02:05	37	191.2	03:35	45	218.9	05:05	50	245.2
00:40	30	145.8	02:10	38	193.5	03:40	45	220.2	05:10	51	246.6
00:45	30	148.5	02:15	38	195.2	03:45	45	221.5	05:15	51	248.0
00:50	31	151.4	02:20	39	197.1	03:50	46	223.0	05:20	51	249.9
00:55	31	154.3	02:25	39	198.4	03:55	46	224.3	05:25	52	251.2
01:00	32	157.2	02:30	40	200.4	04:00	46	226.2	05:30	52	252.6
01:05	32	160.3	02:35	40	202.4	04:05	47	228.3	05:35	52	254.1
01:10	32	163.1	02:40	40	203.4	04:10	47	229.2	05:40	52	255.5
01:15	33	166.0	02:45	41	205.0	04:15	47	230.5	05:45	53	256.8
01:20	33	169.2	02:50	41	207.1	04:20	48	231.9	05:50	53	258.2
01:25	34	171.8	02:55	42	208.4	04:25	48	233.4	05:55	53	260.0
01:30	34	174.8	03:00	42	209.8	04:30	48	234.9	06:00	54	260.8
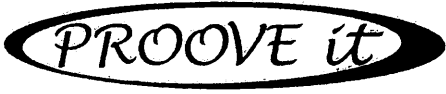
D34

PROOVE it

ASTM C 1202-97

GERMANN INSTRUMENTS

DENMARK
Phone: +45 3967 7117
Fax: +45 3967 3167

USA
Phone: (847)329-9999
Fax: (847)329-8888

Test report

Voltage Used:	60
Testing time:	06:00 hour
Charge passed:	2887
Adjusted Charge passed:	2606
Permeability class:	Moderate
Instrument number:	994704
Channel number:	5
Report date:	7/1/2004
Testing by:	Chris Tuminello
Reference:	LAK-90-23.42
Sample diameter:	100
Comment:	L30 - No SIPMF
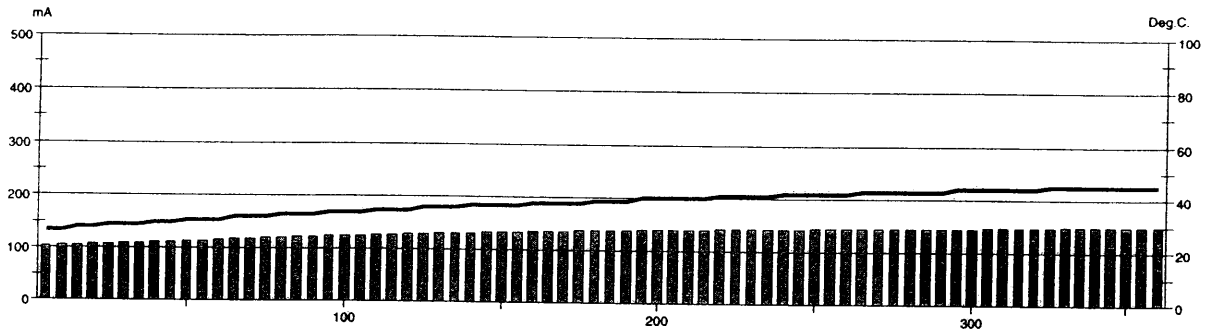
Time	°C	mA	Time	°C	mA	Time	°C	mA	Time	°C	mA
00:05	27	103.3	01:35	34	124.2	03:05	39	138.2	04:35	43	145.3
00:10	27	104.3	01:40	34	125.1	03:10	39	138.9	04:40	43	145.7
00:15	28	105.6	01:45	34	126.1	03:15	40	139.7	04:45	43	145.5
00:20	28	106.8	01:50	35	127.2	03:20	40	140.2	04:50	43	146.0
00:25	29	107.9	01:55	35	128.2	03:25	40	140.3	04:55	44	146.2
00:30	29	108.9	02:00	35	129.0	03:30	40	141.2	05:00	44	146.2
00:35	29	110.0	02:05	36	129.7	03:35	40	141.4	05:05	44	147.0
00:40	30	111.3	02:10	36	130.7	03:40	41	141.8	05:10	44	147.5
00:45	30	112.4	02:15	36	131.8	03:45	41	142.4	05:15	44	147.7
00:50	31	113.7	02:20	37	132.3	03:50	41	143.0	05:20	44	148.2
00:55	31	114.9	02:25	37	133.1	03:55	41	143.0	05:25	45	148.4
01:00	31	116.1	02:30	37	133.6	04:00	42	143.3	05:30	45	148.9
01:05	32	117.5	02:35	37	134.7	04:05	42	143.7	05:35	45	149.0
01:10	32	118.1	02:40	38	135.4	04:10	42	144.2	05:40	45	148.8
01:15	32	119.5	02:45	38	136.1	04:15	42	144.7	05:45	45	148.7
01:20	33	120.9	02:50	38	136.5	04:20	42	144.8	05:50	45	148.8
01:25	33	122.3	02:55	38	137.5	04:25	43	145.0	05:55	45	149.2
01:30	33	123.3	03:00	39	137.8	04:30	43	145.0	06:00	45	149.1
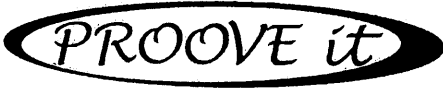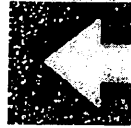
PROOVE it

ASTM C 1202-97

Test report

Voltage Used:	60
Testing time:	06:00 hour
Charge passed:	4767
Adjusted Charge passed:	4302
Permeability class:	High
Instrument number:	994704
Channel number:	5
Report date:	6/29/2004
Testing by:	Chris Tuminello
Reference:	LAK-90-23.42
Sample diameter:	100
Comment:	L33 - No SIPMF
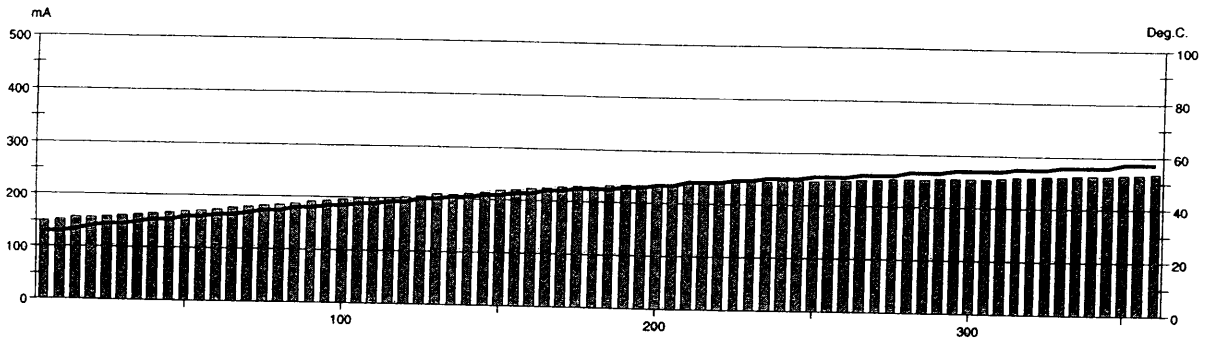
Time	°C	mA	Time	°C	mA	Time	°C	mA	Time	°C	mA
00:05	26	149.1	01:35	37	193.5	03:05	45	232.5	04:35	52	251.2
00:10	26	152.5	01:40	37	195.7	03:10	46	233.6	04:40	53	251.9
00:15	27	155.2	01:45	38	198.0	03:15	46	234.4	04:45	53	252.9
00:20	28	157.2	01:50	38	199.9	03:20	47	236.0	04:50	53	253.7
00:25	29	158.9	01:55	39	201.9	03:25	47	236.6	04:55	54	254.3
00:30	29	160.9	02:00	39	204.0	03:30	48	238.1	05:00	54	255.0
00:35	30	163.0	02:05	40	206.4	03:35	48	239.6	05:05	54	255.3
00:40	31	165.3	02:10	40	209.1	03:40	48	241.0	05:10	54	256.7
00:45	31	167.6	02:15	41	210.3	03:45	49	242.1	05:15	55	258.0
00:50	32	170.1	02:20	41	211.7	03:50	49	242.9	05:20	55	259.1
00:55	32	172.5	02:25	42	215.1	03:55	50	243.6	05:25	55	260.5
01:00	33	175.1	02:30	42	219.3	04:00	50	244.7	05:30	56	262.1
01:05	33	178.0	02:35	43	221.1	04:05	50	246.1	05:35	56	263.6
01:10	34	180.4	02:40	43	223.2	04:10	51	246.4	05:40	56	264.1
01:15	35	183.0	02:45	44	225.2	04:15	51	247.3	05:45	56	264.3
01:20	35	186.0	02:50	44	226.7	04:20	51	248.4	05:50	57	265.1
01:25	36	188.5	02:55	45	228.9	04:25	52	249.2	05:55	57	266.4
01:30	36	191.1	03:00	45	230.6	04:30	52	250.9	06:00	57	267.1
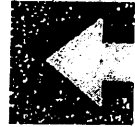
D36

PROOVE it

ASTM C 1202-97

Test report

Voltage Used:	60
Testing time:	06:00 hour
Charge passed:	6865
Adjusted Charge passed:	6196
Permeability class:	High
Instrument number:	994704
Channel number:	4
Report date:	6/30/2004
Testing by:	Chris Tuminello
Reference:	LAK-90-23.42
Sample diameter:	100
Comment:	L35 - No SIPMF
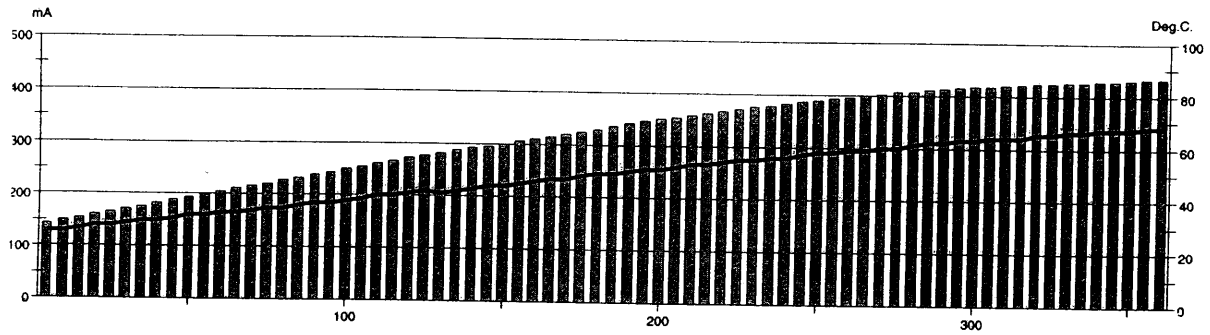
Time	°C	mA	Time	°C	mA	Time	°C	mA	Time	°C	mA
00:05	26	143.1	01:35	37	243.7	03:05	49	335.0	04:35	60	405.5
00:10	26	149.5	01:40	38	249.3	03:10	50	340.7	04:40	61	407.0
00:15	27	155.0	01:45	39	254.8	03:15	51	345.3	04:45	62	409.9
00:20	28	160.6	01:50	40	260.3	03:20	51	350.0	04:50	62	412.0
00:25	28	165.9	01:55	40	266.3	03:25	52	353.7	04:55	63	414.6
00:30	29	171.4	02:00	41	271.8	03:30	53	357.2	05:00	63	416.8
00:35	30	176.7	02:05	42	276.9	03:35	53	362.1	05:05	64	418.1
00:40	30	182.6	02:10	41	281.4	03:40	54	365.8	05:10	64	420.3
00:45	31	188.8	02:15	42	287.0	03:45	55	370.2	05:15	64	421.5
00:50	32	194.1	02:20	43	291.4	03:50	55	374.6	05:20	65	423.8
00:55	32	200.3	02:25	44	295.4	03:55	56	377.8	05:25	65	424.6
01:00	33	206.2	02:30	44	300.1	04:00	56	382.2	05:30	66	425.5
01:05	33	211.7	02:35	45	305.0	04:05	57	385.9	05:35	66	427.4
01:10	34	216.9	02:40	46	309.7	04:10	58	389.3	05:40	67	429.2
01:15	35	222.0	02:45	47	314.4	04:15	58	392.5	05:45	67	429.1
01:20	35	227.2	02:50	47	319.1	04:20	59	395.7	05:50	67	431.3
01:25	36	233.1	02:55	48	324.0	04:25	59	399.4	05:55	68	432.4
01:30	37	238.4	03:00	49	329.1	04:30	60	402.6	06:00	68	432.6

Appendix E
Chloride Ion Test Results

S1

AgNO$_3$	mv	d mL	d mV	d mV/dmL		Temp
0	210.8					22.3
5	236.2	5.00	25.40	5.08		22.4
7	262.6	2.00	26.40	13.20	8.12	22.4
7.5	275.9	0.50	13.30	26.60	13.40	22.4
7.8	290.7	0.30	14.80	49.33	22.73	22.4
8	309.6	0.20	18.90	94.50	45.17	22.4
8.2	326.3	0.20	16.70	83.50	-11.00	22.5
8.4	338.9	0.20	12.60	63.00	-20.50	22.5
8.6	348.5	0.20	9.60	48.00	-15.00	22.5
8.8	354.6	0.20	6.10	30.50	-17.50	22.5

S1 1

E1

S1
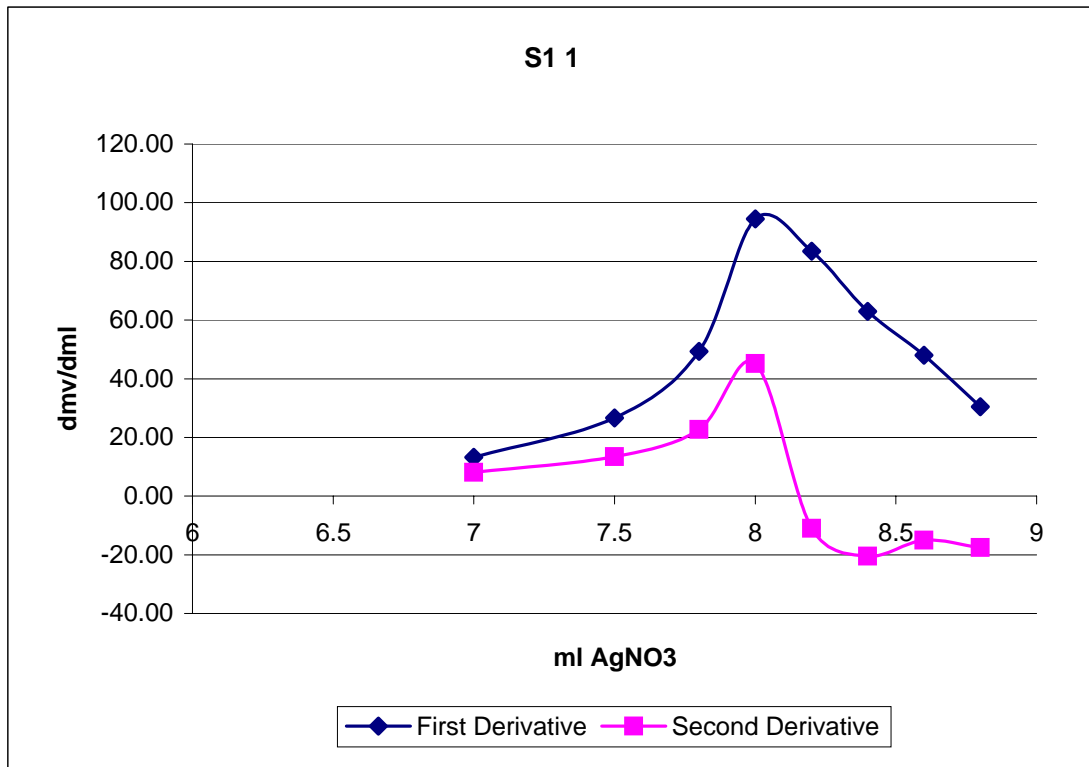
AgNO$_3$	mv	d mL	d mV	d mV/dmL		Temp
0	215.9					22.4
5	254.9	5.00	39.00	7.80		22.5
6	282.7	1.00	27.80	27.80	20.00	22.5
6.2	296.2	0.20	13.50	67.50	39.70	22.5
6.4	312.3	0.20	16.10	80.50	13.00	22.5
6.6	328.8	0.20	16.50	82.50	2.00	22.5
6.8	339.3	0.20	10.50	52.50	-30.00	22.5
7	347.3	0.20	8.00	40.00	-12.50	22.5
7.2	353.5	0.20	6.20	31.00	-9.00	22.5
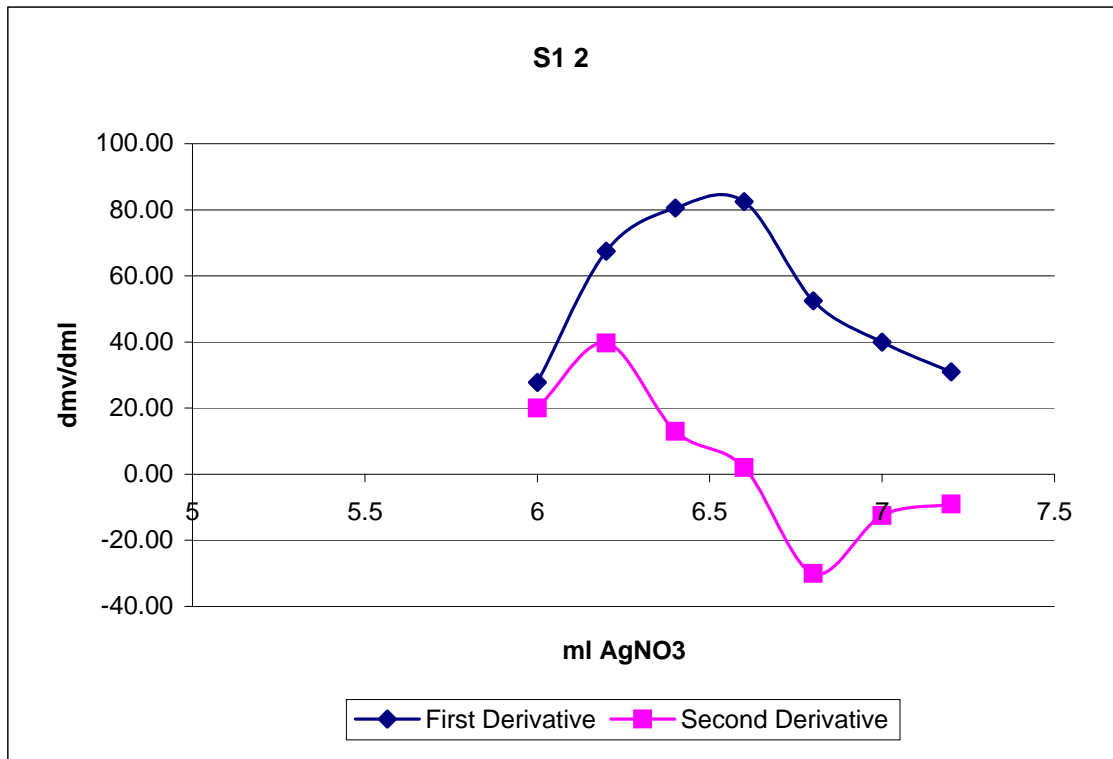
S1

3

AgNO$_3$	mv	d mL	d mV	d mV/dmL		Temp
0	224.3					22.4
4	240.6	4.00	16.30	4.08		22.5
6	255.9	2.00	15.30	7.65	3.58	22.5
7	268.3	1.00	12.40	12.40	4.75	22.5
7.5	277.6	0.50	9.30	18.60	6.20	22.5
7.8	288.2	0.30	10.60	35.33	16.73	22.5
8	295.1	0.20	6.90	34.50	-0.83	22.5
8.2	303.9	0.20	8.80	44.00	9.50	22.5
8.4	313.4	0.20	9.50	47.50	3.50	22.6
8.6	324.8	0.20	11.40	57.00	9.50	22.6
8.8	334.6	0.20	9.80	49.00	-8.00	22.6
9	340.8	0.20	6.20	31.00	-18.00	22.6
9.2	346.1	0.20	5.30	26.50	-4.50	22.6
9.4	352.1	0.20	6.00	30.00	3.50	22.6
9.6	357	0.20	4.90	24.50	-5.50	22.6

E3

S1
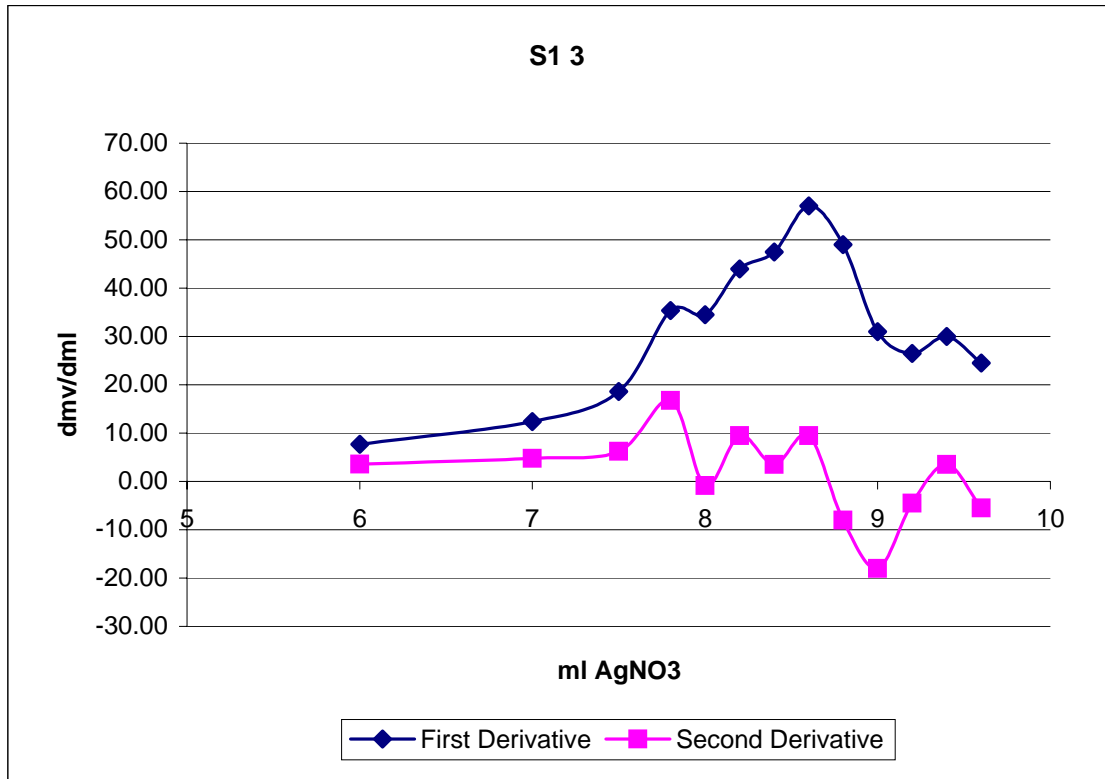
AgNO$_3$	mv	d mL	d mV	d mV/dmL		Temp
0	228.4					22.4
4	253.3	4.00	24.90	6.23		22.5
5	266.3	1.00	13.00	13.00	6.78	22.5
5.3	272.8	0.30	6.50	21.67	8.67	22.5
5.5	277.7	0.20	4.90	24.50	2.83	22.5
5.7	284.1	0.20	6.40	32.00	7.50	22.5
5.9	291.2	0.20	7.10	35.50	3.50	22.5
6.1	298.9	0.20	7.70	38.50	3.00	22.5
6.3	312.6	0.20	13.70	68.50	30.00	22.5
6.5	324.6	0.20	12.00	60.00	-8.50	22.5
6.7	336.5	0.20	11.90	59.50	-0.50	22.5
6.9	346.1	0.20	9.60	48.00	-11.50	22.5
7.1	352.7	0.20	6.60	33.00	-15.00	22.5
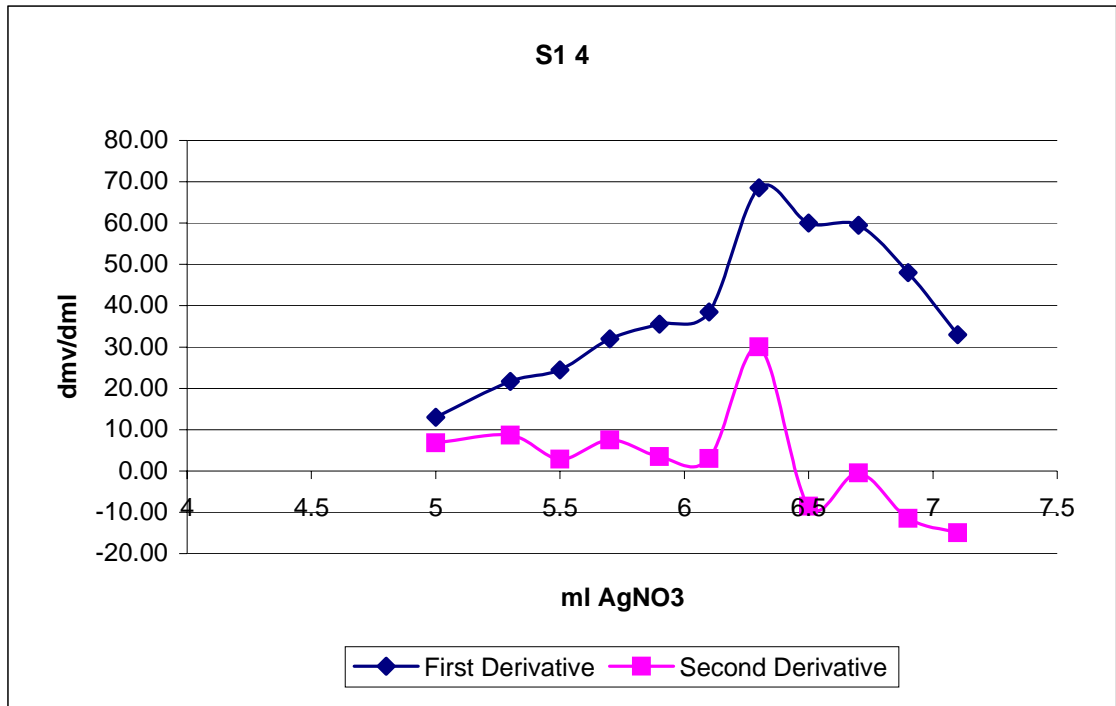
S2

1

AgNO₃ (ml)	mv	d mL	d mV	d mV/dmL		Temp C
0.0	225.0					21.7
2.0	231.2	2.0	6.2	3.1		21.8
4.0	238.7	2.0	7.5	3.8	0.7	21.8
5.0	243.3	1.0	4.6	4.6	0.9	21.8
5.2	244.5	0.2	1.2	6.0	1.4	21.8
5.4	245.7	0.2	1.2	6.0	0.0	21.9
5.6	247.1	0.2	1.4	7.0	1.0	21.9
5.8	248.2	0.2	1.1	5.5	-1.5	21.9
6.0	249.6	0.2	1.4	7.0	1.5	21.9
6.2	251.1	0.2	1.5	7.5	0.5	21.9
6.4	252.8	0.2	1.7	8.5	1.0	21.9
6.6	253.9	0.2	1.1	5.5	-3.0	21.9
6.8	256.3	0.2	2.4	12.0	6.5	22.0
7.0	257.7	0.2	1.4	7.0	-5.0	22.0
7.2	259.8	0.2	2.1	10.5	3.5	22.0
7.4	261.7	0.2	1.9	9.5	-1.0	22.0
7.7	264.9	0.3	3.2	12.8	3.3	22.0
7.8	266.3	0.1	1.4	9.3	-3.5	22.0
8.0	269.1	0.2	2.8	14.0	4.7	22.0
8.2	272.4	0.2	3.3	16.5	2.5	22.0
8.4	276.1	0.2	3.7	18.5	2.0	22.0
8.6	280.1	0.2	4.0	20.0	1.5	22.0
8.8	283.8	0.2	3.7	18.5	-1.5	22.1
9.0	289.4	0.2	5.6	28.0	9.5	22.1
9.2	296.6	0.2	7.2	36.0	8.0	22.1
9.4	303.6	0.2	7.0	35.0	-1.0	22.1
9.7	314.5	0.3	10.9	43.6	8.6	22.1
9.8	321.2	0.2	6.7	44.7	1.1	22.1
10.0	329.7	0.2	8.5	42.5	-2.2	22.1
10.2	337.7	0.2	8.0	40.0	-2.5	22.2
10.4	342.1	0.2	4.4	22.0	-18.0	22.2
10.6	349.2	0.2	7.1	35.5	13.5	22.2
10.8	353.5	0.2	4.3	21.5	-14.0	22.2
11.0	357.3	0.2	3.8	19.0	-2.5	22.2
11.2	361.7	0.2	4.4	22.0	3.0	22.2
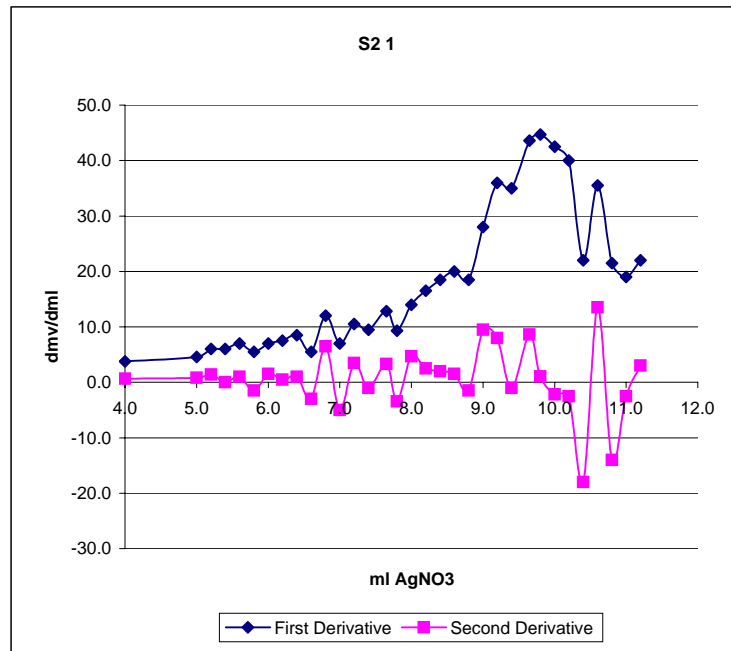
2 AgNO$_3$ (ml)		mv	d mL	d mV	d mV/dmL		Temp C
12.0	0.0	237.9					22.0
13.5	1.5	243.7	1.5	5.8	3.9		22.1
13.7	1.7	244.6	0.2	0.9	4.5	0.6	22.1
13.9	1.9	245.4	0.2	0.8	4.0	-0.5	22.1
14.1	2.1	246.4	0.2	1.0	5.0	1.0	22.1
14.3	2.3	247.4	0.2	1.0	5.0	0.0	22.1
14.5	2.5	248.2	0.2	0.8	4.0	-1.0	22.2
14.7	2.7	249.1	0.2	0.9	4.5	0.5	22.2
14.9	2.9	250.0	0.2	0.9	4.5	0.0	22.2
15.1	3.1	251.3	0.2	1.3	6.5	2.0	22.2
15.3	3.3	252.2	0.2	0.9	4.5	-2.0	22.2
15.5	3.5	253.7	0.2	1.5	7.5	3.0	22.2
15.8	3.8	255.4	0.3	1.7	5.7	-1.8	22.2
16.0	4.0	257.1	0.2	1.7	8.5	2.8	22.2
16.2	4.2	258.4	0.2	1.3	6.5	-2.0	22.2
16.4	4.4	260.1	0.2	1.7	8.5	2.0	22.2
16.6	4.6	261.7	0.2	1.6	8.0	-0.5	22.3
16.8	4.8	263.5	0.2	1.8	9.0	1.0	22.3
17.0	5.0	265.7	0.2	2.2	11.0	2.0	22.3
17.2	5.2	267.7	0.2	2.0	10.0	-1.0	22.3
17.4	5.4	270.3	0.2	2.6	13.0	3.0	22.3
17.6	5.6	272.2	0.2	1.9	9.5	-3.5	22.3
17.8	5.8	275.8	0.2	3.6	18.0	8.5	22.3
18.0	6.0	279.0	0.2	3.2	16.0	-2.0	22.3
18.2	6.2	282.4	0.2	3.4	17.0	1.0	22.3
18.4	6.4	286.7	0.2	4.3	21.5	4.5	22.4
18.6	6.6	291.1	0.2	4.4	22.0	0.5	22.4
18.8	6.8	299.2	0.2	8.1	40.5	18.5	22.4
19.0	7.0	305.1	0.2	5.9	29.5	-11.0	22.4
19.2	7.2	311.9	0.2	6.8	34.0	4.5	22.4
19.4	7.4	321.8	0.2	9.9	49.5	15.5	22.4
19.6	7.6	331.4	0.2	9.6	48.0	-1.5	22.4
19.8	7.8	339.4	0.2	8.0	40.0	-8.0	22.5
20.1	8.1	349.3	0.3	9.9	33.0	-7.0	22.5
20.4	8.4	354.7	0.3	5.4	21.6	-11.4	22.5
20.5	8.5	359.0	0.1	4.3	28.7	7.1	22.5
20.7	8.7	362.5	0.2	3.5	17.5	-11.2	22.5

S2 2

First Derivative   Second Derivative

ml AgNO3
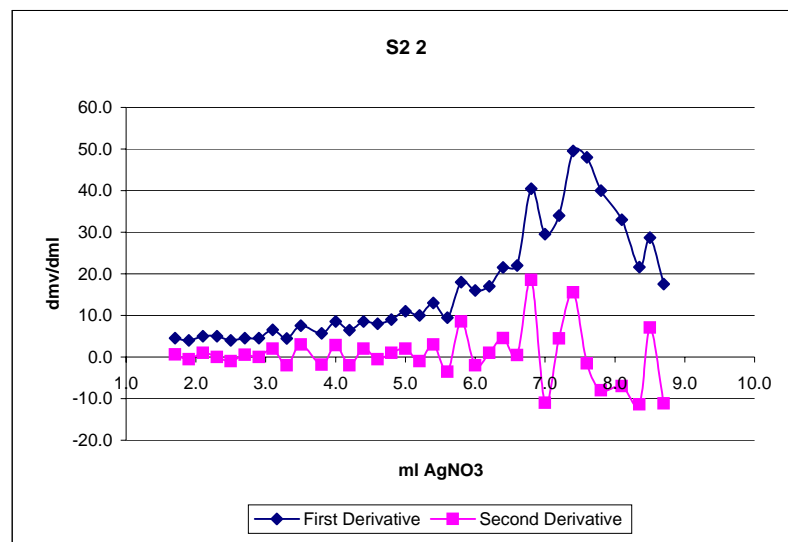
dmv/dml

S2

3

AgNO$_3$ (ml)		mv	d mL	d mV	d mV/dmL		Temp C
21.5	0.0	238.7					22.3
23.0	1.5	244.5	1.5	5.8	3.9		22.3
23.5	2.0	246.8	0.5	2.3	4.6	0.7	22.3
24.0	2.5	248.6	0.5	1.8	3.6	-1.0	22.3
24.5	3.0	251.4	0.5	2.8	5.6	2.0	22.3
25.0	3.5	254.1	0.5	2.7	5.4	-0.2	22.4
25.5	4.0	257.6	0.5	3.5	7.0	1.6	22.4
26.0	4.5	261.1	0.5	3.5	7.0	0.0	22.4
26.2	4.7	262.9	0.2	1.8	9.0	2.0	22.4
26.4	4.9	264.8	0.2	1.9	9.5	0.5	22.4
26.6	5.1	266.8	0.2	2.0	10.0	0.5	22.4
26.8	5.3	269.3	0.2	2.5	12.5	2.5	22.4
27.0	5.5	271.8	0.2	2.5	12.5	0.0	22.4
27.2	5.7	273.6	0.2	1.8	9.0	-3.5	22.4
27.4	5.9	277.1	0.2	3.5	17.5	8.5	22.4
27.6	6.1	280.5	0.2	3.4	17.0	-0.5	22.4
27.8	6.3	286.3	0.2	5.8	29.0	12.0	22.5
28.0	6.5	292.0	0.2	5.7	28.5	-0.5	22.5
28.2	6.7	296.9	0.2	4.9	24.5	-4.0	22.5
28.4	6.9	303.7	0.2	6.8	34.0	9.5	22.5
28.6	7.1	311.9	0.2	8.2	41.0	7.0	22.5
28.8	7.3	320.4	0.2	8.5	42.5	1.5	22.5
29.0	7.5	329.7	0.2	9.3	46.5	4.0	22.5
29.2	7.7	337.0	0.2	7.3	36.5	-10.0	22.5
29.4	7.9	345.0	0.2	8.0	40.0	3.5	22.6
29.7	8.2	351.1	0.3	6.1	24.4	-15.6	22.6
29.9	8.4	355.6	0.3	4.5	18.0	-6.4	22.6
30.1	8.6	359.0	0.2	3.4	17.0	-1.0	22.6
30.3	8.8	362.5	0.2	3.5	17.5	0.5	22.6

S2 3

4
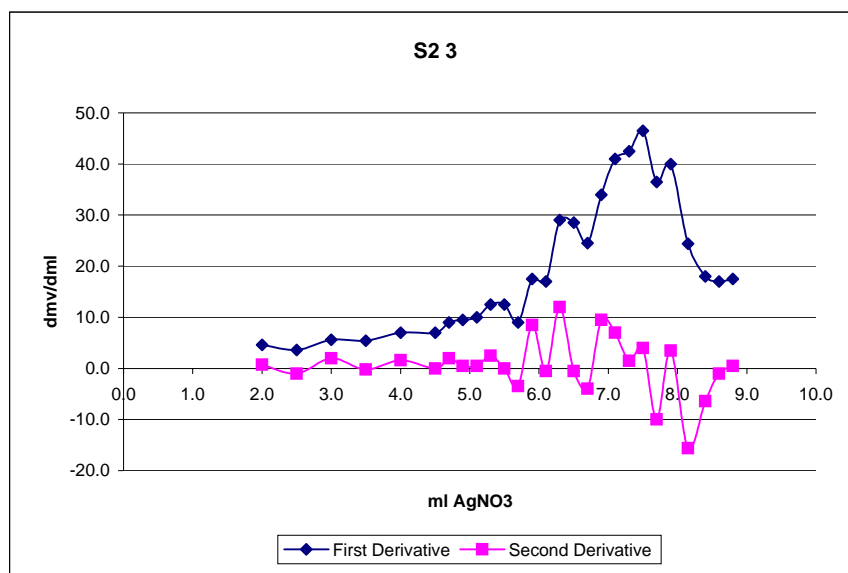
AgNO₃ (ml)		mv	d mL	d mV	d mV/dmL		Temp C
0.8	0.0	234.5					22.5
2.5	1.7	239.5	1.7	5.0	2.9		22.5
3.5	2.7	243.1	1.0	3.6	3.6	0.7	22.5
4.5	3.7	246.9	1.0	3.8	3.8	0.2	22.5
5.5	4.7	251.3	1.0	4.4	4.4	0.6	22.5
6.0	5.2	253.6	0.5	2.3	4.6	0.2	22.5
6.5	5.7	257.0	0.5	3.4	6.8	2.2	22.5
7.0	6.2	260.5	0.5	3.5	7.0	0.2	22.6
7.5	6.7	264.9	0.5	4.4	8.8	1.8	22.6
8.0	7.2	269.4	0.5	4.5	9.0	0.2	22.6
8.5	7.7	275.3	0.5	5.9	11.8	2.8	22.6
8.7	7.9	277.5	0.2	2.2	11.0	-0.8	22.6
9.0	8.2	283.9	0.3	6.4	21.3	10.3	22.6
9.2	8.4	286.4	0.2	2.5	12.5	-8.8	22.6
9.4	8.6	291.8	0.2	5.4	27.0	14.5	22.7
9.6	8.8	297.1	0.2	5.3	26.5	-0.5	22.7
9.8	9.0	302.0	0.2	4.9	24.5	-2.0	22.7
10.0	9.2	310.2	0.2	8.2	41.0	16.5	22.7
10.2	9.4	319.4	0.2	9.2	46.0	5.0	22.7
10.4	9.6	327.5	0.2	8.1	40.5	-5.5	22.7
10.7	9.9	338.5	0.3	11.0	36.7	-3.8	22.8
10.9	10.1	344.3	0.2	5.8	29.0	-7.7	22.8
11.1	10.3	348.6	0.2	4.3	21.5	-7.5	22.8
11.3	10.5	353.6	0.2	5.0	25.0	3.5	22.8
11.5	10.7	357.9	0.2	4.3	21.5	-3.5	22.8
11.7	10.9	360.3	0.2	2.4	12.0	-9.5	22.8
11.9	11.1	363.7	0.2	3.4	17.0	5.0	22.8
12.1	11.3	366.2	0.2	2.5	12.5	-4.5	22.8

S2 4
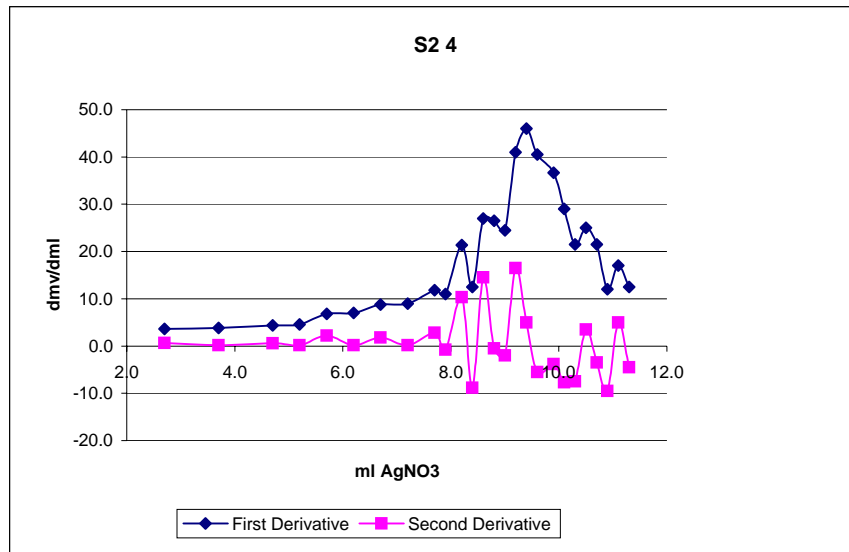
2B

1 AgNO$_3$ (ml)		mv	d mL	d mV	d mV/dmL		Temp C
0.8	0.0	223.4					22.8
2.5	1.7	233.4	1.7	10.0	5.9		22.9
3.5	2.7	239.7	1.0	6.3	6.3	0.4	23.0
4.5	3.7	247.6	1.0	7.9	7.9	1.6	23.0
5.5	4.7	258.6	1.0	11.0	11.0	3.1	23.0
6.0	5.2	265.9	0.5	7.3	14.6	3.6	23.0
6.2	5.4	270.1	0.2	4.2	21.0	6.4	23.0
6.4	5.6	275.1	0.2	5.0	25.0	4.0	23.0
6.6	5.8	280.8	0.2	5.7	28.5	3.5	23.0
6.8	6.0	288.9	0.2	8.1	40.5	12.0	23.0
7.0	6.2	297.4	0.2	8.5	42.5	2.0	23.0
7.2	6.4	311.1	0.2	13.7	68.5	26.0	23.0
7.4	6.6	322.5	0.2	11.4	57.0	-11.5	23.0
7.6	6.8	332.5	0.2	10.0	50.0	-7.0	23.0
7.8	7.0	341.3	0.2	8.8	44.0	-6.0	23.1
8.0	7.2	348.6	0.2	7.3	36.5	-7.5	23.1
8.2	7.4	353.5	0.2	4.9	24.5	-12.0	23.1
8.4	7.6	357.1	0.2	3.6	18.0	-6.5	23.1

2B 1
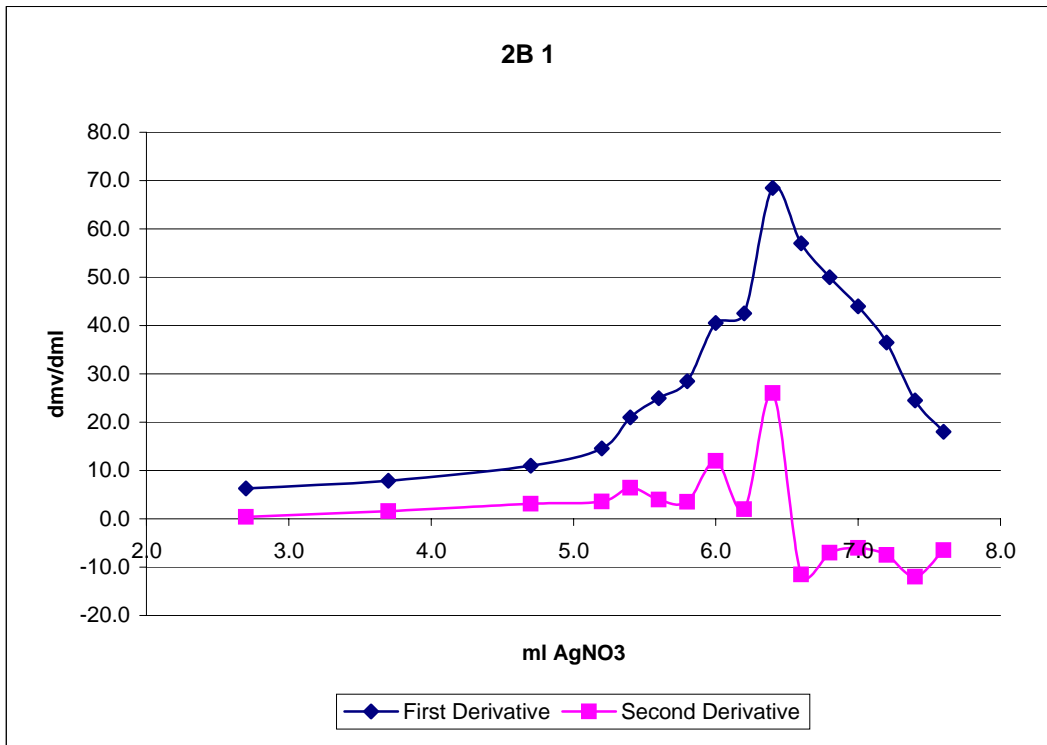
2B

2 AgNO$_3$ (ml)		mv	d mL	d mV	d mV/dmL		Temp C
8.4	0.0	241.6					23.0
9.0	0.6	246.8	0.6	5.2	8.7		23.1
10.0	1.6	249.9	1.0	3.1	3.1	-5.6	23.1
10.5	2.1	253.6	0.5	3.7	7.4	4.3	23.1
11.0	2.6	258.4	0.5	4.8	9.6	2.2	23.1
11.5	3.1	264.1	0.5	5.7	11.4	1.8	23.1
11.8	3.4	268.8	0.3	4.7	15.7	4.3	23.1
12.0	3.6	271.1	0.2	2.3	11.5	-4.2	23.1
12.2	3.8	274.6	0.2	3.5	17.5	6.0	23.1
12.4	4.0	279.9	0.2	5.3	26.5	9.0	23.1
12.6	4.2	286.1	0.2	6.2	31.0	4.5	23.1
12.8	4.4	293.3	0.2	7.2	36.0	5.0	23.1
13.0	4.6	306.7	0.2	13.4	67.0	31.0	23.2
13.2	4.8	318.5	0.2	11.8	59.0	-8.0	23.2
13.4	5.0	326.4	0.2	7.9	39.5	-19.5	23.2
13.6	5.2	334.8	0.2	8.4	42.0	2.5	23.2
13.8	5.4	341.5	0.2	6.7	33.5	-8.5	23.2
14.0	5.6	346.5	0.2	5.0	25.0	-8.5	23.2
14.2	5.8	352.1	0.2	5.6	28.0	3.0	23.2
14.4	6.0	356.4	0.2	4.3	21.5	-6.5	23.2
14.6	6.2	360.2	0.2	3.8	19.0	-2.5	23.2

2B 2

dmv/dml vs ml AgNO3

Legend: First Derivative — Second Derivative
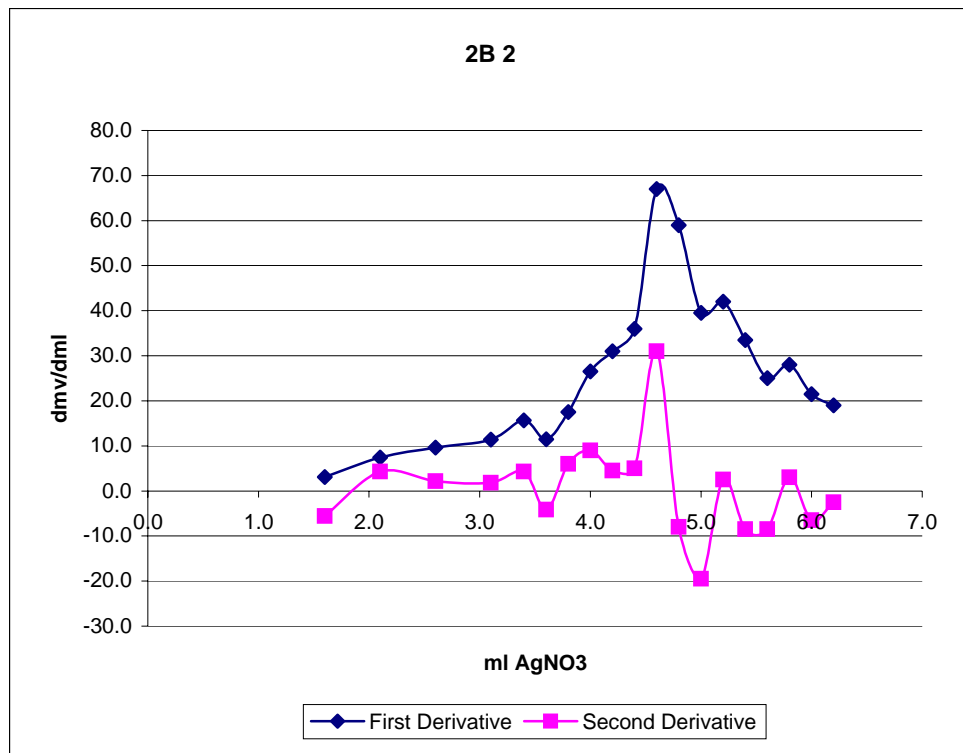
2B

3 AgNO$_3$ (ml)		mv	d mL	d mV	d mV/dmL		Temp C
14.6	0.0	242.9					23.1
15.5	0.9	246.8	0.9	3.9	4.3		23.2
16.5	1.9	252.3	1.0	5.5	5.5	1.2	23.2
17.5	2.9	259.6	1.0	7.3	7.3	1.8	23.2
18.5	3.9	269.4	1.0	9.8	9.8	2.5	23.2
19.0	4.4	276.8	0.5	7.4	14.8	5.0	23.2
19.2	4.6	280.1	0.2	3.3	16.5	1.7	23.2
19.4	4.8	283.5	0.2	3.4	17.0	0.5	23.2
19.6	5.0	288.1	0.2	4.6	23.0	6.0	23.2
19.8	5.2	293.6	0.2	5.5	27.5	4.5	23.3
20.0	5.4	304.5	0.2	10.9	54.5	27.0	23.3
20.2	5.6	317.1	0.2	12.6	63.0	8.5	23.3
20.4	5.8	330.5	0.2	13.4	67.0	4.0	23.3
20.6	6.0	340.8	0.2	10.3	51.5	-15.5	23.3
20.8	6.2	346.5	0.2	5.7	28.5	-23.0	23.3
21.0	6.4	352.9	0.2	6.4	32.0	3.5	23.3
21.2	6.6	357.1	0.2	4.2	21.0	-11.0	23.3

E11
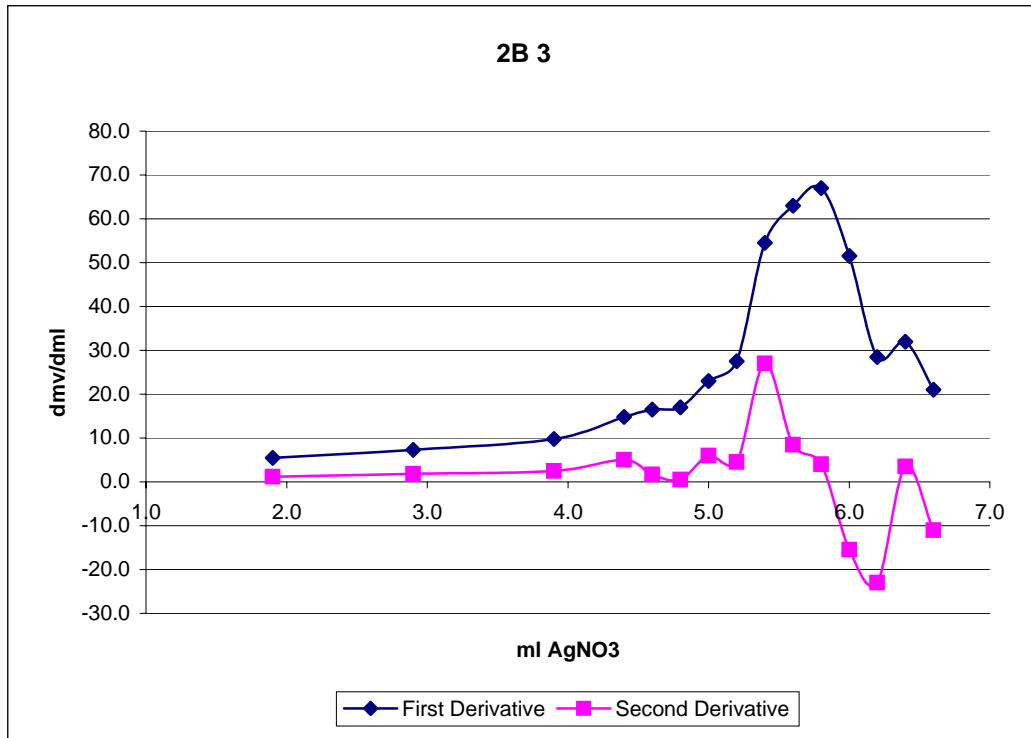
2B

4

AgNO$_3$ (ml)		mv	d mL	d mV	d mV/dmL		Temp C
21.2	0.0	244.2					23.2
23.0	1.8	253.1	1.8	8.9	4.9		23.2
23.5	2.3	258.4	0.5	5.3	10.6	5.7	23.2
24.0	2.8	267.3	0.5	8.9	17.8	7.2	23.2
24.5	3.3	278.1	0.5	10.8	21.6	3.8	23.2
24.7	3.5	283.1	0.2	5.0	25.0	3.4	23.2
24.9	3.7	289.7	0.2	6.6	33.0	8.0	23.3
25.1	3.9	298.2	0.2	8.5	42.5	9.5	23.3
25.3	4.1	312.5	0.2	14.3	71.5	29.0	23.3
25.5	4.3	328.1	0.2	15.6	78.0	6.5	23.3
25.7	4.5	339.7	0.2	11.6	58.0	-20.0	23.3
25.9	4.7	348.4	0.2	8.7	43.5	-14.5	23.3
26.1	4.9	354.7	0.2	6.3	31.5	-12.0	23.3
26.3	5.1	359.1	0.2	4.4	22.0	-9.5	23.3

2B 4

2F
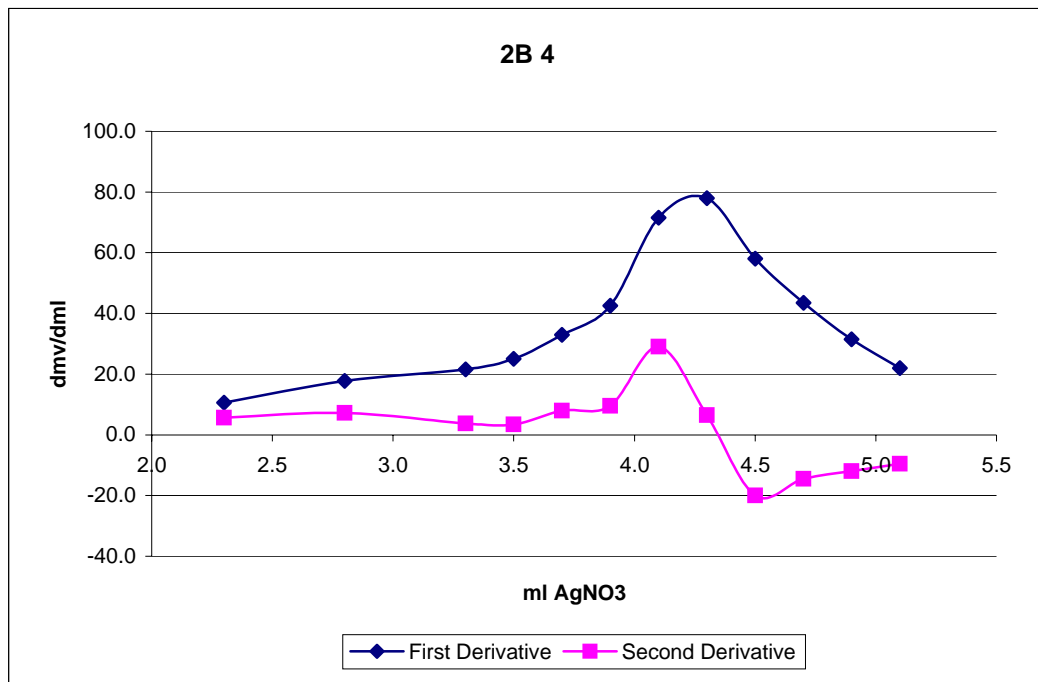
AgNO$_3$	mv	d mL	d mV	d mV/dmL		Temp
0	225.3					22.8
2.5	237.8	2.50	12.50	5.00		22.9
3.5	244.5	1.00	6.70	6.70	1.70	22.9
4.5	254.6	1.00	10.10	10.10	3.40	23
5.5	269.5	1.00	14.90	14.90	4.80	23
6	281.3	0.50	11.80	23.60	8.70	23
6.2	287.9	0.20	6.60	33.00	9.40	23
6.4	296.1	0.20	8.20	41.00	8.00	23
6.6	308.7	0.20	12.60	63.00	22.00	23
6.8	321.5	0.20	12.80	64.00	1.00	23
7	332.6	0.20	11.10	55.50	-8.50	23
7.2	341.9	0.20	9.30	46.50	-9.00	23.1
7.4	348.8	0.20	6.90	34.50	-12.00	23.1
7.6	355.1	0.20	6.30	31.50	-3.00	23.1
7.8	360.5	0.20	5.40	27.00	-4.50	23.1

2F

2
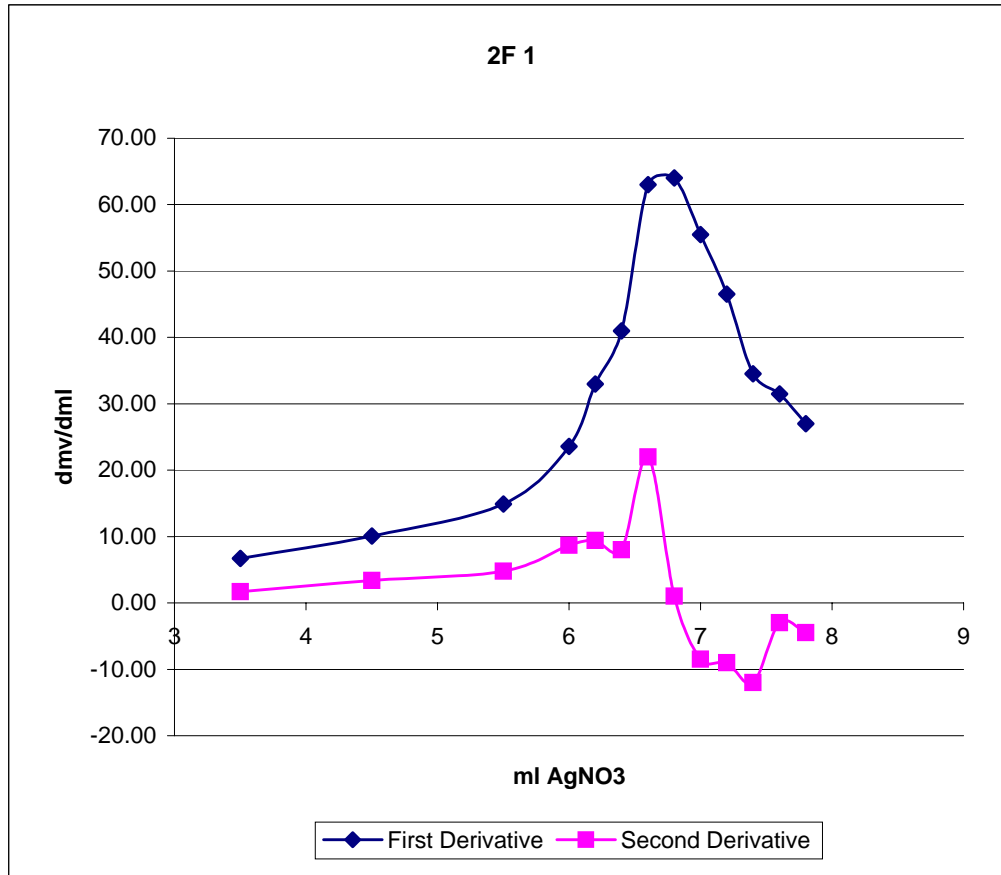
AgNO$_3$		mv	d mL	d mV	d mV/dmL		Temp
7.8	0	217.7					23
11.3	3.5	236.9	3.50	19.20	5.49		23.1
12.8	5	254.5	1.50	17.60	11.73	6.25	23.1
13.8	6	277.1	1.00	22.60	22.60	10.87	23.1
14	6.2	288.5	0.20	11.40	57.00	34.40	23.2
14.2	6.4	300.5	0.20	12.00	60.00	3.00	23.2
14.4	6.6	316.4	0.20	15.90	79.50	19.50	23.2
14.6	6.8	328.4	0.20	12.00	60.00	-19.50	23.2
14.8	7	337.3	0.20	8.90	44.50	-15.50	23.2
15	7.2	344.9	0.20	7.60	38.00	-6.50	23.2
15.2	7.4	349.5	0.20	4.60	23.00	-15.00	23.2

2F 2
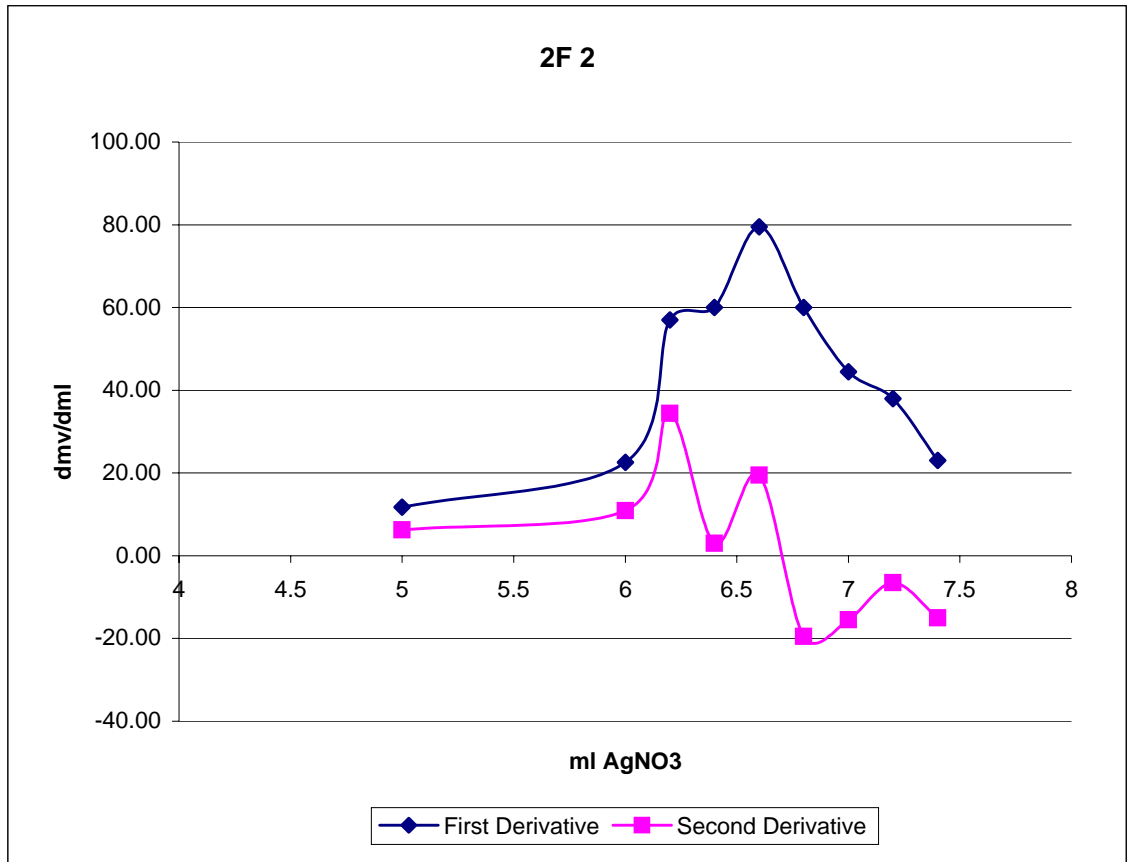
2F

3

AgNO$_3$		mv	d mL	d mV	d mV/dmL		Temp
15.2	0	228.7					23.1
17	1.8	241.3	1.80	12.60	7.00		23.1
18	2.8	250.1	1.00	8.80	8.80	1.80	23.2
19	3.8	263.4	1.00	13.30	13.30	4.50	23.2
19.5	4.3	275.9	0.50	12.50	25.00	11.70	23.2
19.7	4.5	280.6	0.20	4.70	23.50	-1.50	23.2
19.9	4.7	290.1	0.20	9.50	47.50	24.00	23.3
20.1	4.9	304.5	0.20	14.40	72.00	24.50	23.3
20.3	5.1	319.6	0.20	15.10	75.50	3.50	23.3
20.5	5.3	331.1	0.20	11.50	57.50	-18.00	23.3
20.7	5.5	340.5	0.20	9.40	47.00	-10.50	23.3
20.9	5.7	348.1	0.20	7.60	38.00	-9.00	23.3
21.1	5.9	355.3	0.20	7.20	36.00	-2.00	23.3
21.3	6.1	360.1	0.20	4.80	24.00	-12.00	23.3
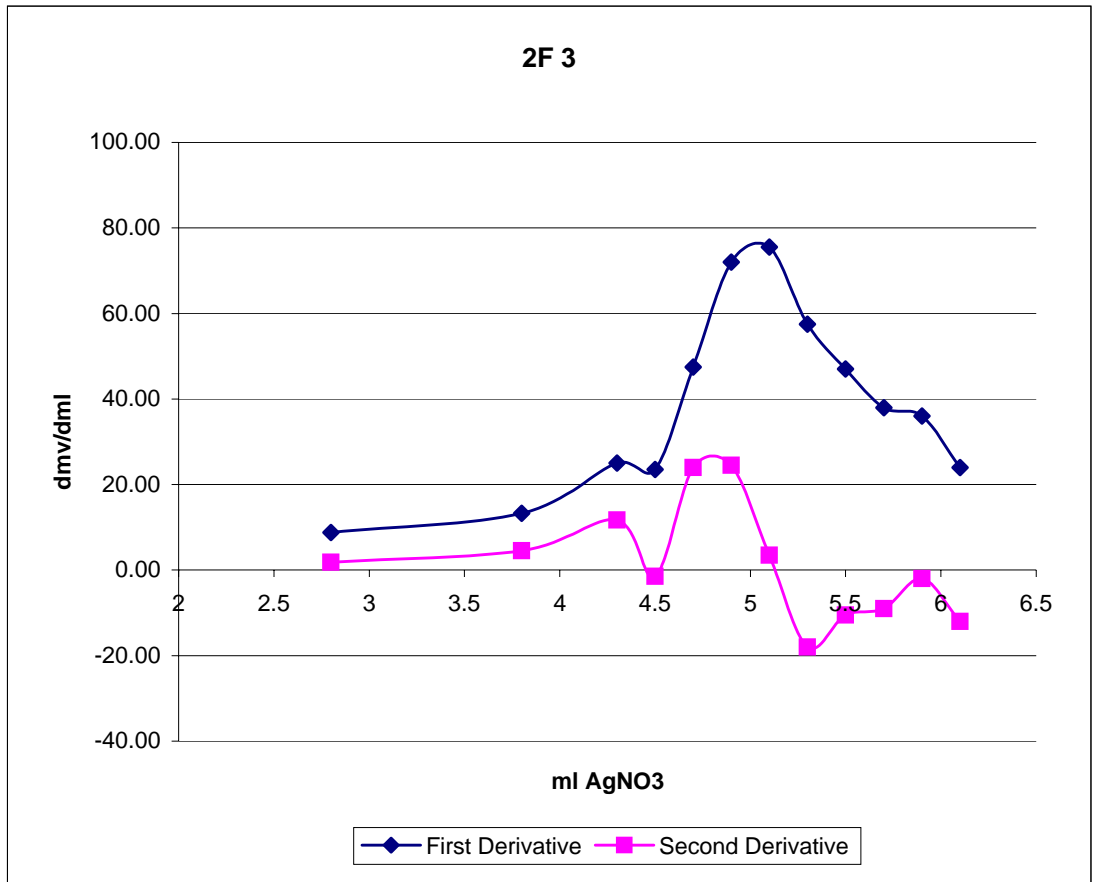
2F

4

AgNO$_3$		mv	d mL	d mV	d mV/dmL		Temp
21.3	0	234.5					23.1
23.2	1.9	247.6	1.90	13.10	6.89		23.2
24.5	3.2	261.1	1.30	13.50	10.38	3.49	23.2
25	3.7	269.9	0.50	8.80	17.60	7.22	23.2
25.5	4.2	282.6	0.50	12.70	25.40	7.80	23.2
25.7	4.4	289.1	0.20	6.50	32.50	7.10	23.2
25.9	4.6	298.3	0.20	9.20	46.00	13.50	23.3
26.1	4.8	312.5	0.20	14.20	71.00	25.00	23.3
26.3	5	326.3	0.20	13.80	69.00	-2.00	23.3
26.5	5.2	336.5	0.20	10.20	51.00	-18.00	23.3
26.7	5.4	345.1	0.20	8.60	43.00	-8.00	23.3
26.9	5.6	352.6	0.20	7.50	37.50	-5.50	23.3
27.1	5.8	359.1	0.20	6.50	32.50	-5.00	23.3
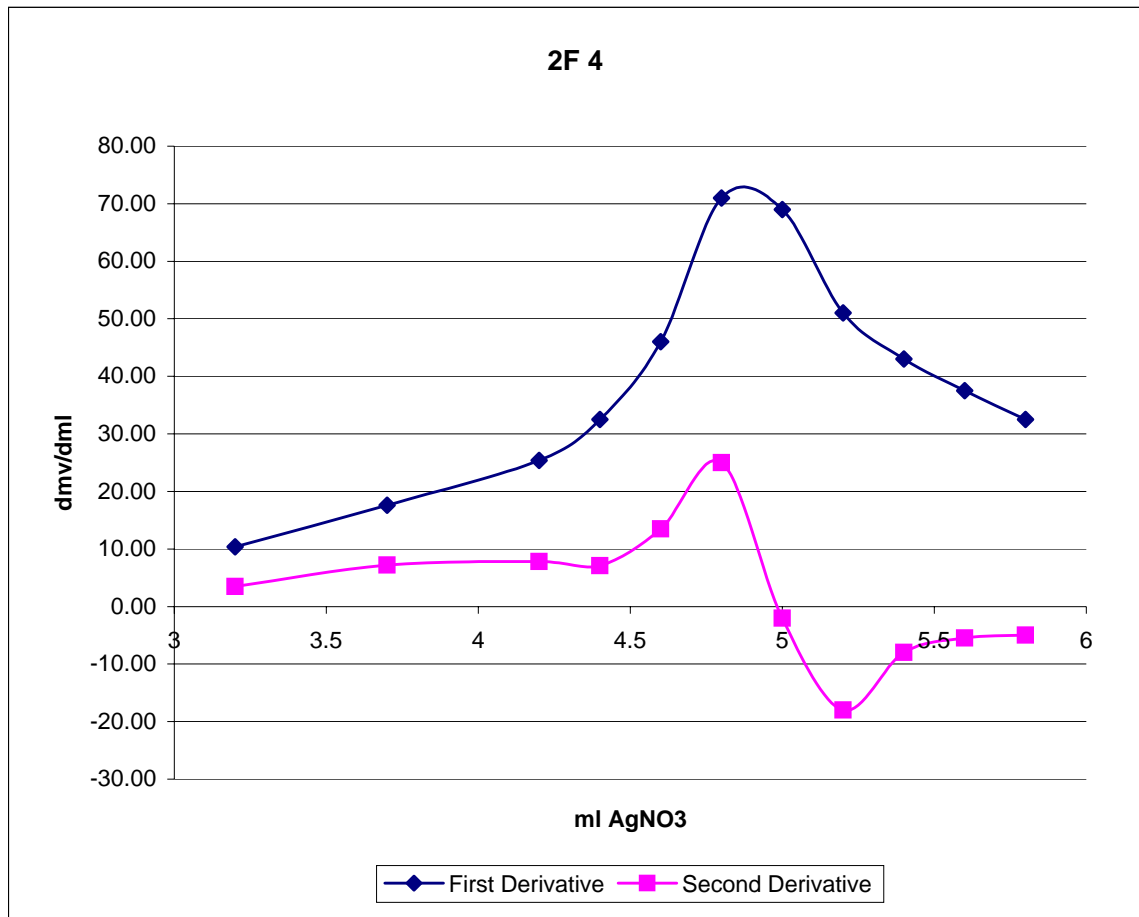
3C

1 AgNO$_3$ (ml)	mv	d mL	d mV	d mV/dmL		Temp C
0.0	215.6					22.2
1.0	219.6	1.0	4.0	4.0		22.3
2.0	223.4	1.0	3.8	3.8	-0.2	22.3
3.0	228.1	1.0	4.7	4.7	0.9	22.3
4.0	234.9	1.0	6.8	6.8	2.1	22.4
5.0	242.8	1.0	7.9	7.9	1.1	22.4
6.0	254.2	1.0	11.4	11.4	3.5	22.4
6.5	262.3	0.5	8.1	16.2	4.8	22.4
7.0	276.5	0.5	14.2	28.4	12.2	22.4
7.5	298.5	0.5	22.0	44.0	15.6	22.4
7.7	309.9	0.2	11.4	57.0	13.0	22.4
7.9	324.3	0.2	14.4	72.0	15.0	22.4
8.1	338.1	0.2	13.8	69.0	-3.0	22.4
8.3	348.1	0.2	10.0	50.0	-19.0	22.4
8.5	354.6	0.2	6.5	32.5	-17.5	22.4
8.7	360.1	0.2	5.5	27.5	-5.0	22.4

E17
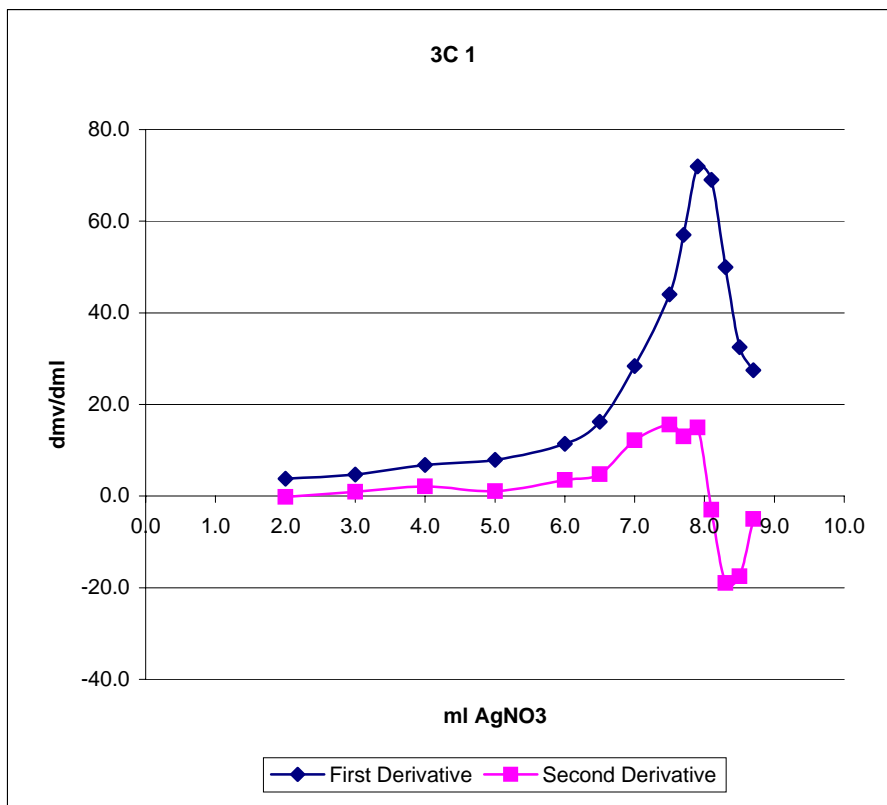
3C

2 AgNO₃ (ml)		mv	d mL	d mV	d mV/dmL		Temp C
8.7	0.0	221.5					22.1
12.0	3.3	238.6	3.3	17.1	5.2		22.2
12.5	3.8	241.6	0.5	3.0	6.0	0.8	22.2
13.0	4.3	246.8	0.5	5.2	10.4	4.4	22.2
13.2	4.5	248.6	0.2	1.8	9.0	-1.4	22.2
13.4	4.7	251.1	0.2	2.5	12.5	3.5	22.3
13.7	5.0	254.9	0.3	3.8	12.7	0.2	22.3
13.9	5.2	257.5	0.2	2.6	13.0	0.3	22.3
14.1	5.4	259.8	0.2	2.3	11.5	-1.5	22.3
14.3	5.6	265.1	0.2	5.3	26.5	15.0	22.3
14.5	5.8	270.1	0.2	5.0	25.0	-1.5	22.3
14.7	6.0	275.9	0.2	5.8	29.0	4.0	22.3
14.9	6.2	282.3	0.2	6.4	32.0	3.0	22.3
15.1	6.4	288.9	0.2	6.6	33.0	1.0	22.3
15.4	6.7	309.9	0.3	21.0	70.0	37.0	22.3
15.6	6.9	326.7	0.2	16.8	84.0	14.0	22.3
15.8	7.1	337.1	0.2	10.4	52.0	-32.0	22.4
16.0	7.3	346.9	0.2	9.8	49.0	-3.0	22.4
16.2	7.5	352.8	0.2	5.9	29.5	-19.5	22.4
16.4	7.7	358.6	0.2	5.8	29.0	-0.5	22.4

3C 2
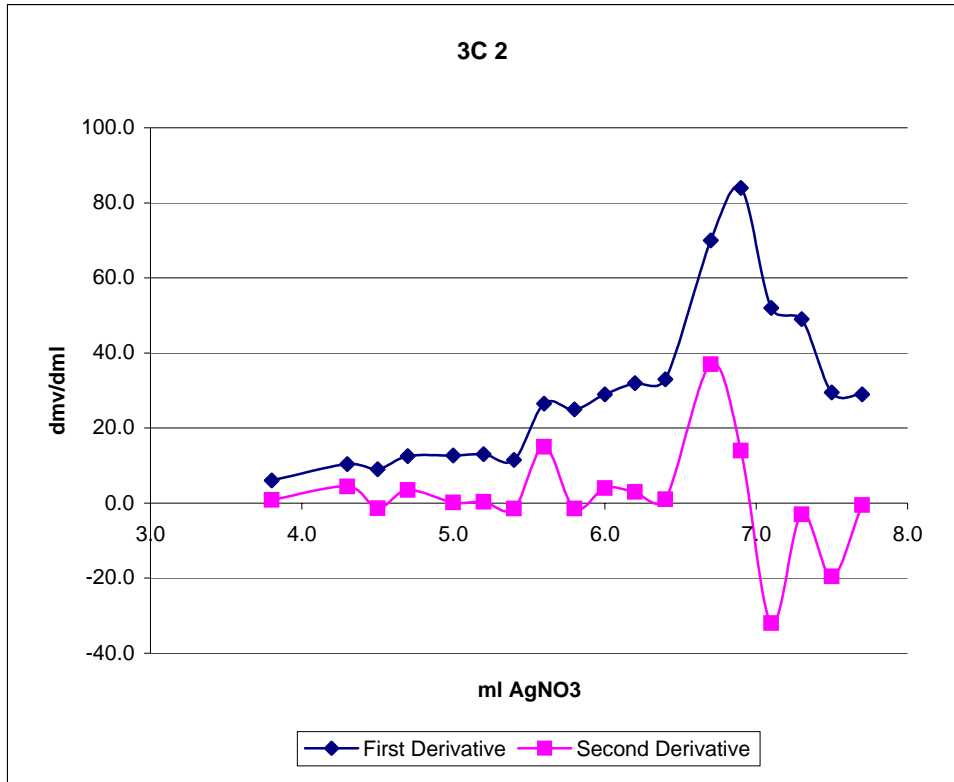
3C

3 AgNO$_3$ (ml)		mv	d mL	d mV	d mV/dmL		Temp C
16.4	0.0	226.9					22.2
19.6	3.2	246.5	3.2	19.6	6.1		22.3
19.8	3.4	249.1	0.2	2.6	13.0	6.9	22.3
20.0	3.6	251.9	0.2	2.8	14.0	1.0	22.3
20.2	3.8	254.6	0.2	2.7	13.5	-0.5	22.3
20.4	4.0	256.3	0.2	1.7	8.5	-5.0	22.3
20.6	4.2	259.1	0.2	2.8	14.0	5.5	22.3
20.8	4.4	262.9	0.2	3.8	19.0	5.0	22.4
21.0	4.6	266.5	0.2	3.6	18.0	-1.0	22.4
21.2	4.8	270.6	0.2	4.1	20.5	2.5	22.4
21.4	5.0	275.6	0.2	5.0	25.0	4.5	22.4
21.6	5.2	280.1	0.2	4.5	22.5	-2.5	22.4
21.8	5.4	287.5	0.2	7.4	37.0	14.5	22.4
22.0	5.6	295.9	0.2	8.4	42.0	5.0	22.4
22.2	5.8	318.1	0.2	22.2	111.0	69.0	22.4
22.4	6.0	332.5	0.2	14.4	72.0	-39.0	22.5
22.6	6.2	341.6	0.2	9.1	45.5	-26.5	22.5
22.8	6.4	350.6	0.2	9.0	45.0	-0.5	22.5
23.0	6.6	357.9	0.2	7.3	36.5	-8.5	22.5

3C 3

E19

3C

3C
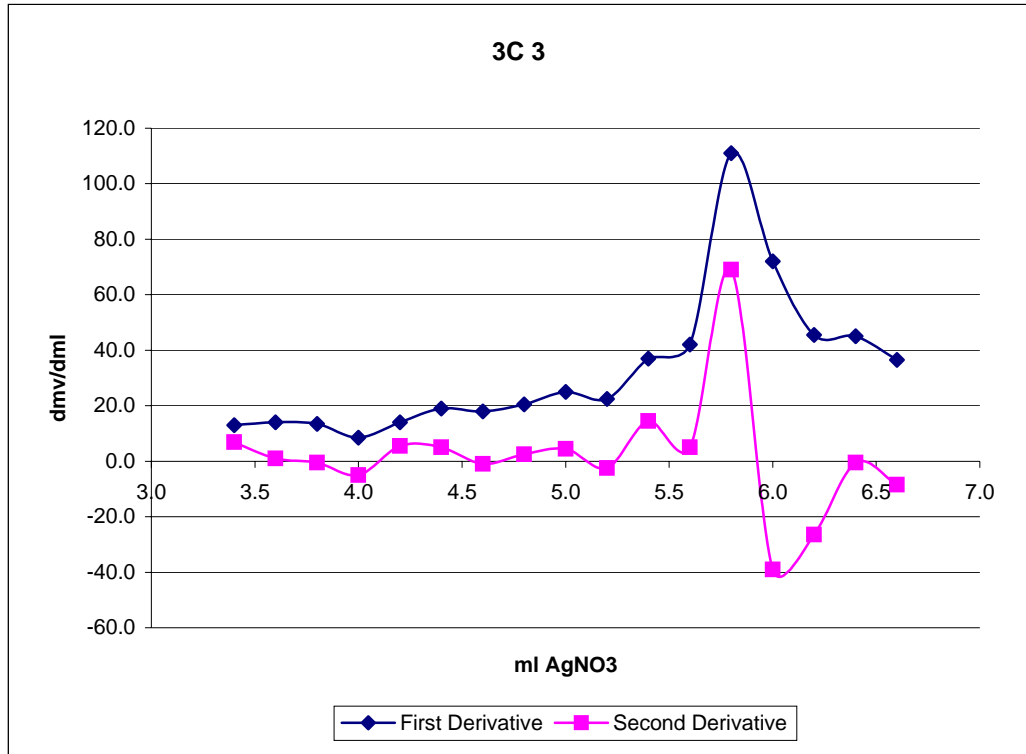
AgNO$_3$ (ml)	mv	d mL	d mV	d mV/dmL		Temp C
0.0	238.1					22.4
2.5	254.3	2.5	16.2	6.5		22.5
2.7	256.1	0.2	1.8	9.0	2.5	22.5
2.9	258.1	0.2	2.0	10.0	1.0	22.5
3.1	260.1	0.2	2.0	10.0	0.0	22.5
3.3	262.3	0.2	2.2	11.0	1.0	22.5
3.5	265.1	0.2	2.8	14.0	3.0	22.5
3.7	268.2	0.2	3.1	15.5	1.5	22.5
3.9	271.5	0.2	3.3	16.5	1.0	22.6
4.1	274.6	0.2	3.1	15.5	-1.0	22.6
4.3	278.1	0.2	3.5	17.5	2.0	22.6
4.5	284.3	0.2	6.2	31.0	13.5	22.6
4.7	291.6	0.2	7.3	36.5	5.5	22.6
4.9	298.3	0.2	6.7	33.5	-3.0	22.6
5.1	308.9	0.2	10.6	53.0	19.5	22.6
5.3	321.8	0.2	12.9	64.5	11.5	22.6
5.6	333.6	0.3	11.8	47.2	-17.3	22.6
5.8	342.6	0.3	9.0	36.0	-11.2	22.6
6.0	350.9	0.2	8.3	41.5	5.5	22.6
6.2	357.1	0.2	6.2	31.0	-10.5	22.6

3C 4

E20

3F
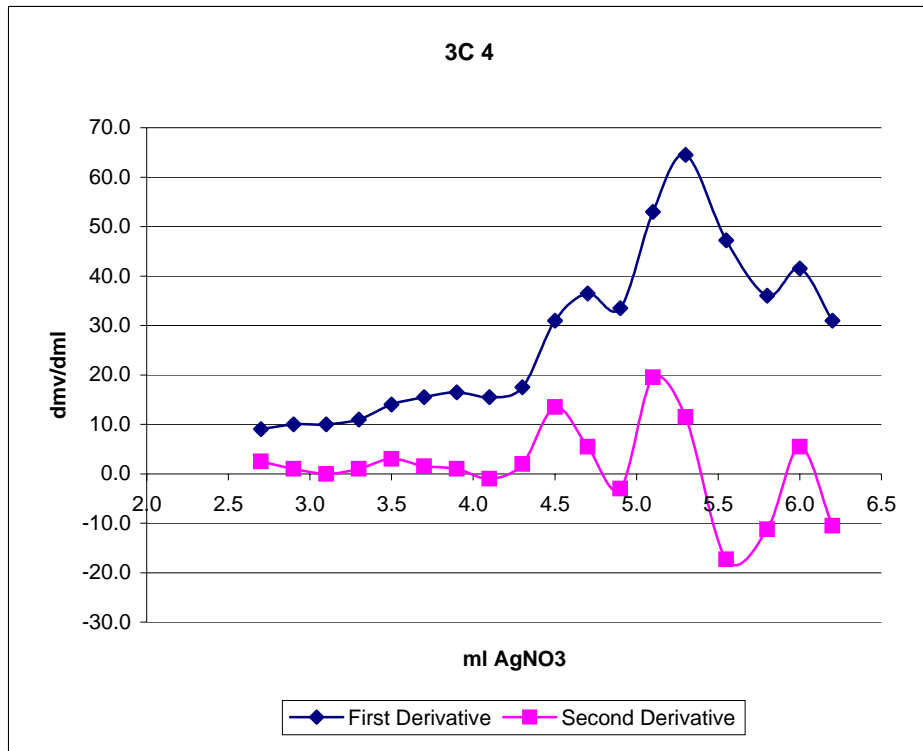
AgNO$_3$		mv	d mL	d mV	d mV/dmL		Temp
0.9	0	213.9					22.4
4.5	3.6	231.8	3.60	17.90	4.97		22.5
6.5	5.6	249.1	2.00	17.30	8.65	3.68	22.5
7.5	6.6	265.5	1.00	16.40	16.40	7.75	22.5
7.8	6.9	274.6	0.30	9.10	30.33	13.93	22.5
8.1	7.2	285.7	0.30	11.10	37.00	6.67	22.6
8.3	7.4	292.8	0.20	7.10	35.50	-1.50	22.6
8.5	7.6	305.6	0.20	12.80	64.00	28.50	22.6
8.7	7.8	321.5	0.20	15.90	79.50	15.50	22.6
8.9	8	332.7	0.20	11.20	56.00	-23.50	22.6
9.1	8.2	342.5	0.20	9.80	49.00	-7.00	22.6
9.3	8.4	350.1	0.20	7.60	38.00	-11.00	22.6
9.5	8.6	356.7	0.20	6.60	33.00	-5.00	22.6
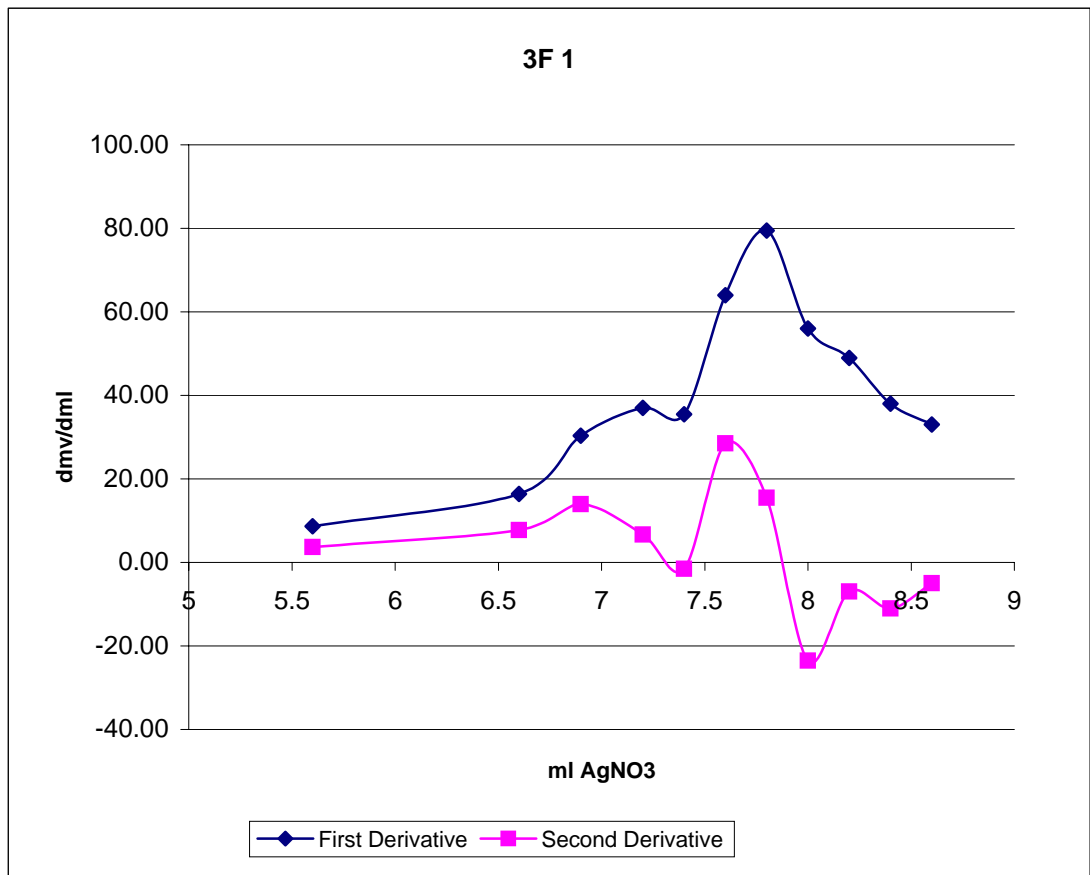
3F

2

AgNO$_3$		mv	d mL	d mV	d mV/dmL		Temp
9.5	0	219.6					22.5
13	3.5	238.1	3.50	18.50	5.29		22.6
14	4.5	249.5	1.00	11.40	11.40	6.11	22.6
15	5.5	261.1	1.00	11.60	11.60	0.20	22.6
15.5	6	273.3	0.50	12.20	24.40	12.80	22.6
15.8	6.3	280.5	0.30	7.20	24.00	-0.40	22.7
16	6.5	287.9	0.20	7.40	37.00	13.00	22.7
16.2	6.7	295.4	0.20	7.50	37.50	0.50	22.7
16.4	6.9	305.8	0.20	10.40	52.00	14.50	22.7
16.6	7.1	316.9	0.20	11.10	55.50	3.50	22.7
16.8	7.3	328.5	0.20	11.60	58.00	2.50	22.8
17	7.5	337.5	0.20	9.00	45.00	-13.00	22.8
17.2	7.7	344.6	0.20	7.10	35.50	-9.50	22.8
17.4	7.9	351.1	0.20	6.50	32.50	-3.00	22.8
17.6	8.1	356.3	0.20	5.20	26.00	-6.50	22.8
17.8	8.3	360.1	0.20	3.80	19.00	-7.00	22.8

3F 2
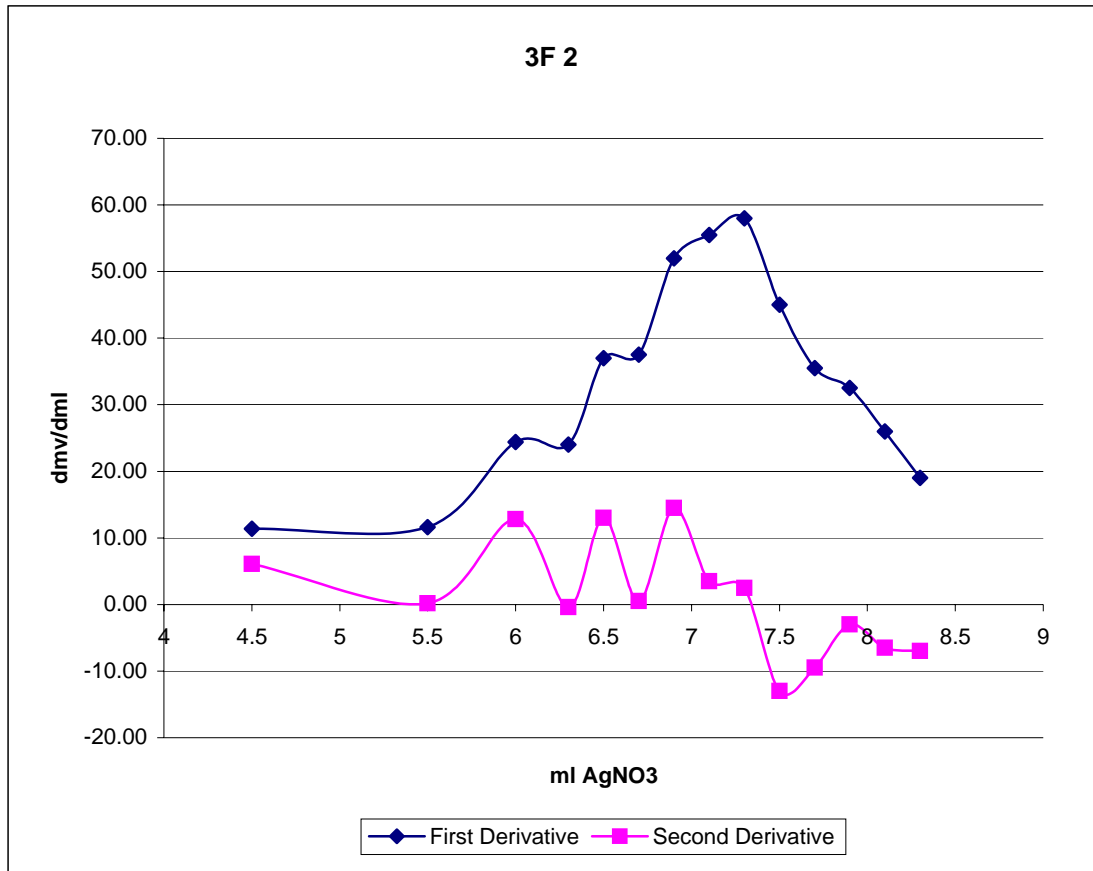
3F

3 AgNO$_3$		mv	d mL	d mV	d mV/dmL		Temp
17.8	0	225.7					22.7
20	2.2	239.6	2.20	13.90	6.32		22.8
21.5	3.7	254.4	1.50	14.80	9.87	3.55	22.9
22.5	4.7	271.8	1.00	17.40	17.40	7.53	22.9
22.8	5	285.4	0.30	13.60	45.33	27.93	22.9
23	5.2	293.1	0.20	7.70	38.50	-6.83	22.9
23.2	5.4	307.5	0.20	14.40	72.00	33.50	22.9
23.4	5.6	321.5	0.20	14.00	70.00	-2.00	22.9
23.6	5.8	333.1	0.20	11.60	58.00	-12.00	22.9
23.8	6	342.5	0.20	9.40	47.00	-11.00	23
24	6.2	351.2	0.20	8.70	43.50	-3.50	23
24.2	6.4	357.2	0.20	6.00	30.00	-13.50	23

3F 3
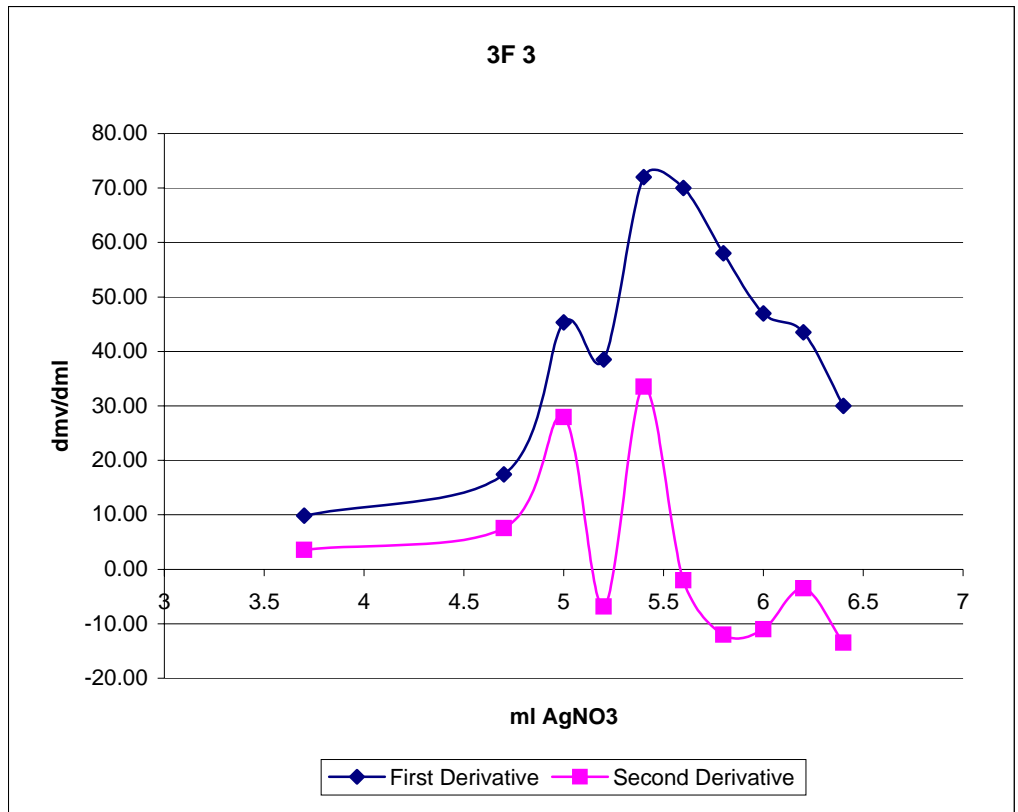
3F

4

AgNO₃		mv	d mL	d mV	d mV/dmL		Temp
17.8	0	228.1					22.8
19.5	1.7	242.3	1.70	14.20	8.35		22.8
20.5	2.7	251.1	1.00	8.80	8.80	0.45	22.9
21.5	3.7	264.8	1.00	13.70	13.70	4.90	22.9
22	4.2	277.5	0.50	12.70	25.40	11.70	22.9
22.3	4.5	287.6	0.30	10.10	33.67	8.27	22.9
22.5	4.7	297.6	0.20	10.00	50.00	16.33	22.9
22.7	4.9	309.6	0.20	12.00	60.00	10.00	23
22.9	5.1	322.6	0.20	13.00	65.00	5.00	23
23.1	5.3	334.1	0.20	11.50	57.50	-7.50	23
23.3	5.5	343.6	0.20	9.50	47.50	-10.00	23
23.5	5.7	349.6	0.20	6.00	30.00	-17.50	23
23.7	5.9	355.1	0.20	5.50	27.50	-2.50	23
23.9	6.1	360.6	0.20	5.50	27.50	0.00	23

3F 4
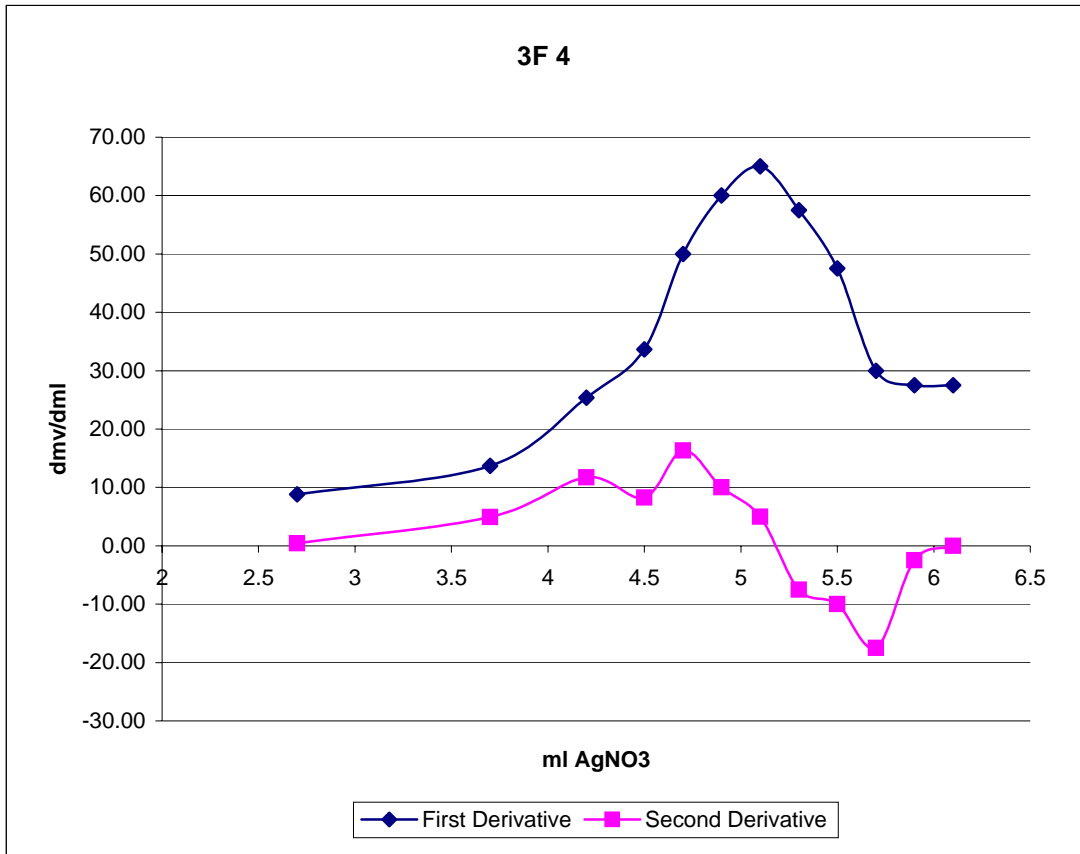
4F

1

AgNO₃ (ml)	mv	d mL	d mV	d mV/dmL		Temp C
0	216.2					23
2	221.6	2	5.4	2.70		23.1
3.5	228.2	1.5	6.6	4.40	1.70	23.2
4.5	233.5	1	5.3	5.30	0.90	23.2
5.5	240.6	1	7.1	7.10	1.80	23.3
6.5	249.6	1	9	9.00	1.90	23.3
7.5	265.8	1	16.2	16.20	7.20	23.3
7.7	269.8	0.2	4	20.00	3.80	23.3
7.9	274.6	0.2	4.8	24.00	4.00	23.3
8.1	280.9	0.2	6.3	31.50	7.50	23.3
8.3	288.6	0.2	7.7	38.50	7.00	23.3
8.5	301.9	0.2	13.3	66.50	28.00	23.3
8.7	316.5	0.2	14.6	73.00	6.50	23.3
8.9	329.1	0.2	12.6	63.00	-10.00	23.3
9.1	338.1	0.2	9	45.00	-18.00	23.3
9.3	347.1	0.2	9	45.00	0.00	23.4
9.5	353.9	0.2	6.8	34.00	-11.00	23.4
9.7	358.5	0.2	4.6	23.00	-11.00	23.4

4F
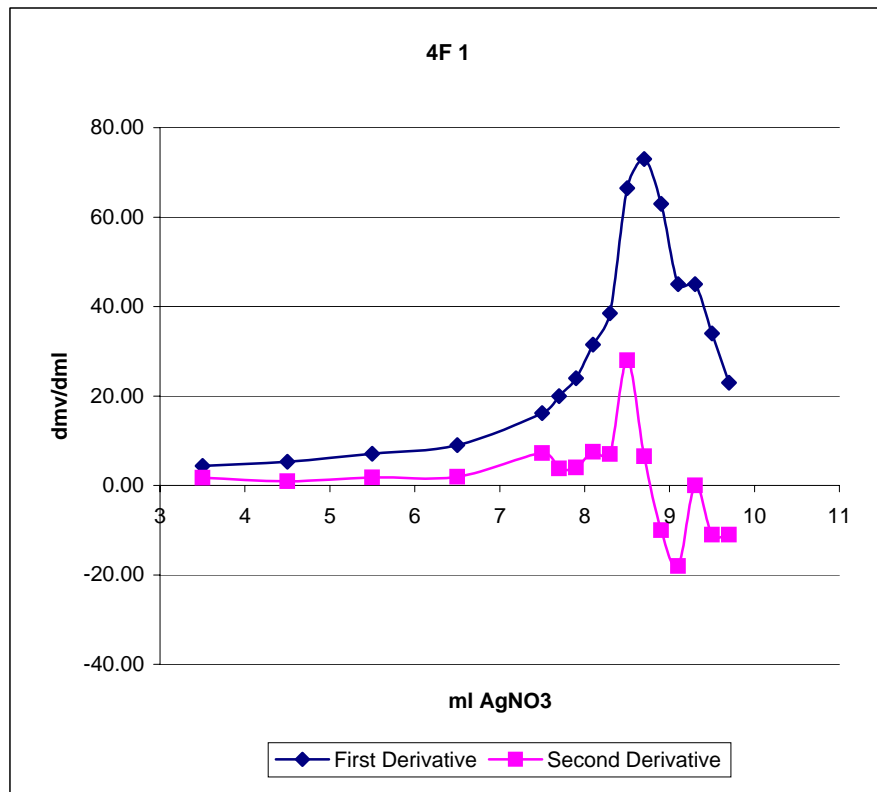
AgNO$_3$ (ml)	mv	d mL	d mV	d mV/dmL		Temp C
0	236.5					23.2
2	247.9	2	11.4	5.7		23.2
3	257.9	1	10	10	4.3	23.2
4	270.1	1	12.2	12.2	2.2	23.2
4.2	274.5	0.2	4.4	22	9.8	23.3
4.4	278.6	0.2	4.1	20.5	-1.5	23.3
4.6	283.9	0.2	5.3	26.5	6	23.3
4.8	290.5	0.2	6.6	33	6.5	23.3
5	298.6	0.2	8.1	40.5	7.5	23.3
5.2	311.2	0.2	12.6	63	22.5	23.3
5.4	325.3	0.2	14.1	70.5	7.5	23.3
5.6	335.1	0.2	9.8	49	-21.5	23.3
5.8	343.9	0.2	8.8	44	-5	23.3
6	350.1	0.2	6.2	31	-13	23.3
6.2	357.6	0.2	7.5	37.5	6.5	23.3

E26
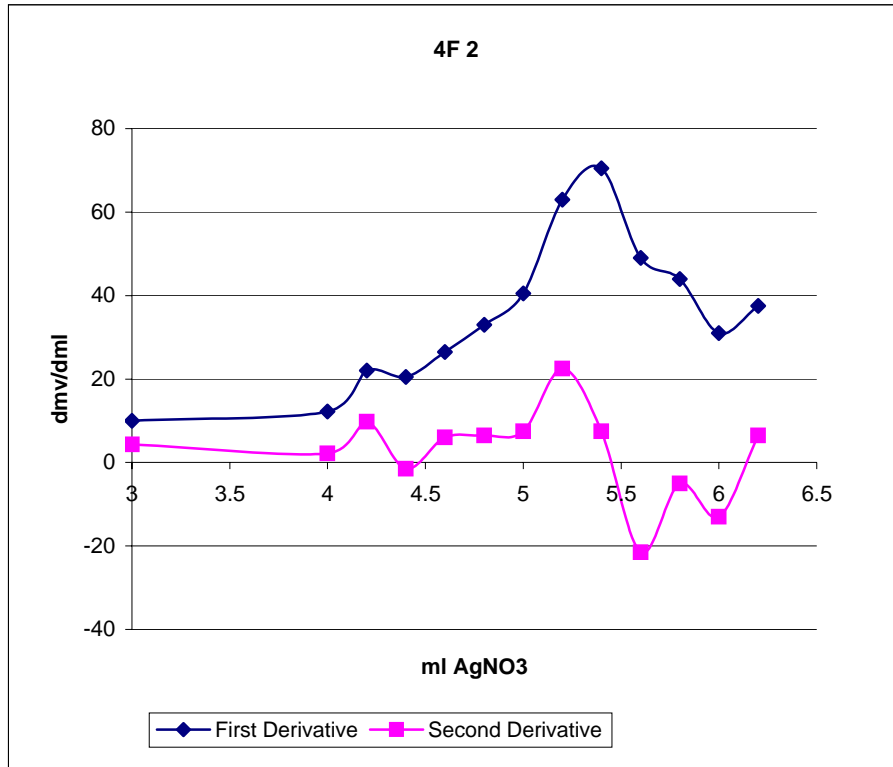
4F

3 AgNO$_3$ (ml)		mv	d mL	d mV	d mV/dmL		Temp C
6.2	0	239.5					23.3
7.5	1.3	246.5	1.3	7	5.38		23.4
8.5	2.3	254.1	1	7.6	7.60	2.22	23.4
9.5	3.3	267.4	1	13.3	13.30	5.70	23.4
9.7	3.5	271.5	0.2	4.1	20.50	7.20	23.4
9.9	3.7	276.2	0.2	4.7	23.50	3.00	23.5
10.1	3.9	281.2	0.2	5	25.00	1.50	23.5
10.3	4.1	288.6	0.2	7.4	37.00	12.00	23.5
10.5	4.3	297.8	0.2	9.2	46.00	9.00	23.5
10.7	4.5	307.5	0.2	9.7	48.50	2.50	23.5
10.9	4.7	319.6	0.2	12.1	60.50	12.00	23.5
11.1	4.9	332.3	0.2	12.7	63.50	3.00	23.5
11.3	5.1	341.1	0.2	8.8	44.00	-19.50	23.5
11.5	5.3	348.6	0.2	7.5	37.50	-6.50	23.5
11.7	5.5	355.4	0.2	6.8	34.00	-3.50	23.5
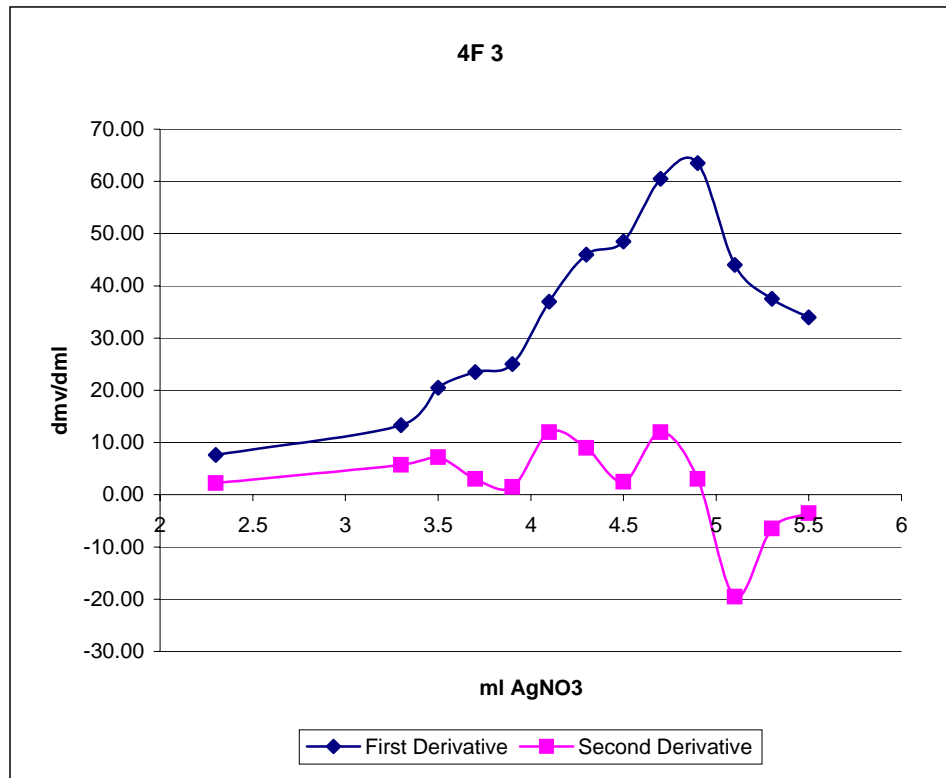
4F

4 AgNO$_3$ (ml)		mv	d mL	d mV	d mV/dmL		Temp C
11.7	0	242.8					23.4
13	1.3	248.2	1.3	5.4	4.15		23.4
14	2.3	254.7	1	6.5	6.50	2.35	23.5
15	3.3	262.9	1	8.2	8.20	1.70	23.5
15.5	3.8	270.1	0.5	7.2	14.40	6.20	23.5
15.7	4	277.2	0.2	7.1	35.50	21.10	23.5
15.9	4.2	282.1	0.2	4.9	24.50	-11.00	23.5
16.1	4.4	289.1	0.2	7	35.00	10.50	23.5
16.3	4.6	302.3	0.2	13.2	66.00	31.00	23.5
16.5	4.8	318.2	0.2	15.9	79.50	13.50	23.6
16.7	5	331.5	0.2	13.3	66.50	-13.00	23.6
16.9	5.2	341.2	0.2	9.7	48.50	-18.00	23.6
17.1	5.4	349.5	0.2	8.3	41.50	-7.00	23.6
17.3	5.6	355.8	0.2	6.3	31.50	-10.00	23.6

E28

5C
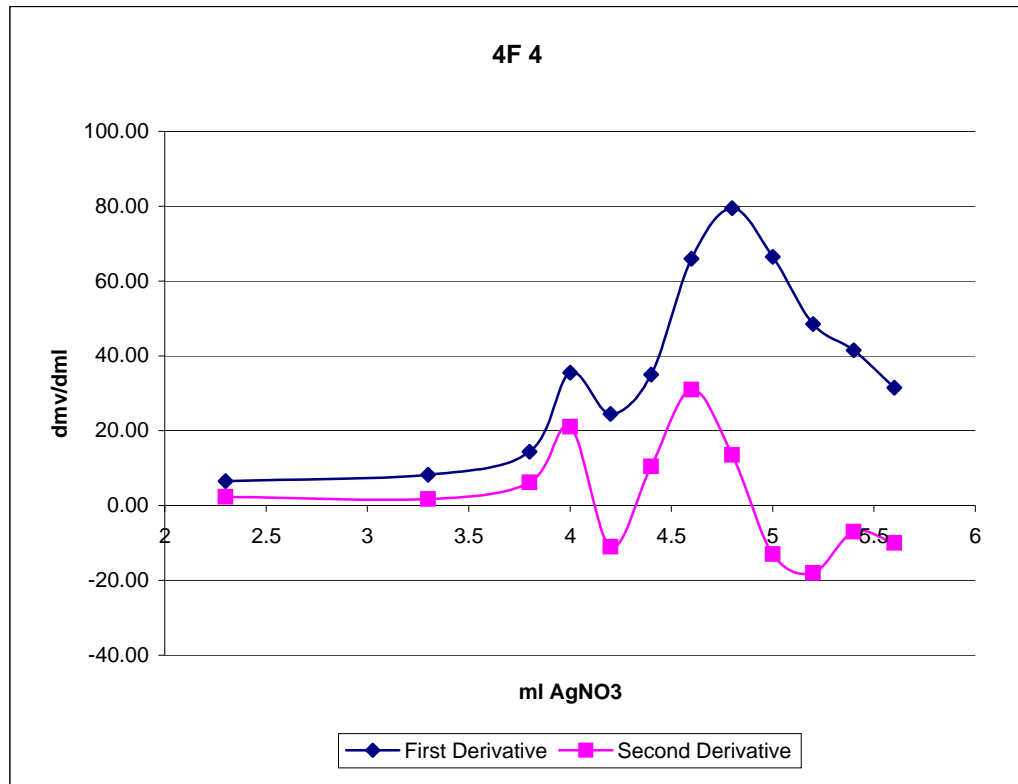
AgNO$_3$ (ml)	mv	d mL	d mV	d mV/dmL		Temp C
0.0	219.8					22.5
1.0	227.2	1.0	7.4	7.4		22.5
2.0	234.9	1.0	7.7	7.7	0.3	22.6
3.0	243.5	1.0	8.6	8.6	0.9	22.6
4.0	255.6	1.0	12.1	12.1	3.5	22.6
5.0	270.8	1.0	15.2	15.2	3.1	22.7
5.2	274.6	0.2	3.8	19.0	3.8	22.7
5.4	279.4	0.2	4.8	24.0	5.0	22.7
5.6	286.4	0.2	7.0	35.0	11.0	22.7
5.8	294.5	0.2	8.1	40.5	5.5	22.7
6.0	308.9	0.2	14.4	72.0	31.5	22.7
6.2	321.6	0.2	12.7	63.5	-8.5	22.7
6.4	332.8	0.2	11.2	56.0	-7.5	22.7
6.6	341.5	0.2	8.7	43.5	-12.5	22.7
6.8	348.9	0.2	7.4	37.0	-6.5	22.7
7.0	355.1	0.2	6.2	31.0	-6.0	22.7
7.2	360.7	0.2	5.6	28.0	-3.0	22.7

5C
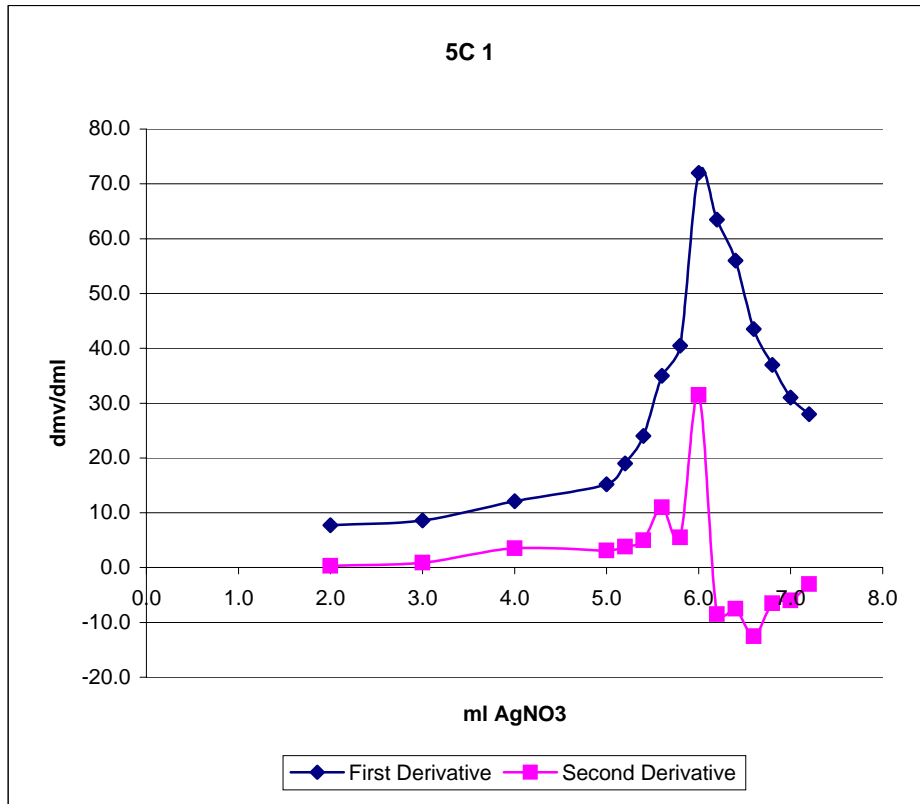
AgNO₃ (ml)	mv	d mL	d mV	d mV/dmL		Temp C
0.0	228.7					22.6
1.5	239.2	1.5	10.5	7.0		22.7
2.5	247.6	1.0	8.4	8.4	1.4	22.7
3.5	258.9	1.0	11.3	11.3	2.9	22.7
4.0	267.6	0.5	8.7	17.4	6.1	22.7
4.2	272.6	0.2	5.0	25.0	7.6	22.7
4.4	278.6	0.2	6.0	30.0	5.0	22.8
4.6	285.1	0.2	6.5	32.5	2.5	22.8
4.8	294.5	0.2	9.4	47.0	14.5	22.8
5.0	306.9	0.2	12.4	62.0	15.0	22.8
5.2	321.8	0.2	14.9	74.5	12.5	22.8
5.4	332.6	0.2	10.8	54.0	-20.5	22.8
5.6	341.5	0.2	8.9	44.5	-9.5	22.8
5.8	349.6	0.2	8.1	40.5	-4.0	22.8
6.0	356.8	0.2	7.2	36.0	-4.5	22.8

5C 2
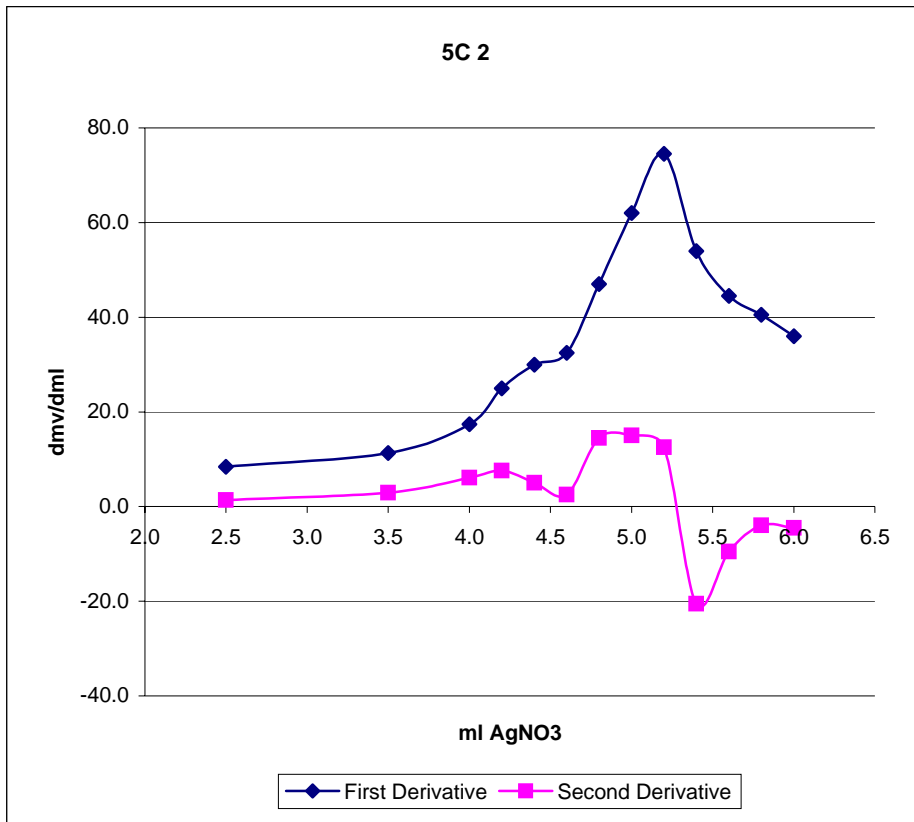
5C

3 AgNO₃ (ml)		mv	d mL	d mV	d mV/dmL		Temp C
6.0	0.0	231.8					22.7
7.0	1.0	236.5	1.0	4.7	4.7		22.8
8.0	2.0	244.1	1.0	7.6	7.6	2.9	22.8
9.0	3.0	254.3	1.0	10.2	10.2	2.6	22.8
9.5	3.5	261.9	0.5	7.6	15.2	5.0	22.8
10.0	4.0	271.1	0.5	9.2	18.4	3.2	22.8
10.2	4.2	276.4	0.2	5.3	26.5	8.1	22.9
10.4	4.4	285.1	0.2	8.7	43.5	17.0	22.9
10.6	4.6	294.3	0.2	9.2	46.0	2.5	22.9
10.8	4.8	305.4	0.2	11.1	55.5	9.5	22.9
11.0	5.0	318.9	0.2	13.5	67.5	12.0	22.9
11.2	5.2	332.5	0.2	13.6	68.0	0.5	22.9
11.4	5.4	343.1	0.2	10.6	53.0	-15.0	22.9
11.6	5.6	350.1	0.2	7.0	35.0	-18.0	23.0
11.8	5.8	357.6	0.2	7.5	37.5	2.5	23.0
12.0	6.0	362.5	0.2	4.9	24.5	-13.0	23.0

5C 3

5C
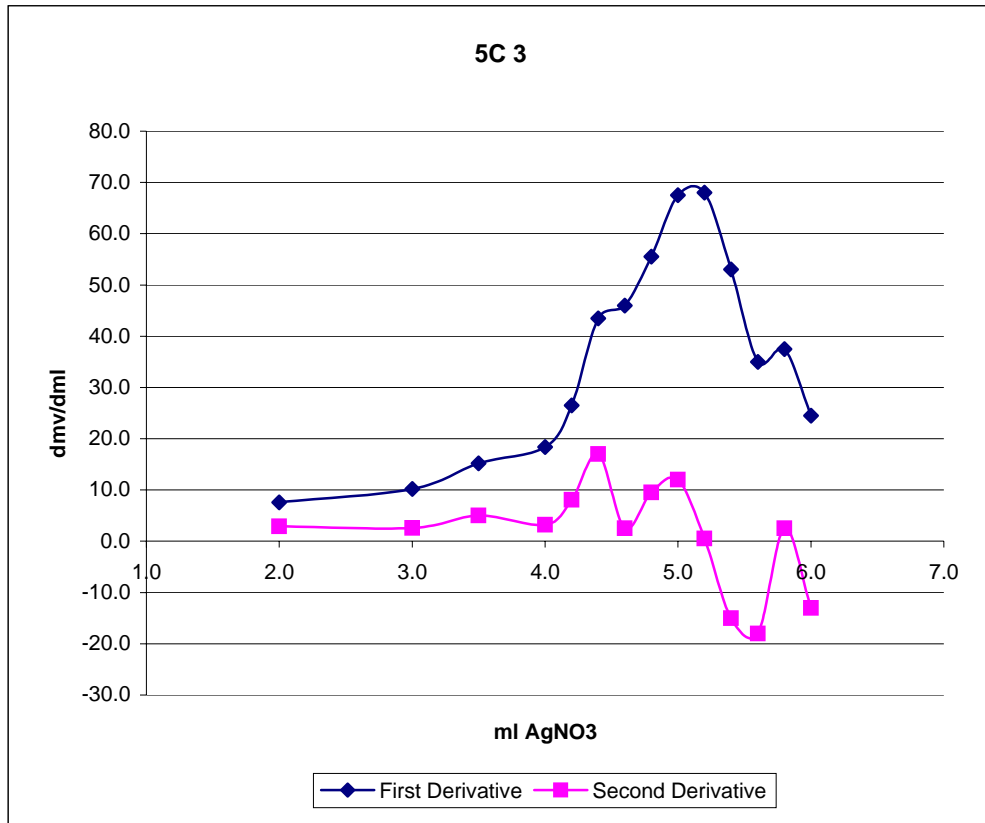
AgNO$_3$ (ml)		mv	d mL	d mV	d mV/dmL		Temp C
12.0	0.0	234.5					22.9
13.5	1.5	242.6	1.5	8.1	5.4		23.0
14.5	2.5	250.9	1.0	8.3	8.3	2.9	23.0
15.0	3.0	255.9	0.5	5.0	10.0	1.7	23.1
15.5	3.5	262.3	0.5	6.4	12.8	2.8	23.1
16.0	4.0	270.5	0.5	8.2	16.4	3.6	23.1
16.2	4.2	274.6	0.2	4.1	20.5	4.1	23.1
16.4	4.4	279.1	0.2	4.5	22.5	2.0	23.1
16.6	4.6	286.4	0.2	7.3	36.5	14.0	23.1
16.8	4.8	295.1	0.2	8.7	43.5	7.0	23.1
17.0	5.0	311.9	0.2	16.8	84.0	40.5	23.2
17.2	5.2	326.5	0.2	14.6	73.0	-11.0	23.2
17.4	5.4	336.8	0.2	10.3	51.5	-21.5	23.2
17.6	5.6	344.3	0.2	7.5	37.5	-14.0	23.2
17.8	5.8	351.2	0.2	6.9	34.5	-3.0	23.2
18.0	6.0	358.1	0.2	6.9	34.5	0.0	23.3
18.2	6.2	363.8	0.2	5.7	28.5	-6.0	23.3

5C 4
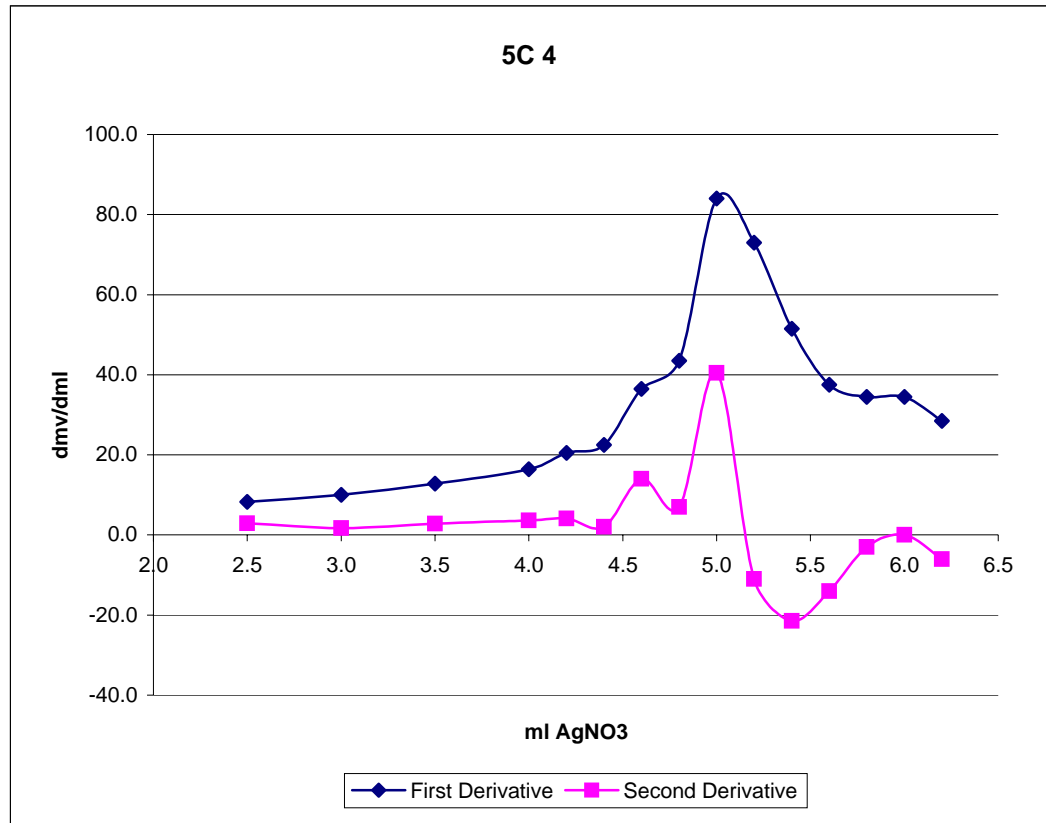
6E

1

AgNO$_3$ (ml)		mv	d mL	d mV	d mV/dmL		Temp C
10.0	0.0	208.6					22.2
14.0	4.0	218.6	4.0	10.0	2.5		22.3
16.5	6.5	227.1	2.5	8.5	3.4	0.9	22.4
17.2	7.2	230.2	0.7	3.1	4.4	1.0	22.4
18.5	8.5	235.6	1.3	5.4	4.2	-0.3	22.4
19.5	9.5	241.3	1.0	5.7	5.7	1.5	22.4
20.5	10.5	247.6	1.0	6.3	6.3	0.6	22.4
21.0	11.0	251.3	0.5	3.7	7.4	1.1	22.4
21.5	11.5	256.4	0.5	5.1	10.2	2.8	22.4
22.0	12.0	261.6	0.5	5.2	10.4	0.2	22.4
22.5	12.5	269.4	0.5	7.8	15.6	5.2	22.5
22.8	12.8	273.9	0.3	4.5	15.0	-0.6	22.5
23.0	13.0	278.6	0.2	4.7	23.5	8.5	22.5
23.2	13.2	284.1	0.2	5.5	27.5	4.0	22.5
23.4	13.4	289.7	0.2	5.6	28.0	0.5	22.5
23.6	13.6	298.6	0.2	8.9	44.5	16.5	22.5
23.8	13.8	309.6	0.2	11.0	55.0	10.5	22.5
24.0	14.0	324.6	0.2	15.0	75.0	20.0	22.5
24.2	14.2	334.6	0.2	10.0	50.0	-25.0	22.6
24.4	14.4	343.1	0.2	8.5	42.5	-7.5	22.6
24.6	14.6	350.2	0.2	7.1	35.5	-7.0	22.6
24.8	14.8	357.6	0.2	7.4	37.0	1.5	22.6

6E 1
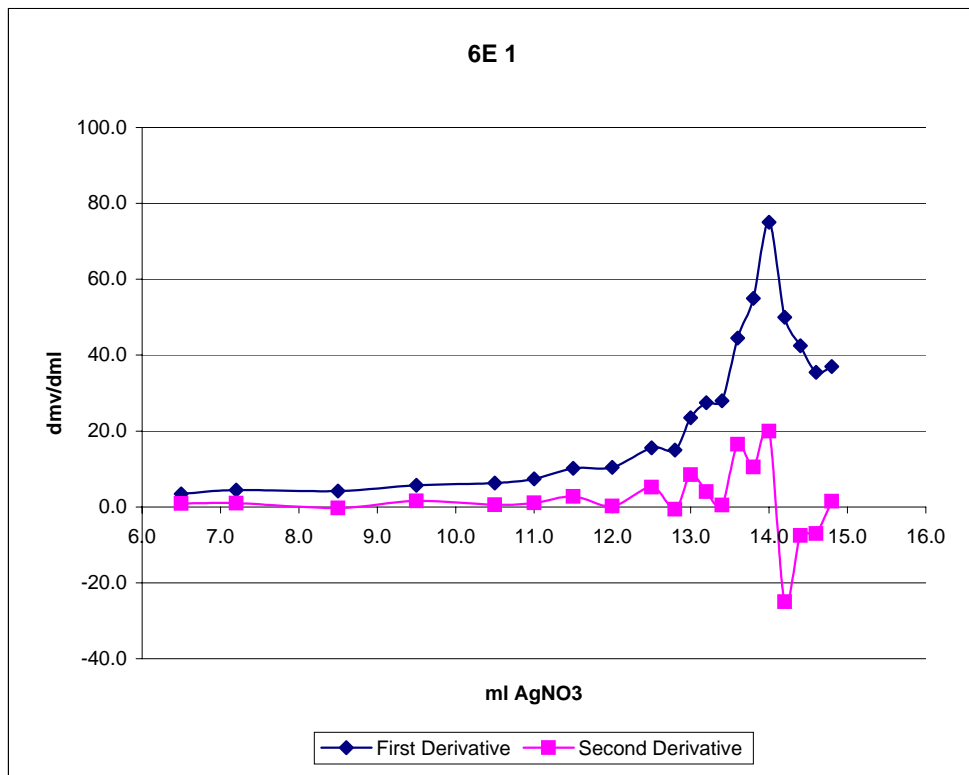
6E

2 AgNO₃ (ml)		mv	d mL	d mV	d mV/dmL		Temp C
24.8	0.0	222.3					22.5
27.0	2.2	228.1	2.2	5.8	2.6		22.6
29.0	4.2	233.9	2.0	5.8	2.9	0.3	22.6
31.0	6.2	243.6	2.0	9.7	4.8	1.9	22.7
32.0	7.2	250.6	1.0	7.0	7.0	2.2	22.7
33.0	8.2	258.9	1.0	8.3	8.3	1.3	22.7
33.5	8.7	264.1	0.5	5.2	10.4	2.1	22.7
34.0	9.2	271.9	0.5	7.8	15.6	5.2	22.7
34.2	9.4	274.6	0.2	2.7	13.5	-2.1	22.7
34.4	9.6	277.9	0.2	3.3	16.5	3.0	22.7
34.6	9.8	283.1	0.2	5.2	26.0	9.5	22.7
34.8	10.0	286.9	0.2	3.8	19.0	-7.0	22.7
35.0	10.2	294.3	0.2	7.4	37.0	18.0	22.7
35.2	10.4	302.5	0.2	8.2	41.0	4.0	22.7
35.4	10.6	313.6	0.2	11.1	55.5	14.5	22.7
35.6	10.8	328.9	0.2	15.3	76.5	21.0	22.7
35.8	11.0	338.9	0.2	10.0	50.0	-26.5	22.8
36.0	11.2	344.5	0.2	5.6	28.0	-22.0	22.8
36.2	11.4	350.6	0.2	6.1	30.5	2.5	22.8
36.4	11.6	356.1	0.2	5.5	27.5	-3.0	22.8

6E 2

y-axis: dmv/dml

x-axis: ml AgNO3

First Derivative   Second Derivative

6E
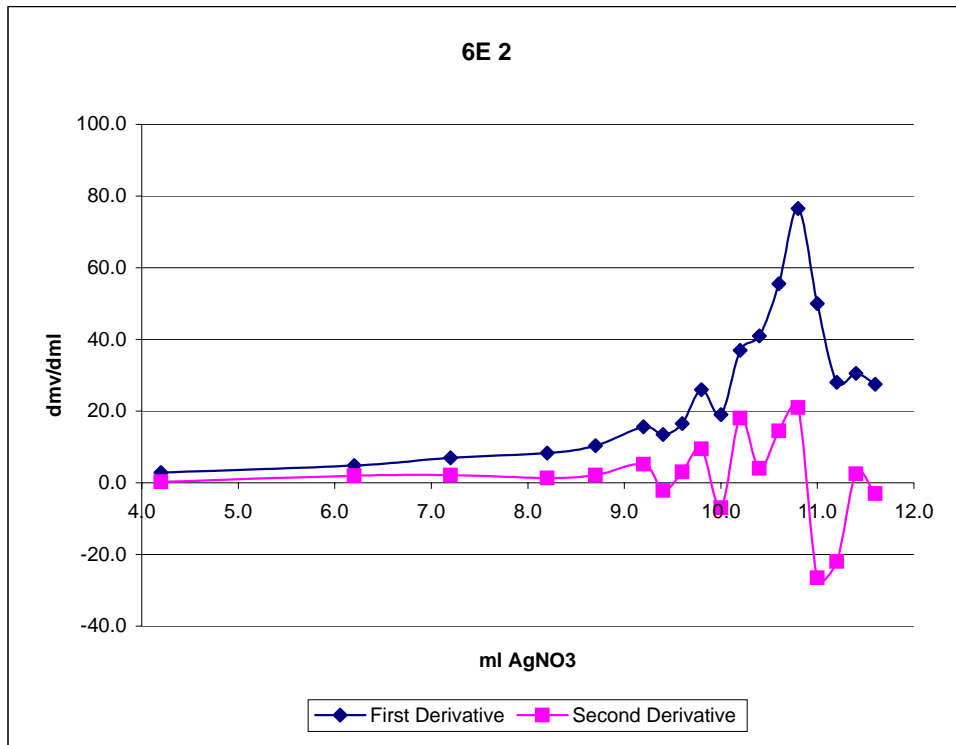
AgNO₃ (ml)	3	mv	d mL	d mV	d mV/dmL		Temp C
10.0	0.0	233.8					22.7
11.5	1.5	239.1	1.5	5.3	3.5		22.8
12.5	2.5	244.2	1.0	5.1	5.1	1.6	22.8
13.5	3.5	249.6	1.0	5.4	5.4	0.3	22.8
14.5	4.5	257.1	1.0	7.5	7.5	2.1	22.8
15.0	5.0	261.3	0.5	4.2	8.4	0.9	22.8
15.5	5.5	268.9	0.5	7.6	15.2	6.8	22.9
16.0	6.0	277.6	0.5	8.7	17.4	2.2	22.9
16.2	6.2	282.8	0.2	5.2	26.0	8.6	22.9
16.4	6.4	288.4	0.2	5.6	28.0	2.0	22.9
16.6	6.6	294.6	0.2	6.2	31.0	3.0	22.9
16.8	6.8	309.1	0.2	14.5	72.5	41.5	22.9
17.0	7.0	326.5	0.2	17.4	87.0	14.5	22.9
17.2	7.2	337.5	0.2	11.0	55.0	-32.0	22.9
17.4	7.4	346.5	0.2	9.0	45.0	-10.0	22.9
17.6	7.6	352.9	0.2	6.4	32.0	-13.0	22.9
17.8	7.8	359.8	0.2	6.9	34.5	2.5	22.9
18.0	8.0	364.6	0.2	4.8	24.0	-10.5	22.9

6E 3

6E
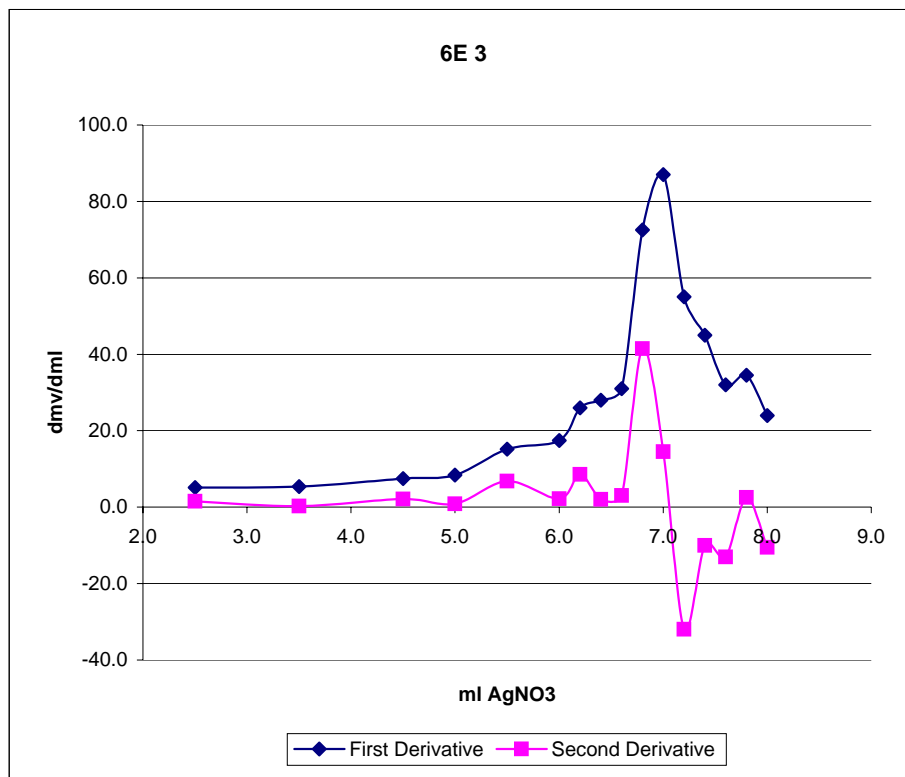
AgNO₃ (ml)		mv	d mL	d mV	d mV/dmL		Temp C
18.0	0.0	238.9					22.9
20.0	2.0	248.6	2.0	9.7	4.8		23.0
21.0	3.0	255.1	1.0	6.5	6.5	1.7	23.0
21.5	3.5	258.6	0.5	3.5	7.0	0.5	23.0
22.0	4.0	263.4	0.5	4.8	9.6	2.6	23.1
22.5	4.5	270.6	0.5	7.2	14.4	4.8	23.1
23.0	5.0	277.9	0.5	7.3	14.6	0.2	23.1
23.2	5.2	281.6	0.2	3.7	18.5	3.9	23.1
23.4	5.4	287.6	0.2	6.0	30.0	11.5	23.1
23.6	5.6	292.5	0.2	4.9	24.5	-5.5	23.1
23.8	5.8	300.1	0.2	7.6	38.0	13.5	23.2
24.0	6.0	313.3	0.2	13.2	66.0	28.0	23.2
24.2	6.2	327.8	0.2	14.5	72.5	6.5	23.2
24.4	6.4	336.5	0.2	8.7	43.5	-29.0	23.2
24.6	6.6	344.6	0.2	8.1	40.5	-3.0	23.2
24.8	6.8	352.1	0.2	7.5	37.5	-3.0	23.2
25.0	7.0	358.9	0.2	6.8	34.0	-3.5	23.2
25.2	7.2	364.1	0.2	5.2	26.0	-8.0	23.2

6E 4

7B
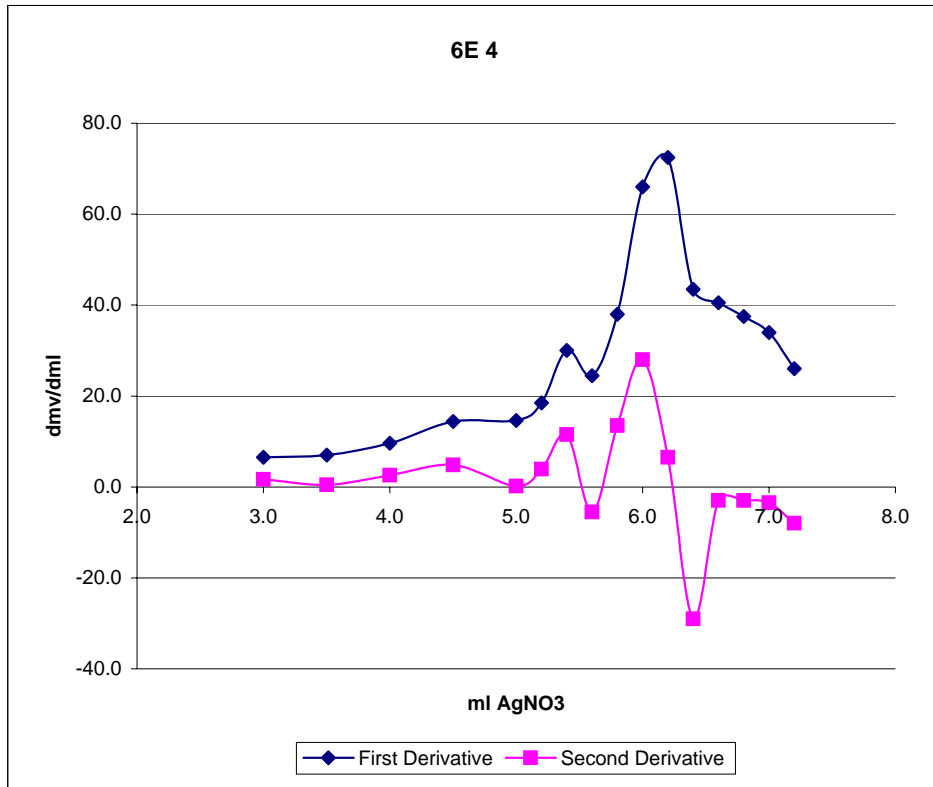
AgNO₃		mv	d mL	d mV	d mV/dmL		Temp
0.9	0	205.2					21.7
3	2.1	210.9	2.10	5.70	2.71		21.8
4.5	3.6	214.6	1.50	3.70	2.47	-0.25	21.8
6.5	5.6	220.4	2.00	5.80	2.90	0.43	21.8
7.5	6.6	223.9	1.00	3.50	3.50	0.60	21.8
8.5	7.6	227.6	1.00	3.70	3.70	0.20	21.8
9.5	8.6	232.9	1.00	5.30	5.30	1.60	21.8
10.5	9.6	239.1	1.00	6.20	6.20	0.90	21.8
11.5	10.6	245.4	1.00	6.30	6.30	0.10	21.8
12.5	11.6	258.1	1.00	12.70	12.70	6.40	21.8
13	12.1	265.4	0.50	7.30	14.60	1.90	21.8
13.2	12.3	269.2	0.20	3.80	19.00	4.40	21.8
13.4	12.5	274.1	0.20	4.90	24.50	5.50	21.8
13.6	12.7	279.9	0.20	5.80	29.00	4.50	21.8
13.8	12.9	285.6	0.20	5.70	28.50	-0.50	21.8
14	13.1	294.5	0.20	8.90	44.50	16.00	21.8
14.2	13.3	305.1	0.20	10.60	53.00	8.50	21.8
14.4	13.5	316.7	0.20	11.60	58.00	5.00	21.8
14.6	13.7	327.6	0.20	10.90	54.50	-3.50	21.8
14.8	13.9	336.1	0.20	8.50	42.50	-12.00	21.8
15	14.1	345	0.20	8.90	44.50	2.00	21.8
15.2	14.3	352.2	0.20	7.20	36.00	-8.50	21.8
15.4	14.5	357.4	0.20	5.20	26.00	-10.00	21.8
15.6	14.7	363.1	0.20	5.70	28.50	2.50	21.9

7B 1

7B

2
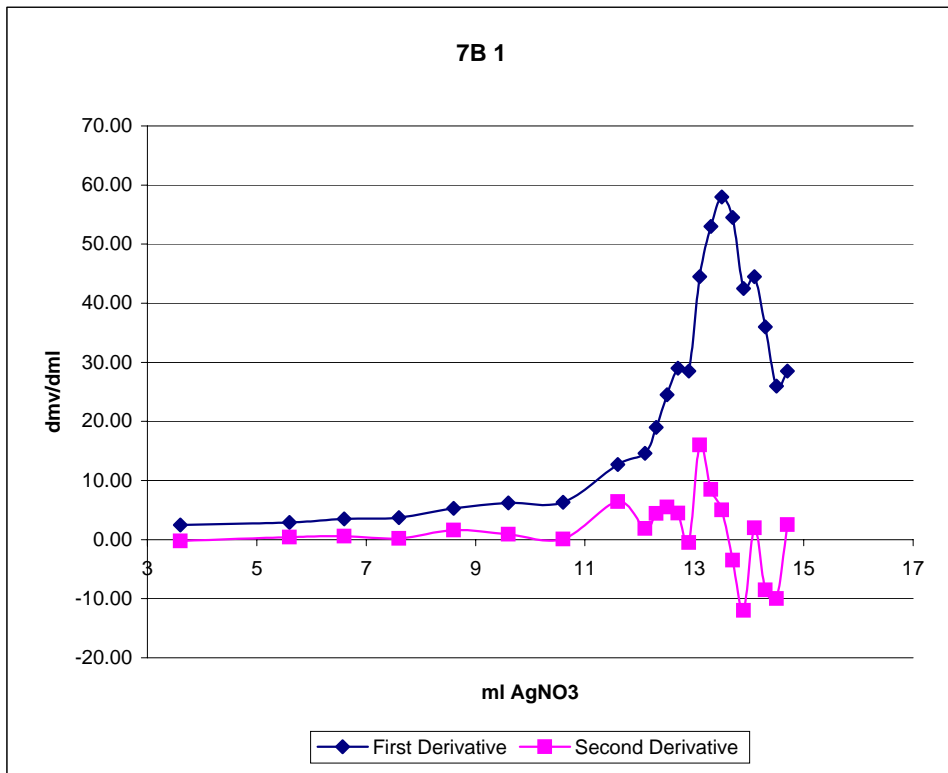
AgNO$_3$		mv	d mL	d mV	d mV/dmL		Temp
15.6	0	221.3					21.8
17.5	1.9	229.4	1.90	8.10	4.26		21.8
19	3.4	236.5	1.50	7.10	4.73	0.47	21.9
20	4.4	244.1	1.00	7.60	7.60	2.87	22
21	5.4	254.3	1.00	10.20	10.20	2.60	22
22	6.4	272.3	1.00	18.00	18.00	7.80	22
22.2	6.6	277.9	0.20	5.60	28.00	10.00	22
22.4	6.8	284.6	0.20	6.70	33.50	5.50	22
22.6	7	295.1	0.20	10.50	52.50	19.00	22.1
22.8	7.2	311.3	0.20	16.20	81.00	28.50	22.1
23	7.4	327.5	0.20	16.20	81.00	0.00	22.1
23.2	7.6	338.9	0.20	11.40	57.00	-24.00	22.1
23.4	7.8	346.9	0.20	8.00	40.00	-17.00	22.1
23.6	8	353.1	0.20	6.20	31.00	-9.00	22.1
23.8	8.2	359.9	0.20	6.80	34.00	3.00	22.1
24	8.4	364.8	0.20	4.90	24.50	-9.50	22.1

7B 2

First Derivative — Second Derivative

dmv/dml (y-axis) vs ml AgNO3 (x-axis)
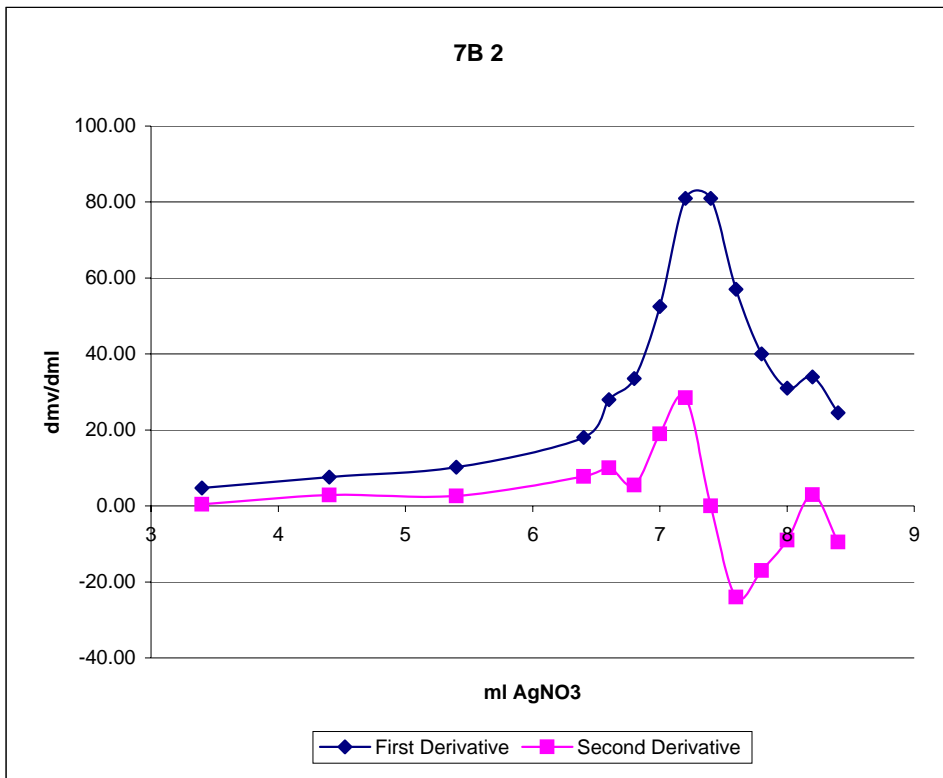
7B

3 AgNO$_3$		mv	d mL	d mV	d mV/dmL		Temp
24	0	227.5					22
25.5	1.5	236.1	1.50	8.60	5.73		22
26.5	2.5	244.6	1.00	8.50	8.50	2.77	22.1
27.5	3.5	254.3	1.00	9.70	9.70	1.20	22.1
28	4	262.5	0.50	8.20	16.40	6.70	22.1
28.5	4.5	272.6	0.50	10.10	20.20	3.80	22.2
28.7	4.7	279.1	0.20	6.50	32.50	12.30	22.2
28.9	4.9	288.6	0.20	9.50	47.50	15.00	22.2
29.1	5.1	299.2	0.20	10.60	53.00	5.50	22.2
29.3	5.3	313.1	0.20	13.90	69.50	16.50	22.2
29.5	5.5	330.2	0.20	17.10	85.50	16.00	22.2
29.7	5.7	340.8	0.20	10.60	53.00	-32.50	22.2
29.9	5.9	349.6	0.20	8.80	44.00	-9.00	22.2
30.1	6.1	355.1	0.20	5.50	27.50	-16.50	22.2
30.3	6.3	360.1	0.20	5.00	25.00	-2.50	22.2
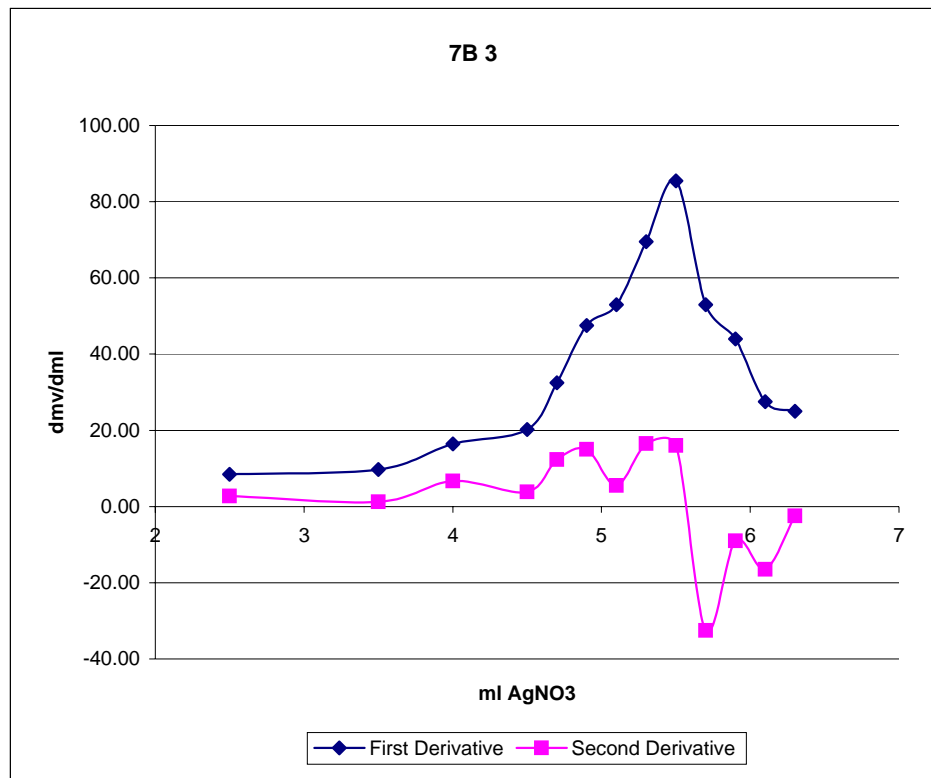
7B

4

AgNO$_3$		mv	d mL	d mV	d mV/dmL		Temp
30.3	0	229.5					22.1
31.8	1.5	236.7	1.50	7.20	4.80		22.2
33	2.7	244.6	1.20	7.90	6.58	1.78	22.2
34	3.7	254	1.00	9.40	9.40	2.82	22.2
35	4.7	267.5	1.00	13.50	13.50	4.10	22.3
35.5	5.2	281.6	0.50	14.10	28.20	14.70	22.3
35.7	5.4	287.9	0.20	6.30	31.50	3.30	22.3
35.9	5.6	299.6	0.20	11.70	58.50	27.00	22.3
36.1	5.8	314.5	0.20	14.90	74.50	16.00	22.3
36.3	6	328.9	0.20	14.40	72.00	-2.50	22.3
36.5	6.2	339.1	0.20	10.20	51.00	-21.00	22.3
36.7	6.4	348.4	0.20	9.30	46.50	-4.50	22.3
36.9	6.6	357.1	0.20	8.70	43.50	-3.00	22.3
37.1	6.8	365.3	0.20	8.20	41.00	-2.50	22.3
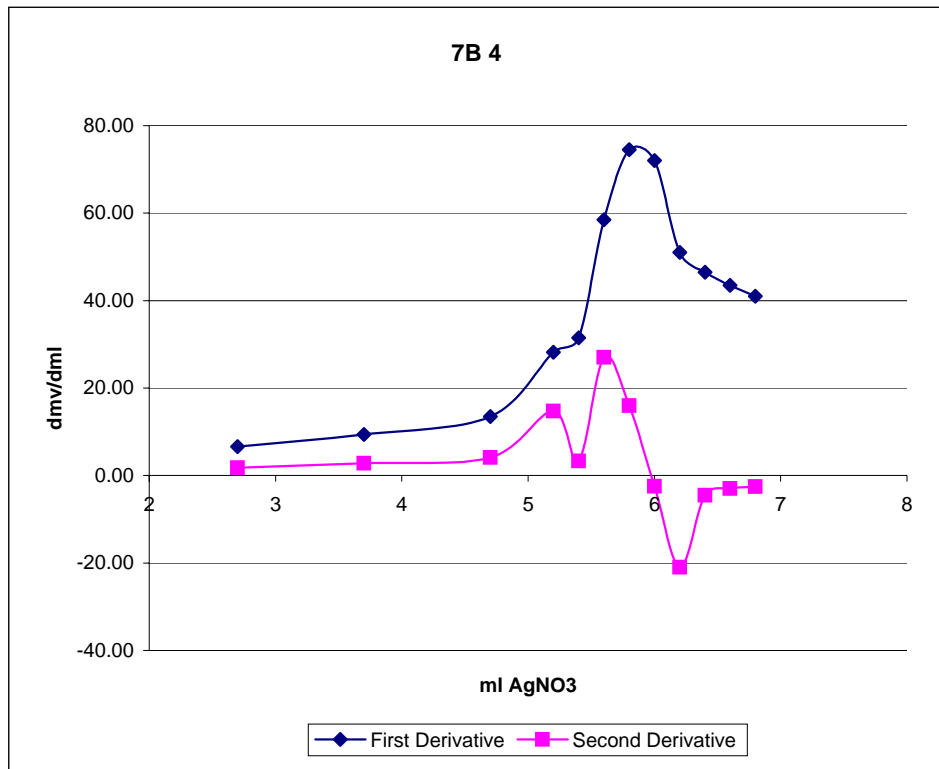
7C

	1					
AgNO$_3$	mv	d mL	d mV	d mV/dmL		Temp
0	193.3					22.4
6	207	6.00	13.70	2.28		22.5
10	220.2	4.00	13.20	3.30	1.02	22.5
13	236.3	3.00	16.10	5.37	2.07	22.6
15	258.1	2.00	21.80	10.90	5.53	22.6
16	281.4	1.00	23.30	23.30	12.40	22.6
16.2	292	0.20	10.60	53.00	29.70	22.6
16.4	308.4	0.20	16.40	82.00	29.00	22.7
16.6	324.2	0.20	15.80	79.00	-3.00	22.7
16.8	337.7	0.20	13.50	67.50	-11.50	22.7
17	348.6	0.20	10.90	54.50	-13.00	22.7
17.2	354.1	0.20	5.50	27.50	-27.00	22.7
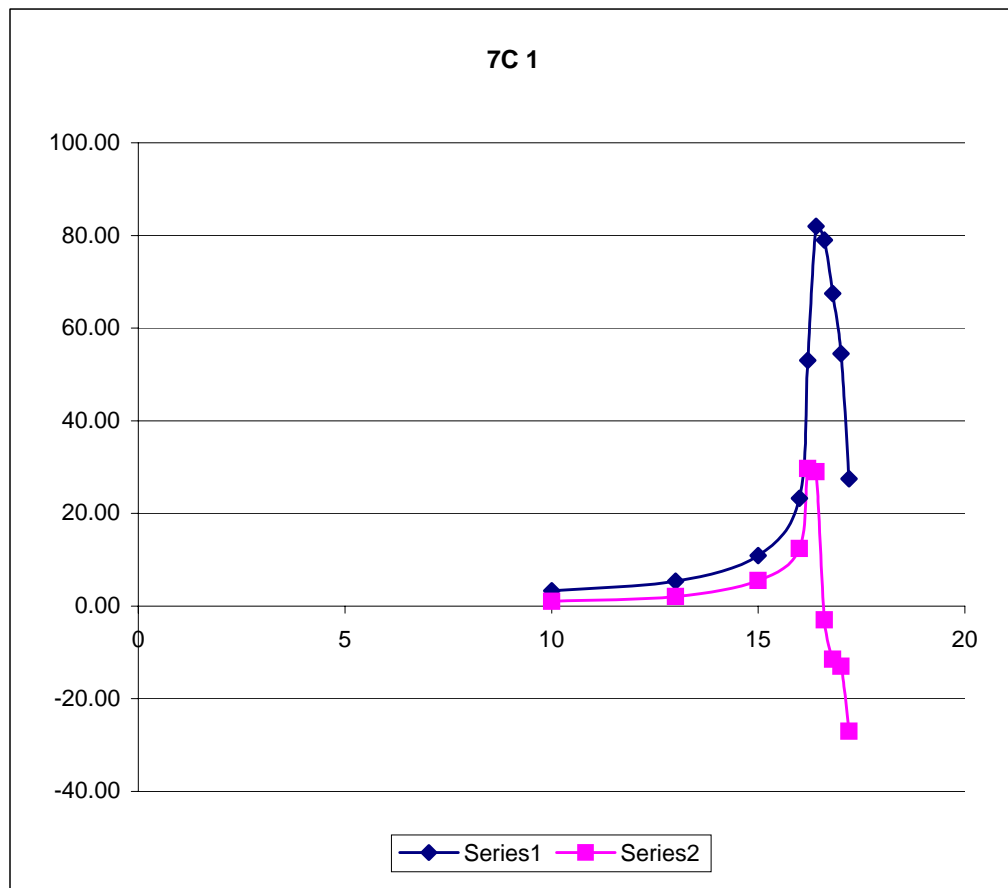
7C

2

AgNO$_3$	mv	d mL	d mV	d mV/dmL		Temp
0	203.4					22.5
6	218.1	6.00	14.70	2.45		22.6
10	234.9	4.00	16.80	4.20	1.75	22.6
12	249.7	2.00	14.80	7.40	3.20	22.6
13	262.3	1.00	12.60	12.60	5.20	22.6
13.5	272.4	0.50	10.10	20.20	7.60	22.6
13.8	280.8	0.30	8.40	28.00	7.80	22.6
14	288.2	0.20	7.40	37.00	9.00	22.6
14.2	298.1	0.20	9.90	49.50	12.50	22.6
14.4	309.7	0.20	11.60	58.00	8.50	22.7
14.6	323.1	0.20	13.40	67.00	9.00	22.7
14.8	332.3	0.20	9.20	46.00	-21.00	22.7
15	340.1	0.20	7.80	39.00	-7.00	22.7
15.2	345.6	0.20	5.50	27.50	-11.50	22.7
15.4	350.7	0.20	5.10	25.50	-2.00	22.7

7C 2

First Derivative   Second Derivative
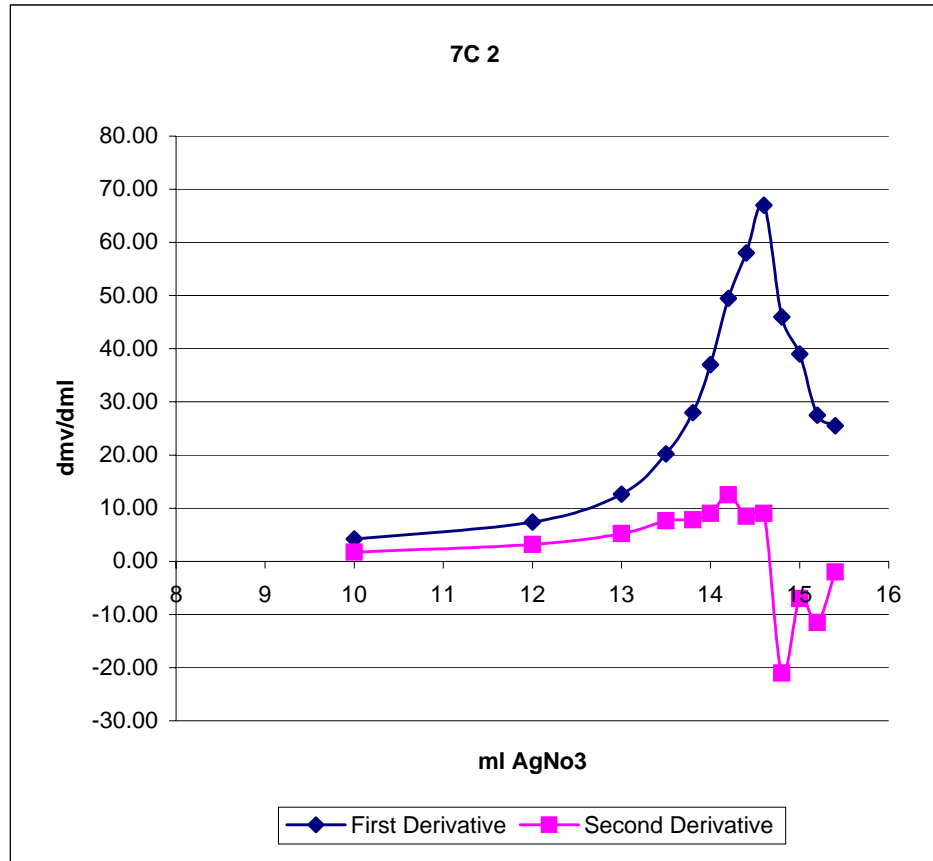
7C

3

AgNO$_3$	mv	d mL	d mV	d mV/dmL		Temp
0	222.4					22.4
4	243.6	4.00	21.20	5.30		22.5
6	269.1	2.00	25.50	12.75	7.45	22.5
6.5	282.1	0.50	13.00	26.00	13.25	22.5
6.7	291.6	0.20	9.50	47.50	21.50	22.5
6.9	302.3	0.20	10.70	53.50	6.00	22.5
7.1	314.1	0.20	11.80	59.00	5.50	22.6
7.3	327.5	0.20	13.40	67.00	8.00	22.6
7.5	335.8	0.20	8.30	41.50	-25.50	22.6
7.7	343.1	0.20	7.30	36.50	-5.00	22.6
7.9	349.6	0.20	6.50	32.50	-4.00	22.6
8.1	354.3	0.20	4.70	23.50	-9.00	22.6
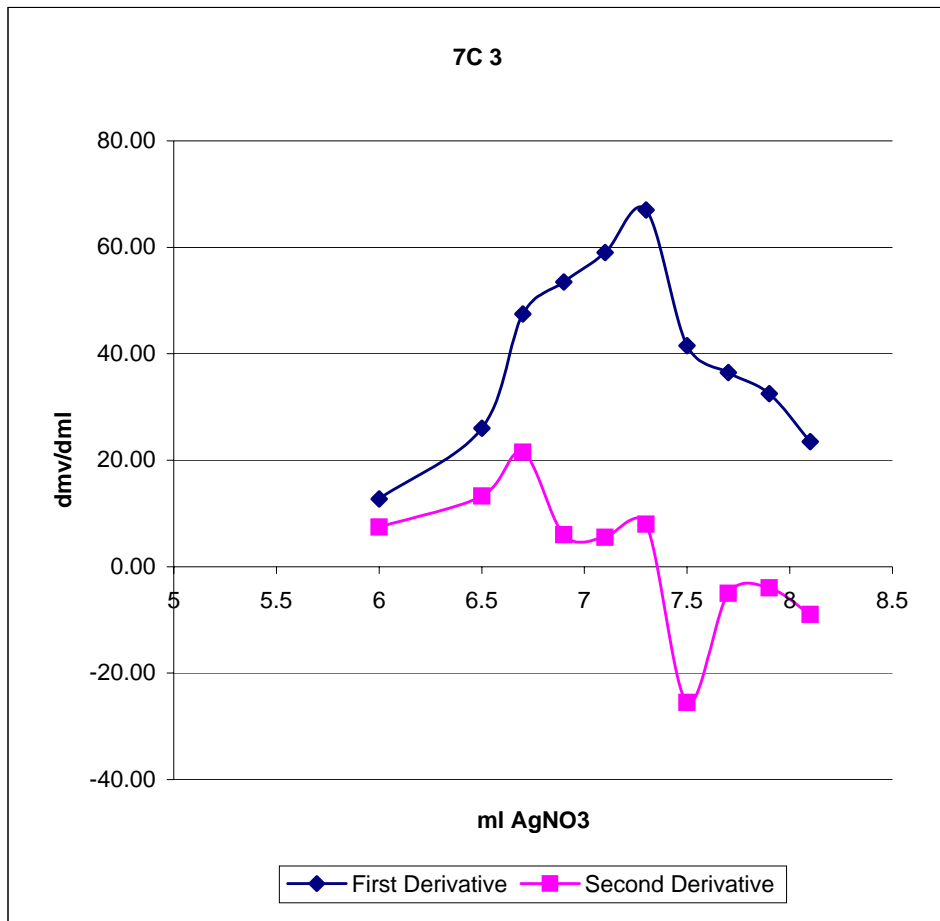
7C

4

AgNO$_3$		mv	d mL	d mV	d mV/dmL		Temp
8.1	0	226.6					22.5
10.9	2.8	246	2.80	19.40	6.93		22.5
12.2	4.1	263.1	1.30	17.10	13.15	6.23	22.6
12.7	4.6	274.2	0.50	11.10	22.20	9.05	22.6
13	4.9	285.9	0.30	11.70	39.00	16.80	22.6
13.2	5.1	298.9	0.20	13.00	65.00	26.00	22.6
13.4	5.3	314.1	0.20	15.20	76.00	11.00	22.6
13.6	5.5	327.5	0.20	13.40	67.00	-9.00	22.6
13.8	5.7	338.6	0.20	11.10	55.50	-11.50	22.6
14	5.9	346.8	0.20	8.20	41.00	-14.50	22.6
14.2	6.1	352.9	0.20	6.10	30.50	-10.50	22.6
14.4	6.3	358.3	0.20	5.40	27.00	-3.50	22.6
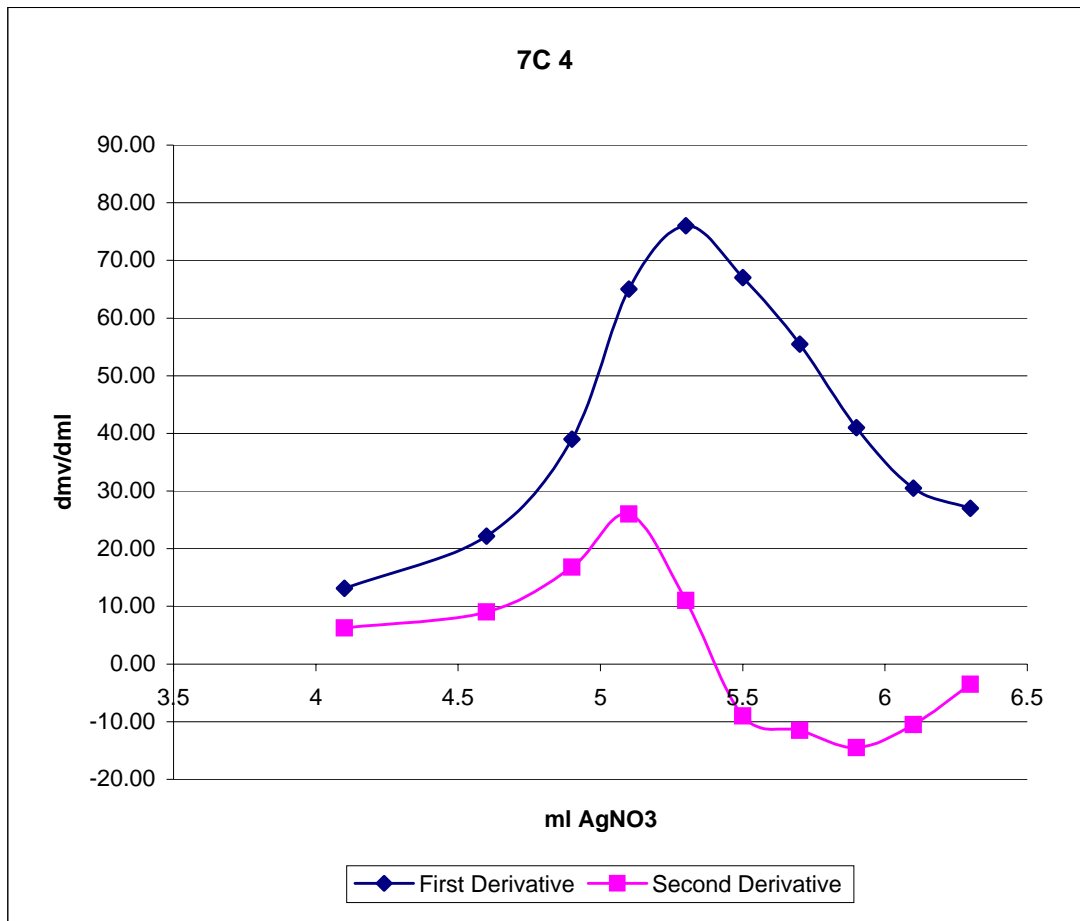
8B

1

AgNO$_3$	mv	d mL	d mV	d mV/dmL		Temp
0	198.2					21.9
5	211.7	5.00	13.50	2.70		22
8	224.6	3.00	12.90	4.30	1.60	22
11	249.5	3.00	24.90	8.30	4.00	22
12	267.2	1.00	17.70	17.70	9.40	22
12.3	277.4	0.30	10.20	34.00	16.30	22
12.6	297.5	0.30	20.10	67.00	33.00	22
12.8	316.8	0.20	19.30	96.50	29.50	22.1
13	330.8	0.20	14.00	70.00	-26.50	22.1
13.2	341.1	0.20	10.30	51.50	-18.50	22.1
13.4	350.8	0.20	9.70	48.50	-3.00	22.1
13.6	356.7	0.20	5.90	29.50	-19.00	22.1

8B
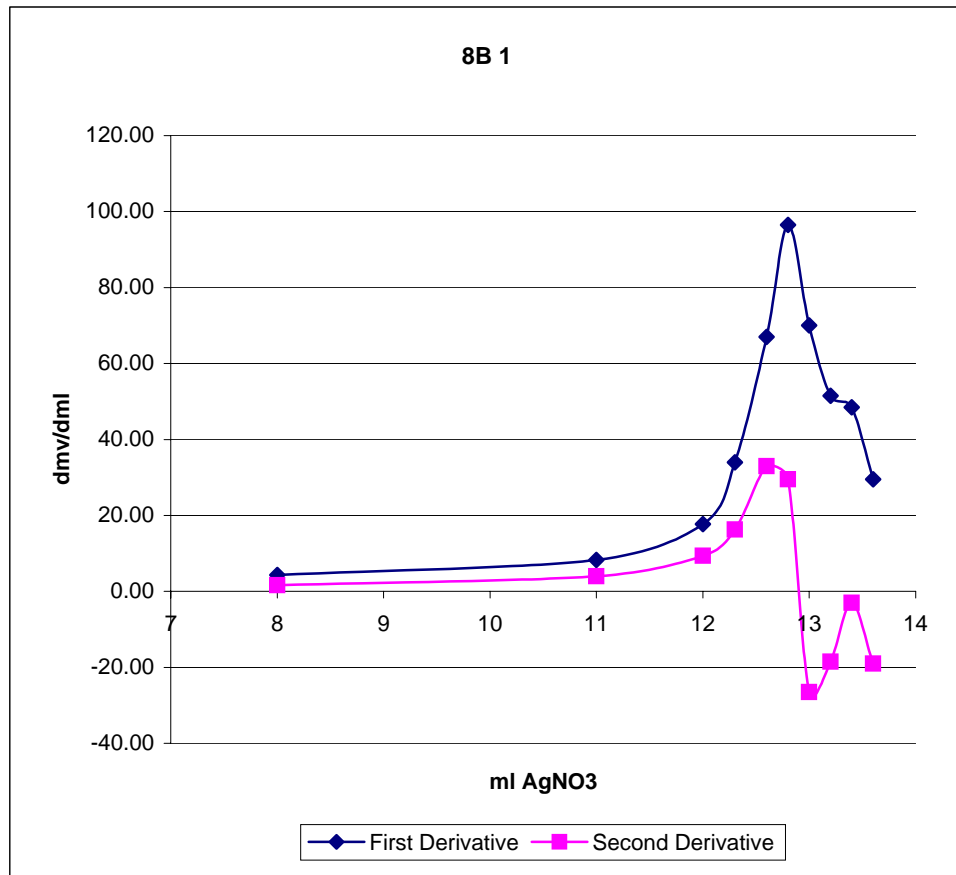
AgNO$_3$		mv	d mL	d mV	d mV/dmL		Temp
1.5	0	216.9					22
6	4.5	237.1	4.50	20.20	4.49		22.1
8	6.5	255.7	2.00	18.60	9.30	4.81	22.1
9	7.5	274.5	1.00	18.80	18.80	9.50	22.1
9.3	7.8	285.4	0.30	10.90	36.33	17.53	22.1
9.5	8	292.4	0.20	7.00	35.00	-1.33	22.2
9.7	8.2	306.7	0.20	14.30	71.50	36.50	22.2
9.9	8.4	320.5	0.20	13.80	69.00	-2.50	22.2
10.1	8.6	330.4	0.20	9.90	49.50	-19.50	22.2
10.3	8.8	341.7	0.20	11.30	56.50	7.00	22.2
10.5	9	349	0.20	7.30	36.50	-20.00	22.3
10.7	9.2	354.7	0.20	5.70	28.50	-8.00	22.3
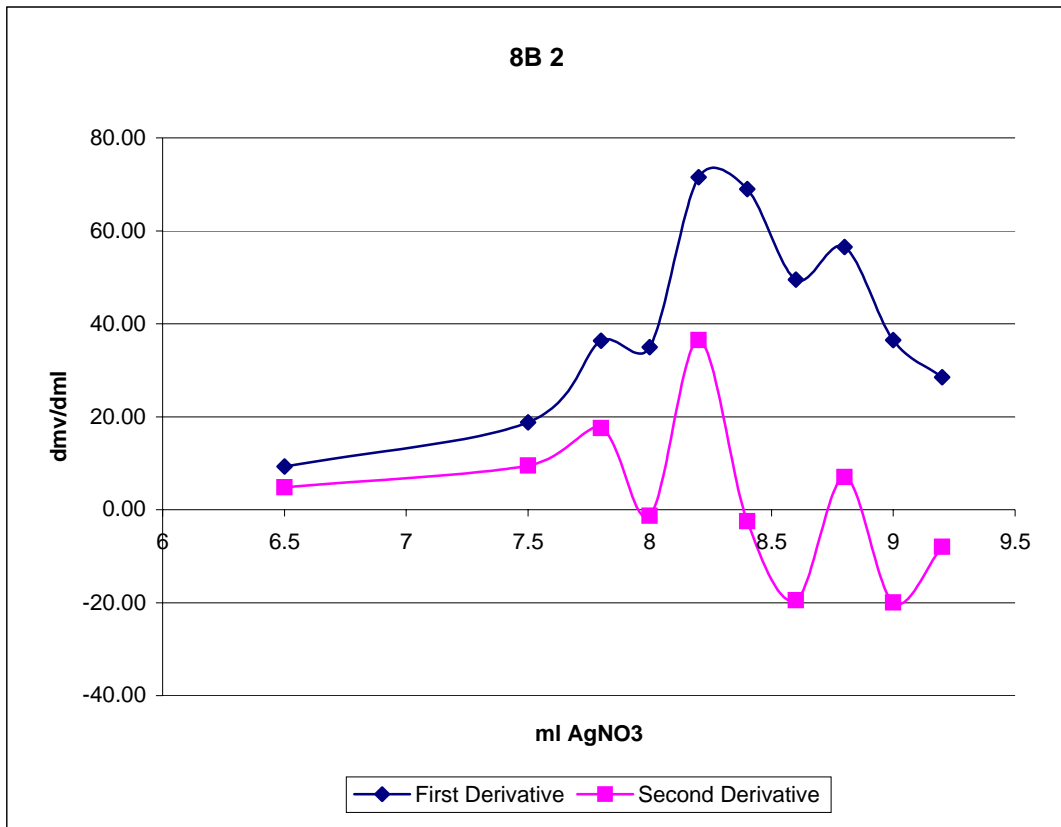
8B

3 AgNO$_3$		mv	d mL	d mV	d mV/dmL		Temp
0.8	0	218.8					22.2
5.3	4.5	254.8	4.50	36.00	8.00		22.2
6.5	5.7	296.9	1.20	42.10	35.08	27.08	22.3
6.7	5.9	316.4	0.20	19.50	97.50	62.42	22.3
6.9	6.1	328.8	0.20	12.40	62.00	-35.50	22.3
7.1	6.3	339.5	0.20	10.70	53.50	-8.50	22.3
7.3	6.5	347.1	0.20	7.60	38.00	-15.50	22.3
7.5	6.7	353.8	0.20	6.70	33.50	-4.50	22.3

8B 3
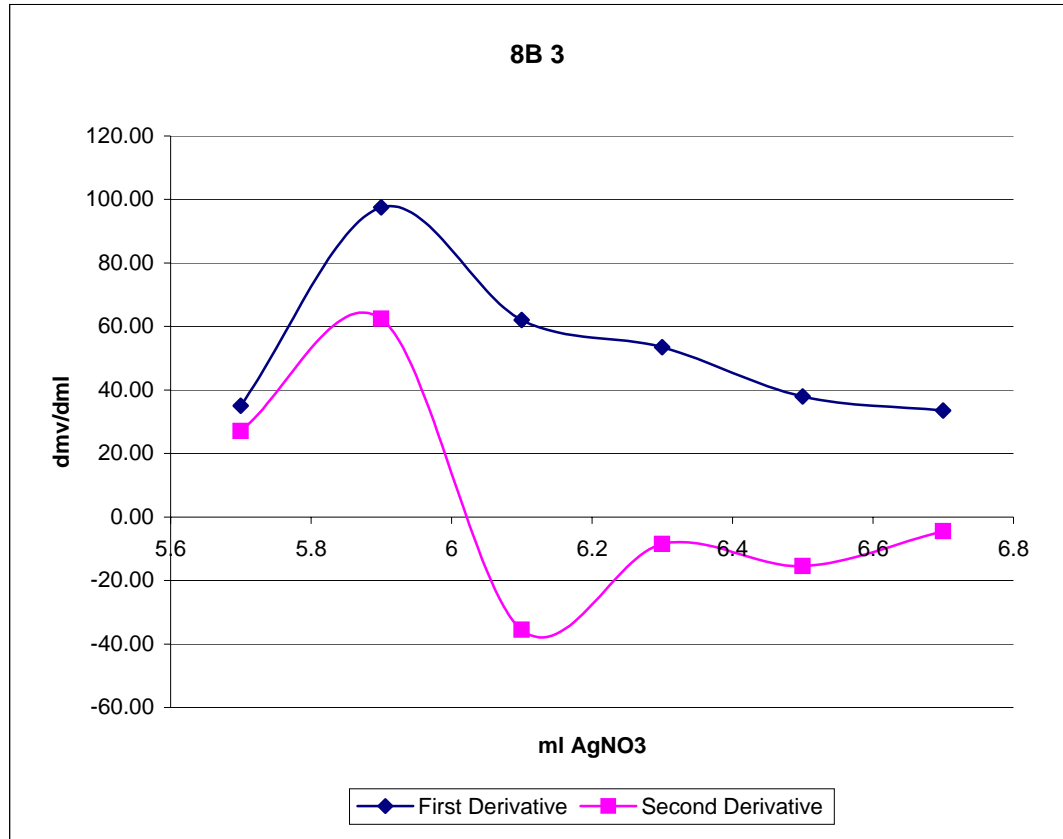
8B

4 AgNO$_3$		mv	d mL	d mV	d mV/dmL		Temp
5.7	0	220.8					22.2
9	3.3	243.2	3.30	22.40	6.79		22.3
10.5	4.8	268.1	1.50	24.90	16.60	9.81	22.3
11	5.3	286.7	0.50	18.60	37.20	20.60	22.3
11.2	5.5	303.1	0.20	16.40	82.00	44.80	22.3
11.4	5.7	319.6	0.20	16.50	82.50	0.50	22.3
11.6	5.9	333.2	0.20	13.60	68.00	-14.50	22.3
11.8	6.1	344.4	0.20	11.20	56.00	-12.00	22.3
12	6.3	350.8	0.20	6.40	32.00	-24.00	22.3
12.2	6.5	356.1	0.20	5.30	26.50	-5.50	22.3

8C1
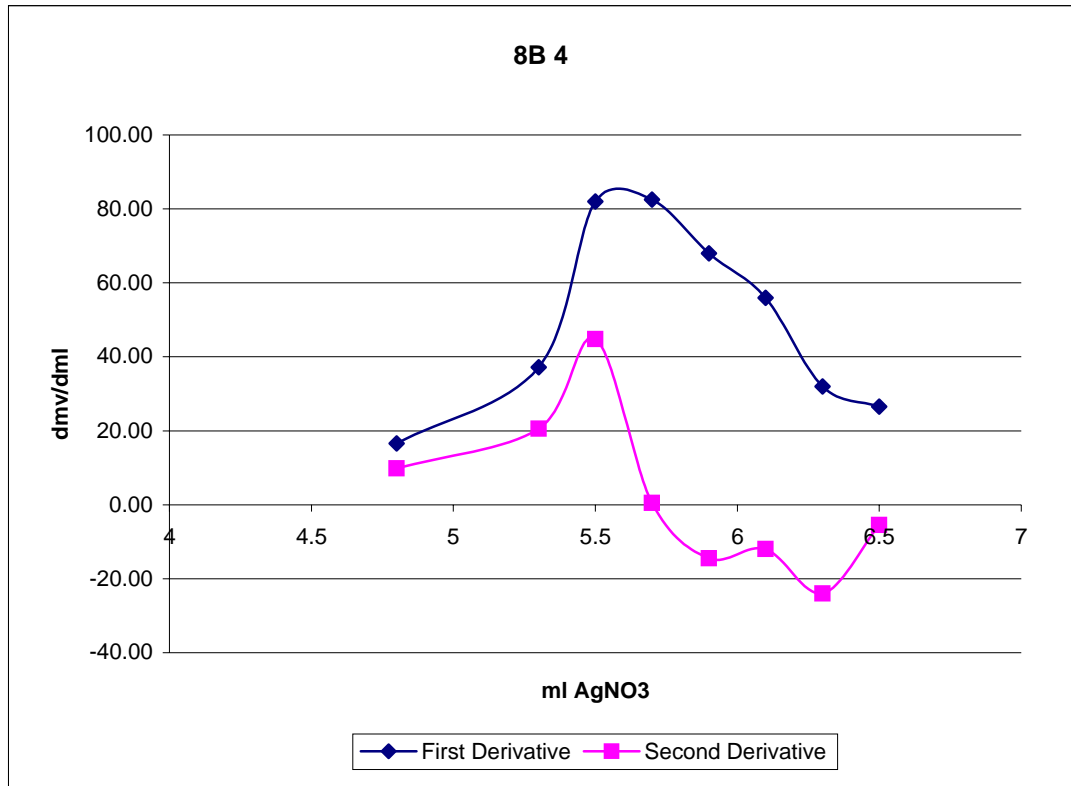
AgNO$_3$	mv	d mL	d mV	d mV/dmL		Temp
0	200.6					22.7
6	217.7	6.00	17.10	2.85		22.8
10	233.4	4.00	15.70	3.93	1.08	22.8
13	256.6	3.00	23.20	7.73	3.81	22.8
13.5	263.8	0.50	7.20	14.40	6.67	22.8
14	274.1	0.50	10.30	20.60	6.20	22.9
14.4	284.3	0.40	10.20	25.50	4.90	22.9
14.65	294.9	0.25	10.60	42.40	16.90	22.9
14.8	302.2	0.15	7.30	48.67	6.27	22.9
15	313.9	0.20	11.70	58.50	9.83	22.9
15.2	326.9	0.20	13.00	65.00	6.50	22.9
15.4	336.6	0.20	9.70	48.50	-16.50	22.9
15.6	344.7	0.20	8.10	40.50	-8.00	22.9
15.8	351.3	0.20	6.60	33.00	-7.50	22.9
16	355.7	0.20	4.40	22.00	-11.00	22.9

8C1 1
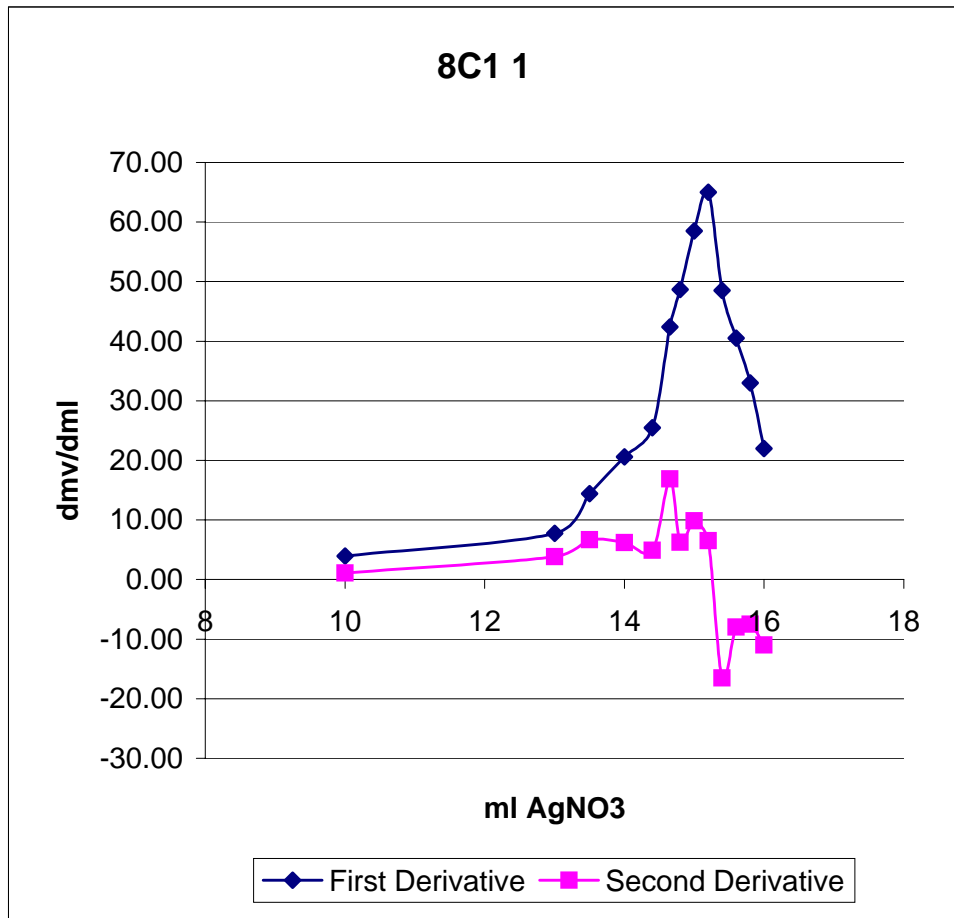
8C1

2

AgNO$_3$	mv	d mL	d mV	d mV/dmL		Temp
0	205.1					22.7
6	219.5	6.00	14.40	2.40		22.8
9	230.7	3.00	11.20	3.73	1.33	22.8
12	249.5	3.00	18.80	6.27	2.53	22.8
13	260.8	1.00	11.30	11.30	5.03	22.8
13.5	268.5	0.50	7.70	15.40	4.10	22.8
13.8	276.2	0.30	7.70	25.67	10.27	22.8
14.1	285.4	0.30	9.20	30.67	5.00	22.8
14.3	293.5	0.20	8.10	40.50	9.83	22.9
14.5	303.7	0.20	10.20	51.00	10.50	22.9
14.7	316.4	0.20	12.70	63.50	12.50	22.9
14.9	327.6	0.20	11.20	56.00	-7.50	22.9
15.1	337.1	0.20	9.50	47.50	-8.50	22.9
15.3	345.3	0.20	8.20	41.00	-6.50	22.9
15.5	351.7	0.20	6.40	32.00	-9.00	22.9

8C1 2
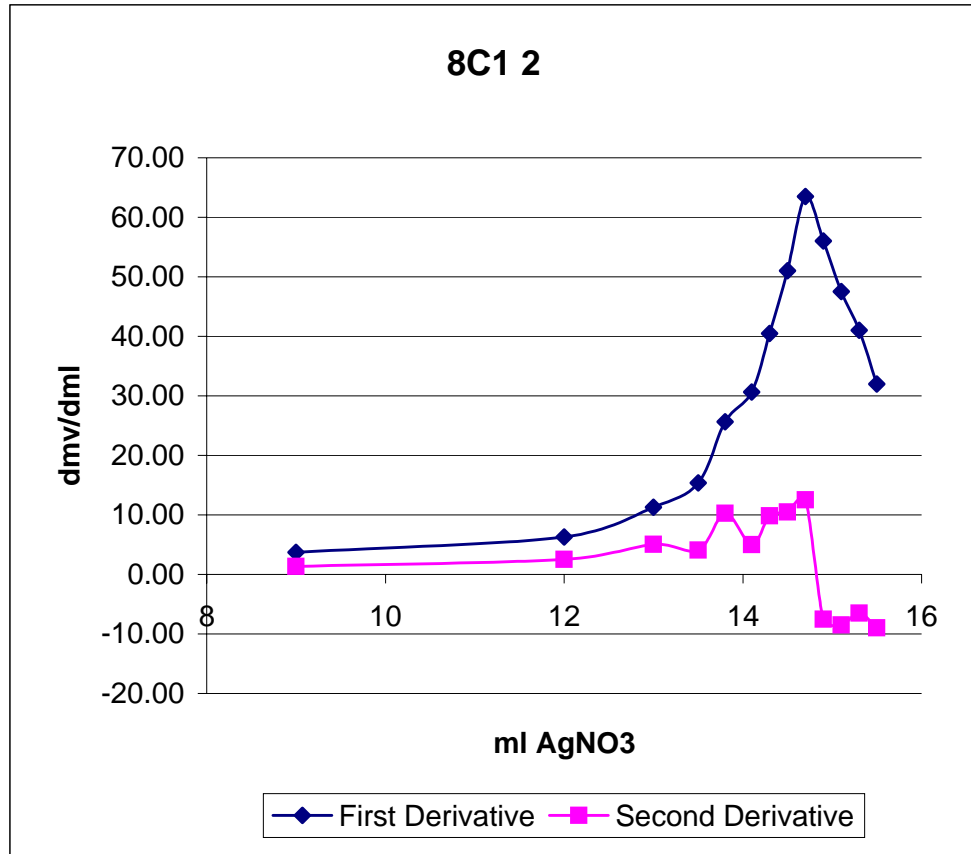
8C1

3 AgNO$_3$	mv	d mL	d mV	d mV/dmL		Temp
0	213.4					22.8
4	232.8	4.00	19.40	4.85		22.9
6	250.2	2.00	17.40	8.70	3.85	22.9
7	266.2	1.00	16.00	16.00	7.30	22.9
7.5	280.1	0.50	13.90	27.80	11.80	22.9
7.7	288.5	0.20	8.40	42.00	14.20	22.9
7.9	299.7	0.20	11.20	56.00	14.00	22.9
8.1	311.9	0.20	12.20	61.00	5.00	23
8.3	324.7	0.20	12.80	64.00	3.00	23
8.5	333.9	0.20	9.20	46.00	-18.00	23
8.7	341.7	0.20	7.80	39.00	-7.00	23
8.9	348.1	0.20	6.40	32.00	-7.00	23
9.1	353.9	0.20	5.80	29.00	-3.00	23
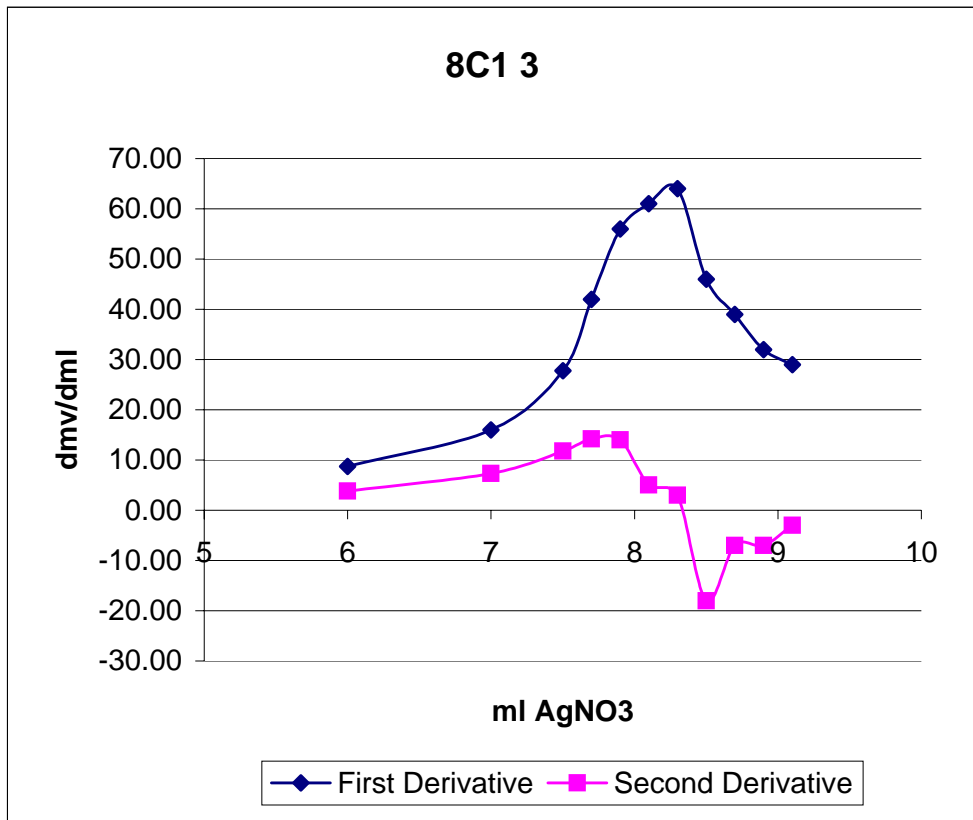
8C1

4

AgNO$_3$	mv	d mL	d mV	d mV/dmL		Temp
0	229.8					22.9
3	253.2	3.00	23.40	7.80		22.9
4	270.3	1.00	17.10	17.10	9.30	23
4.4	284.1	0.40	13.80	34.50	17.40	23
4.6	293.5	0.20	9.40	47.00	12.50	23
4.8	304.8	0.20	11.30	56.50	9.50	23
5	316.5	0.20	11.70	58.50	2.00	23
5.2	332.7	0.20	16.20	81.00	22.50	23
5.4	343.7	0.20	11.00	55.00	-26.00	23
5.6	350.5	0.20	6.80	34.00	-21.00	23
5.8	356.1	0.20	5.60	28.00	-6.00	23

8C1 4

A2
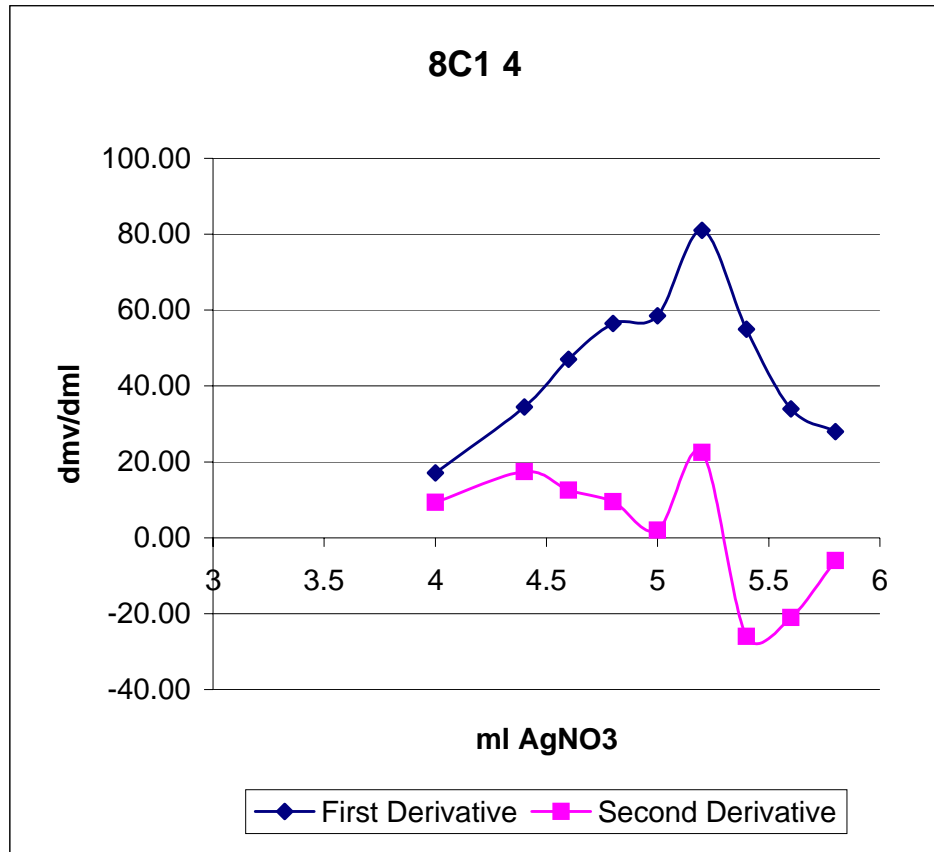
AgNO$_3$		mv	d mL	d mV	d mV/dmL		Temp
0.5	0	218.4					22.5
3.5	3	232.6	3.00	14.20	4.73		22.6
4.5	4	240.8	1.00	8.20	8.20	3.47	22.6
5.5	5	251.9	1.00	11.10	11.10	2.90	22.6
6	5.5	261.5	0.50	9.60	19.20	8.10	22.7
6.2	5.7	264.8	0.20	3.30	16.50	-2.70	22.7
6.4	5.9	268.7	0.20	3.90	19.50	3.00	22.7
6.6	6.1	274.5	0.20	5.80	29.00	9.50	22.7
6.8	6.3	282.5	0.20	8.00	40.00	11.00	22.7
7	6.5	294.5	0.20	12.00	60.00	20.00	22.7
7.2	6.7	309.1	0.20	14.60	73.00	13.00	22.7
7.4	6.9	331.2	0.20	22.10	110.50	37.50	22.7
7.6	7.1	343.5	0.20	12.30	61.50	-49.00	22.7
7.8	7.3	353.4	0.20	9.90	49.50	-12.00	22.7
8	7.5	361.2	0.20	7.80	39.00	-10.50	22.7
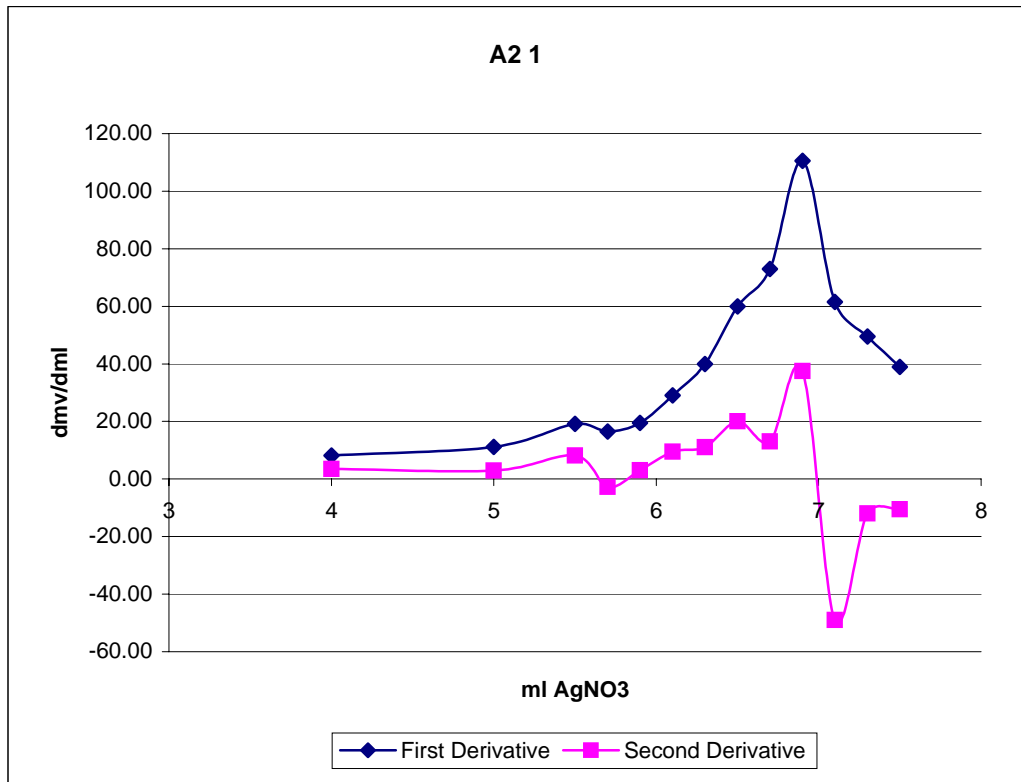
A2

2

AgNO$_3$		mv	d mL	d mV	d mV/dmL		Temp
8	0	225.1					22.6
11.5	3.5	241.3	3.50	16.20	4.63		22.7
12.5	4.5	249.9	1.00	8.60	8.60	3.97	22.7
13	5	253.6	0.50	3.70	7.40	-1.20	22.8
13.5	5.5	259.4	0.50	5.80	11.60	4.20	22.8
14	6	269.1	0.50	9.70	19.40	7.80	22.8
14.2	6.2	273.5	0.20	4.40	22.00	2.60	22.8
14.4	6.4	277.9	0.20	4.40	22.00	0.00	22.8
14.6	6.6	285.4	0.20	7.50	37.50	15.50	22.8
14.8	6.8	297.5	0.20	12.10	60.50	23.00	22.8
15	7	315.1	0.20	17.60	88.00	27.50	22.8
15.2	7.2	332.1	0.20	17.00	85.00	-3.00	22.8
15.4	7.4	343.5	0.20	11.40	57.00	-28.00	22.8
15.6	7.6	351.9	0.20	8.40	42.00	-15.00	22.8
15.8	7.8	358.7	0.20	6.80	34.00	-8.00	22.8
16	8	365.1	0.20	6.40	32.00	-2.00	22.8

A2
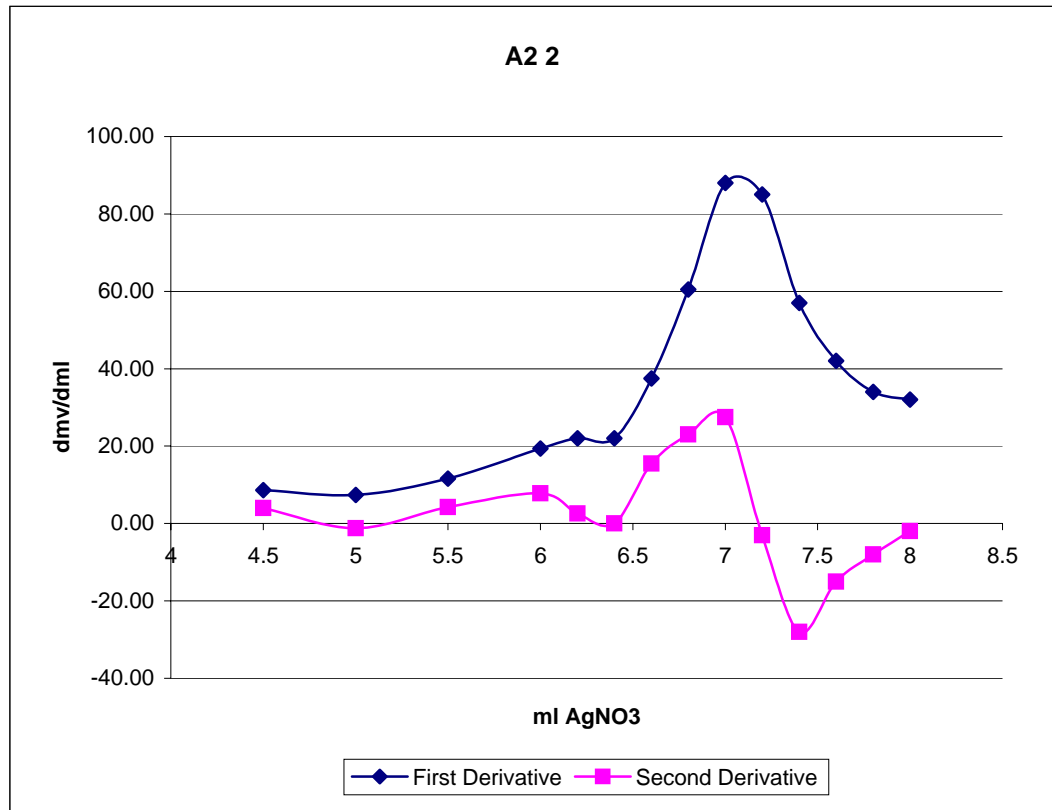
AgNO$_3$		mv	d mL	d mV	d mV/dmL		Temp
16	0	228.1					22.7
19.5	3.5	244.9	3.50	16.80	4.80		22.7
20.5	4.5	254.9	1.00	10.00	10.00	5.20	22.8
21.5	5.5	268.7	1.00	13.80	13.80	3.80	22.8
21.7	5.7	272.8	0.20	4.10	20.50	6.70	22.8
21.9	5.9	279.2	0.20	6.40	32.00	11.50	22.8
22.1	6.1	287.9	0.20	8.70	43.50	11.50	22.8
22.3	6.3	299.1	0.20	11.20	56.00	12.50	22.8
22.5	6.5	317.1	0.20	18.00	90.00	34.00	22.8
22.7	6.7	332.1	0.20	15.00	75.00	-15.00	22.9
22.9	6.9	343.3	0.20	11.20	56.00	-19.00	22.9
23.1	7.1	351.9	0.20	8.60	43.00	-13.00	22.9
23.3	7.3	359.8	0.20	7.90	39.50	-3.50	22.9
23.5	7.5	366.9	0.20	7.10	35.50	-4.00	22.9
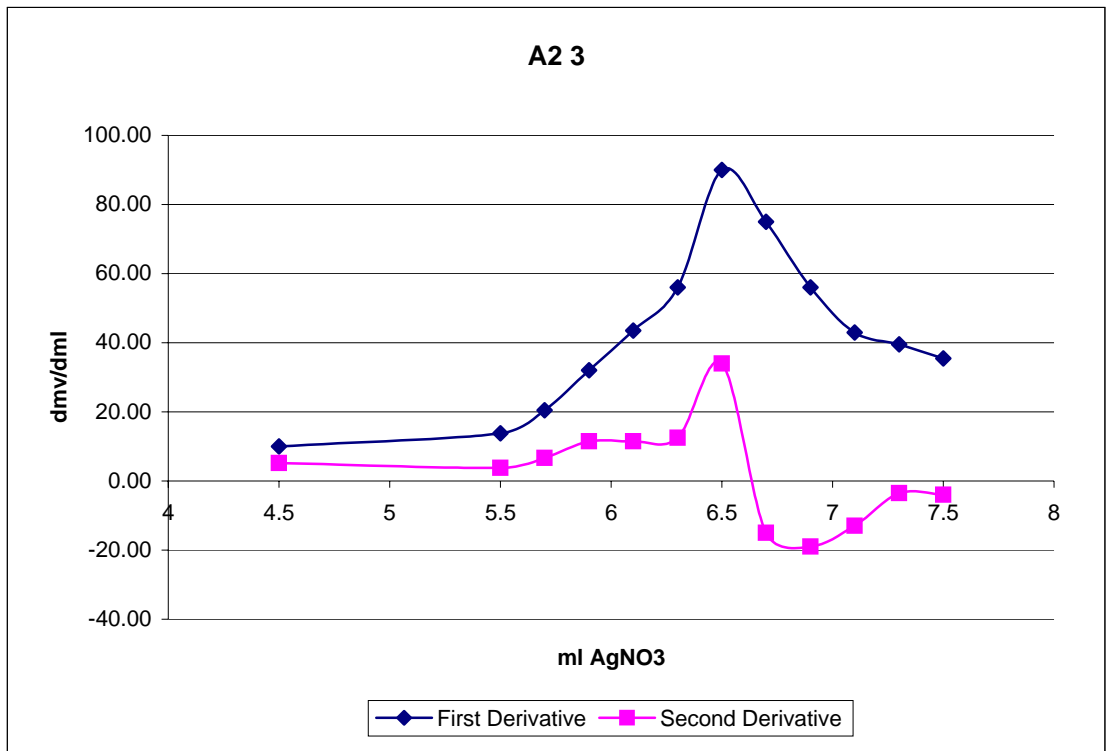
A2

4

AgNO$_3$		mv	d mL	d mV	d mV/dmL		Temp
23.5	0	230.1					23
26	2.5	244.9	2.50	14.80	5.92		23.1
27	3.5	252.9	1.00	8.00	8.00	2.08	23.1
28	4.5	265.4	1.00	12.50	12.50	4.50	23.1
28.5	5	276.9	0.50	11.50	23.00	10.50	23.1
28.7	5.2	281.6	0.20	4.70	23.50	0.50	23.1
28.9	5.4	289.1	0.20	7.50	37.50	14.00	23.2
29.1	5.6	303.4	0.20	14.30	71.50	34.00	23.2
29.3	5.8	322.1	0.20	18.70	93.50	22.00	23.2
29.5	6	335.6	0.20	13.50	67.50	-26.00	23.2
29.7	6.2	346.9	0.20	11.30	56.50	-11.00	23.2
29.9	6.4	355.1	0.20	8.20	41.00	-15.50	23.2
30.1	6.6	363.7	0.20	8.60	43.00	2.00	23.2

A4
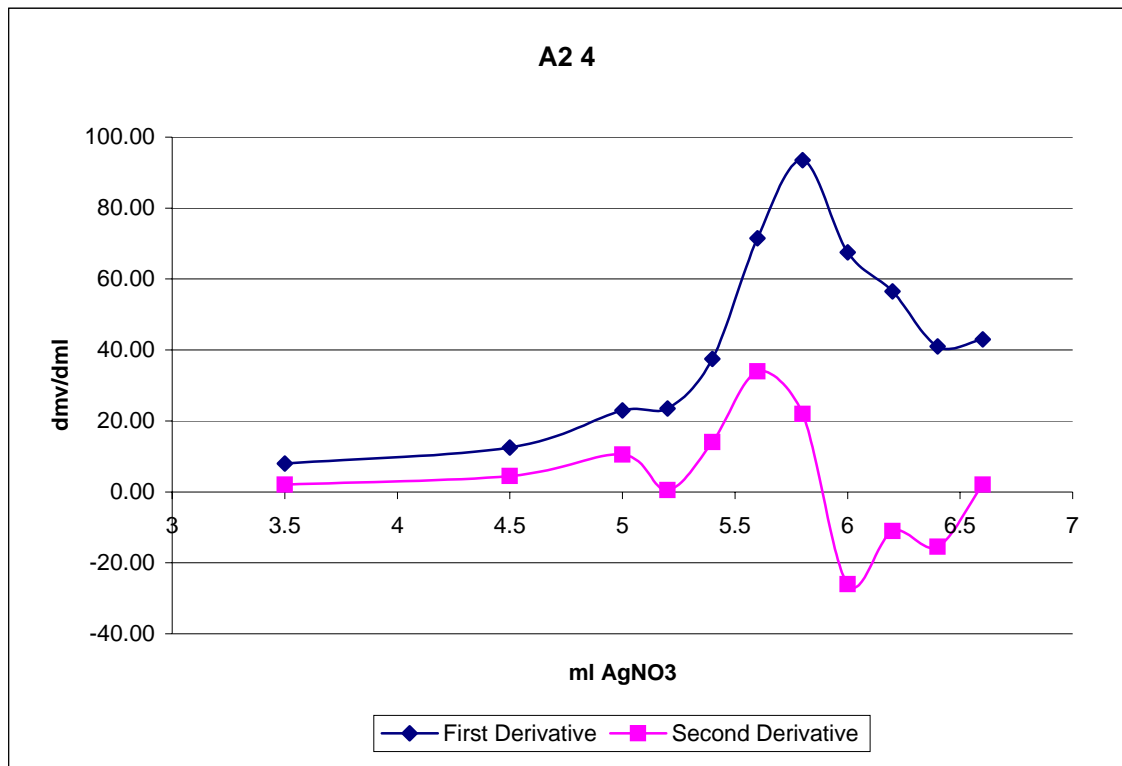
AgNO$_3$ (ml)		mv	d mL	d mV	d mV/dmL		Temp C
1.0	0.0	209.8					23.0
3.5	2.5	217.9	2.5	8.1	3.2		23.1
4.0	3.0	222.2	0.5	4.3	8.6	5.4	23.1
5.5	4.5	227.9	1.5	5.7	3.8	-4.8	23.2
6.5	5.5	231.2	1.0	3.3	3.3	-0.5	23.2
7.5	6.5	236.9	1.0	5.7	5.7	2.4	23.2
8.5	7.5	243.5	1.0	6.6	6.6	0.9	23.2
9.5	8.5	251.2	1.0	7.7	7.7	1.1	23.2
10.5	9.5	266.5	1.0	15.3	15.3	7.6	23.3
11.0	10.0	274.9	0.5	8.4	16.8	1.5	23.3
11.2	10.2	278.9	0.2	4.0	20.0	3.2	23.3
11.4	10.4	283.5	0.2	4.6	23.0	3.0	23.3
11.6	10.6	290.1	0.2	6.6	33.0	10.0	23.3
11.8	10.8	302.1	0.2	12.0	60.0	27.0	23.3
12.0	11.0	322.9	0.2	20.8	104.0	44.0	23.3
12.2	11.2	335.1	0.2	12.2	61.0	-43.0	23.3
12.4	11.4	345.6	0.2	10.5	52.5	-8.5	23.3
12.6	11.6	353.6	0.2	8.0	40.0	-12.5	23.3
12.8	11.8	360.5	0.2	6.9	34.5	-5.5	23.3

A4 1
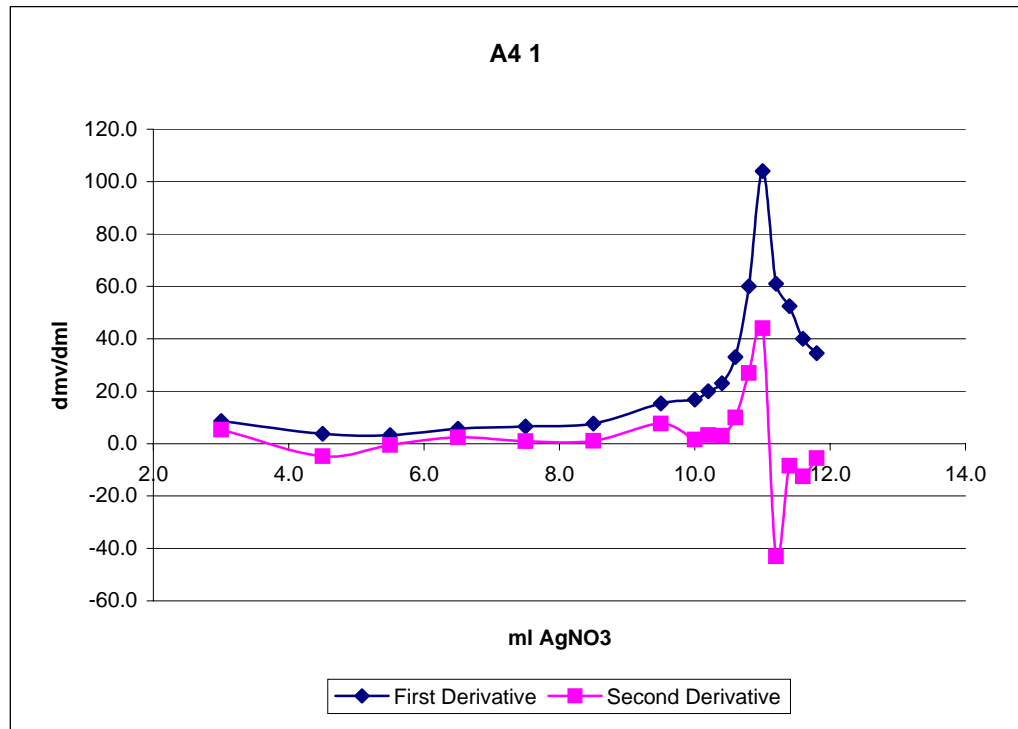
A4

2 AgNO$_3$ (ml)		mv	d mL	d mV	d mV/dmL		Temp C
12.8	0.0	227.1					23.2
15.0	2.2	238.9	2.2	11.8	5.4		23.2
16.0	3.2	245.8	1.0	6.9	6.9	1.5	23.2
17.0	4.2	254.4	1.0	8.6	8.6	1.7	23.2
17.5	4.7	260.1	0.5	5.7	11.4	2.8	23.2
18.0	5.2	267.3	0.5	7.2	14.4	3.0	23.3
18.2	5.4	271.1	0.2	3.8	19.0	4.6	23.3
18.4	5.6	275.9	0.2	4.8	24.0	5.0	23.3
18.6	5.8	282.3	0.2	6.4	32.0	8.0	23.3
18.8	6.0	289.6	0.2	7.3	36.5	4.5	23.3
19.0	6.2	299.1	0.2	9.5	47.5	11.0	23.3
19.2	6.4	315.4	0.2	16.3	81.5	34.0	23.3
19.4	6.6	331.2	0.2	15.8	79.0	-2.5	23.4
19.6	6.8	342.6	0.2	11.4	57.0	-22.0	23.4
19.8	7.0	351.6	0.2	9.0	45.0	-12.0	23.4
20.0	7.2	358.9	0.2	7.3	36.5	-8.5	23.4
20.2	7.4	365.1	0.2	6.2	31.0	-5.5	23.4

A4 2
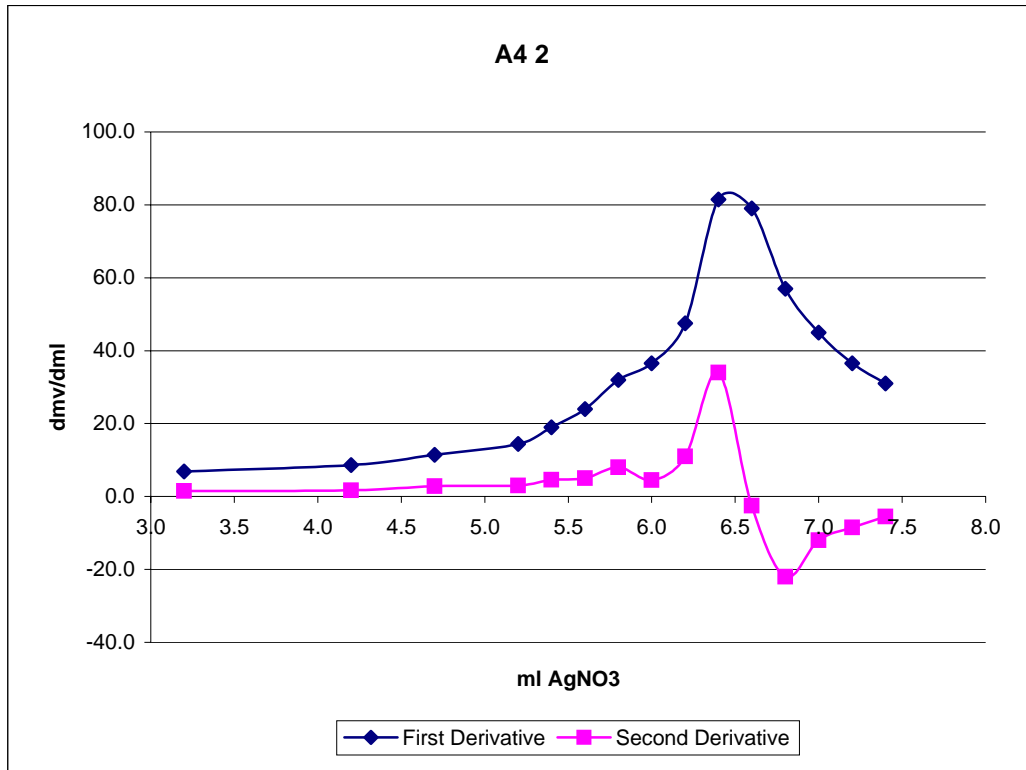
A4

3 AgNO$_3$ (ml)		mv	d mL	d mV	d mV/dmL		Temp C
20.2	0.0	229.2					23.3
22.0	1.8	235.7	1.8	6.5	3.6		23.3
23.0	2.8	241.2	1.0	5.5	5.5	1.9	23.4
24.0	3.8	250.1	1.0	8.9	8.9	3.4	23.4
24.5	4.3	256.8	0.5	6.7	13.4	4.5	23.4
25.0	4.8	263.5	0.5	6.7	13.4	0.0	23.4
25.2	5.0	266.8	0.2	3.3	16.5	3.1	23.4
25.4	5.2	270.6	0.2	3.8	19.0	2.5	23.4
25.6	5.4	277.2	0.2	6.6	33.0	14.0	23.4
25.8	5.6	286.2	0.2	9.0	45.0	12.0	23.4
26.0	5.8	298.5	0.2	12.3	61.5	16.5	23.5
26.2	6.0	315.2	0.2	16.7	83.5	22.0	23.5
26.4	6.2	331.2	0.2	16.0	80.0	-3.5	23.5
26.6	6.4	342.2	0.2	11.0	55.0	-25.0	23.5
26.8	6.6	349.5	0.2	7.3	36.5	-18.5	23.5
27.0	6.8	356.8	0.2	7.3	36.5	0.0	23.5
27.2	7.0	362.5	0.2	5.7	28.5	-8.0	23.5

A4 3
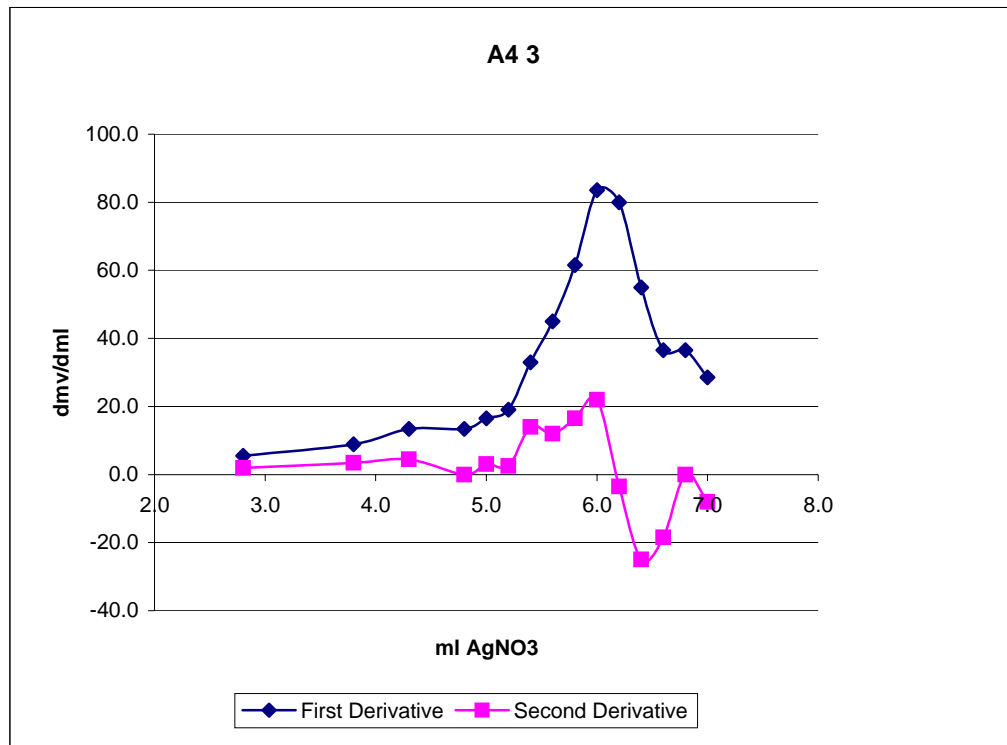
A4

4 AgNO$_3$ (ml)		mv	d mL	d mV	d mV/dmL		Temp C
27.2	0.0	229.2					22.6
29.0	1.8	237.2	1.8	8.0	4.4		22.6
30.0	2.8	245.6	1.0	8.4	8.4	4.0	22.6
30.5	3.3	251.2	0.5	5.6	11.2	2.8	22.7
31.0	3.8	258.5	0.5	7.3	14.6	3.4	22.7
31.5	4.3	266.4	0.5	7.9	15.8	1.2	22.7
31.7	4.5	270.1	0.2	3.7	18.5	2.7	22.7
31.9	4.7	275.2	0.2	5.1	25.5	7.0	22.7
32.1	4.9	281.9	0.2	6.7	33.5	8.0	22.7
32.3	5.1	290.1	0.2	8.2	41.0	7.5	22.7
32.5	5.3	306.1	0.2	16.0	80.0	39.0	22.7
32.7	5.5	321.2	0.2	15.1	75.5	-4.5	22.7
32.9	5.7	333.1	0.2	11.9	59.5	-16.0	22.7
33.1	5.9	344.1	0.2	11.0	55.0	-4.5	22.8
33.3	6.1	353.1	0.2	9.0	45.0	-10.0	22.8
33.5	6.3	361.1	0.2	8.0	40.0	-5.0	22.8
33.7	6.5	367.2	0.2	6.1	30.5	-9.5	22.8
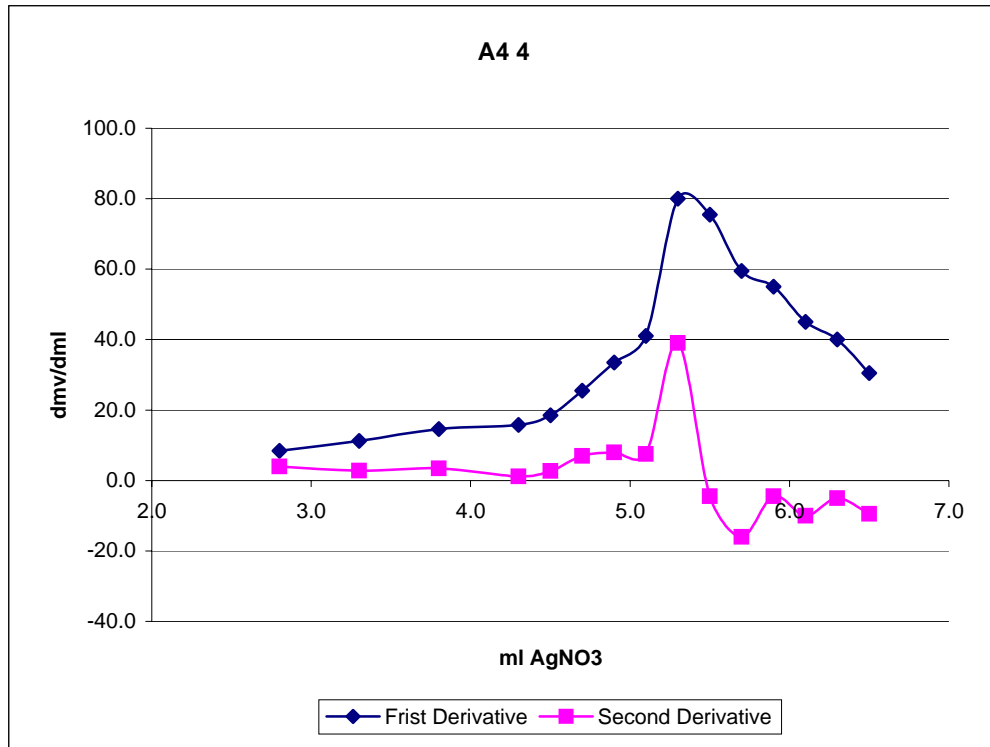
A8

1

AgNO$_3$	mv	d mL	d mV	d mV/dmL		Temp
0	203.2					21.7
6	214.8	6.00	11.60	1.93		21.8
10	227.1	4.00	12.30	3.08	1.14	21.8
13	242.3	3.00	15.20	5.07	1.99	21.8
15	261.5	2.00	19.20	9.60	4.53	21.8
15.5	269.8	0.50	8.30	16.60	7.00	21.8
16	282.3	0.50	12.50	25.00	8.40	21.8
16.2	289.1	0.20	6.80	34.00	9.00	21.8
16.4	297.8	0.20	8.70	43.50	9.50	21.8
16.6	308.5	0.20	10.70	53.50	10.00	21.9
16.8	320.9	0.20	12.40	62.00	8.50	21.9
17	330.9	0.20	10.00	50.00	-12.00	21.9
17.2	340.2	0.20	9.30	46.50	-3.50	21.9
17.4	347.6	0.20	7.40	37.00	-9.50	21.9
17.6	353.2	0.20	5.60	28.00	-9.00	21.9

A8 1
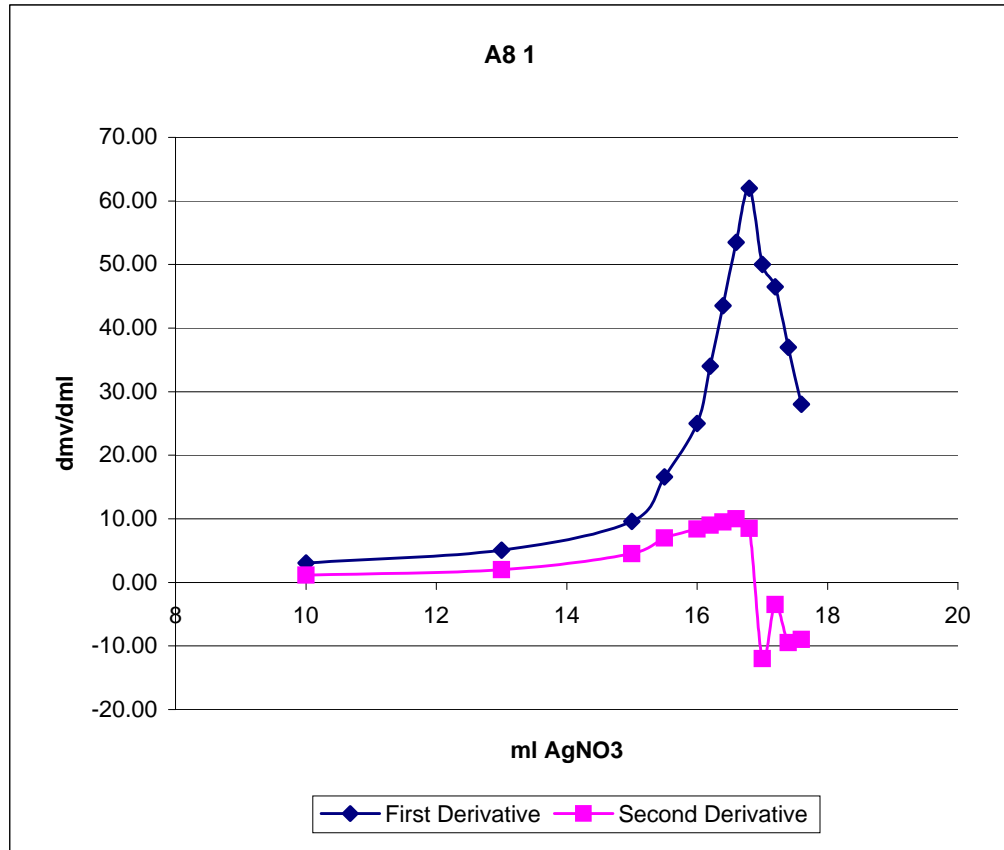
A8

2

AgNO₃		mv	d mL	d mV	d mV/dmL		Temp
1.6	0	215.80					21.8
7	5.4	245.90	5.40	30.10	5.57		21.9
8	6.4	257.30	1.00	11.40	11.40	5.83	21.9
9	7.4	275.50	1.00	18.20	18.20	6.80	21.9
9.4	7.8	290.10	0.40	14.60	36.50	18.30	22
9.6	8	300.80	0.20	10.70	53.50	17.00	22
9.8	8.2	312.20	0.20	11.40	57.00	3.50	22
10	8.4	325.90	0.20	13.70	68.50	11.50	22
10.2	8.6	334.30	0.20	8.40	42.00	-26.50	22
10.4	8.8	344.00	0.20	9.70	48.50	6.50	22
10.6	9	351.60	0.20	7.60	38.00	-10.50	22
10.8	9.2	356.80	0.20	5.20	26.00	-12.00	22

A8
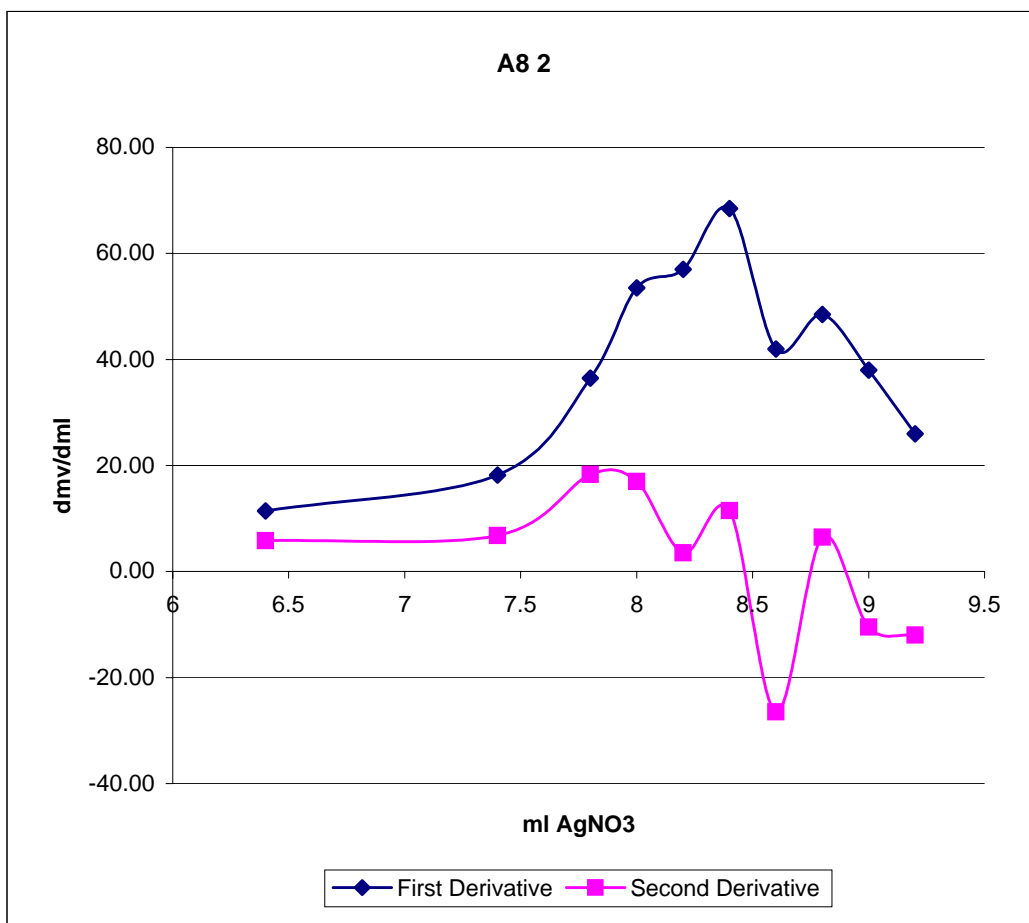
AgNO$_3$		mv	d mL	d mV	d mV/dmL		Temp
1.6	0	222.4					21.7
6	4.4	250.1	4.40	27.70	6.30		21.7
7	5.4	263.5	1.00	13.40	13.40	7.10	21.8
7.5	5.9	275.1	0.50	11.60	23.20	9.80	21.8
7.7	6.1	281.4	0.20	6.30	31.50	8.30	21.8
7.9	6.3	290.1	0.20	8.70	43.50	12.00	21.8
8.1	6.5	300.2	0.20	10.10	50.50	7.00	21.8
8.3	6.7	315.1	0.20	14.90	74.50	24.00	21.8
8.55	6.95	329.1	0.25	14.00	56.00	-18.50	21.8
8.7	7.1	334.7	0.15	5.60	37.33	-18.67	21.9
8.9	7.3	344.3	0.20	9.60	48.00	10.67	21.9
9.1	7.5	352.3	0.20	8.00	40.00	-8.00	21.9
9.3	7.7	357.8	0.20	5.50	27.50	-12.50	21.9

A8
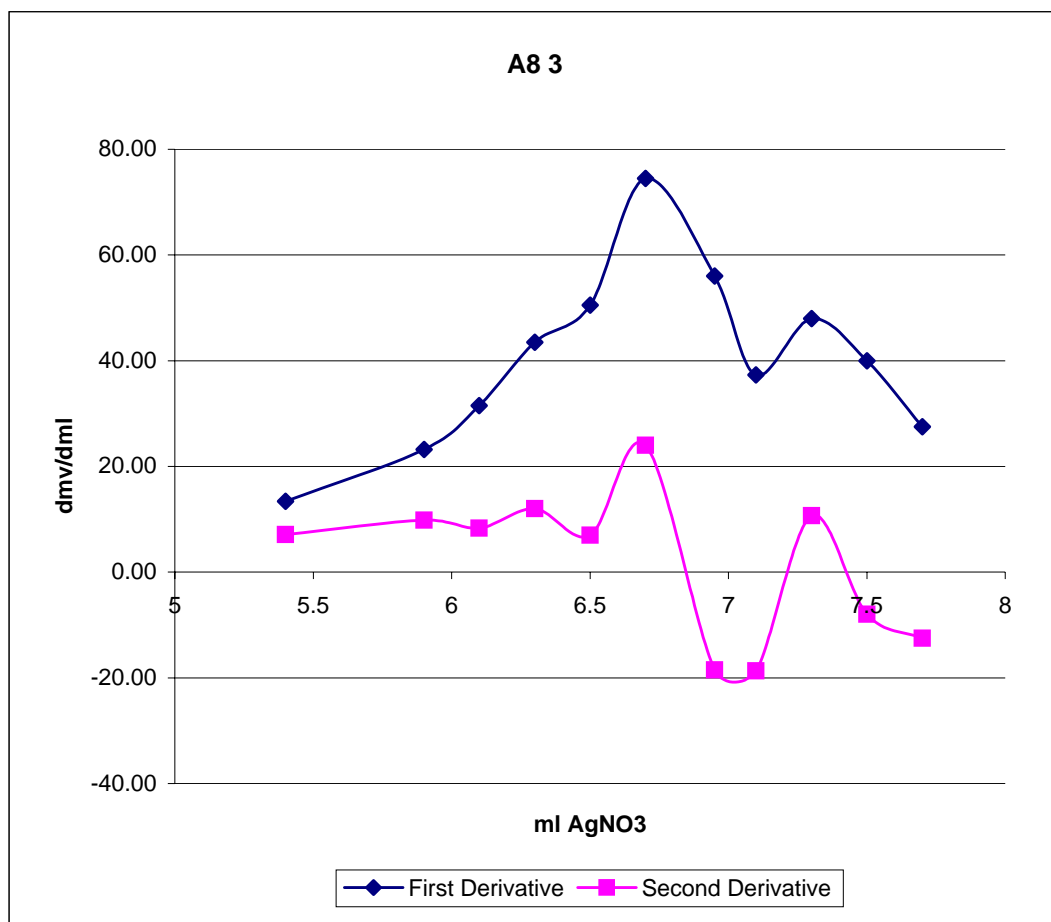
AgNO$_3$		mv	d mL	d mV	d mV/dmL		Temp
9.3	0	222.9					21.8
13.7	4.4	259.6	4.40	36.70	8.34		21.9
14.6	5.3	283.4	0.90	23.80	26.44	18.10	21.9
14.8	5.5	291.1	0.20	7.70	38.50	12.06	21.9
15	5.7	303.9	0.20	12.80	64.00	25.50	21.9
15.2	5.9	318.7	0.20	14.80	74.00	10.00	22
15.4	6.1	330.6	0.20	11.90	59.50	-14.50	22
15.65	6.35	343.3	0.25	12.70	50.80	-8.70	22
15.8	6.5	350.2	0.15	6.90	46.00	-4.80	22
16	6.7	355.1	0.20	4.90	24.50	-21.50	22
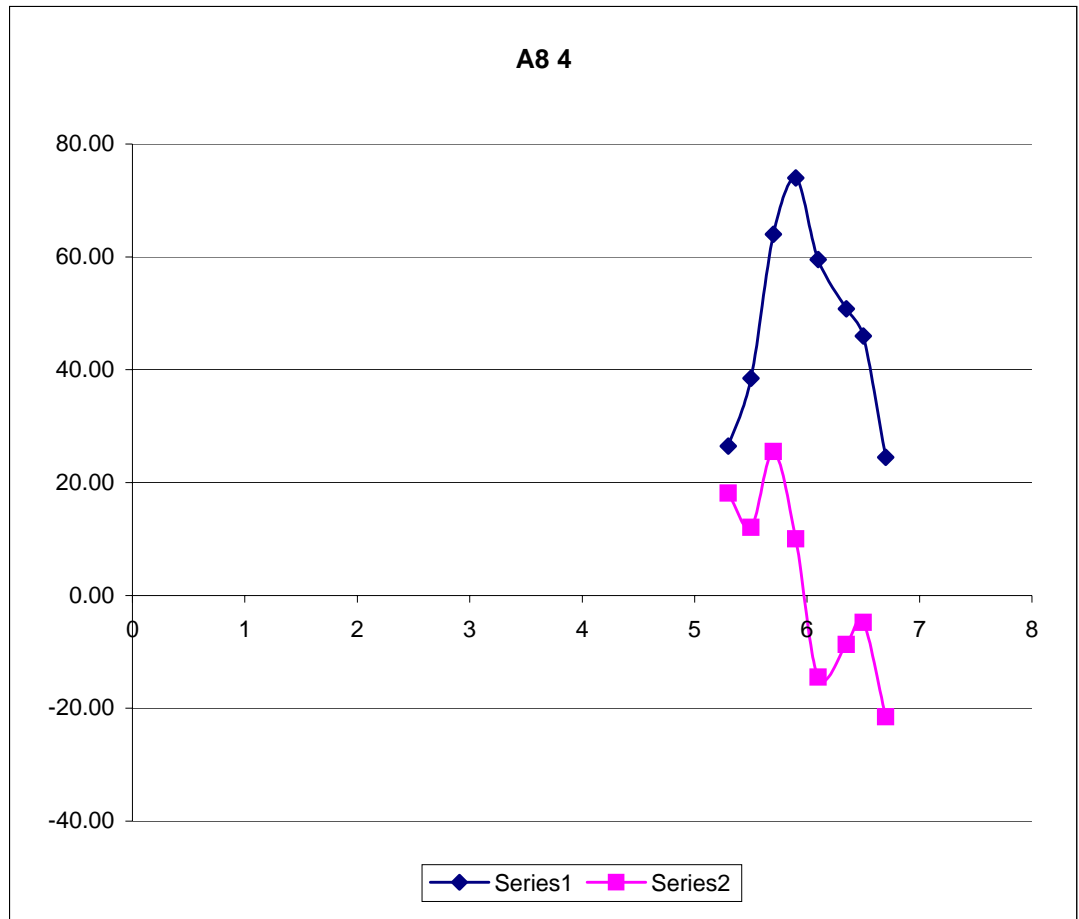
A14

1

AgNO$_3$	mv	d mL	d mV	d mV/dmL		Temp
0	191.5					22.6
7	204.2	7.00	12.70	1.81		22.6
11	214.8	4.00	10.60	2.65	0.84	22.6
15	231.5	4.00	16.70	4.18	1.52	22.6
17	247.1	2.00	15.60	7.80	3.63	22.6
18	260.3	1.00	13.20	13.20	5.40	22.7
18.5	271.8	0.50	11.50	23.00	9.80	22.7
19	288.9	0.50	17.10	34.20	11.20	22.7
19.2	303.9	0.20	15.00	75.00	40.80	22.7
19.4	316.4	0.20	12.50	62.50	-12.50	22.7
19.6	331.4	0.20	15.00	75.00	12.50	22.7
19.8	342.3	0.20	10.90	54.50	-20.50	22.8
20.05	351.4	0.25	9.10	36.40	-18.10	22.8
20.2	354.7	0.15	3.30	22.00	-14.40	22.8
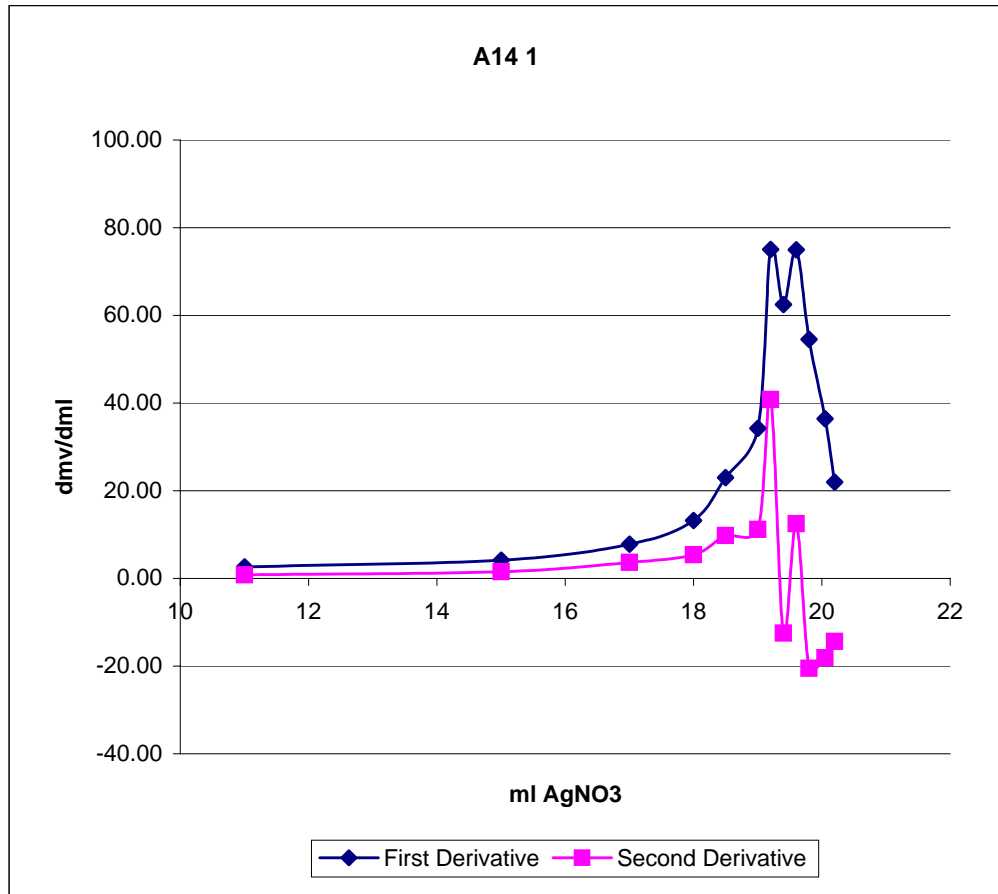
A14

2

AgNO$_3$		mv	d mL	d mV	d mV/dmL		Temp
1.8	0	203.5					22.5
6	4.2	212	4.20	8.50	2.02		22.6
9	7.2	219.7	3.00	7.70	2.57	0.54	22.7
12	10.2	229.9	3.00	10.20	3.40	0.83	22.7
14.5	12.7	243.4	2.50	13.50	5.40	2.00	22.7
16	14.2	255.1	1.50	11.70	7.80	2.40	22.7
17	15.2	268.8	1.00	13.70	13.70	5.90	22.7
17.5	15.7	280.2	0.50	11.40	22.80	9.10	22.7
17.7	15.9	285	0.20	4.80	24.00	1.20	22.7
17.9	16.1	292.4	0.20	7.40	37.00	13.00	22.7
18.1	16.3	303.2	0.20	10.80	54.00	17.00	22.8
18.3	16.5	315.1	0.20	11.90	59.50	5.50	22.8
18.5	16.7	325.3	0.20	10.20	51.00	-8.50	22.8
18.7	16.9	333.5	0.20	8.20	41.00	-10.00	22.8
18.9	17.1	342.5	0.20	9.00	45.00	4.00	22.8
19.1	17.3	350.7	0.20	8.20	41.00	-4.00	22.8
19.3	17.5	356.1	0.20	5.40	27.00	-14.00	22.8

E66
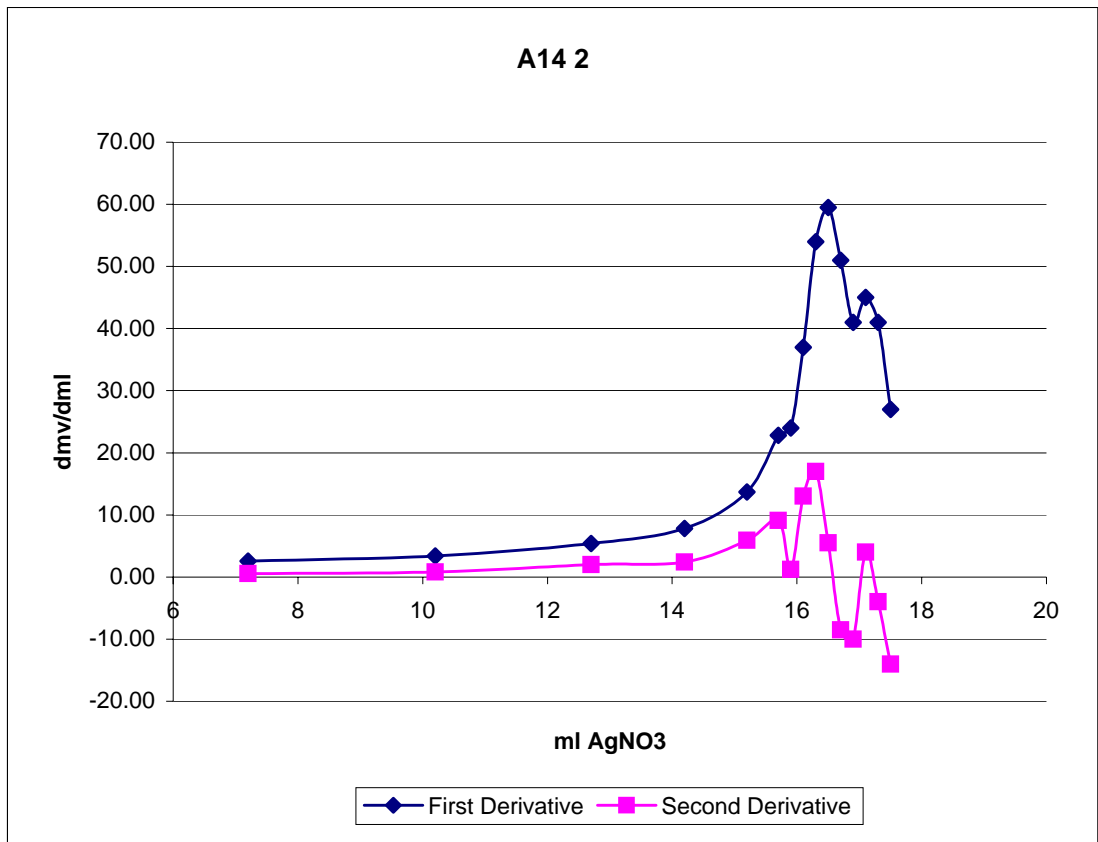
A14

3							
AgNO$_3$		mv	d mL	d mV	d mV/dmL		Temp
19.3	0	214.9					22.6
23	3.7	229.5	3.70	14.60	3.95		22.7
26	6.7	252.1	3.00	22.60	7.53	3.59	22.7
27	7.7	270.8	1.00	18.70	18.70	11.17	22.7
27.5	8.2	282.5	0.50	11.70	23.40	4.70	22.7
27.7	8.4	291.1	0.20	8.60	43.00	19.60	22.7
27.9	8.6	302.7	0.20	11.60	58.00	15.00	22.7
28.1	8.8	316.3	0.20	13.60	68.00	10.00	22.7
28.3	9	328.5	0.20	12.20	61.00	-7.00	22.8
28.5	9.2	338.3	0.20	9.80	49.00	-12.00	22.8
28.7	9.4	346.1	0.20	7.80	39.00	-10.00	22.8
28.9	9.6	352.9	0.20	6.80	34.00	-5.00	22.8
29.1	9.8	358.5	0.20	5.60	28.00	-6.00	22.8

A14 3
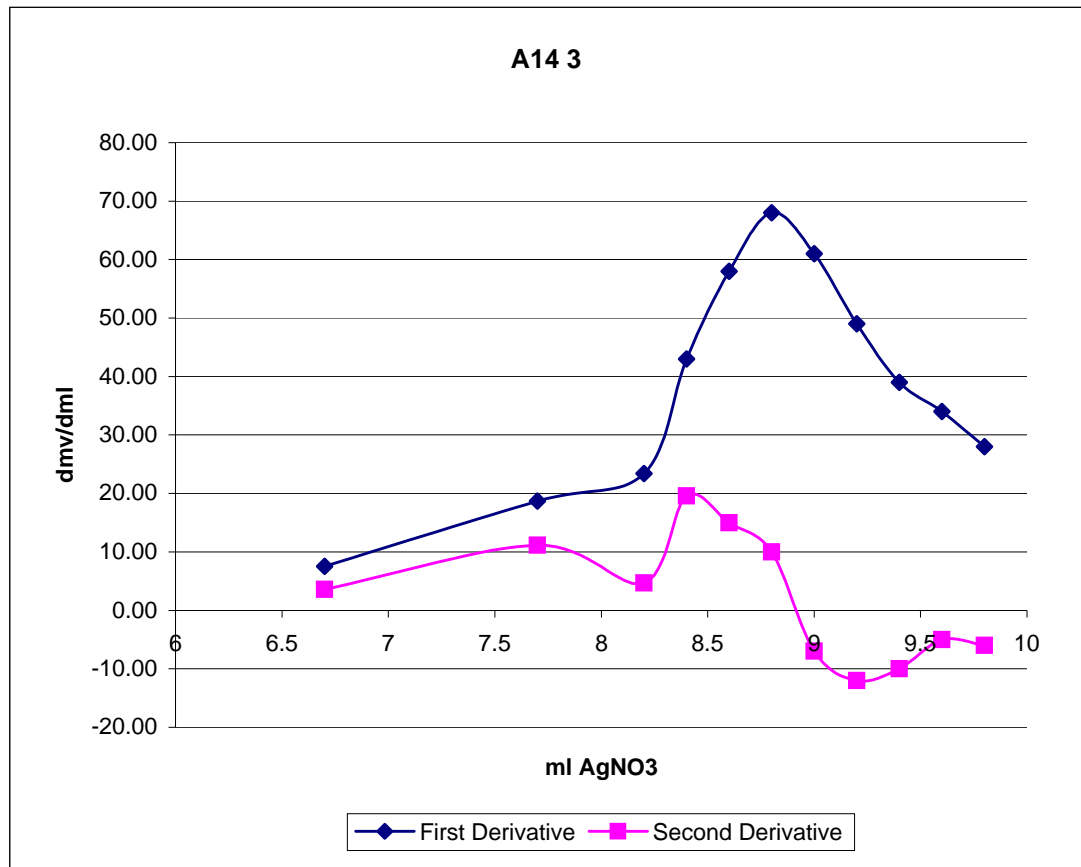
A14

4

AgNO$_3$		mv	d mL	d mV	d mV/dmL		Temp
29.1	0	224.7					22.7
33	3.9	247.9	3.90	23.20	5.95		22.7
34	4.9	259.3	1.00	11.40	11.40	5.45	22.7
35.1	6	282.8	1.10	23.50	21.36	9.96	22.7
35.3	6.2	291.4	0.20	8.60	43.00	21.64	22.7
35.5	6.4	302.9	0.20	11.50	57.50	14.50	22.8
35.7	6.6	314.7	0.20	11.80	59.00	1.50	22.8
35.9	6.8	327.7	0.20	13.00	65.00	6.00	22.8
36.1	7	336.6	0.20	8.90	44.50	-20.50	22.8
36.3	7.2	344.8	0.20	8.20	41.00	-3.50	22.8
36.5	7.4	350.3	0.20	5.50	27.50	-13.50	22.8
36.7	7.6	354.8	0.20	4.50	22.50	-5.00	22.8

A14 4

B7
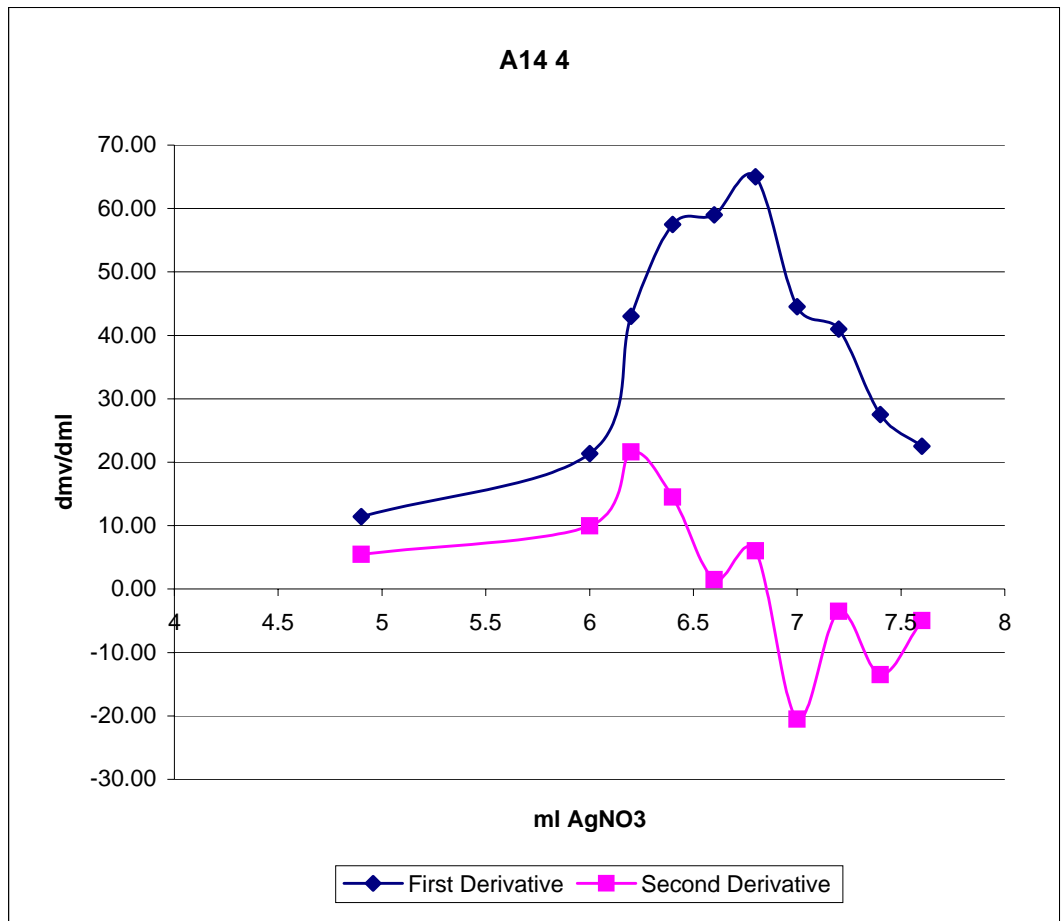
AgNO₃		mv	d mL	d mV	d mV/dmL		Temp
0.6	0	197.6					22.1
6	5.4	207.4	5.40	9.80	1.81		22.2
10	9.4	219.1	4.00	11.70	2.93	1.11	22.2
13	12.4	231.4	3.00	12.30	4.10	1.18	22.3
15	14.4	244.9	2.00	13.50	6.75	2.65	22.3
16	15.4	255.5	1.00	10.60	10.60	3.85	22.3
17	16.4	274.2	1.00	18.70	18.70	8.10	22.3
17.4	16.8	288.2	0.40	14.00	35.00	16.30	22.3
17.6	17	296.2	0.20	8.00	40.00	5.00	22.3
17.8	17.2	310.4	0.20	14.20	71.00	31.00	22.3
18	17.4	323.8	0.20	13.40	67.00	-4.00	22.4
18.25	17.65	338.8	0.25	15.00	60.00	-7.00	22.4
18.4	17.8	346.9	0.15	8.10	54.00	-6.00	22.4
18.6	18	354.5	0.20	7.60	38.00	-16.00	22.4

B7 1

B7
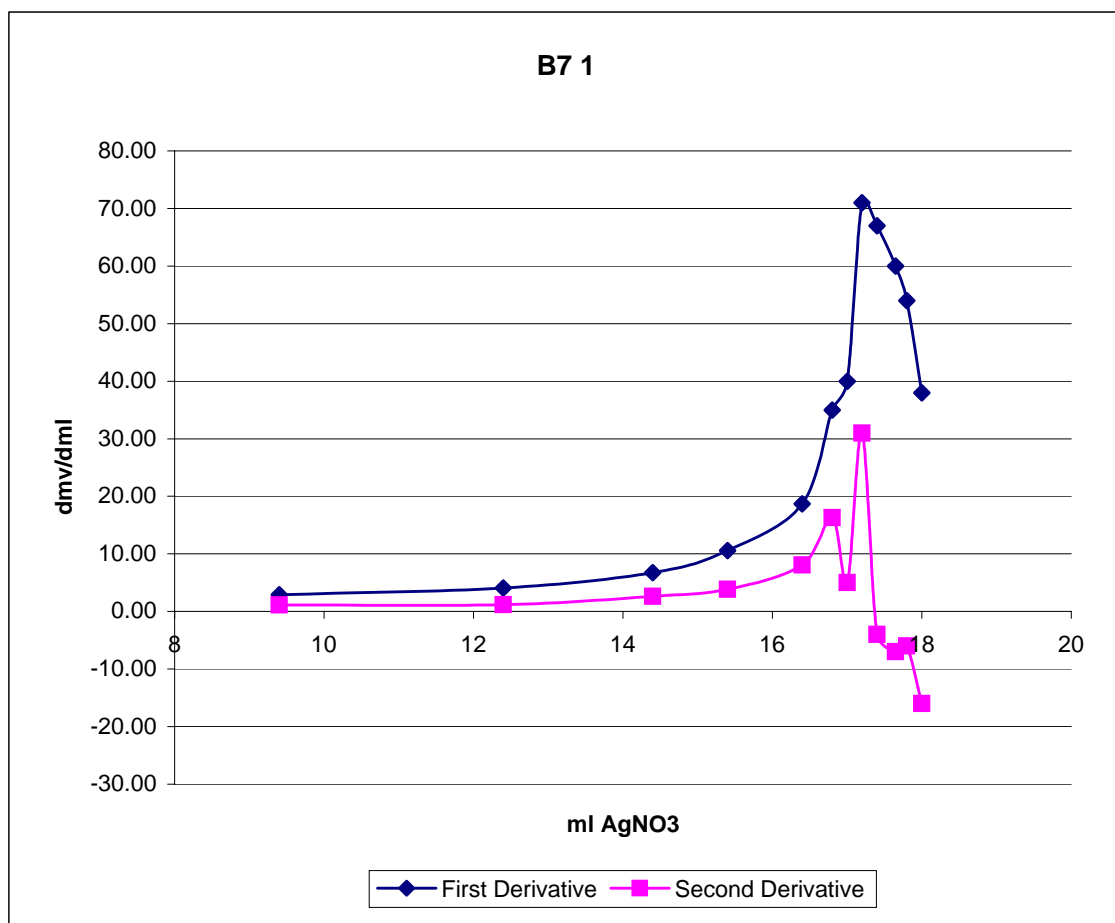
AgNO$_3$		mv	d mL	d mV	d mV/dmL		Temp
0.2	0	199.7					22.1
5	4.8	213.9	4.80	14.20	2.96		22.1
9	8.8	233.1	4.00	19.20	4.80	1.84	22.2
11	10.8	251.7	2.00	18.60	9.30	4.50	22.2
12	11.8	271.9	1.00	20.20	20.20	10.90	22.2
12.5	12.3	296.5	0.50	24.60	49.20	29.00	22.2
12.7	12.5	309.8	0.20	13.30	66.50	17.30	22.2
12.9	12.7	323.9	0.20	14.10	70.50	4.00	22.2
13.1	12.9	334.4	0.20	10.50	52.50	-18.00	22.2
13.3	13.1	343.1	0.20	8.70	43.50	-9.00	22.3
13.5	13.3	350.1	0.20	7.00	35.00	-8.50	22.3
13.7	13.5	356.1	0.20	6.00	30.00	-5.00	22.3

B7
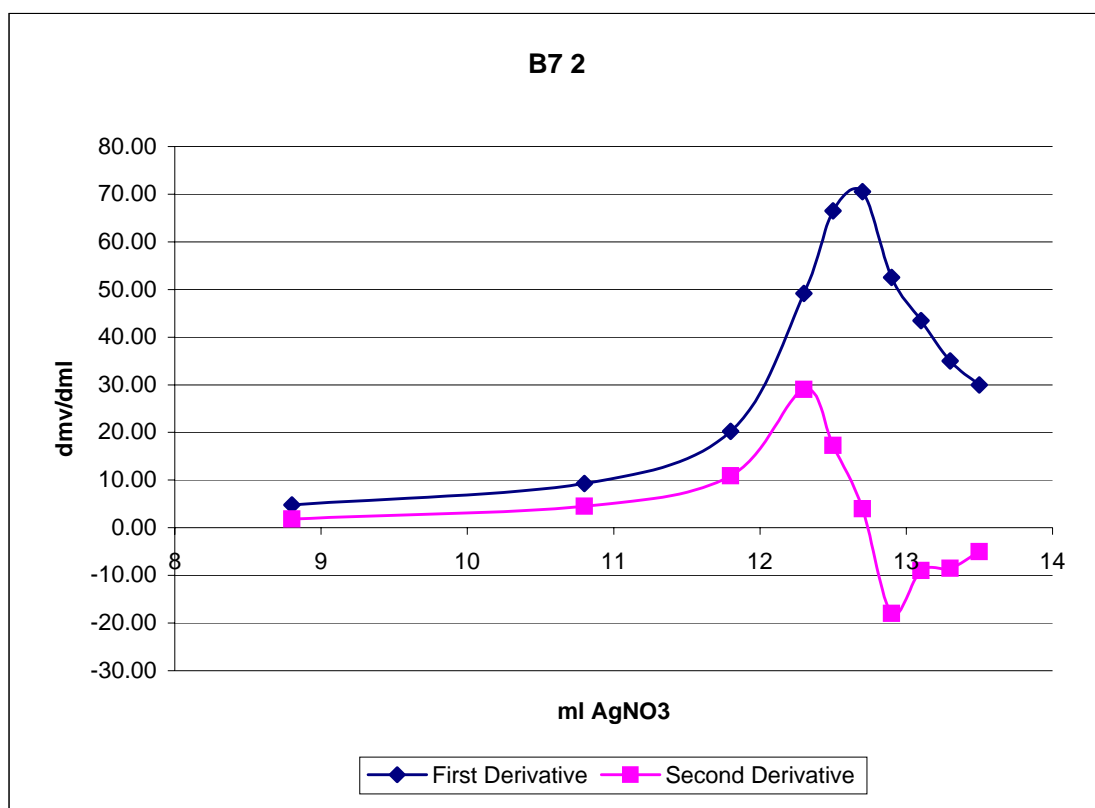
AgNO$_3$		mv	d mL	d mV	d mV/dmL		Temp
0.4	0	208.1					22.3
6	5.6	228.1	5.60	20.00	3.57		22.4
8	7.6	242.2	2.00	14.10	7.05	3.48	22.4
9	8.6	253.4	1.00	11.20	11.20	4.15	22.4
10	9.6	272.2	1.00	18.80	18.80	7.60	22.5
10.5	10.1	291.1	0.50	18.90	37.80	19.00	22.5
10.7	10.3	300.7	0.20	9.60	48.00	10.20	22.5
10.9	10.5	315.5	0.20	14.80	74.00	26.00	22.5
11.1	10.7	331.6	0.20	16.10	80.50	6.50	22.5
11.3	10.9	341.9	0.20	10.30	51.50	-29.00	22.5
11.5	11.1	349.1	0.20	7.20	36.00	-15.50	22.5
11.7	11.3	355.3	0.20	6.20	31.00	-5.00	22.5

B7 3
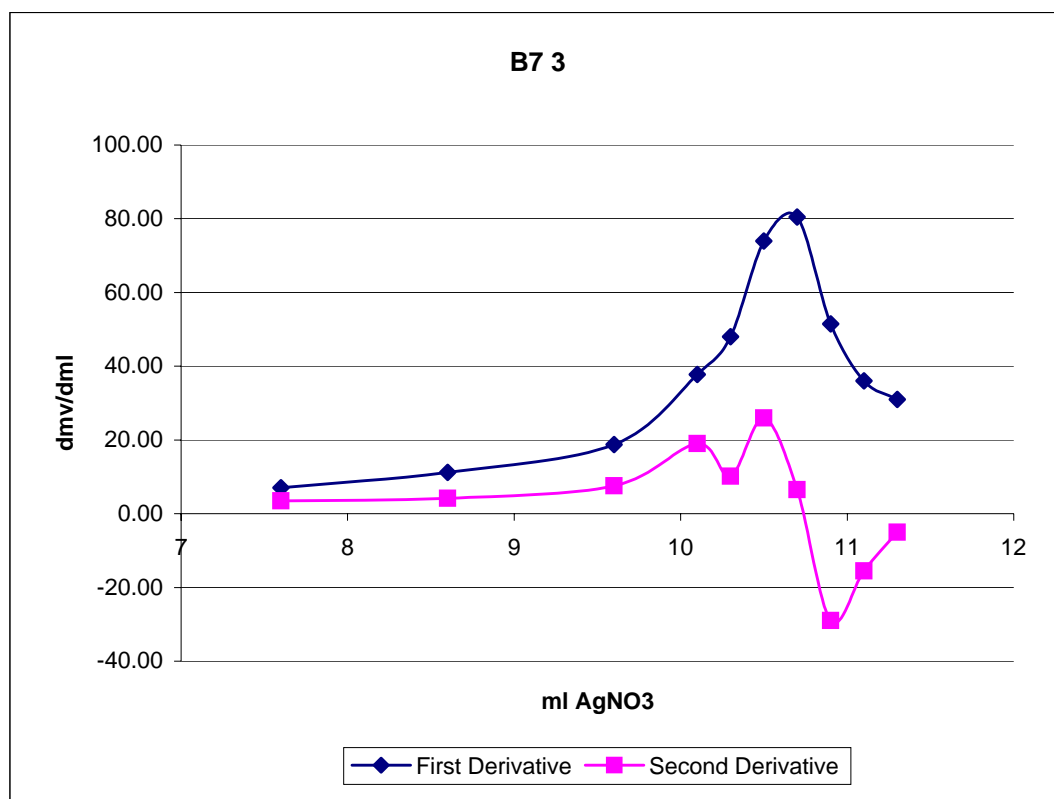
B7

4

AgNO$_3$		mv	d mL	d mV	d mV/dmL		Temp
0.8	0	224.1					22.3
4	3.2	248.3	3.20	24.20	7.56		22.4
5.5	4.7	279.1	1.50	30.80	20.53	12.97	22.4
5.7	4.9	287.6	0.20	8.50	42.50	21.97	22.4
5.9	5.1	300.9	0.20	13.30	66.50	24.00	22.4
6.1	5.3	318.2	0.20	17.30	86.50	20.00	22.5
6.3	5.5	335.4	0.20	17.20	86.00	-0.50	22.5
6.5	5.7	344.3	0.20	8.90	44.50	-41.50	22.5
6.7	5.9	353.8	0.20	9.50	47.50	3.00	22.5
6.9	6.1	360.5	0.20	6.70	33.50	-14.00	22.5

C1
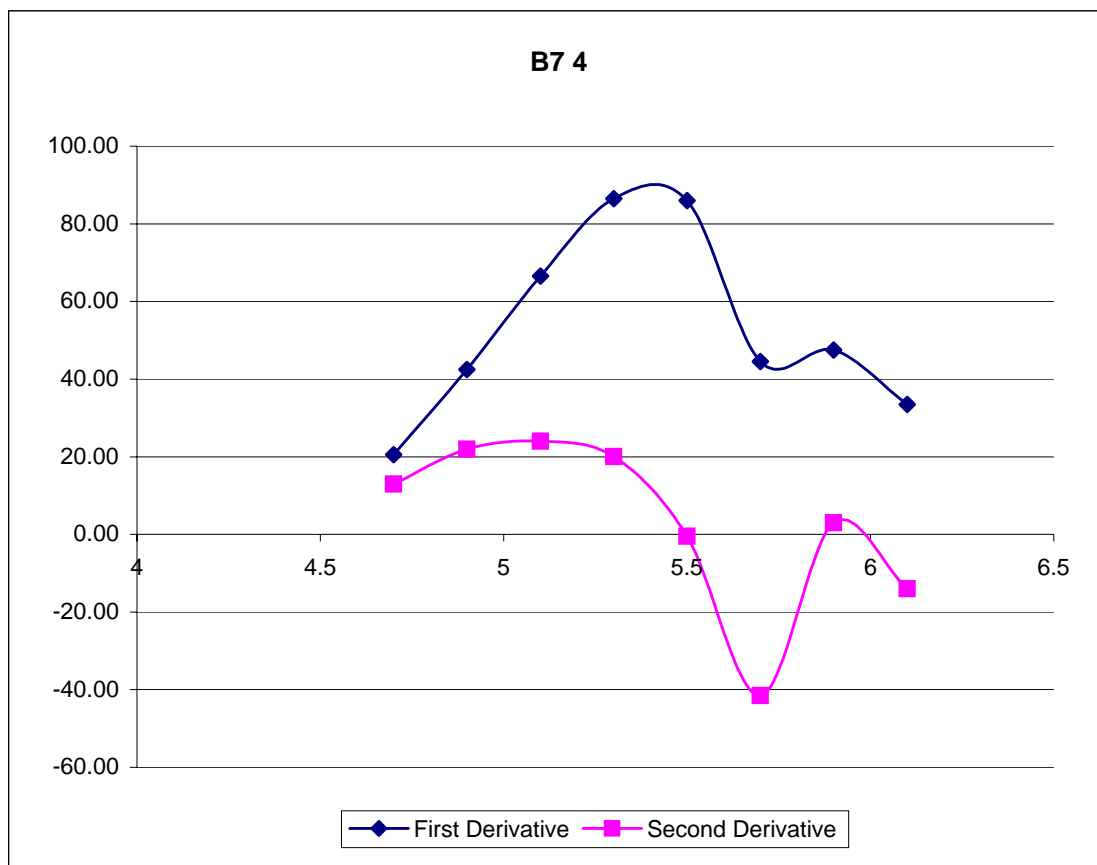
AgNO$_3$	*1*	mv	d mL	d mV	d mV/dmL		Temp
(ml)							C
20.0	0.0	208.2					22.8
21.5	1.5	215.9	1.5	7.7	5.1		22.9
23.0	3.0	221.6	1.5	5.7	3.8	-1.3	23.0
24.0	4.0	226.2	1.0	4.6	4.6	0.8	23.0
25.0	5.0	231.4	1.0	5.2	5.2	0.6	23.0
26.0	6.0	238.8	1.0	7.4	7.4	2.2	23.0
27.0	7.0	247.5	1.0	8.7	8.7	1.3	23.0
28.0	8.0	261.4	1.0	13.9	13.9	5.2	23.1
28.5	8.5	273.1	0.5	11.7	23.4	9.5	23.1
28.7	8.7	278.1	0.2	5.0	25.0	1.6	23.1
28.9	8.9	286.4	0.2	8.3	41.5	16.5	23.1
29.1	9.1	296.1	0.2	9.7	48.5	7.0	23.1
29.3	9.3	312.2	0.2	16.1	80.5	32.0	23.1
29.5	9.5	326.4	0.2	14.2	71.0	-9.5	23.1
29.7	9.7	336.1	0.2	9.7	48.5	-22.5	23.1
29.9	9.9	346.1	0.2	10.0	50.0	1.5	23.1
30.1	10.1	354.2	0.2	8.1	40.5	-9.5	23.1

C1 1

C1
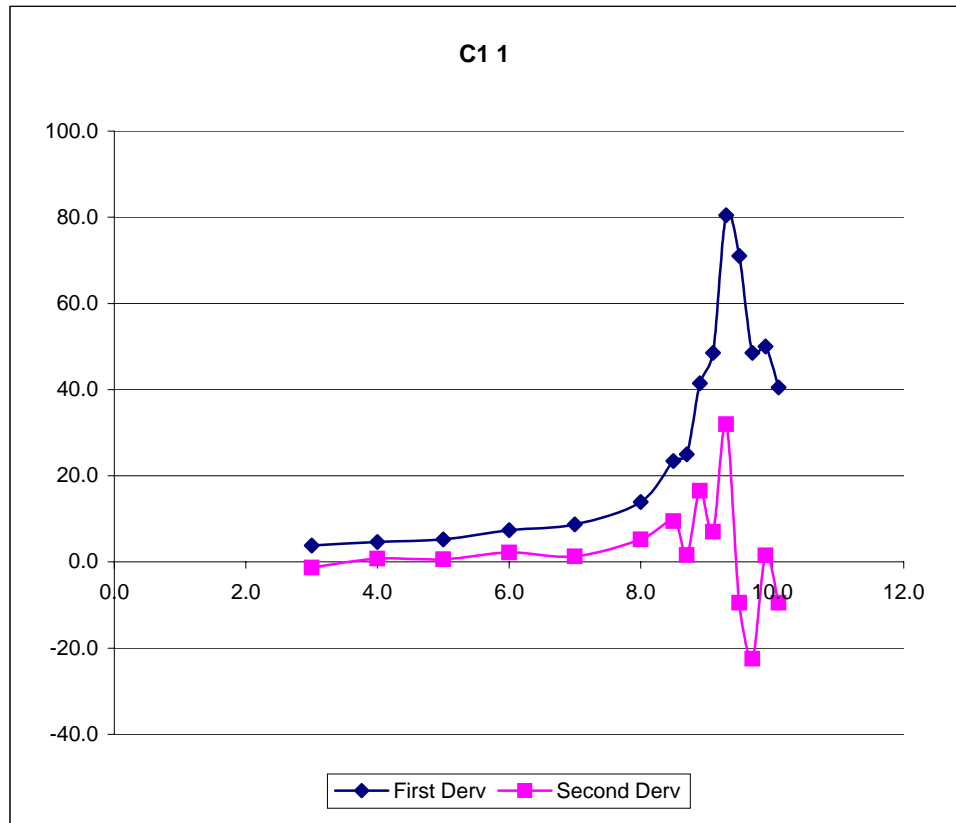
AgNO$_3$ (ml)		mv	d mL	d mV	d mV/dmL		Temp C
0.7	0.0	227.5					23.1
2.5	1.8	234.5	1.8	7.0	3.9		23.2
4.0	3.3	241.1	1.5	6.6	4.4	0.5	23.2
5.0	4.3	247.5	1.0	6.4	6.4	2.0	23.2
6.0	5.3	255.8	1.0	8.3	8.3	1.9	23.2
6.5	5.8	261.1	0.5	5.3	10.6	2.3	23.2
7.0	6.3	268.3	0.5	7.2	14.4	3.8	23.3
7.2	6.5	272.2	0.2	3.9	19.5	5.1	23.3
7.4	6.7	277.1	0.2	4.9	24.5	5.0	23.3
7.6	6.9	283.6	0.2	6.5	32.5	8.0	23.3
7.8	7.1	290.1	0.2	6.5	32.5	0.0	23.3
8.0	7.3	301.1	0.2	11.0	55.0	22.5	23.3
8.2	7.5	313.1	0.2	12.0	60.0	5.0	23.4
8.4	7.7	329.3	0.2	16.2	81.0	21.0	23.4
8.6	7.9	338.6	0.2	9.3	46.5	-34.5	23.4
8.8	8.1	347.5	0.2	8.9	44.5	-2.0	23.4
9.0	8.3	355.4	0.2	7.9	39.5	-5.0	23.4
9.2	8.5	361.1	0.2	5.7	28.5	-11.0	23.4

C1 2

C1
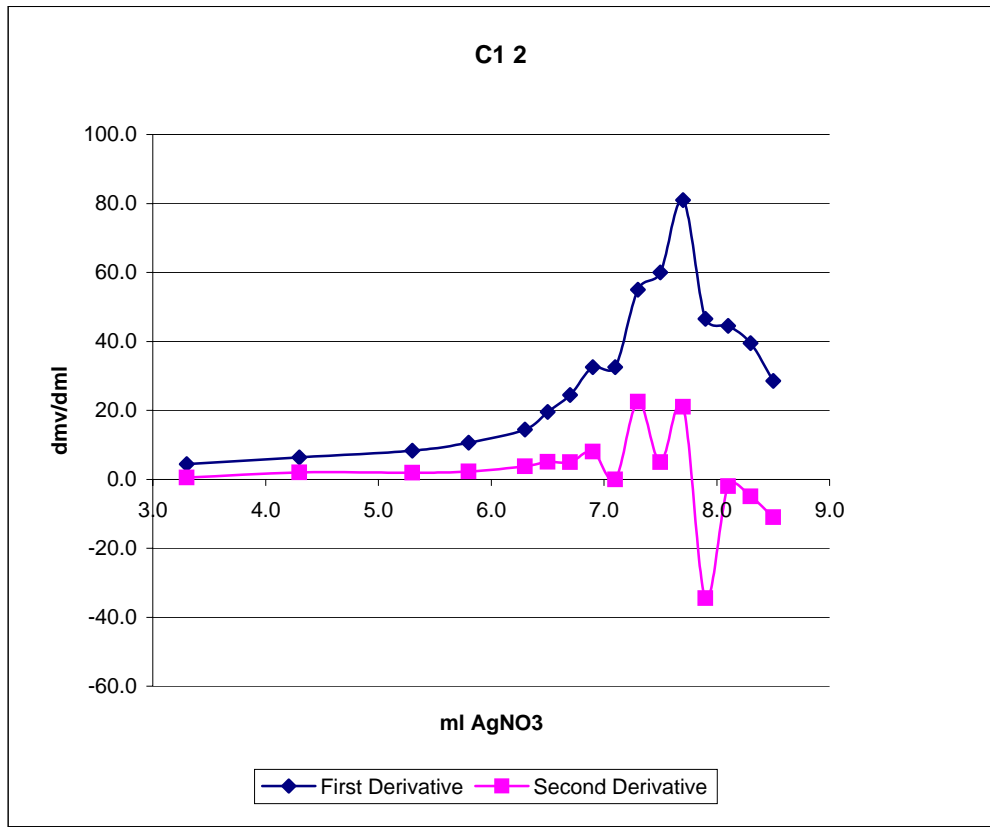
AgNO$_3$ (ml)	*3*	mv	d mL	d mV	d mV/dmL		Temp C
9.2	0.0	235.1					23.3
10.5	1.3	243.3	1.3	8.2	6.3		23.4
11.5	2.3	249.8	1.0	6.5	6.5	0.2	23.4
12.5	3.3	258.1	1.0	8.3	8.3	1.8	23.5
13.5	4.3	271.1	1.0	13.0	13.0	4.7	23.5
13.7	4.5	274.5	0.2	3.4	17.0	4.0	23.5
13.9	4.7	279.1	0.2	4.6	23.0	6.0	23.5
14.1	4.9	285.7	0.2	6.6	33.0	10.0	23.5
14.3	5.1	293.2	0.2	7.5	37.5	4.5	23.5
14.5	5.3	305.4	0.2	12.2	61.0	23.5	23.5
14.7	5.5	320.1	0.2	14.7	73.5	12.5	23.5
14.9	5.7	332.2	0.2	12.1	60.5	-13.0	23.5
15.1	5.9	341.1	0.2	8.9	44.5	-16.0	23.5
15.3	6.1	349.8	0.2	8.7	43.5	-1.0	23.5
15.5	6.3	356.3	0.2	6.5	32.5	-11.0	23.5
15.7	6.5	362.2	0.2	5.9	29.5	-3.0	23.5

C1 3
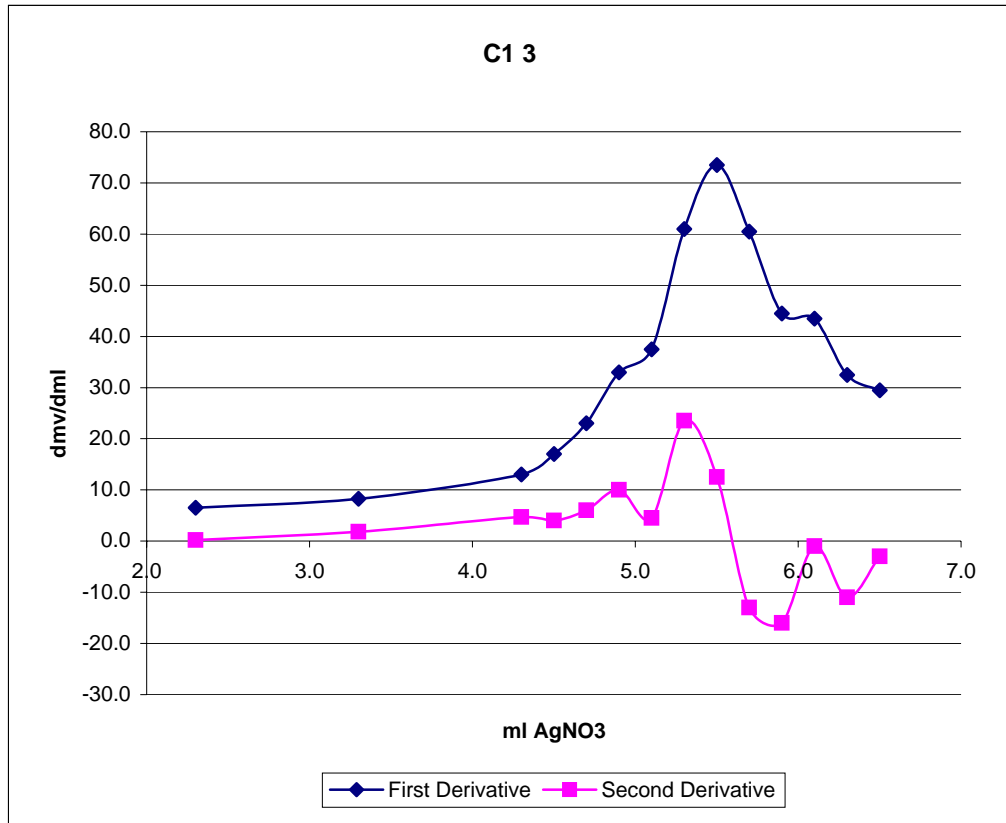
C1

4 AgNO$_3$ (ml)		mv	d mL	d mV	d mV/dmL		Temp C
15.7	0.0	242.9					23.1
17.0	1.3	250.1	1.3	7.2	5.5		23.1
18.0	2.3	257.9	1.0	7.8	7.8	2.3	23.2
18.7	3.0	265.4	0.7	7.5	10.7	2.9	23.2
18.9	3.2	267.8	0.2	2.4	12.0	1.3	23.2
19.1	3.4	271.1	0.2	3.3	16.5	4.5	23.2
19.3	3.6	274.3	0.2	3.2	16.0	-0.5	23.3
19.5	3.8	278.6	0.2	4.3	21.5	5.5	23.3
19.7	4.0	283.4	0.2	4.8	24.0	2.5	23.3
19.9	4.2	289.6	0.2	6.2	31.0	7.0	23.3
20.1	4.4	298.1	0.2	8.5	42.5	11.5	23.3
20.3	4.6	314.9	0.2	16.8	84.0	41.5	23.3
20.5	4.8	331.1	0.2	16.2	81.0	-3.0	23.3
20.7	5.0	340.5	0.2	9.4	47.0	-34.0	23.3
20.9	5.2	348.9	0.2	8.4	42.0	-5.0	23.4
21.1	5.4	356.8	0.2	7.9	39.5	-2.5	23.4
21.3	5.6	362.2	0.2	5.4	27.0	-12.5	23.4

C4
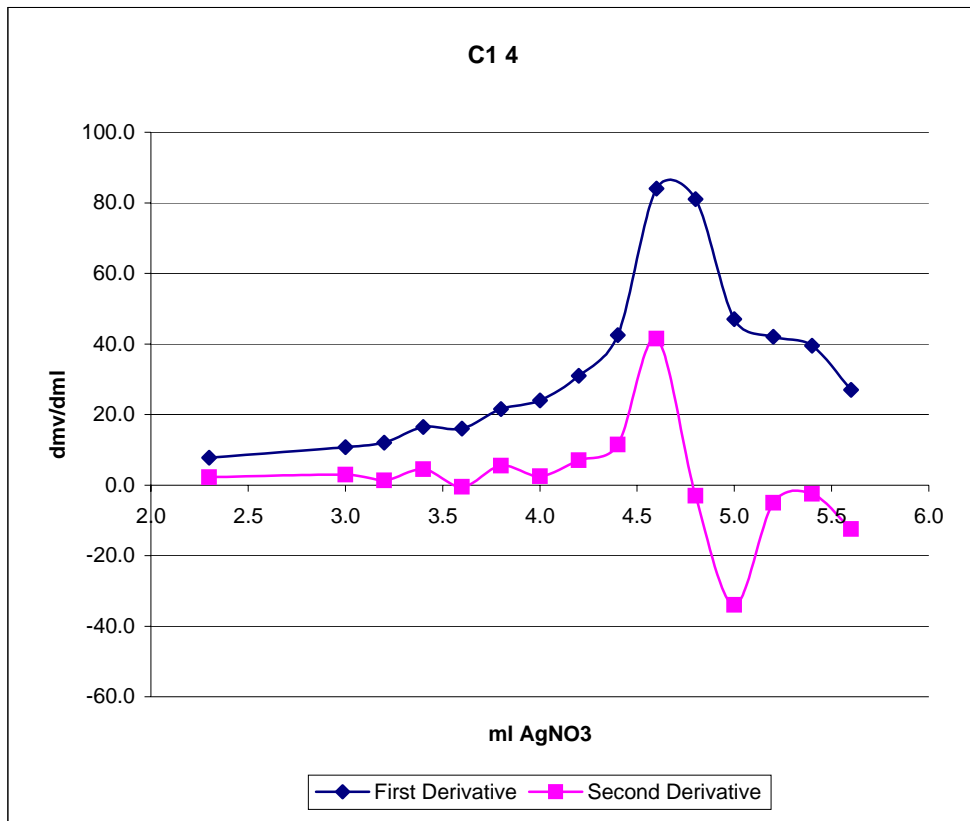
AgNO$_3$ (ml)		mv	d mL	d mV	d mV/dmL		Temp C
10.0	0.0	211.3					22.5
12.0	2.0	216.5	2.0	5.2	2.6		22.6
13.0	3.0	219.8	1.0	3.3	3.3	0.7	22.6
14.0	4.0	223.4	1.0	3.6	3.6	0.3	22.6
15.0	5.0	227.8	1.0	4.4	4.4	0.8	22.7
16.0	6.0	232.9	1.0	5.1	5.1	0.7	22.7
17.0	7.0	238.7	1.0	5.8	5.8	0.7	22.7
18.0	8.0	246.7	1.0	8.0	8.0	2.2	22.7
18.5	8.5	251.3	0.5	4.6	9.2	1.2	22.8
19.0	9.0	257.8	0.5	6.5	13.0	3.8	22.8
19.5	9.5	264.4	0.5	6.6	13.2	0.2	22.8
20.0	10.0	274.8	0.5	10.4	20.8	7.6	22.8
20.2	10.2	280.1	0.2	5.3	26.5	5.7	22.8
20.4	10.4	287.5	0.2	7.4	37.0	10.5	22.9
20.6	10.6	298.1	0.2	10.6	53.0	16.0	22.9
20.8	10.8	313.4	0.2	15.3	76.5	23.5	22.9
21.0	11.0	329.1	0.2	15.7	78.5	2.0	22.9
21.2	11.2	340.1	0.2	11.0	55.0	-23.5	22.9
21.4	11.4	349.5	0.2	9.4	47.0	-8.0	22.9
21.6	11.6	358.0	0.2	8.5	42.5	-4.5	22.9
21.8	11.8	365.1	0.2	7.1	35.5	-7.0	22.9

C4
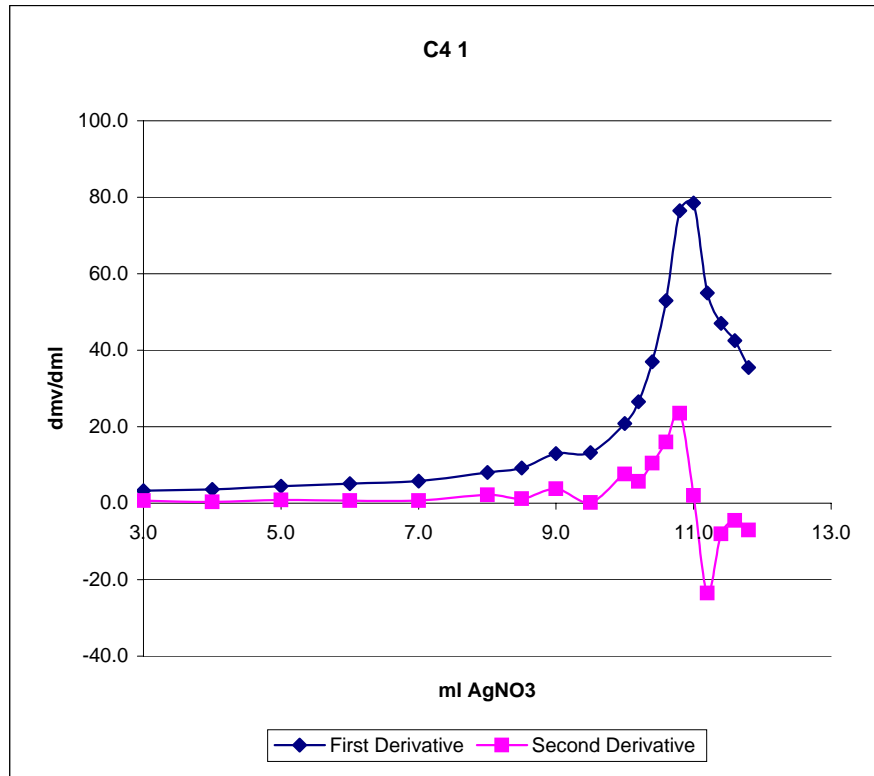
AgNO₃ (ml)	2	mv	d mL	d mV	d mV/dmL		Temp C
21.8	0.0	219.4					22.7
23.0	1.2	223.4	1.2	4.0	3.3		22.8
24.0	2.2	227.9	1.0	4.5	4.5	1.2	22.8
25.0	3.2	233.4	1.0	5.5	5.5	1.0	22.9
26.0	4.2	239.4	1.0	6.0	6.0	0.5	22.9
27.0	5.2	246.9	1.0	7.5	7.5	1.5	22.9
27.5	5.7	252.7	0.5	5.8	11.6	4.1	22.9
28.0	6.2	259.4	0.5	6.7	13.4	1.8	22.9
28.5	6.7	267.4	0.5	8.0	16.0	2.6	22.9
28.7	6.9	270.9	0.2	3.5	17.5	1.5	22.9
28.9	7.1	275.9	0.2	5.0	25.0	7.5	22.9
29.1	7.3	283.1	0.2	7.2	36.0	11.0	23.0
29.3	7.5	291.1	0.2	8.0	40.0	4.0	23.0
29.5	7.7	304.5	0.2	13.4	67.0	27.0	23.0
29.7	7.9	318.1	0.2	13.6	68.0	1.0	23.0
29.9	8.1	330.1	0.2	12.0	60.0	-8.0	23.0
30.1	8.3	340.1	0.2	10.0	50.0	-10.0	23.0
30.3	8.5	349.1	0.2	9.0	45.0	-5.0	23.1
30.5	8.7	356.4	0.2	7.3	36.5	-8.5	23.1
30.7	8.9	362.2	0.2	5.8	29.0	-7.5	23.1

C4 2
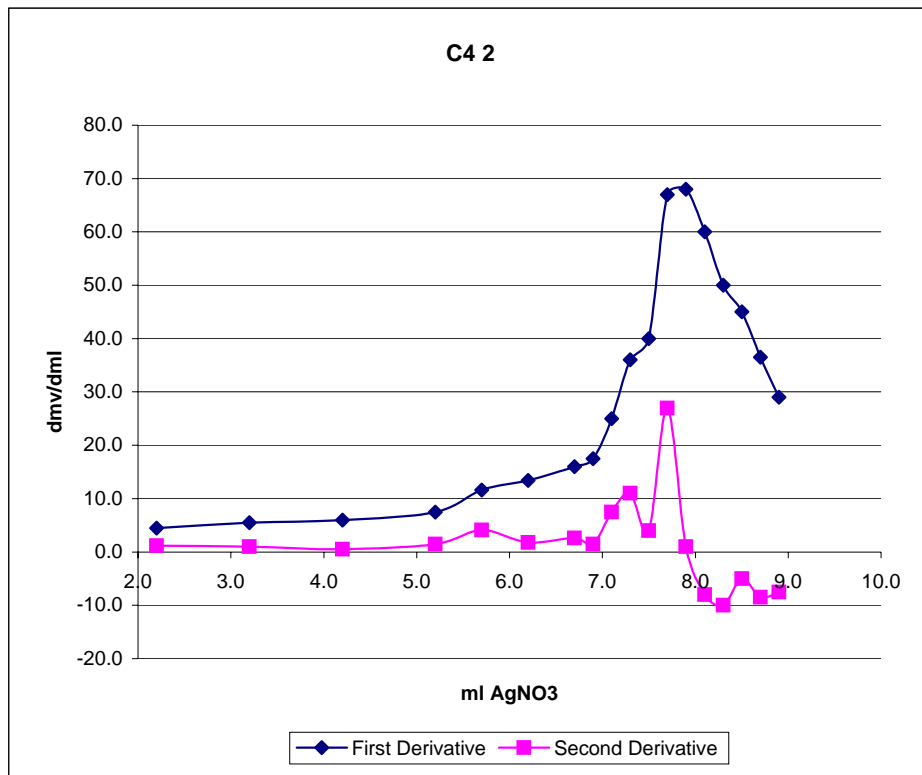
C4

3 AgNO$_3$ (ml)		mv	d mL	d mV	d mV/dmL		Temp C
0.9	0.0	225.1					23.0
3.0	2.1	239.1	2.1	14.0	6.7		23.1
3.5	2.6	243.4	0.5	4.3	8.6	1.9	23.1
4.0	3.1	248.5	0.5	5.1	10.2	1.6	23.1
4.5	3.6	256.2	0.5	7.7	15.4	5.2	23.1
5.0	4.1	263.2	0.5	7.0	14.0	-1.4	23.1
5.2	4.3	266.1	0.2	2.9	14.5	0.5	23.2
5.4	4.5	271.2	0.2	5.1	25.5	11.0	23.2
5.6	4.7	278.4	0.2	7.2	36.0	10.5	23.2
5.8	4.9	284.5	0.2	6.1	30.5	-5.5	23.2
6.0	5.1	295.6	0.2	11.1	55.5	25.0	23.2
6.2	5.3	309.1	0.2	13.5	67.5	12.0	23.2
6.4	5.5	326.2	0.2	17.1	85.5	18.0	23.2
6.6	5.7	337.3	0.2	11.1	55.5	-30.0	23.2
6.8	5.9	347.5	0.2	10.2	51.0	-4.5	23.2
7.0	6.1	354.1	0.2	6.6	33.0	-18.0	23.2
7.2	6.3	360.1	0.2	6.0	30.0	-3.0	23.2
7.4	6.5	364.0	0.2	3.9	19.5	-10.5	23.2

C4 3

C4

AgNO$_3$ (ml)		mv	d mL	d mV	d mV/dmL		Temp C
7.4	0.0	230.2					23.1
9.5	2.1	242.1	2.1	11.9	5.7		23.2
10.0	2.6	247.6	0.5	5.5	11.0	5.3	23.2
10.5	3.1	252.4	0.5	4.8	9.6	-1.4	23.2
11.0	3.6	258.6	0.5	6.2	12.4	2.8	23.2
11.5	4.1	268.7	0.5	10.1	20.2	7.8	23.2
11.7	4.3	272.4	0.2	3.7	18.5	-1.7	23.2
11.9	4.5	277.1	0.2	4.7	23.5	5.0	23.2
12.1	4.7	285.4	0.2	8.3	41.5	18.0	23.3
12.3	4.9	293.9	0.2	8.5	42.5	1.0	23.3
12.5	5.1	310.1	0.2	16.2	81.0	38.5	23.3
12.7	5.3	331.1	0.2	21.0	105.0	24.0	23.3
12.9	5.5	342.2	0.2	11.1	55.5	-49.5	23.3
13.1	5.7	351.1	0.2	8.9	44.5	-11.0	23.3
13.3	5.9	359.9	0.2	8.8	44.0	-0.5	23.3
13.5	6.1	366.4	0.2	6.5	32.5	-11.5	23.3

C4 4

C5
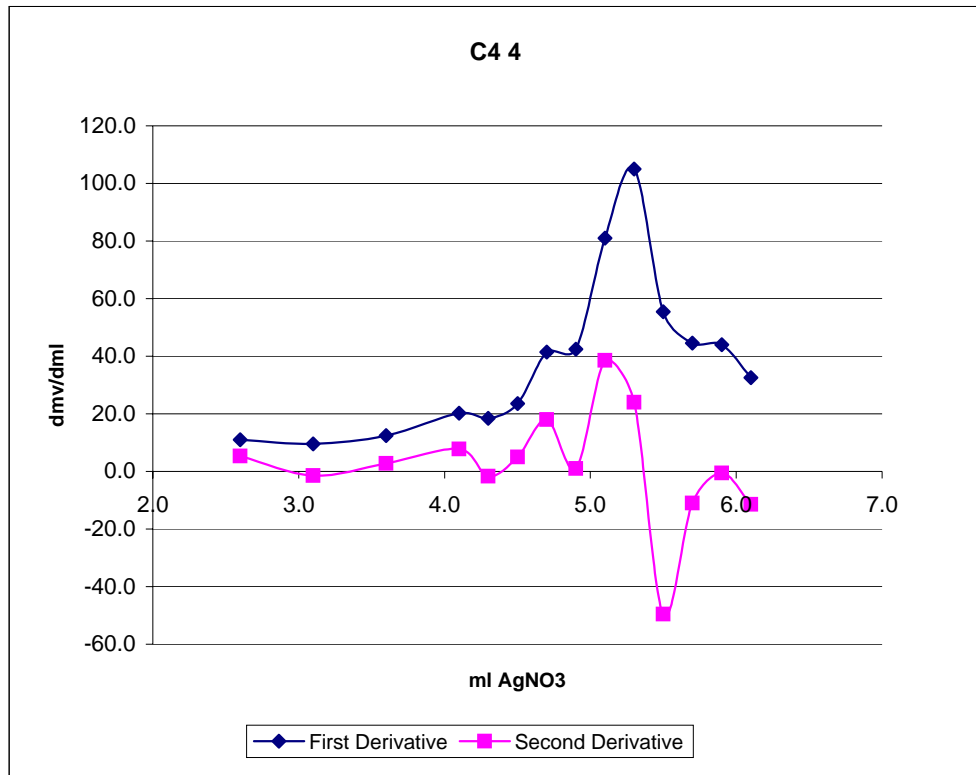
AgNO$_3$	mv	d mL	d mV	d mV/dmL		Temp
0	190.1					22.5
6	200.1	6.00	10.00	1.67		22.6
10	208.5	4.00	8.40	2.10	0.43	22.7
13	215.4	3.00	6.90	2.30	0.20	22.8
16	225.9	3.00	10.50	3.50	1.20	22.9
18	234.5	2.00	8.60	4.30	0.80	22.9
20	249.6	2.00	15.10	7.55	3.25	22.9
21	260.1	1.00	10.50	10.50	2.95	22.9
22	283.1	1.00	23.00	23.00	12.50	22.9
22.2	290.6	0.20	7.50	37.50	14.50	23
22.4	304.5	0.20	13.90	69.50	32.00	23
22.6	319.5	0.20	15.00	75.00	5.50	23
22.8	335.1	0.20	15.60	78.00	3.00	23
23	344.3	0.20	9.20	46.00	-32.00	23
23.2	352.2	0.20	7.90	39.50	-6.50	23
23.4	358.4	0.20	6.20	31.00	-8.50	23
23.6	363.4	0.20	5.00	25.00	-6.00	23

C5
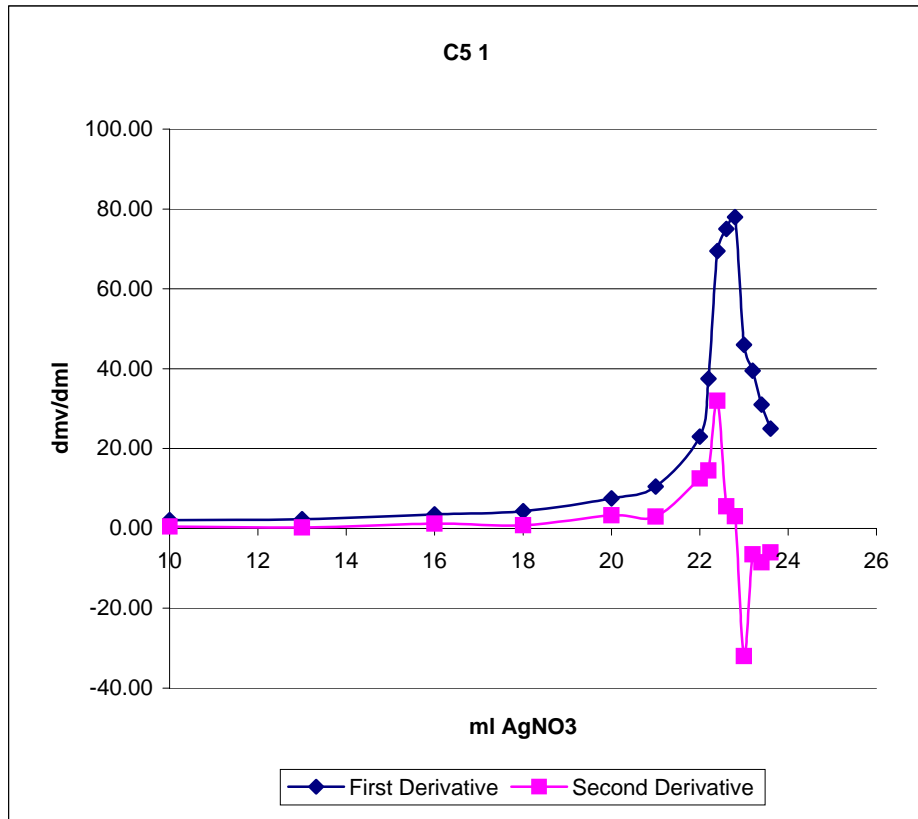
AgNO$_3$		mv	d mL	d mV	d mV/dmL		Temp
23.6	0	221.4					23
30.5	6.9	235.6	6.90	14.20	2.06		23.1
32.5	8.9	250.1	2.00	14.50	7.25	5.19	23.1
34	10.4	271.9	1.50	21.80	14.53	7.28	23.1
34.5	10.9	286.5	0.50	14.60	29.20	14.67	23.1
34.7	11.1	293.1	0.20	6.60	33.00	3.80	23.1
34.9	11.3	305.4	0.20	12.30	61.50	28.50	23.1
35.1	11.5	318.5	0.20	13.10	65.50	4.00	23.2
35.3	11.7	331.1	0.20	12.60	63.00	-2.50	23.2
35.5	11.9	340.3	0.20	9.20	46.00	-17.00	23.2
35.7	12.1	348.6	0.20	8.30	41.50	-4.50	23.2
35.9	12.3	354.8	0.20	6.20	31.00	-10.50	23.2
36.1	12.5	359.8	0.20	5.00	25.00	-6.00	23.2
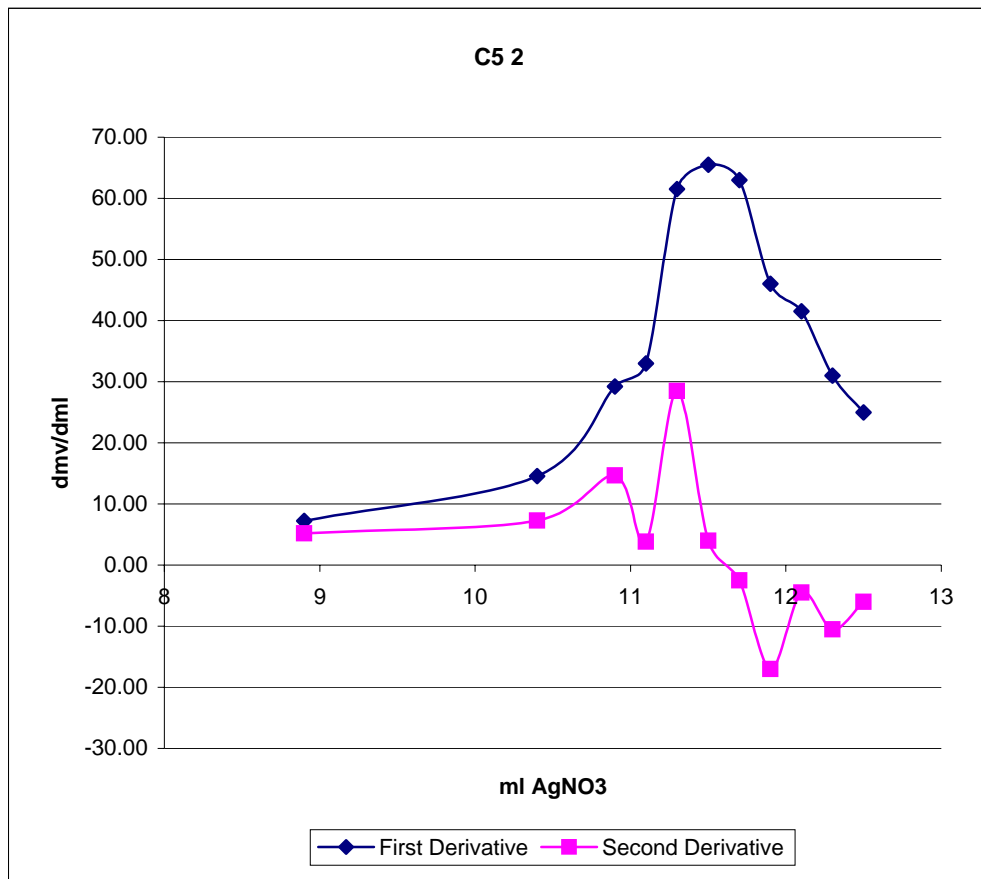
C5

3

AgNO$_3$		mv	d mL	d mV	d mV/dmL		Temp
36.1	0	225.4					23.2
40	3.9	253.2	3.90	27.80	7.13		23.3
41	4.9	271.6	1.00	18.40	18.40	11.27	23.3
41.5	5.4	290.9	0.50	19.30	38.60	20.20	23.3
41.7	5.6	302.4	0.20	11.50	57.50	18.90	23.3
41.9	5.8	315.8	0.20	13.40	67.00	9.50	23.3
42.1	6	328.1	0.20	12.30	61.50	-5.50	23.3
42.3	6.2	339.1	0.20	11.00	55.00	-6.50	23.3
42.5	6.4	347.2	0.20	8.10	40.50	-14.50	23.3
42.7	6.6	353.9	0.20	6.70	33.50	-7.00	23.3
42.9	6.8	359.2	0.20	5.30	26.50	-7.00	23.3

C5
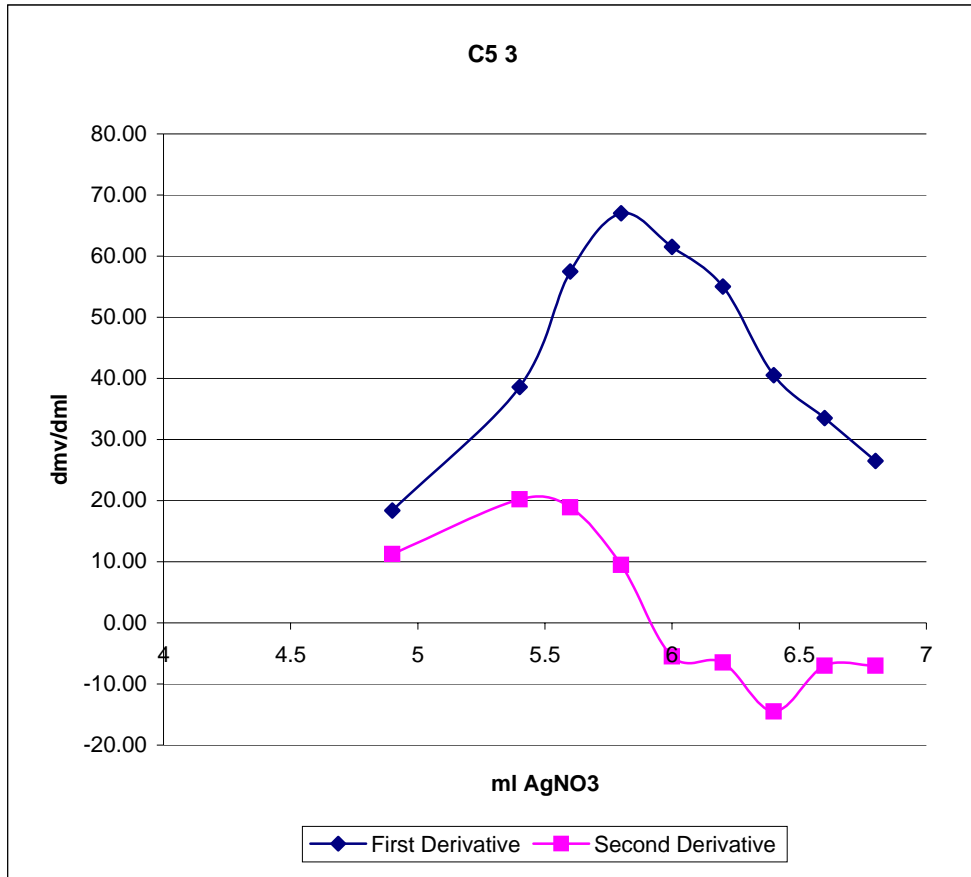
AgNO$_3$		mv	d mL	d mV	d mV/dmL		Temp
2	0	227.1					23
5.5	3.5	260.3	3.50	33.20	9.49		23.1
6	4	269	0.50	8.70	17.40	7.91	23.1
6.5	4.5	285.3	0.50	16.30	32.60	15.20	23.1
7	5	303.3	0.50	18.00	36.00	3.40	23.1
7.2	5.2	319.3	0.20	16.00	80.00	44.00	23.1
7.4	5.4	336.1	0.20	16.80	84.00	4.00	23.2
7.6	5.6	345.2	0.20	9.10	45.50	-38.50	23.2
7.8	5.8	352.3	0.20	7.10	35.50	-10.00	23.2
8	6	359.1	0.20	6.80	34.00	-1.50	23.2
8.2	6.2	364.8	0.20	5.70	28.50	-5.50	23.2

C6
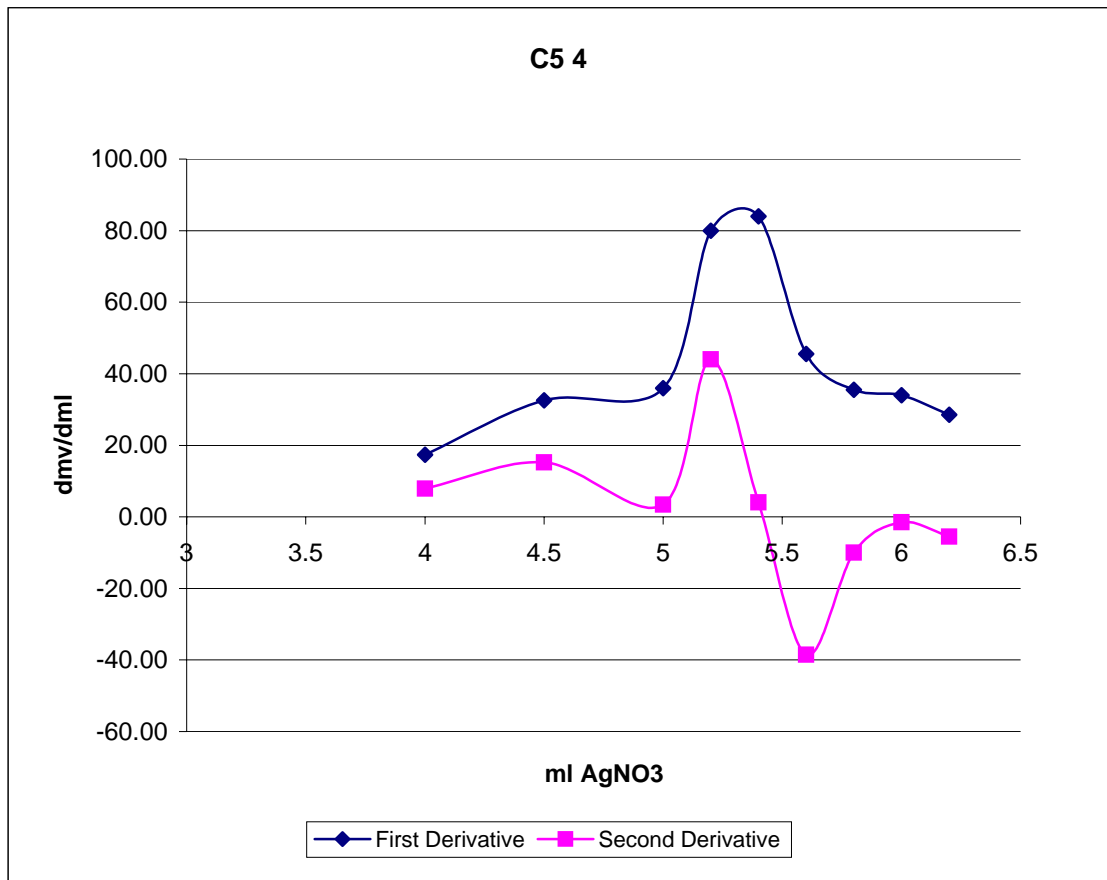
AgNO$_3$		mv	d mL	d mV	d mV/dmL		Temp
0.3	0	197.6					21.9
6	5.7	205.5	5.70	7.90	1.39		22
9	8.7	210.5	3.00	5.00	1.67	0.28	22.1
12	11.7	216.5	3.00	6.00	2.00	0.33	22.1
14	13.7	222.1	2.00	5.60	2.80	0.80	22.1
16	15.7	226.9	2.00	4.80	2.40	-0.40	22.2
18	17.7	234.3	2.00	7.40	3.70	1.30	22.2
20	19.7	244.2	2.00	9.90	4.95	1.25	22.2
22	21.7	259.6	2.00	15.40	7.70	2.75	22.2
23	22.7	272.5	1.00	12.90	12.90	5.20	22.2
23.5	23.2	285.6	0.50	13.10	26.20	13.30	22.3
23.7	23.4	291.3	0.20	5.70	28.50	2.30	22.3
23.9	23.6	299.3	0.20	8.00	40.00	11.50	22.3
24.1	23.8	308.9	0.20	9.60	48.00	8.00	22.3
24.3	24	318.5	0.20	9.60	48.00	0.00	22.3
24.5	24.2	329.2	0.20	10.70	53.50	5.50	22.3
24.7	24.4	338.6	0.20	9.40	47.00	-6.50	22.3
24.9	24.6	345.6	0.20	7.00	35.00	-12.00	22.3
25.1	24.8	350.2	0.20	4.60	23.00	-12.00	22.3

C6
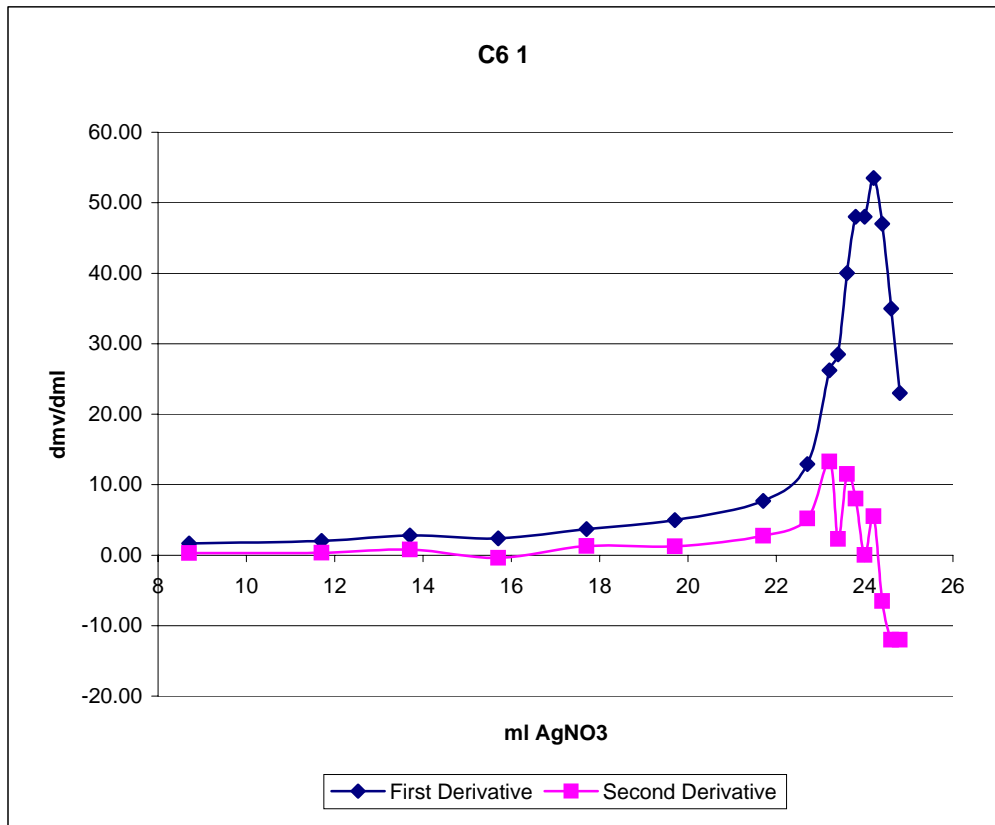
AgNO$_3$		mv	d mL	d mV	d mV/dmL		Temp
0.5	0	198.1					21.7
7	6.5	215.2	6.50	17.10	2.63		21.8
11	10.5	233.2	4.00	18.00	4.50	1.87	21.9
13	12.5	250.9	2.00	17.70	8.85	4.35	21.9
14	13.5	267.3	1.00	16.40	16.40	7.55	22
14.5	14	282.7	0.50	15.40	30.80	14.40	22
14.7	14.2	294.2	0.20	11.50	57.50	26.70	22
14.9	14.4	305.9	0.20	11.70	58.50	1.00	22.1
15.1	14.6	318.9	0.20	13.00	65.00	6.50	22.1
15.3	14.8	331.6	0.20	12.70	63.50	-1.50	22.1
15.5	15	340.2	0.20	8.60	43.00	-20.50	22.1
15.7	15.2	347.4	0.20	7.20	36.00	-7.00	22.1
15.9	15.4	353.1	0.20	5.70	28.50	-7.50	22.1

C6
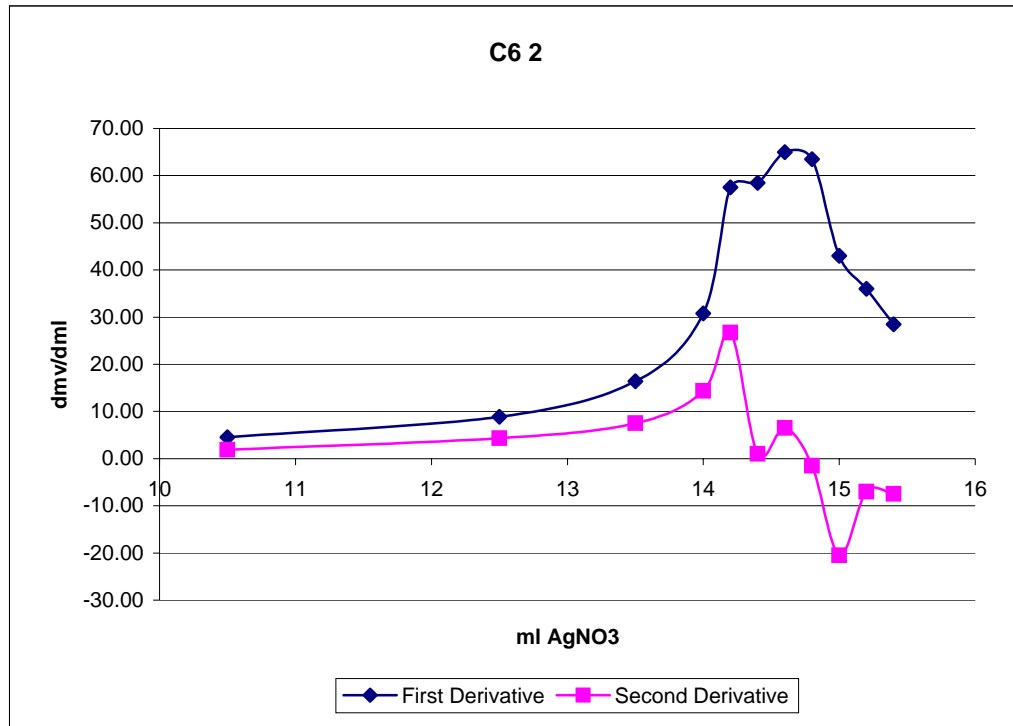
AgNO$_3$		mv	d mL	d mV	d mV/dmL		Temp
0.2	0	218.4					21.8
6.7	6.5	290.7	6.50	72.30	11.12		22
6.9	6.7	297.6	0.20	6.90	34.50	23.38	22
7.1	6.9	316.1	0.20	18.50	92.50	58.00	22
7.3	7.1	331.7	0.20	15.60	78.00	-14.50	22
7.5	7.3	343.7	0.20	12.00	60.00	-18.00	22
7.8	7.6	351.9	0.30	8.20	27.33	-32.67	22
8	7.8	358.9	0.20	7.00	35.00	7.67	22.1
8.2	8	362.5	0.20	3.60	18.00	-17.00	22.1

C6 3
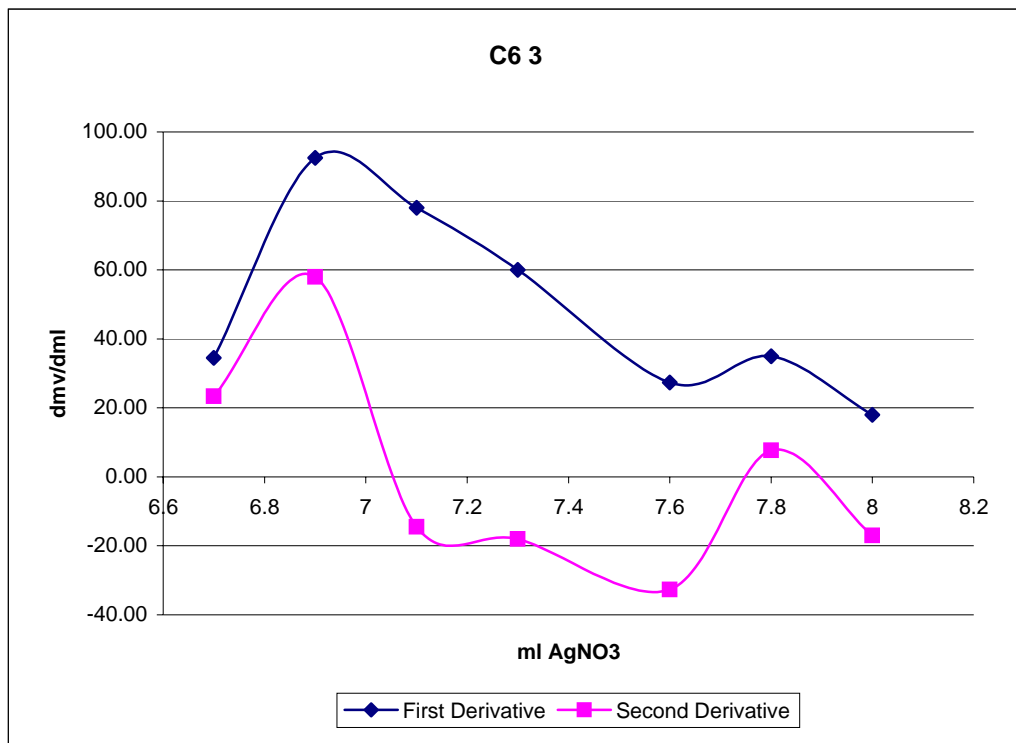
C6

4

AgNO$_3$		mv	d mL	d mV	d mV/dmL		Temp
0.7	0	231.5					21.9
4	3.3	256.9	3.30	25.40	7.70		22
5	4.3	274.8	1.00	17.90	17.90	10.20	22
5.5	4.8	287.9	0.50	13.10	26.20	8.30	22
5.7	5	297.7	0.20	9.80	49.00	22.80	22
5.9	5.2	309.2	0.20	11.50	57.50	8.50	22
6.1	5.4	322.7	0.20	13.50	67.50	10.00	22.1
6.3	5.6	334.9	0.20	12.20	61.00	-6.50	22.1
6.5	5.8	343.1	0.20	8.20	41.00	-20.00	22.1
6.7	6	350.6	0.20	7.50	37.50	-3.50	22.1
6.9	6.2	355.9	0.20	5.30	26.50	-11.00	22.1

C6 4

L4
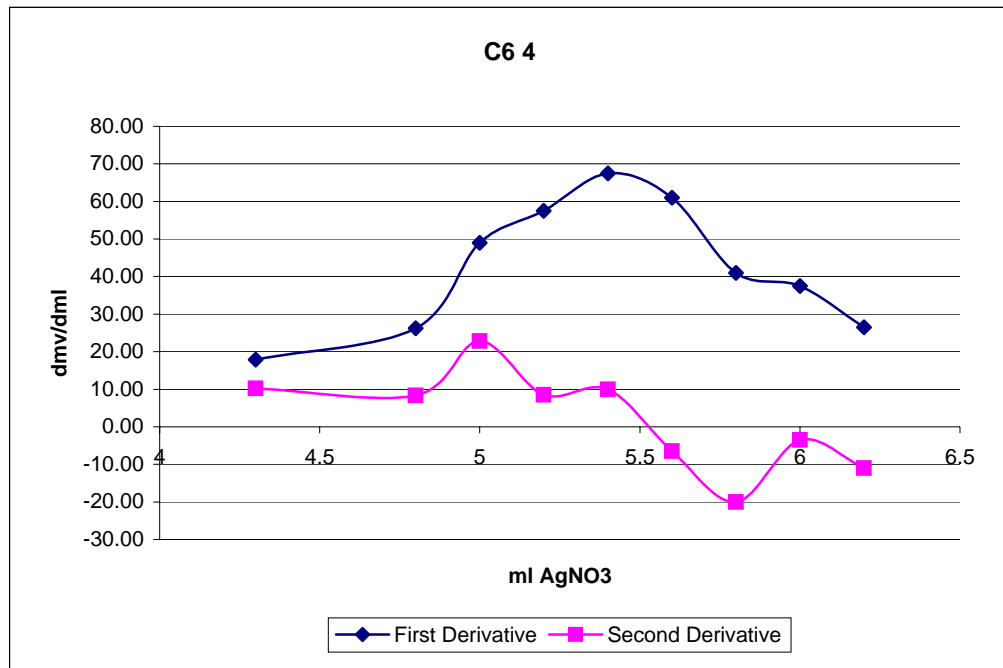
AgNO$_3$		mv	d mL	d mV	d mV/dmL		Temp
0.3	0	179.8					22.5
8	7.7	192.5	7.70	12.70	1.65		22.6
13	12.7	208.6	5.00	16.10	3.22	1.57	22.7
16	15.7	221.8	3.00	13.20	4.40	1.18	22.7
18.5	18.2	237.5	2.50	15.70	6.28	1.88	22.7
20	19.7	248.5	1.50	11.00	7.33	1.05	22.7
21	20.7	265.5	1.00	17.00	17.00	9.67	22.7
21.5	21.2	278.3	0.50	12.80	25.60	8.60	22.7
21.7	21.4	288.6	0.20	10.30	51.50	25.90	22.7
21.9	21.6	299.8	0.20	11.20	56.00	4.50	22.8
22.1	21.8	312.6	0.20	12.80	64.00	8.00	22.8
22.3	22	329.2	0.20	16.60	83.00	19.00	22.8
22.5	22.2	337.8	0.20	8.60	43.00	-40.00	22.8
22.7	22.4	345.9	0.20	8.10	40.50	-2.50	22.8
22.9	22.6	351.7	0.20	5.80	29.00	-11.50	22.8

L4
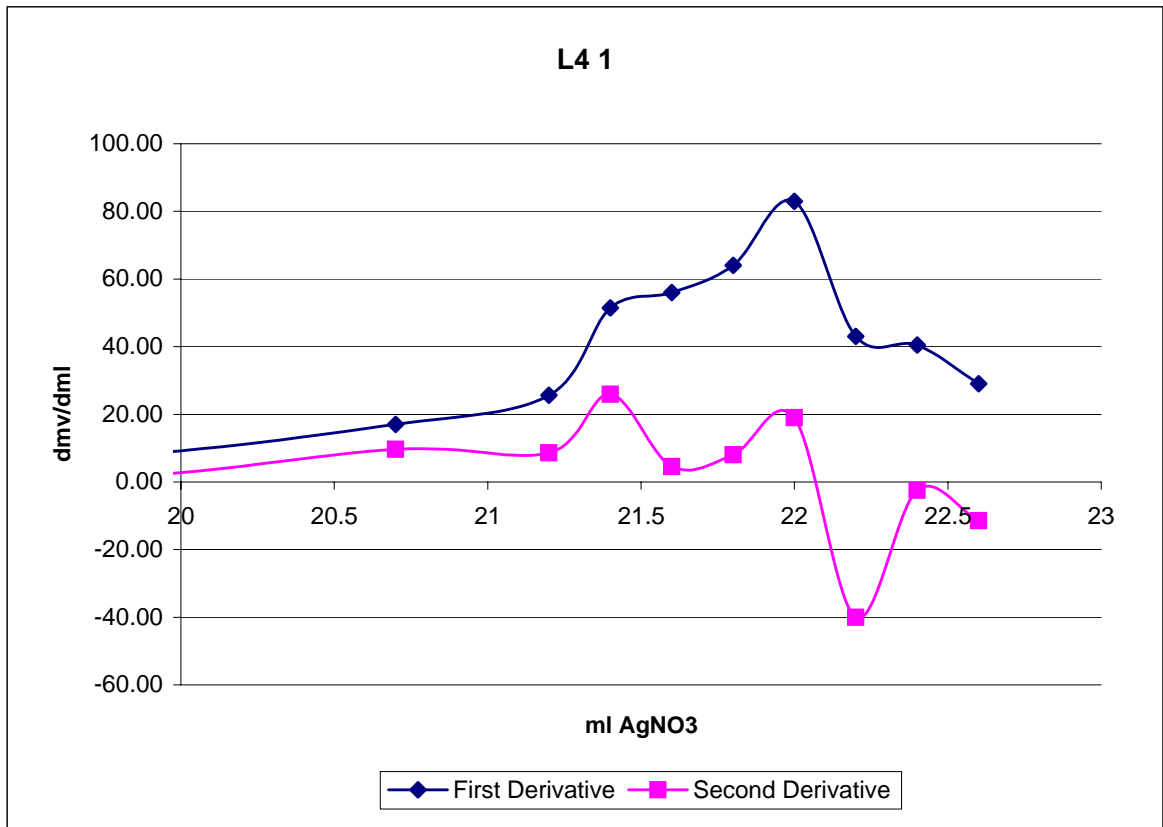
AgNO$_3$		mv	d mL	d mV	d mV/dmL		Temp
0.5	0	192.7					22.7
8	7.5	202.6	7.50	9.90	1.32		22.8
12	11.5	215.1	4.00	12.50	3.13	1.81	22.8
16	15.5	228.7	4.00	13.60	3.40	0.27	22.9
18	17.5	240.1	2.00	11.40	5.70	2.30	22.9
19	18.5	249.3	1.00	9.20	9.20	3.50	22.9
20	19.5	261.7	1.00	12.40	12.40	3.20	22.9
20.5	20	271.1	0.50	9.40	18.80	6.40	22.9
20.8	20.3	279.8	0.30	8.70	29.00	10.20	23
21.1	20.6	291.7	0.30	11.90	39.67	10.67	23
21.3	20.8	301.5	0.20	9.80	49.00	9.33	23
21.5	21	311.9	0.20	10.40	52.00	3.00	23
21.7	21.2	322.3	0.20	10.40	52.00	0.00	23
21.9	21.4	335.1	0.20	12.80	64.00	12.00	23
22.1	21.6	344.7	0.20	9.60	48.00	-16.00	23
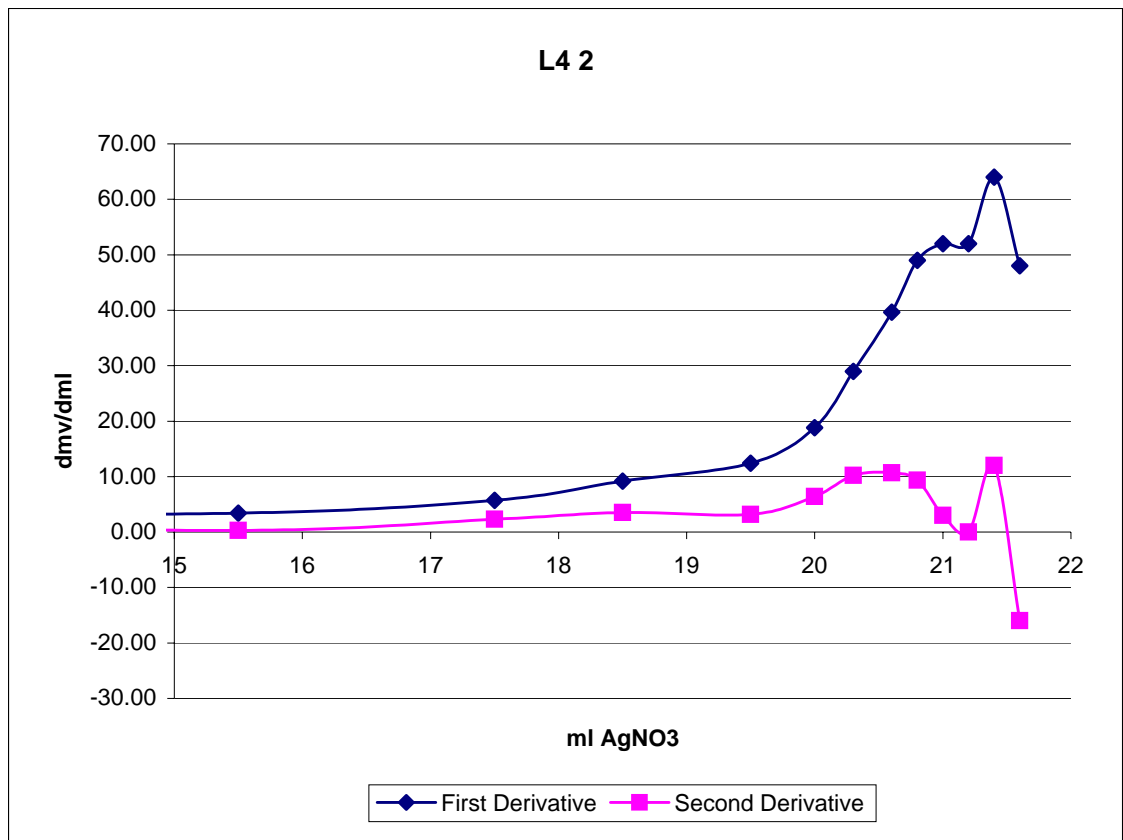
L4

3

AgNO₃		mv	d mL	d mV	d mV/dmL		Temp
1	0	221.7					22.9
4.5	3.5	240.1	3.50	18.40	5.26		22.9
5.5	4.5	258.7	1.00	18.60	18.60	13.34	22.9
6.3	5.3	284.7	0.80	26.00	32.50	13.90	22.9
6.5	5.5	294.3	0.20	9.60	48.00	15.50	23
6.7	5.7	311.9	0.20	17.60	88.00	40.00	23
6.9	5.9	326.7	0.20	14.80	74.00	-14.00	23
7.1	6.1	339.5	0.20	12.80	64.00	-10.00	23
7.3	6.3	347.4	0.20	7.90	39.50	-24.50	23
7.5	6.5	353.1	0.20	5.70	28.50	-11.00	23.1
7.7	6.7	358.7	0.20	5.60	28.00	-0.50	23.1
7.9	6.9	362.8	0.20	4.10	20.50	-7.50	23.1

L4 3
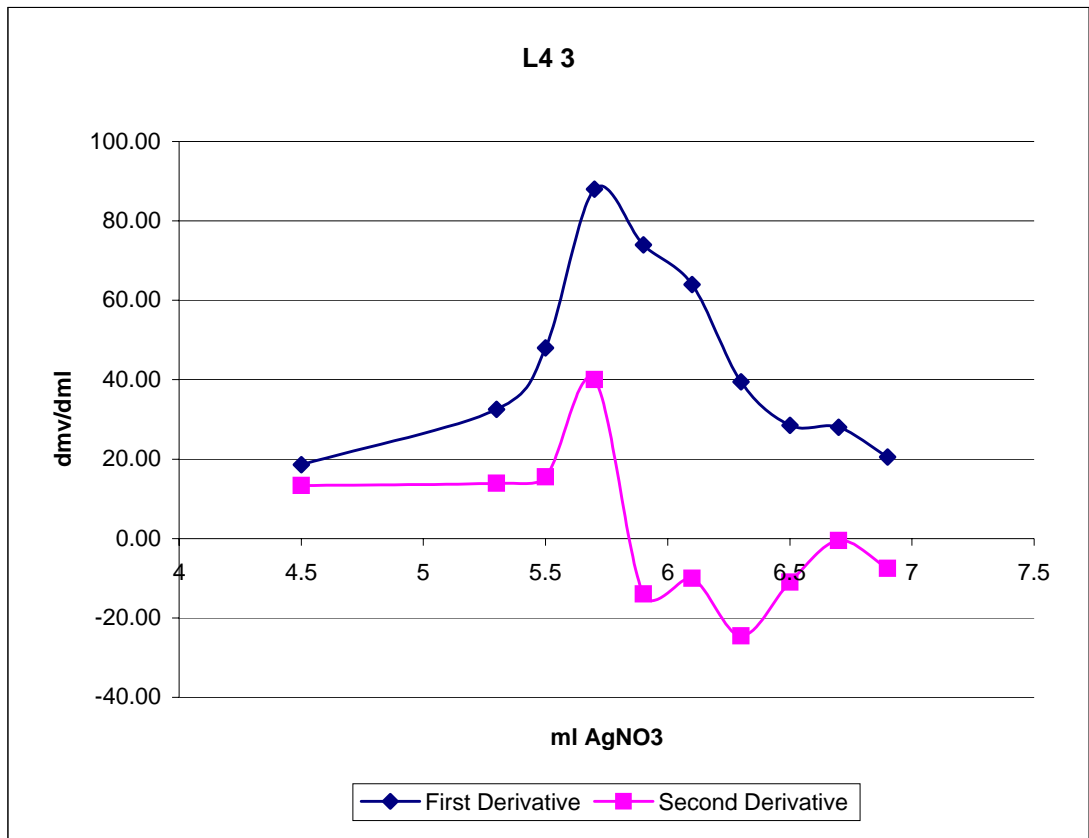
L4

4

AgNO$_3$		mv	d mL	d mV	d mV/dmL		Temp
7.9	0	231.8					23.1
10.5	2.6	247.6	2.60	15.80	6.08		23.1
11	3.1	264.5	0.50	16.90	33.80	27.72	23.2
11.5	3.6	286.7	0.50	22.20	44.40	10.60	23.2
11.7	3.8	296.3	0.20	9.60	48.00	3.60	23.3
11.9	4	307.4	0.20	11.10	55.50	7.50	23.3
12.1	4.2	319.1	0.20	11.70	58.50	3.00	23.3
12.3	4.4	332.7	0.20	13.60	68.00	9.50	23.3
12.5	4.6	341.8	0.20	9.10	45.50	-22.50	23.3
12.7	4.8	349.6	0.20	7.80	39.00	-6.50	23.3
12.9	5	354.3	0.20	4.70	23.50	-15.50	23.3

L7
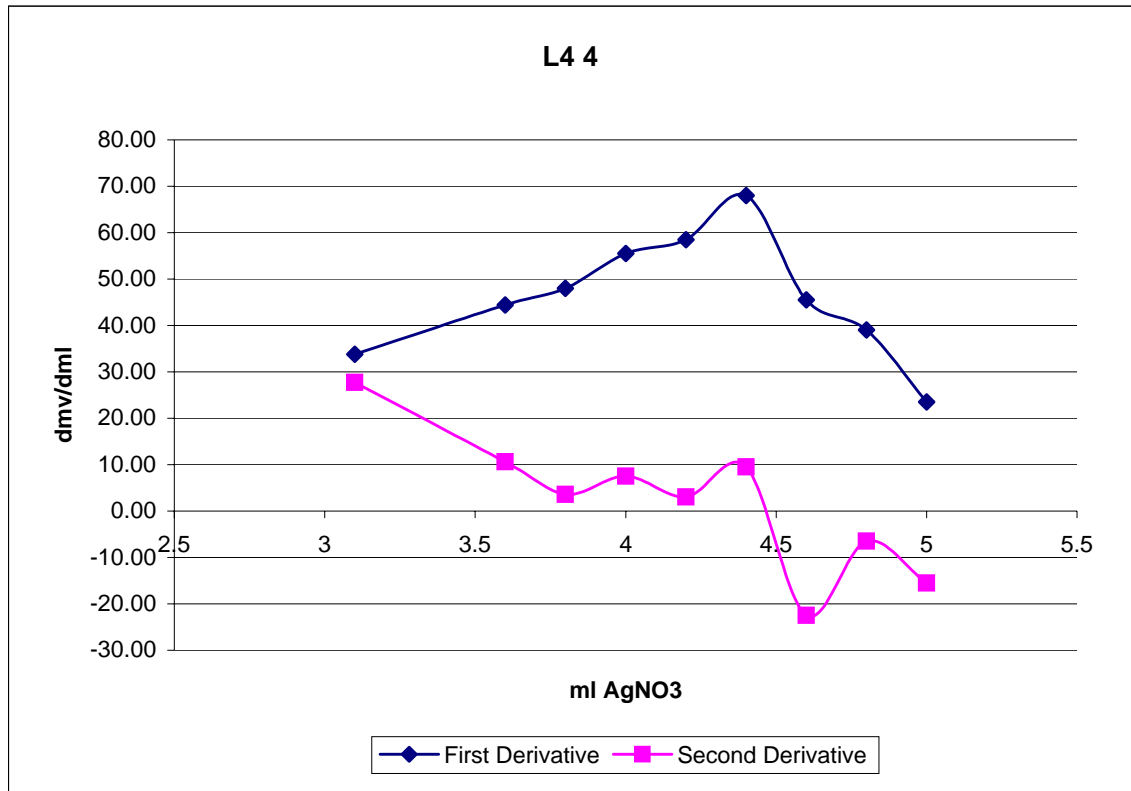
AgNO$_3$	mv	d mL	d mV	d mV/dmL		Temp
0	182.1					21.6
8	198.2	8.00	16.10	2.01		21.7
15	222.8	7.00	24.60	3.51	1.50	21.8
19	271.1	4.00	48.30	12.08	8.56	21.8
19.4	292.3	0.40	21.20	53.00	40.93	21.8
19.6	307.3	0.20	15.00	75.00	22.00	21.8
19.8	329.3	0.20	22.00	110.00	35.00	21.8
20	341.4	0.20	12.10	60.50	-49.50	21.8
20.2	348.5	0.20	7.10	35.50	-25.00	21.8
20.4	355.3	0.20	6.80	34.00	-1.50	21.8
20.6	358.8	0.20	3.50	17.50	-16.50	21.8
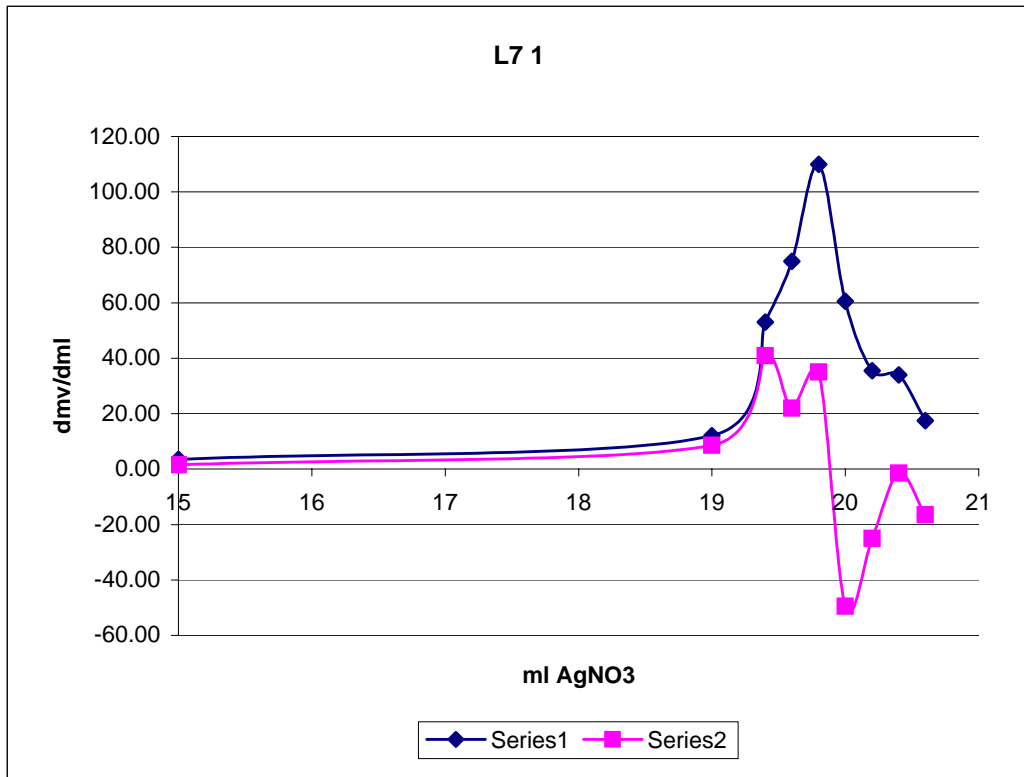
L7

2

AgNO₃		mv	d mL	d mV	d mV/dmL		Temp
1.3	0	207.5					21.8
7	5.7	231.2	5.70	23.70	4.16		21.9
9	7.7	249.4	2.00	18.20	9.10	4.94	21.9
10	8.7	268.4	1.00	19.00	19.00	9.90	21.9
10.5	9.2	283.3	0.50	14.90	29.80	10.80	21.9
10.7	9.4	296.5	0.20	13.20	66.00	36.20	21.9
10.9	9.6	310.2	0.20	13.70	68.50	2.50	21.9
11.1	9.8	323.9	0.20	13.70	68.50	0.00	21.9
11.3	10	336.6	0.20	12.70	63.50	-5.00	22
11.5	10.2	346.1	0.20	9.50	47.50	-16.00	22
11.7	10.4	352.8	0.20	6.70	33.50	-14.00	22
11.9	10.6	358.4	0.20	5.60	28.00	-5.50	22

L7
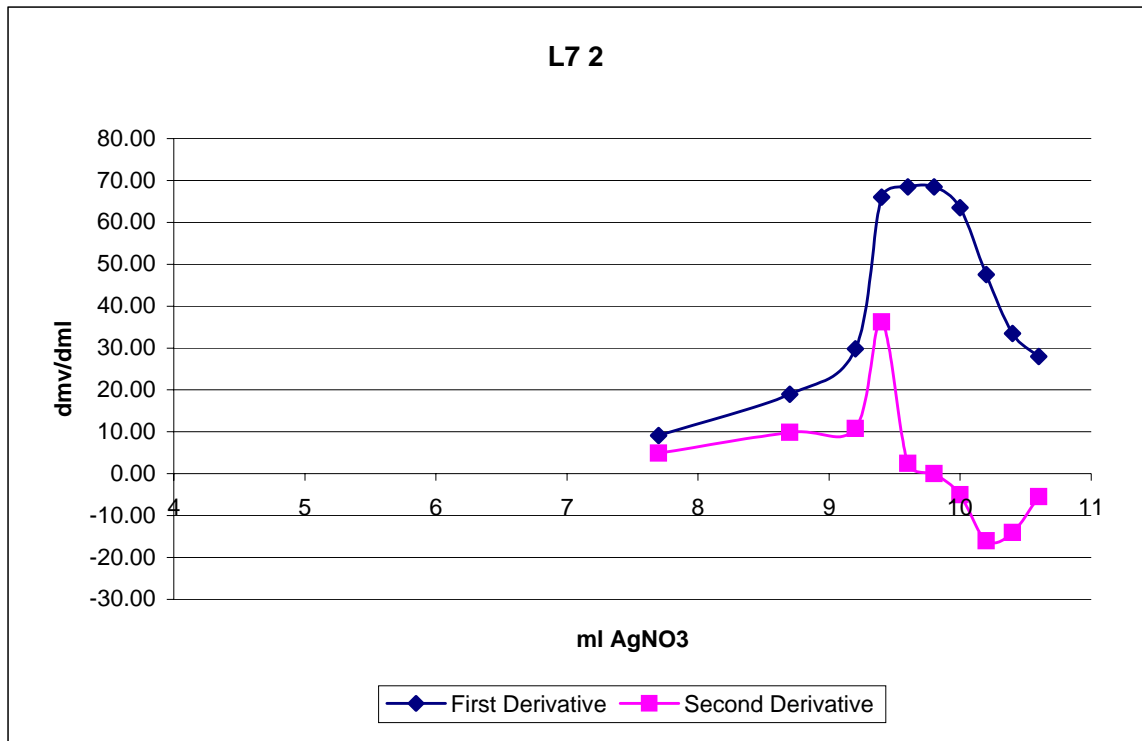
AgNO$_3$		mv	d mL	d mV	d mV/dmL		Temp
1.8	0	224.7					21.9
6	4.2	256.4	4.20	31.70	7.55		21.9
7	5.2	275.7	1.00	19.30	19.30	11.75	21.9
7.5	5.7	296.6	0.50	20.90	41.80	22.50	22
7.7	5.9	311.3	0.20	14.70	73.50	31.70	22
7.9	6.1	324.9	0.20	13.60	68.00	-5.50	22
8.1	6.3	334.4	0.20	9.50	47.50	-20.50	22
8.3	6.5	343.9	0.20	9.50	47.50	0.00	22
8.5	6.7	350.5	0.20	6.60	33.00	-14.50	22
8.7	6.9	356.2	0.20	5.70	28.50	-4.50	22

L7

4
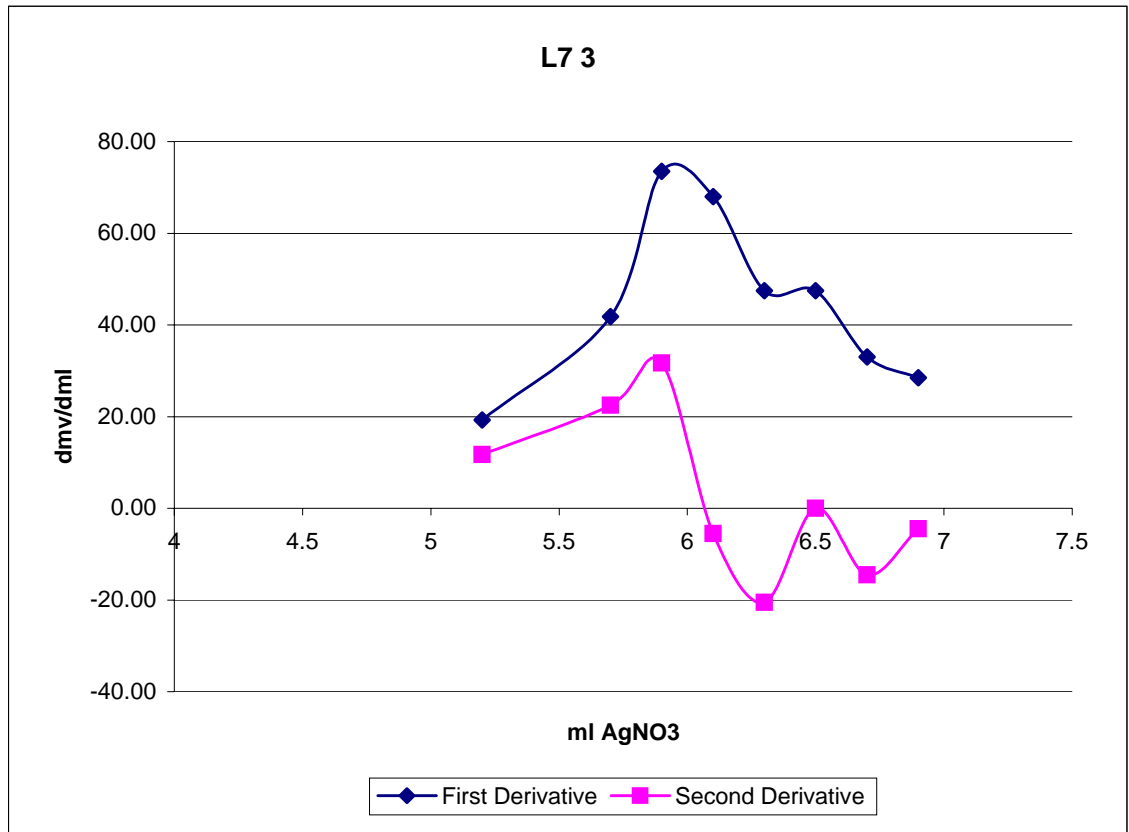
AgNO$_3$		mv	d mL	d mV	d mV/dmL		Temp
8.7	0	228.3					21.9
12.9	4.2	262.2	4.20	33.90	8.07		22
13.5	4.8	275.3	0.60	13.10	21.83	13.76	22
14	5.3	294.5	0.50	19.20	38.40	16.57	22
14.2	5.5	304.3	0.20	9.80	49.00	10.60	22
14.4	5.7	318.5	0.20	14.20	71.00	22.00	22.1
14.6	5.9	330.9	0.20	12.40	62.00	-9.00	22.1
14.8	6.1	340.8	0.20	9.90	49.50	-12.50	22.1
15	6.3	349.3	0.20	8.50	42.50	-7.00	22.1
15.2	6.5	355.3	0.20	6.00	30.00	-12.50	22.1
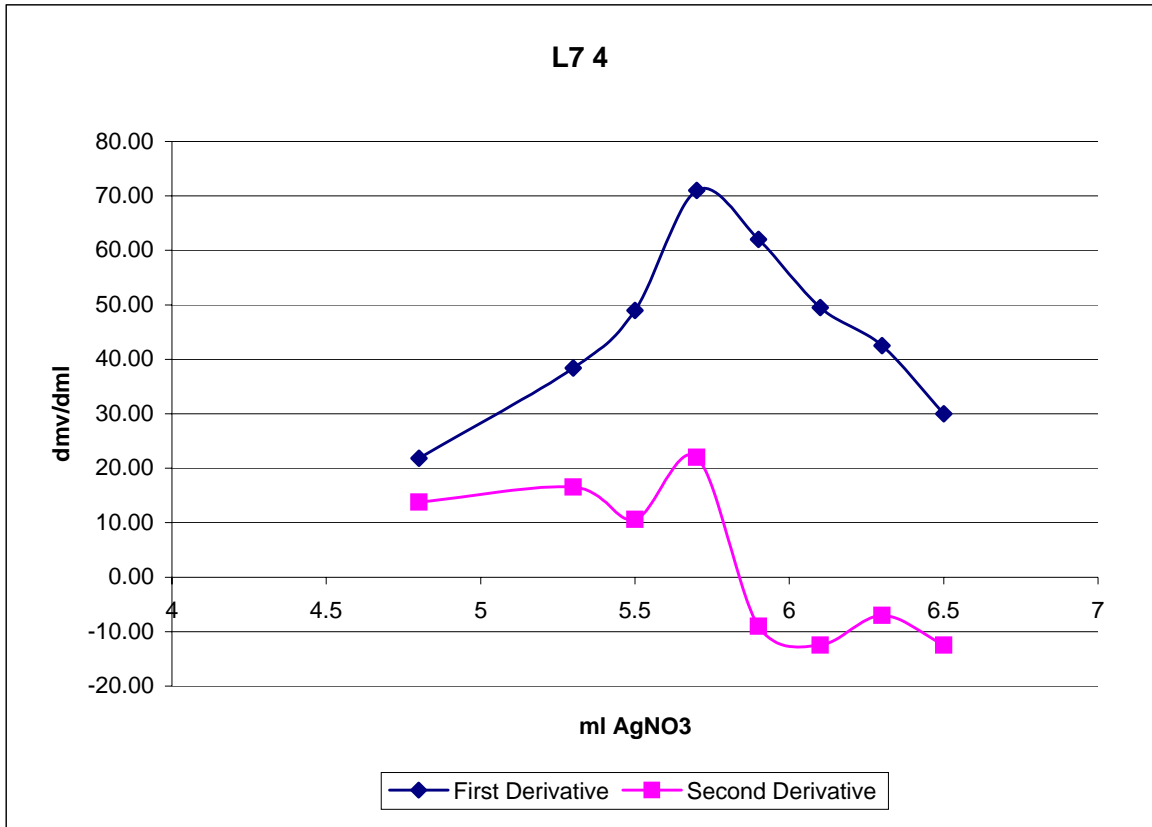
L13

1							
AgNO$_3$		mv	d mL	d mV	d mV/dmL		Temp
0.1	0	199.8					22.5
4.5	4.4	208.1	4.40	8.30	1.89		22.6
7.5	7.4	216.7	3.00	8.60	2.87	0.98	22.7
10.5	10.4	227.1	3.00	10.40	3.47	0.60	22.7
13	12.9	237.5	2.50	10.40	4.16	0.69	22.7
14	13.9	244.3	1.00	6.80	6.80	2.64	22.7
15	14.9	253.7	1.00	9.40	9.40	2.60	22.7
16	15.9	268.1	1.00	14.40	14.40	5.00	22.7
16.2	16.1	273.9	0.20	5.80	29.00	14.60	22.8
16.5	16.4	281.4	0.30	7.50	25.00	-4.00	22.8
16.8	16.7	292.3	0.30	10.90	36.33	11.33	22.8
17	16.9	303.9	0.20	11.60	58.00	21.67	22.8
17.2	17.1	316.3	0.20	12.40	62.00	4.00	22.8
17.4	17.3	329.1	0.20	12.80	64.00	2.00	22.8
17.6	17.5	336.3	0.20	7.20	36.00	-28.00	22.8
17.8	17.7	342.7	0.20	6.40	32.00	-4.00	22.8
18	17.9	350.1	0.20	7.40	37.00	5.00	22.8
18.2	18.1	356.3	0.20	6.20	31.00	-6.00	22.8
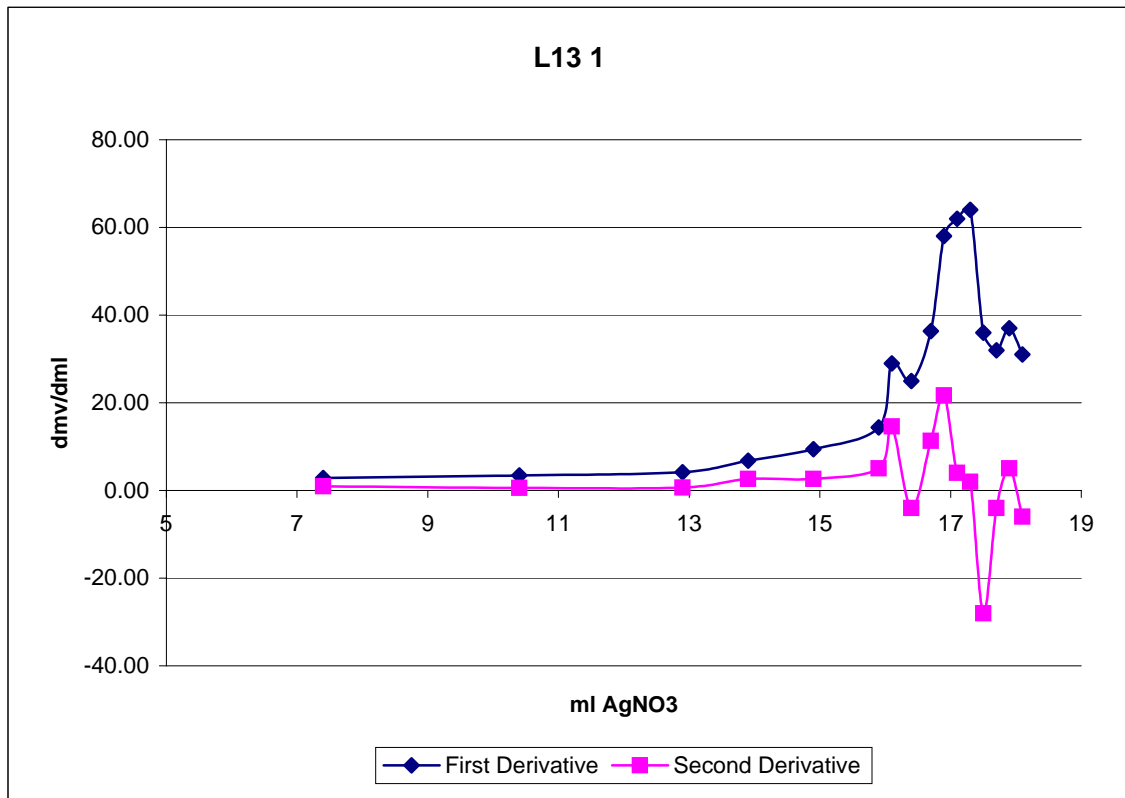
L13

2 AgNO$_3$		mv	d mL	d mV	d mV/dmL		Temp
18.2	0	225.9					22.6
21	2.8	239.1	2.80	13.20	4.71		22.7
22	3.8	247.6	1.00	8.50	8.50	3.79	22.8
23	4.8	262.6	1.00	15.00	15.00	6.50	22.8
23.3	5.1	267.2	0.30	4.60	15.33	0.33	22.8
23.5	5.3	271.9	0.20	4.70	23.50	8.17	22.8
23.7	5.5	276.8	0.20	4.90	24.50	1.00	22.8
23.9	5.7	283	0.20	6.20	31.00	6.50	22.9
24.1	5.9	289.5	0.20	6.50	32.50	1.50	22.9
24.3	6.1	302.4	0.20	12.90	64.50	32.00	22.9
24.5	6.3	314.1	0.20	11.70	58.50	-6.00	22.9
24.7	6.5	325.7	0.20	11.60	58.00	-0.50	22.9
24.9	6.7	336.6	0.20	10.90	54.50	-3.50	22.9
25.1	6.9	343.9	0.20	7.30	36.50	-18.00	22.9
25.3	7.1	349.7	0.20	5.80	29.00	-7.50	22.9
25.5	7.3	355.3	0.20	5.60	28.00	-1.00	22.9

L13 2
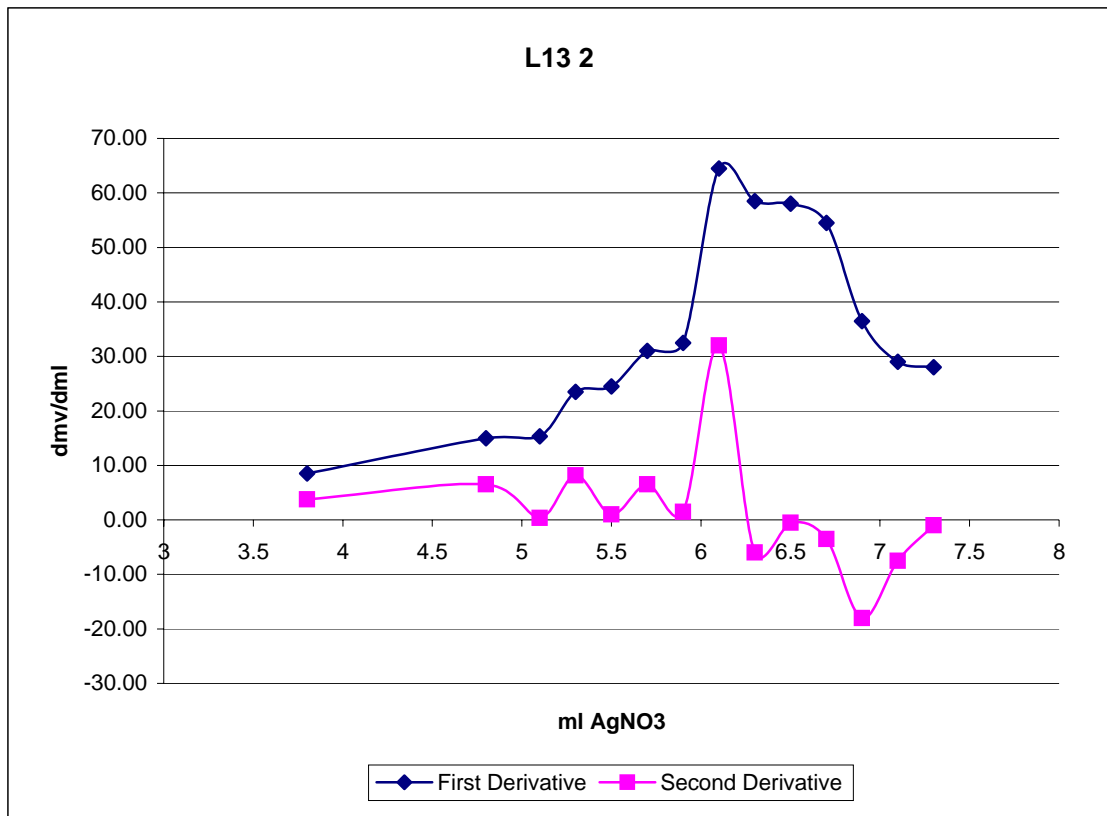
L13

3

AgNO$_3$		mv	d mL	d mV	d mV/dmL		Temp
25.5	0	227.5					22.7
28	2.5	241.2	2.50	13.70	5.48		22.8
29	3.5	251.9	1.00	10.70	10.70	5.22	22.8
29.5	4	258.1	0.50	6.20	12.40	1.70	22.9
30	4.5	266.9	0.50	8.80	17.60	5.20	22.9
30.3	4.8	275.2	0.30	8.30	27.67	10.07	22.9
30.6	5.1	286.3	0.30	11.10	37.00	9.33	22.9
30.8	5.3	297.1	0.20	10.80	54.00	17.00	22.9
31	5.5	309.3	0.20	12.20	61.00	7.00	22.9
31.2	5.7	322.9	0.20	13.60	68.00	7.00	22.9
31.4	5.9	336.3	0.20	13.40	67.00	-1.00	22.9
31.6	6.1	343.7	0.20	7.40	37.00	-30.00	23.0
31.8	6.3	349.6	0.20	5.90	29.50	-7.50	23.0
32	6.5	355.2	0.20	5.60	28.00	-1.50	23.0
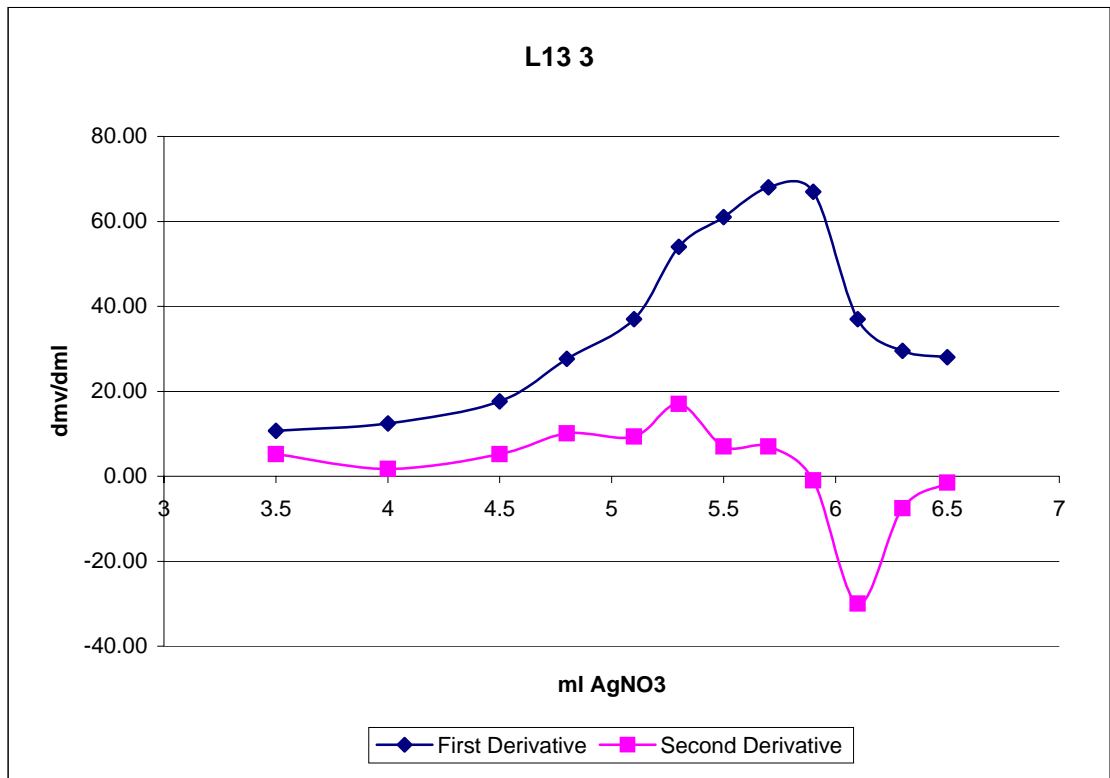
L13

4

AgNO$_3$		mv	d mL	d mV	d mV/dmL		Temp
0.5	0	227.3					22.9
3	2.5	242.1	2.50	14.80	5.92		23
3.5	3	250.3	0.50	8.20	16.40	10.48	23
4.5	4	262.9	1.00	12.60	12.60	-3.80	23.1
5	4.5	275.3	0.50	12.40	24.80	12.20	23.1
5.2	4.7	283.7	0.20	8.40	42.00	17.20	23.1
5.4	4.9	291.9	0.20	8.20	41.00	-1.00	23.1
5.6	5.1	301.3	0.20	9.40	47.00	6.00	23.1
5.8	5.3	313.5	0.20	12.20	61.00	14.00	23.1
6	5.5	327.6	0.20	14.10	70.50	9.50	23.1
6.2	5.7	341	0.20	13.40	67.00	-3.50	23.1
6.4	5.9	347.5	0.20	6.50	32.50	-34.50	23.1
6.6	6.1	355.1	0.20	7.60	38.00	5.50	23.1
6.8	6.3	359.9	0.20	4.80	24.00	-14.00	23.1
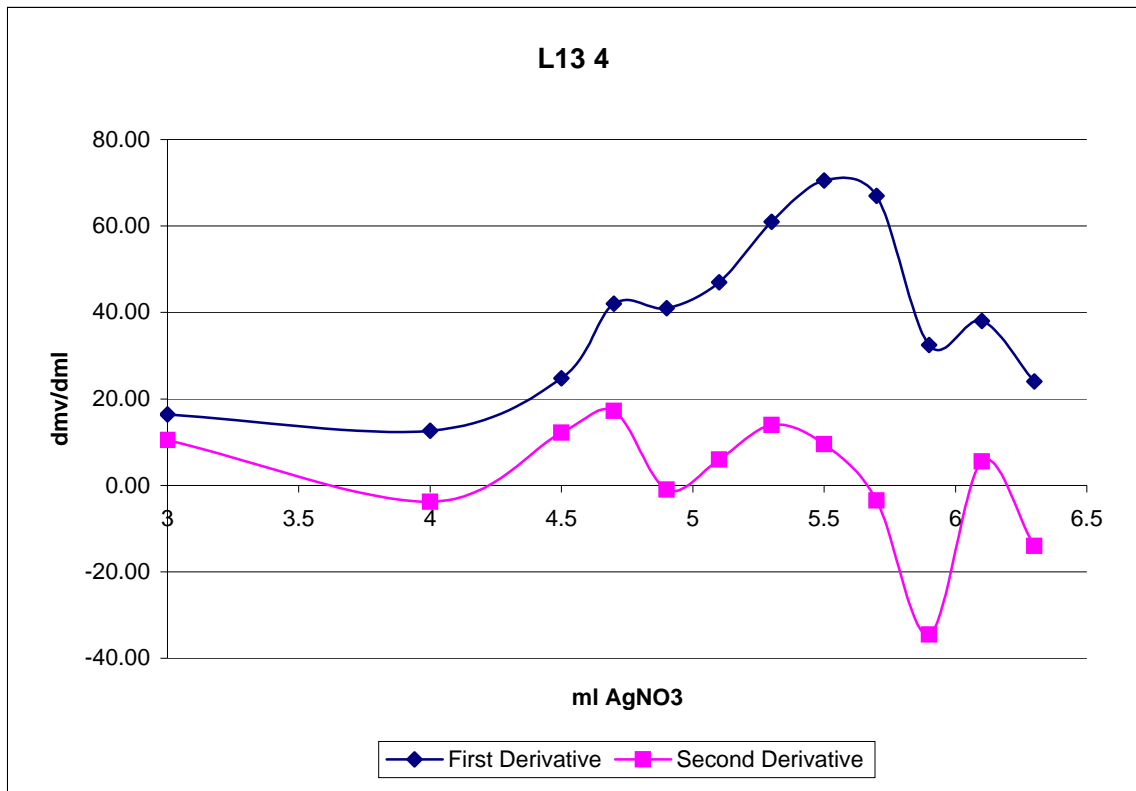
L15

1

AgNO$_3$		mv	d mL	d mV	d mV/dmL		Temp
0.5	0	191.6					22
6.5	6	202.2	6.00	10.60	1.77		22.1
11	10.5	213.1	4.50	10.90	2.42	0.66	22.1
15	14.5	228.1	4.00	15.00	3.75	1.33	22.1
18	17.5	250.1	3.00	22.00	7.33	3.58	22.1
19	18.5	264.5	1.00	14.40	14.40	7.07	22.2
19.4	18.9	274.1	0.40	9.60	24.00	9.60	22.2
19.6	19.1	281.8	0.20	7.70	38.50	14.50	22.2
19.8	19.3	289.5	0.20	7.70	38.50	0.00	22.2
20	19.5	298.2	0.20	8.70	43.50	5.00	22.2
20.2	19.7	310.3	0.20	12.10	60.50	17.00	22.2
20.4	19.9	322.7	0.20	12.40	62.00	1.50	22.3
20.6	20.1	332.9	0.20	10.20	51.00	-11.00	22.3
20.8	20.3	340.9	0.20	8.00	40.00	-11.00	22.3
21	20.5	347.6	0.20	6.70	33.50	-6.50	22.3
21.2	20.7	353.7	0.20	6.10	30.50	-3.00	22.3

L15
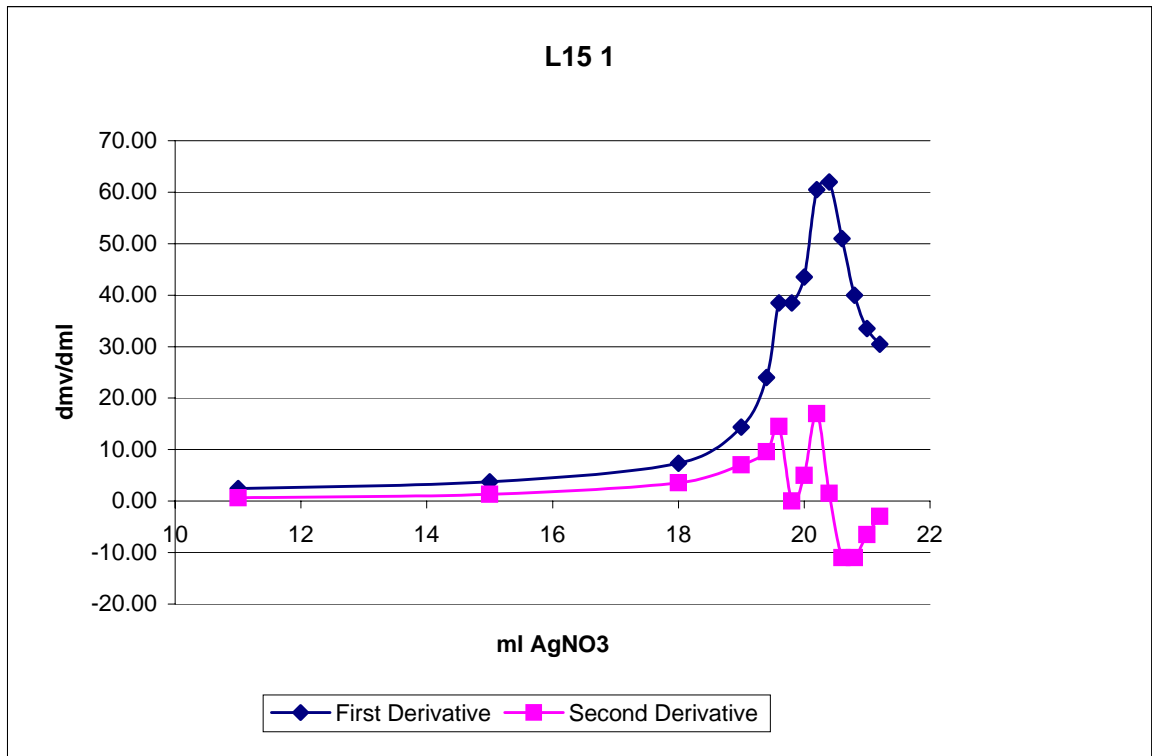
AgNO$_3$	mv	d mL	d mV	d mV/dmL		Temp
0	196.5					22.2
6	212.6	6.00	16.10	2.68		22.3
10	231.1	4.00	18.50	4.63	1.94	22.3
13	263.7	3.00	32.60	10.87	6.24	22.3
13.5	279.9	0.50	16.20	32.40	21.53	22.3
13.8	296.3	0.30	16.40	54.67	22.27	22.3
14	311.3	0.20	15.00	75.00	20.33	22.4
14.2	325.6	0.20	14.30	71.50	-3.50	22.4
14.4	339.1	0.20	13.50	67.50	-4.00	22.4
14.6	346.5	0.20	7.40	37.00	-30.50	22.4
14.8	352.9	0.20	6.40	32.00	-5.00	22.4

E102

L15

3
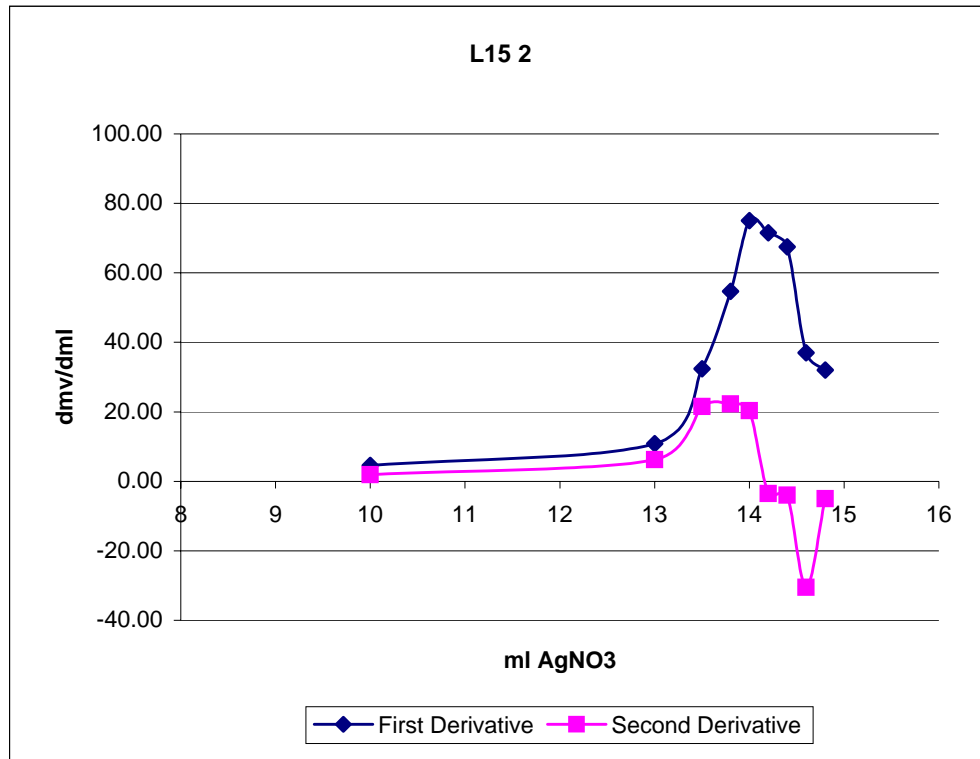
AgNO$_3$		mv	d mL	d mV	d mV/dmL		Temp
0.5	0	228.3					22.3
3	2.5	244.6	2.50	16.30	6.52		22.4
4.1	3.6	255.3	1.10	10.70	9.73	3.21	22.4
5	4.5	269.9	0.90	14.60	16.22	6.49	22.4
5.3	4.8	277.2	0.30	7.30	24.33	8.11	22.4
5.6	5.1	287.4	0.30	10.20	34.00	9.67	22.4
5.8	5.3	296.8	0.20	9.40	47.00	13.00	22.4
6	5.5	307.4	0.20	10.60	53.00	6.00	22.5
6.2	5.7	322.1	0.20	14.70	73.50	20.50	22.5
6.4	5.9	333.9	0.20	11.80	59.00	-14.50	22.5
6.6	6.1	343	0.20	9.10	45.50	-13.50	22.5
6.8	6.3	349.1	0.20	6.10	30.50	-15.00	22.5
7	6.5	354.6	0.20	5.50	27.50	-3.00	22.5
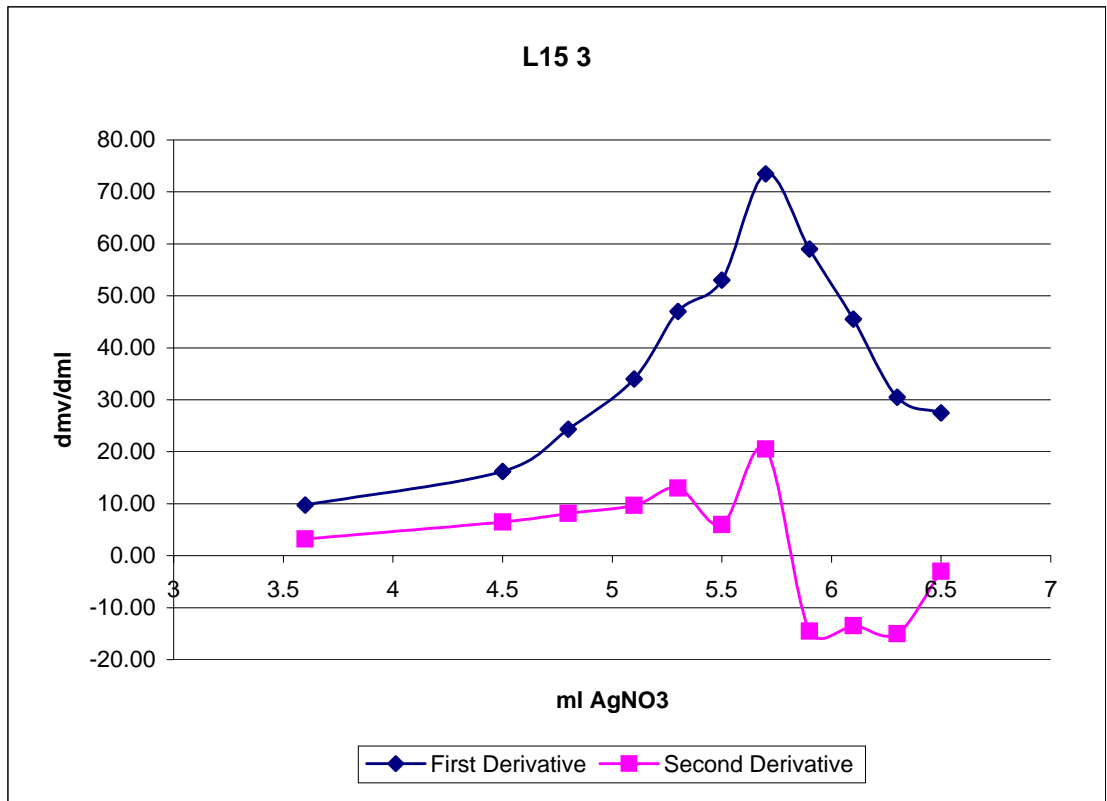
L15

4

AgNO₃	mv	d mL	d mV	d mV/dmL		Temp
0	233.4					22.2
2	247.5	2.00	14.10	7.05		22.3
3	260.8	1.00	13.30	13.30	6.25	22.3
3.4	269.4	0.40	8.60	21.50	8.20	22.3
3.7	277.6	0.30	8.20	27.33	5.83	22.3
3.9	285.1	0.20	7.50	37.50	10.17	22.3
4.1	293.5	0.20	8.40	42.00	4.50	22.3
4.3	305.9	0.20	12.40	62.00	20.00	22.3
4.5	321.6	0.20	15.70	78.50	16.50	22.3
4.7	334.6	0.20	13.00	65.00	-13.50	22.4
4.9	342.8	0.20	8.20	41.00	-24.00	22.4
5.1	348.8	0.20	6.00	30.00	-11.00	22.4
5.3	354.7	0.20	5.90	29.50	-0.50	22.4

L21
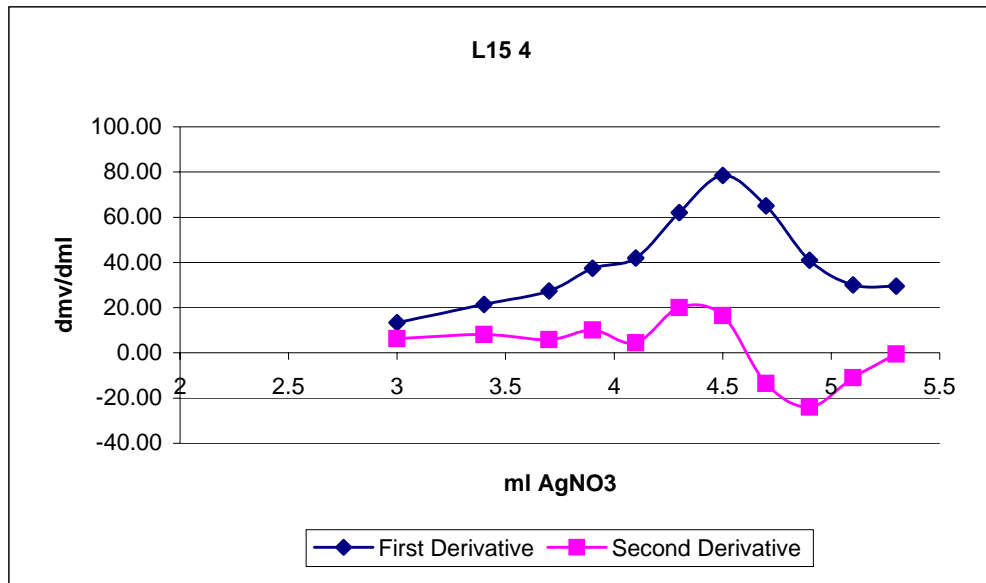
AgNO$_3$		mv	d mL	d mV	d mV/dmL		Temp
0.7	0	190.6					22.3
8	7.3	201.5	7.30	10.90	1.49		22.4
12	11.3	209.4	4.00	7.90	1.98	0.48	22.4
16	15.3	219.9	4.00	10.50	2.63	0.65	22.4
19	18.3	231.6	3.00	11.70	3.90	1.28	22.4
21	20.3	243.4	2.00	11.80	5.90	2.00	22.5
22	21.3	251.9	1.00	8.50	8.50	2.60	22.5
23	22.3	265.2	1.00	13.30	13.30	4.80	22.5
23.5	22.8	277.1	0.50	11.90	23.80	10.50	22.5
23.8	23.1	286.3	0.30	9.20	30.67	6.87	22.5
24	23.3	295.8	0.20	9.50	47.50	16.83	22.5
24.2	23.5	304.6	0.20	8.80	44.00	-3.50	22.5
24.4	23.7	318.2	0.20	13.60	68.00	24.00	22.5
24.6	23.9	330.5	0.20	12.30	61.50	-6.50	22.6
24.8	24.1	339.6	0.20	9.10	45.50	-16.00	22.6
25	24.3	346.4	0.20	6.80	34.00	-11.50	22.6
25.2	24.5	351.6	0.20	5.20	26.00	-8.00	22.6
25.4	24.7	356.5	0.20	4.90	24.50	-1.50	22.6

L21
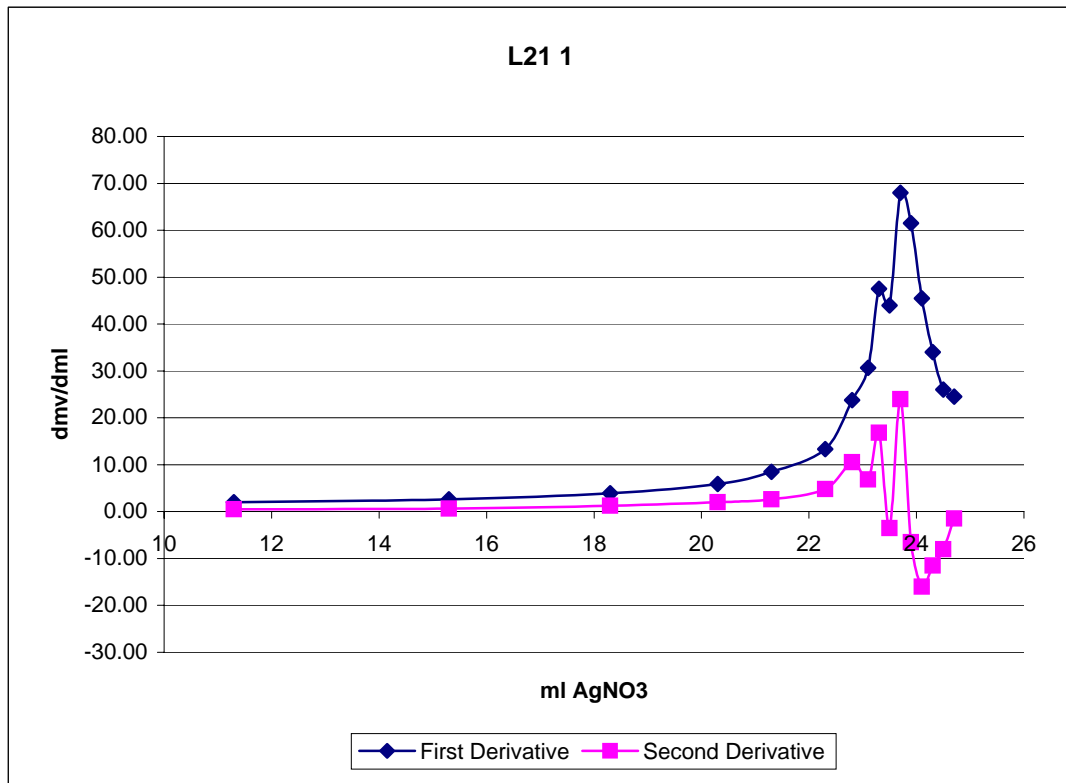
AgNO₃		mv	d mL	d mV	d mV/dmL		Temp
1.8	0	205					22.2
8.5	6.7	231.3	6.70	26.30	3.93		22.3
11	9.2	250.5	2.50	19.20	7.68	3.75	22.3
12	10.2	264.4	1.00	13.90	13.90	6.22	22.3
12.5	10.7	277.1	0.50	12.70	25.40	11.50	22.3
12.8	11	289.7	0.30	12.60	42.00	16.60	22.4
13	11.2	299.7	0.20	10.00	50.00	8.00	22.4
13.2	11.4	312.7	0.20	13.00	65.00	15.00	22.4
13.4	11.6	324.9	0.20	12.20	61.00	-4.00	22.4
13.6	11.8	335	0.20	10.10	50.50	-10.50	22.4
13.8	12	342.8	0.20	7.80	39.00	-11.50	22.4
14	12.2	348.9	0.20	6.10	30.50	-8.50	22.4
14.2	12.4	355.1	0.20	6.20	31.00	0.50	22.4

L21 2

L21

3
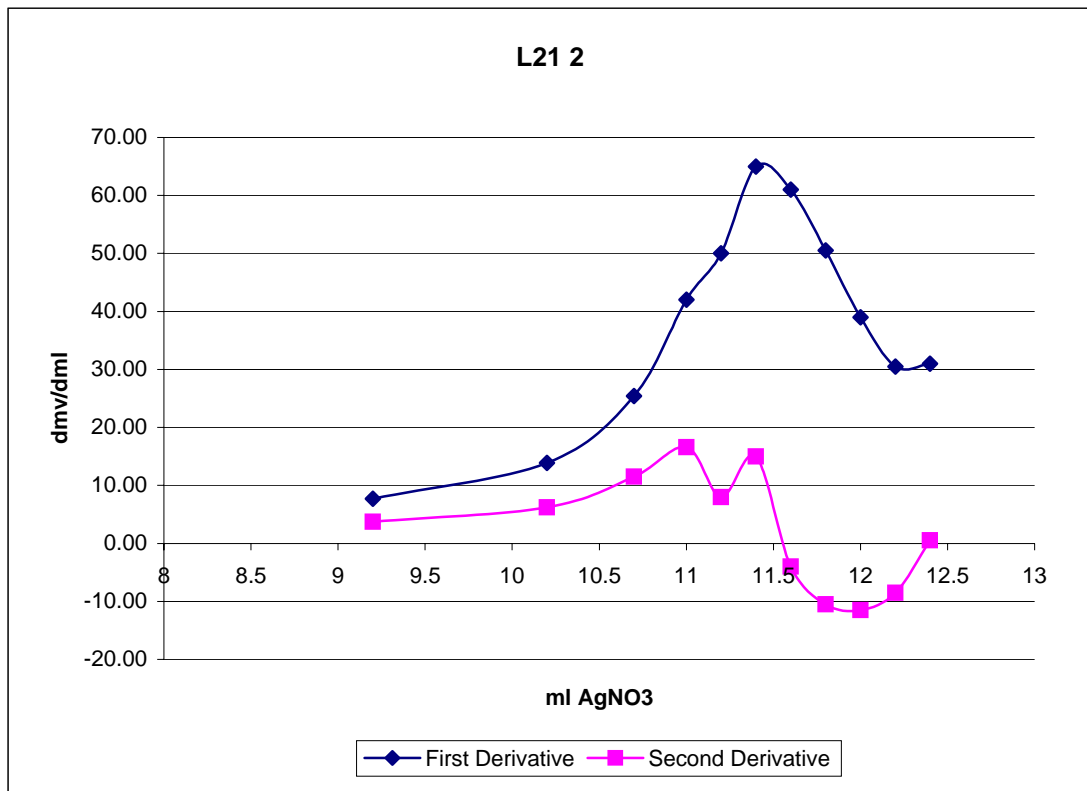
AgNO$_3$		mv	d mL	d mV	d mV/dmL		Temp
0.8	0	215.7					22.3
6	5.2	249.7	5.20	34.00	6.54		22.4
7	6.2	264.4	1.00	14.70	14.70	8.16	22.4
7.5	6.7	279.1	0.50	14.70	29.40	14.70	22.4
7.8	7	288.7	0.30	9.60	32.00	2.60	22.4
8	7.2	299.7	0.20	11.00	55.00	23.00	22.5
8.2	7.4	316.2	0.20	16.50	82.50	27.50	22.5
8.4	7.6	328.1	0.20	11.90	59.50	-23.00	22.5
8.6	7.8	339.9	0.20	11.80	59.00	-0.50	22.5
8.8	8	344.6	0.20	4.70	23.50	-35.50	22.5
9	8.2	350.3	0.20	5.70	28.50	5.00	22.5
9.2	8.4	355.7	0.20	5.40	27.00	-1.50	22.5

L21 3
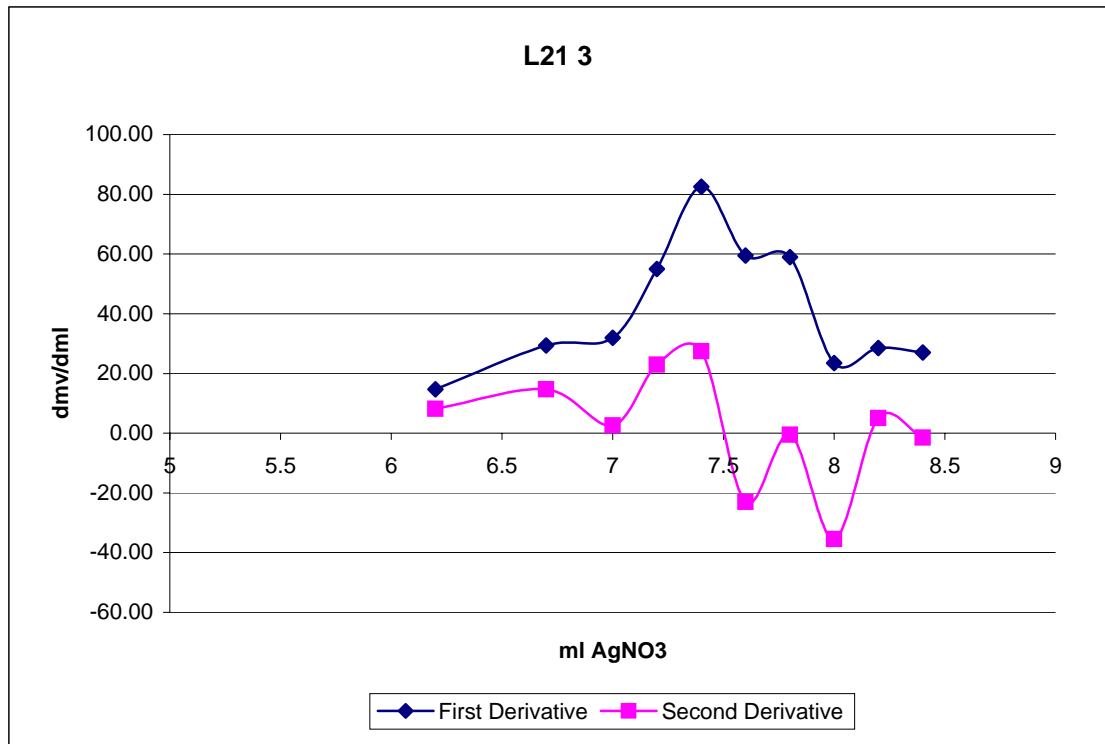
L21

4

AgNO$_3$	mv	d mL	d mV	d mV/dmL		Temp
0	222.1					22.3
3	242.3	3.00	20.20	6.73		22.3
4	253	1.00	10.70	10.70	3.97	22.4
5	272.8	1.00	19.80	19.80	9.10	22.4
5.3	286.6	0.30	13.80	46.00	26.20	22.4
5.5	297.7	0.20	11.10	55.50	9.50	22.4
5.7	313.9	0.20	16.20	81.00	25.50	22.4
5.9	328.8	0.20	14.90	74.50	-6.50	22.4
6.1	342.7	0.20	13.90	69.50	-5.00	22.4
6.3	348.4	0.20	5.70	28.50	-41.00	22.4
6.5	354.1	0.20	5.70	28.50	0.00	22.4
6.7	358.3	0.20	4.20	21.00	-7.50	22.4
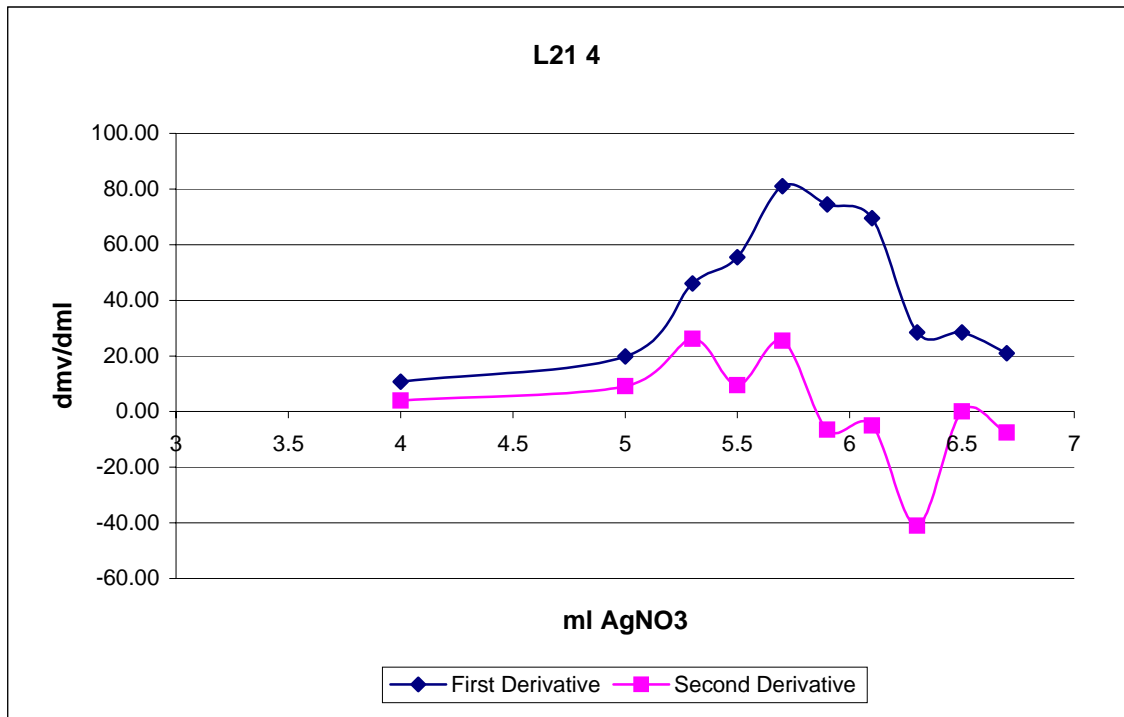
L22

1

AgNO₃		mv	d mL	d mV	d mV/dmL		Temp
0.7	0	187.7					22
8	7.3	201.4	7.30	13.70	1.88		22.1
12	11.3	209.8	4.00	8.40	2.10	0.22	22.1
16	15.3	220.8	4.00	11.00	2.75	0.65	22.1
19	18.3	233.4	3.00	12.60	4.20	1.45	22.1
21	20.3	246.5	2.00	13.10	6.55	2.35	22.2
22.5	21.8	263.2	1.50	16.70	11.13	4.58	22.2
23	22.3	272.8	0.50	9.60	19.20	8.07	22.2
23.4	22.7	284.8	0.40	12.00	30.00	10.80	22.2
23.6	22.9	292.9	0.20	8.10	40.50	10.50	22.2
23.8	23.1	302.6	0.20	9.70	48.50	8.00	22.2
24	23.3	312.7	0.20	10.10	50.50	2.00	22.2
24.2	23.5	323.5	0.20	10.80	54.00	3.50	22.3
24.4	23.7	331.5	0.20	8.00	40.00	-14.00	22.3
24.6	23.9	339.5	0.20	8.00	40.00	0.00	22.3
24.8	24.1	346.5	0.20	7.00	35.00	-5.00	22.3
25	24.3	351.9	0.20	5.40	27.00	-8.00	22.3

L22

AgNO₃		mv	d mL	d mV	d mV/dmL		Temp
0.2	0	212.3					22
5	4.8	236.5	4.80	24.20	5.04		22.1
7	6.8	260.8	2.00	24.30	12.15	7.11	22.1
7.5	7.3	273.6	0.50	12.80	25.60	13.45	22.2
7.8	7.6	285.7	0.30	12.10	40.33	14.73	22.2
8	7.8	297.1	0.20	11.40	57.00	16.67	22.2
8.2	8	312.1	0.20	15.00	75.00	18.00	22.2
8.4	8.2	323.7	0.20	11.60	58.00	-17.00	22.2
8.6	8.4	334.1	0.20	10.40	52.00	-6.00	22.3
8.8	8.6	343.1	0.20	9.00	45.00	-7.00	22.3
9	8.8	349.9	0.20	6.80	34.00	-11.00	22.3
9.2	9	355.3	0.20	5.40	27.00	-7.00	22.3
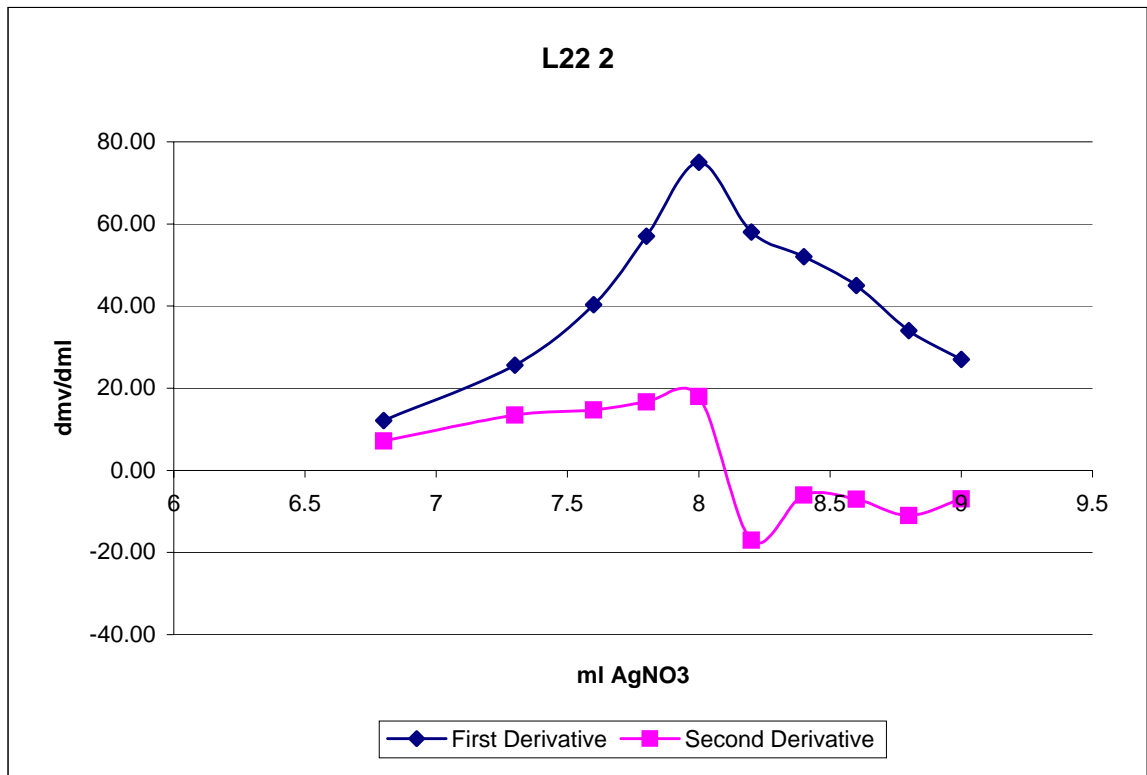
L22

3

AgNO₃		mv	d mL	d mV	d mV/dmL		Temp
9.2	0	219.8					22.1
12	2.8	237.1	2.80	17.30	6.18		22.2
13.5	4.3	253.1	1.50	16.00	10.67	4.49	22.2
14.5	5.3	276.7	1.00	23.60	23.60	12.93	22.2
14.9	5.7	301.6	0.40	24.90	62.25	38.65	22.2
15.1	5.9	318.2	0.20	16.60	83.00	20.75	22.2
15.3	6.1	331.1	0.20	12.90	64.50	-18.50	22.2
15.5	6.3	341.4	0.20	10.30	51.50	-13.00	22.2
15.7	6.5	347.3	0.20	5.90	29.50	-22.00	22.2
15.9	6.7	353.1	0.20	5.80	29.00	-0.50	22.2

L22 3
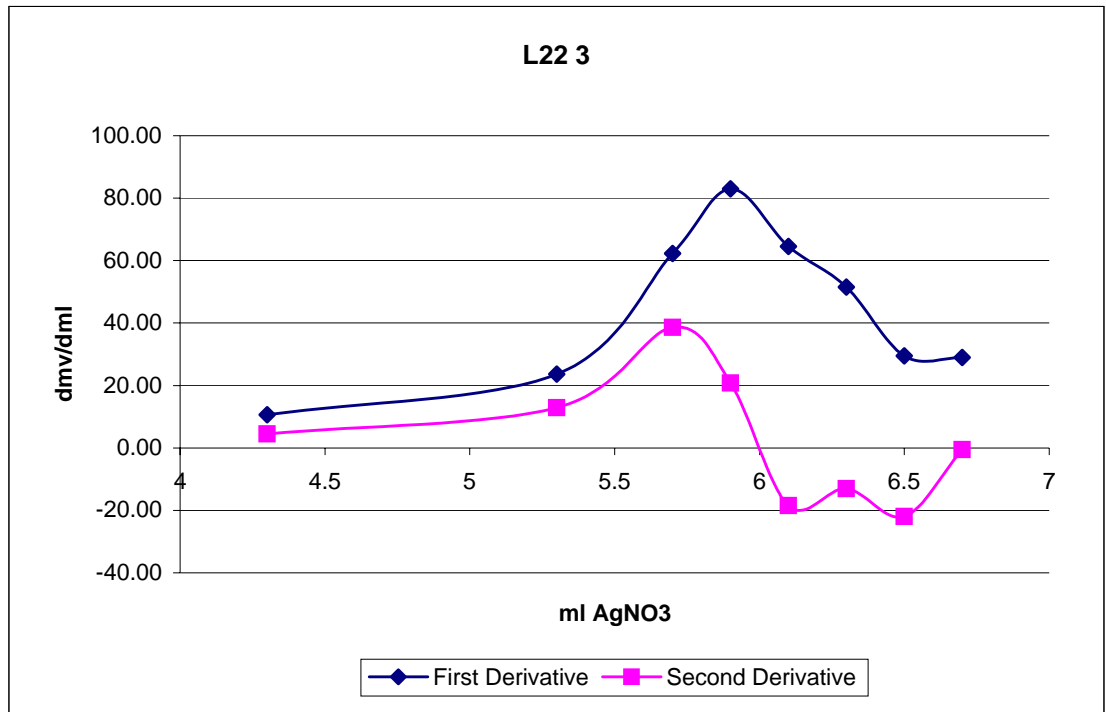
L22

4

AgNO$_3$		mv	d mL	d mV	d mV/dmL		Temp
15.9	0	226.2					22.2
18.7	2.8	246	2.80	19.80	7.07		22.2
20	4.1	263.1	1.30	17.10	13.15	6.08	22.3
20.5	4.6	274.2	0.50	11.10	22.20	9.05	22.3
20.8	4.9	285.9	0.30	11.70	39.00	16.80	22.3
21	5.1	298.9	0.20	13.00	65.00	26.00	22.3
21.2	5.3	314.1	0.20	15.20	76.00	11.00	22.3
21.4	5.5	327.5	0.20	13.40	67.00	-9.00	22.3
21.6	5.7	338.6	0.20	11.10	55.50	-11.50	22.4
21.8	5.9	346.8	0.20	8.20	41.00	-14.50	22.4
22	6.1	352.9	0.20	6.10	30.50	-10.50	22.4
22.2	6.3	358.3	0.20	5.40	27.00	-3.50	22.4
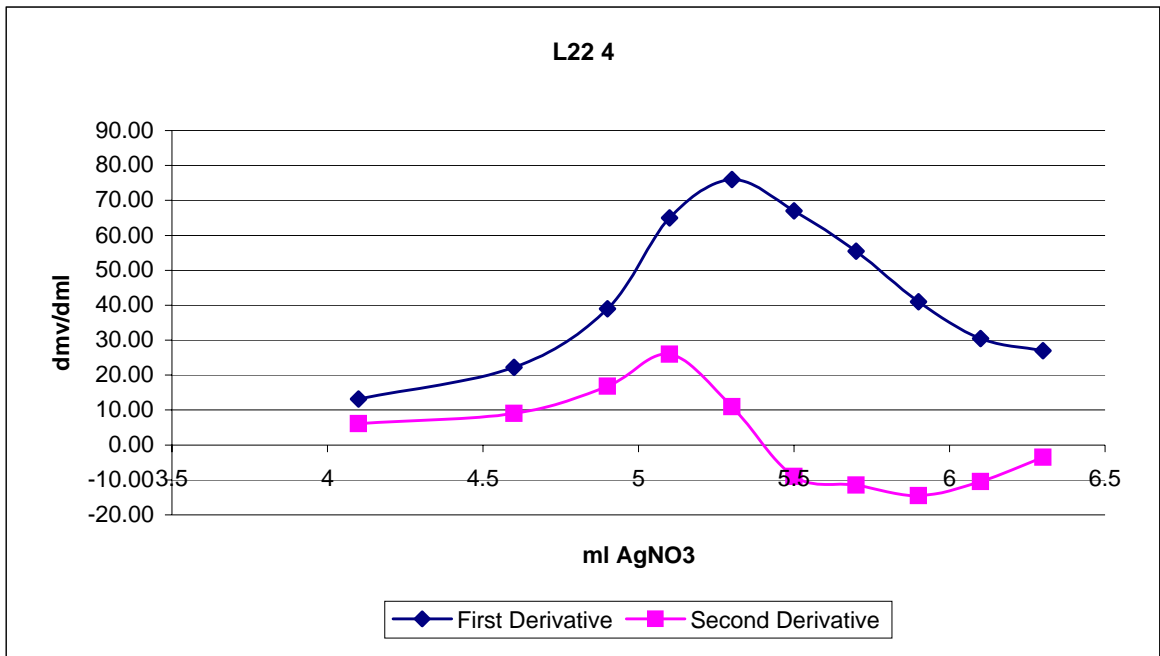
L34

1

AgNO$_3$		mv	d mL	d mV	d mV/dmL		Temp
7.8	0	186.1					21.9
12.8	5	197.5	5.00	11.40	2.28		21.9
24.2	16.4	221.3	11.40	23.80	2.09	-0.19	22
28.5	20.7	240.3	4.30	19.00	4.42	2.33	22
30	22.2	252.8	1.50	12.50	8.33	3.91	22
31.5	23.7	279.1	1.50	26.30	17.53	9.20	22
32	24.2	296.8	0.50	17.70	35.40	17.87	22
32.2	24.4	308.6	0.20	11.80	59.00	23.60	22.1
32.4	24.6	320.4	0.20	11.80	59.00	0.00	22.1
32.6	24.8	330.3	0.20	9.90	49.50	-9.50	22.1
32.8	25	339.1	0.20	8.80	44.00	-5.50	22.1
33	25.2	347.8	0.20	8.70	43.50	-0.50	22.2
33.2	25.4	353.9	0.20	6.10	30.50	-13.00	22.2
33.4	25.6	358.8	0.20	4.90	24.50	-6.00	22.2

L34
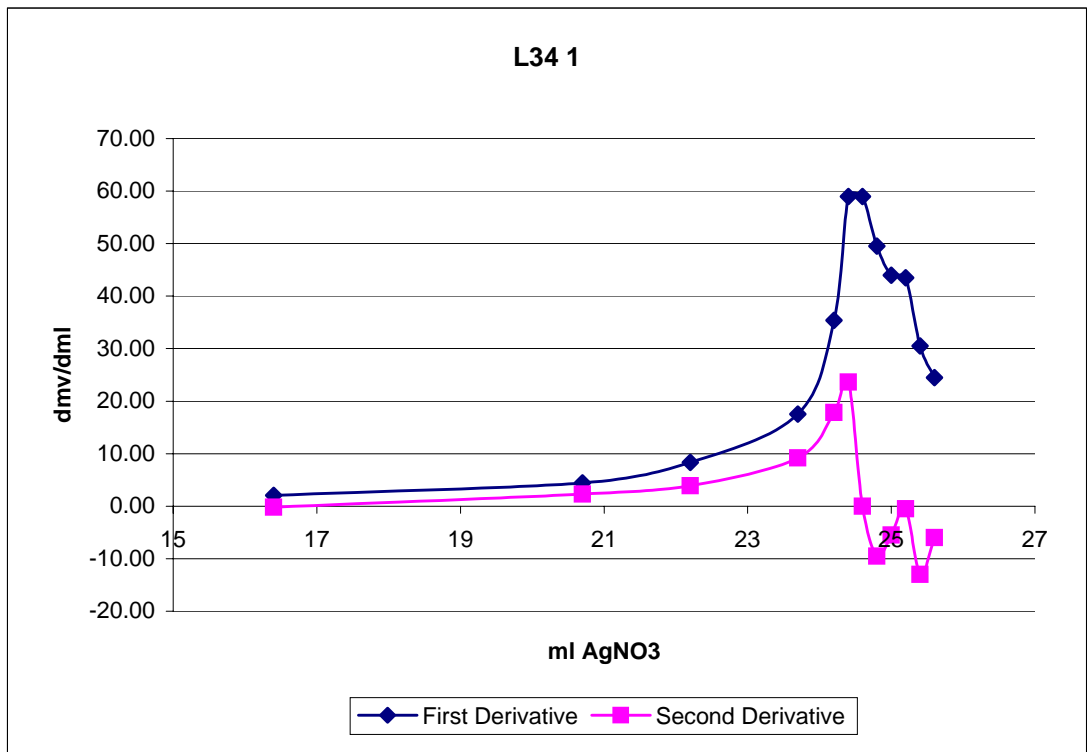
AgNO$_3$		mv	d mL	d mV	d mV/dmL		Temp
0.5	0	212.1					22.1
4	3.5	229.9	3.50	17.80	5.09		22.2
5	4.5	239.1	1.00	9.20	9.20	4.11	22.2
6	5.5	248.5	1.00	9.40	9.40	0.20	22.2
6.6	6.1	256.4	0.60	7.90	13.17	3.77	22.2
7	6.5	263.1	0.40	6.70	16.75	3.58	22.2
7.4	6.9	272.6	0.40	9.50	23.75	7.00	22.2
7.6	7.1	278.8	0.20	6.20	31.00	7.25	22.3
7.8	7.3	288	0.20	9.20	46.00	15.00	22.3
8	7.5	297.7	0.20	9.70	48.50	2.50	22.3
8.2	7.7	311	0.20	13.30	66.50	18.00	22.3
8.4	7.9	329.9	0.20	18.90	94.50	28.00	22.3
8.6	8.1	339.3	0.20	9.40	47.00	-47.50	22.3
8.8	8.3	347.5	0.20	8.20	41.00	-6.00	22.3
9	8.5	353.7	0.20	6.20	31.00	-10.00	22.3

L34
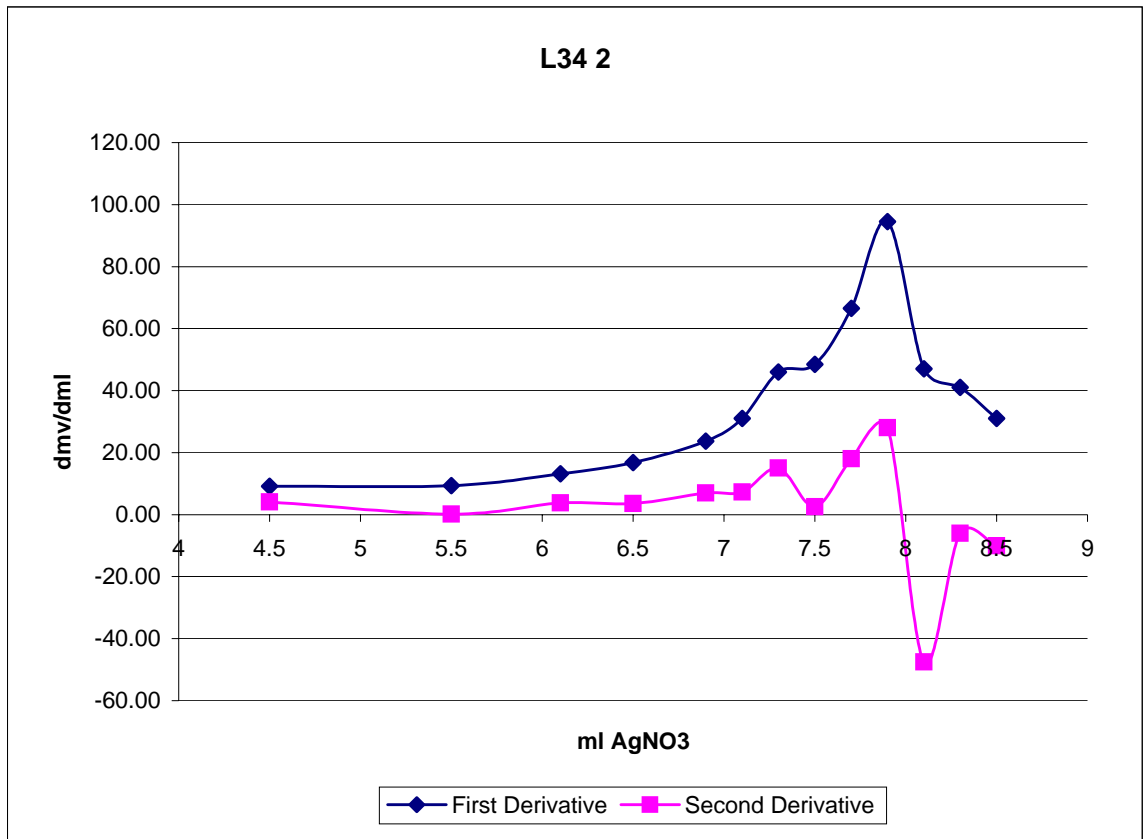
AgNO$_3$		mv	d mL	d mV	d mV/dmL		Temp
0.8	0	217.9					22.3
2.8	2	232.1	2.00	14.20	7.10		22.3
4.3	3.5	245.3	1.50	13.20	8.80	1.70	22.4
4.9	4.1	251.5	0.60	6.20	10.33	1.53	22.4
5.3	4.5	258.1	0.40	6.60	16.50	6.17	22.4
5.8	5	268.5	0.50	10.40	20.80	4.30	22.4
6.2	5.4	274.3	0.40	5.80	14.50	-6.30	22.4
6.4	5.6	281.5	0.20	7.20	36.00	21.50	22.4
6.6	5.8	292	0.20	10.50	52.50	16.50	22.4
6.8	6	305.3	0.20	13.30	66.50	14.00	22.4
7	6.2	318.9	0.20	13.60	68.00	1.50	22.4
7.2	6.4	329.1	0.20	10.20	51.00	-17.00	22.5
7.4	6.6	339.3	0.20	10.20	51.00	0.00	22.5
7.6	6.8	347.8	0.20	8.50	42.50	-8.50	22.5
7.8	7	353.3	0.20	5.50	27.50	-15.00	22.5
8	7.2	358.5	0.20	5.20	26.00	-1.50	22.5

L34

4
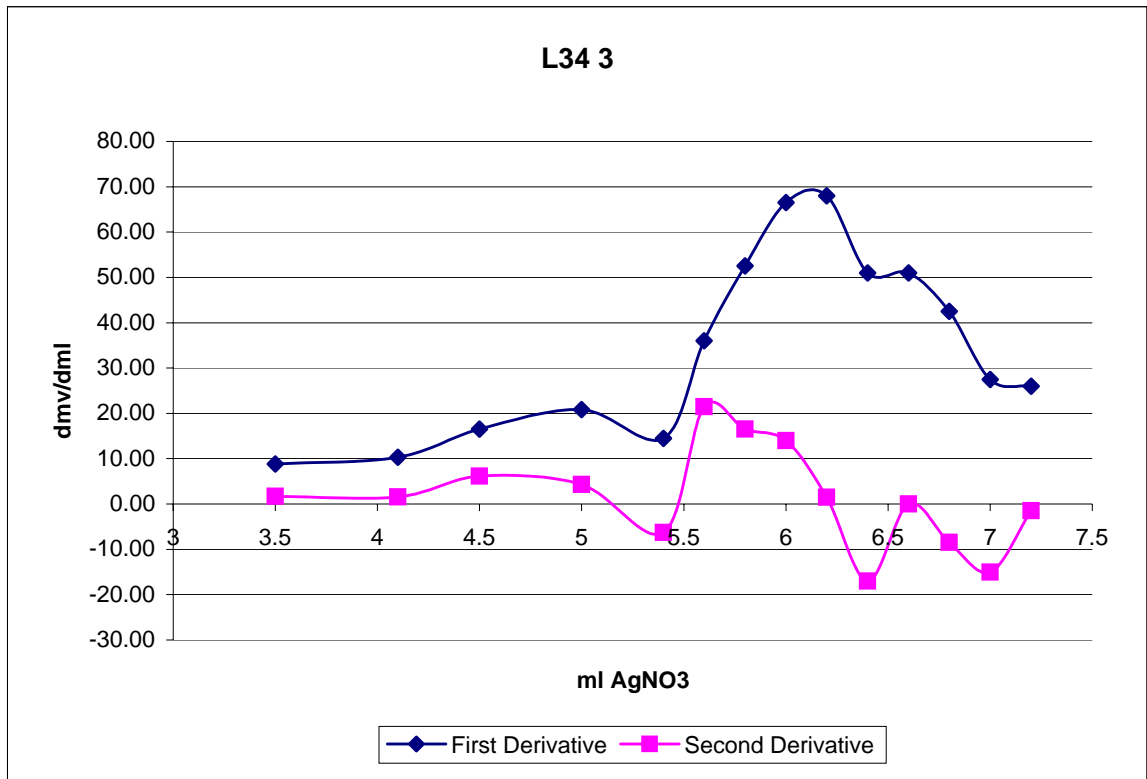
AgNO$_3$		mv	d mL	d mV	d mV/dmL		Temp
0.5	0	229.3					22.4
4	3.5	257.3	3.50	28.00	8.00		22.4
4.5	4	265.3	0.50	8.00	16.00	8.00	22.4
4.9	4.4	271.8	0.40	6.50	16.25	0.25	22.4
5.1	4.6	277.5	0.20	5.70	28.50	12.25	22.5
5.3	4.8	284.3	0.20	6.80	34.00	5.50	22.5
5.5	5	290.3	0.20	6.00	30.00	-4.00	22.5
5.7	5.2	298.3	0.20	8.00	40.00	10.00	22.5
5.9	5.4	309.9	0.20	11.60	58.00	18.00	22.5
6.1	5.6	322.7	0.20	12.80	64.00	6.00	22.5
6.3	5.8	332.7	0.20	10.00	50.00	-14.00	22.5
6.5	6	340.1	0.20	7.40	37.00	-13.00	22.5
6.7	6.2	347.5	0.20	7.40	37.00	0.00	22.5
6.9	6.4	353.5	0.20	6.00	30.00	-7.00	22.5
7.1	6.6	358.1	0.20	4.60	23.00	-7.00	22.5

L34 4

E116

L36
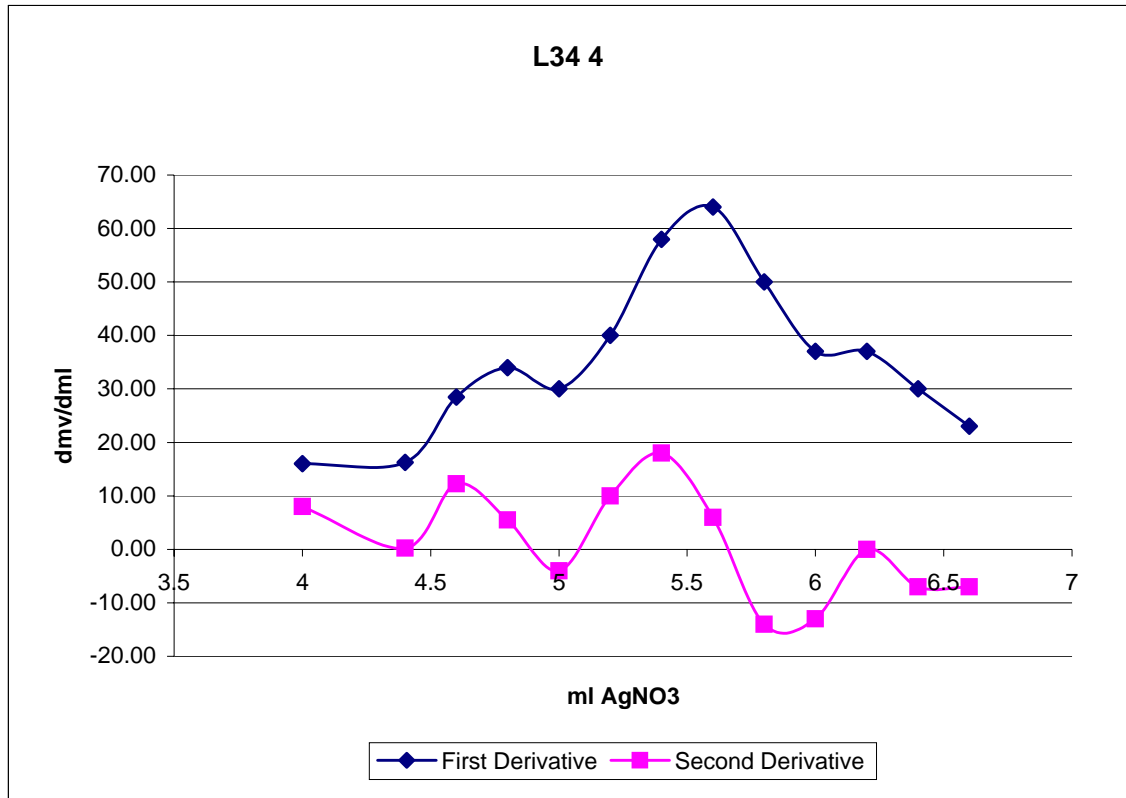
AgNO$_3$		mv	d mL	d mV	d mV/dmL		Temp
0.1	0	174.9					22.5
4.5	4.4	181.1	4.4	6.20	1.41		22.6
8.5	8.4	186.9	4	5.80	1.45	0.04	22.7
12.5	12.4	191.7	4	4.80	1.20	-0.25	22.7
18	17.9	200.5	5.5	8.80	1.60	0.40	22.8
22	21.9	208.5	4	8.00	2.00	0.40	22.8
27	26.9	222.5	5	14.00	2.80	0.80	22.8
29.5	29.4	241	2.5	18.50	7.40	4.60	22.8
30.5	30.4	251.1	1	10.10	10.10	2.70	22.9
31.5	31.4	268.9	1	17.80	17.80	7.70	22.9
32	31.9	285.7	0.5	16.80	33.60	15.80	22.9
32.2	32.1	295.7	0.2	10.00	50.00	16.40	22.9
32.4	32.3	307.1	0.2	11.40	57.00	7.00	22.9
32.6	32.5	321.1	0.2	14.00	70.00	13.00	22.9
32.8	32.7	334.7	0.2	13.60	68.00	-2.00	22.9
33	32.9	341.1	0.2	6.40	32.00	-36.00	22.9
33.2	33.1	348.5	0.2	7.40	37.00	5.00	22.9
33.4	33.3	353.5	0.2	5.00	25.00	-12.00	22.9

E117

L36
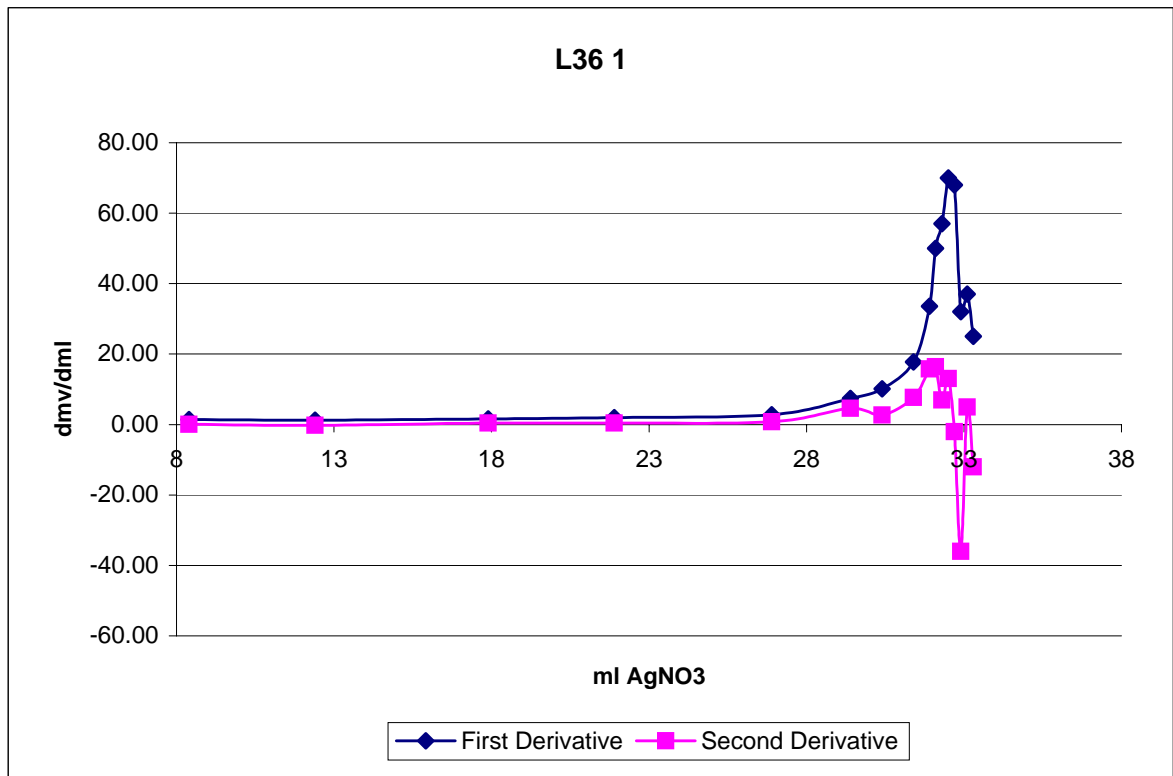
AgNO$_3$		mv	d mL	d mV	d mV/dmL		Temp
0.2	0	184.3					22.7
6.5	6.3	191.6	6.30	7.30	1.16		22.8
11.5	11.3	199.1	5.00	7.50	1.50	0.34	22.9
16.5	16.3	208.5	5.00	9.40	1.88	0.38	22.9
20.5	20.3	219.5	4.00	11.00	2.75	0.87	22.9
24	23.8	231.1	3.50	11.60	3.31	0.56	23
25	24.8	237.5	1.00	6.40	6.40	3.09	23
26.5	26.3	249.6	1.50	12.10	8.07	1.67	23
27.5	27.3	271.9	1.00	22.30	22.30	14.23	23
28.3	28.1	289.2	0.80	17.30	21.63	-0.67	23
28.5	28.3	298.5	0.20	9.30	46.50	24.88	23
28.7	28.5	310.5	0.20	12.00	60.00	13.50	23
28.9	28.7	323.6	0.20	13.10	65.50	5.50	23
29.1	28.9	334.8	0.20	11.20	56.00	-9.50	23.1
29.3	29.1	340.7	0.20	5.90	29.50	-26.50	23.1
29.5	29.3	346.1	0.20	5.40	27.00	-2.50	23.1
29.7	29.5	351.9	0.20	5.80	29.00	2.00	23.1
29.9	29.7	358.3	0.20	6.40	32.00	3.00	23.1

L36 2
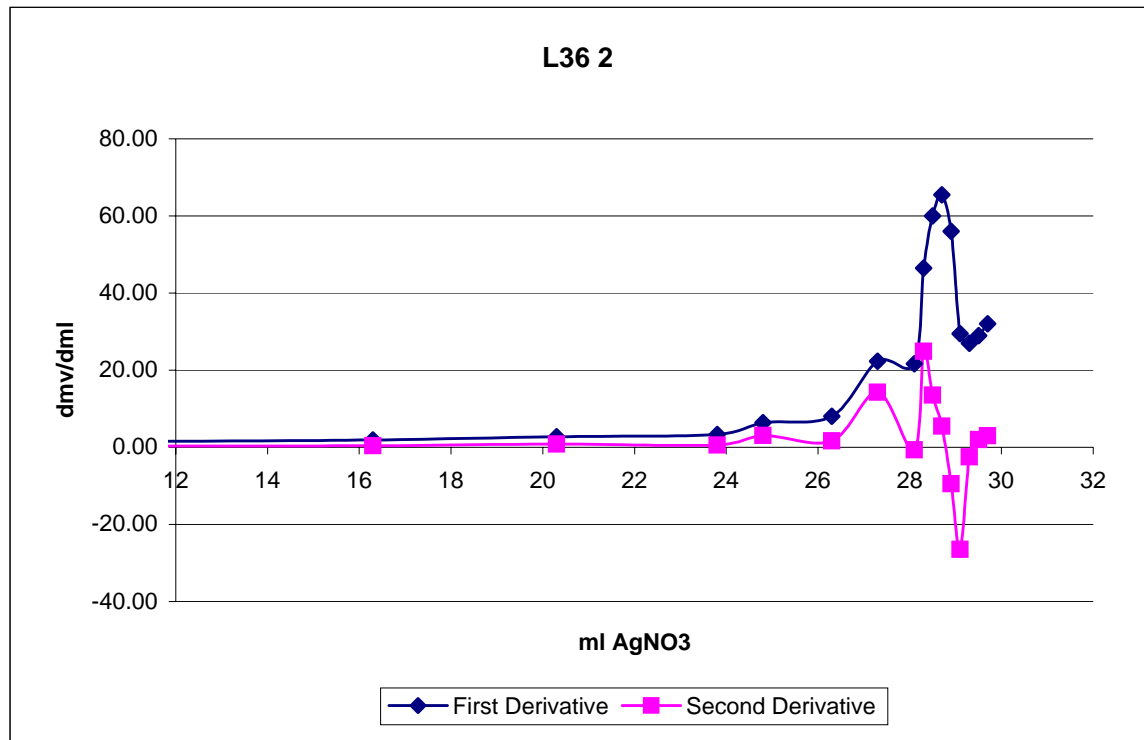
L36

3

AgNO$_3$		mv	d mL	d mV	d mV/dmL		Temp
0.1	0	193.5					22.9
6.5	6.4	203.7	6.40	10.20	1.59		23
11	10.9	211.9	4.50	8.20	1.82	0.23	23
15.1	15	225.3	4.10	13.40	3.27	1.45	23.1
17	16.9	235.6	1.90	10.30	5.42	2.15	23.1
19	18.9	251.6	2.00	16.00	8.00	2.58	23.1
20	19.9	264.7	1.00	13.10	13.10	5.10	23.1
20.8	20.7	294.3	0.80	29.60	37.00	23.90	23.1
21	20.9	307.5	0.20	13.20	66.00	29.00	23.2
21.2	21.1	321	0.20	13.50	67.50	1.50	23.2
21.4	21.3	331.5	0.20	10.50	52.50	-15.00	23.2
21.6	21.5	340.2	0.20	8.70	43.50	-9.00	23.2
21.8	21.7	346.5	0.20	6.30	31.50	-12.00	23.2
22	21.9	351.8	0.20	5.30	26.50	-5.00	23.2
22.2	22.1	356.3	0.20	4.50	22.50	-4.00	23.2
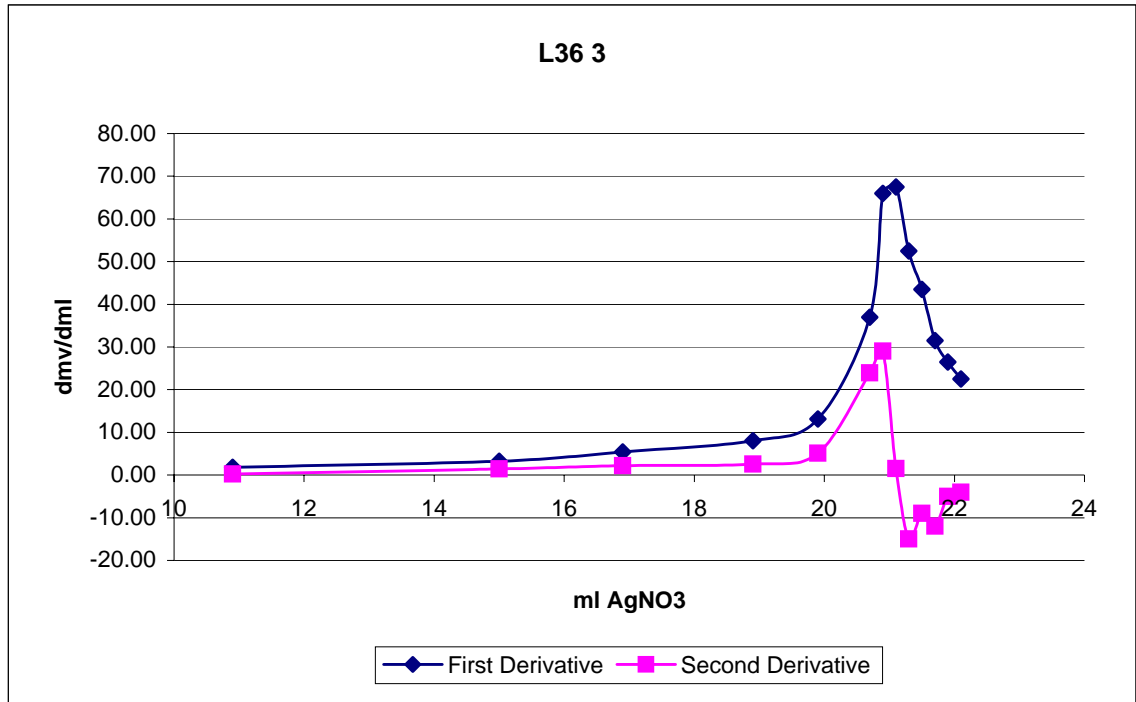
L36

4

AgNO₃	mv	d mL	d mV	d mV/dmL		Temp
0	212.1					23
5	225.8	5.00	13.70	2.74		23.1
8	244.1	3.00	18.30	6.10	3.36	23.2
9	254.9	1.00	10.80	10.80	4.70	23.2
9.8	272.8	0.80	17.90	22.38	11.58	23.2
10	277.1	0.20	4.30	21.50	-0.87	23.2
10.2	285.6	0.20	8.50	42.50	21.00	23.3
10.4	295.9	0.20	10.30	51.50	9.00	23.3
10.6	310.1	0.20	14.20	71.00	19.50	23.3
10.8	321.3	0.20	11.20	56.00	-15.00	23.3
11	331.1	0.20	9.80	49.00	-7.00	23.3
11.2	339.1	0.20	8.00	40.00	-9.00	23.3
11.4	345.6	0.20	6.50	32.50	-7.50	23.3
11.6	351.1	0.20	5.50	27.50	-5.00	23.3
11.8	356.3	0.20	5.20	26.00	-1.50	23.3

L36 4
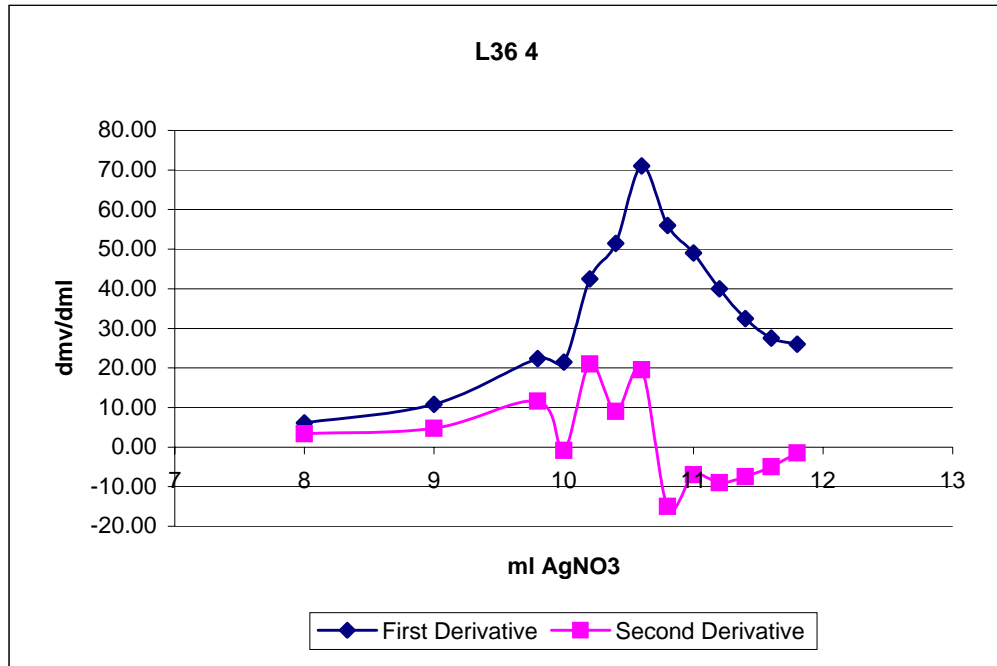
Appendix F
Resource International, Inc.
Bridge Deck Evaluation Report

BRIDGE DECK EVALUATION

Prepared for:

University of Toledo
Department of Civil Engineering
Toledo, Ohio 43606-3390

Prepared by:

Resource International Inc.,
6350 Presidential Gateway
Columbus, Ohio 43231

Rii # W-04-112
July 27, 2005

August 17, 2005

Douglas K. Nims, Ph.D., P.E.
Undergraduate Director and Associate Professor
Department of Civil Engineering
University of Toledo

RE: Ground Penetrating Radar (GPR) Testing Services
        OTT 2   28.47 R
        Sandusky Bay Bridge
        Rii # W-04-112

Dear Dr. Nims:

Enclosed is a report of a Bridge Deck Evaluation located on OTT 2
28.47 R. This report describes the data collected from the field and
the results of the GPR data analysis.

We sincerely appreciate the opportunity to provide GPR testing and
analysis on this project. If you have any questions regarding the
contents of this report, please call at (614) 823-4949.

Sincerely,
Resource International, Inc.

Cherif Amer-Yahia, Ph.D., MSEE
Project Engineer

Todd Majidzadeh
Vice President – Facility Management Services

TABLE OF CONTENTS

Page

II.   LIST OF FIGURES

III   APPENDIX A

DESCRIPTION OF GROUND PENETRATING RADAR (GPR)
AND METHOD OF SURVEY

BRIDGE DECK EVALUATION
OTT 2 28.47 R (Sandusky Bay Bridge)
University of Toledo

_____

1.   INTRODUCTION

Resource International Inc., conducted Ground Penetrating Radar testing and analysis for the subject bridge, OTT 2 28.47 R/Sandusky Bay Bridge (Eastbound only), within the Ottawa and Erie Counties. Initially, the contract purpose was to evaluate approximately 100 linear feet bridge, including the shoulders, to determine the condition of the concrete and rebar immediately above the Stay in Place Metal Forms (SIPMF) and below the lower rebar layer. In accordance with a meeting held on February 14, 2005, additional services were provided. The testing services were completed on November 30, 2004. The GPR data analysis and the results obtained are included in this report.

2.   GPR INSPECTION PROCEDURE

Ground Penetrating Radar (GPR) was used to collect data related to the condition of the deck. GPR equipment used and the procedure to collect deck condition data are described in Appendix A. The GPR data was collected at

   (a) normal speed (25 – 30 MPH) with air launched antennas with 2'' spacing on the sampling rate across the entire structure,
   (b) walking speed (3 – 5 MPH) with air launched antennas with 1'' spacing of the sampling rate for the study area (100 linear feet bridge), and
   (c) walking speed (3 – 5MPH) with ground coupled antenna with a 1'' sampling rate for the study area.

A series of multiple passes on a spacing of two (2) feet longitudinally, have been carried out. Additional passes were taken to assure existing core samples lay on the center of the GPR scan pass. This is shown in Figure 1. The work has been completed in accordance with all applicable segments of ASTM D 6087-97.

Due to the slow data collection speed, lane closures have been required.

3.   ANALYSIS OF GPR DATA

GPR data collected was used to evaluate the condition of the bridge deck. The software developed by the manufacturer of the GPR (GSSI), called RADAN (Radar Data Analyzer for Windows NT), was used to process the field data according to the

procedure developed by GSSI. The results of this analysis were used to determine the bridge deck condition as follows:

Delamination – the areas of the deck where delamination in the concrete was observed from the GPR data, represented by the areas shaded red.

Delamination in Isolated Areas – the areas of the deck where delamination in the concrete is not continuous. The GPR scan indicates that there are isolated areas of developing delaminations, represented by the areas shaded yellow.

No Delamination – the areas of the deck where no delamination in the concrete was observed from the GPR data, represented by the areas shaded light blue.

The GPR Scan analysis results shown in Figures 2 and 3 illustrate typical examples of weak and strong signal returns from the SIPMF.

The results of GPR data analysis are plotted on the plan sheets for the bridge decks, as shown in Figure 4 for the study area, and in Figures 5a, 5b, 5c, and 5d, for the entire structure.

4.   RESULTS OF BRIDGE DECK EVALUATION

The results of bridge deck evaluation shown in Figures 4, 5a, 5b, 5c and 5d indicate that the percent delaminations of the deck areas are as follows:

Study area (100 linear feet bridge)

Description	Top of Deck
Area of Delamination	19.6%
Area of isolated Delaminations	45.2%
Area of No Delamination	35.2%

Description	Bottom form
Area of Delamination	9%
Area of isolated Delaminations	24.5%
Area of No Delamination	66.5%

Entire structure (2050 linear feet bridge)

Description	Top of Deck
Area of Delamination	15.7%
Area of isolated Delaminations	43.7%
Area of No Delamination	40.6%

Description	Bottom form
Area of Delamination	30.8%
Area of isolated Delaminations	51.7%
Area of No Delamination	17.6%

Sandusky Bay Bridge   Resource International, Inc.
University of Toledo   Engineering Consultants
Bridge Deck Evaluation, GPR   3   Rii # W-04-112, 07/27/05
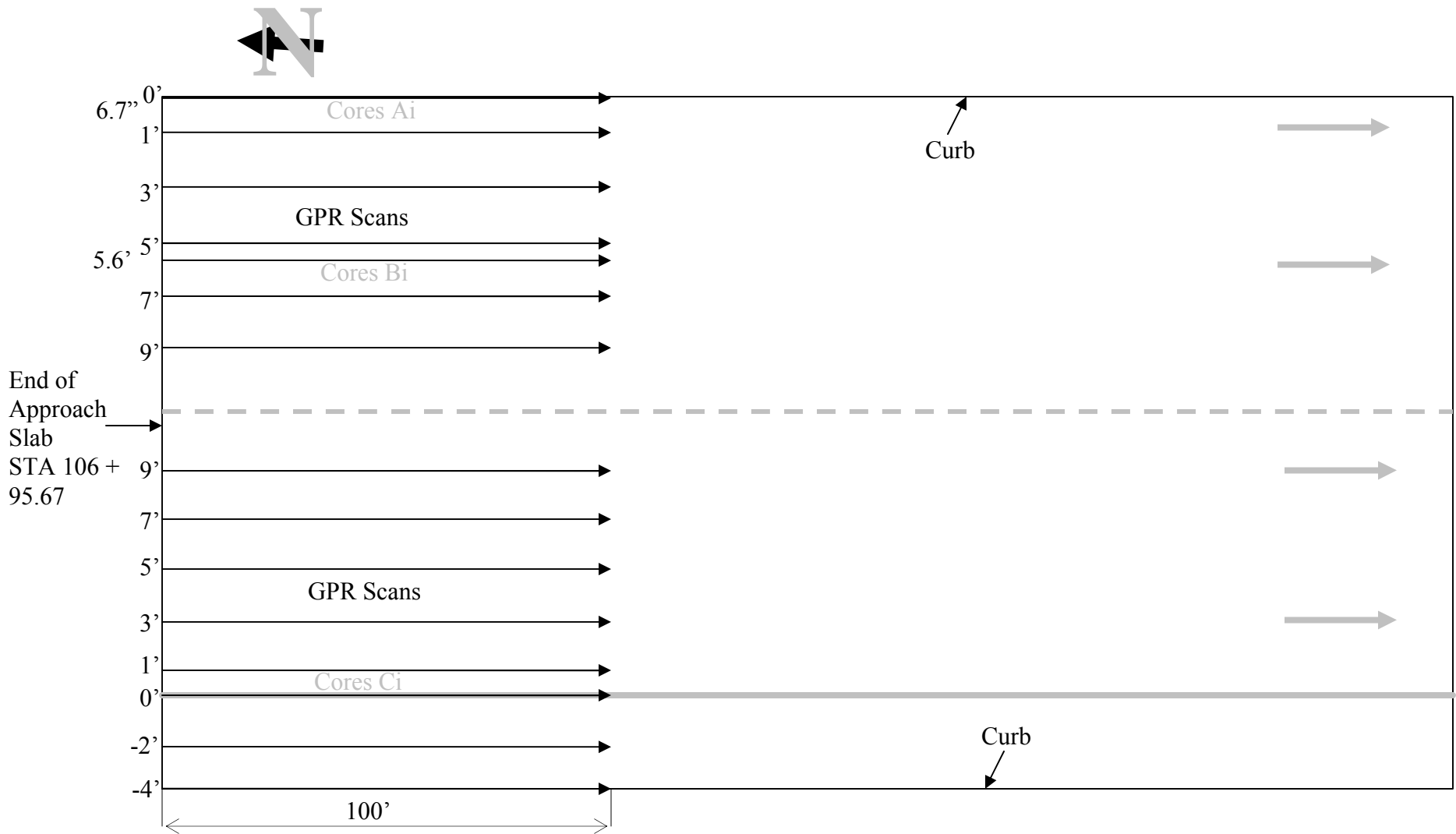
Figure 1. Sketch showing the locations of GPR scan lines (1500 MHz Ground Coupled Antenna)

4
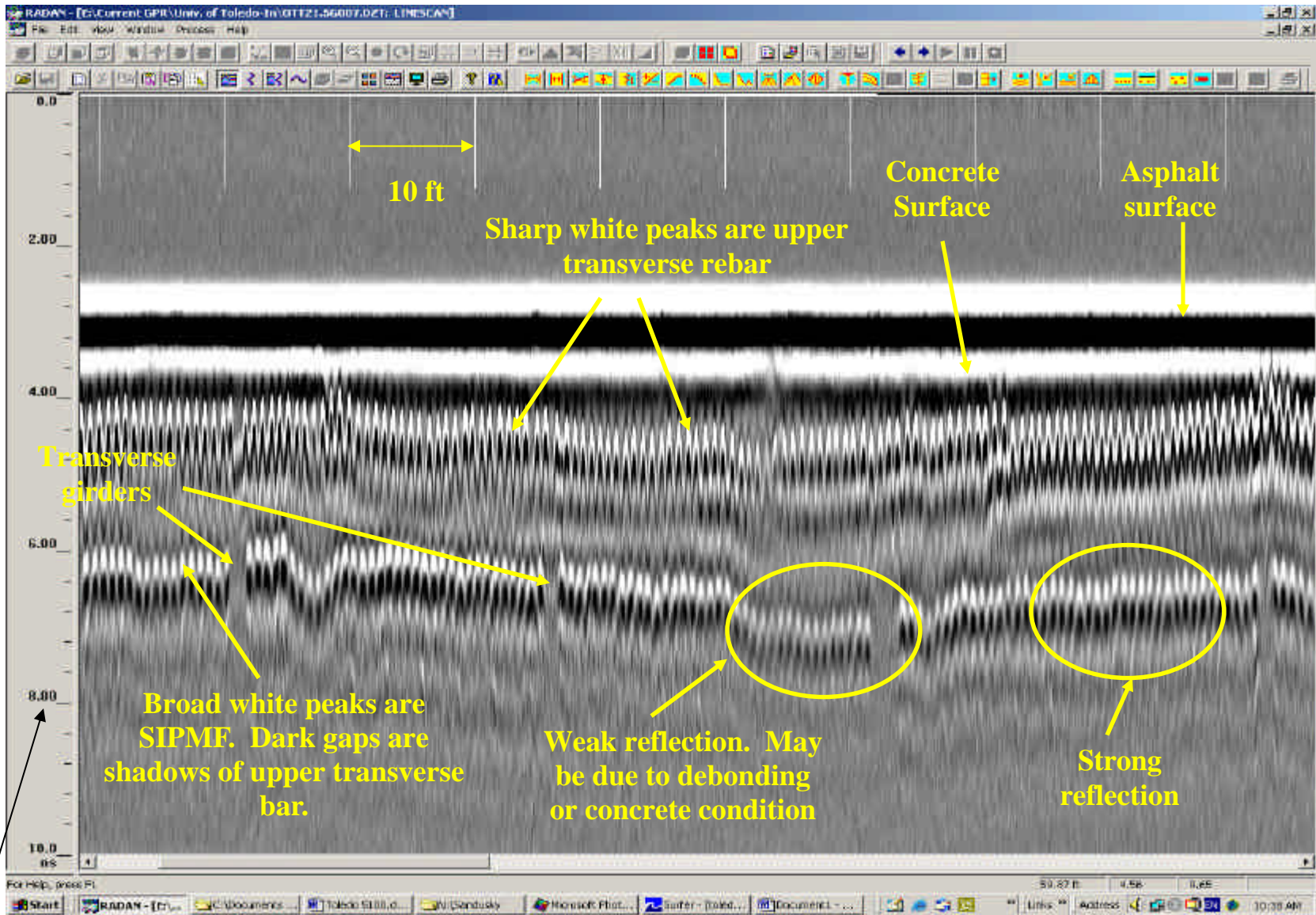
Vertical scale is time in ns. It represents apparent depth.

Figure 2. Typical GPR scan showing strong and weak signal returns from the SIPMF (1500 MHZ Ground Coupled Antenna)

5
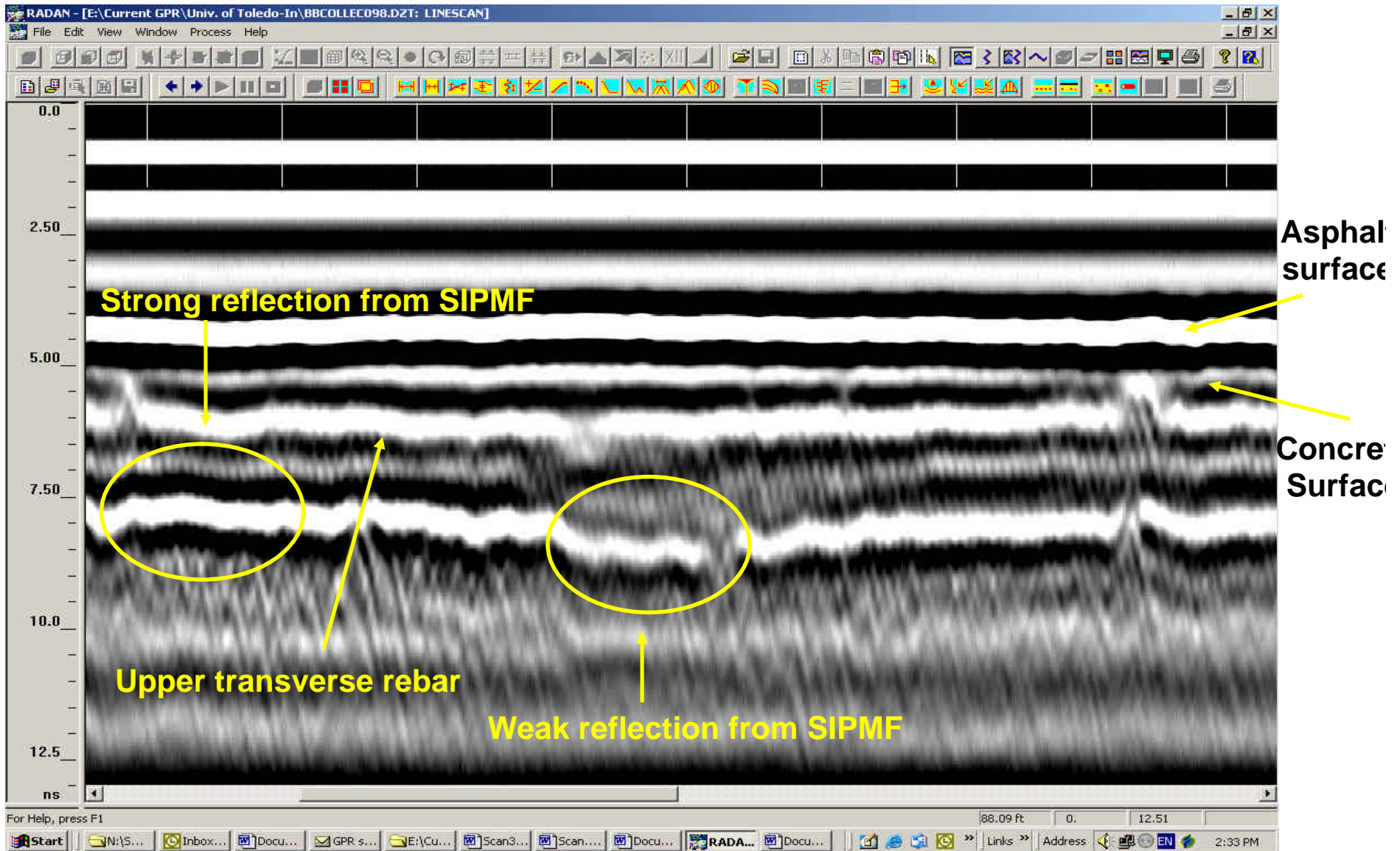
Figure 4. Typical GPR scan showing strong and weak signal returns from the SIPMF (1000 MHZ Air Launched Antenna)

STATE ROUTE 2
SANDUSKY BAY BRIDGE

DELAMINATION MAP \ TOP OF DECK

CORES C1 - C10
CORES B1 - B9
CORES A1 - A18-1

TOP LAYER OF DECK DELAMINATION

Color	Layer	Percent	Area
	DELAMINATION	19.6	389.69 SQ.FT.
	DELAMINATION/ ISOLATED AREAS	45.2	899.77 SQ.FT.
	NO DELAMINATION	35.2	699.26 SQ.FT.

DELAMINATION MAP \ BOTTOM FORM

CORES C1 - C10
CORES B1 - B9
CORES A1 - A18-1

AREA OVER BEAM
AREA OVER BEAM
AREA OVER BEAM

BOTTOM LAYER OF DECK DELAMINATION

Color	Layer	Percent	Area
	DELAMINATION	9.0	130.80 SQ.FT.
	DELAMINATION/ ISOLATED AREAS	24.5	358.81 SQ.FT.
	NO DELAMINATION	66.5	972.82 SQ.FT.

STATE ROUTE 2
SANDUSKY BAY BRIDGE

DELAMINATION MAP \ TOP OF DECK

CORE 16

CORE 15
CORE 14
CORE 13
CORE 12

SOUTH ABUT   PIER 22   PIER 21   PIER 20

TOP LAYER OF DECK DELAMINATION

Color	Layer	Percent	Area
	DELAMINATION	15.7	4808.11 SQ.FT.
	DELAMINATION/ ISOLATED AREAS	43.7	13398.66 SQ.FT.
	NO DELAMINATION	40.6	12466.48 SQ.FT.

DELAMINATION MAP \ BOTTOM FORM

CORE 16

CORE 15
CORE 14
CORE 13
CORE 12

SOUTH ABUT   PIER 22   PIER 21   PIER 20

BOTTOM LAYER OF DECK DELAMINATION

Color	Layer	Percent	Area
	DELAMINATION	30.8	6917.53 SQ.FT.
	DELAMINATION/ ISOLATED AREAS	51.7	11621.46 SQ.FT.
	NO DELAMINATION	17.6	3949.52 SQ.FT.

GRAPHIC SCALE

60 40 20 10 0

(IN FEET)
1 INCH = 20 FT.

DELAMINATION
MAP OF
BRIDGE# OTT-2-28.41
STATE ROUTE 2 OVER
SANDUSKY BAY

DATE:	03/14/05
DRAWN BY:	RCB
CHECKED BY:	CAY
JOB NO.:	W04-112
DRAWING NO.:	00-0
SHEET:	1 OF 4

STATE ROUTE 2
SANDUSKY BAY BRIDGE

DELAMINATION MAP \ TOP OF DECK

CORE 11   CORE 10   CORE 9   CORE 8   CORE 7   CORE 6   CORE 5

PIER 19   PIER 18   PIER 17   PIER 16   PIER 15   PIER 14   PIER 13

TOP LAYER OF DECK DELAMINATION

Color	Layer	Percent	Area
	DELAMINATION	15.7	4808.11 SQ.FT.
	DELAMINATION/ ISOLATED AREAS	43.7	13398.66 SQ.FT.
	NO DELAMINATION	40.6	12466.48 SQ.FT.

DELAMINATION MAP \ BOTTOM FORM

CORE 11   CORE 10   CORE 9   CORE 8   CORE 7   CORE 6   CORE 5

PIER 19   PIER 18   PIER 17   PIER 16   PIER 15   PIER 14   PIER 13
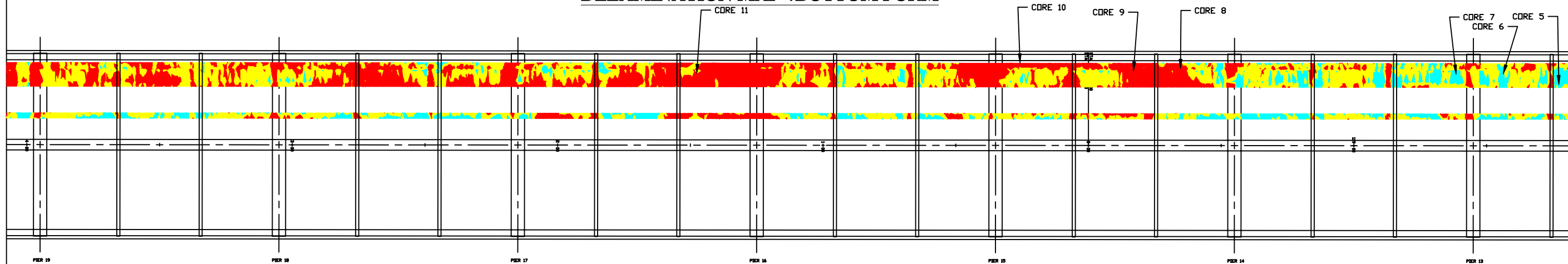
BOTTOM LAYER OF DECK DELAMINATION

Color	Layer	Percent	Area
	DELAMINATION	30.8	6917.53 SQ.FT.
	DELAMINATION/ ISOLATED AREAS	51.7	11621.48 SQ.FT.
	NO DELAMINATION	17.6	3949.52 SQ.FT.

DRAWN BY:	RCB	DATE:	03/14/05
CHECKED BY:	CAY	DRAWING NO.:	00-0
JOB NO.:	W04-112	SHEET:	2 OF 4

STATE ROUTE 2
SANDUSKY BAY BRIDGE

DELAMINATION MAP \ TOP OF DECK

CORE 4   CORE 3   CORE 2   CORE 1

PIER 12   PIER 11   PIER 10   PIER 9   PIER 8   PIER 7

TOP LAYER OF DECK DELAMINATION

Color	Layer	Percent	Area
	DELAMINATION	15.7	4808.11 SQ.FT.
	DELAMINATION/ ISOLATED AREAS	43.7	13398.66 SQ.FT.
	NO DELAMINATION	40.6	12466.48 SQ.FT.

DELAMINATION MAP \ BOTTOM FORM

CORE 4   CORE 3   CORE 2   CORE 1

PIER 12   PIER 11   PIER 10   PIER 9   PIER 8   PIER 7

BOTTOM LAYER OF DECK DELAMINATION

Color	Layer	Percent	Area
	DELAMINATION	30.8	6917.53 SQ.FT.
	DELAMINATION/ ISOLATED AREAS	51.7	11621.48 SQ.FT.
	NO DELAMINATION	17.6	3949.52 SQ.FT.

GRAPHIC SCALE

(IN FEET)
1 INCH = 20 FT.

60 40 20 0 20
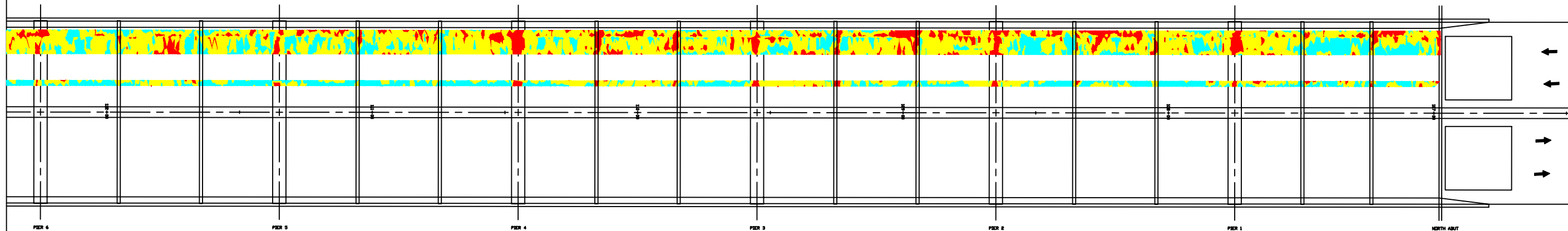
DELAMINATION
MAP OF
BRIDGE# OTT-2-28.41
STATE ROUTE 2 OVER
SANDUSKY BAY

RESOURCE INTERNATIONAL INC.
6350 PRESIDENTIAL GATEWAY
COLUMBUS, OHIO 43231
(614) 823-4949

DATE:	03/14/05	DRAWN BY:	RCB
DRAWING NO.:	00-0	CHECKED BY:	CAY
SHEET:	3 OF 4	JOB NO.:	W04-112

STATE ROUTE 2
SANDUSKY BAY BRIDGE

DELAMINATION MAP \ TOP OF DECK

PIER 6   PIER 5   PIER 4   PIER 3   PIER 2   PIER 1   NORTH ABUT

TOP LAYER OF DECK DELAMINATION

Color	Layer	Percent	Area
	DELAMINATION	15.7	4808.11 SQ.FT.
	DELAMINATION/ ISOLATED AREAS	43.7	13398.66 SQ.FT.
	NO DELAMINATION	40.6	12466.48 SQ.FT.

DELAMINATION MAP \ BOTTOM FORM

PIER 6   PIER 5   PIER 4   PIER 3   PIER 2   PIER 1   NORTH ABUT

BOTTOM LAYER OF DECK DELAMINATION

Color	Layer	Percent	Area
	DELAMINATION	30.8	6917.53 SQ.FT.
	DELAMINATION/ ISOLATED AREAS	51.7	11621.48 SQ.FT.
	NO DELAMINATION	17.6	3949.52 SQ.FT.

GRAPHIC SCALE

(IN FEET)
1 INCH = 20 FT.

DELAMINATION
MAP OF
BRIDGE# OTT-2-28.41
STATE ROUTE 2 OVER
SANDUSKY BAY

DATE:	03/14/05
DRAWING NO.:	00-0
SHEET:	4 OF 4
DRAWN BY:	RCB
CHECKED BY:	CAY
JOB NO.:	W04-112

Background

Ground Penetrating Radar (GPR) manufactured by Geophysical Survey Systems, Inc. (GSSI) is used to conduct non-destructive testing of bridge decks at travel speeds up to 35 miles per hour. This method includes two model 4108 antennas, the SIR-20 with Panasonic Toughbook computer, a distance-measuring instrument (DMI), and a three-camera alignment system. GPR is the state of the art method to evaluate pavement conditions, detect bridge deck delaminations, and estimate quantities of concrete rehab or repair within bridge decks.

The radar transmits a radio pulse with a frequency of 1 GHz into the subsurface. The GPR system uses electromagnetic wave propagation to image, locate, and quantitatively identify changes in electrical and magnetic properties in the surveyed area. The ability to detect a subsurface feature depends upon contrast in electrical and magnetic properties. These electric field data have to be processed to correct for distortions, artifacts of data acquisition, removal of interference, and to provide accurate calibrated positions in time and distance. GPR is capable of locating various materials since the radar signal reflection from these objects depends on contrasting dielectric properties of the material, not just high electrical conductivity.

Experience

Resource international has scanned over 19.75 lane miles of area on 116 bridges. These bridges as well as pavement, parking lots, landfill areas, grave and underground storage tank (UST) scans bring the total area scanned to well over 1.25 million square feet.

Survey Vehicle

The Resource International survey vehicle (pictured above) is equipped with:

- GSSI SIR-20 radar system and two 1 GHz air launched horns attached to the rear of the van on an adjustable mounting system.
- Corrsys-Datron DMI wheel pulse encoder for accurate survey length measurements.
- A three camera alignment system for accurate survey width measurements.

- A workstation inside the van for the operator during data collection.
- Several hazard lights that comply with state and federal standards for this type of survey.
  - Rear facing arrowstick lights.
  - Top mounted strobe light.
  - Red light and flag at end of mounting system.

Method of Survey

The GPR bridge deck survey is performed by making a series of passes over the bridge deck in a continuous loop. Survey scan lines are spaced in 2.0 ft increments over the entire driving surface of the bridge deck (see image on right). In order to accomplish this, six passes are made in each lane (assuming a 12 foot lane). For the safety of equipment, crew, and motorists, the GPR van is always shadowed by a trailing vehicle with truck mounted arrow board. A police vehicle is also used in those areas where traffic is relatively heavy (urban) and/or posted speed limit is high (65 mph).
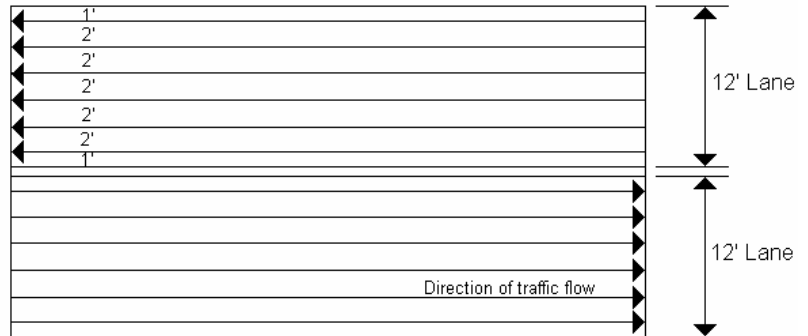
GPR Survey Scan Lines of a 2-Lane Bridge Deck

Camera Positioning

The camera positioning system allows the driving lanes of a bridge width to be surveyed. The survey vehicle is equipped with a three camera positioning system located on either side and in the rear of the vehicle. This system allows the driver to maintain a specified distance from a reference line throughout the survey. The reference lines used are the painted edge lines of each lane surveyed. The bridge deck survey lanes are spaced in 2.0 ft increments over the entire driving surface.

SIR-20 Radar System Control Unit

A trigger pulse is generated in the control unit at a normal repetition rate. The trigger pulse is then sent through the control cable to the transmitter electronics in the transducer (antenna). The transmit pulse then propagates along the antenna and is radiated into the subsurface. In the subsurface, reflections occur at boundaries where there is a dielectric contrast. The reflected portion of the signal travels back to the antenna. The receiver in the antenna detects the returning signal and sends it back to the control unit. Finally, in the control unit the signal is processed and displayed. The SIR-20 Radar System includes:

- Digital system data recording to hard drive and CD.

- Up to 4 antenna channels, typically two are used.
- Advanced gain and filter functions to clarify the data.
- Fast scan rates (500 scans/sec) allow faster survey speeds.
- Size of objects detectable (wire mesh (millimeters) to large geological features).

Distance Measuring Instrument (DMI)

The DMI, manufactured by Corrsys-Datron, allows an entire bridge to be mapped with all features easily located. The DMI correlates radar transmitted pulses to the longitudinal location of the surveyed area. The DMI also allows the vehicle to fluctuate speed from 0 to 122 mph and still accurately record the longitudinal location of the received radar pulses.

Data Collection Limitations

GPR data collection is performed on dry pavement due to the high dielectric constant of water. The settings are optimized for resolution clarity and include only the following limitations:

- The maximum scanning rate limits the GPR van's velocity to less than 35mph for high detail data collection (2-inch increments).
- The air launched antennas must be mounted on the van and therefore survey areas are limited to areas accessible by the van.

Data Collection using a 1500 MHz Ground Coupled antenna